

# Diversity of *Distoseptispora* (Distoseptisporaceae) taxa on submerged decaying wood from the Red River in Yunnan, China

Hong-Wei Shen<sup>1,2,3</sup>, Dan-Feng Bao<sup>1</sup>, Saranyaphat Boonmee<sup>2,3</sup>, Yong-Zhong Lu<sup>4</sup>, Xi-Jun Su<sup>1</sup>, Yun-Xia Li<sup>1</sup>, Zong-Long Luo<sup>1</sup>

<sup>1</sup> College of Agriculture and Biological Science, Dali University, Dali 671003, Yunnan, China

<sup>2</sup> Center of Excellence in Fungal Research, Mae Fah Luang University, Chiang Rai 57100, Thailand

<sup>3</sup> School of Science, Mae Fah Luang University, Chiang Rai 57100, Thailand

<sup>4</sup> School of Food and Pharmaceutical Engineering, Guizhou Institute of Technology, Guiyang 550003, Guizhou, China

Corresponding author: Zong-Long Luo (luozonglongfungi@163.com)

## Abstract

The Red River Basin is located in the Indo-Burma biodiversity hotspot and is rich in lignicolous freshwater fungi, but no systematic research has been conducted. A systematic study on the species diversity of lignicolous freshwater fungi in the basin is ongoing. Seven distoseptispora-like specimens were collected from the Red River Basin in Yunnan. Phylogenetic analysis of ITS, LSU, *tef1*-α, and *rpb2* genes and combined morphological data indicate that there are six distinct species of *Distoseptispora*, including two new species and four known species. Two new species were named *D. suae* and *D. xinpingsensis*, and the four known species were *D. bambusae*, *D. euseptata*, *D. obpyriformis* and *D. pachyconidia*. This study provides detailed descriptions and illustrations of these six species and an updated phylogenetic backbone tree of *Distoseptispora*.

**Key words:** 2 new taxa, lignicolous freshwater fungi, phylogeny, Sordariomycetes, taxonomy



Academic editor: S. Maharachchikumbura

Received: 22 November 2023

Accepted: 19 January 2024

Published: 5 February 2024

**Citation:** Shen H-W, Bao D-F, Boonmee S, Lu Y-Z, Su X-J, Li Y-X, Luo Z-L (2024) Diversity of *Distoseptispora* (Distoseptisporaceae) taxa on submerged decaying wood from the Red River in Yunnan, China. MycoKeys 102: 1–28. <https://doi.org/10.3897/mycokeys.102.116096>

**Copyright:** © Hong-Wei Shen et al.

This is an open access article distributed under terms of the Creative Commons Attribution License (Attribution 4.0 International – CC BY 4.0).

## Introduction

The present study is to establish the species of freshwater fungi along a north-to-south longitudinal gradient (Hyde et al. 2016). Yunnan is one of the hotspots for lignicolous freshwater fungi, where numerous species have been reported (Su et al. 2016; Luo et al. 2017, 2018a, b, 2019; Bao et al. 2020; Dong et al. 2020, 2021). In Yunnan, 278 lignicolous freshwater fungi have been identified in both lentic habitats (Cai et al. 2002; Luo et al. 2004) and lotic habitats, including the Nu Jiang/Salween River, Lancang River/Mekong River, Dulong River, and Jinsha River/Yangtze River (Tsui et al. 2000; Luo et al. 2018a, b, 2019; Bao et al. 2020, 2021; Dong et al. 2020, 2021; Shen et al. 2022). However, the species diversity and distribution of lignicolous freshwater fungi in the Red River Basin remain under-explored.

The Red River, one of the largest rivers in Southeast Asia, originates in Weishan County, Dali Bai Autonomous Prefecture, Yunnan Province, China, it has a total length of 1200 km with a catchment area of 169,000 km<sup>2</sup> (Haruyama 1995; Van den Bergh et al. 2007). Of this area, 50.3% is in Vietnam, 48.8% in China,

and 0.9% in Laos (Van Maren 2007). The portion of the Red River Basin located in China is referred to as “Yuanjiang”. This segment has a length of 677 km and is characterized by a plateau monsoon climate (Gu et al. 2018). Precipitation in the basin generally decreases from downstream to upstream and increases from the valleys to the mountains. The basin boasts a wealth of biological resources (Jiang 1980; Zhou and Cui 1997; Chen and Yu 2013; Gu et al. 2018).

*Distoseptispora* is a well-studied phylogenetic genus introduced by Su et al. (2016) to accommodate some *Sporidesmium* taxa with unbranched, olive green, cylindrical conidiophores, monoblastic, integrated, determinate, terminal, cylindrical conidiogenous cells, and acrogenous, distoseptate, cylindrical, smooth, darker conidia with slightly paler (but not hyaline), rounded apices of indeterminate length (Su et al. 2016; Yang et al. 2018, 2021; Zhang et al. 2022). Based on morphological and phylogenetic analyses, 73 species have been accepted in *Distoseptispora* in recent years (<http://www.indexfungorum.org/Names/Names.asp>; accessed on 2 January 2024; Hu et al. 2023). These include the type species *D. fluminicola* McKenzie, Hong Y. Su, Z.L. Luo & K.D. Hyde and two species transferred from *Ellisembia* as *D. adscendens* (Berk.) R. Zhu & H. Zhang and *D. leonensis* (M.B. Ellis) R. Zhu & H. Zhang. Among them, *D. hyalina* and *D. licualae* are the only two teleomorph taxa in *Distoseptispora* (Yang et al. 2021; Konta et al. 2023). Members of *Distoseptispora* are primarily saprophytes found on woody substrates from freshwater habitats (45 species), predominantly in China and Thailand and some also have been found in terrestrial habitats (23 species); *D. bambusae*, *D. clematidis*, *D. tectonae*, *D. thysanolaenae* and *D. xishuangbannaensis* have been reported in both freshwater and terrestrial habitats (Hyde et al. 2016; Luo et al. 2018a, 2019; Yang et al. 2018, 2021; Monkai et al. 2020; Phukhamsakda et al. 2020; Sun et al. 2020; Dong et al. 2021; Li et al. 2021; Shen et al. 2021; Ma et al. 2022; Zhai et al. 2022; Zhang et al. 2022). The conidia of *Distoseptispora* vary significantly in their characteristics, especially in terms of shape and size. Zhang et al. (2022) reassessed both the generic and specific boundaries of *Distoseptispora*, and summarized the characteristics of species in this genus, encompassing various attributes such as the length of conidiophores, proliferation, and conidiogenesis in conidiogenous cells, and details about conidia, including their type (distoseptate or euseptate), number of septa, shape, length, color, proliferation, rostrate nature, and wall thickness. Even though *Distoseptispora* species formed three distinct clades in phylogenetic analysis results that received strong support, the morphological characters of these species (such as monoblastic/polyblastic, euseptate/distoseptate) only offer species-level differentiation and do not hold taxonomic significance for the broader categorization of *Distoseptispora* (Yang et al. 2021; Zhang et al. 2022).

A systematic investigation of lignicolous freshwater fungal diversity and distribution in the Red River Basin is ongoing. This study represents the first report of *Distoseptispora* species in the Red River Basin. A morphological examination combined with phylogenetic analysis combining internal transcribed spacer (ITS), large subunit nuclear ribosomal RNA (LSU), translation elongation factor 1-alpha (*tef1-α*) and second-largest subunit of RNA polymerase II (*rpb2*) sequence data, established that out of seven *distoseptispora*-like specimens collected in the Red River Basin, six species of *Distoseptispora* were identified, including two new species, named as *D. suae* and *D. xinpingensis* and four known species, viz. *D. bambusae*, *D. euseptata*, *D. obpyriformis* and *D. pachyconidia*.

## Materials and methods

### Specimen collection, examination and isolation

Specimens of submerged decaying wood were collected from the Yuanjiang Basin (Red River) in Yunnan, China. The samples were incubated in a plastic box at room temperature for one week. Morphological observations were conducted following the methods of Luo et al. (2018a) and Senanayake et al. (2020) with a few modifications. Macromorphological characteristics of the samples were observed using an Optec SZ 760 compound stereomicroscope (Chongqing Optec Instrument Co., Ltd, Chongqing, China). Preliminary microscope slides were examined and photographed under a Nikon ECLIPSE Ni-U compound stereomicroscope (Nikon, Tokyo, Japan). Colonies' morphologies on native substrates were captured using a Nikon SMZ1000 stereo-zoom microscope (Nikon, Tokyo, Japan). The measurements of photomicrographs were obtained using Tarosoft (R) Image Frame Work version 0.9.7. Images were edited with Adobe Photoshop CS5 Extended version 12.0.0.0 software (Adobe Systems, San Jose, CA, USA).

Single spore isolations were carried out based on the method described by Luo et al. (2018a). The individually germinated conidia were transferred to fresh potato dextrose agar (PDA, from Beijing Bridge Technology Co., Ltd., Beijing, China) plates and incubated at room temperature in the dark. Some of the remaining germinated spores, along with their agar, were placed on water-mounted glass slides to photograph the origins of the germ tubes.

After observation and isolation, specimens were air-dried naturally, wrapped in absorbent paper, and stored in a ziplock bag with mothballs. These specimens were then deposited in the herbarium of Cryptogams, Kunming Institute of Botany, Chinese Academy of Sciences (**KUN-HKAS**), Kunming, China. The cultures were deposited with the China General Microbiological Culture Collection Center (**CGMCC**), and Kunming Institute of Botany Culture Collection (**KUNCC**). Fungal Names numbers are registered in the Fungal Names database (<https://nmdc.cn/fungalnames/registre>; accessed on 4 August 2023; Wang et al. 2023) and Facesoffungi numbers were obtained as described in Jayasiri et al. (2015).

### DNA extraction, PCR amplification and sequencing

DNA extraction, PCR amplification, sequencing, and phylogenetic analysis were carried out following the methods described by Dissanayake et al. (2020). Mycelia used for DNA extraction were cultivated on PDA for 3–4 weeks at 24 °C. From each isolate, total genomic DNA was extracted from 100–150 mg of axenic mycelium, which was carefully scraped from the edges of the growing culture with a sterile scalpel. This material was transferred to a 1.5 mL microcentrifuge tube using sterilized inoculum needles. Mycelium was ground to a fine powder with liquid nitrogen or quartz sand to break the cells for DNA extraction. DNA was extracted with the Trelief™ Plant Genomic DNA Kit (TSP101) following manufacturer guidelines (Beijing Tsingke Biological Engineering Technology and Services Co., Ltd, Beijing, P.R. China).

Four gene regions, ITS, LSU, *tef1-a* and *rpb2* were amplified using ITS5/ITS4 (White et al. 1990), LR0R/LR7 (Vilgalys and Hester 1990), EF1-983F/EF1-

2218R (Liu et al. 1999) and RPB2-5F/RPB2-7cR (Liu et al. 1999) primer pairs, respectively. Primer sequences are available at the WASABI database at the AFTOL website (aftol.org). The PCR mixture contained 12.5  $\mu$ L of 2 $\times$  GS Taq PCR MasterMix (mixture of DNA Polymerase, dNTPs, Mg<sup>2+</sup> and optimized buffer; Genes and Biotech, Beijing, China), 1  $\mu$ L of each primer including forward primer and reverse primer (10  $\mu$ M), 1  $\mu$ L template DNA extract and 9.5  $\mu$ L double-distilled water (Luo et al. 2018a). The PCR thermal cycling conditions were performed as presented in Table 1. PCR products were purified using mini-columns, purification resin and buffer according to the manufacturer's protocols. The PCR sequences were carried out at Beijing Tsingke Biological Engineering Technology and Services Co., Ltd (Beijing, P.R. China).

### Phylogenetic analysis

BLAST searches using the BLASTn algorithm were performed to retrieve similar sequences from GenBank (<http://www.ncbi.nlm.nih.gov>, accessed on 2 January 2024) and relevant publications (Ma et al. 2022; Zhang et al. 2022; Hu et al. 2023). The sequences were aligned using MAFFT online service: multiple alignment program MAFFT v.7 (Kuraku et al. 2013; Katoh et al. 2019; <http://mafft.cbrc.jp/alignment/server/index.html>, accessed on 2 January 2024), and sequence trimming was performed with trimAl v1.2 with default parameters (<http://trimal.cgenomics.org> for specific operation steps; Capella-Gutiérrez et al. 2009). The sequence dataset was combined using SquenceMatrix v.1.7.8 (Vaidya et al. 2011). FASTA alignment formats were changed to PHYLIP and NEXUS formats by the website: ALignment Transformation EnviRonment (ALTER) (<http://sing.ei.uvigo.es/ALTER/>, accessed on 2 January 2024).

Maximum likelihood (ML) analysis was performed setting RAxML-HPC2 on XSEDE (8.2.12) (Stamatakis 2006; Stamatakis et al. 2008) in CIPRES Science Gateway (Miller et al. 2010; <http://www.phylo.org/portal2>; accessed on 25 January 2022), using the GTR+GAMMA model with 1000 bootstrap repetitions. Bayesian analyses were performed in MrBayes 3.2.6 (Ronquist et al. 2012) and the best-fit model of sequences evolution was estimated via MrModeltest 2.2 (Guindon and Gascuel 2003; Nylander 2004; Darriba et al. 2012). The Markov Chain Monte Carlo (MCMC) sampling approach was used to calculate posterior probabilities (PP) (Rannala and Yang 1996). Bayesian analyses of six simultaneous Markov chains were run for 5 M generations and trees were sampled every thousand generations.

Phylogenetic trees were visualized using FigTree v1.4.0 (<http://tree.bio.ed.ac.uk/software/figtree/>), editing and typesetting using Adobe Illustrator (AI) (Adobe Systems Inc., San Jose, CA, USA). The new sequences were submitted in GenBank and the strain information used in this paper is provided in Table 2.

**Table 1.** PCR thermocycling conditions for genes used in this paper.

Genes	Initial denaturation		Denaturation		Annealing		Extension		No. of cycles	Final extension	
	Temp (°C)	Time (min)	Temp (°C)	Time (s)	Temp (°C)	Time (s)	Temp (°C)	Time (s)		Temp (°C)	Time (min)
ITS	94	3	94	30	56	50	72	60	30	72	10
LSU, <i>tef1-<math>\alpha</math></i>	94	3	94	50	55	60	72	60	30	72	10
<i>rpb2</i>	94	5	94	60	52	90	72	90	38	72	10

**Table 2.** Taxa used in the phylogenetic analyses and their corresponding GenBank accession numbers.

Species	Source	GenBank accession number			
		LSU	ITS	<i>tef1-<math>\alpha</math></i>	<i>rpb2</i>
<i>Aquapteridospora fusiformis</i>	MFLUCC 18-1606 <sup>T</sup>	MK849798	MK828652	MN194056	–
<i>A. lignicola</i>	MFLUCC 15-0377 <sup>T</sup>	KU221018	MZ868774	MZ892980	MZ892986
<i>Distoseptispora adscendens</i>	HKUCC 10820	DQ408561	–	–	DQ435092
<i>D. amniculi</i>	MFLUCC 17-2129 <sup>T</sup>	MZ868761	MZ868770	–	MZ892982
<i>D. appendiculata</i>	MFLUCC 18-0259 <sup>T</sup>	MN163023	MN163009	MN174866	–
<i>D. aqualignicola</i>	KUNCC 21-10729 <sup>T</sup>	ON400845	OK341186	OP413480	OP413474
<i>D. aquamyces</i>	KUNCC 21-10732 <sup>T</sup>	OK341199	OK341187	OP413482	OP413476
<i>D. aquatica</i>	MFLUCC 15-0374 <sup>T</sup>	KU376268	MF077552	–	–
	MFLUCC 18-0646	MK849793	MK828648	–	–
<i>D. aquisubtropica</i>	GZCC 22-0075 <sup>T</sup>	ON527941	ON527933	ON533677	ON533685
<i>D. atroviridis</i>	GZCC 20-0511 <sup>T</sup>	MZ868763	MZ868772	MZ892978	MZ892984
	GZCC 19-0531	MZ227223	MW133915	–	–
<i>D. bambusae</i>	MFLUCC 20-0091 <sup>T</sup>	MT232718	MT232713	MT232880	MT232881
	MFLUCC 14-0583	MT232717	MT232712	–	MT232882
	KUNCC 21-10732	OK341200	OK341188	OP413492	OP413487
<b><i>D. bambusae</i></b>	<b>KUNCC 22-12668</b>	<b>PP068863</b>	<b>PP068486</b>	<b>PP066113</b>	<b>PP066110</b>
<i>D. bambusicola</i>	GZCC 21-0667 <sup>T</sup>	MZ474872	MZ474873	–	–
<i>D. bangkokensis</i>	MFLUCC 18-0262 <sup>T</sup>	MZ518206	MZ518205	–	–
<i>D. cangshanensis</i>	MFLUCC 16-0970 <sup>T</sup>	MG979761	MG979754	MG988419	–
<i>D. caricis</i>	CBS 146041 <sup>T</sup>	MN567632	MN562124	–	MN556805
	CPC 36442 <sup>T</sup>	–	MN562125	–	MN556806
<i>D. chiangraiensis</i>	MFLU 21-0105 <sup>T</sup>	MZ890139	MZ890145	MZ892970	–
	KUNCC 10443	MZ890140	MZ890146	MZ892971	–
<i>D. chinensis</i>	GZCC 21-0665 <sup>T</sup>	MZ474867	MZ474871	MZ501609	–
<i>D. clematidis</i>	MFLUCC 17-2145 <sup>T</sup>	MT214617	MT310661	–	MT394721
	KUMCC 21-10727	OK341197	OK341184	OP413488	OP413483
<i>D. crassispora</i>	KUMCC 21-10726 <sup>T</sup>	OK341196	OK310698	OP413479	OP413473
<i>D. curvularia</i>	KUMCC 21-10725 <sup>T</sup>	OK341195	OK310697	OP413478	OP413472
<i>D. cylindricospora</i>	HKAS 115796 <sup>T</sup>	OK513523	OK491122	OK524220	–
<i>D. dehongensis</i>	KUMCC 18-0090 <sup>T</sup>	MK079662	MK085061	MK087659	–
	MFLUCC 19-0335	OK341201	OK341189	OP413491	OP413486
	MFLUCC 17-2326	OK341193	OK341183	OP413493	–
<i>D. effusa</i>	GZCC 19-0532 <sup>T</sup>	MZ227224	MW133916	MZ206156	–
<i>D. euseptata</i>	MFUCC 20-0154 <sup>T</sup>	MW081544	MW081539	–	MW151860
<i>D. euseptata</i>	DLUCC S2024	MW081545	MW081540	MW084994	MW084996
<b><i>D. euseptata</i></b>	<b>KUNCC 22-12477</b>	<b>PP068864</b>	<b>PP068487</b>	<b>PP066114</b>	–
<i>D. fasciculata</i>	KUMCC 19-0081 <sup>T</sup>	MW287775	MW286501	MW396656	–
<i>D. fluminicola</i>	MFLUCC 15-0417 <sup>T</sup>	KU376270	MF077553	–	–
<i>D. fusiformis</i>	GZCC 20-0512 <sup>T</sup>	MZ868764	MZ868773	MZ892979	MZ892985
<i>D. gasaensis</i>	HJAUP C2034 <sup>T</sup>	OQ942891	OQ942896	OQ944455	–
<i>D. guanshanensis</i>	HJAUP C1063 <sup>T</sup>	OQ942898	OQ942894	OQ944452	OQ944458
<i>D. guizhouensis</i>	GZCC 21-0666 <sup>T</sup>	MZ474869	MZ474868	MZ501610	MZ501611
<i>D. guttulata</i>	MFLUCC 16-0183 <sup>T</sup>	MF077554	MF077543	MF135651	–
	B43	MN163016	MN163011	–	–
<i>D. hyalina</i>	MFLUCC 17-2128 <sup>T</sup>	MZ868760	MZ868769	MZ892976	MZ892981
<i>D. hydei</i>	MFLUCC 20-0115 <sup>T</sup>	MT742830	MT734661	–	MT767128
<i>D. jinghongensis</i>	HJAUP C2120 <sup>T</sup>	OQ942893	OQ942897	OQ944456	–
<i>D. lancangjiangensis</i>	KUN-HKAS 112712 <sup>T</sup>	MW879522	MW723055	–	–
<i>D. leonensis</i>	HKUCC 10822	DQ408566	–	–	DQ435089
<i>D. licualae</i>	MFLUCC 14-1163A <sup>T</sup>	ON650675	ON650686	ON734007	–
	MFLUCC 14-1163B <sup>T</sup>	ON650676	ON650687	ON734008	–

Species	Source	GenBank accession number			
		LSU	ITS	<i>tef1-α</i>	<i>rpb2</i>
<i>D. lignicola</i>	MFLUCC 18-0198 <sup>T</sup>	MK849797	MK828651	–	–
<i>D. longispora</i>	HFJAU 0705 <sup>T</sup>	MH555357	MH555359	–	–
<i>D. longnanensis</i>	HJAUP C1040 <sup>T</sup>	OQ942886	OQ942887	OQ944451	–
<i>D. martinii</i>	CGMCC 3.18651 <sup>T</sup>	KX033566	KU999975	–	–
<i>D. meilingensis</i>	JAUCC 4727 <sup>T</sup>	OK562396	OK562390	OK562408	–
<i>D. menghaiensis</i>	HJAUP C2045 <sup>T</sup>	OQ942900	OQ942890	–	–
	HJAUP C2170 <sup>T</sup>	OQ942888	OQ942899	OQ944457	OQ944461
<i>D. multiseptata</i>	MFLUCC 16-1044	MF077555	MF077544	MF135652	MF135644
<i>D. multiseptata</i>	MFLUCC 15-0609 <sup>T</sup>	KX710140	KX710145	MF135659	–
<i>D. nabanheensis</i>	HJAUP C2003 <sup>T</sup>	OP787877	OP787873	OP961935	–
<i>D. nanchangensis</i>	HJAUP C1074 <sup>T</sup>	OQ942895	OQ942889	OQ944454	OQ944460
<i>D. neurostrata</i>	MFLUCC 18-0376 <sup>T</sup>	MN163017	MN163008	–	–
<i>D. nonrostrata</i>	KUNCC 21-10730 <sup>T</sup>	OK341198	OK310699	OP413481	OP413475
<i>D. obclavata</i>	MFLUCC 18-0329 <sup>T</sup>	MN163010	MN163012	–	–
<i>D. obpyriformis</i>	MFLUCC 17-01694 <sup>T</sup>	MG979764	–	MG988422	MG988415
	DLUCC 0867	MG979765	MG979757	MG988423	MG988416
<b><i>D. obpyriformis</i></b>	<b>KUNCC 23-13047</b>	<b>PP068865</b>	<b>PP068488</b>	<b>PP066115</b>	<b>PP066111</b>
<i>D. pachyconidia</i>	KUMCC 21-10724 <sup>T</sup>	OK341194	OK310696	OP413477	OP413471
	GZCC 22-0074	ON527942	ON527934	ON533678	ON533686
<b><i>D. pachyconidia</i></b>	<b>KUNCC 23-13047</b>	<b>PP068866</b>	<b>PP068489</b>	–	<b>PP066112</b>
<i>D. palmarum</i>	MFLUCC 18-1446 <sup>T</sup>	MK079663	MK085062	MK087660	MK087670
<i>D. phangngaensis</i>	MFLUCC 16-0857 <sup>T</sup>	MF077556	MF077545	MF135653	–
<i>D. phragmiticola</i>	GUCC 220201 <sup>T</sup>	OP749880	OP749887	OP749891	OP752699
	GUCC 220201 <sup>T</sup>	OP749881	OP749888	OP749892	OP752700
<i>D. rayongensis</i>	MFLUCC 18-0415 <sup>T</sup>	MH457137	MH457172	MH463253	MH463255
	MFLUCC 18-0417	MH457138	MH457173	MH463254	MH463256
	MFLU 19-0543	MN163010	MN513037	OP413490	OP413485
<i>D. rostrata</i>	MFLUCC 16-0969 <sup>T</sup>	MG979766	MG979758	MG988424	MG988417
	DLUCC 0885	MG979767	MG979759	MG988425	–
<i>D. saprophytic</i>	MFLUCC 18-1238 <sup>T</sup>	MW287780	MW286506	MW396651	MW504069
<i>D. septata</i>	GZCC 22-0078 <sup>T</sup>	ON527947	ON527939	ON533683	ON533690
<i>D. sinensis</i>	HJAUP C2044 <sup>T</sup>	OP787875	OP787878	OP961936	–
<i>D. songkhlaensis</i>	MFLUCC 18-1234 <sup>T</sup>	MW287755	MW286482	MW396642	–
<i>D. sp.</i>	HKAS 112707	MZ890141	MZ890147	MZ892972	–
	HKAS 112711	MZ890142	MZ890148	MZ892973	–
<b><i>D. suae</i></b>	<b>CGMCC3.24262<sup>T</sup></b>	<b>OQ732679</b>	<b>OQ874968</b>	<b>OR367670</b>	<b>OQ870341</b>
<i>D. suoluensis</i>	MFLUCC 17-0224 <sup>T</sup>	MF077557	MF077546	MF135654	–
	MFLUCC 17-1305	MF077558	MF077547	–	–
<i>D. tectonae</i>	MFLUCC 12-0291 <sup>T</sup>	KX751713	KX751711	KX751710	KX751708
	MFLUCC 16-0946	MG979768	MG979760	MG988426	MG988418
	KUNCC 21-10728	OK348852	OK341185	OP413489	OP413484
	MFLUCC 15-0981	MW287763	MW286489	MW396641	–
	MFLU 20-0262	MT232719	MT232714	–	–
	KUNCC 1093	PP140788	PP140786	–	–
	KUNCC 1094	PP140789	PP140787	–	–
	MFLU 21-0106	MZ890143	MZ890149	MZ892974	–
	MFLU 21-0107	MZ890144	MZ890150	MZ892975	–
<i>D. tectonigena</i>	MFLUCC 12-0292 <sup>T</sup>	KX751714	KX751712	–	KX751709
<i>D. thailandica</i>	MFLUCC 16-0270 <sup>T</sup>	MH260292	MH275060	MH412767	–
<i>D. thysanolaenae</i>	KUN-HKAS 102247 <sup>T</sup>	MK064091	MK045851	MK086031	–
<i>D. tropica</i>	GZCC 22-0076 <sup>T</sup>	ON527943	ON527935	ON533679	ON533687

Species	Source	GenBank accession number			
		LSU	ITS	<i>tef1-<math>\alpha</math></i>	<i>rpb2</i>
<i>D. verrucosa</i>	GZCC 20–0434 <sup>T</sup>	MZ868762	MZ868771	MZ892977	MZ892983
<i>D. wuzhishanensis</i>	GZCC 22–0077 <sup>T</sup>	ON527946	ON527938	ON533682	–
<i>D. xingpingensis</i>	<b>KUNCC 22–12669</b>	<b>OQ732680</b>	<b>OQ874969</b>	–	–
	<b>KUNCC 22–12667<sup>T</sup></b>	<b>OQ732681</b>	<b>OQ874970</b>	<b>OR367671</b>	<b>OQ870340</b>
<i>D. xishuangbannaensis</i>	KUMCC 17–0290 <sup>T</sup>	MH260293	MH275061	MH412768	MH412754
	GZCC 22–0079	ON527944	ON527936	ON533680	ON533688
<i>D. yichunensis</i>	HJAUP C1065 <sup>T</sup>	OQ942892	OQ942885	OQ944453	OQ944459
<i>D. yongxiuensis</i>	JAUCC 4725 <sup>T</sup>	OK562394	OK562388	OK562406	–
<i>D. yunjunshanensis</i>	JAUCC 4723 <sup>T</sup>	OK562398	OK562392	OK562410	–
<i>D. yunnanensis</i>	MFLUCC 20–0153 <sup>T</sup>	MW081546	MW081541	MW084995	MW151861

Notes: The ex-type cultures are indicated using “<sup>T</sup>” after strain numbers; newly generated sequences are indicated in bold. “–” stands for no sequence data in GenBank.

## Results

### Phylogenetic analysis

The dataset comprises the combined LSU, ITS, *tef1- $\alpha$*  and *rpb2* sequences of 113 taxa of Distoseptisporaceae. It encompasses 3,192 characters (including gaps), with *Aquapteridospora fusiformis* (MFLUCC 18–1606) and *A. lignicola* (MFLUCC 15–0377) serving as the outgroup taxon (Fig. 1). Maximum likelihood (ML) and Bayesian analyses resulted similar topologies that were consistent spread the major clades. Likelihood of the final tree is evaluated and optimized under GAMMA. The best RAxML tree with a final likelihood value of -31566.210733 is presented (Fig. 1). The matrix contained 1,517 distinct alignment patterns, with 26.62% undetermined characters or gaps. Estimated base frequencies were as follows: A = 0.238411, C = 0.267281, G = 0.283165, T = 0.211143; substitution rates AC = 1.379525, AG = 3.509297, AT = 1.246498, CG = 0.856966, CT = 7.193589, GT = 1.000000,  $\alpha$  = 0.242260, Tree-Length: 3.349217. Bayesian analyses generated 3,689 trees (average standard deviation of split frequencies: 0.009995) from which 2,767 were sampled after 25% of the trees were discarded as burn-in. The alignment contained a total of 1,517 unique site patterns. Bootstrap support values with a ML greater than 65%, and Bayesian posterior probabilities (PP) greater than 0.96 are given above the nodes.

Multigene phylogenetic analysis results showed that all members of *Distoseptispora* clustered into four stable clades (Fig. 1), Clade 1 contains most species of the genus with more than 50 species; Clade 2 only one species, *D. tropica*; Clade 3 contains eight species, including *D. leonensis* (M.B. Ellis) R. Zhu & H. Zhang; Clade 4 includes 13 species, and the two known teleomorph species of the genus are both in this clade. Four of our seven collections are clustered in clade 1, and the other three are clustered in clade 4. *Distoseptispora suae* (KUNCC 22–12416) is stably aggregated in clade 4 with the teleomorph species *D. hyalina* (MFLUCC 17–2128). *D. xingpingensis* (KUNCC 22–12667 and KUNCC 22–12669) clustered as a sister clade with *D. lignicola* (MFLUCC 18–0198) in clade 1. The new collections, KUNCC 22–12668, KUNCC 22–12477, KUNCC 23–13047 and KUNCC 23–13048 clustered with *D. bambusae*, *D. eu-septata*, *D. obpyriformis* and *D. pachyconidia*, respectively.

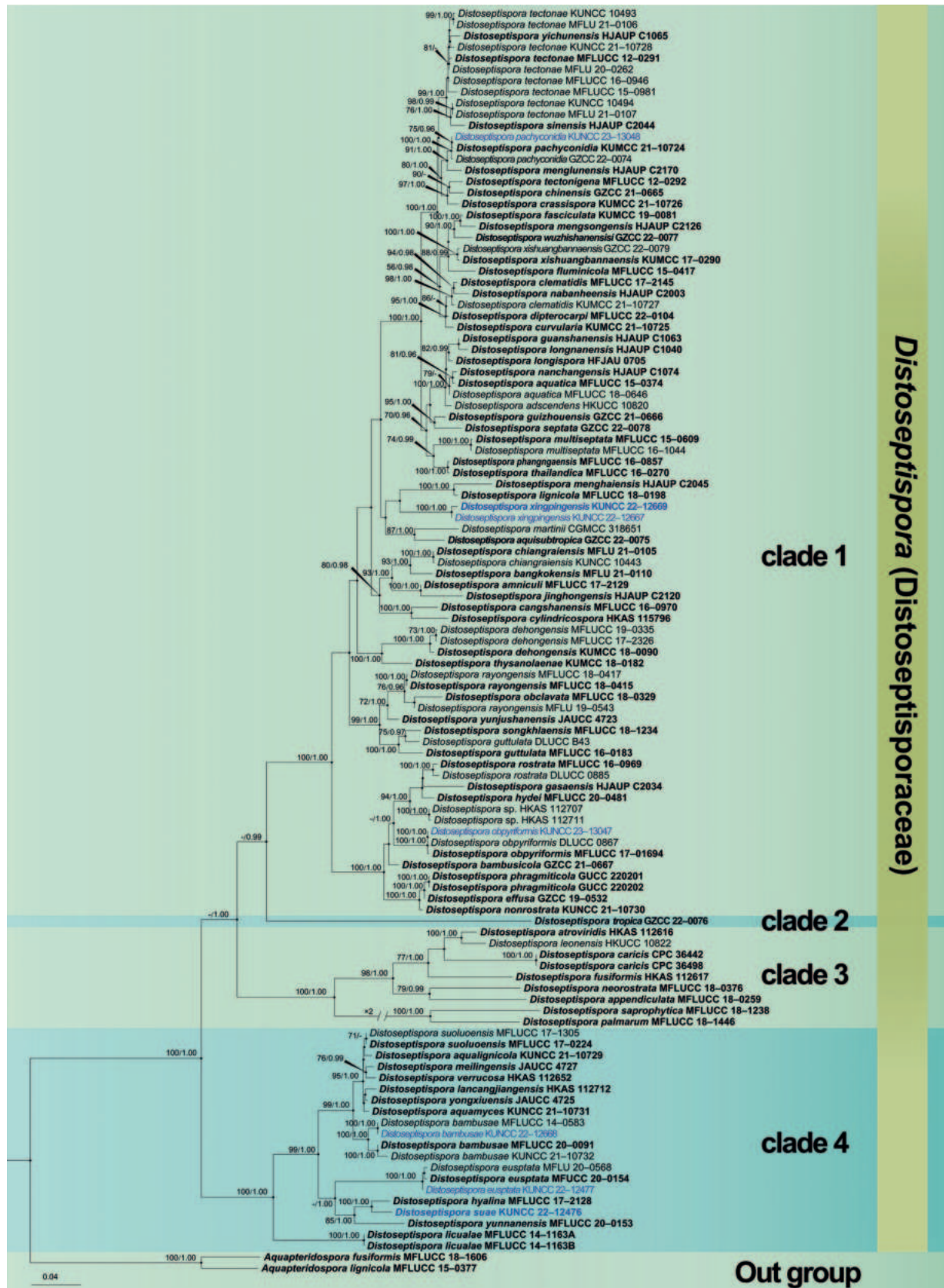


Figure 1. Maximum likelihood (ML) tree is based on combined LSU, ITS, *tef1-α* and *rpb2* sequence data. Bootstrap support values with a ML greater than 65% and Bayesian posterior probabilities (PP) greater than 0.95 are given above the nodes, shown as “ML/PP”. The tree is rooted to *Aquapteridospora fusiformis* (MFLUCC 18–1606) and *A. lignicola* (MFLUCC 15–0377). New species are indicated in blue and type strains are in bold.

## Taxonomy

*Distoseptispora bambusae* Y.R. Sun, I.D. Goonasekara, Yong. Wang bis & K.D. Hyde, *Biodiversity Data Journal* 8(e53678): 6 (2020)

MycoBank No: 557452

Facesoffungi Number: FoF04194

Fig. 2

**Description.** *Saprobic* on submerged decaying wood in a freshwater stream. **Anamorph:** *Colonies* on wood effuse, hairy, dark brown, glistening, solitary or in small group. *Mycelium* immersed, composed of septate, pale brown to



**Figure 2.** *Distoseptispora bambusae* (HKAS 125826) **a, b** colonies on woody substrates **c–e** conidiophores **f, g** conidiogenous cells **h–m** conidia **n** germinated conidium **o** culture on PDA. Scale bars: 50  $\mu$ m (**c–e**); 10  $\mu$ m (**f, g**); 20  $\mu$ m (**h–n**).

brown hyphae, smooth-walled. **Conidiophores** (42–)66–103(–115) × 5–6 μm ( $\bar{x}$  = 84 × 6 μm, n = 20), macronematous, mononematous, solitary or in groups, erect, straight or slightly flexuous, unbranched, cylindrical, 4–6-septate, brown, rounded at the apex, slightly enlarged at the base, smooth and thin-walled. **Conidiogenous cells** (10–)15–22(–25) × 5–6 μm ( $\bar{x}$  = 19 × 5 μm, n = 20), monoblastic, terminal, determinate, subcylindrical, brown, smooth-walled. **Conidia** (55–)69–126(–168) × 10–12 μm ( $\bar{x}$  = 98 × 11 μm, n = 25), acrogenous, solitary, obclavate, rostrate, olivaceous to pale or dark brown, truncate at base, tapering towards the apex, straight or slightly curved, 7–18-euseptate, constricted at the septa, guttulate, verrucose, thick-walled. **Teleomorph**: Undetermined.

**Culture characteristics.** Conidia germinating on PDA within 12 hrs and germ tubes produced from apex and septa of conidium. Colonies growing on PDA reaching 3–4 cm in one month at 26 °C in the dark, flocculent, fluffy, soft white to light brown mycelium from above, dark brown in the middle, light brown at the edges from below.

**Material examined.** CHINA, Yunnan Province, Dali City, Weishan Yi and Hui Autonomous County, 25°29'31"N, 100°06'56"E, on submerged decaying branches in a freshwater stream, 19 February 2022, Z.Q. Zhang & Q.X. Yang YJ 14-24-1 (HKAS 125826, living culture KUNCC 22–12668).

**Notes.** Phylogenetic analysis showed that our new strain KUNCC 22–12668 clusters with the type strain of *Distoseptispora bambusae* (MFLUCC 14–0583) with 100% ML/1.00 PP support (Fig. 1). Furthermore, our new collection (Fig. 2) exhibits morphological characters identical to those of the type strain *Distoseptispora bambusae* (MFLUCC 14–0583). However, our collection has longer conidiophores and conidia. This observation aligns with Yang et al. (2018), suggesting that factors such as incubation time and habitat may influence the lengths of conidiophores and conidia. A comparison of the ITS, LSU, *tef1-α* and *rpb2* sequences between our new strain KUNCC 22–12668 and the type strain (MFLUCC 14–0583) reveals only minimal base pair differences. Therefore, based on morphological evidence and phylogenetic affinity, our new strain KUNCC 22–12668 is identified as *Distoseptispora bambusae* and it is reported from freshwater habitat for the first time in Yunnan, China.

***Distoseptispora euseptata* W.L. Li, H.Y. Su & Jian K. Liu, Phytotaxa 520 (1): 80 (2021)**

MycoBank No: 557967

Facesoffungi Number: FoF09450

Fig. 3

**Description.** **Saprobic** on submerged decaying wood in a freshwater stream. **Anamorph:** **Colonies** on wood effuse, brown, solitary or in small group. **Mycelium** mostly immersed, composed of septate, brown hyphae, smooth-walled. **Conidiophores** (32–)37–59(–73) × 3–4(–5) μm ( $\bar{x}$  = 48 × 4 μm, n = 25), macronematous, mononematous, solitary or in groups, erect, straight or slightly flexuous, branched or unbranched, cylindrical, 2–4(–5)-septate, brown, smooth-walled. **Conidiogenous cells** (11–)13–15(–16) × 5–6 μm ( $\bar{x}$  = 14 × 5 μm, n = 20), monoblastic, terminal, determinate, subcylindrical, brown, smooth-walled. **Conidia** (36–)52–68(–85) × (7–)8–9 μm ( $\bar{x}$  = 60 × 8 μm, n = 30), acrogenous, soli-



**Figure 3.** *Distoseptispora euseptata* (HKAS 125822) **a** colony on woody substrates **b–e** conidiophores **f, g** conidiogenous cells **h–m** conidia **n** germinated conidium **o** culture on PDA. Scale bars: 20  $\mu\text{m}$  (**b–e, h–n**); 10  $\mu\text{m}$  (**f, g**).

tary, obclavate, sometimes rostrate, truncate at base, tapering towards the apex, straight or slightly curved, guttulate, brown to dark brown, 6–9(–11)-euseptate, constricted at the septa, thin and smooth-walled. **Teleomorph:** Undetermined.

**Culture characteristics.** Conidia germinating on PDA within 12 hrs and germ tubes produced from apex of conidium. Colonies growing on PDA reaching 4–5 cm in 20 days at 26 °C in the dark, with dense, velvety, pale brown to dark brown mycelium from above, dark brown from below.

**Material examined.** CHINA, Yunnan Province, Yuxi City, Xinping Yi and Dai Autonomous County, Yuanjiang River, 24°02'16"N, 101°34'05"E, on submerged decaying branches in a freshwater stream, 22 February 2022, S. Luan & W.P. Wang YJ 14-49-1 (HKAS 125822, living culture KUNCC 22-12477).

**Notes.** Polygenetic analysis revealed that our new strain, KUNCC 22-12477, clustered with two strains of *Distoseptispora euseptata* (MFUCC 20-0154 and MFLU 20-0568) with 100% ML/1.00 PP support (Fig. 1). A comparison of the ITS and LSU sequence between strain KUNCC 22-12477 and MFLUCC 20-0153 (from holotype) revealed 0.74% (4/537 bp, including 1 gap), 0.16% (2/1254 bp, including 2 gaps), respectively. And a comparison of the ITS, LSU and *rpb2* sequence between strain KUNCC 22-12477 and DLUCC S2024 (from paratype) revealed 0.74% (4/537 bp, including 1 gap), 0% (0/1274 bp), and 0.23% (2/878 bp), respectively. New collection, KUNCC 22-12477, is morphologically similar to the type species in having obclavate, guttulate, euseptate conidia (Li et al. 2021). Although the conidia size and color of *D. euseptata* KUNCC 22-12477 are slightly different from the type species, and conidia size is also an important basis for distinguishing *Distoseptispora* species, some previous studies in this genus found significant differences in conidial size between different collections of the same species (Yang et al. 2018; Shen et al. 2021; Ma et al. 2022). Based on the currently limited morphological and molecular sequence data, we treat the new collection, KUNCC 22-12477, as *D. euseptata*, which was first discovered in the Red River Basin in Yunnan, China.

***Distoseptispora obpyriformis* Z.L. Luo & H.Y. Su, Mycosphere 9(3): 452 (2018)**

MycoBank No: 554290

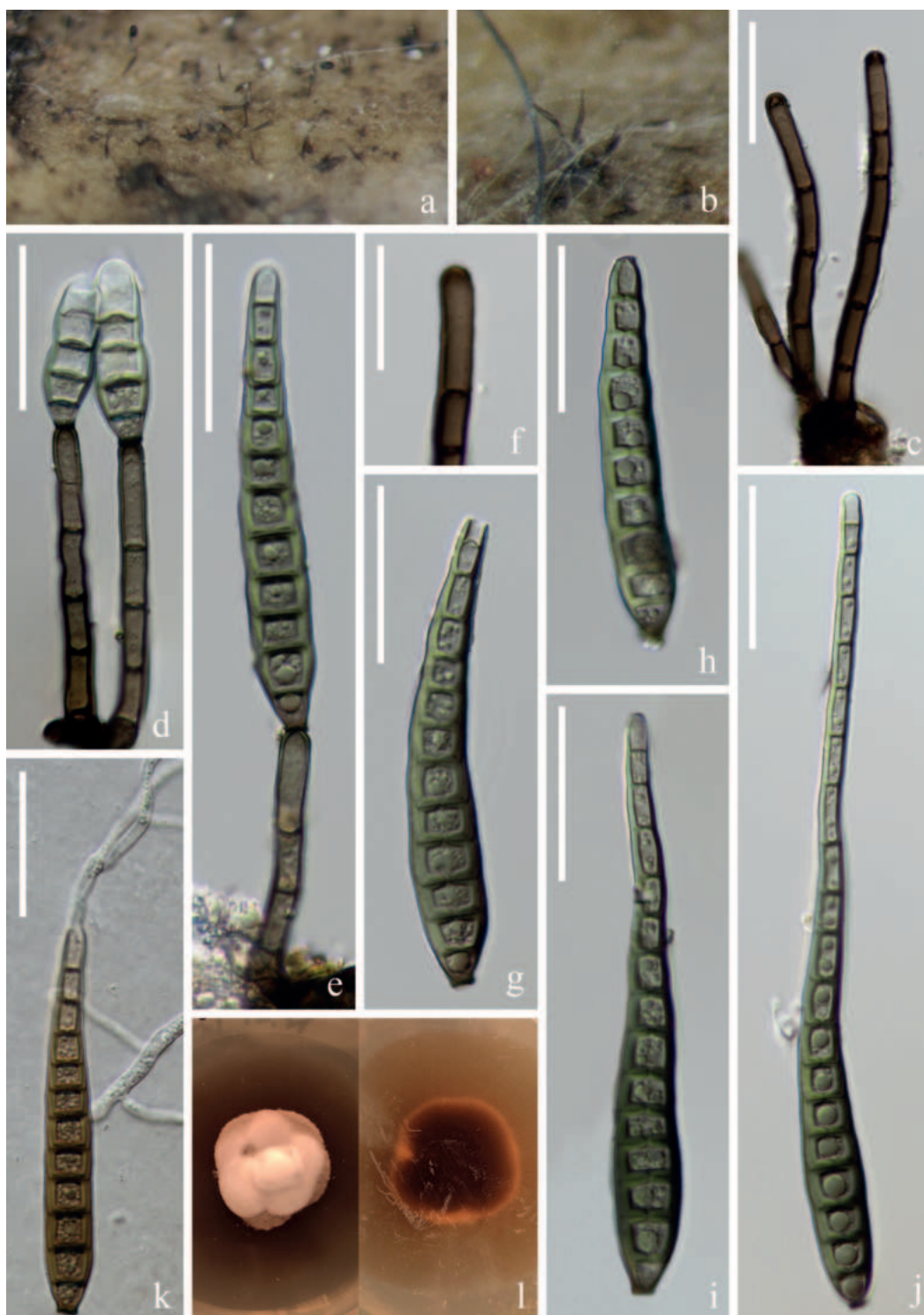
Facesoffungi Number: FoF04194

Fig. 4

**Description.** *Saprobic* on submerged decaying wood in a freshwater stream. **Anamorph:** *Colonies* on wood effuse, hairy, dark brown, glistening, solitary or in small group. *Mycelium* immersed, composed of septate, pale brown to brown hyphae, smooth-walled. **Conidiophores** (42-)66-103(-115) × 5-6 μm ( $\bar{x}$  = 84 × 6 μm, n = 20), macronematous, mononematous, solitary or in groups, erect, straight or slightly flexuous, cylindrical, unbranched, 4-6-septate, brown, rounded at the apex, slightly enlarged at the base, smooth-walled. **Conidiogenous cells** (10-)15-22(-25) × 5-6 μm ( $\bar{x}$  = 19 × 5 μm, n = 20), monoblastic, terminal, determinate, subcylindrical, brown, smooth-walled. **Conidia** (55-)69-126(-168) × 10-12 μm ( $\bar{x}$  = 98 × 11 μm, n = 25), acrogenous, solitary, obclavate, olivaceous to pale or dark brown, truncate at base, tapering towards the apex, straight or slightly curved, constricted at the septa, 7-18-distoseptate, guttulate, thick and smooth-walled. **Teleomorph:** Undetermined.

**Culture characteristics.** Conidia germinating on PDA within 12 hrs and germ tubes produced from apex and septa of conidium. Colonies growing on PDA reaching 4-5 cm in 20 days at 26 °C in the dark, with dense, velvety, middle papillae, pale to dark brown mycelium from above; dark brown from below.

**Material examined.** CHINA, Yunnan Province, Dali City, Weishan Yi and Hui Autonomous County, 25°29'31"N, 100°06'56"E, on submerged decaying branch-



**Figure 4.** *Distoseptispora obpyriformis* (HKAS 125823) **a, b** colonies on woody substrates **c** conidiophores **d, e** conidiophores with conidia **f** conidiogenous cell **g–j** conidia **k** germinating conidium **l** culture on PDA. Scale bars: 30  $\mu\text{m}$  (**c–e, g–k**); 20  $\mu\text{m}$  (**j**).

es in a freshwater stream, 19 February 2022, Z.Q. Zhang & Q.X. Yang YJ 1–19–1 (HKAS 125823, living culture KUNCC 23–13047).

**Notes.** Phylogenetic analysis revealed that our new strain KUNCC 23–13047 clustered with two strains of *Distoseptispora obpyriformis* (MFLUCC 17–1694 (ex-type strain) and DLUCC 0867; Fig. 1). A comparison of the LSU, *tef1-a* and

*rpb2* gene of type strains between KUNCC 23–13047 (this study) and MFLUCC 17–1694 (from holotype) revealed 0% (0/1215 bp), 0.37% (3/812 bp, including 1 gaps), 0% (0/838 bp), 0.29% (3/1034 bp), respectively. Although our collection differs significantly in conidia size from the original description of *D. obpyriformis* (Luo et al. 2018a), multigene sequence data do not support this collection as a separate species. Similar results have been reported in previous studies and were found in several species in this study (Yang et al. 2018; Shen et al. 2021; Ma et al. 2022). Therefore, a new additional record of *D. obpyriformis* is reported from the Red River Basin in Yunnan, China.

***Distoseptispora pachyconidia* R. Zhu & H. Zhang, J. Fungi. 8(10): 22 (2022)**

MycoBank No: 554290

Fig. 5

**Description.** *Saprobic* on submerged decaying wood in a freshwater stream. **Anamorph:** *Colonies* on wood effuse, hairy, dark brown, glistening, solitary or in small group. *Mycelium* immersed, composed of septate, pale brown to brown hyphae, smooth-walled. **Conidiophores** (13–)20–36(–48) × 6–8 μm ( $\bar{x}$  = 28 × 7 μm, n = 30), macronematous, mononematous, solitary or in groups, erect, straight or slightly flexuous, cylindrical, unbranched, 1–3-septate, brown, rounded at the apex, slightly enlarged at the basal, smooth-walled. **Conidiogenous cells** 6–8 × 5–6 μm ( $\bar{x}$  = 7 × 5 μm, n = 25), monoblastic, terminal, determinate, subcylindrical, brown, smooth-walled. **Conidia** (82–)137–246(–296) × (9–)13–16 μm ( $\bar{x}$  = 192 × 15 μm, n = 40), acrogenous, solitary, obclavate, pale brown to brown, truncate at the base, tapering towards the apex, straight or slightly curved, 14–45-distoseptate, constricted at the septa, guttulate, thick and smooth-walled. **Teleomorph:** Undetermined.

**Culture characteristics.** Conidia germinating on PDA within 12 hrs and germ tubes produced from apex and septa of conidium. Colonies growing on PDA reach 2–3 cm in one month at 26 °C in the dark, with dense, velvety, pale brown to dark brown mycelium from above; dark brown from below.

**Material examined.** CHINA, Yunnan Province, Honghe Hani and Yi Autonomous Prefecture, Honghe County, 23°19'32"N, 102°20'52"E, on submerged decaying branches in a freshwater stream, 23 February 2022, Z.Q. Zhang & Q.X. Yang YJ 40–30–1 (HKAS 125824, living culture KUNCC 23–13048).

**Notes.** Phylogenetically, our new strain KUNCC 23–13048 grouped with the strains of *Distoseptispora pachyconidia* (KUMCC 21–10724 and GZCC 22–0074) with 75% ML and 0.96% PP support (Fig. 1). Pairwise comparison of ITS, LSU, *tef1-α* and *rpb2* sequences show negligible base pair differences. As previously reported, the conidia size and color of our new collection HKAS 125824 are significantly different from those originally described for *D. pachyconidia* (137–246 μm vs. 42–136 μm; pale brown to brown vs. pale-brown with a green tinge), as well as the number of conidial septa (14–45-distoseptate vs. 8–21-distoseptate) (Yang et al. 2018; Shen et al. 2021; Ma et al. 2022). Our new collection is also slightly different from the collection described by Ma et al. (2022), especially the number of conidial septa (14–45-distoseptate vs. up to 38-distoseptate) (Ma et al. 2022). However, based on slight differences in molecular data, this collection was not sufficient to qualify as a new species, and therefore, identify this collection as *D. pachyconidia*, which was first discovered in the Red River Basin of Yunnan.



**Figure 5.** *Distoseptispora pachyconidia* (HKAS 125824) **a, b** colonies on woody substrates **c** conidiophores **e** conidiophores with conidia **d** conidiogenous cells **f, g** conidia **h** germinated conidium **i** culture on PDA. Scale bars: 20  $\mu\text{m}$  (**c, d**); 60  $\mu\text{m}$  (**e-h**).

***Distoseptispora suae* H.W. Shen & Z.L. Luo, sp. nov.**

Fungal Names: FN 571689

Figs 6, 7

**Etymology.** “suae” (Lat.) in memory of the Chinese mycologist Prof. Hong-Yan Su (4 April 1967–3 May 2022), who kindly helped the authors in many ways.

**Description.** *Saprobic* on submerged decaying wood in a freshwater stream.

**Anamorph: Colonies** on wood effuse, brown, solitary or in small group. **Mycelium** immersed, septate, brown hyphae, smooth-walled. **Conidiophores** (21–)25–41(–53) × 4–5 μm ( $\bar{x}$  = 33 × 5 μm, n = 20), macronematous, mononematous, solitary or in groups, erect, straight or slightly flexuous, cylindrical, 1–3-septate, brown, unbranched, smooth-walled. **Conidiogenous cells** (11–)13–15(–16) × 5–6 μm ( $\bar{x}$  = 14 × 5 μm, n = 20), monoblastic, terminal, determinate, subcylindrical, brown, smooth-walled. **Conidia** (77–)81–101(–109) × 8–10 μm ( $\bar{x}$  = 91 × 9 μm, n = 30), acrogenous, solitary, obclavate to rostrate, truncate at base, tapering towards the apex, straight or slightly curved, bent at the second or third cell at the base, brown to dark brown, 3–12-euseptate, guttulate, verrucose, thin-walled. **Teleomorph:** Undetermined.

**Culture characteristics.** Conidia germinating on PDA within 12 hrs and germ tubes produced from the apex. Colonies growing on PDA reaching 4–5 cm in one month at 26 °C in the dark, with dense, velvety, brown to dark brown mycelium from above; dark brown from below. Sporulation on PDA after two months, **Mycelium** hyaline to brown, septate, branched, smooth-walled. **Conidiophores** (15–)16–56(–110) × 4–6 μm ( $\bar{x}$  = 36 × 5 μm, n = 30), usually form at the end of the hyphae, cylindrical, straight or slightly curved, yellowish brown to olivaceous-brown, septate. **Conidiogenous cells** (9–)11–14(–16) × 4–5 μm ( $\bar{x}$  = 12 × 5 μm, n = 30) monoblastic, terminal, determinate, cylindrical, brown, sometimes reduce conidiophores. **Conidia** (31–)47–90(–124) × 6–8 μm ( $\bar{x}$  = 68 × 7 μm, n = 40) acrogenous, obclavate, elongated, truncate at base, straight or slightly curved, brown, euseptate, thin-wall, sometimes with a gelatinous sheath around the septum (Fig. 7).

**Material examined.** CHINA, Yunnan Province, Yuxi City, Xinping Yi and Dai Autonomous County, Yuanjiang River, 24°02'16"N, 101°34'05"E, on submerged decaying branches in a freshwater stream, 22 February 2022, H.W. Shen & Q.X. Yang YJ 14–35–2 (HKAS: 125819, holotype, ex-type, CGMCC3.24262 = KUNCC 22–12476).

**Notes.** *Distoseptispora suae* clusters with *D. hyalina* (MFLU 21–0137) with 100% ML/1.00 PP support whereas *D. yunnanensis* (MFLUCC 20–0153) state in a basal lineage (Fig. 1). A comparison of the LSU, ITS, *tef1-α* and *rpb2* nucleotide bases between *D. suae* and *D. hyalina* revealed differences of 8 bp (8/832, including one gap), 11 bp (11/540, including 3 gaps), 21 bp (21/934), and 54 bp (54/1087) sequence similarity, respectively. Morphologically, *D. suae* resembles other species in the genus with its euseptate structure, characterized by acrogenous, solitary, obclavate to rostrate conidia. *D. hyalina*, *D. suae* and *D. yunnanensis* cluster in a stable lineage (Fig. 1). Since only teleomorphs were found in *D. hyalina* (Yang et al. 2021), and only anamorphs were found in *D. suae* (this study), the morphological characteristics of *D. suae* and *D. yunnanensis* were compared here. *D. suae* can be distinguished from *D. yunnanensis* by its shorter conidiophores (25–41(–53) μm vs. 131–175 μm) and guttulate,

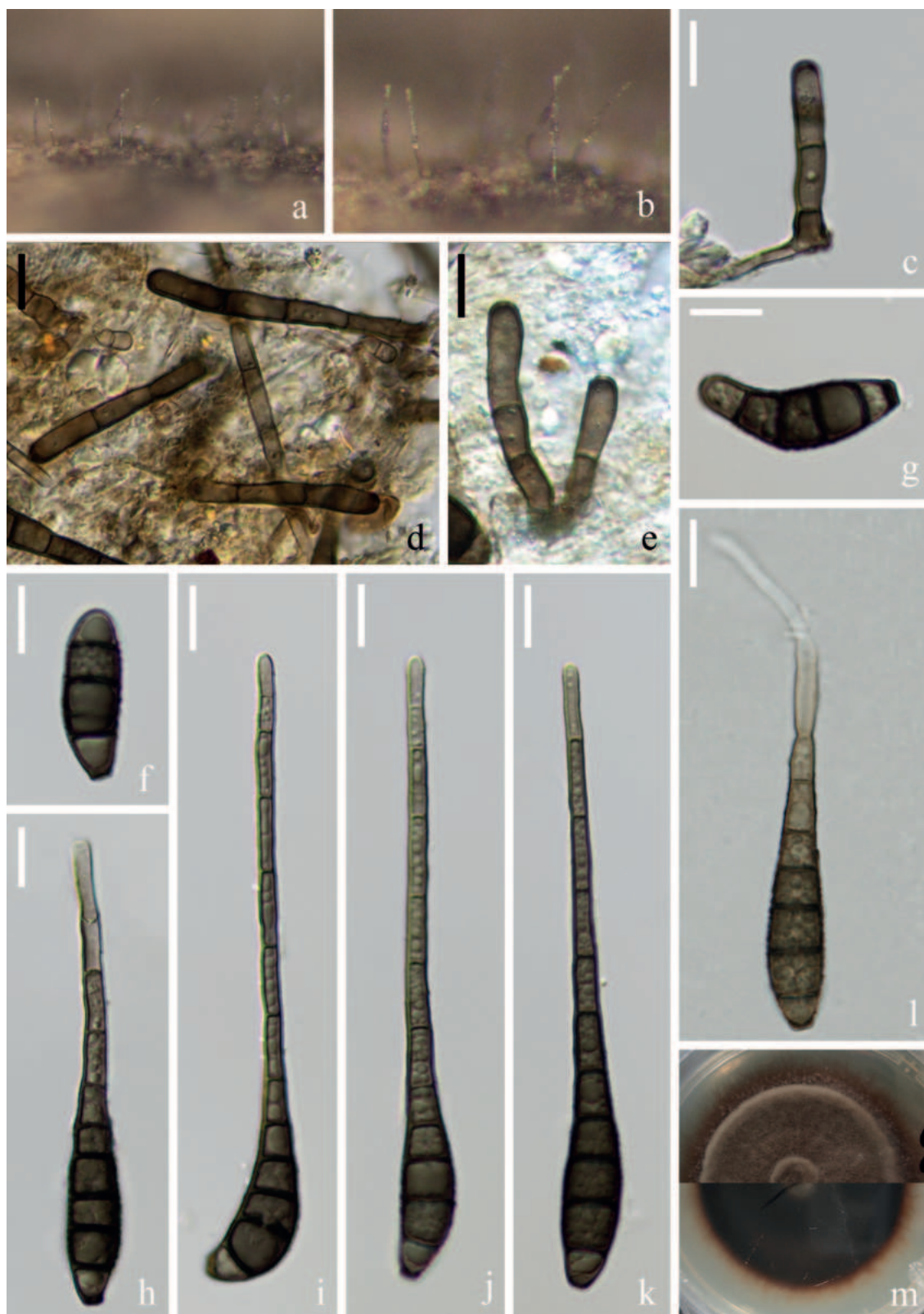


**Figure 6.** *Distoseptispora suae* (HKAS 125819, holotype) **a, b** colonies on woody substrates **c–e** conidiophores and conidiogenous cells **f–k** conidia **l** germinated conidium **m** culture on PDA. Scale bars: 10  $\mu\text{m}$  (**c–l**).

verrucose conidia (Li et al. 2021). Based on phylogenetic analysis and morphological evidence, following the guidelines of Jeewon and Hyde (2016), we therefore introduce *D. suae* as a new species.



**Figure 7.** *Distoseptispora suae* (ex-type culture KUNCC 22–12476) **a** culture on PDA, obverse (left) and reverse (right) **b, c** colonies on PDA **d** mycelium from PDA **e** mycelium, conidiophores and conidia **f** conidiophore **g–j** conidiophores with conidia (Arrow in **i, j** indicate the gelatinous sheath) **k** conidia. Scale bars: 10  $\mu\text{m}$  (**d**); 40  $\mu\text{m}$  (**e**); 20  $\mu\text{m}$  (**f–k**).

***Distoseptispora xinpingensis* H.W. Shen & Z.L. Luo, sp. nov.**

Fungal Names: FN 571753

Fig. 8

**Etymology.** “*xinpingensis*” refers to the Xinping Yi and Dai Autonomous County, Yunnan Province, China, where the species was collected.

**Description.** **Saprobic** on submerged decaying wood in a freshwater stream.

**Anamorph: Colonies** on wood effuse, brown to dark brown, solitary or gregarious. **Mycelium** immersed, composed of septate, hyaline to brown hyphae, smooth-walled. **Conidiophores** (97–)105–149(–175) × 4–5 μm ( $\bar{x}$  = 127 × 5 μm, n = 40), macronematous, mononematous, solitary or in groups, erect, straight or slightly flexuous, cylindrical, brown, unbranched, slightly paler at the apical cell, slightly enlarged at the base, septate, smooth-walled. **Conidiogenous cells** (7–)13–23(–25) × 4–5 μm ( $\bar{x}$  = 18 × 4 μm, n = 30), mono- or poly- blastic, terminal, determinate, subcylindrical, pale brown, smooth-walled. **Conidia** (95–)107–139(–155) × (7–)8–9(–10) μm ( $\bar{x}$  = 123 × 8 μm, n = 40), acrogenous, solitary, obclavate, truncate at base, tapering towards the apex, straight or slightly curved, brown, 8–12-septate, smooth, thin-wall, sometimes a second conidium proliferates at the top of the conidia. **Teleomorph:** Undetermined.

**Culture characteristics.** Conidia germinating on PDA within 24 hrs and swollen germ tubes produced from both ends and some septate. Colonies growing on PDA reaching 2–3 cm in two weeks at 26 °C in the dark, with dense, velvety, dark brown mycelium on the surface; in reverse brown to dark brown with entire margin.

**Material examined.** CHINA, Yunnan Province, Yuxi City, Xinping Yi and Dai Autonomous County, Yuanjiang River, 23°48'12"N, 101°47'21"E, on submerged decaying branch in a freshwater stream, 22 February 2022, S. Luan & W.P Wang YJ 17–2–2 (HKAS: 125818, holotype), ex-type, KUNCC 22–12667; ibid, 23°48'12"N, 101°47'21"E, on submerged decaying branches in a freshwater stream, 22 February 2022, H.W. Shen & Z.Q. Zhang YJ 17–5–2 (HKAS: 125821, paratype), ex-paratype, KUNCC 22–12669.

**Notes.** Phylogenetic analysis showed that the two strains of *Distoseptispora xinpingensis* (KUNCC 22–12669 and KUNCC 22–12667) clustered together and formed a sister clade to *D. lignicola* (MFLUCC 18–0198) and *D. menghaiensis* (HJAUP C2045) with low support (Fig. 1). Based on a megablast search of NCBI's GenBank nucleotide database, the best matching result for ITS sequence of KUNCC 22–12667 is *Distoseptispora* sp. (isolate SICAUCC 22–0049, sequence ID: ON228626; identities: 499/516 (97%), 4 gaps); the best matching result of LSU sequence is *D. lignicola* (strain MFLUCC 18–0198, sequence ID: MK849797; identities: 1223/1245 (98%), no gap); the best matching result of *rpb2* sequence is *D. bambusae* (voucher MFLU 17–1653, sequence ID: MT232882; identities: 1047/1047 (100%), no gap); the best matching result of *tef1-α* sequence is *D. mengsongensis* (strain HJAUP C2126, sequence ID: OP961937; identities: 866/916 (95%), no gap). *Distoseptispora xinpingensis* conforms to the generic concept of *Distoseptispora* (Su et al. 2016; Yang et al. 2018, 2021; Luo et al. 2019; Zhang et al. 2022). The morphological comparison between *Distoseptispora xinpingensis* and the closely related *D. lignicola* and *D. menghaiensis* shows that *D. xinpingensis* has longer conidiophores (105–149 μm vs. 84–124 μm) and conidia (107–139 μm vs. 60–108 μm), and with more conidial septate (8–12 vs. 5–9) than *D. lignicola*. *Distoseptispora xinpingensis* can be distinguished from



**Figure 8.** *Distoseptispora xinpingsensis* (HKAS 125818, holotype) **a, b** colonies on woody substrates **c, d** conidiophores **e, f** conidiogenous cells **g–k** conidia (Arrow in **i–k** indicate proliferating conidia) **l** germinating conidium **m** culture on PDA. Scale bars: 40  $\mu\text{m}$  (**c, d**); 10  $\mu\text{m}$  (**e, f**); 30  $\mu\text{m}$  (**g–l**).

*D. menghaiensis* by its longer conidiophores (105–149  $\mu\text{m}$  vs. 45.7–82.9  $\mu\text{m}$ ) and conidia (107–139  $\mu\text{m}$  vs. 35.7–48.6  $\mu\text{m}$ ), as well as conidial septation (8–12-euseptate vs. 4–8-distoseptate) (Hu et al. 2023). Given the morphological distinctions and evidence from phylogenetic analysis, we introduce *Distoseptispora xinpingsensis* as a new species from the Red River Basin in Yunnan, China.

## Discussion

Systematic research on lignicolous freshwater fungi is ongoing in the Red River Basin. Seven distoseptispora-like species were discovered from submerged decaying wood. Based on multigene phylogenetic analysis and morphological studies, six *Distoseptispora* species were identified, *D. suae* and *D. xinpingsensis* were introduced as new species with their unique morphology and phylogenetic placement. Previously introduced species, *D. bambusae*, *D. euseptata*, *D. obpyriformis* and *D. pachyconidia* were reported in the watershed for the first time. The Red River Basin may contain more interesting, particular, and undiscovered freshwater fungal species, as no studies have been reported on yet.

In the past seven years, more than 70 *Distoseptispora* species have been introduced based on morphological and molecular evidence. These species grow as saprophytes on a variety of decaying wood debris in tropical and subtropical freshwater and terrestrial habitats (Index Fungorum database; Hu et al. 2023). 45 species have been reported on submerged bamboo stems and unknown wood debris in freshwater habitats, and 23 species have been reported on dead leaves, branches, and stems of various plants in terrestrial habitats, such as palms (Hyde et al. 2019), bamboo (Monkai et al. 2020), grasses (Hyde et al. 2023), and unknown broad-leaved trees (Hu et al. 2023), etc., and five species have been reported in both terrestrial and freshwater habitats (Hyde et al. 2016; Tibpromma et al. 2018; Phookamsak et al. 2019; Phukhamsakda et al. 2020; Sun et al. 2020; Shen et al. 2021; Ma et al. 2022; Zhang et al. 2022). China and Thailand are the countries that contribute the most *Distoseptispora* species, with 50 species reported in China and 25 species reported in Thailand.

Species of *Distoseptispora* are usually distinguished based on phylogenetic analysis combined with the morphological characteristics of conidiophores and conidia (Su et al. 2016; Monkai et al. 2020; Zhang et al. 2022). Important morphological characteristics are the color, shape, size, septation type (distoseptate/euseptate) and number of conidia, as well as the length of the conidiophores (Zhang et al. 2022). Phylogenetic studies of *Distoseptispora* are usually based on ITS, LSU, *tef1- $\alpha$* , and *rpb2* gene loci, and currently, all type species are well resolved on the phylogenetic tree (Hu et al. 2023; this study). Several previous studies have shown that new specimens of some species of *Distoseptispora* are significantly different in morphology from original descriptions, especially in the color and size of the conidia (Yang et al. 2018; Luo et al. 2019; Shen et al. 2021; Ma et al. 2022). These new specimens are usually collected from different habitats from the type specimens, and sometimes from the same habitat (Yang et al. 2018; Luo et al. 2019; Shen et al. 2021; Ma et al. 2022). However, the ITS, LSU, *tef1- $\alpha$*  and *rpb2* sequences of these new specimens are not significantly different from the type specimens (Yang et al. 2018; Shen et al. 2021; Ma et al. 2022). Habitat and incubation time may affect the size of conidia, but this has not yet been determined and needs to be resolved in future studies (Yang et al. 2018; Shen et al. 2021; this study). Additionally, the brand and photography mode of the compound microscope may affect the color of the conidia. Of course, another possibility is that the four loci currently used to construct the phylogenetic analysis are not enough to provide more information to explain the morphological differences; combining more loci or a whole-gene phylogenetic study may explain these morphological differences.

The multigene phylogeny indicates that members of *Distoseptispora* are distributed in four distinct clades. However, there are no pronounced morphological differences sufficient to separate them (Zhang et al. 2022). Morphologically, *Distoseptispora martinii* stands apart from other species within the genus due to its ellipsoid, oblate or subglobose and muriform conidia. These characteristics align more closely with the general concept of *Junewangia*. Therefore, the phylogenetic placement of *D. martinii* requires further examination through nucleotide base sequence analysis. In subsequent studies, the culture of *D. martinii* (CGMCC 3.18651) could be encouraged to sporulate to determine if similar conidiophores and conidia are produced. Notably, in our study, the ex-type strain of *D. suae* (KUNCC 22–12476) produced conidiophores and conidia that mirrored those observed on the natural substrate, confirming this approach as promising.

## Acknowledgments

Hong-Wei Shen thanks Qiu-Xia Yang, Sha Luan, Wen-Peng Wang and Zheng-Quan Zhang for their help with the sample collection, DNA extraction and PCR amplification. Thanks to Rong-Ju Xu for his help with the specimen and culture preservation.

## Additional information

### Conflict of interest

The authors have declared that no competing interests exist.

### Ethical statement

No ethical statement was reported.

### Funding

We would like to thank the National Natural Science Foundation of China (project ID: 32060005), National Science and Technology Fundamental Resources Investigation Program of China (2021FY100900), and the Yunnan Fundamental Research Project (Grant No. 202201AW070001) for financial support. This work was also supported by the Foundation of Yunnan Province Science and Technology Department (202305AM070003).

### Author contributions

Conceptualization: SB, YZL, ZLL. Formal analysis: HWS. Funding acquisition: ZLL. Investigation: XJS, HWS, YXL. Methodology: YXL, DFB. Resources: HWS, XJS. Software: DFB. Supervision: ZLL, SB. Writing – original draft: XJS, HWS. Writing – review and editing: DFB, ZLL, YXL, YZL, SB.

### Author ORCIDs

Hong-Wei Shen  <https://orcid.org/0000-0003-2508-1970>

Dan-Feng Bao  <https://orcid.org/0000-0002-5697-4280>

Saranyaphat Boonmee  <https://orcid.org/0000-0001-5202-2955>

Yong-Zhong Lu  <https://orcid.org/0000-0002-1033-5782>

Xi-Jun Su  <https://orcid.org/0000-0002-6357-7750>

Yun-Xia Li  <https://orcid.org/0009-0007-5645-8861>

Zong-Long Luo  <https://orcid.org/0000-0001-7307-4885>

## Data availability

All of the data that support the findings of this study are available in the main text.

## References

- Bao DF, McKenzie EH, Bhat DJ, Hyde KD, Luo ZL, Shen HW, Su HY (2020) *Acrogenospora* (Acrogenosporaceae, Minutisphaerales) appears to be a very diverse genus. *Frontiers in Microbiology* 11: e1606. <https://doi.org/10.3389/fmicb.2020.01606>
- Bao DF, Hyde KD, McKenzie EH, Jeewon R, Su HY, Nalumpang S, Luo ZL (2021) Biodiversity of lignicolous freshwater hyphomycetes from China and Thailand and description of sixteen species. *Journal of Fungi* 7(8): e669. <https://doi.org/10.3390/jof7080669>
- Cai L, Tsui CKM, Zhang KQ, Hyde KD (2002) Aquatic fungi from Lake Fuxian, Yunnan, China. *Fungal Diversity* 9: 57–70.
- Capella-Gutiérrez S, Silla-Martínez JM, Gabaldón T (2009) trimAl: A tool for automated alignment trimming in large-scale phylogenetic analyses. *Bioinformatics* 25(15): 1972–1973. <https://doi.org/10.1093/bioinformatics/btp348>
- Chen J, Yu X (2013) Odonata diversity of the middle and lower reaches of the Red River basin, Yunnan, China. *Journal of Insect Biodiversity* 1(9): 1–11. <https://doi.org/10.12976/jib/2013.1.9>
- Darriba D, Taboada GL, Doallo R, Posada D (2012) jModelTest 2: More models, new heuristics and parallel computing. *Nature Methods* 9(8): 772–772. <https://doi.org/10.1038/nmeth.2109>
- Dissanayake PD, Choi SW, Igalavithana AD, Yang X, Tsang DC, Wang CH, Kua HW, Lee KB, Ok YS (2020) Sustainable gasification biochar as a high efficiency adsorbent for CO<sub>2</sub> capture: A facile method to designer biochar fabrication. *Renewable & Sustainable Energy Reviews* 124: e109785. <https://doi.org/10.1016/j.rser.2020.109785>
- Dong W, Wang B, Hyde KD, McKenzie EHC, Raja HA, Tanaka K, Abdel-Wahab MA, Abdel-Aziz FA, Doilom M, Phookamsak R, Hongsanan S, Wanasinghe DN, Yu X-D, Wang G-N, Yang H, Yang J, Thambugala KM, Tian Q, Luo Z-L, Yang J-B, Miller AN, Fournier J, Boonmee S, Hu D-M, Nalumpang S, Zhang H (2020) Freshwater Dothideomycetes. *Fungal Diversity* 105(1): 319–575. <https://doi.org/10.1007/s13225-020-00463-5>
- Dong W, Hyde KD, Jeewon R, Doilom M, Yu XD, Wang GN, Liu NG, Hu DM, Nalumpang S, Zhang H (2021) Towards a natural classification of Annulatascaceae-like taxa II: Introducing five new genera and eighteen new species from freshwater. *Mycosphere* 12(1): 1–88. <https://doi.org/10.5943/mycosphere/12/1/1>
- Gu Z, Duan X, Shi Y, Li Y, Pan X (2018) Spatiotemporal variation in vegetation coverage and its response to climatic factors in the Red River Basin, China. *Ecological Indicators* 93: 54–64. <https://doi.org/10.1016/j.ecolind.2018.04.033>
- Guindon S, Gascuel O (2003) A simple, fast, and accurate algorithm to estimate large phylogenies by maximum likelihood. *Systematic Biology* 52(5): 696–704. <https://doi.org/10.1080/10635150390235520>
- Haruyama S (1995) Geomorphic environment of Tonkin delta. *The Study of International Relations. Tsuda College* 21: 1–13.
- Hu YF, Liu JW, Luo XX, Xu ZH, Xia JW, Zhang XG, Castañeda-Ruiz RF, Ma J (2023) Multi-locus phylogenetic analyses reveal eight novel species of *Distoseptispora* from southern China. *Microbiology Spectrum* 11(6): e02468–e23. <https://doi.org/10.1128/spectrum.02468-23>

- Hyde KD, Hongsanan S, Jeewon R, Bhat DJ, McKenzie EHC, Jones EBG, Phookamsak R, Ariyawansa HA, Boonmee S, Zhao Q, Abdel-Aziz FA, Abdel-Wahab MA, Banmai S, Chomnunti P, Cui BK, Daranagama DA, Das K, Dayarathne MC, de Silva NI, Dissanayake AJ, Doilom M, Ekanayaka AH, Gibertoni TB, Góes-Neto A, Huang SK, Jayasiri SC, Jayawardena RS, Konta S, Lee HB, Li WJ, Lin CG, Liu JK, Lu YZ, Luo ZL, Manawasinghe IS, Manimohan P, Mapook A, Niskanen T, Norphanphoun C, Papizadeh M, Perera RH, Phukhamsakda C, Richter C, André ALCM, Drechsler-Santos ER, Senanayake IC, Tanaka K, Tennakoon TMDS, Thambugala KM, Tian Q, Tibpromma S, Thongbai B, Vizzini A, Wanasinghe DN, Wijayawardene NN, Wu HX, Yang J, Zeng XY, Zhang H, Zhang JF, Bulgakov TS, Camporesi E, Bahkali AH, Amoozegar MA, Araujo-Neta LS, Ammirati JF, Baghela A, Bhatt RP, Bojantchev D, Buyck B, da Silva GA, de Lima CLF, de Oliveira RJV, de Souza CAF, Dai YC, Dima B, Duong TT, Ercole E, Mafalda-Freire F, Ghosh A, Hashimoto A, Kamolhan S, Kang JC, Karunarathna SC, Kirk PM, Kytövuori I, Lantieri A, Liimatainen K, Liu ZY, Liu XZ, Lücking R, Medardi G, Mortimer PE, Nguyen TTT, Promputtha I, Raj KNA, Reck MA, Lumyong S, Shahzadeh-Fazeli SA, Stadler M, Soudi MR, Su HY, Takahashi T, Tangthirasunun N, Uniyal P, Wang Y, Wen TC, Xu JC, Zhang ZK, Zhao YC, Zhou JL, Zhu L (2016) Fungal diversity notes 367–490: Taxonomic and phylogenetic contributions to fungal taxa. *Fungal Diversity* 80: 1–270. <https://doi.org/10.1007/s13225-016-0373-x>
- Hyde KD, Tennakoon DS, Jeewon R, Bhat DJ, Maharachchikumbura SSN, Rossi W, Leonardi M, Lee HB, Mun HY, Houbraken J, Nguyen TTT, Jeon SJ, Frisvad JC, Wanasinghe DN, Lücking R, Aptroot A, Cáceres MES, Karunarathna SC, Hongsanan S, Phookamsak R, de Silva NI, Thambugala KM, Jayawardena RS, Senanayake IC, Boonmee S, Chen J, Luo ZL, Phukhamsakda C, Pereira OL, Abreu VP, Rosado AWC, Bart B, Randrianjohany E, Hofstetter V, Gibertoni TB, da Soares AMS, Plautz HL, Sotão HMP, Xavier WKS, Bezerra JDP, de Oliveira TGL, de Souza-Motta CM, Magalhães OMC, Bundhun D, Harishchandra D, Manawasinghe IS, Dong W, Zhang SN, Bao DF, Samarakoon MC, Pem D, Karunarathna A, Lin CG, Yang J, Perera RH, Kumar V, Huang SK, Dayarathne MC, Ekanayaka AH, Jayasiri SC, Xiao Y, Konta S, Niskanen T, Liimatainen K, Dai YC, Ji XH, Tian XM, Mešić A, Singh SK, Phutthacharoen K, Cai L, Sorvongxay T, Thiyagaraja V, Norphanphoun C, Chaiwan N, Lu YZ, Jiang HB, Zhang JF, Abeywickrama PD, Aluthmuhandiram JVS, Brahmanage RS, Zeng M, Chethana T, Wei D, Réblová M, Fournier J, Někviňová J, do Nascimento Barbosa R, dos Santos JEF, de Oliveira NT, Li GJ, Ertz D, Shang QJ, Phillips AJL, Kuo CH, Camporesi E, Bulgakov TS, Lumyong S, Jones EBG, Chomnunti P, Gentekaki E, Bungartz F, Zeng XY, Fryar S, Tkalčec Z, Liang J, Li G, Wen TC, Singh PN, Gafforov Y, Promputtha I, Yasanthika E, Goonasekara ID, Zhao RL, Zhao Q, Kirk PM, Liu JK, Yan JY, Mortimer PE, Xu J, Doilom M (2019) Fungal diversity notes 1036–1150: Taxonomic and phylogenetic contributions on genera and species of fungal taxa. *Fungal Diversity* 96(1): 1–242. <https://doi.org/10.1007/s13225-019-00429-2>
- Hyde KD, Norphanphoun C, Ma J, Yang HD, Zhang JY, Du TY, Gao Y, Gomes de Farias AR, He SC, He YK, Li CJY, Li JY, Liu XF, Lu L, Su HL, Tang X, Tian XG, Wang SY, Wei DP, Xu RF, Xu RJ, Yang YY, Zhang F, Zhang Q, Bahkali AH, Boonmee S, Chethana KWT, Jayawardena RS, Lu YZ, Karunarathna SC, Tibpromma S, Wang Y, Zhao Q (2023) *Mycosphere* notes 387–412 – novel species of fungal taxa from around the world. *Mycosphere* 14(1): 663–744. <https://doi.org/10.5943/mycosphere/14/1/8>
- Jayasiri SC, Hyde KD, Ariyawansa HA, Bhat DJ, Buyck B, Cai L, Dai YC, Abd-Elsalam KA, Ertz D, Hidayat I, Jeewon R, Jones EBG, Bahkali AH, Karunarathna SC, Liu JK, Luangsa-ard JJ, Lumbsch HT, Maharachchikumbura SSN, McKenzie EHC, Moncalvo JM,

- Ghobad-Nejhad M, Nilsson H, Pang KL, Pereira OL, Phillips AJL, Raspé O, Rollins AW, Romero AI, Etayo J, Selçuk F, Stephenson SL, Suetrong S, Taylor JE, Tsui CKM, Vizzini A, Abdel-Wahab MA, Wen TC, Boonmee S, Dai DQ, Daranagama DA, Dissanayake AJ, Ekanayaka AH, Fryar SC, Hongsanan S, Jayawardena RS, Li WJ, Perera RH, Phookamsak R, Silva NI, Thambugala KM, Tian Q, Wijayawardene NN, Zhao RL, Zhao Q, Kang JC, Promputtha I (2015) The Faces of Fungi database: Fungal names linked with morphology, phylogeny and human impacts. *Fungal Diversity* 74(1): 3–18. <https://doi.org/10.1007/s13225-015-0351-8>
- Jeewon R, Hyde KD (2016) Establishing species boundaries and new taxa among fungi: Recommendations to resolve taxonomic ambiguities. *Mycosphere* 7(11): 1669–1677. <https://doi.org/10.5943/mycosphere/7/11/4>
- Jiang HQ (1980) Distributional features and zonal regularity of vegetation in Yunnan. *Yunnan Zhi Wu Yan Jiu* 2(2): 142–151.
- Katoh K, Rozewicki J, Yamada KD (2019) MAFFT online service: Multiple sequence alignment, interactive sequence choice and visualization. *Briefings in Bioinformatics* 20(4): 1160–1166. <https://doi.org/10.1093/bib/bbx108>
- Konta S, Tibpromma S, Karunarathna SC, Samarakoon MC, Steven LS, Mapook A, Boonmee S, Senwannana C, Balasuriya A, Eungwanichayapant PD, Hyde KD (2023) Morphology and multigene phylogeny reveal ten novel taxa in Ascomycota from terrestrial palm substrates (Arecaceae) in Thailand. *Mycosphere* 14: 107–152. <https://doi.org/10.5943/mycosphere/14/1/2>
- Kuraku S, Zmasek CM, Nishimura O, Katoh K (2013) aLeaves facilitates on-demand exploration of metazoan gene family trees on MAFFT sequence alignment server with enhanced interactivity. *Nucleic Acids Research* 41(W1): W22–W28. <https://doi.org/10.1093/nar/gkt389>
- Li WL, Liu ZP, Zhang T, Dissanayake AJ, Luo ZL, Su HY, Liu JK (2021) Additions to *Distoseptispora* (Distoseptisporaceae) associated with submerged decaying wood in China. *Phytotaxa* 520(1): 75–86. <https://doi.org/10.11646/phytotaxa.520.1.5>
- Liu YJ, Whelen S, Hall BD (1999) Phylogenetic relationships among ascomycetes: Evidence from an RNA polymerase II subunit. *Molecular Biology and Evolution* 16(12): 1799–1808. <https://doi.org/10.1093/oxfordjournals.molbev.a026092>
- Luo J, Yin J, Cai L, Zhang KQ, Hyde KD (2004) Freshwater fungi in Lake Dianchi, a heavily polluted lake in Yunnan, China. *Fungal Diversity* 16: 93–112.
- Luo ZL, Bhat DJ, Jeewon R, Boonmee S, Bao DF, Zhao YC, Chai HM, Su HY, Su XJ, Hyde KD (2017) Molecular phylogeny and morphological characterization of asexual fungi (Tubeufiaceae) from freshwater habitats in Yunnan, China. *Cryptogamie. Mycologie* 38(1): 27–53. <https://doi.org/10.7872/crym/v38.iss1.2017.27>
- Luo ZL, Hyde KD, Liu JK, Bhat DJ, Bao DF, Li WL, Su HY (2018a) Lignicolous freshwater fungi from China II: Novel *Distoseptispora* (Distoseptisporaceae) species from northwestern Yunnan Province and a suggested unified method for studying lignicolous freshwater fungi. *Mycosphere* 9(3): 444–461. <https://doi.org/10.5943/mycosphere/9/3/2>
- Luo ZL, Hyde KD, Bhat DJ, Jeewon R, Maharachchikumbura SSN, Bao DF, Li WL, Su XJ, Yang XY, Su HY (2018b) Morphological and molecular taxonomy of novel species Pleurotheciaceae from freshwater habitats in Yunnan, China. *Mycological Progress* 17(5): 511–530. <https://doi.org/10.1007/s11557-018-1377-6>
- Luo ZL, Hyde KD, Liu JK, Maharachchikumbura SS, Jeewon R, Bao DF, Bhat DJ, Lin CG, Li WL, Yang J, Liu NG, Lu YZ, Jayawardena RS, Li JF, Su HY (2019) Freshwater Sordariomycetes. *Fungal Diversity* 99(1): 451–660. <https://doi.org/10.1007/s13225-019-00438-1>

- Ma J, Zhang JY, Xiao XJ, Xiao YP, Tang X, Boonmee S, Kang JC, Lu YZ (2022) Multi-gene phylogenetic analyses revealed five new species and two new records of *Distoseptisporales* from China. *Journal of Fungi* 8(11): e1202. <https://doi.org/10.3390/jof8111202>
- Miller MA, Pfeiffer W, Schwartz T (2010) Creating the CIPRES Science Gateway for Inference of Large Phylogenetic Trees. 2010 gateway computing environments workshop (GCE), 8 pp. <https://doi.org/10.1109/GCE.2010.5676129>
- Monkai J, Boonmee S, Ren GC, Wei DP, Phookamsak R, Mortimer PE (2020) *Distoseptispora hydei* sp. nov. (Distoseptisporaceae), a novel lignicolous fungus on decaying bamboo in Thailand. *Phytotaxa* 459(2): 93–107. <https://doi.org/10.11646/phytotaxa.459.2.1>
- Nylander J (2004) MrModeltest v2. Program distributed by the author: Evolutionary Biology Centre. Uppsala University, Sweden. <http://www.ebc.uu.se/systzoo/staff/nylander.html>
- Phookamsak R, Hyde KD, Jeewon R, Bhat DJ, Jones EBG, Maharachchikumbura SSN, Raspé O, Karunarathna SC, Wanasinghe DN, Hongsanan S, Doilom M, Tennakoon DS, Machado AR, Firmino AL, Ghosh A, Karunarathna A, Mešić A, Dutta AK, Thongbai B, Devadatha B, Norphanphoun C, Senwannana C, Wei DP, Pem D, Ackah FK, Wang GN, Jiang HB, Madrid H, Lee HB, Goonasekara ID, Manawasinghe IS, Kušan I, Cano J, Gené J, Li JF, Das K, Acharya K, Raj KNA, Latha KPD, Chethana KWT, He MQ, Dueñas M, Jadan M, Martín MP, Samarakoon MC, Dayarathne MC, Raza M, Park MS, Telleria MT, Chaiwan N, Matočec N, de Silva NI, Pereira OL, Singh PN, Manimohan P, Uniyal P, Shang QJ, Bhatt RP, Perera RH, Alvarenga RLM, Nogal-Prata S, Singh SK, Vadthananat S, Oh SY, Huang SK, Rana S, Konta S, Paloi S, Jayasiri SC, Jeon SJ, Mehmood T, Gibertoni TB, Nguyen TTT, Singh U, Thiyagaraja V, Sarma VV, Dong W, Yu XD, Lu YZ, Lim YW, Chen Y, Tkalčec Z, Zhang ZF, Luo ZL, Daranagama DA, Thambugala KM, Tibpromma S, Camporesi E, Bulgakov TS, Dissanayake AJ, Senanayake IC, Dai DQ, Tang LZ, Khan S, Zhang H, Promputtha I, Cai L, Chomnunti P, Zhao RL, Lumyong S, Boonmee S, Wen TC, Mortimer PE, Xu JC (2019) Fungal diversity notes 929–1035: Taxonomic and phylogenetic contributions on genera and species of fungi. *Fungal Diversity* 95(1): 1–273. <https://doi.org/10.1007/s13225-019-00421-w>
- Phukhamsakda C, McKenzie EHC, Phillips AJL, Gareth Jones EB, Jayarama Bhat D, Stadler M, Bhunjun CS, Wanasinghe DN, Thongbai B, Camporesi E, Ertz D, Jayawardena RS, Perera RH, Ekanayake AH, Tibpromma S, Doilom M, Xu J, Hyde KD (2020) Microfungi associated with *Clematis* (Ranunculaceae) with an integrated approach to delimiting species boundaries. *Fungal Diversity* 102(1): 1–203. <https://doi.org/10.1007/s13225-020-00448-4>
- Rannala B, Yang Z (1996) Probability distribution of molecular evolutionary trees: A new method of phylogenetic inference. *Journal of Molecular Evolution* 43(3): 304–311. <https://doi.org/10.1007/BF02338839>
- Ronquist F, Teslenko M, van der Mark P, Ayres DL, Darling A, Höhna S, Larget B, Liu L, Suchard MA, Huelsenbeck JP (2012) MrBayes 3.2: Efficient Bayesian phylogenetic inference and model choice across a large model space. *Systematic Biology* 61(3): 539–542. <https://doi.org/10.1093/sysbio/sys029>
- Senanayake IC, Rathnayaka AR, Marasinghe DS, Calabon MS, Gentekaki E, Lee HB, Hurdeal VG, Pem D, Dissanayake LS, Wijesinghe SN, Bundhun D, Nguyen TT, Goonasekara ID, Abeywickrama PD, Bhunjun CS, Jayawardena RS, Wanasinghe DN, Jeewon R, Bhat DJ, Xiang MM (2020) Morphological approaches in studying fungi: Collection, examination, isolation, sporulation and preservation. *Mycosphere* 11(1): 2678–2754. <https://doi.org/10.5943/mycosphere/11/1/20>

- Shen HW, Bao DF, Bhat DJ, Su HY, Luo ZL (2022) Lignicolous freshwater fungi in Yunnan Province, China: an overview. *Mycology* 13(2): 119–132. <https://doi.org/10.1080/21501203.2022.2058638>
- Shen HW, Bao DF, Hyde KD, Su HY, Bhat DJ, Luo ZL (2021) Two novel species and two new records of *Distoseptispora* from freshwater habitats in China and Thailand. *MycKeys* 84: 79–101. <https://doi.org/10.3897/mycokeys.84.71905>
- Stamatakis A (2006) RAxML-VI-HPC: Maximum likelihood-based phylogenetic analyses with thousands of taxa and mixed models. *Bioinformatics* 22(21): 2688–2690. <https://doi.org/10.1093/bioinformatics/btl446>
- Stamatakis A, Hoover P, Rougemont J (2008) A rapid bootstrap algorithm for the RAxML web servers. *Systematic Biology* 57(5): 758–771. <https://doi.org/10.1080/10635150802429642>
- Su H, Hyde KD, Maharachchikumbura SSN, Ariyawansa HA, Luo Z, Promputtha I, Tian Q, Lin C, Shang Q, Zhao Y, Chai H, Liu X, Bahkali AH, Bhat JD, McKenzie EHC, Zhou D (2016) The families *Distoseptisporaceae* fam. nov., *Kirschsteinioteliaceae*, *Sporormiaceae* and *Torulaceae*, with new species from freshwater in Yunnan Province, China. *Fungal Diversity* 80(1): 375–409. <https://doi.org/10.1007/s13225-016-0362-0>
- Sun YR, Goonasekara ID, Thambugala KM, Jayawardena RS, Wang Y, Hyde KD (2020) *Distoseptispora bambusae* sp. nov. (*Distoseptisporaceae*) on bamboo from China and Thailand. *Biodiversity Data Journal* 8: e53678. <https://doi.org/10.3897/BDJ.8.e53678>
- Tibpromma S, Hyde KD, McKenzie EH, Bhat DJ, Phillips AJ, Wanasinghe DN, Samarakoon MC, Jayawardena RS, Dissanayake AJ, Tennakoon DS, Doilom M, Phookamsak R, Tang AMC, Xu J, Mortimer PE, Promputtha I, Maharachchikumbura SSN, Khan S, Karunaratna SC (2018) Fungal diversity notes 840–928: Micro-fungi associated with Pandanaceae. *Fungal Diversity* 93(1): 1–60. <https://doi.org/10.1007/s13225-018-0408-6>
- Tsui KM, Hyde KD, Hodgkiss IJ (2000) Biodiversity of fungi on submerged wood in Hong Kong streams. *Aquatic Microbial Ecology* 21: 289–298. <https://doi.org/10.3354/ame021289>
- Vaidya G, Lohman DJ, Meier R (2011) SequenceMatrix: Concatenation software for the fast assembly of multi-gene datasets with character set and codon information. *Cladistics* 27(2): 171–180. <https://doi.org/10.1111/j.1096-0031.2010.00329.x>
- Van den Bergh GD, Boer W, Schaapveld MA, Duc DM, Van Weering TC (2007) Recent sedimentation and sediment accumulation rates of the Ba Lat prodelta (Red River, Vietnam). *Journal of Asian Earth Sciences* 29(4): 545–557. <https://doi.org/10.1016/j.jseaes.2006.03.006>
- Van Maren DS (2007) Water and sediment dynamics in the Red River mouth and adjacent coastal zone. *Journal of Asian Earth Sciences* 29(4): 508–522. <https://doi.org/10.1016/j.jseaes.2006.03.012>
- Vilgalys R, Hester M (1990) Rapid genetic identification and mapping of enzymatically amplified ribosomal DNA from several *Cryptococcus* species. *Journal of Bacteriology* 172(8): 4238–4246. <https://doi.org/10.1128/jb.172.8.4238-4246.1990>
- Wang F, Wang K, Cai L, Zhao M, Kirk PM, Fan G, Sun Q, Li B, Wang S, Yu Z, Han D, Ma J, Wu L, Yao Y (2023) Fungal names: A comprehensive nomenclatural repository and knowledge base for fungal taxonomy. *Nucleic Acids Research* 51(D1): D708–D716. <https://doi.org/10.1093/nar/gkac926>
- White TJ, Bruns T, Lee SJ, Taylor J (1990) Amplification and direct sequencing of fungal ribosomal RNA genes for phylogenetics. *PCR protocols: A guide to methods and applications* 18(1): 315–322. <https://doi.org/10.1016/B978-0-12-372180-8.50042-1>

- Yang J, Maharachchikumbura SSN, Liu JK, Hyde KD, Jones EBG, Al-Sadi AM, Liu ZY (2018) *Pseudostanjehughesia aquitropica* gen. et sp. nov. and *Sporidesmium sensu lato* species from freshwater habitats. *Mycological Progress* 17(5): 591–616. <https://doi.org/10.1007/s11557-017-1339-4>
- Yang J, Liu LL, Jones EB, Li WL, Hyde KD, Liu ZY (2021) Morphological variety in *Distoseptispora* and introduction of six novel species. *Journal of Fungi* 7(11): e945. <https://doi.org/10.3390/jof7110945>
- Zhai ZJ, Yan JQ, Li WW, Gao Y, Hu HJ, Zhou JP, Song HY, Hu DM (2022) Three novel species of *Distoseptispora* (Distoseptisporaceae) isolated from bamboo in Jiangxi Province, China. *MycKeys* 88: 35–54. <https://doi.org/10.3897/mycokeys.88.79346>
- Zhang H, Zhu R, Qing Y, Yang H, Li C, Wang G, Zhang D, Ning P (2022) Polyphasic Identification of *Distoseptispora* with six new species from fresh water. *Journal of Fungi* 8(10): e1063. <https://doi.org/10.3390/jof8101063>
- Zhou W, Cui GH (1997) Fishes of the genus *Triplophysa* in the Yuanjiang River (upper Red River) basin of Yunnan, China, with description of a new species. *Ichthyological Exploration of Freshwaters* 8: 177–183.

# New species of *Tropicoporus* (Basidiomycota, Hymenochaetales, Hymenochaetaceae) from India, with a key to Afro-Asian *Tropicoporus* species

Sugantha Gunaseelan<sup>1</sup>, Kezhocuyi Kezo<sup>1</sup>, Samantha C. Karunarathna<sup>2,3</sup>, Erfu Yang<sup>2,4</sup>, Changlin Zhao<sup>5</sup>, Abdallah M. Elgorban<sup>6</sup>, Saowaluck Tibpromma<sup>2</sup>, Malarvizhi Kaliyaperumal<sup>1</sup>

1 Centre for Advanced Studies in Botany, University of Madras, Guindy Campus, Chennai 600025, Tamil Nadu, India

2 Center for Yunnan Plateau Biological Resources Protection and Utilization, College of Biological Resource and Food Engineering, Qujing Normal University, Qujing, Yunnan 655011, China

3 National Institute of Fundamental Studies (NIFS), Kandy, Sri Lanka

4 Department of Biology, Faculty of Science, Chiang Mai University, Chiang Mai 50200, Thailand

5 College of Biodiversity Conservation, Southwest Forestry University, Kunming 650224, China

6 Department of Botany and Microbiology, College of Science, King Saud University, Riyadh 11451, Saudi Arabia

Corresponding authors: Sugantha Gunaseelan ([suganthagunaseelan@gmail.com](mailto:suganthagunaseelan@gmail.com)); Malarvizhi Kaliyaperumal ([malar.kaliyaperumal@gmail.com](mailto:malar.kaliyaperumal@gmail.com))



Academic editor: Ajay Kumar Gautam

Received: 8 December 2023

Accepted: 21 January 2024

Published: 5 February 2024

Citation: Gunaseelan S, Kezo K, Karunarathna SC, Yang E, Zhao C, Elgorban AM, Tibpromma S, Kaliyaperumal M (2024)

New species of *Tropicoporus* (Basidiomycota, Hymenochaetales, Hymenochaetaceae) from India, with a key to Afro-Asian *Tropicoporus* species. MycoKeys 102: 29–54. <https://doi.org/10.3897/mycokeys.102.117067>

Copyright: © Sugantha Gunaseelan et al.

This is an open access article distributed under terms of the Creative Commons Attribution License (Attribution 4.0 International – CC BY 4.0).

## Abstract

The *Inonotus linteus* complex, predominantly reported from East Asia, Mesoamerica and Caribbean countries, was circumscribed into *Tropicoporus* as one of the new genera, based on morphological and phylogenetic data. The present paper describes four new species of *Tropicoporus* from India. Morphological characteristics and phylogenetic analyses, based on ITS and nLSU data, delimited the new species, which are named *T. cleistanthicola*, *T. indicus*, *T. pseudoindicus* and *T. tamilnaduensis*. The pairwise homoplasy index (PHI) test was done to confirm the distinctive nature of the new species. The traits of Indian species remain distinct from one another, except for the pileate basidiome with the mono-dimitic hyphal system, cystidioles and broadly ellipsoid basidiospores. Descriptions, illustrations, PHI test results and a phylogenetic tree to show the position of the new species are provided. In addition, an identification key to *Tropicoporus* in Asia and an African species is given.

**Key words:** DNA, *Inonotus linteus* complex, mushroom, new species, taxonomy, wood decaying fungi

## Introduction

The morpho-taxonomy and phylogenetic analyses, based on the nLSU and ITS genetic markers, revealed that the *Inonotus linteus* complex comprises two clades and are respectively treated as two new genera, *Sanghuangporus* and *Tropicoporus* (Zhou et al. 2015). *Tropicoporus* is characterised by their annual to perennial, resupinate, effused-reflexed to pileate basidiome with glabrous, uncracked to radially cracked pilear surface, homogeneous to duplex context, with or without a black line. A mono-dimitic or dimitic hyphal system with simple septate generative hyphae, presence or absence of cystidioles, presence

of hymenial setae with smooth, fairly thick-walled to thick-walled, yellowish, subglobose to ellipsoid basidiospores are microscopic characteristic features of *Tropicoporus* (Zhou et al. 2015; Wu et al. 2022).

A total of forty-eight *Tropicoporus* species have been recorded in MycoBank with fifteen new species and thirty-three new combinations (as of 12 January 2024). Two new species, namely *Tropicoporus excentrodendri* L.W. Zhou & Y.C. Dai and *T. guanacastensis* L.W. Zhou, Y.C. Dai & Vlasák have been delimited, based on nLSU and ITS datasets (Zhou et al. 2015). In addition, *Tropicoporus boehmeriae* (L.W. Zhou & F. Wu) Y. C. Dai & F. Wu, *T. drechsleri* Salvador-Montoya & Popoff, *T. flabellatus* V.R.T. Oliveira, J.R.C. Oliveira-Filho, Xavier de Lima & Gibertoni, *T. nullisetus* Xavier de Lima, V.R.T. Oliveira & Gibertoni, *T. stratificans* Y.C. Dai & F. Wu. and *T. texanus* A.A. Brown, D.P. Lawr. & K. Baumgartner were reported across the world, based on the morphological and molecular data (Wu et al. 2015; Coelho et al. 2016; Salvador-Montoya et al. 2018; Brown et al. 2019; Lima et al. 2022). Recently, seven new species viz., *T. angustisulcatus* Y.C. Dai & F. Wu, *T. hainanicus* Y.C. Dai & F. Wu, *T. lineatus* Y.C. Dai & F. Wu, *T. minus* Y.C. Dai & F. Wu, *T. ravidus* Y.C. Dai & F. Wu, *T. substratificans* Y.C. Dai & F. Wu and *T. tenuis* Y.C. Dai & F. Wu with twenty-four new combinations were reported, based on the combined dataset of ITS and nLSU sequences (Wu et al. 2022). Of the forty-eight legitimate *Tropicoporus* species, only *T. nullisetus* was reported without setae (Lima et al. 2022).

*Tropicoporus linteus* (also known as *Phellinus linteus*) is used as a renowned Chinese medicine. Due to the presence of *P. linteus* polysaccharides (PLPs), it may play a vital role in anti-aging, anti-bacterial, anti-inflammation, anti-tumour, anti-oxidant, hepatoprotective and hypoglycaemic processes (Chen et al. 2019). On the other hand, *Tropicoporus tropicalis* has been reported to cause diseases in humans (Sutton et al. 2005; Haidar et al. 2017; Gupta et al. 2022).

In India, hymenochaetoid fungi from Himachal Pradesh were studied (Kaur et al. 2022). Fourteen hymenochaetoid members were documented from Tamil Nadu (Natarajan and Kolandavelu 1998). Nevertheless, studies on Indian hymenochaetoid fungi, based on molecular data have not been attempted, which makes it difficult to understand their evolutionary history, phylogenetic relationships and accuracy of species delimitation. This study is the first attempt to describe new *Tropicoporus* species from India, based on morphology and molecular evidence. In addition, an identification key to Afro-Asian *Tropicoporus* is given.

## Materials and methods

### Morphological analyses

Eight specimens were collected from parts of Eastern Ghats and the plain region of Tamil Nadu, southern India. Macro-morphological characteristics such as shape, size of basidiome, perennial or annual, colour, texture, margin (acute or obtuse), context (homogenous, duplex with or without black line), tube layer (colour, length, stratification) and pores (size and shape) were examined in the fresh sample and recorded. Colour descriptions were based on the Methuen Handbook (Kornerup and Wanscher 1978). To analyse the micro-morphological

characteristics, free-hand sections of dry specimens were mounted in water, 5% potassium hydroxide (KOH) (v/w), cotton blue (CB) and Melzer's reagent (IK). Sections were studied and photos were taken at magnification up to 1000× using a LABOMED OPTIC-CX BINO LED microscope. The drawings were made using LABOMED CxL2 compound microscope. Microscopic measurements and illustrations were made in 5% KOH solution. Basidiospores measurements (as minimum-mean-maximum) and Q values (length/width ratios) were recorded. The following abbreviations are used: IKI<sup>-</sup> (inamyloid), IKI<sup>+</sup> (amyloid), CB<sup>-</sup> (acyanophilous), CB<sup>+</sup> (cyanophilous), L = mean spore length (arithmetic average of all spores), W = mean spore width (arithmetic average of all spores), Q = (variation in the L/W ratios; and basidium length excludes the lengths of the sterigmata) and n = number of spores measured. For measuring the spores, an average of 50 spores were considered. Specimens in this study were deposited in the Madras University Botany Laboratory (**MUBL**), Centre for Advanced Studies in Botany, University of Madras, India.

### Genomic DNA extraction, PCR amplification and sequencing

Extraction of total genomic DNA from mycelium and dried basidiome followed the protocol of Doyle and Doyle (1987), modified by Góes-Neto et al. (2005). The ITS and nLSU regions were amplified and sequenced with the primers ITS1/ITS4 and LR0R/LR7, respectively (Vilgalys and Hester 1990; White et al. 1990). The polymerase chain reaction (PCR) procedure for ITS was as follows: initial denaturation at 95 °C for 3 min, followed by 32 cycles at 95 °C for 30 s, 52 °C for 30 s and 72 °C for 1 min and a final extension of 72 °C for 3 min. The PCR procedure followed for nLSU was as follows: initial denaturation at 94 °C for 1 min, followed by 34 cycles at 94 °C for 30 s, 45 °C for 30 s and 72 °C for 1.5 min and final extension at 72 °C for 10 min. The PCR products were sequenced at Eurofins Genomics India Pvt. Ltd., Karnataka, India.

### Phylogenetic analyses

The dataset comprised ITS and nLSU sequences of *Fulvifomes*, *Inonotus*, *Phellinus*, *Phylloporia*, *Sanghuangporus* and *Tropicoporus* retrieved from GenBank (NCBI), along with the outgroup (*Fomitiporella caryophylli*, CBS 448.76) and the newly-generated sequences (deposited at GenBank (Sayers et al. 2023); for accession numbers, see Table 1). The dataset was aligned using MEGA X v.10.0.2 configured for Windows and edited manually to increase the alignment similarity (Kumar et al. 2018). The Maximum Likelihood (ML) tree was constructed using raxmlGUI 2.0 (Edler et al. 2020) with the best-fit evolutionary model estimated by jModelTest 2.1.10 with 1000 rapid bootstrap inferences (BS) (Guindon and Gascuel 2003; Darriba et al. 2012). Bayesian Inference (BI) was performed using MrBayes 3.2.7a with two independent runs and six chains of Metropolis-coupled Markov Chain Monte Carlo iterations for 2,000,000 generations and trees were sampled every 100 generations (Ronquist et al. 2012). A proportion of 0.25% of all trees (nLSU+ITS, ITS, nLSU) were discarded as burn-in. The final alignments and the retrieved topologies were deposited in TreeBASE (<http://purl.org/phylo/treebase/phyloids/study/TB2:S31000>).

**Table 1.** Names, strain numbers, countries of collection and the corresponding GenBank accession numbers of the sequences used in this study.

Species	Strain numbers	Country	Accession numbers	
			ITS	nLSU
<i>Fomitiporella caryophylli</i>	CBS 448.76	–	AY558611	AY558611
<i>Fulvifomes centroamericanus</i> <sup>T</sup>	JV0611_III	Guatemala	KX960763	KX960764
<i>F. elaeodendri</i>	CMW47825	South Africa	MH599094	MH599134
<i>F. nilgherensis</i>	CBS 209.36	USA	AY558633	AY059023
<i>F. thailandicus</i> <sup>T</sup>	LWZ 2014073-11	Thailand	KR905672	KR905665
<i>Inonotus pachyphloeus</i>	Wu 0407.6	Taiwan	KP030785	KP030770
<i>Phellinus laevigatus</i>	CBS 122.40	USA	MH856059	MH867554
<i>P. populicola</i> <sup>T</sup>	CBS 638.75	Finland	MH860960	MH872729
<i>Phylloporia nodostipitata</i>	FLOR:51153	Brazil	KJ639057	KJ631414
<i>Sanguangporus alpinus</i>	Cui12485	China	MF772781	MF772799
<i>S. baumii</i>	Cui 11769	China	MF772784	MF772803
<i>S. lonicericola</i>	Dai 8376	China	JQ860308	MF772805
<i>S. lonicerinus</i>	Dai 17093	China	MF772788	MF772807
<i>S. quercicola</i>	Dai 13947	China	KY328309	MF772809
<i>S. sanghuang</i>	Cui 14419	China	MF772789	MF772810
<i>S. vaninii</i>	DMR 95-1-T	North America	KU139198	KU139258
<i>S. vitexicola</i>	Wu 2006-21	–	MT906620	MZ437416
<i>S. weigelaie</i>	Dai 16077	China	MF772794	MF772815
<i>S. zonatus</i>	Dai 10841	China	JQ860306	KP030775
<i>Tropicoporus angustisulcatus</i>	Dai 17409	Brazil	MZ484584	MZ437417
<i>T. angustisulcatus</i> <sup>T</sup>	JV 1808/83	French Guiana	MZ484585	MZ437418
<i>T. boehmeriae</i> <sup>T</sup>	LWZ 20140729-10	Thailand	KT223640	MT319393
<i>T. boehmeriae</i>	LWZ 20140729-13	Thailand	KT223641	MT319394
	Dai 20522	China	MZ484586	MZ437419
	Dai 20617	China	MZ484587	MZ437420
<b><i>T. cleistanthicola</i><sup>T</sup></b>	<b>MUBL1089</b>	<b>India</b>	<b>OR272292</b>	<b>OR272337</b>
<b><i>T. cleistanthicola</i></b>	<b>MUBL1090</b>	<b>India</b>	<b>OR272291</b>	<b>OR272336</b>
<i>T. cubensis</i>	MUCL 47113	Cuba	JQ860324	KP030777
	MUCL 47079	Cuba	JQ860325	KP030776
<i>T. dependens</i>	JV 0409/12-J	USA	KC778777	MF772818
<i>T. detonsus</i>	CBS 617.89	–	AF534077	AY059037
	IDR 1300012986	USA	KF695121	KF695122
<i>T. drechsleri</i> <sup>T</sup>	CTES:570140	Argentina	MG242439	MG242444
<i>T. drechsleri</i>	CTES:570144	Argentina	MG242437	MG242442
<i>T. excentrodendri</i>	Yuan 6234	China	KP030791	–
	Yuan 6229	China	KP030789	–
<i>T. flabellatus</i> <sup>T</sup>	VRT0873	Brazil	MT908376	MT906643
<i>T. guanacastensis</i>	O 19228	Costa Rica	KP030794	–
<i>T. guanacastensis</i> <sup>T</sup>	JV 1408_25	Costa Rica	KP030793	KP030778
<i>T. hainanicus</i> <sup>T</sup>	Dai 17705	China	MZ484588	MZ437421
<b><i>T. indicus</i><sup>T</sup></b>	<b>MUBL1083</b>	<b>India</b>	<b>OR272293</b>	<b>OR272338</b>
<b><i>T. indicus</i></b>	<b>MUBL1084</b>	<b>India</b>	<b>OR272294</b>	<b>OR272339</b>
<i>T. lineatus</i> <sup>T</sup>	Dai 21196	Malaysia	MZ484594	MZ437426
<i>T. linteus</i>	JV 0904/64	USA	JQ860322	JX467701

Species	Strain numbers	Country	Accession numbers	
			ITS	nLSU
<i>T. linteus</i>	JV 0904/140	USA	JQ860323	KP030780
<i>T. minor</i> <sup>T</sup>	Dai 21139	China	MZ484592	MZ437424
<i>T. minus</i>	Dai 18487A	China	MZ484590	MZ437422
	Dai 21183	China	MZ484593	MZ437425
<i>T. nullisetus</i> <sup>T</sup>	VXLF616	Brazil	MN795129	MN812261
<i>T. nullisetus</i>	VRT0195	Brazil	MN795118	MN812254
<b><i>T. pseudoindicus</i><sup>T</sup></b>	<b>MUBL1087</b>	<b>India</b>	<b>OR272295</b>	<b>OR272340</b>
<b><i>T. pseudoindicus</i></b>	<b>MUBL1088</b>	<b>India</b>	<b>OR272296</b>	<b>OR272341</b>
<i>T. pseudolinteus</i>	JV0402/35-K	Venezuela	KC778781	MF772820
	JV 0312/22.10-J	Venezuela	KC778780	–
<i>T. ravidus</i> <sup>T</sup>	Dai 18165	China	MZ484595	MZ437427
<i>T. rudis</i>	O 915614	Rwanda	KP030796	–
	O 915617	Tanzania	KP030797	MH101016
<i>T. sideroxylicola</i>	JV 1207/4.3-J	USA	KC778783	–
<i>T. sideroxylicola</i> <sup>T</sup>	JV 0409/30-J	USA	KC778782	–
<i>T. stratificans</i> <sup>T</sup>	SMDB 14732	Brazil	KM199689	–
<i>T. stratificans</i>	VRT0884	Brazil	MN795124	MN812266
<i>T. substratificans</i> <sup>T</sup>	JV 1908/80	French Guiana	MZ484597	MZ437429
<b><i>T. tamilnaduensis</i><sup>T</sup></b>	<b>MUBL1085</b>	<b>India</b>	<b>OR272297</b>	<b>OR272343</b>
<b><i>T. tamilnaduensis</i></b>	<b>MUBL1086</b>	<b>India</b>	–	<b>OR272344</b>
<i>T. tenuis</i> <sup>T</sup>	Dai 19699	China	MZ484598	MZ437430
<i>T. tenuis</i>	Dai 19724	China	MZ484599	MZ437431
<i>T. texanus</i> <sup>T</sup>	CBS 145357	USA	NR_168219	NG_068906
<i>T. texanus</i>	TX8	USA	MN108123	MN113949
<i>T. tropicalis</i>	UTHSC 02-617	USA	AY641432	–
	UAMH 10376	USA	AY599487	–

<sup>T</sup> = Type material and “–” refers to the data unavailability. Sequences generated from the present study are indicated in bold.

## Genealogical concordance phylogenetic species recognition analysis

Genealogical concordance phylogenetic species recognition analysis (GCPSR) by the pairwise homoplasy index (PHI) test was used to determine the recombination level within closely-related species (Bruen et al. 2006). The data were analysed by the software SplitsTree 4 (Bruen et al. 2006; Huson and Bryant 2006). The relationships between closely related taxa were visualised by constructing split graphs from concatenated datasets, using the LogDet transformation and splits decomposition options. If the PHI test value is  $(\Phi_w) \leq 0.05$ , it indicates significant recombination within the dataset. This is an important method to provide further evidence to justify a species. All results are shown in Fig. 1.

## Results

### Phylogenetic analyses

In total, eight new sequences of the ITS and seven new sequences of the nLSU regions were generated and submitted to GenBank (Table 1). Additionally, 62 taxa (52 nLSU and 62 ITS sequences) were retrieved from GenBank

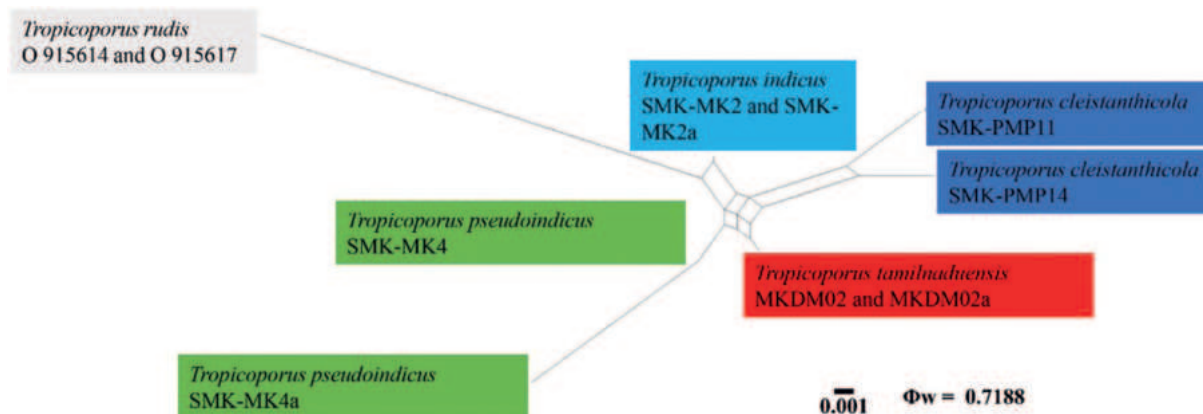


**Figure 1.** Split graphs show the results of the PHI test of the new species, *Tropicoporus indicus*, *T. tamilnaduensis*, *T. pseudoindicus*, *T. cleistanthicola* and their most closely-related species *T. rudis*, using LogDet transformation and split decomposition options. The PHI test result  $\Phi_w \leq 0.05$  indicates that there is a significant recombination within the dataset.

(Table 1). The combined nLSU and ITS dataset were aligned and the multiple sequence alignment consists of 1,820 characters (914 for nLSU and 902 for ITS) of which 1,017 were constant, 962 were variable and 570 (31%) were parsimony informative. The best-fit evolutionary model (GAMMA+P-Invar Model) was estimated by jModelTest 2.1.10 for the combined datasets. The Maximum Likelihood (ML) trees were constructed using raxmlGUI 2.0 with 1,000 rapid bootstrap inferences (BS). The Bayesian analysis was run for 2,000,000 generations and the average standard deviation reached 0.010166. The phylogenetic topology was selected from Bayesian analysis. The Maximum Likelihood bootstrap values  $\geq 60\%$  and the Bayesian posterior probabilities  $\geq 0.90$  are summarised in Fig. 2.

### Taxonomical descriptions of the four novel species of *Tropicoporus*

#### *Tropicoporus cleistanthicola* S. Gunaseelan & M. Kaliyaperumal, sp. nov.

Mycobank No: 849484

Figs 3, 4

**Etymology.** The specific epithet *cleistanthicola* (Lat.) refers to the host *Cleistanthus collinus*.

**Diagnosis.** *Tropicoporus cleistanthicola* is characterised by perennial, effused-reflexed to pileate, applanate to triquetrous basidiome with narrowly zonate, glabrous, meagrely warted pileal surface, acute margin, homogenous context, mono-dimitic hyphal system, presence of cystidioles and subglobose to broadly ellipsoid basidiospores measuring  $4.7\text{--}5.4 \times 4.2\text{--}4.9 \mu\text{m}$ .

**Type.** INDIA, Tamil Nadu, Thiruvannamalai District, Jawadhu Hills,  $12^{\circ}54'24''\text{N}$ ,  $78^{\circ}87'75''\text{E}$ ; 15 Nov 2019; Sugantha Gunaseelan; on a living angiosperm tree (*Cleistanthus collinus*); SMK-PMP11 (MUBL1089; Holotype); GenBank: OR272292 (ITS); OR272337 (nLSU).

**Description.** **Basidiome** perennial, pileate, solitary, hard corky and without distinctive odour or taste when fresh, woody hard and light in weight when dry. **Pilei** effused-reflexed to pileate, dimidiate, triquetrous in section, projecting up to 4 cm, 6.5 cm wide and 3 cm thick at the base; Pileal surface narrowly zonate, glabrous, meagrely warted near attachment, yellowish-brown (5E6; 5E8) to dark

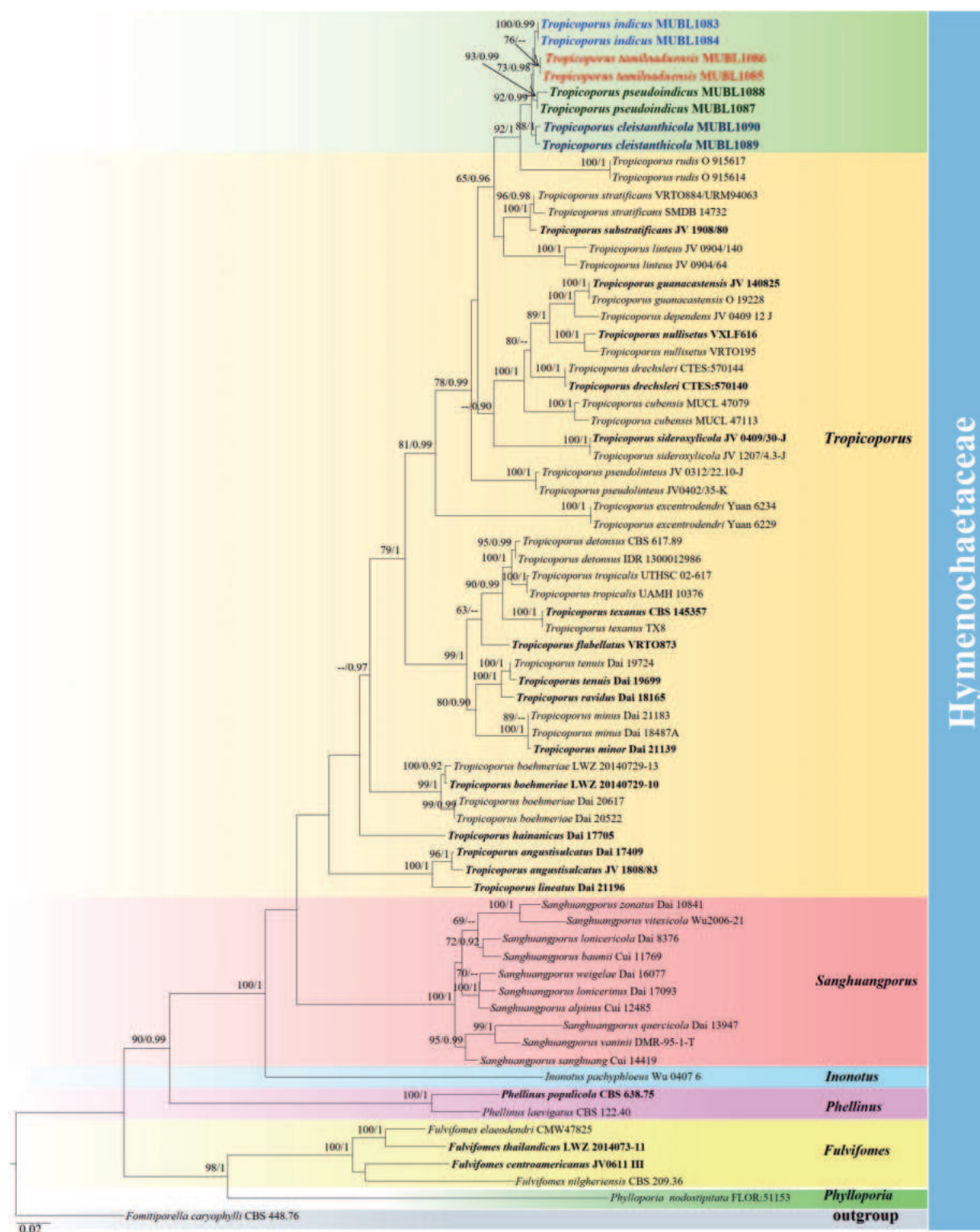


**Figure 2.** Molecular phylogeny of four new Indian *Tropicoporus* species and other hymenochaetoid species inferred from combined ITS and nLSU sequences. The topology is from the Bayesian analysis. Maximum Likelihood bootstrap values and Bayesian posterior probabilities, above 60% and 0.9, respectively, are labelled at the nodes. The newly-generated sequences are coloured and bold; the type specimens are in bold.

brown (6F5), turning dark brown (7F4) to greyish-brown (6F3). **Margin** acute, 1 mm thick, light brown (6D5). **Pore surface** brown (6E6) to dark brown (6F7); sterile margin up to 2 mm wide, light brown (6D5); pores circular, 5–7 per mm.

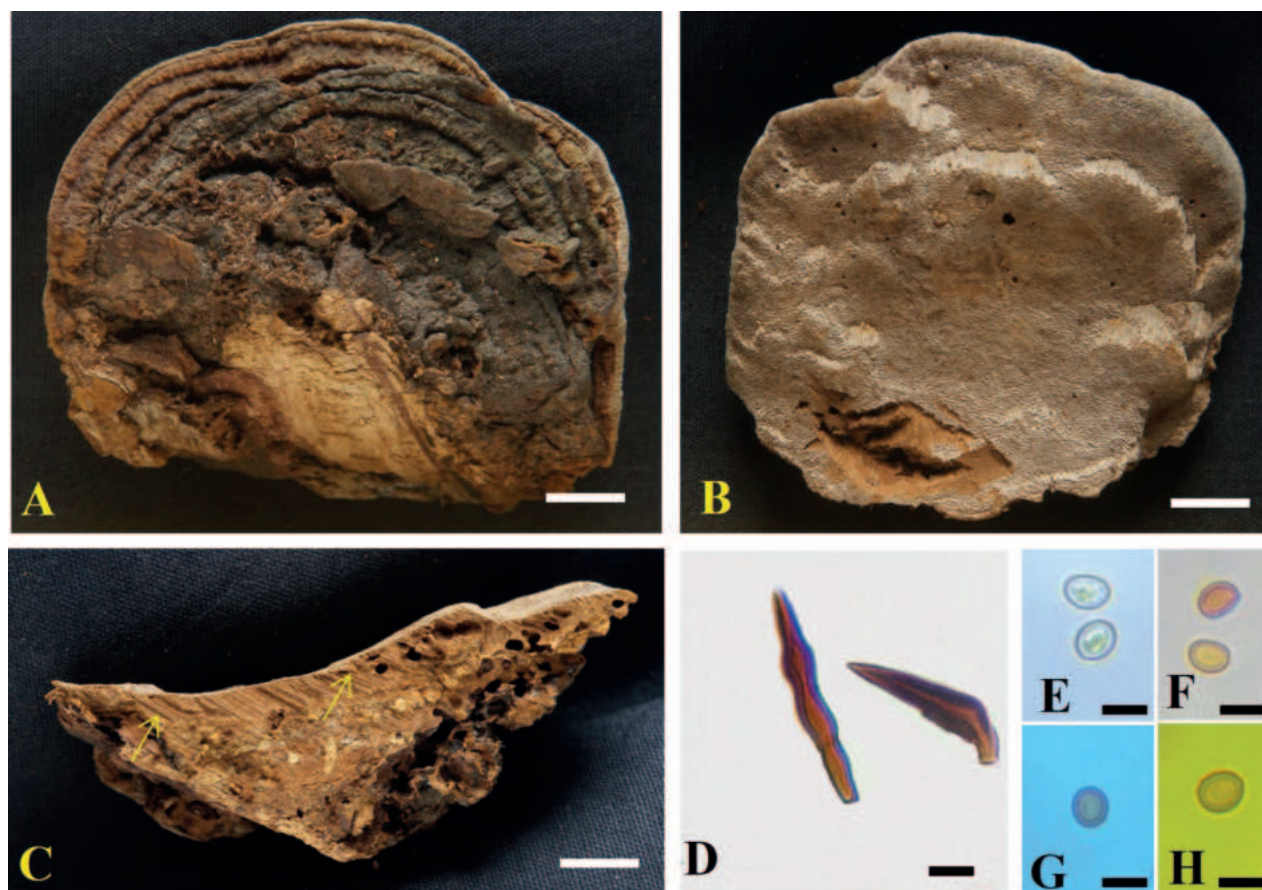


**Figure 3.** *Tropicoporus cleistanthicola* (MUBL1089 holotype) **A** basidiomata (Holotype) **B** pore surface **C** cross-section of basidiome (arrows indicating stratified tube layers) **D** hymenial setae **E–H** basidiospores: **E** basidiospores in water **F** basidiospores in KOH **G** basidiospore in cotton blue **H** basidiospore in Melzer's reagent. Scale bars: 1 cm (**A–C**); 5 µm (**D–H**).

**Context** homogenous, up to 1.5 cm thick, brown (6E8). **Tubes** up to 0.5 cm long, tube layers distinctly stratified, each stratum up to 2 mm, brown (6E7).

**Hyphal structures.** Hyphal system monomitic in the context and dimitic in the trama, tissue darkening with KOH without hyphal swelling.

**Context.** Generative hyphae, thin to thick-walled, hyaline to golden yellow, simple septate, rarely branched, 2–5 µm diam.

**Trama.** Generative hyphae, dominant, thin to thick-walled, hyaline to pale yellow, septate, occasionally branched, 2–4 µm diam. Skeletal hyphae thick-walled with narrow to wide lumen, yellowish-brown, aseptate, unbranched, 2–3.5 µm diam.

**Hymenium.** Hymenial setae dark brown, thick-walled, ventricose to subulate with sharp to blunt tips, 5–32 × 4–5.5 µm. Cystidia absent. Cystidioles hyaline, thin-walled, ventricose to fusoid with elongated tapering apical portion, 7–45 × 2–5 µm. Basidia clavate to broadly clavate, 7–15 × 2.7–6.2 µm, with four sterigmata and a simple septum at the base. Basidioles clavate, 5–13 × 3.5–6 µm. Basidiospores broadly ellipsoid to subglobose, pale yellow in water, turning golden yellow to brown in KOH, thick-walled, smooth, CB<sup>-</sup>, IKI<sup>-</sup>, (4.7–) 4.9–5.2 (–5.4) × (4.2–) 4.5–4.7 (–4.9) µm (n = 50/2), Q = 1.1 (Q range 1.05–1.2).

**Habitat and distribution.** Basidiomes were found on living trees of *Cleistanthus collinus* (Phyllanthaceae), distributed in Jawadhu Hills, Thiruvannamalai District, Tamil Nadu, India.

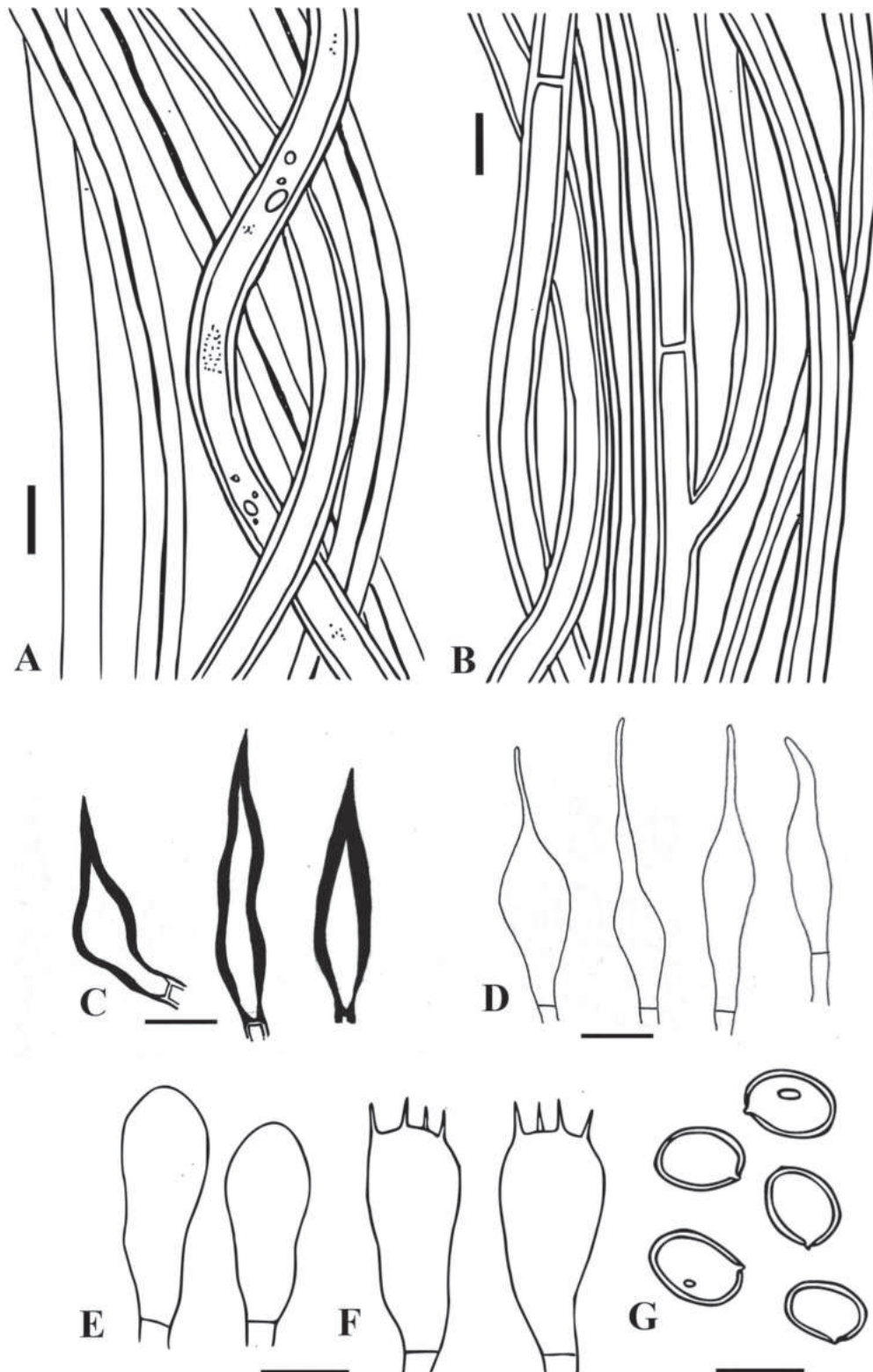


**Figure 4.** *Tropicoporus cleistanthicola* (MUBL1089 holotype) **A** contextual hyphae **B** tramal hyphae **C** hymenial setae **D** cystidioles **E** basidioles **F** basidia **G** basidiospores. Scale bars: 5  $\mu$ m.

**Additional material examined.** INDIA, Tamil Nadu, Thiruvannamalai District, Jawadhu Hills; 12°51'20"N, 78°73'71"E; 15 Nov 2019; Sugantha Gunaseelan; on a living angiosperm tree (*Cleistanthus collinus*); SMK-PMP14 (MUBL1090, Paratype); GenBank: OR272291 (ITS); OR272336 (nLSU).

**Notes.** The present phylogenetic study indicated that *T. cleistanthicola* is sister to *T. rudis* with significant support (92% ML/0.9 BPP). However, *T. rudis* has appanate basidiomes with fulvous, velvety, concentrically zonate, matted, rimose pilear surface, whereas *T. cleistanthicola* has triquetrous basidiome and glabrous pilear surface with infrequent warts without cracks. *Tropicoporus cleistanthicola* and *T. rudis* are comparable only in mono-dimitic hyphal system and *T. rudis* lacks cystidioles and has larger basidiospores ( $4.9\text{--}6 \times 4\text{--}4.8 \mu\text{m}$ ) (Wu et al. 2022). Despite sharing pileate basidiomes, mono-dimitic hyphal system and presence of cystidioles in *T. linteus*, *T. cleistanthicola* differs by having effused-reflexed to pileate, narrowly zonate, meagrely warted pilear surface (Tian et al. 2013; Wu et al. 2022). *Tropicoporus cleistanthicola* resembles *T. angustisulcatus*, *T. dependens*, *T. excentrodendri*, *T. substratificans* and *T. lineatus* by sharing pileate, triquetrous basidiomes with concentrically zonation and presence of cystidioles, but *T. cleistanthicola* differs by having a mono-dimitic hyphal system and spore size ( $4.7\text{--}5.4 \times 4.2\text{--}4.9 \mu\text{m}$ ) (Zhou et al. 2015; Wu et al. 2022). *Tropicoporus cleistanthicola* and *T. drechleri* are similar in having pileate basidiomes and a mono-dimitic hyphal system with the presence of cystidioles, but *T. cleistanthicola* differs by having smaller pores (5–7 pores/mm) and larger basidiospores (Salvador-Montoya et al. 2018). Except for sharing a mono-dimitic hyphal system and indistinctly stratified tube layers, *T. cleistanthicola* differs from *T. flabellatus* and *T. guanacastensis* in pores (size and shape), basidiospore shape and absence of cystidioles (Zhou et al. 2015; Lima et al. 2022).

***Tropicoporus indicus* S. Gunaseelan & M. Kaliyaperumal, sp. nov.**

MycoBank No: 849482

Figs 5, 6

**Etymology.** The species epithet "*indicus*" (Lat.): referring to the species being collected from India.

**Diagnosis.** *Tropicoporus indicus* is characterised by appanate to meagrely triquetrous basidiome with concentrically zonate, sulcate, glabrous, deeply cracked to rimose pilear surface, homogenous context, acute margin, mono-dimitic hyphal system, presence of cystidioles, subglobose to broadly ellipsoid basidiospores measuring  $5\text{--}6 \times 4.2\text{--}4.9 \mu\text{m}$ .

**Type.** INDIA, Tamil Nadu, Kallakurichi District, Kalvarayan Hills;  $11^{\circ}91'30''\text{N}$ ,  $78^{\circ}57'86''\text{E}$ ; 29 Sep 2022; Sugantha Gunaseelan; on living angiosperm tree of *Albizia amara*; SMK- MK2 (MUBL1083, Holotype); GenBank: OR272293 (ITS); OR272338 (nLSU).

**Description.** **Basidiome** perennial, pileate, woody and without distinctive odour or taste when fresh, hard when dry. **Pilei** appanate to meagrely triquetrous, projecting up to 5.5 cm, 7 cm wide and 4 cm thick at the base; pileal surface concentrically zonate, sulcate, glabrous, deeply cracked to rimose near attachment, dark brown (7E4), greyish-brown (7F3). **Margin** velutinate, 2 mm thick, acute, brown (6E7). **Pore surface** light brown (5D5) to yellowish-brown (5E7); pores circular, 4–6 per mm. **Context** homogenous, up to 0.8 cm thick, brown (6E8) to dark brown (6F8). **Tubes** woody hard, up to 2.5 cm long, brown (6E7); tube layers stratified, each stratum up to 0.5 cm long.



Figure 5. *Tropicoporus indicus* (MUBL1083 holotype) **A** basidiomata (Holotype) **B** basidiome (SMK-MK2a- Isotype) **C** pore surface **D** cross-section of basidiome (arrows indicating stratified tube layers) **E** hymenial setae **F** cystidioles **G–J** basidiospores: **G** basidiospores in water **H** basidiospores in KOH **I** basidiospores in cotton blue **J** basidiospores in Melzer's reagent. Scale bars: 1 cm (**A–D**); 5  $\mu$ m (**E–J**).

**Hyphal structures.** Hyphal system monomitic in the context and dimitic in the trama, tissue darkening with KOH without swelling

**Context.** Generative hyphae, thin to thick-walled, hyaline to golden yellow, simple septate, rarely branched, 2–5  $\mu$ m diam.

**Trama.** Generative hyphae dominant, thin to thick-walled, hyaline to pale yellow, septate, occasionally branched, 2–4.5  $\mu$ m diam. Skeletal hyphae thick-walled with narrow to wide lumen, yellowish-brown, aseptate, unbranched, 2–4  $\mu$ m diam.

**Hymenium.** Hymenial setae dark brown, thick-walled, ventricose to subulate with sharp to blunt tips, 7–28  $\times$  3–5  $\mu$ m. Cystidia absent. Cystidioles hyaline, thin-walled, ventricose to fusoid with elongated tapering apical portion, 5–21  $\times$  3–5  $\mu$ m. Basidia clavate to broadly clavate, 7–17  $\times$  3–6  $\mu$ m, with four sterigmata and a simple septum at the base. Basidioles clavate, 5–14  $\times$  3–5  $\mu$ m. Basidiospores broadly ellipsoid to subglobose, pale yellow in water, turning golden

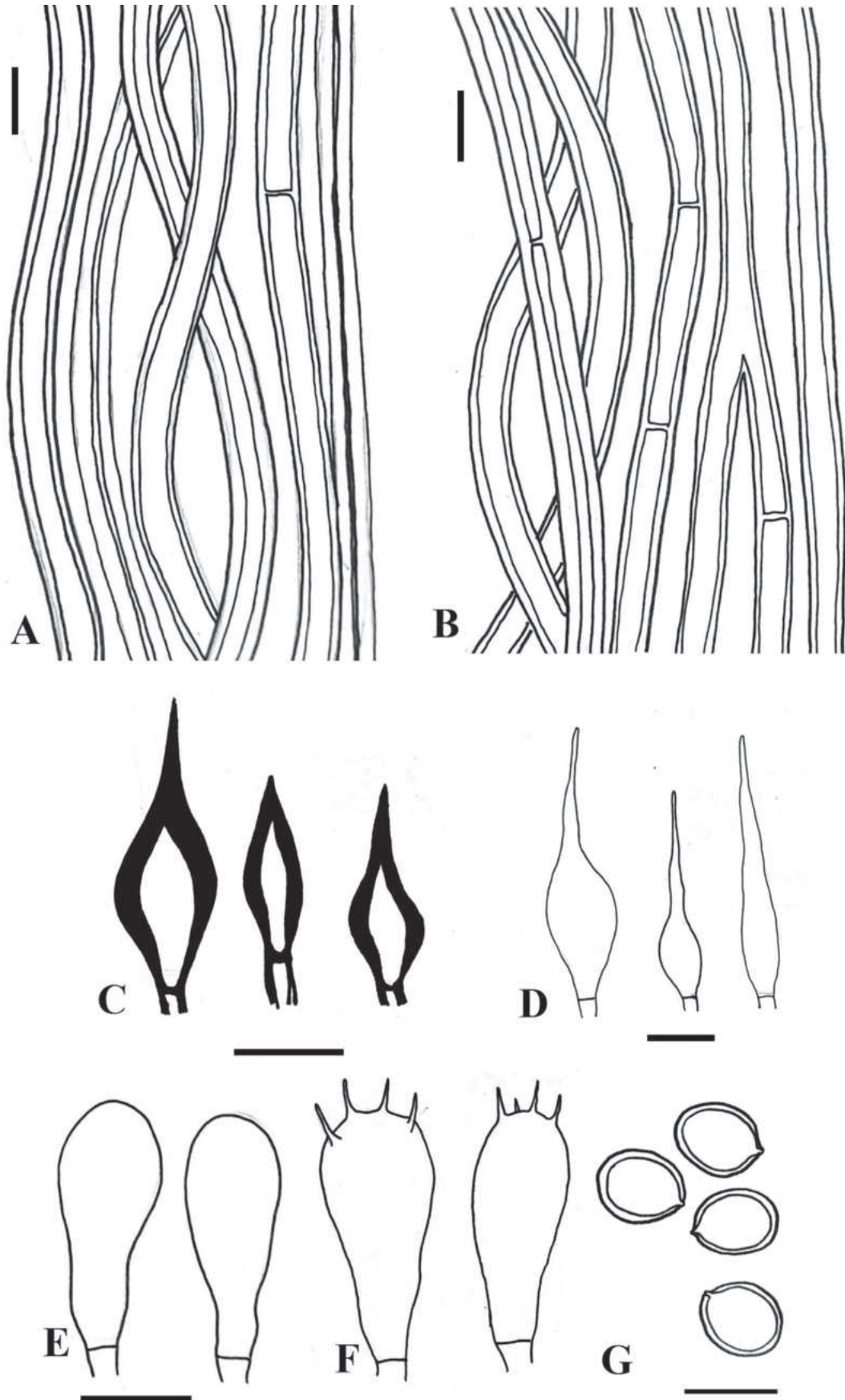


**Figure 6.** *Tropicoporus indicus* (MUBL1083 holotype) **A** contextual hyphae **B** tramal hyphae **C** hymenial setae **D** cystidioles **E** basidioles **F** basidia **G** basidiospores. Scale bars: 5  $\mu$ m.

yellow to brown in KOH, thick-walled, smooth, CB<sup>-</sup>; IKI<sup>-</sup>; (5–) 5.3–5.8 (– 6) × (4.2–) 4.7–4.9 μm (n = 50/2), Q = 1.16 (Q range 1.05–1.3).

**Habitat and distribution.** Basidiomes were found on living trees of Fabaceae members (*Albizia amara* and *Prosopis cineraria*), distributed in Kalvarayan Hills, Kallakurichi District, Tamil Nadu, India.

**Additional material examined.** INDIA, Tamil Nadu, Kallakurichi District, Kalvarayan Hills; 11°90'39"N, 78°55'69"E; on a living angiosperm tree (*Prosopis cineraria*); 29 Sep 2022; Kezhocuyi Kezo; SMK-MK2a (MUBL1084, Paratype); GenBank: OR272294 (ITS); OR272339 (nLSU).

**Notes.** Phylogenetically, *Tropicoporus indicus* was recovered in the *T. linteus* clade. *Tropicoporus indicus* is similar to *T. linteus* by sharing, pileate, dimidiate basidiomes, concentrically sulcate pilear surface, zonate context, smaller pores (5–7/mm), a mono-dimitic hyphal system and presence of cystidioles. While varying in the nature of cracks, *T. linteus* has more or less cracked basidiomes, *T. indicus* has irregular deep cracks in basidiomes, with larger basidiospores (*T. linteus* 4.8–5.7 × 3.8–4.8 μm and *T. indicus* 5–6 × 4.2–4.9 μm) (Tian et al. 2013; Wu et al. 2022). *Tropicoporus indicus* and *T. rudis* share a mono-dimitic hyphal system, but *T. indicus* differs from *T. rudis* in having zonate, sulcate, deeply cracked to rimose basidiomes and larger pores (4–6/mm). In these regards, *T. rudis* is characterised by fulvous, velvety, concentrically zonate, matted, rimose basidiome and smaller pores (6–7/mm) (Wu et al. 2022). *Tropicoporus indicus* differs from *T. angustisulcatus*, *T. excentrodendri*, *T. lineatus* and *T. substratificans* in having mono-dimitic hyphal system and a cracked basidiome (Zhou et al. 2015; Wu et al. 2022). *Tropicoporus indicus* and *T. flabellatus* are similar in having a mono-dimitic hyphal system, but differ significantly by having concentric zones, sulcate, glabrous, deeply-cracked to rimose pilear surface with larger pores (4–6/mm) and broadly ellipsoid to subglobose spores (5–6 × 4.2–4.9 μm). *Tropicoporus flabellatus*, in contrast, has a velutinate pilear surface, uncracked basidiomes with smaller pores (7–9/mm) and smaller basidiospores (4.5–5 × 3.5–4 μm) (Lima et al. 2022). *Tropicoporus indicus* and *T. guanacastensis* are similar in having sulcate, cracked basidiome, stratified tube, mono-dimitic hyphal system and ventricose setae. However, the former differs in larger pores (4–6/mm) and larger basidiospores (*T. indicus* 5–6 × 4.2–4.9 μm vs. *T. guanacastensis* 4.1–5 × 3.1–4 μm) (Zhou et al. 2015). *Tropicoporus indicus* and *T. drechsleri* share concentrically sulcate deeply-cracked pilei with mono-dimitic hyphal system, larger pores (< 6/mm) and presence of cystidioles, but the South American species differs in basidiospore size (4–5.5 × 3–4.5 μm) (Salvador-Montoya et al. 2018).

***Tropicoporus pseudoindicus* S. Gunaseelan & M. Kaliyaperumal, sp. nov.**

MycoBank No: 849483

Figs 7, 8

**Etymology.** The species *pseudoindicus* signifies the close morphological and phylogenetic relationships with the species *Tropicoporus indicus*.

**Diagnosis.** *Tropicoporus pseudoindicus* is characterised by applanate to meagrely unguulate to triquetrous basidiome with broadly zonate, distinctly cracked by radial fissures, sulcate pilear surface, duplex context with black line,

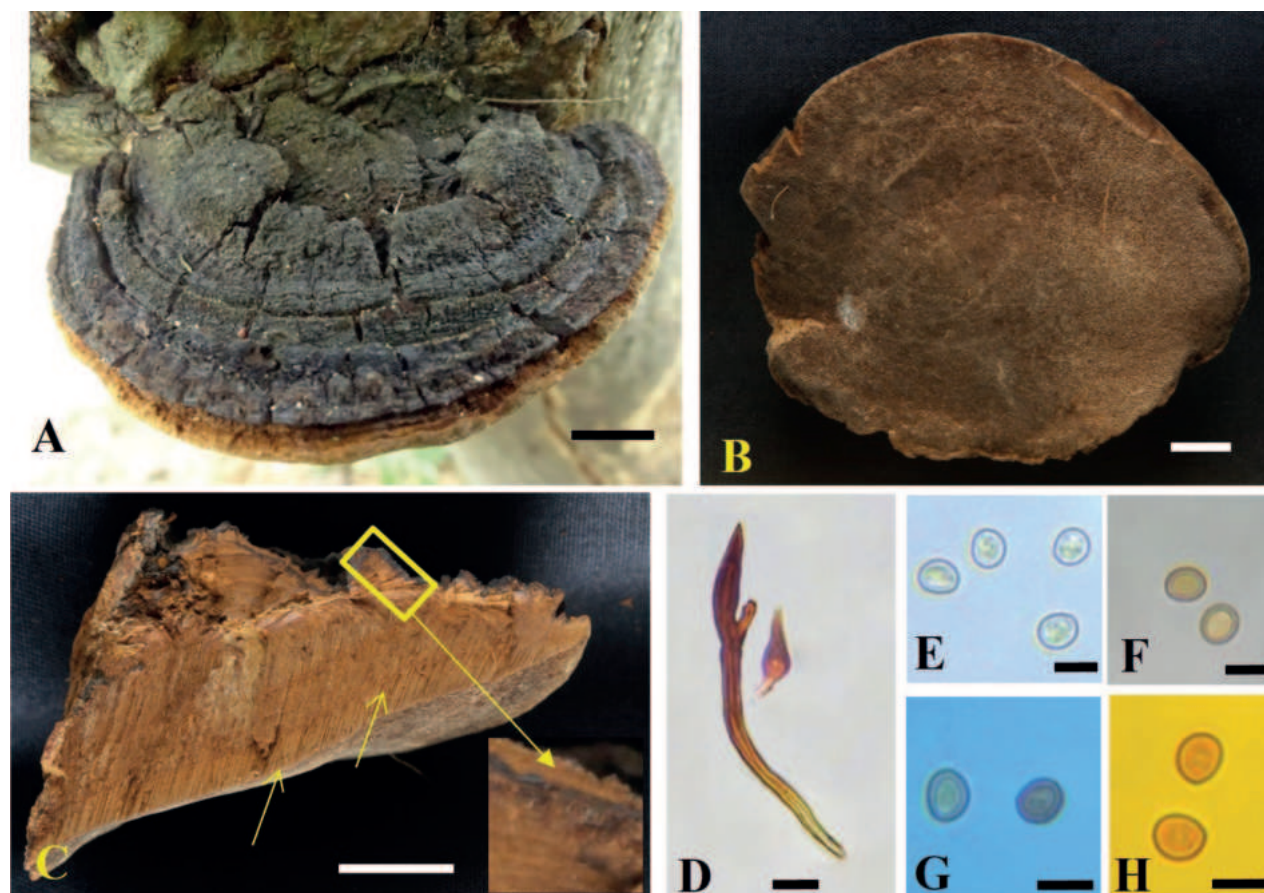


**Figure 7.** *Tropicoporus pseudoindicus* (MUBL1085 holotype) **A** basidiomata (Holotype) **B** pore surface **C** cross-section of basidiome (arrows indicating stratified tube layers and duplex context with black line) **D** hymental setae **E–H** basidiospores: **E** basidiospores in water **F** basidiospores in KOH **G** basidiospores in cotton blue **H** basidiospores in Melzer's reagent. Scale bars: 1 cm (**A–C**); 5 µm (**D–H**).

acute to obtuse margin, pores 6–8/mm, mono-dimitic hyphal system, presence of cystidioles, subglobose to broadly ellipsoid basidiospores measuring 4–5.2 × 3.7–4.7 µm.

**Type.** INDIA, Tamil Nadu, Kallakurichi District, Kalvarayan Hills; 11°86'98"N, 78°55'68"E; 29 Sep. 2022; Sugantha Gunaseelan; on a living angiosperm tree (*Albizia amara*); SMK-MK4 (MUBL1087, Holotype); GenBank: OR272295 (ITS); OR272340 (nLSU).

**Description.** **Basidiome** perennial, pileate, woody and without distinctive odour or taste when fresh, hard and light in weight when dry. **Pilei** applanate, meagrely unguulate to triquetrous, dimidiate, projecting up to 5 cm, 8 cm wide and 3.5 cm thick at base; pileal surface broadly zonate, distinctly cracked by radial fissures, sulcate, brown (6E8), dark brown (7F4) to greyish-brown (6F3).

**Margin** acute to obtuse, up to 3 mm thick, light brown (6D5). **Pore surface** brown (6E6) to dark brown (7E6); sterile margin brown (6E6), up to 2 mm wide; pores circular, 6–8 per mm. **Context** duplex with black line, woody hard, up to 1.2 cm thick, several black lines present along context, brown (6E7) to dark brown (7F6). **Tubes** up to 1.5 cm long, annual layers distinct, each stratum up to 0.3 cm, brown (7E8) to dark brown (6F8).

**Hyphal structures.** Hyphal system monomitic in the context and dimitic in the trama, tissue darkening with KOH without swelling.

**Context.** Generative hyphae, thin to thick-walled, hyaline to golden yellow, simple septate, rarely branched, 2–5 µm diam.

**Trama.** Generative hyphae, dominant, thin to thick-walled, hyaline to pale yellow, septate, occasionally branched, 2–4 µm diam. Skeletal hyphae, thick-walled with narrow to wide lumen, yellowish-brown, aseptate, unbranched, 2–3.5 µm diam.

**Hymenium.** Hymenial setae dark brown, thick-walled, ventricose to subulate with sharp to blunt tips, rarely with lateral appendage, 5–18 × 3–5.5 µm. Cystidia absent. Cystidioles hyaline, thin-walled, ventricose to fusoid with elongated tapering apical portion, 7–52 × 2.5–5.2 µm. Basidia clavate to broadly clavate, 7–15 × 2.7–6.2 µm, with four sterigmata and a simple septum at the base. Basidioles clavate, 5–13 × 3.5–6 µm. Basidiospores broadly ellipsoid to subglobose, pale yellow in water, turning golden yellow to brown in KOH, thick-walled, smooth, CB<sup>-</sup>, IKI<sup>-</sup>, (4–) 4.2–5 (–5.2) × (3.7–) 4–4.5 (–4.7) µm (n = 50/2) and Q = 1.14 (Q range 1.05–1.25).

**Habitat and distribution.** Basidiomes were found on living trees of Fabaceae members (*Albizia amara* and *Peltophorum pterocarpum*), distributed in Kalvarayan Hills, Kallakurichi District, Tamil Nadu, India.

**Additional material examined.** INDIA, Tamil Nadu, Kallakurichi District, Kalvarayan Hills; 11°87'33"N, 78°42'78"E; 29 Sep 2022; Kezhocuyi Kezo; on a living angiosperm tree (*Peltophorum pterocarpum*); SMK-MK4a (MUBL1088, Paratype); GenBank: OR272296 (ITS); OR272341 (nLSU).

**Notes.** *Tropicoporus pseudoindicus* and *T. drechsleri*, share similar characteristics, such as applanate basidiomes with mono-dimitic hyphal system and the presence of cystidioles; however, *T. pseudoindicus* differs in having smaller pores (6–8/mm) and larger basidiospores (*T. pseudoindicus* 4–5.2 × 3.7–4.7 µm vs. *T. drechsleri* 4–5.5 × 3–4.5 µm) (Salvador-Montoya et al. 2018). *Tropicoporus pseudoindicus* resembles *T. rudis* in having a mono-dimitic hyphal system, presence of cystidioles, and basidiospore shape, but differs from *T. rudis* in having distinctly cracked, fissured to sulcate pilei, duplex context and smaller basidiospores (4–5.2 × 3.7–4.7 µm) (Vlasák et al. 2013). *Tropicoporus pseudoindicus* differs from *T. guanacastensis* in having cystidioles and subglobose to broadly ellipsoidal spores (*T. pseudoindicus* 4–5.2 × 3.7–4.7 µm vs. *T. guanacastensis* 4.1–5.0 × 3.1–4.0 µm) (Tian et al. 2013). *Tropicoporus pseudoindicus* and *T. linteus* share similar pileate basidiomes with sulcate pilear surface, smaller pores (5–7/mm), mono-dimitic hyphal system and presence of cystidioles. However, the former differs in basidiospore size (*T. linteus* 4.8–5.7 × 3.8–4.8 µm vs. *T. pseudoindicus* 4–5.2 × 3.7–4.7 µm) (Tian et al. 2013; Wu et al. 2022). *Tropicoporus pseudoindicus* and *T. flabellatus* are similar in their mono-dimitic hyphal system, but differ significantly in pilear characteristics, absence of cystidioles and size and shape of basidiospores (*T. flabellatus* 4.5–5 × 3.5–4 µm vs. *T. pseudoindicus* (4–) 4.2–5 (–5.2) × (3.7–) 4–4.5 (–4.7) µm) (Lima et al. 2022). *Tropicoporus pseudoindicus* differs from some other reported *Tropicoporus* species (namely *T. angustisulcatus*, *T. excentrodendri*, *T. lineatus* and *T. substratificans*) in having concentrically zonate, glabrous, distinctly cracked pileal surface and a mono-dimitic hyphal system (Zhou et al. 2015; Wu et al. 2022).

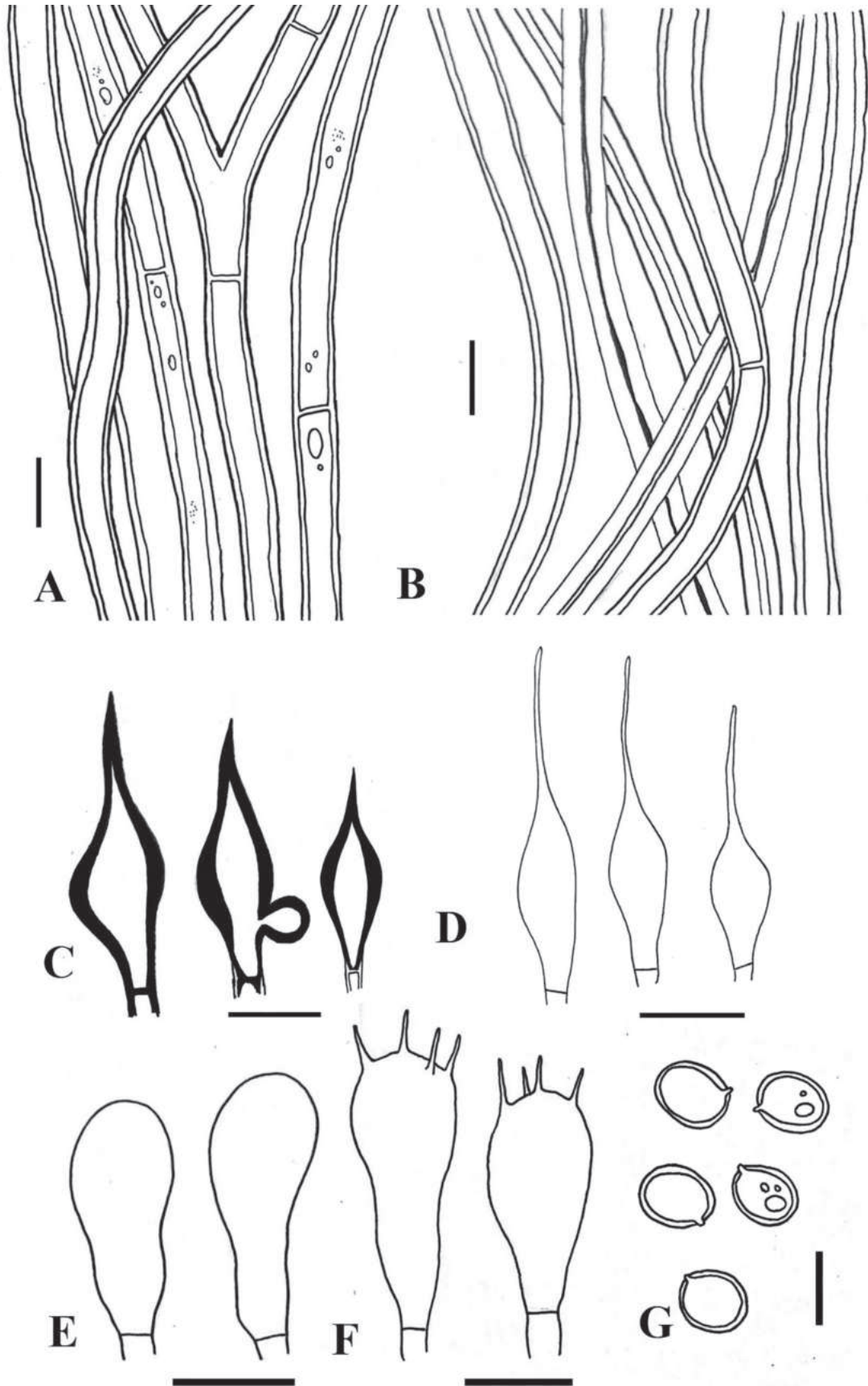


**Figure 8.** *Tropicoporus pseudoindicus* (MUBL1085 holotype) **A** contextual hyphae **B** tramal hyphae **C** hymenial setae **D** cystidioles **E** basidioles **F** basidia **G** basidiospores. Scale bars: 5 µm.

***Tropicoporus tamilnaduensis* M. Kaliyaperumal & S. Gunaseelan, sp. nov.**

MycoBank No: 849481

Figs 9, 10

**Etymology.** The species epithet *tamilnaduensis* refers to the locality of the type specimen (Tamil Nadu).

**Diagnosis.** *Tropicoporus tamilnaduensis* is characterised by applanate to meagrely unguulate basidiome with glabrous, broadly zonate, sulcate and deeply irregularly cracked pilear surface, homogenous context, obtuse margin, pores 4–5/mm, mono-dimitic hyphal system, presence of cystidioles, subglobose to broadly ellipsoid basidiospores measuring 4.5–5.7 × 3.5–4.7 µm.

**Type.** INDIA, Tamil Nadu, Cuddalore District, Thaiyalkunampattinam, Kanni Tamil Nadu; 11°59'18"N, 79°60'17"E; 31 Dec 2022; Malarvizhi Kaliyaperumal; on a living angiosperm tree (*Madhuca longifolia*); MKDM02 (MUBL1085, holotype); GenBank: OR272297 (ITS); OR272343 (nLSU).

**Description.** **Basidiome** perennial, pileate, without distinctive odour or taste when fresh, woody hard and light in weight when dry. **Pilei** applanate to meagrely unguulate, projecting up to 5 cm, 8 cm wide and 4 cm thick at base; pileal surface glabrous, broadly zonate, sulcate, deeply irregularly cracked near attachment, brown (6E7), yellowish-brown (5F4) to golden brown (7F7) turning greyish-brown (5F3). **Margin** obtuse, 4 mm thick, light brown (6D5). **Pore surface** brown (6E6), sterile margin yellowish-brown (5E6), up to 2 mm wide; pores circular, 4–5 per mm; dissepiments thick, entire. **Context** homogenous, zonate, brown (6D7) to dark brown (6F8), woody hard, up to 2 cm thick. **Tubes** brown (6E6), up to 2 cm long, annual layers distinct, each stratum up to 0.3 cm long.

**Hyphal structures.** Hyphal system monomitric in the context and dimitic in the trama, tissue darkening with KOH without hyphal swelling.

**Context.** Generative hyphae, thin to thick-walled, hyaline to golden yellow, simple septate, rarely branched, 2–5 µm diam.

**Trama.** Generative hyphae, dominant, thin to thick-walled, hyaline to pale yellow, septate, occasionally branched, 2–4 µm diam. Skeletal hyphae, thick-walled with narrow to wide lumen, yellowish-brown, aseptate, unbranched, 2–3.5 µm diam.

**Hymenium.** Hymenial setae dark brown, thick-walled, ventricose to subulate with sharp to blunt tips, 6–19 × 3.8–5 µm. Cystidia absent. Cystidioles hyaline, thin walled, ventricose to fusoid with elongated tapering apical portion, 10–45 × 2–5 µm. Basidia clavate to broadly clavate, 7–15 × 2.7–6.2 µm, with four sterigmata and a simple septum at the base. Basidioles clavate, 5–13 × 3.5–6 µm. Basidiospores broadly ellipsoid to subglobose, pale yellow in water, turning golden yellow to brown in KOH, thick-walled, smooth, CB<sup>+</sup>, IKI<sup>-</sup>, (4.5–) 4.7–5.5 (–5.7) × (3.5–) 3.7–4.5 (–4.7) µm (n = 50/2), Q = 1.13 (Q range 1.05–1.25).

**Habitat and distribution.** Basidiomes are found on living trees of *Madhuca longifolia* and *Prosopis cineraria*, distributed in Cuddalore District, Tamil Nadu, India.

**Additional material examined.** INDIA, Tamil Nadu, Cuddalore District, Thaiyalkunampattinam, Kanni Tamil Nadu; 11°50'14"N, 79°54'14"E; 31 Dec 2022; Malarvizhi Kaliyaperumal; on a living angiosperm tree (*Prosopis cineraria*); MKDM02a (MUBL1086, Paratype); GenBank: OR272344 (nLSU).

**Notes.** *Tropicoporus tamilnaduensis* and *T. linteus* are similar in having pileate sulcate basidiomes, zonate context and a mono-dimitic hyphal system

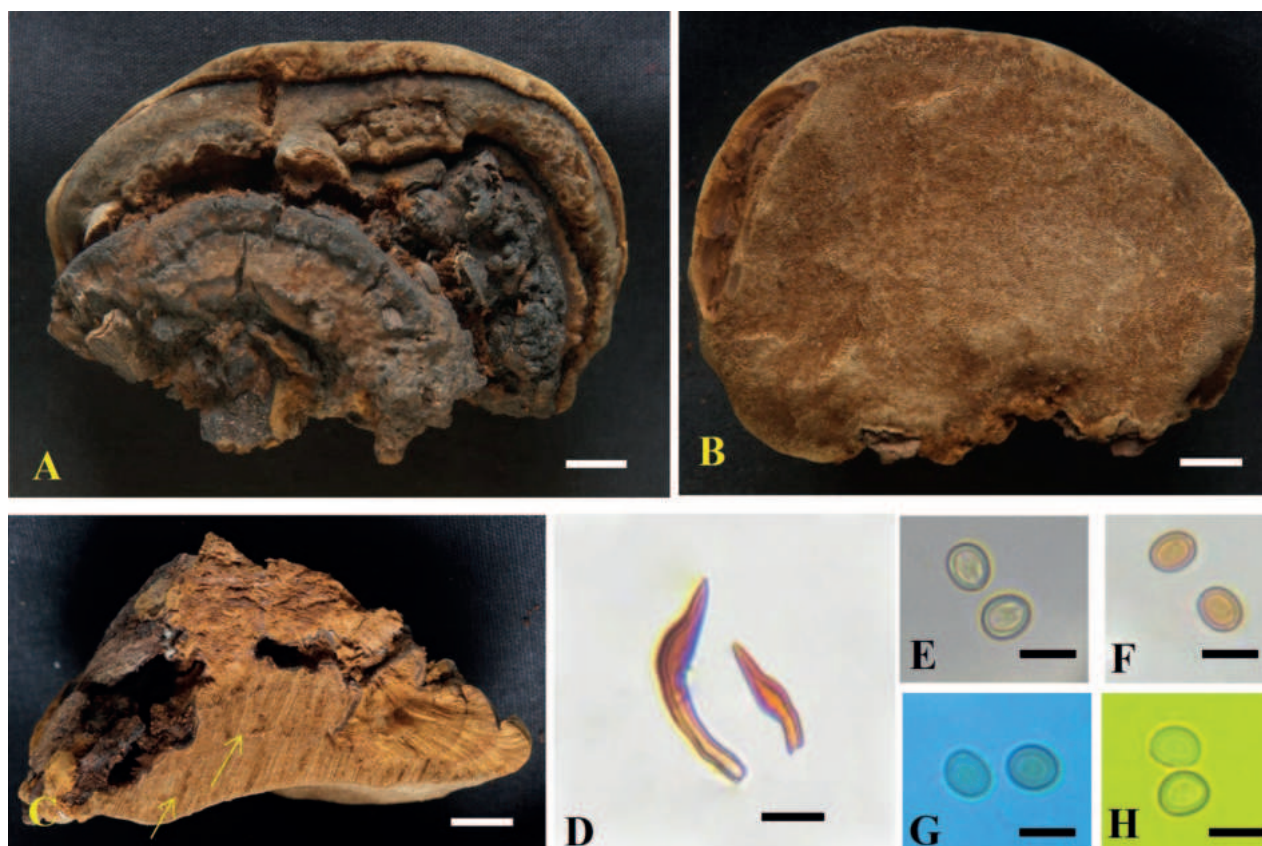


**Figure 9.** *Tropicoporus tamilnaduensis* (MUBL1085 holotype) **A** basidiomata (Holotype) **B** pore surface **C** cross-section of basidiome (arrows indicating stratified tube layers) **D** hymental setae **E–H** basidiospores: **E** basidiospore in water **F** basidiospores in KOH **G** basidiospores in cotton blue **H** basidiospores in Melzer's reagent. Scale bars: 1 cm (**A–C**); 5  $\mu$ m (**D–H**).

with cystidioles. However, *T. tamilnaduensis* differs from *T. linteus* in deeply-cracked basidiomes and smaller basidiospores (Tian et al. 2013; Wu et al. 2022). *Tropicoporus tamilnaduensis* and *T. rudis* share a homogenous context, a mono-dimitic hyphal system and subglobose to broadly ellipsoid basidiospores, but *T. tamilnaduensis* differs in having zonate, sulcate, deeply irregularly-cracked basidiome and larger pores (4–5/mm) (Wu et al. 2022). *Tropicoporus tamilnaduensis* differs from *T. angustisulcatus*, *T. lineatus* and *T. substratificans* in having sulcate and deeply cracked basidiomes and a mono-dimitic hyphal system, while *T. angustisulcatus*, *T. lineatus* and *T. substratificans* have basidiomes with velutinate to glabrous, uncracked pilear surface and a dimitic hyphal system (Zhou et al. 2015; Wu et al. 2022). *Tropicoporus tamilnaduensis* resembles *T. excentrodendri*, *T. dependens* and *T. sideroxylicola* by sharing concentrically zonate, sulcate, cracked to rimose pilear surface; however, the former differs by having a mono-dimitic hyphal system (Zhou et al. 2015; Salvador-Montoya et al. 2018). *Tropicoporus tamilnaduensis* and *T. guanacastensis* are similar in having a mono-dimitic hyphal system; however, *T. tamilnaduensis* has unguulate, sulcate, deeply irregularly cracked basidiomes with larger pores (4–7/mm) and broadly ellipsoid to subglobose spores (4.5–5.7  $\times$  3.5–4.7  $\mu$ m) (Zhou et al. 2015). Although sharing a mono-dimitic hyphal system, *T. tamilnaduensis* differs from *T. flabellatus* by having sulcate, deeply irregularly cracked basidiomes, cystidioles and larger pores (4–7/mm) with homogenous context (Lima et al. 2022). *Tropicoporus tamilnaduensis*

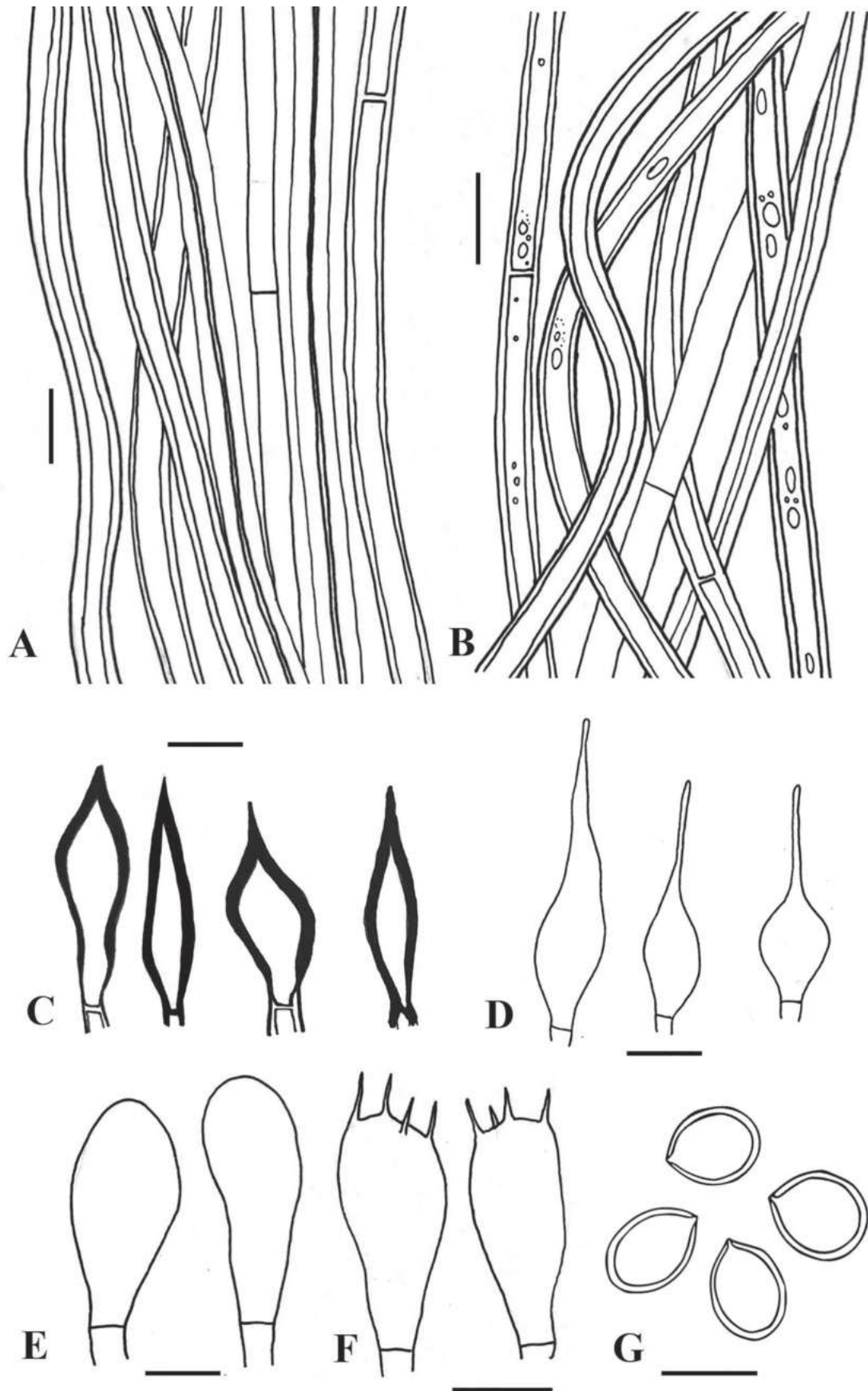


**Figure 10.** *Tropicoporus tamilnaduensis* (MUBL1085 holotype) **A** tramal hyphae **B** contextual hyphae **C** hymenial setae **D** cystidioles **E** basidioles **F** basidia **G** Basidiospores. Scale bars: 5  $\mu$ m.

varies from *T. drechsleri* by having sulcate, deeply irregularly cracked basidiomes and broadly ellipsoid to ellipsoid basidiospores ( $4.5\text{--}5.7 \times 3.5\text{--}4.7 \mu\text{m}$ ) (Salvador-Montoya et al. 2018).

## Discussion

Recently, the *Inonotus linteus* complex has gained attention because of its medicinal values and as an emerging potential pathogen in plants (Dai et al. 2009; Dai 2010), humans (Sutton et al. 2005; Haidar et al. 2017; Gupta et al. 2022) and dogs (Hevia et al. 2019). Zhou et al. (2015) segregated the *I. linteus* complex into two new genera viz. *Sanghuangporus* Sheng H. Wu, L.W. Zhou & Y.C. Dai and *Tropicoporus* L.W. Zhou, Y.C. Dai & Shen. H. Wu. Since then, many new species/combinations from tropical countries, especially from China followed by the Americas were introduced (Salvador-Montoya et al. 2018; Brown et al. 2019; Wu et al. 2022). *Tropicoporus* is characterised by its annual to perennial, resupinate, effused-reflexed to pileate basidiomes with mono-dimitic, dimitic hyphal system, ellipsoid to subglobose basidiospores. To date, twenty-three legitimate species are accepted under *Tropicoporus*, of which eleven were from tropical American countries, seven were from East Asian countries and one each from Africa, Costa Rica, Cuba and French Guiana.

The Bayesian phylogram illustrated in the present study is consistent with the previous studies (Coelho et al. 2016; Salvador-Montoya et al. 2018; Brown et al. 2019; Lima et al. 2022). The four new *Tropicoporus* species from Tamil Nadu, India, fit well within the *Tropicoporus* clade but formed a unique, distinct lineage that was the sister clade to *T. rudis* (earlier treated as *Xanthochrous rudis*). The *T. rudis* clade consists of strictly African collections (92% BS, 1.00 BPP) in the phylogeny (Fig. 1). This clade, in turn, forms the sister clade to a clade composed of *T. stratificans*, *T. substratificans* and *T. linteus* with 62% BS, 0.96 BPP.

The Eastern Ghats has discontinuous mountain ranges with hills ranging from 1,100 to 1,600 m with luxuriant vegetation of tropical evergreen to deciduous, thorn forest or scrub jungle that harbours diverse groups of wood rot fungi. This is the first report of the genus *Tropicoporus* from the Eastern Ghats of Tamil Nadu with three novel species, viz. *T. cleistanthicola*, *T. indicus* and *T. pseudoindicus*.

*Tropicoporus cleistanthicola*, *T. tamilnaduensis*, *T. indicus* and *T. pseudoindicus* are characterised by their perennial, pileate basidiomes with mono-dimitic hyphal system, presence of cystidioles and hymenial setae, smooth, thick-walled, coloured and inamyloid basidiospores (Table 2). However, there is significant variation in their basidiome characteristics, pore (shape and size) and basidiospore (shape and size). *Tropicoporus cleistanthicola* differs from the other three species in having effused-reflexed to pileate, sulcate, and narrowly zonate basidiome with infrequent warts. *Tropicoporus tamilnaduensis* differs in irregularly cracked basidiome with glabrous, sulcate and irregularly cracked, un-gulate basidiome and smaller basidiospores ( $4.5\text{--}5.4 \times 3.5\text{--}4.7 \mu\text{m}$ ), while *T. indicus* has regularly cracked and concentric zonate basidiome, glancing pore surface and larger basidiospores ( $5\text{--}6 \times 4.2\text{--}4.9 \mu\text{m}$ ). Morphologically, *T. pseudoindicus* is similar to *T. indicus* in sharing concentric zonate, glabrous and rimose with maturity, mono-dimitic hyphal system and presence of cystidioles,

**Table 2.** Synoptic comparison of characteristics amongst species of the newly-reported *Tropicoporus* from India.

Species	Basidiomata	Context	Margin	Pores /mm	Hyphal system	Setae (in $\mu\text{m}$ )	Cystidioles (in $\mu\text{m}$ )	Basidiospores (in $\mu\text{m}$ )	Q value (Q range)
<i>T. cleistanthicola</i>	Effused-reflexed to pileate, applanate to triquetrous basidiome with narrowly zonate, glabrous, meagrely warted pilear surface	Homogenous	Acute	5–7	Mono-Di	5–32 × 4–5.5	7–45 × 2–5	(4.7–) 4.9–5.2 (–5.4) × (4.2–) 4.5–4.7 (–4.9)	1.1 (1.05–1.2)
<i>T. indicus</i>	Applanate to meagrely triquetrous basidiome with concentrically zonate, sulcate, glabrous, deeply cracked to rimose pilear surface	Homogenous	Acute	4–6	Mono-Di	7–28 × 3–5	5–21 × 3–5	(5–) 5.3–5.8 (–6) × (4.2–) 4.7–4.9	1.16 (1.05–1.3)
<i>T. pseudoindicus</i>	Applanate, meagrely unguulate to triquetrous basidiome with broadly zonate, distinctly cracked by radial fissures, sulcate pilear surface	Duplex with blackline	Acute to obtuse	6–8	Mono-Di	5–18 × 3–5.5	7–52 × 2.5–5.2	(4–) 4.2–5 (–5.2) × (3.7–) 4–4.5 (–4.7)	1.14 (1.05–1.25)
<i>T. tamilnaduensis</i>	Applanate to meagrely unguulate basidiome with glabrous, broadly zonate, sulcate and deeply irregularly cracked pilear surface	Homogenous	Obtuse	4–5	Mono-Di	6–19 × 3.8–5	10–45 × 2–5	(4.5–) 4.7–5.4 (–5.7) × (3.5–) 3.7–4.5 (–4.7)	1.13 (1.05–1.25)

while *T. pseudoindicus* differs by having sulcate deeply cracked, radially fissured basidiome, homogenous context and smaller basidiospores. Our Indian *Tropicoporus* species (*Tropicoporus cleistanthicola*, *T. tamilnaduensis*, *T. indicus* and *T. pseudoindicus*) could be easily distinguished by its pileate basidiomes and mono-dimitic hyphal system from the other *Tropicoporus* resupinate species (*T. boehmeriae*, *T. hainanicus*, *T. minus*, *T. ravidus*, *T. stratificans*, *T. tenuis* and *T. texanus*) (Wu et al. 2015; Coelho et al. 2016; Brown et al. 2019; Wu et al. 2022).

### Key to species of *Tropicoporus* in the Afro-Asian region

- 1 Basidiocarps resupinate to effused-reflexed.....**2**
- Basidiocarps distinctly pileate.....**7**
- 2 Basidiocarps annual to biennial .....**3**
- Basidiocarps perennial .....**6**
- 3 Basidiospores cyanophilic.....***T. tenuis***
- Basidiospores acyanophilic.....**4**
- 4 Basidiocarp resupinate to effused reflexed, pileal surface tomentose to hispid basidiospores > 3  $\mu\text{m}$  in length .....***T. excentrodendri***
- Basidiocarp resupinate, basidiospores < 3  $\mu\text{m}$  in length.....**5**
- 5 Dissepiments lacerate, context layer present between tube layers.....***T. hainanicus***
- Dissepiments entire, context layer absent between tub layers.....***T. boehmeriae***
- 6 Basidiocarp resupinate, cystidioles present, pores 10–12/mm.....***T. minus***
- Basidiocarp cushion-shaped, cystidioles absent, pores 8–10/mm.....***T. ravidus***
- 7 Hyphal system strictly dimitic .....***T. lineatus***
- Hyphal system mono-dimitic, dimitic in trama.....**8**

- 8 Context homogenous..... 9  
– Context duplex with black line..... *T. pseudoindicus*  
9 Effused reflexed to pileate, uncracked basidiome ..... *T. cleistanthicola*  
– Applanate to unguulate or triquetrous, cracked pilear surface ..... 10  
10 Pores > 6/mm, cyanophilic basidiospores ..... *T. rudis*  
– Pores < 6/mm, acyanophilic basidiospores ..... 11  
11 Applanate to triquetrous basidiome with acute velutinate margin, regularly cracked pilear surface..... *T. indicus*  
– Applanate to meagrely unguulate basidiome with obtuse margin and deeply irregularly cracked pilear surface ..... *T. tamilnaduensis*

## Acknowledgements

Malarvizhi Kaliyaperumal and Sugantha Gunaseelan thank EMR-SERB, DST (EMR/2016/003078), Government of India for the financial assistance. MK and GS are grateful to 'The PCCF' of Tamil Nadu Forest Department for providing permission (E2/20458/2017), assistance and support during the field visits in Eastern Ghats of Tamil Nadu. MK, SG and KK thank Prof N. Mathivanan, The Director, Centre for Advanced Studies in Botany, University of Madras, Chennai, for providing the laboratory facilities. Samantha Chandranath Karunarathna thanks the National Natural Science Foundation of China (Numbers NSFC 32260004) and the High-Level Talent Recruitment Plan of Yunnan Provinces ("High-End Foreign Experts" programme) for their support. The authors extend their appreciation to the Researchers Supporting Project number (RSP2024R56), King Saud University, Riyadh, Saudi Arabia.

## Additional information

### Conflict of interest

The authors have declared that no competing interests exist.

### Ethical statement

No ethical statement was reported.

### Funding

EMR-SERB, DST (EMR/2016/003078), Government of India; National Natural Science Foundation of China (Numbers NSFC 32260004). High-Level Talent Recruitment Plan of Yunnan Provinces ("High-End Foreign Experts" programme) and Researchers Supporting Project number (RSP2024R56), King Saud University, Riyadh, Saudi Arabia.

### Author contributions

Conceptualisation: MK, SG, KK; Data Curation: MK, SG, KK, SK, EY, CZ, AME, ST; Formal analysis: MK, EY, SK, CZ, AME, ST; Funding acquisition: SG, MK, SK, EY, CZ, AME, ST; Investigation: MK, SG, KK; Methodology: MK, SG, KK; Project administration: MK; Resources: MK, SG, KK; Software: MK, SK, EY, ST; Supervision: MK, SK; Validation: MK, SG, KK, SK; Visualisation: MK; Writing – original draft: MK, SG, KK; Writing – review & editing: MK, SK, EY, CZ, AME, ST.

### Author ORCIDs

Sugantha Gunaseelan  <https://orcid.org/0000-0001-7089-2292>

Kezhocuyi Kezo  <https://orcid.org/0000-0002-3723-0462>

Samantha C. Karunarathna  <https://orcid.org/0000-0001-7080-0781>

Erfu Yang  <https://orcid.org/0000-0003-2385-6402>

Changlin Zhao  <https://orcid.org/0000-0002-1395-591X>

Abdallah M. Elgorban  <https://orcid.org/0000-0003-3664-7853>

Saowaluck Tibpromma  <https://orcid.org/0000-0002-4706-6547>

Malarvizhi Kaliyaperumal  <https://orcid.org/0000-0002-1218-3778>

## Data availability

All holotype and paratype collections of the new species are deposited at Madras University Botany Laboratory (MUBL), Centre for Advanced Studies in Botany, University of Madras, Chennai-600 025, Tamil Nadu, India. The sequences generated during this study are deposited in NCBI GenBank. The ITS and nLSU alignment is deposited in TreeBase.

## References

- Brown AA, Lawrence DP, Baumgartner K (2019) Role of basidiomycete fungi in the grapevine trunk disease esca. *Plant Pathology* 69(2): 205–220. <https://doi.org/10.1111/ppa.13116>
- Bruen TC, Philippe H, Bryant D (2006) A simple and robust statistical test for detecting the presence of recombination. *Genetics* 172(4): 2665–2681. <https://doi.org/10.1534/genetics.105.048975>
- Chen W, Tan H, Liu Q, Zheng X, Zhang H, Liu Y, Xu L (2019) A review: The bioactivities and pharmacological applications of *Phellinus linteus*. *Molecules* 24(10): e1888. <https://doi.org/10.3390/molecules24101888>
- Coelho G, Silveira ADO, Antonioli ZI, Yurchenko E (2016) *Tropicoporus stratificans* sp. nov. (Hymenochaetales, Basidiomycota) from southern Brazil. *Phytotaxa* 245(2): 144–152. <https://doi.org/10.11646/phytotaxa.245.2.5>
- Dai YC (2010) Hymenochaetales (Basidiomycota) in China. *Fungal Diversity* 45(1): 131–343. <https://doi.org/10.1007/s13225-010-0066-9>
- Dai YC, Yang ZL, Cui BK, Yu CJ, Zhou LW (2009) Species diversity and utilization of medicinal mushrooms and fungi in China. *International Journal of Medicinal Mushrooms* 11(3): 287–302. <https://doi.org/10.1615/IntJMedMushr.v11.i3.80> [Review]
- Darriba D, Taboada GL, Doallo R, Posada D (2012) jModelTest 2: More models, new heuristics and parallel computing. *Nature Methods* 9(8): e772. <https://doi.org/10.1038/nmeth.2109>
- Doyle JJ, Doyle JL (1987) A rapid isolation procedure for small quantities of fresh tissue. *Phytochemical Bulletin*. Botanical Society of America 19: 11–15.
- Edler D, Klein J, Antonelli A, Silvestro D (2020) raxmlGUI 2.0: A graphical interface and toolkit for phylogenetic analyses using RAxML. *Methods in Ecology and Evolution* 12(2): 373–377. <https://doi.org/10.1111/2041-210X.13512>
- Góes-Neto A, Loguercio-Leite C, Guerrero RT (2005) DNA extraction from frozen field-collected and dehydrated herbarium fungal basidiome: Performance of SDS and CTAB-based methods. *Biotemas* 18: 19–32. <https://periodicos.ufsc.br/index.php/biotemas/article/download/21410/19377/68437>
- Guindon S, Gascuel O (2003) A simple, fast and accurate algorithm to estimate large phylogenies by maximum likelihood. *Systematic Biology* 52(5): 696–704. <https://doi.org/10.1080/10635150390235520>
- Gupta P, Kaur H, Dwivedi S, Agnihotri S, Rudramurthy SM (2022) First case of *Tropicoporus tropicalis* keratitis in an immunocompetent host from India and review of the

- literature. *Journal de Mycologie Médicale* 32(1): e101205. <https://doi.org/10.1016/j.mycmed.2021.101205>
- Haidar G, Zerbe CS, Cheng M, Zelazny AM, Holland SM, Sheridan KR (2017) *Phellinus* species: An emerging cause of refractory fungal infections in patients with X-linked chronic granulomatous disease. *Mycoses* 60(3): 155–160. <https://doi.org/10.1111/myc.12573>
- Hevia A, Iachini R, Fernández J, Lazzari J, Suárez-Alvarez R, Abrantes R, Toranzo A, Refojo N, Canteros C (2019) Mycosis due to *Tropicoporus tropicalis* (= *Inonotus tropicalis*) in a domestic dog. *Mycopathologia* 184(5): 701–706. <https://doi.org/10.1007/s11046-019-00368-1>
- Huson DH, Bryant D (2006) Application of phylogenetic networks in evolutionary studies. *Molecular Biology and Evolution* 23(2): 254–267. <https://doi.org/10.1093/molbev/msj030>
- Kaur R, Kaur M, Singh AP, Ghuman NK, Dhingra GS (2022) Diversity of some colourful poroid and non-poroid Agaricomycetous fungi. In: Rajpal VR, Singh I, Navi SS (Eds) *Fungal Diversity, Ecology and Control Management Fungal Biology*. Springer, Singapore, 199–254. [https://doi.org/10.1007/978-981-16-8877-5\\_11](https://doi.org/10.1007/978-981-16-8877-5_11)
- Kornerup A, Wanscher JH (1978) *Methuen Handbook of Colour* (3<sup>rd</sup> edn.). Eyre Methuen, London.
- Kumar S, Stecher G, Li M, Knyaz C, Tamura K (2018) MEGA X: Molecular evolutionary genetics analysis across computing platforms. *Molecular Biology and Evolution* 35(6): 1547–1549. <https://doi.org/10.1093/molbev/msy096>
- Lima VX, de Oliveira VRT, de Lima-Júnior NC, Oliveira-Filho JRC, Santos C, Lima N, Gibertoni TB (2022) Taxonomy and phylogenetic analysis reveal one new genus and three new species in *Inonotus s.l.* (Hymenochaetales) from Brazil. *Cryptogamie. Mycologie* 43(1): 1–21. <https://doi.org/10.5252/cryptogamie-mycologie2022v43a1>
- Natarajan K, Kolandavelu K (1998) Resupinate Aphyllophorales of Tamil Nadu, India. *CAS in Botany, University of Madras*. <https://koeltz.com/en/resupinate-aphyllophorales-of-tamilnadu-india-1998-133-p>
- Ronquist F, Teslenko M, van der Mark P, Ayres DL, Darling A, Höhna S, Larget B, Liu L, Suchard MA, Huelsenbeck JP (2012) MrBayes 3.2: Efficient Bayesian phylogenetic inference and model choice across a large model space. *Systematic Biology* 61(3): 539–542. <https://doi.org/10.1093/sysbio/sys029>
- Salvador-Montoya CA, Costa-Rezende DH, Ferreira-Lopes V, Borba-Silva MA, Popoff OF (2018) *Tropicoporus drechsleri* (Hymenochaetales, Basidiomycota), a new species in the “*Inonotus linteus*” complex from Northern Argentina. *Phytotaxa* 338: 075–089. <https://doi.org/10.11646/phytotaxa.338.1.6>
- Sayers ER, Bolton EE, Brister JR, Canese K, Chan J, Comeau DC, Farrell CM, Feldgarden M, Fine AM, Funk K, Hatcher E, Kannan S, Kelly C, Kim S, Klimke W, Landrum MJ, Lathrop S, Lu Z, Madden TM, Malheiro A, Marchler-Bauer A, Murphy TD, Phan L, Pujar S, Rangwala SH, Schneider VA, Tse T, Wang J, Ye J, Trawick BW, Kim D, Pruitt KD, Sherry ST (2023) Database resources of the National Centre for Biotechnology Information in 2023. *Nucleic Acids Research* 51(D1): D29–D38. <https://doi.org/10.1093/nar/gkac1032>
- Sutton DA, Thompson EH, Rinaldi MG, Iwen PC, Nakasone KK, Jung HS, Rosenblatt HM, Paul ME (2005) Identification and first report of *Inonotus (Phellinus) tropicalis* as an etiologic agent in a patient with chronic granulomatous disease. *Journal of Clinical Microbiology* 43(2): 982–987. <https://doi.org/10.1128/JCM.43.2.982-987.2005>

- Tian XM, Yu HY, Zhou LW, Decock C, Vlasák J, Dai YC (2013) Phylogeny and taxonomy of the *Inonotus linteus* complex. *Fungal Diversity* 58(1): 159–169. <https://doi.org/10.1007/s13225-012-0202-9>
- Vilgalys R, Hester M (1990) Rapid genetic identification and mapping of enzymatically amplified ribosomal DNA from several *Cryptococcus* species. *Journal of Bacteriology* 172(8): 4238–4246. <https://doi.org/10.1128/jb.172.8.4238-4246.1990>
- Vlasák J, Li HJ, Zhou LW, Dai YC (2013) A further study on *Inonotus linteus* complex (Hymenochaetales, Basidiomycota) in tropical America. *Phytotaxa* 124(1): 25–36. <https://doi.org/10.11646/phytotaxa.124.1.3>
- White TJ, Bruns T, Lee S, Taylor J (1990) Amplification and direct sequencing of fungal ribosomal RNA genes for phylogenetics. In: Innis MA, Gelfand DH, Sninsky JJ, White TJ (Eds) *PCR Protocols: A Guide to Methods and Applications*. Academic Press, San Diego, 315–322. <https://doi.org/10.1016/B978-0-12-372180-8.50042-1>
- Wu F, Qin WM, Eutrakool O, Zhou LW (2015) *Tropicoporus boehmeriae* sp. nov. (Hymenochaetales, Basidiomycota) from Thailand, a new member of the *Inonotus linteus* complex. *Phytotaxa* 231(1): 73–80. <https://doi.org/10.11646/phytotaxa.231.1.7>
- Wu F, Zhou LW, Vlasák J, Dai YC (2022) Global diversity and systematics of Hymenochaetales with poroid hymenophore. *Fungal Diversity* 113(1): 1–192. <https://doi.org/10.1007/s13225-021-00496-4>
- Zhou LW, Vlasák J, Decock C, Assefa A, Stenlid J, Abate D, Wu SH, Dai YC (2015) Global diversity and taxonomy of the *Inonotus linteus* complex (Hymenochaetales, Basidiomycota): *Sanghuangporus* gen. nov., *Tropicoporus excentrodendri* and *T. guanacastensis* gen. et spp. nov., and 17 new combinations. *Fungal Diversity* 77(1): 335–347. <https://doi.org/10.1007/s13225-015-0335-8>

## Supplementary material 1

### Pairwise distance matrix, based on nucleotide sequences of four new *Tropicoporus* spp. and its related species

Authors: Sugantha Gunaseelan, Kezhocuyi Kezo, Samantha C. Karunarathna, Erfu Yang, Changlin Zhao, Abdallah M. Elgorban, Saowaluck Tibpromma, Malarvizhi Kaliyaperumal  
Data type: xls

Explanation note: Pairwise distance matrix, based on nucleotide sequences of four new *Tropicoporus* spp. and its related species (Pairwise distances calculations were accomplished using MEGA X v.10.0.2. Distances and standard errors are respectively displayed in the lower-left matrix and the upper-right matrix).

Copyright notice: This dataset is made available under the Open Database License (<http://opendatacommons.org/licenses/odbl/1.0/>). The Open Database License (ODbL) is a license agreement intended to allow users to freely share, modify, and use this Dataset while maintaining this same freedom for others, provided that the original source and author(s) are credited.

Link: <https://doi.org/10.3897/mycokeys.102.117067.suppl1>

## Supplementary material 2

### Molecular Phylogeny of four new Indian *Tropicoporus* species inferred from ITS sequences

Authors: Sugantha Gunaseelan, Kezhocuyi Kezo, Samantha C. Karunarathna, Erfu Yang, Changlin Zhao, Abdallah M. Elgorban, Saowaluck Tibpromma, Malarvizhi Kaliyaperumal

Data type: jpg

Explanation note: The topology is from Bayesian analysis. Bootstrap values and Bayesian posterior probabilities, equal to or above 60% and 0.90, respectively, are labelled at the nodes. The newly-generated sequences are coloured and bold, and the type specimens are in bold.

Copyright notice: This dataset is made available under the Open Database License (<http://opendatacommons.org/licenses/odbl/1.0/>). The Open Database License (ODbL) is a license agreement intended to allow users to freely share, modify, and use this Dataset while maintaining this same freedom for others, provided that the original source and author(s) are credited.

Link: <https://doi.org/10.3897/mycokeys.102.117067.suppl2>

## Supplementary material 3

### Molecular Phylogeny of four new Indian *Tropicoporus* species inferred from nLSU sequences

Authors: Sugantha Gunaseelan, Kezhocuyi Kezo, Samantha C. Karunarathna, Erfu Yang, Changlin Zhao, Abdallah M. Elgorban, Saowaluck Tibpromma, Malarvizhi Kaliyaperumal

Data type: jpg

Explanation note: The topology is from Bayesian analysis. Bootstrap values and Bayesian posterior probabilities, equal to or above 60% and 0.90, respectively, are labelled at the nodes. The newly-generated sequences are coloured and bold and the type specimens are in bold.

Copyright notice: This dataset is made available under the Open Database License (<http://opendatacommons.org/licenses/odbl/1.0/>). The Open Database License (ODbL) is a license agreement intended to allow users to freely share, modify, and use this Dataset while maintaining this same freedom for others, provided that the original source and author(s) are credited.

Link: <https://doi.org/10.3897/mycokeys.102.117067.suppl3>

# Morphology and multigene phylogeny reveal three new species of *Distoseptispora* (Distoseptisporales, Distoseptisporaceae) on palms (Arecaceae) from peatswamp areas in southern Thailand

Omid Karimi<sup>1,2,3</sup>, K. W. Thilini Chethana<sup>2,3</sup>, Antonio R. G. de Farias<sup>3</sup>, Raheleh Asghari<sup>2,3</sup>,  
Saithong Kaewchai<sup>4</sup>, Kevin D. Hyde<sup>2,3,5,6</sup>, Qirui Li<sup>1</sup>

1 State Key Laboratory of Functions and Applications of Medicinal Plants, Guizhou Medical University, Guiyang 550004, China

2 School of Science, Mae Fah Luang University, Chiang Rai 57100, Thailand

3 Center of Excellence in Fungal Research, Mae Fah Luang University, Chiang Rai 57100, Thailand

4 Princess of Naradhiwas University, 99 Moo 8, Kok Kian, Muang District, Narathiwat Province, 9600 Thailand

5 Mushroom Research Foundation, 128 M.3 Ban Pa Deng T. Pa Pae, A. Mae Taeng, Chiang Mai 50150, Thailand

6 Innovative Institute for Plant Health, Zhongkai University of Agriculture and Engineering, Haizhu District, Guangzhou 510225, China

Corresponding author: Qirui Li (lqrd2008@163.com)

## Abstract

Peatswamp forest is a unique habitat that supports high biodiversity, particularly fungal diversity. The current study collected submerged and dead plant parts from *Eleiodoxa conferta*, *Eugeissona tristis* and *Licuala paludosa* from a peatswamp forest in Narathiwat Province, Thailand. Morphological features coupled with multigene phylogenetic analyses of ITS, LSU, *rpb2* and *tef1-α* sequence data identified our isolates as new *Distoseptispora* species (viz. *D. arecearum* **sp. nov.**, *D. eleiodoxae* **sp. nov.** and *D. narathiwatensis* **sp. nov.**). Morphological descriptions, illustrations and notes are provided.

**Key words:** asexual morph, molecular phylogeny, novel taxa, saprobic fungi, Sordariomycetes, taxonomy



Academic editor: Nalin Wijayawardene

Received: 16 September 2023

Accepted: 15 November 2023

Published: 9 February 2024

**Citation:** Karimi O, Chethana KWT, de Farias ARG, Asghari R, Kaewchai S, Hyde KD, Li Q (2024) Morphology and multigene phylogeny reveal three new species of *Distoseptispora* (Distoseptisporales, Distoseptisporaceae) on palms (Arecaceae) from peatswamp areas in southern Thailand. MycoKeys 102: 55–81. <https://doi.org/10.3897/mycokeys.102.112815>

**Copyright:** © Omid Karimi et al.

This is an open access article distributed under terms of the Creative Commons Attribution License (Attribution 4.0 International – CC BY 4.0).

## Introduction

Most peatswamp forests can be found in tropical rainforests where peat is submerged for most of the year and characterised by low nutrient contents and high acidity due to lack of fully decomposed plant materials (Page et al. 1999, 2011; Jackson et al. 2009; Lampela et al. 2016; Ratnayake 2020). Peatswamp forests are unique ecosystems due to their high species diversity and significant role in maintaining a stable global climate. They function as carbon sinks, storing twice as much carbon as all global forest biomass (Hakim et al. 2017; Fujimoto et al. 2019; Shuhada et al. 2020). Beyond carbon storage, peatlands offer valuable benefits. They play vital roles in the water cycle, storing and filtering water and mitigating floods by slowing peak flows. Home to diverse plants and animals, these wetlands support millions of people. Additionally, they hold archaeological relics and provide insights into past environmental conditions

through their peat layers, aiding predictions about the future climate (Parish et al. 2008; Posa et al. 2011; Minayeva and Sirin 2012; UNEP 2022). Asian peatlands are amongst the most diverse and geographically extensive in the world, with over 160 million hectares and the majority of tropical peatlands are found in Southeast Asia (e.g. Brunei, Indonesia, Malaysia, Papua New Guinea and Thailand) (UNEP 2022).

These habitats support many flora, including an extensive number of bryophytes, ferns and palms (Arecaceae) (Prentice 2011; Rieley 2016). Arecaceae comprises iconic monocotyledonous flowering plants belonging to 188 genera and 2,585 species that are distributed throughout tropical and subtropical areas of the world. However, they are most diverse in highly threatened moist tropical forest habitats (Dransfield et al. 2008; Palmweb 2023; POWO 2023). In peat swamp forests, many palm species, such as *Areca macrocalyx* Zipp. ex Blume, *Calamus concinnus* Mart, *Cyrtostachys renda* Blume, *Eugeissona tristis* Griff, *Eleiodoxa conferta* (Griff.) Burret, *Licuala longicalycata* Furtado, *L. paludosa* Griff, *Metroxylon sagu* Rottb and *Nenga pumila* (Blume) H.Wendl. ex Schaedtler can be found (Calabon et al. 2022), exerting different biological functions.

Several studies on palm fungi have focused on saprobic, endophytic and plant pathogenic life modes from different habitats worldwide (Hyde 1988; Taylor et al. 1999; Fröhlich and Hyde 2000; Fröhlich et al. 2000; Hyde et al. 2000; Taylor and Hyde 2003; Pilantanapak et al. 2005; Lumyong et al. 2009; Liu et al. 2010; Wikee et al. 2013; Konta et al. 2016a, 2016b, 2016c, 2017, 2020a, 2020b, 2020c, 2021a, 2021b, 2023; Chou et al. 2019; El Meleigi et al. 2019; Kinge et al. 2019; Marin-Felix et al. 2019; Chen et al. 2020; Mapook et al. 2020; Zhang et al. 2020; Tian et al. 2022). Even though many palm trees grow in peat swamp forests, there are few records of fungal studies in these environments, mostly reported from Thailand (Pinruan et al. 2002, 2004a, 2004b, 2004c, 2004d, 2007, 2008, 2010a, 2010b, 2014; Pinnoi et al. 2003a, 2003b, 2004, 2006, 2009, 2010; Voglmayr and Yule 2006; Sivichai and Boonyuen 2010; Boonyuen et al. 2012), of which many lack molecular data. Pinnoi et al. (2006) studied saprobic fungi on dead palm material in the Sirindhorn peat swamp forest, Narathiwat Province, Thailand and listed 462 ascomycetous and basidiomycetous taxa from various parts of palm materials (such as dry, damp and submerged palm materials), based on morphological identification and also recorded five sporidesmium-like taxa. Pinnoi et al. (2009) identified 88 fungal species from 212 collections of *Calamus* sp. in Thailand, with six records resembling sporidesmium-like taxa.

*Distoseptispora* K.D. Hyde, McKenzie & Maharachch belongs to Distoseptisporaceae, Distoseptisporales, Sordariomycetes, Ascomycota and comprises sporidesmium-like taxa (Wijayawardene et al. 2022). Su et al. (2016) proposed Distoseptisporaceae to accommodate sporidesmium-like taxa with *Distoseptispora* as the type genus and *D. fluminicola* McKenzie, Hong Y. Su, Z.L. Luo & K.D. Hyde as the type species. Subsequently, Luo et al. (2019) introduced Distoseptisporales to accommodate Distoseptisporaceae, based on multigene phylogenetic analyses of LSU, SSU, *rpb2* and *tef1-a* sequence data. *Distoseptispora* is characterised by short, septate, olivaceous to brown conidiophores. The conidiogenous cells are monoblastic and determinate, bearing acrogenous conidia that are brown, euseptate, distoseptate or muriform and cut off by cross

walls at the basal cell with a basal scar (Yang et al. 2018). The genus exhibits morphology similar to *Sporidesmium*, but can be distinguished by having shorter conidiophores and darker conidia with pale round apexes (Su et al. 2016). To date, *Distoseptispora* comprises 65 species listed in the MycoBank database (<https://www.mycobank.org/>; Accessed in August 2023), with molecular data available for all reported species in the GenBank. The estimated divergence time for Distoseptisporaceae is approximately 44.21 million years ago (MYA), after the Tertiary–Cretaceous extinction event (Hyde et al. 2020), which could have created conducive conditions for *Distoseptispora* to thrive as a saprobe on various hosts (Phukhamsakda et al. 2022).

Peatswamp forests are unique, endangered ecosystems and their fungal biodiversity is little known. Therefore, in the current study, we aimed to study fungal species on different palm materials from peatswamp forests in Thailand, based on morphology and phylogeny. This study introduces three new species, *Distoseptispora arecacearum*, *D. eleiodoxae* and *D. narathiwatensis*, associated with *Eleiodoxa conferta*, *Eugeissona tristis* and *Licuala paludosa* from a peatswamp forest in Narathiwat Province, Thailand, based on morphological characteristics coupled with multigene phylogenetic analyses (ITS, LSU, *rpb2* and *tef1-a*).

## Materials and methods

### Sample collection, morphological study and isolation

Decaying leaves of *Eleiodoxa conferta*, *Eugeissona tristis* and *Licuala paludosa* were collected from a peatswamp forest in Narathiwat Province, Thailand, in April 2022. Wet (submerged) and dry (aerial part) palm specimens were placed in plastic bags and brought to the laboratory. The submerged materials were kept moist and examined periodically for fungal fruiting structures and the dry materials were examined immediately or incubated in moisture chambers. Small pieces of the collected specimens were examined under a Leica EZ4 stereomicroscope and isolated into axenic culture using a single spore technique (Choi et al. 1999) in the Difco potato dextrose agar (PDA) media supplemented with Streptomycin 0.5 g/l. Germinating spores were transferred to new PDA and incubated at  $25 \pm 1$  °C in dark conditions for two weeks. The micro-morphological characters were examined and photographed using a digital camera (Canon 600D, Japan) fitted to a compound microscope (Nikon ECLIPSE Ni, Japan) and the measurements were obtained using the Tarosoft (R) Image Frame Work programme version 0.9.7 (Tarosoft, Thailand). The ex-type living cultures were deposited at the Mae Fah Luang University Culture Collection (MFLUCC) and the herbarium specimens at the Mae Fah Luang University Herbarium (MFLU). The Facesoffungi (FoF) and Index Fungorum numbers were obtained, as explained in Jayasiri et al. (2015) and Index Fungorum (<http://www.indexfungorum.org>), respectively.

### DNA extraction, PCR amplification and sequencing

Genomic DNA was extracted from fresh fungal mycelia using the Biospin Fungus Genomic DNA Extraction Kit (BioFlux, P.R. China), according to the

**Table 1.** Primers and PCR protocols.

Gene regions	Primers	PCR conditions	References
ITS	ITS5/ITS4	95 °C for 4 min, 40 cycles of 94 °C for 45 s, 56 °C for 1 min and 72 °C for 2 min, 72 °C for 10 min	White et al. (1990)
LSU	LR0R/LR5	94 °C for 3 min, 40 cycles of 94 °C for 30 s, 50 °C for 45 s and 72 °C for 2 min, 72 °C for 10 min	Vilgalys and Hester (1990), Rehner and Samuels (1994)
<i>rpb2</i>	fRPB2-5f/fRPB2-7cR	95 °C for 5 min, 35 cycles of 95 °C for 1 min, 55 °C for 1.25 min and 72 °C for 2 min, 72 °C for 10 min	Liu et al. (1999)
<i>tef1-a</i>	EF1-983F/EF1-2218R	94 °C for 3 min, 40 cycles of 94 °C for 30 s, 54 °C for 50 s and 72 °C for 2 min, 72 °C for 10 min	Rehner (2001)

manufacturer's standard protocol. Polymerase chain reactions (PCR) were conducted to amplify the internal transcribed spacer region rDNA (ITS), 28S large subunit rDNA (LSU), RNA polymerase II second largest subunit (*rpb2*) and translation elongation factor 1-alpha (*tef1-a*) using primers and conditions listed in Table 1. The PCR products were visualised on 1% agarose gels, stained with 4S Green Stain and sequenced at SolGent Co., Ltd (South Korea).

### Sequence alignment and Phylogenetic analyses

The obtained sequences of ITS, LSU, *rpb2* and *tef1-a* were assembled using SeqMan software version 7.1.0 (DNASTAR Inc., WI) and subjected to BLASTn search against the GenBank nucleotide database at National Center for Biotechnology Information (NCBI) to identify closely-related sequences. Sequence data of related taxa were obtained from previous publications (Su et al. 2016; Yang et al. 2018, 2021; Crous et al. 2019; Hyde et al. 2019; Luo et al. 2019; Monkai et al. 2020; Phukhamsakda et al. 2020; Sun et al. 2020; Ma et al. 2022; Zhai et al. 2022; Zhang et al. 2022; Afshari et al. 2023) and downloaded from the GenBank database (Table 2). The sequences were aligned using MAFFT v.7 online web server (<http://mafft.cbrc.jp/alignment/server/index.html>, Katoh et al. 2019) under default settings and the alignments were trimmed in NGPhylogeny online web server (<https://ngphylogeny.fr/workflows/wkmake/3a4ab-1bef8e7ff3c>, Lemoine et al. 2019). The sequence datasets were combined using SequenceMatrix software version 1.9 (Vaidya et al. 2011). The Maximum Likelihood (ML) phylogenetic analysis was run in the CIPRES Science Gateway platform (Miller et al. 2010), using RAxMLHPC2 on the XSEDE (v. 8.2.10) tool (Stamatakis 2014) under the GTRCAT substitution model and 1,000 non-parametric bootstrap replicates. For Bayesian Inference (BI) analysis, the optimal substitution model of each region was determined using jModelTest2 on the CIPRES Science Gateway under the Akaike Information Criterion (AIC) (Darriba et al. 2012). Bayesian analysis was performed using MrBayes v. 3.2.6 on XSEDE at the CIPRES Science Gateway with four simultaneous Markov Chain runs for 1,000,000 generations. The resulting trees were visualised in FigTree v. 1.4.0 (Rambaut 2012) and edited in Microsoft PowerPoint 2019 (Forethought, Inc., The United States).

**Table 2.** GenBank accession numbers used in the phylogenetic analyses.

Taxon	Identifier	GenBank accession number			
		ITS	LSU	<i>rpb2</i>	<i>tef1-a</i>
<i>Aquapteridospora aquatica</i>	MFLUCC 17-2371*	NR172447	NG075413	–	–
<i>A. fusiformis</i>	MFLU 18-1601*	MK828652	MK849798	–	MN194056
<i>Distoseptispora adscendens</i>	HKUCC 10820	–	DQ408561	DQ435092	–
<i>D. amniculi</i>	MFLUCC 17-2129*	MZ868770	MZ868761	MZ892982	–
<i>D. appendiculata</i>	MFLUCC 18-0259*	MN163009	MN163023	–	MN174866
<i>D. aqualignicola</i>	KUNCC 21-10729*	OK341186	ON400845	OP413474	OP413480
<i>D. aquamyces</i>	KUNCC 21-10732*	OK341187	OK341199	OP413476	OP413482
<i>D. aquatica</i>	MFLUCC 15-0374*	MF077552	KU376268	–	–
<i>D. aquatica</i>	MFLUCC 16-0904	MK828649	MK849794	–	MN194053
<i>D. aquatica</i>	MFLUCC 18-0646	MK828648	MK849793	–	MN194052
<i>D. aquatica</i>	S-965	MK828647	MK849792	MN124537	MN194051
<i>D. aquisubtropica</i>	GZCC 22-0075*	ON527933	ON527941	ON533685	ON533677
<b><i>D. arecacearum</i></b>	<b>MFLUCC 23-0211*</b>	<b>OR234707</b>	<b>OR510857</b>	<b>OR250439</b>	<b>OR250442</b>
<b><i>D. arecacearum</i></b>	<b>MFLUCC 23-0212</b>	<b>OR354399</b>	<b>OR510860</b>	<b>OR481048</b>	<b>OR481045</b>
<i>D. atroviridis</i>	GZCC 20-0511*	MZ868772	MZ868763	MZ892984	MZ892978
<i>D. atroviridis</i>	GZCC 19-0531	MW133915	MZ227223	–	–
<i>D. bambusae</i>	MFLUCC 20-0091*	NR170068	NG074430	MT232881	MT232880
<i>D. bambusae</i>	MFLU 17-1653	MT232712	MT232717	MT232882	–
<i>D. bangkokensis</i>	MFLUCC 18-0262*	MZ518205	MZ518206	–	–
<i>D. cangshanensis</i>	MFLUCC 16-0970*	MG979754	MG979761	–	MG988419
<i>D. caricis</i>	CPC: 36498*	NR166325	MN567632	MN556805	–
<i>D. caricis</i>	CPC: 36442	MN562125	–	MN556806	–
<i>D. chinensis</i>	GZCC 21-0665	MZ474871	MZ474867	–	MZ501609
<i>D. clematidis</i>	MFLUCC 17-2145*	MT310661	MT214617	MT394721	–
<i>D. clematidis</i>	KUN-HKAS:112708	MW723056	MW879523	–	–
<i>D. crassispora</i>	KUMCC 21-10726*	OK310698	OK341196	OP413473	OP413479
<i>D. curvularia</i>	KUMCC 21-10725*	OK310697	OK341195	OP413472	OP413478
<i>D. cylindricospora</i>	KUN-HKAS:115796*	OK491122	OK513523	–	OK524220
<i>D. dehongensis</i>	KUMCC 18-0090*	MK085061	MK079662	–	MK087659
<i>D. dipteroearpi</i>	MFLUCC 22-0104 *	OP600053	OP600052	OP595140	–
<i>D. effusa</i>	GZCC 19-0532*	MW133916	MZ227224	–	–
<b><i>D. eleiodoxae</i></b>	<b>MFLUCC 23-0213*</b>	<b>OR234706</b>	<b>OR510856</b>	<b>OR250438</b>	<b>OR250441</b>
<b><i>D. eleiodoxae</i></b>	<b>MFLUCC 23-0214</b>	<b>OR354398</b>	<b>OR510859</b>	<b>OR481047</b>	<b>OR481044</b>
<i>D. euseptata</i>	MFLUCC 20-0154*	MW081539	MW081544	MW151860	–
<i>D. euseptata</i>	MFLU 20-0568	MW081540	MW081545	MW084996	MW084994
<i>D. fasciculata</i>	KUMCC 19-0081*	NR172452	NG075417	–	MW396656
<i>D. fluminicola</i>	MFLUCC 15-0417*	MF077553	KU376270	–	–
<i>D. fusiformis</i>	GZCC 20-0512*	MZ868773	MZ868764	MZ892985	MZ892979
<i>D. guizhouensis</i>	GZCC 21-0666*	MZ474868	MZ474869	MZ501611	MZ501610
<i>D. guttulata</i>	MFLUCC 16-0183*	MF077543	MF077554	–	MF135651
<i>D. hyalina</i>	MFLUCC 17-2128*	MZ868769	MZ868760	MZ892981	MZ892976
<i>D. hydei</i>	MFLUCC 20-0115*	MT734661	MT742830	MT767128	–
<i>D. lancangjiangensis</i>	DLUCC 1864*	MW723055	MW879522	–	–
<i>D. leonensis</i>	HKUCC 10822	–	DQ408566	DQ435089	–

Taxon	Identifier	GenBank accession number			
		ITS	LSU	<i>rpb2</i>	<i>tef1-a</i>
<i>D. licualae</i>	MFLUCC 14-1163*	ON650686	ON650675	–	ON734007
<i>D. lignicola</i>	MFLUCC 18-0198*	MK828651	MK849797	–	–
<i>D. longispora</i>	HFJAU 0705*	MH555359	MH555357	–	–
<i>D. martinii</i>	CGMCC 3.18651	KU999975	KX033566	–	–
<i>D. meilingensis</i>	JAUCC 4728	OK562391	OK562397	–	OK562409
<i>D. mengsongensis</i>	HJAUP C2126*	OP787876	OP787874	–	OP961937
<i>D. multiseptata</i>	MFLUCC 15-0609*	KX710145	KX710140	–	MF135659
<i>D. nabanheensis</i>	HJAUP C2003*	OP787877	OP787873	–	OP961935
<b><i>D. narathiwatensis</i></b>	<b>MFLUCC 23-0215*</b>	<b>OR234708</b>	<b>OR510858</b>	<b>OR250440</b>	<b>OR250443</b>
<b><i>D. narathiwatensis</i></b>	<b>MFLUCC 23-0216</b>	<b>OR354400</b>	<b>OR510861</b>	<b>OR481049</b>	<b>OR481046</b>
<i>D. neurostrata</i>	MFLUCC 18-0376*	MN163008	MN163017	–	–
<i>D. nonrostrata</i>	KUNCC 21-10730*	OK310699	OK341198	OP413475	OP413481
<i>D. obclavata</i>	MFLUCC 18-0329*	MN163012	MN163010	–	–
<i>D. obpyriformis</i>	MFLUCC 17-1694*	–	MG979764	MG988415	MG988422
<i>D. obpyriformis</i>	DLUCC 0867	MG979757	MG979765	MG988416	MG988423
<i>D. pachyconidia</i>	KUMCC 21-10724*	OK310696	OK341194	OP413471	OP413477
<i>D. palmarum</i>	MFLUCC 18-1446*	MK085062	MK079663	MK087670	MK087660
<i>D. palmarum</i>	MFLU 18-0588	NR165897	NG067856	–	–
<i>D. phangngaensis</i>	MFLUCC 16-0857*	NR166230	–	–	MF135653
<i>D. rayongensis</i>	MFLUCC 18-0415*	NR171938	NG073624	–	MH463253
<i>D. rayongensis</i>	MFLU 18-1045	MH457172	MH457137	MH463255	–
<i>D. rostrata</i>	MFLUCC 16-0969*	MG979758	MG979766	MG988417	MG988424
<i>D. rostrata</i>	DLUCC 0885	MG979759	MG979767	–	MG988425
<i>D. rostrata</i>	MFLU 18-0479	NR157552	NG064513	–	–
<i>D. saprophytica</i>	MFLUCC 18-1238*	NR172454	NG075419	MW504069	MW396651
<i>D. septata</i>	GZCC 22-0078*	ON527939	ON527947	ON533690	ON533683
<i>D. sinensis</i>	HJAUP C2044*	OP787878	OP787875	–	OP961936
<i>D. songkhlaensis</i>	MFLUCC 18-1234*	MW286482	MW287755	–	MW396642
<i>D. submersa</i>	MFLUCC 16-0946	MG979760	MG979768	MG988418	MG988426
<i>D. suoluensis</i>	MFLUCC 17-0224*	NR168764	NG068552	–	MF135654
<i>D. tectonae</i>	MFLUCC 12-0291*	KX751711	KX751713	KX751708	KX751710
<i>D. tectonigena</i>	MFLUCC 12-0292*	NR154018	KX751714	KX751709	–
<i>D. thailandica</i>	MFLUCC 16-0270*	MH275060	MH260292	–	MH412767
<i>D. thysanolaenae</i>	KUN-HKAS: 112710	MW723057	MW879524	–	MW729783
<i>D. thysanolaenae</i>	KUMCC 18-0182	MK045851	MK064091	–	MK086031
<i>D. tropica</i>	GZCC 22-0076*	ON527935	ON527943	ON533687	ON533679
<i>D. verrucosa</i>	GZCC 20-0434*	MZ868771	MZ868762	MZ892983	MZ892977
<i>D. wuzhishanensis</i>	GZCC 22-0077*	ON527938	ON527946	–	ON533682
<i>D. xishuangbannaensis</i>	KUMCC 17-0290*	MH275061	MH260293	MH412754	MH412768
<i>D. yongxiensis</i>	JAUCC 4725	OK562388	OK562394	–	OK562406
<i>D. yongxiensis</i>	JAUCC 4726	OK562389	OK562395	–	OK562407
<i>D. yunjushanensis</i>	JAUCC 4723	OK562392	OK562398	–	OK562411
<i>D. yunjushanensis</i>	JAUCC 4724	OK562393	OK562399	–	OK562410
<i>D. yunnanensis</i>	MFLUCC 20-0153*	MW081541	MW081546	MW151861	MW081541

Ex-type strains are indicated with an asterisk (\*) after the collection number; “–” indicates unavailable sequences; sequences produced in the current study are in bold.

## Abbreviations

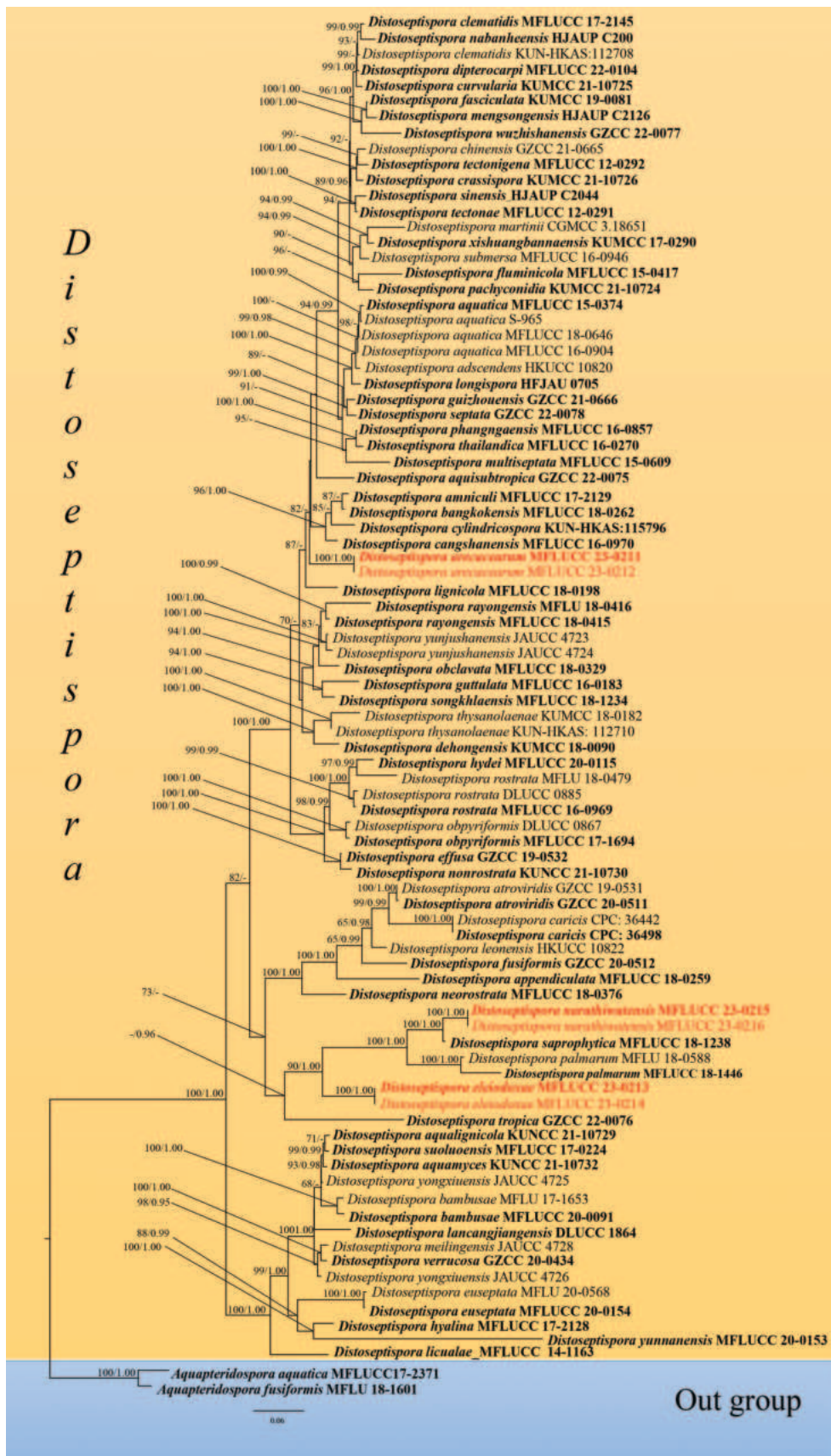
**CGMCC**: China General Microbiological Culture Collection Center, Chinese Academy of Sciences, Beijing, China; **CPC**: Collection of P.W. Crous, Utrecht, The Netherlands; **DLUCC**: Dali University Culture Collection, Yunnan, China; **GZCC**: Guizhou Culture Collection, Gui Yang, China; **HFJAU**: Herbarium of Fungi, Jiangxi Agricultural University, Nanchang, China; **HKUCC**: The University of Hong Kong Culture Collection, Hong Kong, China; **JAUCC**: Jiangxi Agricultural University Culture Collection, Nanchang, China; **KUMCC**: Kunming Institute of Botany Culture Collection, Kunming, China; **KUN-HKAS**: Herbarium of Cryptogams, Kunming Institute of Botany Academia Sinica; **MFLU**: Mae Fah Luang University Herbarium, Chiang Rai, Thailand; **MFLUCC**: Mae Fah Luang University Culture Collection, Chiang Rai, Thailand.

## Results

### Phylogenetic analyses

The combined ITS, LSU, *rpb2* and *tef1- $\alpha$*  dataset consisted of 83 strains, with *Aquapteridospora aquatica* X.D. Yu, W. Dong & H. Zhang (MFLUCC 17-2371) and *A. fusiformis* Z.L. Luo, D.F. Bao, H.Y. Su & K.D. Hyde (MFLU 18-1601) as outgroup taxa (Table 2). The final alignment comprised 3,383 characters (ITS: 567 bp, LSU: 855 bp, *rpb2*: 1,051 bp, *tef1- $\alpha$* : 909 bp), including gaps. The final ML optimisation likelihood value of the best RAxML tree was -33894.57 and the matrix had 1,637 distinct alignment patterns, with 29.85% undetermined characters or gaps. Estimated base frequencies were as follows: A = 0.240315, C = 0.262752, G = 0.283175, T = 0.213758; substitution rates AC = 1.324179, AG = 3.427671, AT = 1.239665, CG = 0.914354, CT = 6.950002, GT = 1.0; gamma distribution shape parameter  $\alpha$  = 0.273123. The RAxML and Bayesian analyses yielded a similar tree topology.

The topology of our phylogenetic tree is nearly identical to previous publications, but there are some differences, which may be due to different taxon sampling. As new species are introduced into this genus frequently, taxon sampling conducted for different studies varies. In our phylogenetic analyses, two strains of the new species *Distoseptispora arecacearum* (MFLUCC 23-0211 and MFLUCC 23-0212) formed a robust subclade (100% ML, 1.00 PP) independently. The species has close relationships with *D. amniculi* (MFLUCC 17-2129), *D. bangkokensis* (MFLUCC 18-0262), *D. cangshanensis* (MFLUCC 16-0970) and *D. cylindricospora* (KUN-HKAS:115796) with 82% ML bootstrap support. The other two new species, *D. eleiodoxae* and *D. narathiwatensis*, clustered with *D. saprophytica* (MFLUCC 18-1238), *D. palmarum* (MFLU 18-0588 and MFLUCC 18-1446) and *D. tropica* (GZCC 22-0076) with 0.96 PP support. *Distoseptispora eleiodoxae* (strains MFLUCC 23-0213 and MFLUCC 23-0214) formed a robust subclade (100% ML, 1.00 PP) basal to *D. narathiwatensis* (MFLUCC 23-0215 and MFLUCC 23-0216), *D. saprophytica* (MFLUCC 18-1238) and *D. palmarum* (MFLU 18-0588 and MFLUCC 18-1446) with 90% ML and 1.00 PP support. *Distoseptispora narathiwatensis* (MFLUCC 23-0215 and MFLUCC 23-0216) formed a sister clade with *D. saprophytica* (MFLUCC 18-1238) with 100% ML and 1.00 PP support (Fig. 1).



## Taxonomy

***Distoseptispora areacearum* O. Karimi, Q.R. Li & K.D. Hyde, sp. nov.**

Index Fungorum number: IF900843

Facesoffungi number: FoF14756

Fig. 2

**Etymology.** The epithet “*areacearum*” refers to host family, Aceraceae.

**Holotype.** MFLU 23-0276.

**Description.** **Saprobic** on submerged rachis of *Licuala paludosa* in peatswamp forest. **Sexual morph:** Undetermined. **Asexual morph:** Hyphomycetous. Colonies gregarious or scattered, effuse, hairy, dark brown to black. **Mycelium** mostly immersed, composed of branched, septate, smooth hyphae. **Conidiophores** 70–140 × 5.1–6.3 μm ( $\bar{x}$  = 110 × 5.5 μm, n = 20), macronematous, mononematous, unbranched, erect, straight or flexuous, cylindrical, smooth, thick-walled, brown, 4–7 septa, sometimes consists a swollen cell in the middle or towards the apex. **Conidiogenous cells** 13–25 × 4.5–6 μm ( $\bar{x}$  = 17 × 5 μm, n = 20), monoblastic or polyblastic, terminal or subterminal, determinate, cylindrical, brown. **Conidia** 25–60 × 7–17 μm ( $\bar{x}$  = 44 × 10 μm, n = 30), acrogenous, solitary, cylindrical, obclavate to obpyriform or irregular, straight or curved, 4–10-distoseptate, brown, thick-walled, smooth, round apex, truncated base, sometimes with percurrent regeneration forming a secondary conidium from the conidial apex.

**Culture characteristics.** Colonies grown on PDA, reaching 50 mm in diameter after 15 days at 25 °C, under dark conditions, circular, fimbriate edge, flat, dull surface, radiating outwards, felted, medium dense, without pigment diffusion and sporulation, brown on the top, reverse dark brown to black.

**Material examined.** Thailand. Narathiwat Province: Yi-ngo District, peatswamp forest, on submerged rachis of *Licuala paludosa*, 06 April 2022, Omid Karimi, S5PP3SG (MFLU 23-0276, **holotype**); ex-type culture MFLUCC 23-0211, additional living culture MFLUCC 23-0212.

**Notes.** Morphologically, our proposed new species is similar to *Distoseptispora dehongensis* W. Dong, H. Zhang & K.D. Hyde and *D. obpyriformis* Z.L. Luo & H.Y. Su in having macronematous, mononematous, unbranched, erect, straight or flexuous, cylindrical, septate conidiophores, terminal, determinate, cylindrical, brown conidiogenous cells and acrogenous, distoseptate, straight or curved conidia (Luo et al. 2018; Hyde et al. 2019). However, our isolate differs from *D. dehongensis* (HKAS 101738) in having longer and wider conidiophores (70–140 × 5.1–6.3 μm vs. 45–80 × 4–5 μm), with swollen cells, longer and wider conidia (25–60 × 7–17 μm vs. 17–30 × 7.5–10 μm) and more distosepta (4–10-distoseptate vs. 3–5-distoseptate). *Distoseptispora areacearum* (MFLU 23-0276) differs from *D. obpyriformis* (MFLU 18-0476) in having conidiophores with swollen cells and shorter conidia (25–60 μm vs. 53–71 μm) (Luo et al. 2018). The BLASTn searches of the ITS sequence of *D. areacearum* (MFLUCC 23-0211) resulted in *D. aquatica* Z.L. Luo, H.Y. Su & K.D. Hyde (MFLUCC 18-0646) with 92.21% similarity across 100% of the query sequence coverage, while the LSU sequence of *D. areacearum* has 99.09% similarity across 100% of the sequence coverage with *D. phangngaensis* J. Yang, Maharachch. & K.D. Hyde (MFLUCC 16-0857). *Distoseptispora areacearum* (MFLU 23-0276) is easily distinguishable from *D. aquatica* (HKAS 83991) in having longer



**Figure 2.** *Distoseptispora arecacearum* (MFLU 23-0276, holotype) **a** host material **b** colonies on the substrate **c–e** conidiophores and conidia **f–i** conidia **j, k** culture on PDA. Scale bars: 200 µm (**b**); 50 µm (**c–e**); 10 µm (**f–i**).

conidiophores (70–140  $\mu\text{m}$  vs. 29–41  $\mu\text{m}$ ) and shorter conidia (25–60  $\mu\text{m}$  vs. 110–157  $\mu\text{m}$ ) with less distosepta (4–10-distoseptate vs. 15–28-distoseptate) (Su et al. 2016). *Distoseptispora areacearum* (MFLU 23-0276) differs from *D. phangngaensis* (MFLU 17-0855) in having longer conidiophores (70–140  $\mu\text{m}$  vs. 18–30(–40)  $\mu\text{m}$ ) and shorter conidia (25–60  $\mu\text{m}$  vs. 165–350  $\mu\text{m}$ ) (Yang et al. 2018). Therefore, we introduced *D. areacearum* (MFLU 23-0276) as a novel species, based on morphological and phylogenetic analyses.

***Distoseptispora eleiodoxae* O. Karimi, Q.R. Li & K.D. Hyde, sp. nov.**

Index Fungorum number: IF900844

Facesoffungi number: FoF14757

Fig. 3

**Etymology.** The epithet “*eleiodoxae*” refers to the name of the host genus, *Eleiodoxa conferta*.

**Holotype.** MFLU 23-0277.

**Description.** *Saprobic* on submerged rachis of *Eleiodoxa conferta* in peatswamp forest. **Sexual morph:** Undetermined. **Asexual morph:** Hyphomycetous. **Mycelium** immersed to superficial, septate, smooth, brown to dark brown. **Colonies** on submerged rachis, solitary, scattered, dark brown to black. **Conidiophores** 71–161  $\times$  5–6.5  $\mu\text{m}$  ( $\bar{x}$  = 110  $\times$  5.7  $\mu\text{m}$ ,  $n$  = 20), macronematous, mononematous, cylindrical, erect, straight to flexuous, unbranched, smooth or finely verrucose, thick-walled, dark brown, 5–10-septate with lobed basal cells, percurrent proliferations at the apex. **Conidiogenous cells** 13.5–18.8  $\times$  5–6.8  $\mu\text{m}$  ( $\bar{x}$  = 15.96  $\times$  5.6  $\mu\text{m}$ ,  $n$  = 20), holoblastic, monoblastic, terminal, integrated, cylindrical to ampulliform, percurrent, brown to dark brown, smooth. **Conidia** 31.5–48  $\times$  13.5–15.8  $\mu\text{m}$  ( $\bar{x}$  = 40.8  $\times$  14.8  $\mu\text{m}$ ,  $n$  = 30), secession schizolytic, solitary, obpyriform, rostrate, truncated base, 6–7-euseptate, verrucose, thick-walled, brown with dark brown to black cells in the middle, paler towards the apex.

**Culture characteristics.** Colonies grown on PDA, reaching 30 mm in diameter after 15 days at 25 °C, under dark conditions, circular, entire to radially with lobate edge, well-defined margin, low convex, dull surface, felted, dense, mycelium superficial to immersed, without pigment diffusion and sporulation, greyish-brown on the top with dark brown margin, reverse brown with dark brown centre and margin.

**Material examined.** Thailand. Narathiwat Province: Yi-ngo District, peatswamp forest, on submerged rachis of *Eleiodoxa conferta*, 06 April 2022, Omid Karimi, S5PP8N1SG (MFLU 23-0277, **holotype**); ex-type culture MFLUCC 23-0213, additional living culture MFLUCC 23-0214.

**Notes.** *Distoseptispora eleiodoxae* (MFLU 23-0277) shares similar characteristics with *D. tropica* J. Ma & Y.Z. Lu (HKAS 123761), in having macronematous, mononematous, cylindrical, erect, straight, unbranched conidiophores with holoblastic, monoblastic, terminal, cylindrical, thick-walled conidiogenous cells and verrucose, rostrate conidia (Ma et al. 2022). However, *D. eleiodoxae* (MFLU 23-0277) differs from *D. tropica* (HKAS 123761) in having shorter and wider obpyriform conidia (31.5–48  $\times$  13.5–15.8  $\mu\text{m}$  vs. 39–75  $\times$  7.5–10.5  $\mu\text{m}$ ), with broad and darker middle cells, no guttules and lacking conspicuous hyphae attachment to conidia. The BLAST search against GenBank showed that the

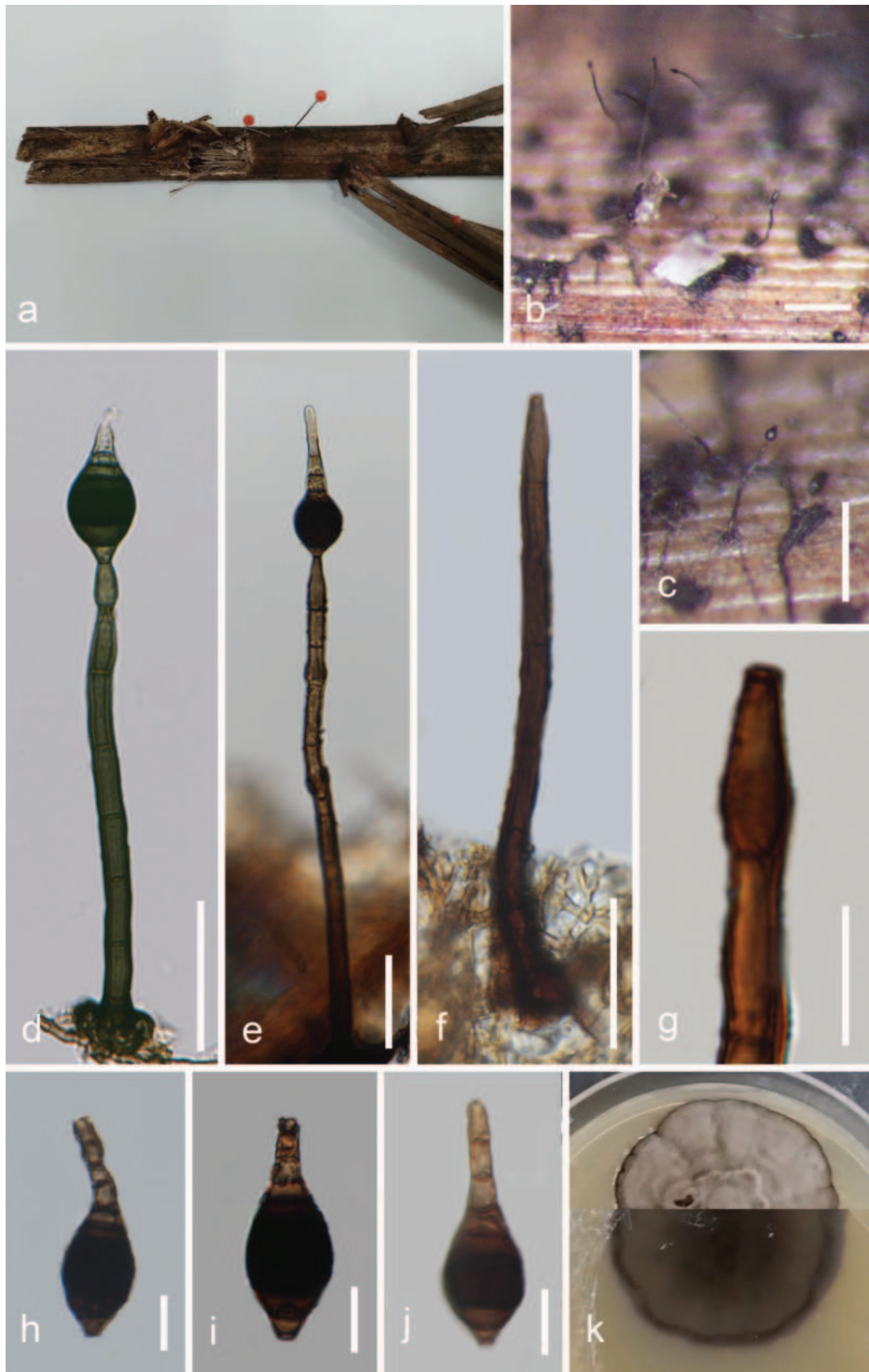


**Figure 3.** *Distoseptispora eleiodoxae* (MFLU 23-0277, holotype) **a** host material **b, c** colonies on the substrate **d–f** conidiophores and conidia **g** conidiogenous cell **h–j** conidia **k** culture on PDA (top and reverse). Scale bars: 100 µm (**b, c**); 30 µm (**d–f**); 10 µm (**g–j**).

ITS and LSU sequences of the new isolate, *D. eleiodoxae* (MFLUCC 23-0213), share 84.25% similarity across 100% sequence coverage with *D. tropica* (GZCC 22-0076) and 96.09% similarity across 100% sequence coverage with *D. effusa* L.L. Liu & Z.Y. Liu, respectively. *Distoseptispora eleiodoxae* (MFLU 23-0277) differs from *D. effusa* (GZAAS 20-0427) in having shorter conidia (31.5–48 vs. 35.5–113  $\mu\text{m}$ ) (Yang et al. 2021). Based on a pairwise comparison of ITS, LSU, *rpb2* and *tef1-a* nucleotides, *D. eleiodoxae* (MFLUCC 23-0213) differs from *D. tropica* (GZCC 22-0076) in 70/536 bp (13.05%) for ITS, 50/834 bp (5.99%) for LSU, 141/1052 bp (13.40%) for *rpb2* and 96/888 bp (10.8%) for *tef1-a* (without including gaps). Therefore, we introduced *D. eleiodoxae* (MFLU 23-0277) as a novel species, based on the morphological evidence and according to the species delimitation guidelines proposed by Chethana et al. (2021) and Maharachchikumbura et al. (2021).

***Distoseptispora narathiwatensis* O. Karimi, Q.R. Li & K.D. Hyde, sp. nov.**

Index Fungorum number: IF900845

Facesoffungi number: FoF14758

Fig. 4

**Etymology.** The epithet “*narathiwatensis*” refers to Narathiwat Province, where the holotype was collected.

**Holotype.** MFLU 23-0278.

**Description.** *Saprobic* on dead petiole of *Eugeissona tristis* in peat swamp forest. **Sexual morph:** Undetermined. **Asexual morph:** Hyphomycetous. **Colonies** superficial, effuse, hairy, gregarious, brown. **Mycelium** immersed to superficial, composed of septate, branched, pale brown hyphae. **Conidiophores** 27–155  $\times$  3–6.5(–7)  $\mu\text{m}$  ( $\bar{x}$  = 104  $\times$  5  $\mu\text{m}$ , n = 50), macronematous, mononematous, cylindrical, straight or flexuous, occasionally slightly curved in the middle and near the base and the apex, up to 10 septa, slightly constricted at septa, unbranched, brown, thin-walled, smooth, often containing inflated or constricted cells at the apex or middle, sometimes percurrent with annellations. **Conidiogenous** cells 7–17  $\times$  4–5.5  $\mu\text{m}$  ( $\bar{x}$  = 12.5  $\times$  5  $\mu\text{m}$ , n = 30), holoblastic, mono- to polyblastic, integrated, determinate, terminal and intercalary, subcylindrical, brown, smooth. **Conidia** 12–38  $\times$  4.5–8  $\mu\text{m}$  ( $\bar{x}$  = 27  $\times$  6.5  $\mu\text{m}$ , n = 30), secession schizolytic, solitary or occasionally catenate, dry, thin-walled, smooth, subcylindrical to obclavate to conical, straight or curved, 1–7-distoseptate, slightly constricted at septa, olivaceous to brown, apex rounded, truncated base with slightly pigmented scar, often the primary cells of conidia are narrower than the second ones which are often inflated.

**Culture characteristics.** Colonies grown on PDA, reaching 50 mm in diameter after 15 days at 25 °C, under dark conditions, circular, entire margin, well-defined margin, low convex, dull surface, felted, dense, mycelium mostly superficial, without pigment diffusion and sporulation, medium brown to reddish-brown with dark brown edge on the top, reverse-side dark brown to black.

**Material examined.** Thailand. Narathiwat Province: Yi-ngo District, peat swamp forest, on dead petiole of *Eugeissona tristis*, 06 April 22, Omid Karimi, 35Y (MFLU 23-0278, **holotype**); ex-type culture MFLUCC 23-0215, additional living culture MFLUCC 23-0216.



**Figure 4.** *Distoseptispora narathiwatensis* (MFLU 23-0278, holotype) **a** host material **b** colonies on the substrate **c–e** conidiophores and conidia **f** conidiogenous cell **g–j** conidia **k, l** culture on PDA. Scale bars: 100  $\mu\text{m}$  (**b**); 50  $\mu\text{m}$  (**c–e**); 10  $\mu\text{m}$  (**f–j**).

**Notes.** *Distoseptispora narathiwatensis* (MFLU 23-0278) is similar to *D. saprophytica* (MFLU 18-1568), but it can be distinguished in having longer and wider conidiophores ( $27\text{--}155 \times 3\text{--}6.5$  ( $-7$ )  $\mu\text{m}$  vs.  $50\text{--}140 \times 3.2\text{--}4.2$   $\mu\text{m}$ ) and conidiogenous cells ( $7\text{--}17 \times 4\text{--}5.5$   $\mu\text{m}$  vs.  $5\text{--}11.5 \times 3\text{--}4.5$   $\mu\text{m}$ ). In *D. narathiwatensis* (MFLU 23-0278), the conidiophore is slightly curved at the base, middle and near the top in contrast to *D. saprophytica* (MFLU 23-0278), which is characterised by sharp curving near the base; also in *D. narathiwatensis*, the conidiophore cells are often inflated or constricted at the apex or middle which is not observed in *D. saprophytica* (Dong et al. 2021). Conidiogenous cells of *D. narathiwatensis* are terminal and intercalary and their conidia are not acrogenous as in *D. saprophytica*. The primary cell in the conidium is often narrower than the second one and the second cell is often inflated, which is not observed in *D. saprophytica*. The BLAST search against the GenBank showed that the ITS and *rpb2* sequences of the new isolate, *D. narathiwatensis* (MFLUCC 23-0215), share 98.33% similarity across 100% sequence coverage and 98.63% similarity across 78% sequence coverage with *D. saprophytica* (MFLUCC 18-1238), respectively. In a BLAST search against GenBank, the LSU and *tef1-a* sequences of *D. narathiwatensis* (MFLUCC 23-0215) share 99.3% similarity across 85% sequence coverage and 94.12% similarity across 94% sequence coverage with *D. palmarum* (MFLU 18-0588), respectively. However, *D. palmarum* is distinguished in having longer ( $12\text{--}38$   $\mu\text{m}$  vs.  $35\text{--}180$   $\mu\text{m}$ ), elongated, greenish-black to brown conidia (Hyde et al. 2019). Based on a pairwise comparison of ITS and LSU nucleotides, *D. narathiwatensis* (MFLUCC 23-0215) differs from *D. saprophytica* (MFLUCC 18-1238) by 22/580 bp (3.8%), 16/870 bp (1.8%) differences, respectively (without including gaps). Therefore, we introduced *D. narathiwatensis* (MFLU 23-0278) as a novel species, based on the morphological evidence and according to the species delimitation guidelines proposed by Chethana et al. (2021) and Maharachchikumbura et al. (2021).

## Discussion

Peatswamp forests are unique habitats found in only a few regions worldwide (Jackson et al. 2009). The destruction caused by humans threatens them; hence more extensive studies on fungal identification are needed before the extinction of fungal species. Pinnoi et al. (2006, 2009) recorded sporidesmium-like taxa on the palm species *Eleiodoxa conferta* and *Calamus* sp. in Sirindhorn peatswamp forest, Narathiwat, Thailand, based on morphological data. In this study, three new *Distoseptispora* species (*D. arecacearum*, *D. eleiodoxae* and *D. narathiwatensis*) from peatswamp forest in Thailand are introduced, based on multilocus phylogenetic analysis (ITS, LSU, *rpb2* and *tef1-a*) (Fig. 1) and morphology (Figs 2–4).

The fungal diversity in peatswamp forest has not been well studied and a few previously studies (Pinruan et al. 2002, 2004a, 2004b, 2007, 2008, 2010a, 2010b, 2014; Pinnoi et al. 2003a, 2003b, 2004, 2006, 2009, 2010; Voglmayr and Yule 2006; Sivichai and Boonyuen 2010; Boonyuen et al. 2012) show a high fungal diversity in this habitat, especially in Thailand, but some of the previous studies (Pinruan et al. 2002, 2007, 2014; Pinnoi et al. 2003a, 2003b, 2004, 2006, 2009; Sivichai and Boonyuen 2010) lack molecular data. As only morphological data are insufficient to identify a fungal species (Chethana et al. 2021; Maharachchikumbura et al.

2021), studying the fungal diversity by combining morphological and molecular data are required and this has been followed in this study.

Except for *Distoseptispora hyalina* J. Yang & K.D. Hyde and *D. licualae* Kanta & K.D. Hyde, most *Distoseptispora* species have been recorded as having an asexual morph and their characters, such as size, shape, colour and the number of septa in conidiophores and conidia, are crucial for distinguishing species. Morphologically, *Distoseptispora* is similar to *Ellisembia* Subram and *Sporidesmium* Link; therefore, it is problematic to recognise *Distoseptispora* species by only morphological signatures (Su et al. 2016; Hyde et al. 2019; Luo et al. 2019; Yang et al. 2021). Different studies have explored the taxonomy of *Distoseptispora* using various combinations of gene regions, such as combined ITS, LSU (Tibpromma et al. 2018), combined LSU, ITS, *rpb2* (Monkai et al. 2020) or combined LSU, ITS, *tef1-a* and *rpb2* (Zhang et al. 2022). In our study, we constructed the phylogenetic tree using concatenated ITS, LSU, *rpb2* and *tef1-a*. In this study, *Distoseptispora clematidis* (MFLUCC 17-2145) and *D. nabanheensis* Jing W. Liu, X.G. Zhang & Jian Ma (HJAUP C2003) formed a sister clade, consistent with previous research (Liu et al. 2023). However, *D. clematidis* (KUN-HKAS:112708) appeared separated from these two taxa, presenting an unresolved relationship. The phylogenetic relationship amongst these three taxa is not comparable with the previous studies due to the lack of all these taxa together in their phylogenetic trees (Afshari et al. 2023; Liu et al. 2023). The unresolved clade's origin may stem from the lack of *rpb2* sequence data for *D. clematidis* (KUN HKAS:112708) in contrast to the other two taxa where this gene region is available. This suggests that different taxon sampling and protein-coding sequences can influence the topology of the tree. However, further studies are essential to validate this hypothesis.

Morphologically, some taxa that share similarities exhibit distinct phylogenies. For instance, *D. arecearum* shares a morphological resemblance with *D. dehongensis*, although they are phylogenetically distinct. Similarly, *D. eleiodoxae* shows morphological similarities to *D. tropica*, but resides in a separate clade in the phylogenetic tree. *Distoseptispora narathiwatensis* forms a sister clade with *D. saprophytica* despite the differences highlighted by the pairwise comparison of ITS, LSU and other genetic markers. These encompass 22/580 bp (3.8%) and 16/870 bp (1.8%) differences for ITS and LSU, respectively, excluding gaps. Moreover, distinctions in the morphology of conidiophores and the absence of acrogenous conidia further contribute to the differentiation between *D. narathiwatensis* and *D. saprophytica*. Our study confirmed the necessity of associating molecular data with morphological characters to distinguish them, as previously demonstrated in other studies (Su et al. 2016; Hyde et al. 2019; Luo et al. 2019; Yang et al. 2021; Ma et al. 2022).

To date, the majority of *Distoseptispora* species have been reported from China (42 species) and Thailand (23 species), primarily on dead plant materials in freshwater (44 species) and terrestrial (21 species) habitats. In most cases, the hosts are unknown. Although in 19 cases, their hosts have been identified, two of which have been reported from palm, including *D. palmarum* from *Cocos nucifera* and *D. licualae* from dead leaves of *Licuala glabra* in terrestrial habitats (Hyde et al. 2016, 2021; Su et al. 2016; Xia et al. 2017; Tibpromma et al. 2018; Yang et al. 2018; Luo et al. 2019; Phookamsak et al. 2019; Monkai et al. 2020; Phukhamsakda et al. 2020, 2022; Song et al. 2020; Sun et al. 2020; Dong et al.

2021; Li et al. 2021; Shen et al. 2021; Jayawardena et al. 2022; Ma et al. 2022; Zhai et al. 2022; Zhang et al. 2022; Konta et al. 2023; Liu et al. 2023). *Distoseptispora* species have been recorded as saprophytes and their reported limited geographic distribution (China and Thailand) is most likely due to increased attention by mycologists in these areas on saprophytic fungi in aquatic and terrestrial habitats. This study shows that there is much to be done in this regard. Ongoing and future investigations will reveal the diversity and functions of these microorganisms in this ecosystem.

## Acknowledgements

Omid Karimi would like to thank the National Science, Research and Innovation Fund: Thailand Science Research Innovation (Basic Research Fund 2023) entitled 'Taxonomy, Phylogeny and Chemo-profiling of selected families in *Xylariales* (662A01003)' for the financial support and Mr. Arttapon Walker for his valuable help in collecting samples. Shaun Pennycook is thanked for advising to give epithets for the new taxa. Omid Karimi and Raheleh Asghari would like to thank the Mae Fah Luang University Partial Scholarship for the doctoral degree programme and Mushroom Research Foundation. Kevin D. Hyde would like to thank the National Research Council of Thailand (NRCT) grant "Total fungal diversity in a given forest area with implications towards species numbers, chemical diversity and biotechnology" (grant no. N42A650547). Qirui Li would like to thank the China National Natural Science Foundation (31960005 and 32000009).

## Additional information

### Conflict of interest

The authors have declared that no competing interests exist.

### Ethical statement

No ethical statement was reported.

### Funding

The National Science, Research and Innovation Fund: Thailand Science Research Innovation (Basic Research Fund 2023) entitled 'Taxonomy, Phylogeny and chemo-profiling of selected families in *Xylariales* (662A01003), China National Natural Science Foundation (31960005 and 32000009), National Research Council of Thailand (NRCT) grant "Total fungal diversity in a given forest area with implications towards species numbers, chemical diversity and biotechnology" (grant no. N42A650547)

### Author contributions

Morphological identification, photo-plates, and phylogenetic analyzes were completed by Omid Karimi and Raheleh Asghari. The original draft was written by Omid Karimi, and K.W. Thilini Chethana, Antonio R.G. Farias, Saithong Kaewchai, Kevin D. Hyde, Qirui Li revised the paper.

### Author ORCIDs

Omid Karimi  <https://orcid.org/0000-0001-9652-2222>

K.W. Thilini Chethana  <https://orcid.org/0000-0002-5816-9269>

Antonio R.G. de Farias  <https://orcid.org/0000-0003-4768-1547>

Raheleh Asghari  <https://orcid.org/0009-0006-4897-5327>

Saithong Kaewchai  <https://orcid.org/0009-0004-9335-7697>

Kevin D. Hyde  <https://orcid.org/0000-0002-2191-0762>

Qirui Li  <https://orcid.org/0000-0001-8735-2890>

## Data availability

All of the data that support the findings of this study are available in the main text.

## References

- Afshari N, Gomes de Farias AR, Bhunjun CS, Phukhamsakda C, Hyde KD, Lumyong S (2023) *Distoseptispora dipteroearpi* sp. nov. (Distoseptisporaceae), a lignicolous fungus on decaying wood of *Dipteroearpus* in Thailand. *Current Research in Environmental & Applied Mycology* 13(1): 68–78. <https://doi.org/10.5943/cream/13/1/5>
- Boonyuen N, Sri-indrasutdhi V, Suetrong S, Sivichai S, Jones EBG (2012) *Annulatascus aquatorba* sp. nov., a lignicolous freshwater ascomycete from Sirindhorn Peat Swamp Forest, Narathiwat, Thailand. *Mycologia* 104(3): 746–757. <https://doi.org/10.3852/11-238>
- Calabon MS, Hyde KD, Jones EBG, Luo ZL, Dong W, Hurdeal VG, Gentekaki E, Rossi W, Leonardi M, Thiyagaraja V, Lestari AS, Shen HW, Bao DF, Boonyuen N, Zeng M (2022) Freshwater fungal numbers. *Fungal Diversity* 114(1): 3–235. <https://doi.org/10.1007/s13225-022-00503-2>
- Chen YJ, Jayawardena RS, Bhunjun CS, Harishchandra DL, Hyde KD (2020) *Pseudocercospora dypsidis* sp. nov. (Mycosphaerellaceae) on *Dypsis lutescens* leaves in Thailand. *Phytotaxa* 474(3): 218–234. <https://doi.org/10.11646/phytotaxa.474.3.2>
- Chethana KWT, Manawasinghe IS, Hurdeal VG, Bhunjun CS, Appadoo MA, Gentekaki E, Raspé O, Promputtha I, Hyde KD (2021) What are fungal species and how to delineate them? *Fungal Diversity* 109(1): 1–25. <https://doi.org/10.1007/s13225-021-00483-9>
- Choi YW, Hyde KD, Ho WWH (1999) Single spore isolation of fungi. *Fungal Diversity* 3: 29–38.
- Chou T, Xu W, Mukhtar I, Quan X, Jiang S, Huang R, Xie B, Xu W (2019) First report of leaf spot disease caused by *Colletotrichum siamense* on *Chrysalidocarpus lutescens* in China. *Plant Disease* 103(6): 1–5. <https://doi.org/10.1094/PDIS-11-18-2049-PDN>
- Crous PW, Wingfield MJ, Lombard L, Roets F, Swart WJ, Alvarado P, Carnegie AJ, Moreno G, Luangsaard J, Thangavel R, Alexandrova AV, Baseia IG, Bellanger JM, Bessette AE, Bessette AR, De la Peña-Lastra S, García D, Gené J, Pham THG, Heykoop M, Malysheva E, Malysheva V, Martín MP, Morozova OV, Noisripoom W, Overton BE, Rea AE, Sewall BJ, Smith ME, Smyth CW, Tasanathai K, Visagie CM, Adamčík S, Alves A, Andrade JP, Aninat MJ, Araújo RVB, Bordallo JJ, Bouffleur T, Baroncelli R, Barreto RW, Bolin J, Cabero J, Caboň M, Cafà G, Caffot MLH, Cai L, Carlavilla JR, Chávez R, de Castro RRL, Delgat L, Deschuyteneer D, Dios MM, Domínguez LS, Evans HC, Eyssartier G, Ferreira BW, Figueiredo CN, Liu F, Fournier J, Galli-Terasawa LV, Gil-Durán C, Glienke C, Gonçalves MFM, Gryta H, Guarro J, Himaman W, Hywel-Jones N, Iturrieta-González I, Ivanushkina NE, Jargeat P, Khalid AN, Khan J, Kiran M, Kiss L, Kochkina GA, Kolařík M, Kubátová A, Lodge DJ, Loizides M, Luque D, Manjón JL, Marbach PAS, Massola Jr NS, Mata M, Miller AN, Mongkolsamrit S, Moreau PA, Morte A, Mujic A, Navarro-Ródenas A, Németh MZ, Nóbrega TF, Nováková A, Olariaga I, Ozerskaya SM, Palma MA, Petters-Vandresen DAL, Piontelli E, Popov ES, Rodríguez A, Requejo Ó, Rodrigues ACM, Rong

- IH, Roux J, Seifert KA, Silva BDB, Sklenář F, Smith JA, Sousa JO, Souza HG, De Souza JT, Švec K, Tanchaud P, Tanney JB, Terasawa F, Thanakitpipattana D, Torres-Garcia D, Vaca I, Vaghefi N, van Iperen AL, Vasilenko OV, Verbeken A, Yilmaz N, Zamora JC, Zapata M, Jurjević Ž, Groenewald JZ (2019) Fungal Planet description sheets: 951–1041. *Persoonia* 43(1): 223–425. <https://doi.org/10.3767/persoonia.2019.43.06>
- Darriba D, Taboada GL, Doallo R, Posada D (2012) JModelTest 2: More models, new heuristics and parallel computing. *Nature Methods* 9(8): 772. <https://doi.org/10.1038/nmeth.2109>
- Dong W, Hyde HD, Jeewon R, Doilom M, Yu XD, Wang GN, Liu NG, Hu DM, Nalumpang S, Zhang H (2021) Towards a natural classification of annulatasceae-like taxa II: Introducing five new genera and eighteen new species from freshwater. *Mycosphere: Journal of Fungal Biology* 12(1): 1–88. <https://doi.org/10.5943/mycosphere/12/1/1>
- Dransfield J, Uhl NW, Asmussen CB, Baker WJ, Harley MM, Lewis CE (2008) *Genera Palmarum – The evolution and classification of the palms*. Royal Botanic Gardens, Kew, UK, London, 732 pp.
- El Meleigi MA, Omar AF, Al Rokibah AA, Alsohim A, Al Jamhan KA, Sukar NA (2019) Molecular identification and pathogenicity of phytophthora nicotianae-caused bud rot disease of washingtonia palms in saudi arabia and use of Lysobacter enzymes as a bioagent in an in vitro study. *Egyptian Journal of Biological Pest Control* 29(1): 1–9. <https://doi.org/10.1186/s41938-019-0107-y>
- Fröhlich J, Hyde KD (2000) *Palm microfungi*. Fungal Diversity Press, Hong Kong, 1–393.
- Fröhlich J, Hyde KD, Petrini O (2000) Endophytic fungi associated with palms. *Mycological Research* 104(10): 1202–1212. <https://doi.org/10.1017/S095375620000263X>
- Fujimoto K, Miura M, Kobayashi S, Simbolon H (2019) Habitat evolution of a peat swamp forest and belowground carbon sequestration during the Holocene along the coastal lowland in Central Sumatra, Indonesia. *Progress in Earth and Planetary Science* 6(1): 1–13. <https://doi.org/10.1186/s40645-019-0288-8>
- Hakim SS, Yuwati TW, Nurulita S (2017) Isolation of peat swamp forest foliar endophyte fungi as biofertiliser. *Journal of Wetlands Environmental Management* 5(1): 10–17. <https://doi.org/10.20527/jwem.v5i1.111>
- Hyde KD (1988) The genus *Linocarpon* from the mangrove palm *Nypa fruticans*. *Nippon Kingakkai Kaiho* 29: 338–350.
- Hyde KD, Taylor JE, Fröhlich J (2000) *Genera of Ascomycetes from palm*. Fungal Diversity Press, Hong Kong, 247 pp.
- Hyde KD, Hongsanan S, Jeewon R, Bhat DJ, McKenzie EHC, Jones EBG, Phookamsak R, Ariyawansa HA, Boonmee S, Zhao Q, Abdel-Aziz FA, Abdel-Wahab MA, Banmai S, Chomnunti P, Cui BK, Daranagama DA, Das K, Dayarathne MC, de Silva NI, Dissanayake AJ, Doilom M, Ekanayaka AH, Gibertoni TB, Góes-Neto A, Huang SK, Jayasiri SC, Jayawardena RS, Konta S, Lee HB, Li WJ, Lin CG, Liu JK, Lu YZ, Luo ZL, Manawasinghe IS, Manimohan P, Mapook A, Niskanen T, Norphanphoun C, Papizadeh M, Perera RH, Phukhamsakda C, Richter C, André ALCM, Drechsler-Santos ER, Senanayake IC, Tanaka K, Tennakoon TMDS, Thambugala KM, Tian Q, Tibpromma S, Thongbai B, Vizzini A, Wanasinghe DN, Wijayawardene NN, Wu HX, Yang J, Zeng XY, Zhang H, Zhang JF, Bulgakov TS, Camporesi E, Bahkali AH, Amoozegar MA, Araujo-Neta LS, Ammirati JF, Baghela A, Bhatt RP, Bojantchev D, Buyck B, da Silva GA, de Lima CLF, de Oliveira RJV, de Souza CAF, Dai YC, Dima B, Duong TT, Ercole E, Mafalda-Freire F, Ghosh A, Hashimoto A, Kamolhan S, Kang JC, Karunarathna SC, Kirk PM, Kytövuori I, Lantieri A, Liimatainen K, Liu ZY, Liu XZ, Lücking R, Medardi G, Mortimer PE, Nguyen TTT, Promputtha I, Raj KNA, Reck MA, Lumyong S, Shahzadeh-Fazeli SA,

- Stadler M, Soudi MR, Su HY, Takahashi T, Tangthirasunun N, Uniyal P, Wang Y, Wen TC, Xu JC, Zhang ZK, Zhao YC, Zhou JL, Zhu L (2016) Fungal diversity notes 367–490: Taxonomic and phylogenetic contributions to fungal taxa. *Fungal Diversity* 80: 1–270. <https://doi.org/10.1007/s13225-016-0373-x>
- Hyde KD, Tennakoon DS, Jeewon R, Bhat DJ, Maharachchikumbura SSN, Rossi W, Leonardi M, Lee HB, Mun HY, Houbraken J, Nguyen TTT, Jeon SJ, Frisvad JC, Wanasinghe DN, Lücking R, Aptroot A, Cáceres MES, Karunarathna SC, Hongsanan S, Phookamsak R, de Silva NI, Thambugala KM, Jayawardena RS, Senanayake IC, Boonmee S, Chen J, Luo ZL, Phukhamsakda C, Pereira OL, Abreu VP, Rosado AWC, Bart B, Randrianjohany E, Hofstetter V, Gibertoni TB, Soares AM da S, Plautz Jr HL, Sotão HMP, Xavier WKS, Bezerra JDP, de Oliveira TGL, de Souza-Motta CM, Magalhães OMC, Bundhun D, Harishchandra D, Manawasinghe IS, Dong W, Zhang SN, Bao DF, Samarakoon MC, Pem D, Karunarathna A, Lin CG, Yang J, Perera RH, Kumar V, Huang SK, Dayarathne MC, Ekanayaka AH, Jayasiri SC, Xiao Y, Konta S, Niskanen T, Liimatainen K, Dai YC, Ji XH, Tian XM, Mešić A, Singh SK, Phutthacharoen K, Cai L, Sorvongxay T, Thiyagaraja V, Norphanphoun C, Chaiwan N, Lu YZ, Jiang HB, Zhang JF, Abeywickrama PD, Aluthmuhandiram JVS, Brahmanage RS, Zeng M, Chethana T, Wei D, Réblová M, Fournier J, Nekvindová J, do Nascimento Barbosa R, dos Santos JEF, de Oliveira NT, Li G-J, Ertz D, Shang Q-J, Phillips AJL, Kuo C-H, Camporesi E, Bulgakov TS, Lumyong S, Jones EBG, Chomnunti P, Gentekaki E, Bungartz F, Zeng X-Y, Fryar S, Tkalčec Z, Liang J, Li G, Wen T-C, Singh PN, Gafforov Y, Promputtha I, Yasanthika E, Goonasekara ID, Zhao R-L, Zhao Q, Kirk PM, Liu J-K, Yan JY, Mortimer PE, Xu J, Doilom M (2019) Fungal diversity notes 1036–1150: Taxonomic and phylogenetic contributions on genera and species of fungal taxa. *Fungal Diversity* 96(1): 1–242. <https://doi.org/10.1007/s13225-019-00429-2>
- Hyde KD, de Silva NI, Jeewon R, Bhat DJ, Phookamsak R, Doilom M, Boonmee S, Jayawardena RS, Maharachchikumbura SSN, Senanayake IC, Manawasinghe IS, Liu NG, Abeywickrama PD, Chaiwan N, Karunarathna A, Pem D, Lin CG, Sysouphanthong P, Luo ZL, Wei DP, Wanasinghe DN, Norphanphoun C, Tennakoon DS, Samarakoon MC, Jayasiri SC, Jiang HB, Zeng XY, Li JF, Wijesinghe SN, Devadatha B, Goonasekara ID, Brahmanage RS, Yang EF, Aluthmuhandiram JVS, Dayarathne MC, Marasinghe DS, Li WJ, Dissanayake LS, Dong W, Huanraluek N, Lumyong S, Liu JK, Karunarathna SC, Jones EBG, Al-Sadi AM, Xu JC, Harishchandra D, Sarma VV, Bulgakov TS (2020) AJOM new records and collections of fungi: 1–100. *Asian Journal of Mycology* 3(1): 22–294. <https://doi.org/10.5943/ajom/3/1/3>
- Hyde KD, Suwannarach N, Jayawardena RS, Manawasinghe IS, Liao CF, Doilom M, Cai L, Zhao P, Buyck B, Phukhamsakda C, Su WX, Fu YP, Li Y, Zhao RL, He MQ, Li JX, Tibpromma S, Lu L, Tang X, Kang JC, Ren GC, Gui H, Hofstetter V, Ryoo R, Antonín V, Hurdeal VG, Gentekaki E, Zhang JY, Lu YZ, Senanayake IC, Yu FM, Zhao Q, Bao DF (2021) Mycosphere notes 325–344 – Novel species and records of fungal taxa from around the world. *Mycosphere* 12(1): 1101–1156. <https://doi.org/10.5943/mycosphere/12/1/14>
- Jackson CR, Liew KC, Yule CM (2009) Structural and functional changes with depth in microbial communities in a tropical malaysian peat swamp forest. *Microbial Ecology* 57(3): 402–412. <https://doi.org/10.1007/s00248-008-9409-4>
- Jayasiri SC, Hyde KD, Ariyawansa HA, Bhat J, Buyck B, Cai L, Dai YC, Abd-Elsalam KA, Ertz D, Hidayat I, Jeewon R, Jones EBG, Bahkali AH, Karunarathna SC, Liu JK, Luangsa-ard JJ, Lumbsch HT, Maharachchikumbura SSN, McKenzie EHC, Moncalvo JM, Ghobad-Nejhad M, Nilsson H, Pang KL, Pereira OL, Phillips AJL, Raspé O, Rollins AW,

- Romero AI, Etayo J, Selçuk F, Stephenson SL, Suetrong S, Taylor JE, Tsui CKM, Vizzini A, Abdel-Wahab MA, Wen TC, Boonmee S, Dai DQ, Daranagama DA, Dissanayake AJ, Ekanayaka AH, Fryar SC, Hongsanan S, Jayawardena RS, Li WJ, Perera RH, Phookamsak R, de Silva NI, Thambugala KM, Tian Q, Wijayawardene NN, Zhao RL, Zhao Q, Kang JC, Promputtha I (2015) The Faces of Fungi database: Fungal names linked with morphology, phylogeny and human impacts. *Fungal Diversity* 74(1): 3–18. <https://doi.org/10.1007/s13225-015-0351-8>
- Jayawardena RS, Hyde KD, Wang S, Sun YR, Suwannarach N, Sysouphanthong P, Abdel-Wahab MA, Abdel-Aziz FA, Abeywickrama PD, Abreu VP, Armand A, Aptroot A, Bao DF, Begerow D, Bellanger JM, Bezerra JDP, Bundhun D, Calabon MS, Cao T, Cantillo T, Carvalho JLVR, Chaiwan N, Chen CC, Courtecuisse R, Cui BK, Damm U, Denchev CM, Denchev TT, Deng CY, Devadatha B, de Silva NI, dos Santos LA, Dubey NK, Dumez S, Fernandez HS, Firmino AL, Gafforov Y, Gajanayake AJ, Gomdola D, Gunaseelan S, Shucheng-He, Htet ZH, Kaliyaperumal M, Kemler M, Kezo K, Kularathnagen ND, Leonardi M, Li J-P, Liao C, Liu S, Loizides M, Luangharn T, Ma J, Madrid H, Mahadevakumar S, Maharachchikumbura SSN, Manamgoda DS, Martín MP, Mekala N, Moreau P-A, Mu Y-H, Pahoua P, Pem D, Pereira OL, Phonrob W, Phukhamsakda C, Raza M, Ren G-C, Rinaldi AC, Rossi W, Samarakoon BC, Samarakoon MC, Sarma VV, Senanayake IC, Singh A, Souza MF, Souza-Motta CM, Spielmann AA, Su W, Tang X, Tian XG, Thambugala KM, Thongklang N, Tennakoon DS, Wannathes N, Wei DP, Welti S, Wijesinghe SN, Yang H, Yang Y, Yuan H-S, Zhang H, Zhang J, Balasuriya A, Bhunjun CS, Bulgakov TS, Cai L, Camporesi E, Chomnunti P, Deepika YS, Doilom M, Duan W-J, Han S-L, Huanraluek N, Jones EBG, Lakshmidhevi N, Li Y, Lumyong S, Luo Z-L, Khuna S, Kumla J, Manawasinghe IS, Mapook A, Punyaboon W, Tibpromma S, Lu Y-Z, Yan JY, Wang Y (2022) Fungal diversity notes 1512–1610: Taxonomic and phylogenetic contributions on genera and species of fungal taxa. *Fungal Diversity* 117(1): 1–272. <https://doi.org/10.1007/s13225-022-00513-0>
- Katoh K, Rozewicki J, Yamada KD (2019) MAFFT online service: Multiple sequence alignment, interactive sequence choice and visualisation. *Briefings in Bioinformatics* 20(4): 1160–1166. <https://doi.org/10.1093/bib/bbx108>
- Kinge TR, Moforcha ZL, Mih AM (2019) Cultural Variability of *Fusarium oxysporum* f. sp. *elaedis* Isolates from Oil Palm in South Western Cameroon and Sensitivity to Four Plant Extracts. *Plant Pathology & Quarantine Journal of Fungal Biology* 9(1): 116–127. <https://doi.org/10.5943/ppq/9/1/10>
- Konta S, Phillips AJ, Bahkali AH, Jones EBG, Eungwanichayapant DP, Hyde KD, Boonmee S (2016a) Botryosphaeriaceae from palms in Thailand-*Barriopsis archontophoenicis* sp. nov, from *Archontophoenix alexandrae*. *Mycosphere: Journal of Fungal Biology* 7(7): 921–932. <https://doi.org/10.5943/mycosphere/si/1b/1>
- Konta S, Hongsanan S, Phillips AJ, Jones EB, Boonmee S, Hyde KD (2016b) Botryosphaeriaceae from palms in Thailand II-two new species of *Neodeightonia*, *N. rattanica* and *N. rattanicola* from *Calamus* (rattan palm). *Mycosphere: Journal of Fungal Biology* 7(7): 950–961. <https://doi.org/10.5943/mycosphere/si/1b/6>
- Konta S, Hongsanan S, Tibpromma S, Thongbai B, Maharachchikumbura SSN, Bahkali AH, Hyde KD, Boonmee S (2016c) An advance in the endophyte story: *Oxydothidaceae* fam. nov. with six new species of *Oxydothis*. *Mycosphere: Journal of Fungal Biology* 7(9): 1425–1446. <https://doi.org/10.5943/mycosphere/7/9/15>
- Konta S, Hongsanan S, Liu JK, Eungwanichayapant PD, Jeewon R, Hyde KD, Maharachchikumbura SSN, Boonmee S (2017) *Leptospora* (*Leptosporaceae* fam. nov.) and *Linocarpon* and *Neolinocarpon* (*Linocarpaceae* fam. nov.) are accommodated

- in Chaetosphaeriales. *Mycosphere: Journal of Fungal Biology* 8(10): 1943–1974. <https://doi.org/10.5943/mycosphere/8/10/16>
- Konta S, Maharachchikumbura SSN, Senanayake IC, McKenzie EHC, Stadler M, Boonmee S, Phookamsak R, Jayawardena RS, Senwana C, Hyde KD, Elgorban AM, Eungwanichayapant PD (2020a) A new genus *Allodiatrype*, five new species and a new host record of diatrypaceous fungi from palms (Arecaceae). *Mycosphere: Journal of Fungal Biology* 11(1): 239–268. <https://doi.org/10.5943/mycosphere/11/1/4>
- Konta S, Hyde KD, Eungwanichayapant PD, Doilom M, Tennakoon DS, Senwana C, Boonmee S (2020b) *Fissuroma* (Aigialaceae: Pleosporales) appears to be hyperdiverse on Arecaceae: evidence from two new species from Southern Thailand. *Acta Botanica Brasiliensis* 34(2): 384–393. <https://doi.org/10.1590/0102-33062020abb0021>
- Konta S, Hyde KD, Phookamsak R, Xu JC, Maharachchikumbura SSN, Daranagama DA, McKenzie EHC, Boonmee S, Tibpromma S, Eungwanichayapant PD, Samarakoon MC (2020c) Polyphyletic genera in Xylariaceae (Xylariales): *Neoxylaria* gen. nov. and *Stilbohypoxyton*. *Mycosphere: Journal of Fungal Biology* 11(1): 2629–2651. <https://doi.org/10.5943/mycosphere/11/1/17>
- Konta S, Hyde KD, Karunarathna SC, Mapook A, Senwana C, Dauner LAP, Nanayakkara CM, Xu J, Tibpromma S, Lumyong S (2021a) Multigene phylogeny and morphology reveal *Haplohelminthosporium* gen. nov. and *Helminthosporiella* gen. nov. associated with palms in Thailand and a checklist for *Helminthosporium* reported worldwide. *Life (Basel, Switzerland)* 11(5): 454. <https://doi.org/10.3390/life11050454>
- Konta S, Hyde KD, Eungwanichayapant PD, Karunarathna SC, Samarakoon MC, Xu J, Dauner LAP, Aluthwattha ST, Lumyong S, Tibpromma S (2021b) Multigene phylogeny reveals *Haploanthostomella elaeidis* gen. et sp. nov. and familial replacement of *Endocalyx* (Xylariales, Sordariomycetes, Ascomycota). *Life (Basel, Switzerland)* 11(6): 486. <https://doi.org/10.3390/life11060486>
- Konta S, Tibpromma S, Karunarathna SC, Samarakoon MC, Steven LS, Mapook A, Boonmee S, Senwana C, Balasuriya A, Eungwanichayapant PD, Hyde KD (2023) Morphology and multigene phylogeny reveal ten novel taxa in Ascomycota from terrestrial palm substrates (Arecaceae) in Thailand. *Mycosphere* 14(1): 107–152. <https://doi.org/10.5943/mycosphere/14/1/2>
- Lampela M, Jauhiainen J, Kämäri I, Koskinen M, Tanhuanpää T, Valkeapää A, Vasander H (2016) Ground surface microtopography and vegetation patterns in a tropical peat swamp forest. *Catena* 139: 127–136. <https://doi.org/10.1016/j.catena.2015.12.016>
- Lemoine F, Correia D, Lefort V, Doppelt-Azeroual O, Mareuil F, Cohen-Boulakia S, Gascuel O (2019) NGPhylogeny.fr: New generation phylogenetic services for non-specialists. *Nucleic Acids Research* 47(W1): W260–W265. <https://doi.org/10.1093/nar/gkz303>
- Li W-L, Liu Z-P, Zhang T, Dissanayake AJ, Luo Z-L, Su H-Y, Liu J-K (2021) Additions to *Distoseptispora* (Distoseptisporaceae) associated with submerged decaying wood in China. *Phytotaxa* 520(1): 75–86. <https://doi.org/10.11646/phytotaxa.520.1.5>
- Liu YJ, Whelen S, Hall BD (1999) Phylogenetic relationships among Ascomycetes: Evidence from an RNA polymerase II subunit. *Molecular Biology and Evolution* 16(12): 1799–1808. <https://doi.org/10.1093/oxfordjournals.molbev.a026092>
- Liu JK, Chomnunti P, Cai L, Phookamsak R, Chukeatirote E, Jones EBG, Moslem M, Hyde KD (2010) Phylogeny and morphology of *Neodeightonia palmicola* sp. nov. from palms. *Sydowia* 62: 261–276.
- Liu J, Hu Y, Luo X, Xu Z, Castañeda-Ruiz RF, Xia J, Zhang X, Zhang L, Cui R, Ma J (2023) Morphological and Phylogenetic Analyses Reveal Three New Species of

- Distoseptispora* (Distoseptisporaceae, Distoseptisporales) from Yunnan, China. *Journal of Fungi* 9(4): 470. <https://doi.org/10.3390/jof9040470>
- Lumyong S, Techa W, Lumyong P, McKenzie EHC, Hyde KD (2009) Endophytic fungi from *calamus kerrianus* and *Wallichia caryotoides* (Arecaceae) at Doi Suthep-Pui National Park, Thailand. *Warasan Khana Witthayasat Maha Witthayalai Chiang Mai* 36: 158–167.
- Luo ZL, Hyde KD, Liu JK, Bhat DJ, Bao DF, Li WL, Su HY (2018) Lignicolous freshwater fungi from China II: Novel *Distoseptispora* (Distoseptisporaceae) species from northwestern Yunnan Province and a suggested unified method for studying lignicolous freshwater fungi. *Mycosphere* 9(3): 444–461. <https://doi.org/10.5943/mycosphere/9/3/2>
- Luo ZL, Hyde KD, Liu JK, Maharachchikumbura SSN, Jeewon R, Bao DF, Bhat DJ, Lin CG, Li WL, Yang J, Liu NG, Lu YZ, Jayawardena RS, Li JF, Su HY (2019) Freshwater Sordariomycetes. *Fungal Diversity* 99(1): 451–660. <https://doi.org/10.1007/s13225-019-00438-1>
- Ma J, Zhang JY, Xiao XJ, Xiao YP, Tang X, Boonmee S, Kang JC, Lu YZ (2022) Multi-gene Phylogenetic Analyses Revealed Five New Species and Two New Records of Distoseptisporales from China. *Journal of Fungi (Basel, Switzerland)* 8(11): 1202. <https://doi.org/10.3390/jof8111202>
- Maharachchikumbura SSN, Chen Y, Ariyawansa HA, Hyde KD, Haelewaters D, Perera RH, Samarakoon MC, Wanasinghe DN, Bustamante DE, Liu JK, Lawrence DP, Cheewangkoon R, Stadler M (2021) Integrative approaches for species delimitation in Ascomycota. *Fungal Diversity* 109(1): 155–179. <https://doi.org/10.1007/s13225-021-00486-6>
- Mapook A, Macabeo APG, Thongbai B, Hyde KD, Stadler M (2020) Polyketide-derived secondary metabolites from a Dothideomycetes fungus, *Pseudopalawania siamensis* gen. et sp. nov., (Muyocoprionales) with antimicrobial and cytotoxic activities. *Biomolecules* 10(4): 569. <https://doi.org/10.3390/biom10040569>
- Marin-Felix Y, Hernández-Restrepo M, Iturrieta-González I, García D, Gené J, Groenewald JZ, Cai L, Chen Q, Quaedvlieg W, Schumacher RK, Taylor PWJ, Ambers C, Bonthond G, Edwards J, Krueger-Hadfield SA, Luangsa-ard JJ, Morton L, Moslemi A, Sandoval-Denis M, Tan YP, Thangavel R, Vaghefi N, Cheewangkoon R, Crous PW (2019) Genera of phytopathogenic fungi: GOPHY 3. *Studies in Mycology* 94(1): 1–124. <https://doi.org/10.1016/j.simyco.2019.05.001>
- Miller MA, Pfeiffer W, Schwartz T (2010) Creating the CIPRES Science Gateway for inference of large phylogenetic trees. *Gateway Computing Environments Workshop, GCE 2010*: 1–8. <https://doi.org/10.1109/GCE.2010.5676129>
- Minayeva TY, Sirin AA (2012) Peatland biodiversity and climate change. *Biology Bulletin Reviews* 2(2): 164–175. <https://doi.org/10.1134/S207908641202003X>
- Monkai J, Boonmee S, Ren GC, Wei DP, Phookamsak R, Mortimer PE (2020) *Distoseptispora hydei* sp. nov. (Distoseptisporaceae), a novel lignicolous fungus on decaying bamboo in Thailand. *Phytotaxa* 459(2): 93–107. <https://doi.org/10.11646/phytotaxa.459.2.1>
- Page SE, Rieley JO, Shotyk ØW, Weiss D (1999) Interdependence of peat and vegetation in a tropical peat swamp forest. *Philosophical Transactions of the Royal Society of London, Series B, Biological Sciences* 354(1391): 1885–1897. <https://doi.org/10.1098/rstb.1999.0529>
- Page SE, Rieley JO, Banks CJ (2011) Global and regional importance of the tropical peatland carbon pool. *Global Change Biology* 17(2): 798–818. <https://doi.org/10.1111/j.1365-2486.2010.02279.x>

- Palmweb (2023) Palms of the World Online. <https://palmweb.org/node/4?q=node/5> [Accessed on 27 May 2023]
- Parish F, Sirin A, Charman D, Joosten H, Minayeva T, Silvius M, Stringer L (2008) Assessment on Peatlands, Biodiversity, and Climate Change: Main Report. Kuala Lumpur: Global Environment Centre & Wetlands International. [http://www.imcg.net/media/download\\_gallery/books/assessment\\_peatland.pdf](http://www.imcg.net/media/download_gallery/books/assessment_peatland.pdf)
- Phookamsak R, Hyde KD, Jeewon R, Bhat DJ, Jones EBG, Maharachchikumbura SSN, Raspé O, Karunarathna SC, Wanasinghe DN, Hongsanan S, Doilom M, Tennakoon DS, Machado AR, Firmino AL, Ghosh A, Karunarathna A, Mešić A, Dutta AK, Thongbai B, Devadatha B, Norphanphoun C, Senwannan C, Wei D, Pem D, Ackah FK, Wang G-N, Jiang H-B, Madrid H, Lee HB, Goonasekara ID, Manawasinghe IS, Kušan I, Cano J, Gené J, Li J, Das K, Acharya K, Raj KNA, Latha KPD, Chethana KWT, He M-Q, Dueñas M, Jadan M, Martín MP, Samarakoon MC, Dayarathne MC, Raza M, Park MS, Telleria MT, Chaiwan N, Matočec N, de Silva NI, Pereira OL, Singh PN, Manimohan P, Uniyal P, Shang Q-J, Bhatt RP, Perera RH, Alvarenga RLM, Nogal-Prata S, Singh SK, Vadthanarat S, Oh S-Y, Huang S-K, Rana S, Konta S, Paloi S, Jayasiri SC, Jeon SJ, Mehmood T, Gibertoni TB, Nguyen TTT, Singh U, Thiyagaraja V, Sarma VV, Dong W, Yu X-D, Lu Y-Z, Lim YW, Chen Y, Tkalčec Z, Zhang Z-F, Luo Z-L, Daranagama DA, Thambugala KM, Tibpromma S, Camporesi E, Bulgakov TS, Dissanayake AJ, Senanayake IC, Dai DQ, Tang L-Z, Khan S, Zhang H, Promputtha I, Cai L, Chomnunti P, Zhao R-L, Lumyong S, Boonmee S, Wen T-C, Mortimer PE, Xu J (2019) Fungal diversity notes 929–1035: Taxonomic and phylogenetic contributions on genera and species of fungi. *Fungal Diversity* 95(1): 1–273. <https://doi.org/10.1007/s13225-019-00421-w>
- Phukhamsakda C, McKenzie EHC, Phillips AJL, Jones EBG, Bhat DJ, Stadler M, Bhunjun CS, Wanasinghe DN, Thongbai B, Camporesi E, Ertz D, Jayawardena RS, Perera RH, Ekanayake AH, Tibpromma S, Doilom M, Xu J, Hyde KD (2020) Microfungi associated with *Clematis* (Ranunculaceae) with an integrated approach to delimiting species boundaries. *Fungal Diversity* 102(1): 1–203. <https://doi.org/10.1007/s13225-020-00448-4>
- Phukhamsakda C, Nilsson RH, Bhunjun CS, de Farias ARG, Sun YR, Wijesinghe SN, Raza M, Bao DF, Lu L, Tibpromma S, Dong W, Tennakoon DS, Tian XG, Xiong YR, Karunarathna SC, Cai L, Luo ZL, Wang Y, Manawasinghe IS, Camporesi E, Kirk PM, Promputtha I, Kuo CH, Su HY, Doilom M, Li Y, Fu YP, Hyde KD (2022) The numbers of fungi: contributions from traditional taxonomic studies and challenges of metabarcoding. *Fungal Diversity* 114: 327–386. <https://doi.org/10.1007/s13225-022-00502-3>
- Pilantanapak A, Jones EBG, Eaton RA (2005) Marine fungi on *Nypa fruticans* in Thailand. *Botanica Marina* 48(5–6): 365–373. <https://doi.org/10.1515/bot.2005.049>
- Pinnoi A, Jones EBG, McKenzie EHC, Hyde KD (2003a) Aquatic fungi from peat swamp palms: *Unisetosphaeria penguinoides* gen. et sp. nov., and three new *Dactylaria* species. *Mycoscience* 44(5): 377–382. <https://doi.org/10.1007/S10267-003-0124-1>
- Pinnoi A, McKenzie EHC, Jones EBG, Hyde KD (2003b) Palm fungi from Thailand: *Custingophora undulatistipes* sp. nov. and *Vanakripa minutiellipsoidea* sp. nov. *Nova Hedwigia* 77(1–2): 213–219. <https://doi.org/10.1127/0029-5035/2003/0077-0213>
- Pinnoi A, Pinruan U, Hyde KD, McKenzie EHC, Lumyong S (2004) *Submersisphaeria palmae* sp. nov. with a key to species, and notes on *Helicoubsisia*. *Sydowia* 56: 72–78.
- Pinnoi A, Lumyong S, Hyde KD, Jones EBG (2006) Biodiversity of fungi on the palm *Eleiodoxa conferta* in Sirindhorn peat swamp forest, Narathiwat, Thailand. *Fungal Diversity* 22: 205–218.
- Pinnoi A, Phongpaichit S, Hyde KD, Jones EBG (2009) Biodiversity of fungi on *Calamus* (Palmae) in Thailand. *Cryptogamie. Mycologie* 30: 181–190.

- Pinnoi A, Phongpaichit P, Jeewon R, Tang AMC, Hyde KD, Jones EBG (2010) Phylogenetic relationships of *Astrocystis eleiodoxae* sp. nov. (Xylariaceae). *Mycosphere* 1: 1–9.
- Pinruan U, Jones EBG, Hyde KD (2002) Aquatic fungi from peat swamp palms: *Jahnula appendiculata* sp. nov. *Sydowia* 54: 242–247.
- Pinruan U, Sakayaroj J, Jones EBG, Hyde KD (2004a) Aquatic fungi from peat swamp palms: *Phruensis brunneispora* gen. et sp. nov. and its hyphomycete anamorph. *Mycologia* 96(5): 1163–1170. <https://doi.org/10.1080/15572536.2005.11832916>
- Pinruan U, Sakayaroj J, Jones EBG, Hyde KD (2004b) *Flammispora* gen. nov., a new freshwater ascomycete from decaying palm leaves. *Studies in Mycology* 50: 381–386.
- Pinruan U, McKenzie EHC, Jones EBG, Hyde KD (2004c) Two new species of *Stachybotrys*, and a key to the genus. *Fungal Diversity* 17: 145–157.
- Pinruan U, Lumyong S, McKenzie EHC, Jones EBG, Hyde KD (2004d) Three new species of *Craspedodidymum* from palm in Thailand. *Mycoscience* 45(3): 177–180. <https://doi.org/10.1007/S10267-003-0173-5>
- Pinruan U, Hyde KD, Lumyong S, McKenzie EHC, Jones EBG (2007) Occurrence of fungi on tissues of the peat swamp palm *Licuala longicalycata*. *Fungal Diversity* 25: 157–173.
- Pinruan U, Sakayaroj J, Hyde KD, Jones EBG (2008) *Thailandiomyces bisetulosus* gen. et sp. nov. (Diaporthales, Sordariomycetidae, Sordariomycetes) and its anamorph *Craspedodidymum*, is described based on nuclear SSU and LSU rDNA sequences. *Fungal Diversity* 29: 89–98.
- Pinruan U, Rungjindamai N, Choeyklin R, Lumyong S, Hyde KD, Jones EBG (2010a) Occurrence and diversity of basidiomycetous endophytes from the oil palm, *Elaeis guineensis* in Thailand. *Fungal Diversity* 41(1): 71–88. <https://doi.org/10.1007/s13225-010-0029-1>
- Pinruan U, Rungjindamai N, Sakayaroj J, Lumyong S, Hyde KD, Jones EBG (2010b) *Baipadisphaeria* gen. nov., a freshwater ascomycete (Hypocreales, Sordariomycetes) from decaying palm leaves in Thailand. *Mycosphere* 1: 53–63.
- Pinruan U, Pinnoi A, Hyde KD, Jones EBG (2014) Tropical peat swamp fungi with special reference to palms. *Freshwater Fungi and Fungal-like Organisms*, Dee Gruyter Press, Berlin, 371–386. <https://doi.org/10.1515/9783110333480.371>
- Posa MRC, Wijedasa LS, Corlett RT (2011) Biodiversity and conservation of tropical peat swamp forests. *Bioscience* 61(1): 49–57. <https://doi.org/10.1525/bio.2011.61.1.10>
- POWO (2023) Plants of the World Online. Facilitated by the Royal Botanic Gardens, Kew. <http://www.plantsoftheworldonline.org/> [Accessed on 27 May 2023]
- Prentice RC (2011) The Peatland Biodiversity Management Toolbox: A Handbook for the Conservation and Management of Peatland Biodiversity in Southeast Asia. A Compilation. ASEAN Peatland Forests Project: Rehabilitation and Sustainable Use of Peatland Forests in Southeast Asia. Association of Southeast Asian Nations (ASEAN) and the Global Environment Centre. [http://www.aseanpeat.net/ebook/toolbox/The\\_Peatland\\_Biodiversity\\_Management\\_Toolbox.Pdf](http://www.aseanpeat.net/ebook/toolbox/The_Peatland_Biodiversity_Management_Toolbox.Pdf)
- Rambaut A (2012) FigTree, version 1.4.2. University of Edinburgh, Edinburgh.
- Ratnayake AS (2020) Characteristics of Lowland Tropical Peatlands: Formation, Classification, and Decomposition. *Journal of Tropical Forestry and Environment* 10(1): 1–16. <https://doi.org/10.31357/jtfe.v10i1.4685>
- Rehner SA (2001) Primers for elongation factor 1-alpha (EF1-alpha).
- Rehner SA, Samuels GJ (1994) Taxonomy and phylogeny of *Gliocladium* analysed from nuclear large subunit ribosomal DNA sequences. *Mycological Research* 98(6): 625–634. [https://doi.org/10.1016/S0953-7562\(09\)80409-7](https://doi.org/10.1016/S0953-7562(09)80409-7)

- Rieley JO (2016) Biodiversity of Tropical Peatland in Southeast Asia. 15<sup>th</sup> International Peat Congress, 707–711. <https://peatlands.org/assets/uploads/2019/06/ipc16p707-711a213rieley.pdf>
- Shen H-W, Bao D-F, Hyde KD, Su H-Y, Bhat DJ, Luo Z-L (2021) Two novel species and two new records of *Distoseptispora* from freshwater habitats in China and Thailand. *MycKeys* 84: 79–101. <https://doi.org/10.3897/mycokeys.84.71905>
- Shuhada SN, Salim S, Nobilly F, Lechner AM, Azhar B (2020) Conversion of peat swamp forest to oil palm cultivation reduces the diversity and abundance of macrofungi. *Global Ecology and Conservation* 23: e01122. <https://doi.org/10.1016/j.gecco.2020.e01122>
- Sivichai S, Boonyuen N (2010) *Jahnula morakotii* sp. nov. and *J. appendiculata* from a peat swamp in Thailand. *Mycotaxon* 112(1): 475–481. <https://doi.org/10.5248/112.475>
- Song H, El Sheikha AF, Zhai Z, Zhou J-P, Chen M-H, Huo G-H, Huang X-G, Hu D-M (2020) *Distoseptispora longispora* sp. nov. from freshwater habitats in China. *Mycotaxon* 135(3): 513–523. <https://doi.org/10.5248/135.513>
- Stamatakis A (2014) RAxML version 8: A tool for phylogenetic analysis and post-analysis of large phylogenies. *Bioinformatics (Oxford, England)* 30(9): 1312–1313. <https://doi.org/10.1093/bioinformatics/btu033>
- Su HY, Hyde KD, Maharachchikumbura SSN, Ariyawansa HA, Luo Z, Promputtha I, Tian Q, Lin C, Shang Q, Zhao Y, Chai H, Liu XY, Bahkali AH, Bhat DJ, McKenzie EHC, Zhou D (2016) The families Distoseptisporaceae fam. nov., Kirschsteinotheliaceae, Sporormiaceae and Torulaceae, with new species from freshwater in Yunnan Province, China. *Fungal Diversity* 80(1): 375–409. <https://doi.org/10.1007/s13225-016-0362-0>
- Sun Y, Goonasekara ID, Thambugala KM, Jayawardena RS, Wang Y, Hyde KD (2020) *Distoseptispora bambusae* sp. nov. (Distoseptisporaceae) on bamboo from China and Thailand. *Biodiversity Data Journal* 8: e53678. <https://doi.org/10.3897/BDJ.8.e53678>
- Taylor JE, Hyde KD (2003) Microfungi of tropical and temperate palms. Fungal Diversity Press, Hong Kong, 459 pp.
- Taylor JE, Hyde KD, Jones EBG (1999) Endophytic fungi associated with the temperate palm, *Trachycarpus fortunei*, within and outside its natural geographic range. *The New Phytologist* 142(2): 335–346. <https://doi.org/10.1046/j.1469-8137.1999.00391.x>
- Tian X, Tibpromma S, Karunarathna SC, Dai D, Lu Y, Mapook A, Jayawardena RS (2022) A new species and a new host record of *Pseudoberkleasium* (Pseudoberkleasmiaceae, Dothideomycetes) from *Cocos nucifera* and *Zea mays* in northern Thailand. *Phytotaxa* 547(3): 232–242. <https://doi.org/10.11646/phytotaxa.547.3.2>
- Tibpromma S, Hyde KD, McKenzie EHC, Bhat DJ, Phillips AJL, Wanasinghe DN, Samarakoon MC, Jayawardena RS, Dissanayake AJ, Tennakoon DS, Doilom M, Phookamsak R, Tang AMC, Xu J, Mortimer PE, Promputtha I, Maharachchikumbura SSN, Khan S, Karunarathna SC (2018) Fungal diversity notes 840–928: Microfungi associated with Pandanaceae. *Fungal Diversity* 93(1): 1–160. <https://doi.org/10.1007/s13225-018-0408-6>
- UNEP (2022) Global Peatlands Assessment – The State of the World’s Peatlands: Evidence for action toward the conservation, restoration, and sustainable management of peatlands. Main Report. Global Peatlands Initiative. United Nations Environment Programme, Nairobi.
- Vaidya G, Lohman DJ, Meier R (2011) SequenceMatrix: Concatenation software for the fast assembly of multigene datasets with character set and codon information. *Cladistics* 27(2): 171–180. <https://doi.org/10.1111/j.1096-0031.2010.00329.x>

- Vilgalys R, Hester M (1990) Rapid genetic identification and mapping of enzymatically amplified ribosomal DNA from several *Cryptococcus* species. *Journal of Bacteriology* 172(8): 4238–4246. <https://doi.org/10.1128/jb.172.8.4238-4246.1990>
- Voglmayr H, Yule CM (2006) *Polyancora globosa* gen. sp. nov., an aeroaquatic fungus from Malaysian peat swamp forests. *Mycological Research* 110(10): 1242–1252. <https://doi.org/10.1016/j.mycres.2006.07.001>
- White TJ, Bruns T, Lee S, Taylor J (1990) Amplification and direct sequencing of fungal ribosomal RNA genes for phylogenetics. In: Innis MA, Gelfand DH, Sninsky JJ, White TJ (Eds) *PCR protocols: a guide to methods and applications*. Academic Press, San Diego, 315–322. <https://doi.org/10.1016/B978-0-12-372180-8.50042-1>
- Wijayawardene NN, Hyde KD, Dai DQ, Sánchez-García M, Goto BT, Saxena RK, Erdoğdu M, Selçuk F, Rajeshkumar KC, Aptroot A, Błaszczowski J, Boonyuen N, da Silva GA, de Souza FA, Dong W, Ertz D, Haelewaters D, Jones EBG, Karunaratna SC, Kirk PM, Kukwa M, Kumla J, Leontyev DV, Lumbsch HT, Maharachchikumbura SSN, Marguno F, Martínez-Rodríguez P, Mešić A, Monteiro JS, Oehl F, Pawłowska J, Pem D, Pfliegler WP, Phillips AJL, Pošta A, He MQ, Li JX, Raza M, Sruthi OP, Suetrong S, Suwannarach N, Tedersoo L, Thiyagaraja V, Tibpromma S, Tkáčec Z, Tokarev YS, Wanasinghe DN, Wijesundara DSA, Wimalaseena SDMK, Madrid H, Zhang GQ, Gao Y, Sánchez-Castro I, Tang LZ, Stadler M, Yurkov A, Thines M (2022) Outline of Fungi and fungus-like taxa – 2021. *Mycosphere: Journal of Fungal Biology* 13(1): 53–453. <https://doi.org/10.5943/mycosphere/13/1/2>
- Wikee S, Lombard L, Nakashima C, Motohashi K, Chukeatirote E, Cheewangkoon R, McKenzie EHC, Hyde KD, Crous PW (2013) A phylogenetic re-evaluation of *Phyllosticta* (Botryosphaerales). *Studies in Mycology* 76: 1–29. <https://doi.org/10.3114/sim0019>
- Xia JW, Ma YR, Li Z, Zhang XG (2017) Acrodictys-like wood decay fungi from southern China, with two new families Acrodictyceae and Junewangiaceae. *Scientific Reports* 7(1): 7888. <https://doi.org/10.1038/s41598-017-08318-x>
- Yang J, Maharachchikumbura SSN, Liu JK, Hyde KD, Jones EBG, Al-Sadi AM, Liu ZY (2018) *Pseudostanjehughesia aquitropica* gen. et sp. nov. and *Sporidesmium* sensu lato species from freshwater habitats. *Mycological Progress* 17(5): 591–616. <https://doi.org/10.1007/s11557-017-1339-4>
- Yang J, Liu LL, Gareth Jones EBG, Li WL, Hyde KD, Liu ZY (2021) Morphological variety in *Distoseptispora* and introduction of six novel species. *Journal of Fungi* (Basel, Switzerland) 7(11): 945. <https://doi.org/10.3390/jof7110945>
- Zhai ZJ, Yan JQ, Li WW, Gao Y, Hu HJ, Zhou JP, Song HY, Hu DM (2022) Three novel species of *Distoseptispora* (Distoseptisporaceae) isolated from bamboo in Jiangxi Province, China. *MycKeys* 88: 35–54. <https://doi.org/10.3897/mycokeys.88.79346>
- Zhang SN, Hyde KD, Jones EBG, Cheewangkoon R, Liu JK (2020) Additions to *Fissuroma* and *Neoastrophaeriella* (Aigialaceae, Pleosporales) from palms. *Mycosphere* 11(1): 269–284. <https://doi.org/10.5943/mycosphere/11/1/5>
- Zhang H, Zhu R, Qing Y, Yang H, Li C, Wang G, Zhang D, Ning P (2022) Polyphasic Identification of *Distoseptispora* with Six New Species from Fresh Water. *Journal of Fungi* (Basel, Switzerland) 8(10): 1036. <https://doi.org/10.3390/jof8101063>



# Identification of two new species and a new host record of *Distoseptispora* (Distoseptisporaceae, Distoseptisporales, Sordariomycetes) from terrestrial and freshwater habitats in Southern China

Xue-Mei Chen<sup>1,2</sup>, Xia Tang<sup>3,4</sup>, Jian Ma<sup>1,4</sup>, Ning-Guo Liu<sup>1</sup>, Saowaluck Tibpromma<sup>2</sup>,  
Samantha C. Karunaratna<sup>2,5</sup>, Yuan-Pin Xiao<sup>1</sup>, Yong-Zhong Lu<sup>1,3</sup>

1 School of Food and Pharmaceutical Engineering, Guizhou Institute of Technology, Guiyang 550003, China

2 Center for Yunnan Plateau Biological Resources Protection and Utilization, College of Biological Resource and Food Engineering, Qujing Normal University, Qujing, Yunnan 655011, China

3 Engineering and Research Center for Southwest Biopharmaceutical Resource of National Education Ministry of China, Guizhou University, Guiyang, 550025, Guizhou Province, China

4 Center of Excellence in Fungal Research, Mae Fah Luang University, Chiang Rai, 57100, Thailand

5 National Institute of Fundamental Studies, Kandy, Sri Lanka

Corresponding author: Yong-Zhong Lu (yzlu@git.edu.cn)



Academic editor: Xinlei Fan  
Received: 8 November 2023  
Accepted: 29 December 2023  
Published: 9 February 2024

Citation: Chen X-M, Tang X, Ma J, Liu N-G, Tibpromma S, Karunaratna SC, Xiao Y-P, Lu Y-Z (2024) Identification of two new species and a new host record of *Distoseptispora* (Distoseptisporaceae, Distoseptisporales, Sordariomycetes) from terrestrial and freshwater habitats in Southern China. MycoKeys 102: 83–105. <https://doi.org/10.3897/mycokeys.102.115452>

Copyright: © Xue-Mei Chen et al.  
This is an open access article distributed under terms of the Creative Commons Attribution License (Attribution 4.0 International – CC BY 4.0).

## Abstract

During our investigation of saprophytic fungi in Guizhou and Hainan provinces, China, three hyphomycetes were collected from terrestrial and freshwater habitats. Based on morphological characteristics and phylogenetic analyses of combined ITS, LSU, *tef1-α*, and *rpb2* sequence data, two new species are introduced: *Distoseptispora hainanensis* and *D. lanceolatispora*. Additionally, one known species, *D. tectonae*, previously unreported from *Edgeworthia chrysantha*, is newly reported. Detailed descriptions, illustrations, and a phylogenetic tree to show the two new species and the new host record of *Distoseptispora* are provided. In addition, a checklist of *Distoseptispora* species with their locations, lifestyles, habitats, and hosts is provided.

**Key words:** 2 new taxa, asexual morph, phylogeny, taxonomy

## Introduction

*Distoseptispora* K.D. Hyde, McKenzie & Maharachch. was introduced by Su et al. (2016) with *D. fluminicola* McKenzie, Hong Y. Su, Z.L. Luo & K.D. Hyde, as the type species. Most *Distoseptispora* species are reported as saprophytes, typically found on decaying wood in terrestrial and freshwater habitats (Hyde et al. 2016, 2019; Su et al. 2016; Xia et al. 2017; Yang et al. 2018; Crous et al. 2019; Luo et al. 2019). The initial descriptions of *Distoseptispora* are derived from its asexual morphology (Hyde et al. 2016, 2019, 2020; Su et al. 2016; Yang et al. 2018, 2021; Luo et al. 2019; Sun et al. 2020). The first description of a sexual morph of *Distoseptispora* was described by Yang et al. (2021). Recently, Konta et al. (2023) identified the second sexual species on dead leaves of *Licuala glabra*, and provided detailed explanations, enhancing our understanding of *Distoseptispora*

sexual morphology. This sexual morph is characterized by solitary or gregarious, immersed to semi-immersed, subglobose to ellipsoidal, perithecial, dark brown ascomata with a short neck; 8-spored, cylindrical, short pedicellate asci with non-amyloid apical annuli; and fusiform, 0–3-septate, hyaline ascospores with mucilaginous sheaths (Yang et al. 2021; Konta et al. 2023). The asexual morph of *Distoseptispora* was recently expanded upon by Yang et al. (2021), incorporating macronematous, mononematous, solitary or fasciculate conidiophores, blastic, terminal, percurrent, cylindrical conidiogenous cells; and acrogenous, solitary, obclavate, ellipsoidal, obovoid or fusiform, rostrate or not, euseptate, distoseptate or rarely muriform conidia with or without a septal pore and mucilaginous sheath.

*Distoseptispora* has been found on various hosts viz. *Tectona*, *Pandanus*, bamboo, *Clematis*, *Carex*, *Dipterocarpus*, *Licuala glabra*, *Cocos nucifera*, *Phragmites australis*, *Thysanolaena maxima*, *Platanus orientalis*, and decaying wood and grasses (Shoemaker and White 1985; McKenzie 1995; Hyde et al. 2016, 2019, 2021, 2023; Su et al. 2016; Tibpromma et al. 2018; Crous et al. 2019; Phookamsak et al. 2019; Phukhamsakda et al. 2020, 2022; Sun et al. 2020; Zhai et al. 2022; Afshari et al. 2023; Hu et al. 2023; Konta et al. 2023). Most *Distoseptispora* species have been described in Asia, mainly in China, Thailand, and Malaysia, and only a few have been described in Europe (Shoemaker and White 1985; McKenzie 1995; Phookamsak et al. 2019; Ma et al. 2022; Zhai et al. 2022; Zhang et al. 2022; Konta et al. 2023). *Distoseptispora* comprises 74 accepted species in Index Fungorum (2024), but there is an ambiguity in the taxonomic status of *D. submersa* Z.L. Luo, K.D. Luo et al. (2019) stated that *D. submersa* is phylogenetically closely related to *D. tectonae*, and there are only minor size differences in conidiophores and conidia between *D. tectonae* and *D. submersa*. Dong et al. (2021) synonymized *D. submersa* under *D. tectonae*, thus, *Distoseptispora* comprises 73 accepted saprobic species, of which 44 were from freshwater habitats, 29 from terrestrial habitats, and five from both terrestrial and freshwater environments (Hyde et al. 2016, 2019; Luo et al. 2019; Monkai et al. 2020; Yang et al. 2021; Ma et al. 2022; Zhang et al. 2022; Afshari et al. 2023; Hu et al. 2023; Konta et al. 2023; Liu et al. 2023).

In this study, three fresh hyphomycetous fungal collections were encountered during a microfungus investigation in Hainan and Guizhou provinces. Based on multi-gene phylogeny and morphological comparison, two new species, *Distoseptispora hainanensis* and *D. lanceolatispora* are introduced. In addition, a new host record of *D. tectonae* from *Edgeworthia chrysantha* is also reported.

## Materials and methods

### Sample collection, isolation, and morphological study

Fresh specimens were collected from Hainan and Guizhou provinces in China. Fungal colonies were mounted on a slide with distilled water and were observed and examined using a stereomicroscope (SMZ 745, Nikon, Tokyo, Japan). Micro-morphological characteristics were captured with a Nikon EOS 90D digital camera combined with an ECLIPSE Ni-U compound microscope (Nikon, Tokyo, Japan). The sizes of the fungal structures were measured using the Tarosoft (R) Image Frame Work program (IFW 0.97 version), and the photo plates were processed with Adobe Photoshop CC 2019 (Adobe Systems, San Jose, CA, USA).

Single spore isolations were carried out following the methods described in Senanayake et al. (2020). Germinated conidia were transferred to fresh potato dextrose agar (PDA) plates and incubated at 25–27 °C for four weeks. Culture characteristics, including color, shape, and size, were recorded. Herbarium specimens were deposited in the herbarium of the Guizhou Academy of Agriculture Sciences (**GZAAS**), Guiyang, China, and the living cultures were deposited at the Guizhou Culture Collection, China (**GZCC**). Faces of Fungi and Index Fungorum numbers were obtained following the protocols outlined by Jayasiri et al. (2015) and Index Fungorum (2024), respectively.

### **DNA extraction, PCR amplification, and sequencing**

Fresh mycelia were scraped from cultures that were incubated at 25–27 °C for 28 days. Fungal genomic DNA was extracted using the Biospin Fungus Genomic DNA Extraction Kit (BioFlux, Shanghai, China), following the manufacturer's instructions. Four gene regions: internal transcribed spacer (ITS), large subunit ribosomal DNA (LSU), translation elongation factor 1-alpha (*tef1-α*), and RNA polymerase II second largest subunit (*rpb2*) were selected. The primers used in this study for each gene region were as follows: ITS4 and ITS5 for ITS (White et al. 1990), LR0R and LR5 for LSU (Vilgalys and Hester 1990; Cubeta et al. 1991), EF1-983F and EF1-2218R for *tef1-α* (Rehner and Samuels 1994), and *rpb2* with fRPB2-5F and fRPB2-7cR (Liu et al. 1999).

Polymerase chain reaction (PCR) amplifications were carried out in a 50 µL reaction volume containing 44 µL of 1.1 × T3 Super PCR Mix (TsingKe Biotech, Chongqing, China), 2 µL of DNA template, and 2 µL of each forward and reverse primer. The amplification condition for LSU and ITS consisted of initial denaturation at 94 °C for 3 min, followed by 35 cycles of 45 s at 94 °C, 50 s at 56 °C, and 1 min at 72 °C, and a final extension period of 10 min at 72 °C. The amplification condition for the *tef1-α* gene consisted of initial denaturation at 94 °C for 3 min, followed by 30 cycles of 30 s at 94 °C, 50 s at 56 °C, and 1 min at 72 °C, a final extension period of 10 min at 72 °C. The amplification condition for the *rpb2* gene consisted of initial denaturation at 95 °C for 5 min, followed by 35 cycles of 15 s at 95 °C, 50 s at 56 °C, and 1 min at 72 °C, a final extension period of 10 min at 72 °C. The quality of PCR amplification products was examined with 1% agarose electrophoresis gels stained with ethidium bromide, and the PCR products were sent to TsingKe Biotech, Chongqing, China for purification and sequencing.

### **Phylogenetic analyses**

The raw sequences were initially checked with BioEdit v 7.0.5.3 (Hall 1999). Forward and reverse sequences were assembled using SeqMan v. 7.0.0 (DNASTAR, Madison, WI, USA). Sequence data (LSU, ITS, *tef1-α*, and *rpb2*) for *Distoseptispora* were downloaded from GenBank based on the blast results and recent publications (Table 1). Each individual gene dataset was aligned using the online program MAFFT version 7 with the “auto” option (Hall 1999; Katoh and Standley 2013). These alignments were visually inspected and manually improved in BioEdit v 7.0.5.3. Multi-gene alignments were combined by SequenceMatrix (Vaidya et al. 2011). In this study, phylogenetic analyses were performed using maximum likelihood (ML), maximum parsimony (MP),

**Table 1.** Names, strain numbers, and corresponding GenBank accession numbers of taxa used in this study.

Taxa names	Strain	GenBank Accessions				References
		LSU	ITS	<i>tef1-α</i>	<i>rpb2</i>	
<i>Aquapteridospora aquatica</i>	MFLUCC 17-2371 <sup>T</sup>	MW287767	MW286493	N/A	N/A	Dong et al. (2021)
<i>Distoseptispora adscendens</i>	HKUCC 10820	DQ408561	N/A	N/A	DQ435092	Shenoy et al. (2006)
<i>D. amniculi</i>	MFLU 17-2129 <sup>T</sup>	MZ868761	MZ868770	N/A	MZ892982	Yang et al. (2021)
<i>D. appendiculata</i>	MFLUCC 18-0259 <sup>T</sup>	MN163023	MN163009	MN174866	N/A	Luo et al. (2019)
<i>D. aqualignicola</i>	KUNCC 21-10729 <sup>T</sup>	ON400845	OK341186	OP413480	OP413474	Zhang et al. (2022)
<i>D. aquamyces</i>	KUNCC 21-10731 <sup>T</sup>	OK341199	OK341187	OP413482	OP413476	Zhang et al. (2022)
<i>D. aquatica</i>	MFLUCC 15-0374 <sup>T</sup>	KU376268	MF077552	N/A	N/A	Su et al. (2016)
	MFLUCC 18-0646	MK849793	MK828648	N/A	N/A	Luo et al. (2019)
<i>D. aquisubtropica</i>	GZCC 22-0075 <sup>T</sup>	ON527941	ON527933	ON533677	ON533685	Ma et al. (2022)
<i>D. atroviridis</i>	GZCC 20-0511 <sup>T</sup>	MZ868763	MZ868772	MZ892978	MZ892984	Yang et al. (2021)
<i>D. bambusae</i>	MFLUCC 20-0091 <sup>T</sup>	MT232718	MT232713	MT232880	MT232881	Sun et al. (2020)
	MFLUCC 14-0583	MT232717	MT232712	N/A	MT232882	Sun et al. (2020)
<i>D. bambusicola</i>	GZCC 21-0667 <sup>T</sup>	MZ474872	MZ474873	N/A	N/A	Hyde et al. (2023)
<i>D. bangkokensis</i>	MFLUCC 18-0262 <sup>T</sup>	MZ518206	MZ518205	N/A	N/A	Shen et al. (2021)
<i>D. cangshanensis</i>	MFLUCC 16-0970 <sup>T</sup>	MG979761	MG979754	MG988419	N/A	Luo et al. (2018)
<i>D. caricis</i>	CPC 36498 <sup>T</sup>	MN567632	MN562124	N/A	MN556805	Crous et al. (2019)
	CPC 36442	N/A	MN562125	N/A	MN556806	Crous et al. (2019)
<i>D. chinensis</i>	GZCC 21-0665 <sup>T</sup>	MZ474867	MZ474871	MZ501609	N/A	Hyde et al. (2021)
<i>D. clematidis</i>	MFLUCC 17-2145 <sup>T</sup>	MT214617	MT310661	N/A	MT394721	Phukhamsakda et al. (2020)
<i>D. crassispora</i>	KUMCC 21-10726 <sup>T</sup>	OK341196	OK310698	OP413479	OP413473	Zhang et al. (2022)
<i>D. curvularia</i>	KUMCC 21-10725 <sup>T</sup>	OK341195	OK310697	OP413478	OP413472	Zhang et al. (2022)
<i>D. cylindricospora</i>	DLUCC 1906 <sup>T</sup>	OK513523	OK491122	OK524220	N/A	Phukhamsakda et al. (2022)
<i>D. dehongensis</i>	KUMCC 18-0090 <sup>T</sup>	MK079662	MK085061	MK087659	N/A	Hyde et al. (2019)
<i>D. dipteroearpi</i>	MFLUCC 22-0104 <sup>T</sup>	OP600052	OP600053	N/A	OP595140	Afshari et al. (2023)
<i>D. effusa</i>	GZCC 19-0532 <sup>T</sup>	MZ227224	MW133916	N/A	N/A	Yang et al. (2021)
<i>D. eusptata</i>	MFLUCC 20-0154 <sup>T</sup>	MW081544	MW081539	N/A	MW151860	Li et al. (2021)
	MFLU 20-0568	MW081545	MW081540	MW084994	MW084996	Li et al. (2021)
<i>D. fasciculata</i>	KUMCC 19-0081 <sup>T</sup>	MW287775	MW286501	MW396656	N/A	Dong et al. (2021)
<i>D. fluminicola</i>	MFLUCC 15-0417 <sup>T</sup>	KU376270	MF077553	N/A	N/A	Su et al. (2016)
<i>D. fusiformis</i>	GZCC 20-0512 <sup>T</sup>	MZ868764	MZ868773	MZ892979	MZ892985	Yang et al. (2021)
<i>D. gasaensis</i>	HJAUP C2034 <sup>T</sup>	OQ942891	OQ942896	OQ944455	N/A	Hu et al. (2023)
<i>D. guanshanensis</i>	HJAUP C1063 <sup>T</sup>	OQ942898	OQ942894	OQ944452	OQ944458	Hu et al. (2023)
<i>D. guizhouensis</i>	GZCC 21-0666 <sup>T</sup>	MZ474869	MZ474868	MZ501610	MZ501611	Hyde et al. (2021)
<i>D. guttulata</i>	MFLUCC 16-0183 <sup>T</sup>	MF077554	MF077543	MF135651	N/A	Yang et al. (2018)
	DLUCC B43	MN163016	MN163011	N/A	N/A	Luo et al. (2019)
<b><i>D. hainanensis</i></b>	<b>GZCC 22-2047<sup>T</sup></b>	<b>OR438894</b>	<b>OR427328</b>	<b>OR449122</b>	<b>OR449119</b>	<b>This study</b>
<i>D. hyalina</i>	MFLUCC 17-2128 <sup>T</sup>	MZ868760	MZ868769	MZ892976	MZ892981	Yang et al. (2021)
<i>D. hydei</i>	MFLUCC 20-0481 <sup>T</sup>	MT742830	MT734661	N/A	MT767128	Monkai et al. (2020)
<i>D. jinghongensis</i>	HJAUP C2120 <sup>T</sup>	OQ942893	OQ942897	OQ944456	N/A	Hu et al. (2023)
<i>D. lancangjiangensis</i>	KUN-HKAS 112712 <sup>T</sup>	MW879522	MW723055	N/A	MW882260	Shen et al. (2021)
<b><i>D. lanceolatispora</i></b>	<b>GZCC 22-2045<sup>T</sup></b>	<b>OR43BB95</b>	<b>OR427329</b>	<b>OR449123</b>	<b>OR449120</b>	<b>This study</b>
<i>D. leonensis</i>	HKUCC 10822	DQ408566	N/A	N/A	DQ435089	Shenoy et al. (2006)
<i>D. licualae</i>	MFLUCC 14-1163A <sup>T</sup>	ON650675	ON650686	ON734007	N/A	Konta et al. (2023)
	MFLUCC 14-1163B <sup>T</sup>	ON650676	ON650687	ON734008	N/A	Konta et al. (2023)

Taxa names	Strain	GenBank Accessions				References
		LSU	ITS	<i>tef1-α</i>	<i>rpb2</i>	
<i>D. lignicola</i>	MFLUCC 18-0198 <sup>T</sup>	MK849797	MK828651	N/A	N/A	Luo et al. (2019)
<i>D. longispora</i>	HFAU 0705 <sup>T</sup>	MH555357	MH555359	N/A	N/A	Song et al. (2020)
<i>D. longnanensis</i>	HJAUP C1040 <sup>T</sup>	OQ942886	OQ942887	OQ944451	N/A	Hu et al. (2023)
<i>D. martinii</i>	CGMCC 3.18651 <sup>T</sup>	KX033566	KU999975	N/A	N/A	Xia et al. (2017)
<i>D. meilingensis</i>	JAUCC 4727 <sup>T</sup>	OK562396	OK562390	OK562408	N/A	Zhai et al. (2022)
<i>D. menghaiensis</i>	HJAUP C2045 <sup>T</sup>	OQ942900	OQ942890	N/A	N/A	Hu et al. (2023)
	HJAUP C2170 <sup>T</sup>	OQ942888	OQ942899	OQ944457	OQ944461	Hu et al. (2023)
<i>D. mengsongensis</i>	HJAUP C2126 <sup>T</sup>	OP78784	OP787876	OP961937	N/A	Liu et al. (2023)
<i>D. multiseptata</i>	MFLUCC 16-1044	MF077555	MF077544	MF135652	MF135644	Yang et al. (2018)
	MFLUCC 15-0609 <sup>T</sup>	KX710140	KX710145	MF135659	N/A	Hyde et al. (2016)
<i>D. nabanheensis</i>	HJAUP C2003 <sup>T</sup>	OP787877	OP787873	OP961935	N/A	Liu et al. (2023)
<i>D. nanchangensis</i>	HJAUP C1074 <sup>T</sup>	OQ942895	OQ942889	OQ944454	OQ944460	Hu et al. (2023)
<i>D. neorostrata</i>	MFLUCC 18-0376 <sup>T</sup>	MN163017	MN163008	N/A	N/A	Luo et al. (2019)
<i>D. nonrostrata</i>	KUNCC 21-10730 <sup>T</sup>	OK341198	OK310699	OP413481	OP413475	Zhang et al. (2022)
<i>D. obclavata</i>	MFLUCC 18-0329 <sup>T</sup>	MN163010	MN163012	N/A	N/A	Luo et al. (2019)
<i>D. obpyriformis</i>	MFLUCC 17-1694 <sup>T</sup>	MG979764	N/A	MG988422	MG988415	Luo et al. (2018)
	DLUCC 0867	MG979765	MG979757	MG988423	MG988416	Luo et al. (2018)
<i>D. pachyconidia</i>	KUMCC 21-10724 <sup>T</sup>	OK341194	OK310696	OP413477	OP413471	Zhang et al. (2022)
<i>D. palmarum</i>	MFLUCC 18-1446 <sup>T</sup>	MK079663	MK085062	MK087660	MK087670	Hyde et al. (2019)
<i>D. phangngaensis</i>	MFLUCC 16-0857 <sup>T</sup>	MF077556	MF077545	MF135653	N/A	Yang et al. (2018)
<i>D. phragmiticola</i>	GUCC 22-0202 <sup>T</sup>	OP749881	OP749888	OP749892	OP752700	Hyde et al. (2023)
<i>D. rayongensis</i>	MFLUCC 18-0415 <sup>T</sup>	MH457137	MH457172	MH463253	MH463255	Hyde et al. (2020)
	MFLUCC 18-0417	MH457138	MH457173	MH463254	MH463256	Hyde et al. (2020)
<i>D. rostrata</i>	MFLUCC 16-0969 <sup>T</sup>	MG979766	MG979758	MG988424	MG988417	Luo et al. (2018)
	DLUCC 0885	MG979767	MG979759	MG988425	N/A	Luo et al. (2018)
<i>D. saprophytica</i>	MFLUCC 18-1238 <sup>T</sup>	MW287780	MW286506	MW396651	MW504069	Dong et al. (2021)
<i>D. septata</i>	GZCC 22-0078 <sup>T</sup>	ON527947	ON527939	ON533683	ON533690	Ma et al. (2022)
<i>D. sinensis</i>	HJAUP C2044 <sup>T</sup>	OP787875	OP787878	OP961936	N/A	Liu et al. (2023)
<i>D. songkhlaensis</i>	MFLUCC 18-1234 <sup>T</sup>	MW287755	MW286482	MW396642	N/A	Dong et al. (2021)
<i>D. suoluensis</i>	MFLUCC 17-0224 <sup>T</sup>	MF077557	MF077546	MF135654	N/A	Yang et al. (2018)
	MFLUCC 17-1305	MF077558	MF077547	N/A	N/A	Yang et al. (2018)
<i>D. tectonae</i>	MFLUCC 12-0291 <sup>T</sup>	KX751713	KX751711	KX751710	KX751708	Hyde et al. (2016)
	MFLU 20-0262	MT232719	MT232714	N/A	N/A	Sun et al. (2020)
	MFLUCC 16-0946	MG979768	MG979760	MG988426	MG988418	Dong et al. (2021)
<b><i>D. tectonae</i></b>	<b>GZCC 22-2046</b>	<b>OR348896</b>	<b>OR427330</b>	<b>OR449124</b>	<b>OR449121</b>	<b>This study</b>
<i>D. tectonigena</i>	MFLUCC 12-0292 <sup>T</sup>	KX751714	KX751712	N/A	KX751709	Hyde et al. (2016)
<i>D. thailandica</i>	MFLUCC 16-0270 <sup>T</sup>	MH260292	MH275060	MH412767	N/A	Tibpromma et al. (2018)
<i>D. thysanolaenae</i>	KUN-HKAS 102247 <sup>T</sup>	MK064091	MK045851	MK086031	N/A	Phukhamsak et al. (2019)
<i>D. tropica</i>	GZCC 22-0076 <sup>T</sup>	ON527943	ON527935	ON533679	ON533687	Ma et al. (2022)
<i>D. verrucosa</i>	GZCC20-0434 <sup>T</sup>	MZ868762	MZ868771	MZ892977	MZ892983	Yang et al. (2021)
<i>D. wuzhishanensis</i>	GZCC 22-0077 <sup>T</sup>	ON527946	ON527938	ON533682	N/A	Ma et al. (2022)
<i>D. xishuangbannaensis</i>	KUMCC 17-0290 <sup>T</sup>	MH260293	MH275061	MH412768	MH412754	Tibpromma et al. (2018)
<i>D. yichunensis</i>	HJAUP C1065 <sup>T</sup>	OQ942892	OQ942885	OQ944453	OQ944459	Hu et al. (2023)
<i>D. yongxiuensis</i>	JAUCC 4725 <sup>T</sup>	OK562394	OK562388	OK562406	N/A	Zhai et al. (2022)
<i>D. yunshanshanensis</i>	JAUCC 4723 <sup>T</sup>	OK562398	OK562392	OK562410	N/A	Zhai et al. (2022)
<i>D. yunnanensis</i>	MFLUCC 20-0153 <sup>T</sup>	MW081546	MW081541	MW084995	MW151861	Li et al. (2021)

Note: "T" denotes ex-type strain. Newly generated sequences are indicated in black bold. "N/A": no data available in GenBank.

and Bayesian posterior probability (BYPP) methods. The analyses were based on LSU, ITS, *tef1- $\alpha$* , and *rpb2* combined sequence datasets.

The phylogenetic analyses were conducted using the CIPRES Science Gateway V. 3.3. “RAxML-HPC v.8 on XSEDE”, “PAUP on XSEDE”, and “MrBayes on XSEDE (3.2.7a)” were utilized for ML, MP, and BYPP methods, respectively (Huelsenbeck and Ronquist 2001; Swofford 2002; Stamatakis et al. 2008; Miller et al. 2010; Ronquist et al. 2012). For the ML analysis, the GTRGAMMA model of nucleotide evolution was employed, and RAxML rapid bootstrapping with 1,000 bootstrap replicates was obtained (Stamatakis et al. 2008).

The MP analysis employed 1,000 random taxa additions to infer trees. Branches of zero length were collapsed, and all multiple parsimonious trees were saved. The maxtrees value was set to 5,000. For trees generated using different optimal criteria, parsimony score values were determined for tree length (TL), consistency index (CI), retention index (RI), and homoplasy index (HI). To assess clade stability, the bootstrap (BT) method was used with 1,000 iterations, each consisting of 100 trials of random stepwise addition of taxa (Hillis and Bull 1993).

The posterior probabilities (PP) were determined based on Bayesian Markov chain Monte Carlo sampling (Huelsenbeck and Ronquist 2001). The best nucleotide substitution model for each data partition was determined using the program MrModeltest 2.2 (Nylander 2004). The GTR + I + G substitution model with gamma rates and Dirichlet base frequencies was selected for all LSU, ITS, *tef1- $\alpha$* , and *rpb2* sequences. To calculate the posterior probabilities, four simultaneous Markov chains were run for one million generations, with trees sampled every 100<sup>th</sup> generation, resulting in a total of 10,000 trees. A burn-in parameter of 0.25 was set, indicating that 75% of the trees were removed during the burn-in phase, and the remaining trees were used for calculating the posterior probabilities in the majority rule consensus tree.

FigTree v. 1.4.4. was used for visualizing the phylogenetic trees, and Adobe Illustrator CC 2019v. 23.1.0 was used to edit trees and figure layout.

## Phylogenetic analyses results

This study utilized a combined multi-gene dataset encompassing ITS, LSU, *tef1- $\alpha$* , and *rpb2* sequences to assess the phylogenetic relationships among *Distoseptispora* species. The analyses included a total of 90 taxa, designating *Aquapteridospora aquatica* X.D. Yu, W. Dong & H. Zhang (MFLUCC 17-2371) as the outgroup taxon. The combined aligned sequence matrix comprised 3,360 characters, including gaps: LSU (1–840 bp), ITS (841–1406 bp), *tef1- $\alpha$*  (1407–2321 bp), and *rpb2* (2322–3360 bp). The ML, MP, and Bayesian trees analyzed exhibited a high degree of similarity in topology and showed no significant conflicts. The RAxML analysis yielded a best-scoring tree (ln = -31666.963504), which is presented in Fig. 1. The matrix encompassed 1572 distinct alignment patterns, with 27.15% constituted by undetermined characters or gaps. The estimated base frequencies were as follows: A = 0.239306, C = 0.265297, G = 0.281926, T = 0.213472; substitution rates AC = 1.429077, AG = 3.512798, AT = 1.204511, CG = 0.845859, CT = 6.948345, GT = 1.000000; gamma distribution shape parameter  $\alpha$  = 0.244431. For the MP analysis, 3360 characters remained unchanged, 330 were variable and parsimoniously uninformative, and

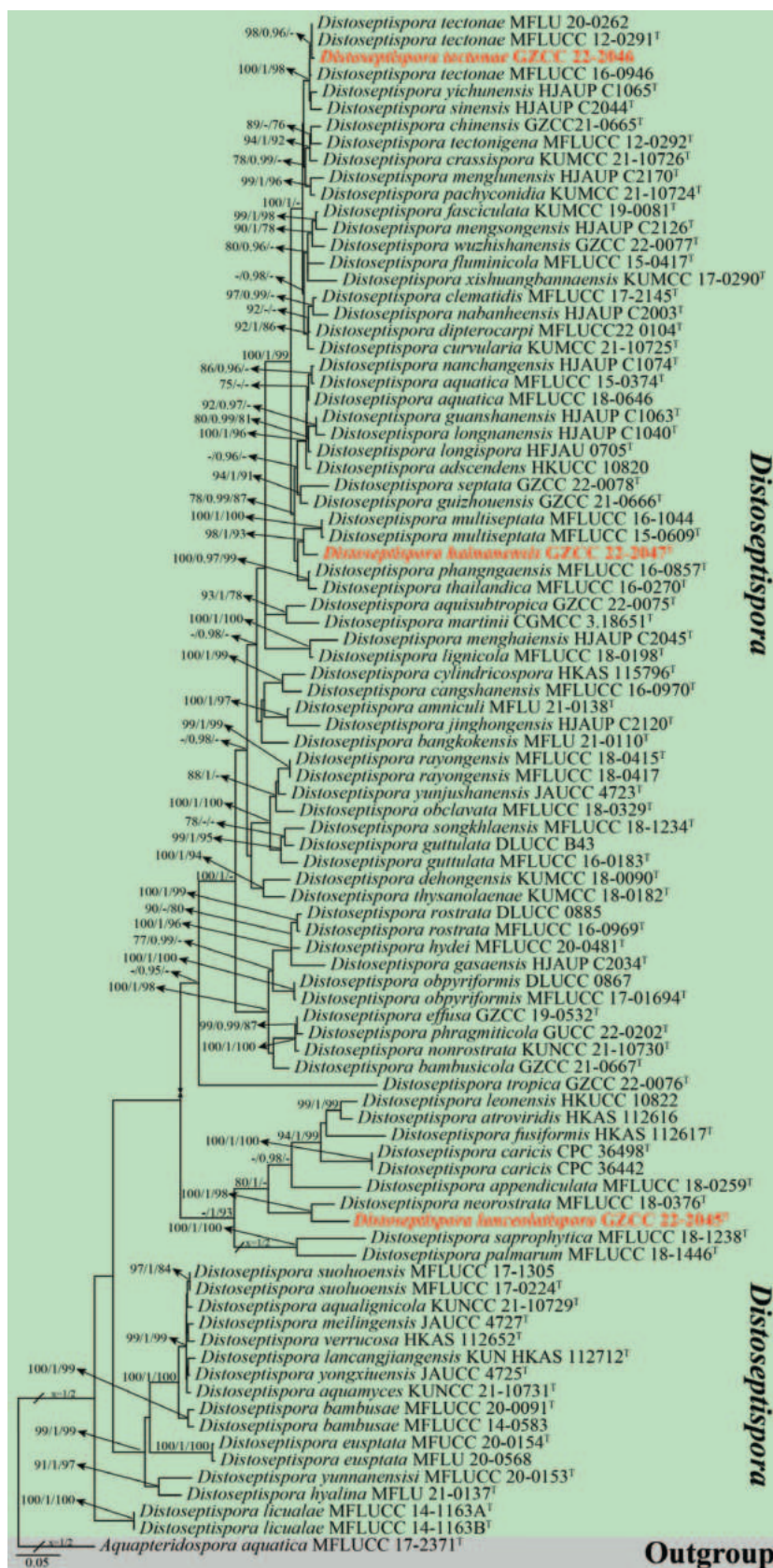


**Figure 1.** Phylogenetic tree generated from ML analysis based on a combination of LSU, ITS, *tef1-a*, and *rpb2* sequence data. Bootstrap support values of ML and MP equal to or greater than 75%, and PP value equal to or greater than 0.95 are given near the nodes as ML/PP/MP. The tree is rooted with *Aquapteridospora aquatica* (MFLUCC 17-2371). Ex-type strains are indicated by the superscript T. The new collections are in bold red text.

1074 were parsimoniously informative. The most parsimonious tree yielded the following values: TL = 5624, CI = 0.400, RI = 0.738, RC = 0.295, HI = 0.600. For BYPP analysis, Bayesian posterior probabilities from MCMC were evaluated with a final average standard deviation of split frequencies of 0.009754.

In the phylogenetic analyses (Fig. 1), all our newly identified taxa nested within *Distoseptispora*, affirming their classification within this genus. *Distoseptispora hainanensis* (GZCC 22-047) formed a sister clade to *D. multiseptata* strains (MFLUCC 16-1044 and MFLUCC 15-0609) with 98% ML, 1.00 PP, and 93% MP statistical support. *Distoseptispora lanceolatispora* (GZCC 22-2045) formed a sister clade to *D. neurostrata* (MFLUCC 18-0376) with 100% ML, 1.00 PP, and 98% MP statistical support. In addition, our new collection GZCC 22-2046 clustered together with three *D. tectonae* strains (MFLU 20-0262 and MFLUCC 12-0291) with 98% ML and 0.96 PP statistical support, indicating they represent the same species.

## Taxonomy

### *Distoseptispora hainanensis* X.M. Chen & Y.Z. Lu, sp. nov.

Index Fungorum: IF900953

Facesoffungi Number: FoF14663

Fig. 2

**Etymology.** The epithet refers to the location “Hainan Province” where the holotype was collected.

**Holotype.** GZAAS 22-2047.

**Description.** *Saprobic* on decaying wood in terrestrial habitat. **Sexual morph:** Undetermined. **Asexual morph: Colonies** on natural substrate superficial, effuse, dark brown, and hairy. **Mycelium** mostly immersed, composed of branched, septate, brown to dark brown, smooth hyphae. **Conidiophores** 70–130 × 5–8.5 μm ( $\bar{x}$  = 103 × 7 μm, n = 20), macronematous, mononematous, erect, solitary, straight or slightly flexuous, brown to dark brown, paler towards the apex, cylindrical, 4–6-septate, slightly constricted and darkened at septa, unbranched, thick-walled. **Conidiogenous cells** 6–13 × 3.5–6.5 μm ( $\bar{x}$  = 10 × 5 μm, n = 20), holoblastic, monoblastic, integrated, terminal, indeterminate, cylindrical, slightly tapering towards the apex, brown, percurrent. **Conidia** 44–117 μm × 9–18.5 μm ( $\bar{x}$  = 90 × 14 μm, n = 20), acrogenous, solitary, obclavate or obpyriform, rostrate, truncate at the base, straight or slightly curved, up to 22-distoseptate, slightly constricted at septa, brown, verrucose.

**Culture characteristics.** Colonies grown on PDA circular, dense, fluffy, with raised center and lobate edge, pale gray in the center, grayish brown in the outer ring from the front view, dark brown in the center, and blackish brown in the outer ring from the reverse view.

**Material examined.** CHINA, Hainan Province, on unidentified decaying wood, 15 May 2021, Xia Tang, HN02 (GZAAS 22-2047, holotype), ex-type living culture, GZCC 22-2047.

**Notes.** Morphologically, *Distoseptispora hainanensis* is similar to *D. effusa* L.L. Liu & Z.Y. Liu in having macronematous conidiophores, monoblastic conidiogenous cells, and acrogenous, obclavate, rostrate conidia (Yang et al. 2021). However, conidia of *D. hainanensis* are up to 22-distoseptate, whereas those of *D. effusa* are only 4–9-distoseptate. In the phylogenetic analyses, *D. hainan-*



**Figure 2.** *Distoseptispora hainanensis* (GZAAS 22-2047, holotype) **a, b** colonies on substrate **c–e** conidiophores and conidia **f–h** conidiogenous cells bearing conidia **i, j** conidiophores **k–q** conidia **r, s** colony on PDA (**r** from front **s** from reverse). Scale bars: 50  $\mu\text{m}$  (**c, d, f–j, l–q**); 30  $\mu\text{m}$  (**e, k**).

*ensis* formed a distinct clade sister to *D. multiseptata* Jiao Yang & K.D. Hyde with 98% ML, 1 PP, and 93% MP statistical support (Fig. 1). *Distoseptispora hainanensis* differs from *D. multiseptata* in having brown, longer conidiophores (70–130  $\mu\text{m}$  vs. 23–65  $\mu\text{m}$ ) and obclavate or obpyriform, brown, verrucose, smaller conidia (44–117  $\mu\text{m}$  vs. up to 290  $\mu\text{m}$ ) (Hyde et al. 2016). Comparing DNA sequence data, *D. hainanensis* diverges from *D. multiseptata* (MFLUCC 15-0609) in the ITS by 21/552 bp (3.8% difference), in the LSU by 1/812 bp (0.01% difference), in *tef1*- $\alpha$  by 33/912 bp (3.6% difference), and no data is available for *rpb2* of *D. multiseptata* (MFLUCC 15-0609) in GenBank. Hence, the novel species, *D. hainanensis*, is introduced, following the guidelines of Jeewon and Hyde (2016) and Chethana et al. (2021).

***Distoseptispora lanceolatispora* X.M. Chen & Y.Z. Lu, sp. nov.**

Index Fungorum: IF900954

Facesoffungi Number: FoF14664

Fig. 3

**Etymology.** Referring to the lanceolate conidia.

**Holotype.** GZAAS 22-2045.

**Description.** *Saprobic* on submerged decaying wood in freshwater habitat.

**Sexual morph:** Undetermined. **Asexual morph: Colonies** on substrate effuse, gregarious, hairy, pale brown to brown. **Mycelium** mostly immersed, composed of septate, yellow-brown to brown, smooth hyphae. **Conidiophores** 120–190  $\times$  4–8  $\mu\text{m}$  ( $\bar{x}$  = 155  $\times$  6.5  $\mu\text{m}$ ,  $n$  = 20), macronematous, mononematous, erect, solitary, straight or slightly flexuous, grayish brown to dark brown, slightly tapering towards the apex, cylindrical, 7–8-septate, unbranched, thick-walled, smooth-walled. **Conidiogenous cells** 15–27  $\times$  3–5.5  $\mu\text{m}$  ( $\bar{x}$  = 20.5  $\times$  4.5  $\mu\text{m}$ ,  $n$  = 20), monoblastic, integrated, terminal, cylindrical, slightly tapering towards the apex, pale brown, percurrent. **Conidia** 31–90  $\times$  9.5–15  $\mu\text{m}$  ( $\bar{x}$  = 58.5  $\times$  13  $\mu\text{m}$ ,  $n$  = 20), acrogenous, solitary, fusiform or lanceolate, rostrate, truncate at the base, straight or slightly curved, 5–13-distoseptate, slightly constricted at septa, olivaceous to olivaceous brown, slightly paler at the apex, verrucous, with or without apical, hyaline appendages.

**Culture characteristics.** Colonies grown on PDA circular, dense, flat, dry, gray to dark gray, radially striated, and a ring in the middle of the colonies with an entire edge from the front view, dark brown to black with a circular, gray edge from reverse view, not pigmented.

**Material examined.** CHINA, Hainan Province, on submerged decaying wood in a freshwater stream, 23 October 2021, Jian Ma, J13 (GZAAS 22-2045, holotype), ex-type living culture, GZCC 22-2045.

**Notes.** *Distoseptispora lanceolatispora* is morphologically similar to *D. leonensis* (M.B. Ellis) R. Zhu & H. Zhang. However, compared to *D. lanceolatispora*, *D. leonensis* has longer conidiophores (120–190  $\mu\text{m}$  vs. 110–130  $\mu\text{m}$ ), longer conidiogenous cells (15–27  $\mu\text{m}$  vs. 5–15  $\mu\text{m}$ ), and 5–13-distoseptate, fusiform or lanceolate conidia (Zhang et al. 2022). In the phylogenetic analyses (Fig. 1), *D. lanceolatispora* forms a unique clade adjacent to *D. neurostrata* D.F. Bao, Z.L. Luo & H.Y. Su with 100% ML, 1 PP, and 98% MP support. Based on a pairwise nucleotide comparison of ITS and LSU sequences, *D. lanceolatispora* deviates from



**Figure 3.** *Distoseptispora lanceolatispora* (GZAAS 22-2045, holotype) **a, b** colonies on substrate **c–e** conidiophores and conidia **f, g** conidiogenous cells bearing conidia **h–k** conidia **l** germinated conidium **m, n** colony on PDA (**m** from front **n** from reverse). Scale bars: 50 µm (**c–g**); 30 µm (**h–l**).

*D. neurostrata* by 39/529 bp (6.8%) for ITS and 14/850 bp (1.6%) for LSU, and there is no data available for *tef1-α* and *rpb2* for *D. neurostrata* (MFLUCC 18-0376) in GenBank. Hence, we introduce the new species, *D. lanceolatispora*, based on the criteria established by Jeewon and Hyde (2016) and Chethana et al. (2021).

***Distoseptispora tectonae* Doilom & K.D. Hyde, Fungal Diversity 80: 222 (2016)**

Index Fungorum: IF552223

Facesoffungi number: FoF01877

Fig. 4

**Description.** **Saprobic** on dead twigs of *Edgeworthia chrysantha*. **Sexual morph:** Undetermined. **Asexual morph: Colonies** on natural substrate abundant, superficial, dark brown, hairy. **Conidiophores** 35–80 μm × 4–7.5 μm ( $\bar{x}$  = 58 × 5.5 μm, n = 20), macronematous, mononematous, simple, erect to slightly curved, solitary, pale brown to dark brown, cylindrical, 2–4-septate, slightly constricted at the septa, unbranched, thick-walled. **Conidiogenous cells** 6–10 μm × 3.5–6.5 μm ( $\bar{x}$  = 8 × 4.5 μm, n = 20), holoblastic, monoblastic, integrated, terminal, cylindrical, slightly tapering towards the apex, brown to reddish brown, percurrent. **Conidia** 190–255 μm × 9.5–16 μm ( $\bar{x}$  = 220 μm × 13 μm, n = 20), 5–16 μm ( $\bar{x}$  = 13 μm, n = 20) wide at the protruding truncate base; 4.5–8 μm ( $\bar{x}$  = 6.5 μm, n = 20) wide in the tapering part, acrogenous, solitary, obclavate, elongate, rostrate, straight or curved, tapering towards the apex, 9–39-distoseptate, olivaceous-green when young, dark reddish brown at maturity, verrucose.

**Culture characteristics.** Conidia germinating on PDA within 24 h, colonies circular, dense, umbonate, spreading, fluffy. The surface is slightly rough with reddish-gray mycelium, colonies somewhat raised in the middle, and with a filiform edge. The reverse side is dark gray with a circular, pale reddish-gray edge, not pigmented.

**Material examined.** CHINA, Guizhou Province, Guiyang City, Guiyang Medicinal Botanical Garden, on dead twigs of *Edgeworthia chrysantha*, 20 August 2022, Xia Tang, JX30 (GZAAS 22-2046), living culture, GZCC 22-2046.

**Known host and distribution.** *Tectona grandis* (Thailand, Hyde et al. 2016), on dead stems (Thailand, Sun et al. 2020), on dead, submerged, decaying wood of unidentified plants (China & Thailand, Luo et al. 2019; Dong et al. 2021; Zhang et al. 2022), and dead twig and branch of *Edgeworthia chrysantha* (China, this study).

**Notes.** *Distoseptispora tectonae* was first isolated from a dead twig of *Tectona grandis* in Thailand (Hyde et al. 2016). Since then, this species has been identified in various countries on different substrates and hosts (Hyde et al. 2016; Sun et al. 2020; Dong et al. 2021; Zhang et al. 2022). In the phylogenetic tree (Fig. 1), our new isolate forms a close lineage to *D. tectonae* (GZCC 22-2046) with statistical support of 98% ML and 0.96 PP. Based on pairwise nucleotide comparisons of ITS, LSU, *tef1-α*, and *rpb2*, our new isolate diverges from *D. tectonae* (MFLUCC 12-0291, ex-type) by 6/554 bp (1%) for ITS, 1/852 bp (0.01%) for LSU, 0/980 bp (0%) for *tef1-α*, and 2/899 bp (0.2%) for *rpb2*. In addition, the morphological characteristics of our isolate match well with the holotype description of *D. tectonae* (Hyde et al. 2016). This study reports a new host record of *Distoseptispora tectonae* on dead twigs of *Edgeworthia chrysantha* in China.

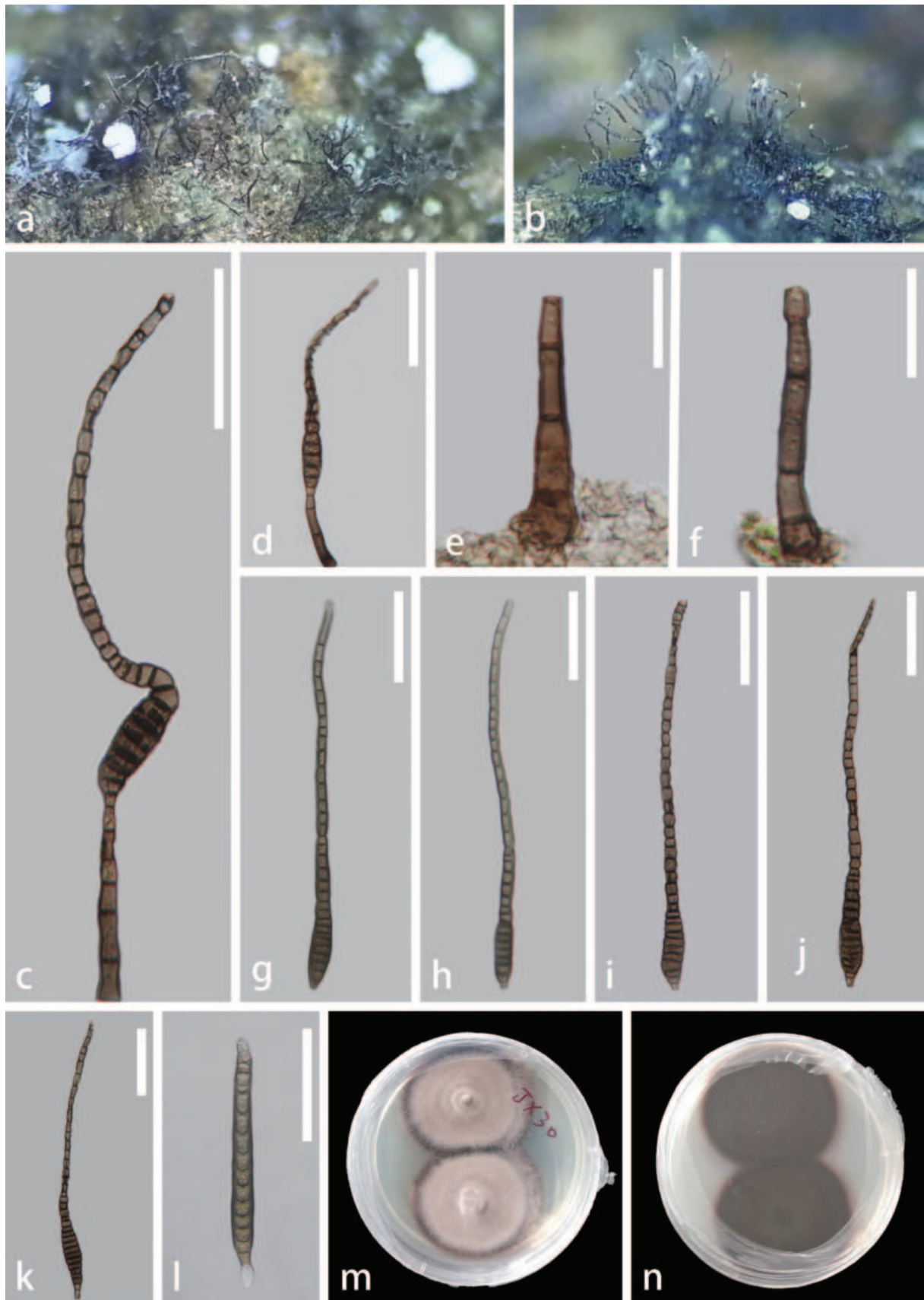


**Figure 4.** *Distoseptispora tectonae* (GZAAS 22-2046) **a, b** colonies on substrate **c, d** conidiophores and conidia **e, f** conidiophores **g–k** conidia **l** germinated conidium **m, n** colonies on PDA (**m** from front **n** from reverse) Scale bars: 50  $\mu\text{m}$  (**c, d, g–l**); 20  $\mu\text{m}$  (**e, f**).

## Discussion

*Distoseptispora* is one of the sporidesmium-like taxa and is well-known for its asexual morph, which has considerable morphological variations (Su et al. 2016; Yang et al. 2018, 2021). However, the phylogenetic analyses suggest a lack of correlation between phylogenetic relationships and morphological analyses. For instance, species such as *D. appendiculata* D.F. Bao, Z.L. Luo & H.Y. Su, *D. atroviridis* J. Yang & K.D. Hyde, *D. caricis* Crous, *D. fusiformis* J. Yang & K.D. Hyde, *D. lanceolatispora*, *D. leonensis*, *D. neurostrata*, *D. palmarum* S.N. Zhang, K.D. Hyde & J.K. Liu, and *D. saprophytica* W. Dong, H. Zhang & K.D. Hyde cluster together as a subclade in the phylogenetic tree (see Fig. 1). In contrast, morphological analysis reveals significant differences, especially in the characteristics of conidiophores, conidiogenous cells, and conidia (Crous et al. 2019; Hyde et al. 2019; Luo et al. 2019; Dong et al. 2021; Yang et al. 2021; Zhang et al. 2022). This disparity is common within the genus. We recommend adopting a combination approach using molecular and morphological methods for more effective identification within this genus.

Worth noting, among the various species of *Distoseptispora*, *D. martinii* (J.L. Crane & Dumont) J.W. Xia & X.G. Zhang stands out due to its unique morphological characteristics, especially its oblate or subglobose conidia, distinguishing it from other species within *Distoseptispora* (Xia et al. 2017). The species was initially introduced as *Acrodictys martinii* J.L. Crane & Dumont by Crane and Dumont (1975) based on morphological characteristics. Then, it underwent several taxonomic revisions based solely on morphology (Baker et al. 2002; Delgado 2009). Later, Xia et al. (2017) reclassified *Acrodictys martinii* as *D. martinii* based on genetic analysis. However, the morphological traits of *D. martinii* greatly diverge from typical *Distoseptispora* features (Crane and Dumont 1975; Xia et al. 2017). Therefore, we suggest additional collections and analysis of *D. martinii* specimens to ensure the reliability of the provided DNA sequence data.

In recent years, *Distoseptispora* species have been reported worldwide, such as in China, Hungary, Hawaii, Malaysia, and Thailand (Shoemaker and White 1985; McKenzie 1995; Wu and Zhuang 2005; Zhang et al. 2022). Studies on *Distoseptispora* have been particularly extensive in China and Thailand (Hyde et al. 2016, 2019, 2020; Su et al. 2016; Yang et al. 2018, 2021; Luo et al. 2019; Sun et al. 2020; Hu et al. 2023). To date, 73 species of *Distoseptispora* have been documented, of which 55 have been recorded in China (including known species, see Table 2). Our collections further highlight the distribution of the genus in

**Table 2.** *Distoseptispora* species and their locations, lifestyles, habitats, hosts, and corresponding references.

Species	Country	Habitat	Host	References
<i>D. adscendens</i>	China; Hungary; Hawaii	Terrestrial	Decaying wood and decaying branches of many woody plant species; <i>Platanus orientalis</i>	Shoemaker et al. (1985); McKenzie et al. (1995); Wu et al. (2005); Zhang et al. (2022)
<i>D. amniculi</i>	Thailand	Freshwater	Submerged decaying wood	Yang et al. (2021)
<i>D. appendiculata</i>	Thailand	Freshwater	Submerged decaying wood	Luo et al. (2019)
<i>D. aqualignicola</i>	China	Freshwater	Submerged decaying wood	Zhang et al. (2022)
<i>D. aquamyces</i>	China	Freshwater	Submerged decaying wood	Zhang et al. (2022)
<i>D. aquatica</i>	China	Freshwater	Submerged decaying wood	Su et al. (2016); Luo et al. (2019); Li et al. (2021)
<i>D. aquisubtropica</i>	China	Freshwater	Submerged decaying wood	Ma et al. (2022)

Species	Country	Habitat	Host	References
<i>D. atroviridis</i>	China	Freshwater	Submerged decaying wood	Yang et al. (2021)
<i>D. bambusae</i>	China	Terrestrial	Decaying bamboo culms	Sun et al. (2020)
<i>D. bambusicola</i>	China	Freshwater	Submerged bamboo culms	Jayawardena et al. (2022)
<i>D. bangkokensis</i>	Thailand	Freshwater	Submerged decaying wood	Shen et al. (2021)
<i>D. cangshanensis</i>	China	Freshwater	Submerged decaying wood	Luo et al. (2018)
<i>D. caricis</i>	Thailand	Terrestrial	Leaves of <i>Carex</i> sp.	Crous et al. (2019)
<i>D. chinensis</i>	China	Freshwater	Submerged decaying wood	Hyde et al. (2021)
<i>D. clematidis</i>	China; Thailand	Freshwater; Terrestrial	Dried stem of <i>Clematis sikkimensis</i> ; submerged decaying wood	Phukhamsakda et al. (2020); Shen et al. (2021)
<i>D. crassispora</i>	China	Freshwater	Submerged decaying wood	Zhang et al. (2022)
<i>D. curvularia</i>	China	Freshwater	Submerged decaying wood	Zhang et al. (2022)
<i>D. cylindricospora</i>	China	Freshwater	Submerged decaying wood	Phukhamsakda et al. (2022)
<i>D. dehongensis</i>	China; Thailand	Freshwater	Submerged decaying wood	Hyde et al. (2019); Zhang et al. (2022)
<i>D. dipterocarpi</i>	Thailand	Terrestrial	Woody litter of <i>Dipterocarpus</i> sp.	Afshari et al. (2023)
<i>D. effusa</i>	China	Freshwater	Submerged decaying wood	Yang et al. (2021)
<i>D. euseptata</i>	China	Freshwater	Submerged decaying wood	Li et al. (2021)
<i>D. fasciculata</i>	Thailand	Freshwater	Submerged decaying wood	Dong et al. (2021)
<i>D. fluminicola</i>	China	Freshwater	Submerged decaying wood	Su et al. (2016); Luo et al. (2018)
<i>D. fusiformis</i>	China	Freshwater	Submerged decaying wood	Yang et al. (2021)
<i>D. gasaensis</i>	China	Terrestrial	Decaying branches of broadleaf tree	Hu et al. (2023)
<i>D. guanshanensis</i>	China	Terrestrial	Decaying branches of broadleaf tree	Hu et al. (2023)
<i>D. guizhouensis</i>	China	Terrestrial	Decaying wood	Hyde et al. (2021)
<i>D. guttulata</i>	Thailand	Freshwater	Submerged decaying wood	Yang et al. (2018); Luo et al. (2019)
<i>D. hainanensis</i>	China	Terrestrial	Decaying wood	This study
<i>D. hyalina</i>	Thailand	Freshwater	Submerged decaying wood	Yang et al. (2021)
<i>D. hydei</i>	Thailand	Terrestrial	Decaying bamboo culms	Monkai et al. (2020)
<i>D. jinghongensis</i>	China	Terrestrial	Decaying branches of broadleaf tree	Hu et al. (2023)
<i>D. lancangjiangensis</i>	China	Freshwater	Submerged decaying wood	Shen et al. (2021)
<i>D. lanceolatispora</i>	China	Freshwater	Submerged decaying wood	This study
<i>D. leonensis</i>	China; Malaysia	Terrestrial	Decaying culms of grasses or decaying branches	McKenzie et al. (1995); Wu et al. (2005); Zhang et al. (2022)
<i>D. licualae</i>	Thailand	Terrestrial	Decaying leaves of <i>Licuala glabra</i>	Konta et al. (2023)
<i>D. lignicola</i>	China; Thailand	Freshwater	Submerged decaying wood	Luo et al. (2019); Yang et al. (2021)
<i>D. longispora</i>	China	Freshwater	Submerged decaying wood	Song et al. (2020)
<i>D. longnanensis</i>	China	Terrestrial	Decaying branches of broadleaf tree	Hu et al. (2023)
<i>D. martinii</i>	China	Terrestrial	Decaying branches	Xia et al. (2017)
<i>D. meilingensis</i>	China	Freshwater	Decaying bamboo culms	Zhai et al. (2022)
<i>D. menghaiensis</i>	China	Terrestrial	Decaying branches of broadleaf tree	Hu et al. (2023)
<i>D. menglunensis</i>	China	Terrestrial	Decaying branches of broadleaf tree	Hu et al. (2023)
<i>D. mongsongensis</i>	China	Terrestrial	Decaying branches	Liu et al. (2023)
<i>D. multiseptata</i>	Thailand	Freshwater	Submerged decaying wood	Hyde et al. (2016); Yang et al. (2018)
<i>D. nabanheensis</i>	China	Terrestrial	Decaying branches	Liu et al. (2023)
<i>D. nanchangensis</i>	China	Terrestrial	Decaying branches of broadleaf tree	Hu et al. (2023)
<i>D. neostrata</i>	Thailand	Freshwater	Submerged decaying wood	Luo et al. (2019)
<i>D. nonrostrata</i>	China	Freshwater	Submerged decaying wood	Zhang et al. (2022)
<i>D. obclavata</i>	Thailand	Freshwater	Submerged decaying wood	Luo et al. (2019)
<i>D. obpyriformis</i>	China	Freshwater	Submerged decaying wood	Luo et al. (2018)
<i>D. pachyconidia</i>	China	Freshwater; Terrestrial	Submerged decaying wood; decaying wood	Ma et al. (2022); Zhang et al. (2022)
<i>D. palmarum</i>	Thailand	Terrestrial	Rachis of <i>Cocos nucifera</i>	Hyde et al. (2019)
<i>D. phangngaensis</i>	Thailand	Freshwater	Submerged decaying wood	Yang et al. (2018)
<i>D. phragmiticola</i>	China	Terrestrial	Decaying <i>Phragmites australis</i>	Hyde et al. (2023)
<i>D. rayongensis</i>	Thailand	Freshwater	Submerged decaying wood	Hyde et al. (2020)
<i>D. rostrata</i>	China	Freshwater	Submerged decaying wood	Luo et al. (2018)
<i>D. saprophytica</i>	Thailand	Freshwater	Submerged decaying wood	Dong et al. (2021)

Species	Country	Habitat	Host	References
<i>D. septata</i>	China	Freshwater	Submerged decaying wood	Ma et al. (2022)
<i>D. sinensis</i>	China	Terrestrial	Decaying branches	Liu et al. (2023)
<i>D. songkhlaensis</i>	Thailand	Freshwater	Submerged decaying wood	Dong et al. (2021)
<i>D. suoluensis</i>	China	Freshwater	Submerged decaying wood	Yang et al. (2018)
<i>D. tectonae</i>	China; Thailand	Terrestrial; Freshwater	Decaying twig of <i>Tectona grandis</i> ; stems of dead wood; submerged decaying wood; decaying twigs of <i>Edgeworthia chrysantha</i>	Hyde et al. (2016); Luo et al. (2018); Sun et al. (2020); Dong et al. (2021); Li et al. (2021); Zhang et al. (2022); This study
<i>D. tectonigena</i>	Thailand	Terrestrial	Decaying twig of <i>Tectona grandis</i>	Hyde et al. (2016)
<i>D. thailandica</i>	Thailand	Terrestrial	Decaying leaves of <i>Pandanus</i> sp.	Tibpromma et al. (2018)
<i>D. thysanolaenae</i>	China	Terrestrial; Freshwater	Decaying culms of <i>Thysanolaena maxima</i> ; Submerged decaying wood	Phookamsak et al. (2019); Shen et al. (2021)
<i>D. tropica</i>	China	Terrestrial	Decaying wood	Ma et al. (2022)
<i>D. verrucosa</i>	China	Freshwater	Submerged decaying wood	Yang et al. (2021)
<i>D. wuzhishanensis</i>	China	Freshwater	Submerged decaying wood	Ma et al. (2022)
<i>D. xishuangbannaensis</i>	China	Terrestrial; Freshwater	Decaying leaves of <i>Pandanus utilis</i> ; submerged decaying wood	Tibpromma et al. (2018); Ma et al. (2022)
<i>D. yichunensis</i>	China	Terrestrial	Decaying branches of broadleaf tree	Hu et al. (2023)
<i>D. yongxiensis</i>	China	Freshwater	Decaying bamboo culms	Zhai et al. (2022)
<i>D. yunjushanensis</i>	China	Freshwater	Decaying bamboo culms	Zhai et al. (2022)
<i>D. yunnanensis</i>	China	Freshwater	Submerged decaying wood	Li et al. (2021)

China, and we speculate that the country may harbor a greater diversity of the genus. Thus, future studies are needed to validate this hypothesis.

## Acknowledgments

The authors thank Shaun Pennycook, Manaaki Whenua – Landcare Research, New Zealand, for his guidance on the fungal nomenclature and the suggestion on naming the new taxa. The authors also thank the Guizhou Institute of Technology for its support of the experiment. Samantha Chandranath Karunarathna thanks the National Natural Science Foundation of China (Numbers 32260004) and the High-Level Talent Recruitment Plan of Yunnan Province (“High-End Foreign Experts” program) for their support.

## Additional information

### Conflict of interest

The authors have declared that no competing interests exist.

### Ethical statement

No ethical statement was reported.

### Funding

This work was funded by the National Natural Science Foundation of China (NSFC 32360011).

### Author contributions

Conceptualization - Xue-Mei Chen and Yong-Zhong Lu; data curation - Xue-Mei Chen, Xia Tang, Jian Ma, Ning-Guo Liu; formal analysis - Yuan-Pin Xiao, Xue-Mei Chen, Xia Tang, Jian Ma; funding acquisition - Yong-Zhong Lu; investigation - Saowaluck Tibpromma, Sa-

mantha C. Karunaratna, Yuan-Pin Xiao, Yong-Zhong Lu; methodology - Xue-Mei Chen, Yong-Zhong Lu; project administration - Yuan-Pin Xiao, Yong-Zhong Lu; resources - Yong-Zhong Lu, Saowaluck Tibpromma, Samantha C. Karunaratna; software - Xue-Mei Chen; supervision - Yong-Zhong Lu, Saowaluck Tibpromma, Samantha C. Karunaratna; validation - Xue-Mei Chen, Xia Tang, Jian Ma, Ning-Guo Liu; visualization - Saowaluck Tibpromma, Samantha C. Karunaratna; writing original draft - Xue-Mei Chen; writing, review and editing - Xue-Mei Chen, Xia Tang, Jian Ma, Ning-Guo Liu, Saowaluck Tibpromma, Samantha C. Karunaratna, Yuan-Pin Xiao, Yong-Zhong Lu. All authors have read and agreed to the published version of the manuscript.

### Author ORCIDs

Xue-Mei Chen  <https://orcid.org/0009-0004-8631-0735>

Xia Tang  <https://orcid.org/0000-0003-2705-604X>

Jian Ma  <https://orcid.org/0009-0008-1291-640X>

Ning-Guo Liu  <https://orcid.org/0000-0002-9169-2350>

Saowaluck Tibpromma  <https://orcid.org/0000-0002-4706-6547>

Samantha C. Karunaratna  <https://orcid.org/0000-0001-7080-0781>

Yuan-Pin Xiao  <https://orcid.org/0000-0003-1730-3545>

Yong-Zhong Lu  <https://orcid.org/0000-0002-1033-5782>

### Data availability

All of the data that support the findings of this study are available in the main text.

### References

- Afshari N, Gomes de Farias AR, Bhunjun CS, Phukhamsakda C, Hyde KD, Lumyong S (2023) *Distoseptispora dipterocarpi* sp. nov. (Distoseptisporaceae), a lignicolous fungus on decaying wood of *Dipterocarpus* in Thailand. *Current Research in Environmental & Applied Mycology* 13(1): 68–78. <https://doi.org/10.5943/cream/13/1/5>
- Baker WA, Partridge EC, Morgan-Jones G (2002) Notes on hyphomycetes LXXXV. *Junewangia*, a genus in which to classify four *Acrodictys* species and a new taxon. *Mycotaxon* 81: 293–319.
- Chethana KWT, Manawasinghe IS, Hurdeal VG, Bhunjun CS, Appadoo MA, Gentekaki E, Raspé O, Promputtha I, Hyde KD (2021) What are fungal species and how to delineate them? *Fungal Diversity* 109(1): 1–25. <https://doi.org/10.1007/s13225-021-00483-9>
- Crane JL, Dumont KP (1975) Hyphomycetes from the West Indies and Venezuela. *Canadian Journal of Botany* 53(9): 843–851. <https://doi.org/10.1139/b75-102>
- Crous PW, Wingfield MJ, Lombard L, Roets F, Swart WJ, Alvarado P, Carnegie AJ, Moreno G, Luangsaard J, Thangavel R, Alexandrova AV, Baseia IG, Bellanger JM, Bessette AJ, Bessette AR, Peña-Lastra SDL, García D, Gené J, Pham THG, Heykoop M, Malysheva E, Malysheva V, Martín MP, Morozova OV, Noisripoom W, Overton BE, Rea AE, Sewall BJ, Smith ME, Smyth CW, Tasanathai K, Visagie CM, Adamčík S, Alves A, Andrade JP, Aninat MJ, Araújo RVB, Bordallo JJ, Bouffleur T, Baroncelli R, Barreto RW, Bolin J, Cabero J, Caboñ M, Cafà G, Caffot MLH, Cai L, Carlavilla JR, Chávez R, Castro RRLD, Delgat L, Deschuyteneer D, Dios MM, Domínguez LS, Evans HC, Eyssartier G, Ferreira BW, Figueiredo CN, Liu F, Fournier J, Galli-Terasawa LV, Gil-Durán C, Glienke C, Gonçalves MFM, Gryta H, Guarro J, Himaman W, Hywel-Jones N, Iturrieta-González I, Ivanushkina NE, Jargeat P, Khalid AN, Khan J, Kiran M, Kiss L, Kochkina JA, Kolařík M, Kubátová A, Lodge DJ, Loizides M, Luque D, Manjón JL, Marbach PAS, Massola NS, Mata M, Miller

- AN, Mongkolsamrit S, Moreau PA, Morte A, Mujic A, Navarro-Ródenas A, Németh MZ, Nóbrega TF, Nováková A, Olariaga I, Ozerskaya SM, Palma MA, Petters-Vandresen DAL, Piontelli E, Popov ES, Rodríguez A, Requejo Ó, Rodrigues ACM, Rong IH, Roux J, Seifert KA, Silva BDB, Sklenář F, Smith JA, Sousa JO, Souza HG, Souza JTD, Švec K, Tanchaud P, Tanney JB, Terasawa F, Thanakitpipattana D, Torres-García D, Vaca I, Vaghefi N, Iperen ALV, Vasilenko OV, Verkleen A, Yilmaz N, Zamora JC, Zapata M, Jurjević Ž, Groenewald JZ (2019) Fungal Planet description sheets: 951–1041. *Persoonia* 43(1): 223–425. <https://doi.org/10.3767/persoonia.2019.43.06>
- Cubeta MA, Echandi E, Abernethy T, Vilgalys R (1991) Characterization of anastomosis groups of binucleate *Rhizoctonia* species using restriction analysis of an amplified ribosomal RNA gene. *Phytopathology* 81(11): 1395–1400. <https://doi.org/10.1094/Phyto-81-1395>
- Delgado G (2009) South Florida microfungi: *Veramycella bispora*, a new palmicolous, anamorphic genus and species, with some new records for the continental USA. *Mycotaxon* 107(1): 357–373. <https://doi.org/10.5248/107.357>
- Dong W, Hyde KD, Jeewon R, Doilom M, Yu XD, Wang GN, Liu NG, Hu DM, Nalumpang S, Zhang H (2021) Towards a natural classification of annulatasceae-like taxa II: Introducing five new genera and eighteen new species from freshwater. *Mycosphere* 12(1): 1–88. <https://doi.org/10.5943/mycosphere/12/1/1>
- Hall TA (1999) BioEdit: A user-friendly biological sequence alignment editor and analysis program for windows 95/98/NT. *Nucleic Acids Symposium Series* 41: 95–98. <https://doi.org/10.1021/bk-1999-0734.ch008>
- Hillis DM, Bull JJ (1993) An empirical test of bootstrapping as a method for assessing confidence in phylogenetic analysis. *Systematic Biology* 42(2): 182–192. <https://doi.org/10.1093/sysbio/42.2.182>
- Hu YF, Liu JW, Luo XX, Xu ZH, Xia JW, Zhang XG, Castañeda-Ruiz RF, Ma J (2023) Multi-locus phylogenetic analyses reveal eight novel species of *Distoseptispora* from southern China. *Microbiology Spectrum* 11(6): e02468–e23. <https://doi.org/10.1128/spectrum.02468-23>
- Huelsenbeck JP, Ronquist FJB (2001) MRBAYES: Bayesian inference of phylogenetic trees. *Bioinformatics* 17(8): 754–755. <https://doi.org/10.1093/bioinformatics/17.8.754>
- Hyde KD, Hongsanan S, Jeewon R, Bhat DJ, McKenzie EHC, Jones EBG, Phookamsak R, Ariyawansa HA, Boonmee S, Zhao Q, Abdel-Aziz FA, Abdel-Wahab MA, Banmai S, Chomnunti P, Cui BK, Daranagama DA, Das K, Dayarathne MC, Silva NID, Goes-Neto AA, Huang SK, Jayasiri SC, Jayawardena RS, Konta S, Lee HB, Li WJ, Lin CG, Liu JK, Lu YZ, Luo ZL, Manawasinghe IS, Manimohan P, Mapook A, Niskanen T, Norphanphoun C, Papizadeh M, Perera RH, Phukhamsakda C, Richter C, Santiago ALCMDA, Drechsler-Santos ER, Senanayake IC, Tanaka K, Tennakoon TMDS, Thambugala KM, Tian Q, Tibpromma S, Thongbai B, Vizzini A, Wanasinghe DN, Wijayawardene NN, Wu HX, Yang J, Zeng XY, Zhang H, Zhang JF, Bulgakov TS, Camporesi E, Bahkali AH, Amoozegar MA, Araujo-Neta LS, Ammirati JF, Baghela A, Bhatt RP, Bojantchev D, Buyck B, Silva GAD, Lima CLFD, Oliveira RJVD, Souza CAFD, Dai YC, Dima B, Duong TT, Ercole E, Mafalda-Freire F, Ghosh A, Hashimoto A, Kamolhan S, Kang JC, Karunarathna SC, Kirk PM, Kytovuori I, Lantieri A, Liimatainen K, Liu ZY, Liu XY, Lucking R, Medardi G, Mortimer PE, Nguyen TTT, Promputtha I, Raj KNA, Reck MA, Lumyong S, Shahzadeh-Fazeli SA, Stadler M, Soudi MR, Su HY, Takahashi T, Tangthirasunun N, Uniyal P, Wang Y, Wen TC, Xu JC, Zhang ZK, Zhao YC, Zhou JL, Zhu L (2016) Fungal diversity

- notes 367–490: taxonomic and phylogenetic contributions to fungal taxa. *Fungal Diversity* 80: 1–270. <https://doi.org/10.1007/s13225-016-0373-x>
- Hyde KD, Tennakoon DS, Jeewon R, Bhat DJ, Maharachchikumbura SSN, Rossi W, Leonardi M, Lee HB, Mun HY, Houbraken J, Nguyen TTT, Jeon SJ, Frisvad JC, Wanasinghe DN, Lücking R, Aptroot A, Cáceres MES, Karunarathna SC, Hongsanan S, Phookamsak R, Silva NI, Thambugala KM, Jayawardena RS, Senanayake IC, Boonmee S, Chen J, Luo ZL, Phukhamsakda C, Pereira OL, Abreu VP, Rosado AWC, Bart B, Randrianjohany E, Hofstetter V, Gibertoni TB, Soares AWS, Plautz Jr HL, Sotão HMP, Xavier WKS, Bezerra JDP, Oliveira TGL, Souza-Motta CM, Magalhães OMC, Bundhun D, Harishchandra D, Manawasinghe IS, Dong W, Zhang SN, Bao DF, Samarakoon MC, Pem D, Karunarathna A, Lin CG, Yang J, Perera RH, Kumar V, Huang SK, Dayarathne MC, Ekanayaka AH, Jayasiri SC, Xiao YP, Konta S, Niskanen T, Liimatainen K, Dai YC, Ji XH, Tian XM, Mešić A, Singh SK, Phuththacharoen K, Cai L, Sorvongxay T, Thiagaraja V, Norphanphoun C, Chaiwan N, Lu YZ, Jiang HB, Zhang JF, Abeywickrama PD, Aluthmuhandiram JVS, Brahmanage RS, Zeng M, Chethana T, Wei DP, Réblová M, Fournier J, Nekvindová J, Barbosa RN, Santos JEF, Oliveira NT, Li GJ, Ertz D, Shang QJ, Phillips AJL, Kuo CH, Camporesi E, Bulgakov TS, Lumyong S, Jones EBG, Chomnunti P, Gentekaki E, Bungartz F, Zeng XY, Fryar S, Kralčec Z, Liang JM, Li GS, Wen TC, Singh PN, Gafforov Y, Promputtha I, Yasanthika E, Goonasekara ID, Zhao RL, Zhao Q, Kirk PM, Liu JK, Yan JY, Mortimer PE, Xu JC, Doilom M (2019) Fungal diversity notes 1036–1150: Taxonomic and phylogenetic contributions on genera and species of fungal taxa. *Fungal Diversity* 96: 1–242. <https://doi.org/10.1007/s13225-019-00429-2>
- Hyde KD, Jeewon R, Chen YJ, Bhunjun CS, Calabon MS, Jiang HB, Lin CG, Norphanphoun C, Sysouphanthong P, Pem D, Tibpromma S, Zhang Q, Doilom M, Jayawardena RS, Liu JK, Maharachchikumbura SSN, Phukhamsakda C, Phookamsak R, Al-Sadi AM, Thongklang N, Wang Y, Gafforov Y, Jones EBG, Lumyong S (2020) The numbers of fungi: Is the descriptive curve flattening? *Fungal Diversity* 103: 219–271. <https://doi.org/10.1007/s13225-020-00458-2>
- Hyde KD, Suwannarach N, Jayawardena RS, Manawasinghe IS, Liao CF, Doilom M, Cai L, Zhao P, Buyck B, Phukhamsakda C, Su WX, Fu YP, Li Y, Zhao RL, He MQ, Li JX, Tibpromma S, Lu L, Tang X, Kang JC, Ren GH, Hofstetter V, Ryoo R, Antonín V, Hurdeal VG, Gentekaki E, Zhang JY, Lu YZ, Senanayake IC, Yu FM, Zhao Q, Bao DF (2021) Mycosphere notes 325–344—Novel species and records of fungal taxa from around the world. *Mycosphere* 12: 1101–1156. <https://doi.org/10.5943/mycosphere/12/1/14>
- Hyde KD, Norphanphoun C, Ma J, Yang HD, Zhang JY, Du TY, Gao Y, Gomes de Farias AR, Gui H, He SC, He YK, Li CJY, Liu XF, Lu L, Su HL, Tang X, Tian XG, Wang SY, Wei DP, Xu RF, Xu RJ, Yang Q, Yang YY, Zhang F, Zhang Q, Bahkali AH, Boonmee S, Chethana KWT, Jayawardena RS, Lu YZ, Karunarathna SC, Tibpromma S, Wang Y, Zhao Q (2023) Mycosphere notes 387–412—novel species of fungal taxa from around the world. *Mycosphere* 14(1): 663–744. <https://doi.org/10.5943/mycosphere/14/1/8>
- Index Fungorum (2024) Index Fungorum. <https://www.indexfungorum.org/Names/Names.asp> [Accessed 2 January 2024]
- Jayasiri SC, Hyde KD, Ariyawansa HA, Bhat J, Buyck B, Cai L, Dai YC, Abd-Elsalam KA, Ertz D, Hidayat I, Jeewon R, Jones EBG, Bahkali AH, Karunarathna SC, Liu JK, Luangsa-ard JJ, Lumbsch HT, Maharachchikumbura SSN, McKenzie EHC, Moncalvo JM, Ghobad-Nejhad M, Nilsson H, Pang KL, Pereira OL, Phillips AJL, Raspé O, Rollins AW, Romero AI, Etayo J, Selçuk F, Stephenson SL, Suetrong S, Taylor JE, Tsui CKM, Vizzini A, Abdel-Wahab MA, Wen TC, Boonmee S, Dai DQ, Daranagama DA, Dissanayake AJ,

- Ekanayaka AH, Fryar SC, Hongsanan S, Jayawardena RS, Li WJ, Perera RH, Phookamsak R, de Silva NI, Thambugala KM, Tian Q, Wijayawardene NN, Zhao RL, Zhao Q, Kang JC, Promputtha I (2015) The Faces of Fungi database: fungal names linked with morphology, phylogeny and human impacts. *Fungal Diversity* 74: 3–18. <https://doi.org/10.1007/s13225-015-0351-8>
- Jayawardena RS, Hyde KD, Wang S, Sun YR, Suwannarach N, Sysouphanthong P, Abdel-Wahab MA, Abdel-Aziz FA, Abeywickrama PD, Abreu VP, Armand A, Aptroot A, Bao DF, Begerow D, Bellanger JM, Bezerra JDP, Bundhun D, Calabon MS, Cao T, Cantillo T, Carvalho JLVR, Chaiwan N, Chen CC, Courtecuisse R, Cui BK, Damm U, Denchev CM, Denchev TT, Deng CY, Devadatha B, de Silva NI, dos Santos LA, Dubey NK, Dumez S, Fernandez HS, Firmino AL, Gafforov Y, Gajanayake AJ, Gomdola D, Gunaseelan S, He SC, Htet ZH, Kaliyaperumal M, Kemler M, Kezo K, Kularathnage ND, Leonardi M, Li JP, Liao CF, Liu S, Loizides M, Luangharn T, Ma J, Madrid H, Mahadevakumar S, Maharachchikumbura SSN, Manamgoda DS, Martín MP, Mekala N, Moreau PA, Mu YH, Pahoua P, Pem D, Pereira OL, Phonrob W, Phukhamsakda C, Raza M, Ren GC, Rinaldi AC, Rossi W, Samarakoon BC, Samarakoon MC, Sarma VV, Senanayake IC, Singh A, Souza MF, Souza-Motta CM, Spielmann AA, Su WX, Tang X, Tian XG, Thambugala KM, Thongklang N, Tennakoon DS, Wannathes N, Wei DP, Welti S, Wijesinghe SN, Yang HD, Yang YH, Yuan HS, Zhang H, Zhang JY, Balasuriya A, Bhunjun CS, Bulgakov TS, Cai L, Camporesi E, Chomnunti P, Deepika YS, Doilom M, Duan WJ, Han SL, Huanraluek N, Jones EBG, Lakshmidhevi N, Li Y, Lumyong S, Luo ZL, Khuna S, Kumla J, Manawasinghe IS, Mapook A, Punyaboon W, Tibpromma S, Lu YZ, Yan JY, Wang Y (2022) Fungal diversity notes 1512–1610: Taxonomic and phylogenetic contributions on genera and species of fungal taxa. *Fungal Diversity* 117: 1–272. <https://doi.org/10.1007/s13225-022-00513-0>
- Jeewon R, Hyde KD (2016) Establishing species boundaries and new taxa among fungi: Recommendations to resolve taxonomic ambiguities. *Mycosphere* 7(11): 1669–1677. <https://doi.org/10.5943/mycosphere/7/11/4>
- Katoh K, Standley DM (2013) Evolution MAFFT multiple sequence alignment software version 7: Improvements in performance and usability. *Molecular Biology and Evolution* 30(4): 772–780. <https://doi.org/10.1093/molbev/mst010>
- Konta S, Tibpromma S, Karunarathna SC, Samarakoon MC, Steven LS, Mapook A, Boonmee S, Senwanna C, Balasuriya A, Eungwanichayapant PD, Hyde KD (2023) Morphology and multigene phylogeny reveal ten novel taxa in Ascomycota from terrestrial palm substrates (Arecaceae) in Thailand. *Mycosphere* 14(1): 107–152. <https://doi.org/10.5943/mycosphere/14/1/2>
- Li WL, Liu ZP, Zhang T, Dissanayake AJ, Luo ZL, Su HY, Liu JK (2021) Additions to *Distoseptispora* (Distoseptisporaceae) associated with submerged decaying wood in China. *Phytotaxa* 520: 75–86. <https://doi.org/10.11646/phytotaxa.520.1.5>
- Liu YJ, Whelen S, Hall BD (1999) Phylogenetic relationships among ascomycetes: evidence from an RNA polymerase II subunit. *Molecular Biology and Evolution* 16: 1799–1808. <https://doi.org/10.1093/oxfordjournals.molbev.a026092>
- Liu JW, Hu YF, Luo XX, Xu ZH, Castañeda-Ruíz RF, Xia JW, Zhang XG, Zhang LH, Cui RQ, Ma J (2023) Morphological and phylogenetic analyses reveal three new species of *Distoseptispora* (Distoseptisporaceae, Distoseptisporales) from Yunnan, China. *Journal of Fungi* 9(4): 470. <https://doi.org/10.3390/jof9040470>
- Luo ZL, Hyde KD, Liu JK, Bhat DJ, Su H, Bao DF, Li WL (2018) Lignicolous freshwater fungi from China II: Novel *Distoseptispora* (Distoseptisporaceae) species from northwest-

- ern Yunnan Province and a suggested unified method for studying lignicolous freshwater fungi. *Mycosphere* 9: 444–461. <https://doi.org/10.5943/mycosphere/9/3/2>
- Luo ZL, Hyde KD, Liu JK, Maharachchikumbura SSN, Jeewon R, Bao DF, Bhat DJ, Lin CG, Li WL, Yang J, Liu NG, Lu YZ, Jayawardena RS, Li JF, Su HY (2019) Freshwater Sordariomycetes. *Fungal Diversity* 99: 451–660. <https://doi.org/10.1007/s13225-019-00438-1>
- Ma J, Zhang JY, Xiao XJ, Xiao YP, Tang X, Boonmee S, Kang JC, Lu YZ (2022) Multi-gene phylogenetic analyses revealed five new species and two new records of *Distoseptisporales* from China. *Journal of Fungi* 8(11): e1202. <https://doi.org/10.3390/jof8111202>
- McKenzie EHC (1995) Dematiaceous hyphomycetes on Pandanaceae 5 *Sporidesmium sensu lato*. *Mycotaxon* 56: 9–29.
- Miller MA, Pfeiffer W, Schwartz T (2010) Creating the CIPRES Science Gateway for inference of large phylogenetic trees. Gateway Computing Environments Workshop (GCE), New Orleans (USA), November 2010, IEEE, 8 pp. <https://doi.org/10.1109/GCE.2010.5676129>
- Monkai J, Boonmee S, Ren G, Wei D, Phookamsak R, Mortimer PE (2020) *Distoseptispora hydei* sp. nov. (Distoseptisporaceae), a novel lignicolous fungus on decaying bamboo in Thailand. *Phytotaxa* 459: 93–107. <https://doi.org/10.11646/phytotaxa.459.2.1>
- Nylander JAA (2004) MrModeltest 20 Program Distributed by the Author. Evolutionary Biology Centre, Uppsala University, Uppsala.
- Phookamsak R, Hyde KD, Jeewon R, Bhat DJ, Jones EBG, Maharachchikumbura SSN, Raspé O, Karunarathna SC, Wanasinghe DN, Hongsanan S, Doilom M, Tennakoon DS, Machado AR, Firmino AL, Ghosh A, Karunarathna A, Mešić A, Dutta AK, Thongbai B, Devadatha B, Norphanphoun C, Senwantha C, Wei DP, Pem D, Ackah FK, Wang GN, Jiang HB, Madrid H, Lee HB, Goonasekara ID, Manawasinghe IS, Kušan I, Cano J, Gené J, Li JF, Das K, Acharya K, Raj KNA, Latha KPD, Chethana KWT, He MQ, Dueñas M, Jadan M, Martín MP, Samarakoon MC, Dayarathne MC, Raza M, Park MS, Telleria MT, Chaiwan N, Matočec N, Silva NI, Pereira OL, Singh PN, Manimohan P, Uniya P, Shang QJ, Bhatt RP, Perera RH, Alvarenga RLM, Nogal-Prata S, Singh SK, Vadthananat S, Oh SY, Huang SK, Rana S, Konta S, Paloi S, Jayasiri SC, Jeon SJ, Mehmood T, Gibertoni TB, Nguyen TTT, Singh U, Thiyagaraja V, Sarma VV, Dong W, Yu XD, Lu YZ, Lim YW, Chen Y, Tkalčec Z, Zhang ZF, Luo ZL, Daranagama DA, Thambugala KM, Tibpromma S, Camporesi E, Bulgakov TS, Dissanayake AJ, Senanayake IC, Dai DQ, Tang LZ, Khan S, Zhang H, Promputtha I, Cai L, Chomnunti P, Zhao RL, Lumyong S, Boonmee S, Wen TC, Mortimer PE, Xu JC (2019) Fungal diversity notes 929–1035: Taxonomic and phylogenetic contributions on genera and species of fungi. *Fungal Diversity* 95: 1–273. <https://doi.org/10.1007/s13225-019-00421-w>
- Phukhamsakda C, McKenzie EHC, Phillips AJL, Jones EBG, Bhat DJ, Marc S, Bhunjun CS, Wanasinghe DN, Thongbai B, Camporesi E, Ertz D, Jayawardena RS, Perera RH, Ekanayake AH, Tibpromma S, Doilom M, Xu JC, Hyde KD (2020) Microfungi associated with *Clematis* (Ranunculaceae) with an integrated approach to delimiting species boundaries. *Fungal Diversity* 102: 1–203. <https://doi.org/10.1007/s13225-020-00448-4>
- Phukhamsakda C, Nilsson RH, Bhunjun CS, Farias ARGD, Sun YR, Wijesinghe SN, Raza M, Bao DF, Lu L, Tibpromma S, Dong W, Tennakoon DS, Tian XG, Xiong YR, Karunarathna SC, Cai L, Luo ZL, Wang Y, Manawasinghe IS, Camporesi I, Kirk PM, Promputtha I, Kuo CH, Su HY, Doilom M, Li Y, Fu YP, Hyde KD (2022) The numbers of fungi: Contri-

- butions from traditional taxonomic studies and challenges of metabarcoding. *Fungal Diversity* 114: 327–386. <https://doi.org/10.1007/s13225-022-00502-3>
- Rehner SA, Samuels GJ (1994) Taxonomy and phylogeny of *Gliocladium* analysed from nuclear large subunit ribosomal DNA sequences. *Mycological Research* 98: 625–634. [https://doi.org/10.1016/S0953-7562\(09\)80409-7](https://doi.org/10.1016/S0953-7562(09)80409-7)
- Ronquist F, Teslenko M, Van Der Mark P, Ayres DL, Darling A, Höhna S, Larget B, Liu L, Suchard MA, Huelsenbeck JP (2012) MrBayes 3.2: Efficient Bayesian Phylogenetic Inference and model choice across a large model space. *Systematic Biology* 61: 539–542. <https://doi.org/10.1093/sysbio/sys029>
- Senanayake IC, Rathnayaka AR, Marasinghe DS, Calabon MS, Gentekaki E, Lee HB, Hurdeal VG, Pem D, Dissanayake LS, Wijesinghe SN, Bundhun D, Goonasekara ID, Abeywickrama PD, Bhunjun CS, Jayawardena RS, Wanasinghe DN, Jeewon R, Bhat DJ, Xiang MM (2020) Morphological approaches in studying fungi: collection, examination, isolation, sporulation and preservation. *Mycosphere* 11: 2678–2754. <https://doi.org/10.5943/mycosphere/11/1/20>
- Shen HW, Bao DF, Hyde KD, Su HY, Bhat DJ, Luo ZL (2021) Two novel species and two new records of *Distoseptispora* from freshwater habitats in China and Thailand. *MycKeys* 84: 79–101. <https://doi.org/10.3897/mycokeys.84.71905>
- Shenoy BD, Jeewon R, Wu WP, Bhat DJ, Hyde KD (2006) Ribosomal and RPB2 DNA sequence analyses suggest that *Sporidesmium* and morphologically similar genera are polyphyletic. *Mycological Research* 110: 916–928. <https://doi.org/10.1016/j.mycres.2006.06.004>
- Shoemaker RA, White GP (1985) *Lasiosphaeria caesariata* with *Sporidesmium hormiscioides* and *L. triseptata* with *S. adscendens*. *Sydowia* 38: 278–283.
- Song HY, El Sheikha AF, Zhai ZJ, Zhou JP, Chen MH, Huo GH, Huang XG, Hu DM (2020) *Distoseptispora longispora* sp. Nov. from freshwater habitats in China. *Mycotaxon* 135(3): 513–523. <https://doi.org/10.5248/135.513>
- Stamatakis A, Hoover P, Rougemont J (2008) A rapid bootstrap algorithm for the RAxML web servers. *Systematic Biology* 57(5): 758–771. <https://doi.org/10.1080/10635150802429642>
- Su HY, Hyde KD, Maharachchikumbura SSN, Ariyawansa HA, Luo ZL, Promputtha I, Tian Q, Lin CG, Shang QJ, Zhao YC, Chai HM, Liu XY, Bahkali AH, Bhat JD, McKenzie EHC, Zhou DQ (2016) The families Distoseptisporaceae fam. Nov., Kirschsteinioteliaceae, Sporormiaceae, and Torulaceae, with new species from freshwater in Yunnan Province, China. *Fungal Diversity* 80: 375–409. <https://doi.org/10.1007/s13225-016-0362-0>
- Sun Y, Goonasekara ID, Thambugala KM, Jayawardena RS, Wang Y, Hyde KD (2020) *Distoseptispora bambusae* sp. nov. (Distoseptisporaceae) on bamboo from China and Thailand. *Biodiversity Data Journal* 8: e53678. <https://doi.org/10.3897/BDJ.8.e53678.figure2>
- Swofford DL (2002) PAUP\*: Phylogenetic analysis using parsimony (and other methods), version 4.0 b10 MA: Sinauer Associates, Sunderland.
- Tibpromma S, Hyde KD, McKenzie EHC, Bhat DJ, Phillips AJL, Wanasinghe DN, Samarakoon MC, Jayawardena RS (2018) Fungal diversity notes 840–928: Micro-fungi associated with Pandanaceae. *Fungal Diversity* 100: 1–160. <https://doi.org/10.1007/s13225-018-0408-6>
- Vaidya G, Lohman DJ, Meier R (2011) SequenceMatrix: Concatenation software for the fast assembly of multi-gene datasets with character set and codon information. *Cladistics* 27: 171–180. <https://doi.org/10.1111/j.1096-0031.2010.00329.x>

- Vilgalys R, Hester M (1990) Rapid genetic identification and mapping of enzymatically amplified ribosomal DNA from several *Cryptococcus* species. *Journal of Bacteriology* 172: 4238–4246. <https://doi.org/10.1128/jb.172.8.4238-4246.1990>
- White TJ, Bruns T, Lee SJWT, Taylor J (1990) Amplification and direct sequencing of fungal ribosomal RNA genes for phylogenetics. *PCR protocols: A guide to methods and applications* 18(1): 315–322. <https://doi.org/10.1016/B978-0-12-372180-8.50042-1>
- Wu WP, Zhuang WY (2005) *Sporidesmium*, *Endophragmiella* and related genera from China. *Fungal Diversity Research Series* 15: 1–351.
- Xia JW, Ma YR, Li Z, Zhang XG (2017) Acrodictys-like wood decay fungi from southern China, with two new families Acrodictyceae and Junewangiaceae. *Scientific Reports* 7: e7888. <https://doi.org/10.1038/s41598-017-08318-x>
- Yang J, Maharachchikumbura SSN, Liu JK, Hyde KD, Jones EBG, Al-Sadi AM, Liu ZY (2018) *Pseudostanjehughesia aquitropica* gen. et sp. nov. and *Sporidesmium sensu lato* species from freshwater habitats. *Mycological Progress* 17: 591–616. <https://doi.org/10.1007/s11557-017-1339-4>
- Yang J, Liu LL, Jones EBG, Li WL, Hyde KD, Liu ZY (2021) Morphological variety in *Distoseptispora* and introduction of six novel species. *Journal of Fungi* 7: e945. <https://doi.org/10.3390/jof7110945>
- Zhai ZJ, Yan JQ, Li WW, Gao Y, Hu HJ, Zhou JP, Song HY, Hu DM (2022) Three novel species of *Distoseptispora* (Distoseptisporaceae) isolated from bamboo in Jiangxi Province, China. *MycKeys* 88: 35–54. <https://doi.org/10.3897/mycokeys.88.79346>
- Zhang H, Zhu R, Qing Y, Yang H, Li CX, Wang GN, Zhang D, Ning P (2022) Polyphasic identification of *Distoseptispora* with six new species from freshwater. *Journal of Fungi* 8: e1063. <https://doi.org/10.3390/jof8101063>



# Three new *Pyrenula* species with 3-septate ascospores with red or orange oil when over-mature (Ascomycota, Pyrenulales, Pyrenulaceae) from China

Mingzhu Dou<sup>1</sup>, Shengnan Liu<sup>1</sup>, Jiechen Li<sup>1</sup>, André Aptroot<sup>2</sup>, Zefeng Jia<sup>1</sup>

<sup>1</sup> College of Life Sciences, Liaocheng University, Liaocheng 252059, China

<sup>2</sup> Laboratório de Botânica, Liquenologia, Instituto de Biociências, Universidade Federal de Mato Grosso do Sul, Avenida Costa e Silva s/n, Bairro Universitário, CEP 79070-900, Campo Grande, Mato Grosso do Sul, Brazil

Corresponding author: Zefeng Jia (zjia2008@163.com)

## Abstract

The lichenised fungal genus *Pyrenula* is a very common crustose lichen element in tropical to subtropical forests, but little research has been done on this genus in China. During our study on *Pyrenula* in China, based on morphological characteristics, chemical traits and molecular phylogenetic analysis (ITS and nuLSU), three new 3-septate species with red or orange oil in over-mature ascospores were found: *Pyrenula inspersa* **sp. nov.**, *P. thailandicoides* **sp. nov.** and *P. apiculata* **sp. nov.** Compared to the known 3-septate species of *Pyrenula* with red or orange oil, *P. inspersa* is characterised by the inspersed hamathecium; *P. thailandicoides* is characterised by the IKI+ red hamathecium and the existence of an unknown lichen substance; and *P. apiculata* is characterised by the absence of endospore layers in the spore tips and the absence of pseudocyphellae. It is reported for the first time that the presence of a gelatinous halo around the ascospores of *Pyrenula* is common. A word key for the *Pyrenula* species with red or orange oil in over-mature ascospores is provided.

**Key words:** morphology, new species, phylogeny, Pyrenulaceae, taxonomy



Academic editor: Thorsten Lumbsch

Received: 4 October 2023

Accepted: 30 January 2024

Published: 12 February 2024

**Citation:** Dou M, Liu S, Li J, Aptroot A, Jia Z (2024) Three new *Pyrenula* species with 3-septate ascospores with red or orange oil when over-mature (Ascomycota, Pyrenulales, Pyrenulaceae) from China. MycoKeys 102: 107–125. <https://doi.org/10.3897/mycokeys.102.113619>

**Copyright:** © Mingzhu Dou et al.

This is an open access article distributed under terms of the Creative Commons Attribution License (Attribution 4.0 International – CC BY 4.0).

## Introduction

The lichen genus *Pyrenula* Ach. (Pyrenulaceae) was first established by Acharius, with *Pyrenula nitida* (Weigel) Ach. as the type species (Acharius 1814). *Pyrenula* is mainly a tropical and subtropical genus (Mendonça et al. 2016) and the Neotropics are the centre of diversity of the genus, which typically grow on bark (Aptroot 2012). The genus is characterised by UV– or UV+ yellow thallus, with or without pseudocyphellae, with or without lichexanthone or anthraquinones, perithecioid ascomata, occasionally inspersed hamathecia, unbranched filaments and distoseptate, transversely septate or (sub)muriform ascospores (Aptroot 2012; Mendonça et al. 2016).

In a world key of *Pyrenula* species, Aptroot (2012) accepted 169 species out of the ca. 745 named taxa in the genus. Since then, many new species of *Pyrenula* have been described and the genus now comprises ca. 238 species

(Aptroot 2012, 2021; Aptroot et al. 2018; Ingle et al. 2018; Miranda-González et al. 2022; Mishra et al. 2022; Lücking et al. 2023; Soto-Medina et al. 2023), of which 41 species have so far been found in China (Aptroot 2012, 2021; Wang et al. 2018; Fu et al. 2018, 2019; Wei 2020; Xie et al. 2021).

Harris (1989) was the first to recognise the presence of red or orange oily granules in over-mature ascospores of some *Pyrenula* species and to point out the significance of the degradation stage of spores for the taxonomy of *Pyrenula*. Aptroot et al (2013) described the degradation process in detail: in a few species, the old spores assume a reddish tinge, the wall becomes red-brown and the remains of the lumina develop into red or orange granules. Now, a total of seven species with red or orange oil in over-mature ascospores have been reported, of which four have transverse distoseptate ascospores, viz. *P. concastroma* R.C. Harris, *P. bahiana* Malme, *P. sexlocularis* (Nyl.) Müll. Arg. and *P. thailandica* Aptroot; three have (sub)muriform ascospores, viz. *P. seminuda* (Müll. Arg.) Sipman & Aptroot, *P. breutelii* (Müll. Arg.) Aptroot and *P. macularis* (Zahlbr.) R.C. Harris. Our study adds three septate *Pyrenula* species with red or orange oily granules in over-mature ascospores.

As far as we can tell, there have been no reports of a gelatinous halo around the ascospores in *Pyrenula*. This could mislead lichen taxonomists into believing that ascospore gelatinous haloes are absent in this genus. However, during our study of *Pyrenula* in southern China, we found that gelatinous haloes are common in this genus and present in all the three new species described here.

In term of molecular data, the attempts to infer relationships within Pyrenulaceae presented two well-supported groups that do not seem to differ based on their morphology, apart from the presence/absence of pseudocyphellae; meanwhile, delimitation problems in few taxa, for instance, *P. quassiicola* and *P. mamillana*, were highlighted (Weerakoon et al. 2012; Gueidan et al. 2016). Our phylogenetic analysis using ribosomal genes (nuLSU and ITS) confirmed the above conclusions and supported the description of three new species.

## Materials and methods

### Morphological and chemical analyses

The specimens were collected in southern China and deposited in the Fungarium, College of Life Sciences, Liaocheng University, China (LCUF). Morphological and anatomical characters of thalli and apothecia were examined and photographed under an Olympus SZX16 dissecting microscope and an Olympus BX53 compound microscope. The lichen secondary metabolites were detected and identified by thin-layer chromatography using solvent C and B (Orange et al. 2010; Jia and Wei 2016).

### DNA extraction, PCR sequencing and phylogenetic analysis

Genomic DNA was extracted from ascomata using the Hi-DNA-secure Plant Kit (Tiangen, Beijing, China) according to the manufacturer's protocol. The nuLSU and ITS regions were amplified using the primer pair AL2R/LR6 (Vilgalys and Hester 1990; Mangold et al. 2008) and ITS1F/ITS4 (White et al. 1990; Gardes and Bruns 1993). The PCR amplification progress followed Dou et al. (2018)

and the PCR products were sequenced by Biosune Inc. (Shanghai). The newly-generated sequences were submitted to GenBank (Table 1).

Multi-locus (ITS and nuLSU) phylogenetic analysis was performed. The combined analysis included 187 sequences (Table 1), of which nine sequences were newly generated and 178 were downloaded in GenBank (Lutzoni et al. 2001; Geiser et al. 2006; Weerakoon et al. 2012; Gueidan et al. 2016). The dataset represented 121 taxa, amongst which two out-group species, *Endocarpon pusillum* and *Cyphellophora europaea*, were chosen, based on previous studies (Weerakoon et al. 2012; Gueidan et al. 2016). All *Pyrenula* taxa that could be found in GenBank were included in our data matrix.

The alignment of sequences for each marker (ITS and nuLSU) was undertaken independently by applying MAFFT 7 (Kato and Standley 2013). We used the “maskSegment” function in the R package AlignmentFilter (Zhang et al. 2023) to mask ambiguously-aligned or overly-divergent segments (stringency-controlling parameter prob set to 0.05) and then used the “degap” function to remove sites with more than 50% gaps. The congruence of the two datasets was tested using a 70% reciprocal bootstrap criterion (Mason-Gamer and Kellogg 1996): the two matrices (nuLSU, ITS) were analysed separately with RAxML v.8.2.12 (Stamatakis 2014) using 100 bootstrap pseudoreplicates and implementing a GTRGAMMA model on the CIPRES Web Portal (<http://www.phylo.org>). The resulting trees were compared and any hard conflicts detected were eliminated by pruning sequences or taxa out of the datasets. The two single-locus alignments were concatenated in PhyloSuite v.1.2.2 (Zhang et al. 2020). The concatenated data matrix comprised 1581 characters (674 for ITS and 907 for nuLSU). For BI (Bayesian Inference) analysis, PartitionFinder 2 (Lanfear et al. 2017) was used to determine the best-fit model for each partition. The dataset was partitioned into gene groups, with the GTR+I+G and SYM+I+G substitution models applied to ITS gene and nuLSU gene, respectively. BI analysis was performed with MrBayes 3.2.7 (Ronquist et al. 2012). Two runs of four chains were carried out for 10,000,000 generations and trees were sampled every 1000 generations. The convergence of parameters was checked with the programme Tracer v.1.6 (Rambaut et al. 2014). The first 25% of the convergence runs were discarded as burn-in. Construction of the ML (Maximum Likelihood) tree was undertaken by applying RAxML v.8.2.12 (Stamatakis 2014), using 100 bootstrap pseudoreplicates and a GTRGAMMA model on the CIPRES Web Portal (<http://www.phylo.org>). ML bootstrap values (BS)  $\geq 70\%$  and Bayesian posterior probabilities (PP)  $\geq 0.95$  were considered as significantly supported. The datasets/alignments were deposited in TreeBase (<http://purl.org/phylo/treebase/phyloids/study/TB2:S31046>).

## Results and discussion

### Phylogenetic analyses

The dataset includes 105 ITS sequences and 82 LSU sequences, of which five ITS sequences and four LSU sequences are newly generated in this study. The BI and ML trees showed similar topologies, so only the BI tree is provided here as Fig. 1. Compared with the dataset of Gueidan et al. (2016), our phylogenetic analysis includes nine additional species (*Pyrenula punctella*, *P. nitidella*,

**Table 1.** Information for the sequences used in this study. Newly-generated sequences are shown in bold.

Species Name	Specimen No.	Locality	GenBank accession number	
			ITS	nuLSU
<i>P. thailandicoides</i> M.Z. Dou & Z.F. Jia	FJ220208	China Fujian	<b>OR578593</b>	–
	YN18212	China Yunnan	<b>OR578589</b>	<b>OR578570</b>
	YN18015	China Yunnan	<b>OR578590</b>	<b>OR578571</b>
<i>P. inspersa</i> M.Z. Dou & Z.F. Jia	HN17058	China Hainan	<b>OR578591</b>	<b>OR578572</b>
<i>P. apiculata</i> M.Z. Dou & Z.F. Jia	YN18172	China Yunnan	<b>OR578592</b>	<b>OR578573</b>
<i>P. cf. acutalis</i> R.C. Harris	F_19092_b	Australia	–	DQ329026
<i>P. aff. aggregataspistea</i> Aptroot & M. Cáceres	AA11618	Brazil	–	KT808561
<i>P. aggregataspistea</i> Aptroot & M. Cáceres	AA11216	Brazil	KT820112	KT808557
<i>P. anomala</i> (Ach.) A. Massal.	AA11222	Brazil	KT820168	KT808607
	AA11607	Brazil	KT820116	–
	AA15591	Brazil	KT820113	–
<i>P. arthoniotheca</i> Upreti	AA11887	Brazil	KT820120	–
<i>P. aspistea</i> (Ach.) Ach	AA11263	Brazil	KT820121	KT808560
	AA13547	Brazil	KT820123	–
	CBS_109078	Hong Kong	–	EF411063
	CG3030	Vietnam	KT820124	KT808562
	CG3060	Vietnam	KT820125	KT808564
	CG3070	Vietnam	KT820126	–
	CG3071	Vietnam	KT820127	–
	GW1042	Sri Lanka	JQ927450	JQ927469
	GW1044	Sri Lanka	JQ927451	JQ927470
	RAMK17271	Thailand	KT820128	–
	RAMK17277	Thailand	KT820129	KT808563
<i>P. astroidea</i> (Fée) R.C. Harris	RAMK17281	Thailand	KT820088	–
<i>P. bahiana</i> Malme	RVH1	Laos	KT820090	–
	RVH2	Laos	KT820091	KT808614
	RVH3	Laos	KT820092	KT808605
<i>P. balia</i> (Kremp.) R.C. Harris	CG3063	Vietnam	KT820130	KT808566
<i>P. brunnea</i> Fée	CG3023	Vietnam	KT820093	–
<i>P. cf. subglabrata</i> (Nyl.) Müll. Arg	CG3028	Vietnam	KT820140	KT808574
<i>P. chlorospila</i> (Nyl.) Arnol	CG1520b	England	JQ927452	JQ927471
<i>P. cornutispora</i> Aptroot & M. Cáceres	AA11938	Brazil	KT820131	KT808618
	ISE_AA11938	Brazil	NR_158911	NG_060160
<i>P. corticata</i> (Müll. Arg.) R.C. Harris	AA11443	Brazil	KT820132	KT808568
	AA11466	Brazil	KT820133	KT808569
<i>P. confinis</i> (Nyl.) R.C. Harris	AA13575	Brazil	–	KT808567
<i>P. cruenta</i> (Mont.) Vain	Green_PYCR12	USA	KC592268	–
	Green_PYCR16	USA	KC592269	–
	Green_PYCR4	USA	KC592267	–
	Lutzoni_9806174	Puerto Rico	–	AF279407
<i>P. fetivica</i> (Kremp.) Müll. Arg	CG1963	Vietnam	KT820134	–
<i>P. fetivica</i> (Kremp.) Müll. Arg	GW307A	Sri Lanka	JQ927453	JQ927472
	GW835	Sri Lanka	JQ927454	–

Species Name	Specimen No.	Locality	GenBank accession number	
			ITS	nuLSU
<i>P. infraleucotrypa</i> Aptroot & M. Cáceres	AA11105	Brazil	KT820114	KT808558
	AA11468	Brazi	KT820136	–
	AA11499	Brazi	KT820115	–
	AA15450	Brazi	KT820142	KT808575
	AA15451	Brazi	KT820117	KT808559
<i>P. inframamillana</i> Aptroot & M. Cáceres	AA11220	Brazi	KT820137	KT808572
	AA11272	Brazi	KT820138	KT808571
	AA11897	Brazi	KT820139	KT808573
<i>P. laevigata</i> (Pers.) Arnold	OL_206758	Norway	MK812685	–
	OL_206773	Norway	MK812185	–
	Palice 5608	Slovakia	–	AY607736
<i>P. cf. leucostoma</i> Ach.	F_19082	Australia	–	DQ329024
<i>P. macrospora</i> (Degel.) Coppins & P. James	CG1520a	England	JQ927455	JQ927473
<i>P. mamillana</i> (Ach.) Trevis.	AA11342	Brazil	KT820143	KT808576
	AA11610	Brazil	KT820144	KT808615
	AA11846	Brazil	KT820145	KT808617
	AA15465	Brazil	KT820146	KT808579
	CG3014	Vietnam	KT820147	KT808580
	CG3034	Vietnam	KT820149	KT808582
	CG3058	Vietnam	KT820150	KT808583
	CG3059	Vietnam	KT820151	KT808584
<i>P. aff. mamillana</i> (Ach.) Trevis.	GW818A	Sri Lank	JQ927456	JQ927474
<i>P. massariospora</i> (Starbäck) R.C. Harris	CG3061	Vietnam	KT820153	KT808585
	CG3062	Vietnam	KT820154	KT808586
	GW1028	Sri Lanka	JQ927457	JQ927475
<i>P. minor</i> Fée	AA11505	Brazil	KT820155	KT808620
	AA13516	Brazil	–	KT808587
<i>P. minutispora</i> Aptroot & M. Cáceres	AA11877	Brazil	KT820119	–
	ABL_AA11877	Brazil	NR_136140	–
<i>P. nitida</i> (Weigel) Ach.	17076	Poland	MN387114	–
	17081	Poland	MN387115	–
	17146	Poland	MN387116	–
	17189	Poland	MN387117	–
	F_5929	Czech Republic	JQ927458	DQ329023
	s. n.	Germany	–	AY607737
<i>P. nitidella</i> (Flörke) Müll. Arg.	17082	Poland	MN387139	–
	CG3027	Vietnam	KT820156	–
<i>P. occidentalis</i> (R.C. Harris) R.C. Harris	OL_206777	Norway	MK811633	–
<i>P. ochraceoflava</i> (Nyl.) R.C. Harris	Gaya_160308_EGB11	USA	KC592275	–
<i>P. punctella</i> (Nyl.) Trevis.	Tripp4522	–	KT232213	–
<i>P. pyrenuloides</i> (Mont.) R.C. Harris	CG1545	Vietnam	KT820094	–
<i>P. quassiicola</i> Fée	CG3001	Vietnam	KT820098	KT808588
	CG3019	Vietnam	KT820101	KT808591
	CG3032	Vietnam	KT820104	KT808592
	CG3033	Vietnam	KT820105	KT808593
	RVH6	Laos	KT820107	KT808595

Species Name	Specimen No.	Locality	GenBank accession number	
			ITS	nuLSU
<i>P. sanguinea</i> Aptroot, M. Cáceres & Lücking	15707F	Brazil	–	KF697129
<i>P. leucostoma</i> Aptroot & Gueidan	AFTOL_ID387	USA	DQ782845	–
	DUKE_0047599	–	NR_119610	NG_068722
	Reeb VR 14 VI 025	USA	–	AY640962
<i>P. reginae</i> E.L. Lima, Aptroot & M. Cáceres	ELL0010	Brazil	–	KT808596
<i>P. rubronitidula</i> Aptroot & M. Cáceres	AA11332	Brazil	KT820157	KT808597
	AA15603	Brazil	KT820158	–
	AA11697	Brazil	KT820159	KT808616
	ISE_AA11697	Brazil	NR_158913	NG_06015
<i>P. scutata</i> (Stirt.) Zahlbr	CG1635	Vietnam	KT820160	KT808598
<i>P. septicollaris</i> (Eschw.) R.C. Harris	AA13534	Brazil	KT820166	KT808610
	AA13546	Brazil	KT820161	–
	AA13555	Brazil	KT820167	–
	AA15009	Brazil	–	KT808599
	AA15012	Brazil	KT820162	KT808600
	AA15021	Brazil	KT820163	KT808601
	AA15023	Brazil	KT820164	KT808602
	AA15038	Brazil	–	KT808603
	AA15042	Brazil	KT820165	KT808604
<i>P. sexocularis</i> (Eschw.) R.C. Harris	RAMK17261	Thailand	KT820108	KT808606
<i>P. sp.</i>	F19113n	Australia	–	DQ329027
	CG3009	Vietnam	KT820110	KT808611
	F19082r	Australia	JQ927461	DQ329025
	LHD210	Vietnam	AB935436	–
<i>P. subelliptica</i> (Tuck.) R.C. Harris	RVH5	Laos	KT820106	KT808594
<i>P. subglabrata</i> (Nyl.) Müll. Arg.	CG3069	Vietnam	KT820169	KT808608
<i>P. subpraelucida</i> Müll. Arg.	F_17550_f	Costa Rica	–	DQ329015
<i>P. theleomorpha</i> Tuck.	F_19082	Australia	JQ927460	–
<i>P. viridipyrgilla</i> Aptroot & M. Cáceres	AA11864	Brazil	KT820170	KT808619
	ISE_AA11864	Brazil	NR_158914	–
<i>Cyphellophora europaea</i> (de Hoog, Mayser & Haase) Réblová & Unter.	CBS129_96	–	EF551553	FJ358248
<i>Endocarpon pusillum</i> Hedw.	CG470	–	JQ927447	EF643754

*P. cf. acutalis*, *P. cf. leucostoma*, *P. sanguinea*, *P. occidentalis* and three new species) and confirms the presence of two main well-supported monophyletic groups in accord with the presence/absence of pseudocyphellae as shown in Weerakoon et al. (2012) and Gueidan et al. (2016). Our phylogenetic results also indicate that delimitation problems affect several taxa, for example, *P. mamillana*, *P. quassiicola* and *P. rubrostigma*, which is consistent with Gueidan et al. (2016).

The three specimens of *Pyrenula thailandicoides* form a well-supported monophyletic group (1/100 and 0.99/83). *Pyrenula thailandicoides* is sister to *P. sexocularis*, but with very low support (0.52/-, Suppl. material 1). *Pyrenula inspersa* is sister to *P. quassiicola* clade 1 with low support (0.79/-) and *P. apiculata* forms the first diverging lineage in Group 1 with strong support (1/100). The three new species all belong to Group 1.

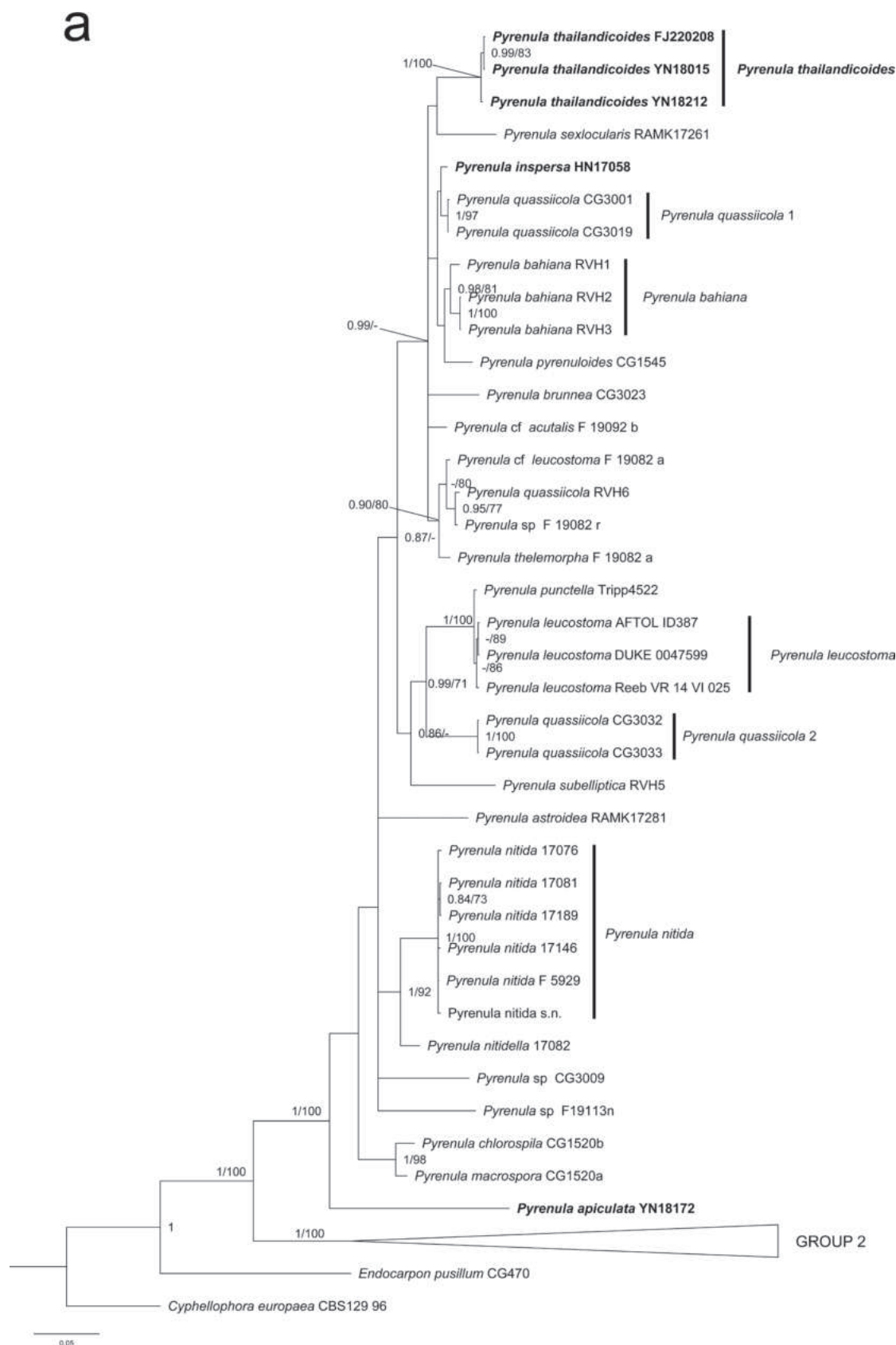


**Figure 1.** Phylogeny of the family Pyrenulaceae, based on a two-gene dataset (ITS and nuLSU) and 121 taxa **a** overview of the entire tree and details of Group 1 **b** details of Group 2. Most likely tree obtained using MrBayes. Support values are reported above the branches [posterior probability (PP)/bootstrap value (BS)]. Only significant values (higher than 95% PP and higher than 70% BS) are shown. *Cyphellophora europaea* and *Endocarpon pusillum* are the out-group taxa.

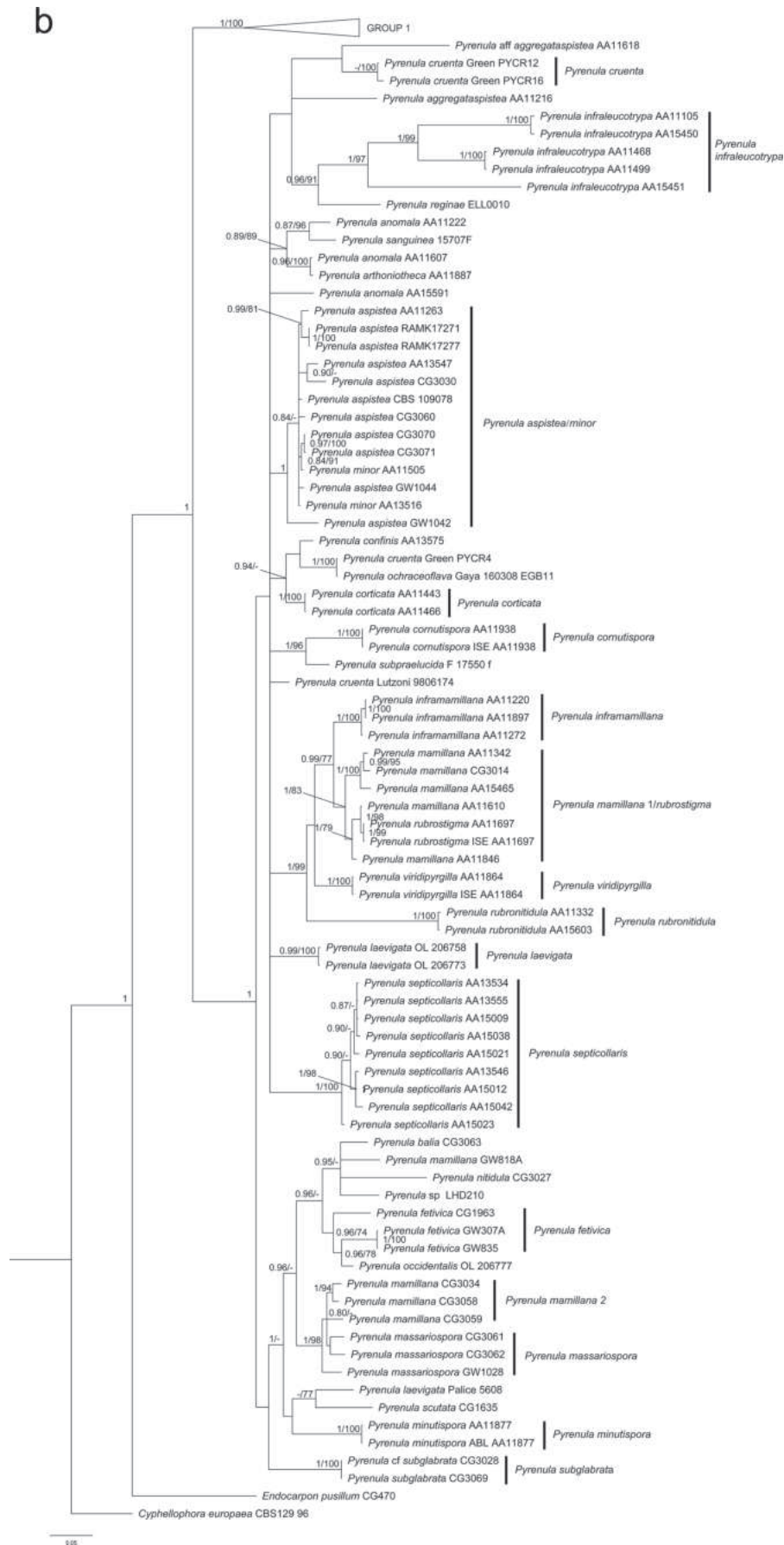


Figure 1. Continued.

## Taxonomy

### 1. *Pyrenula inspersa* M.Z. Dou & Z.F. Jia, sp. nov.

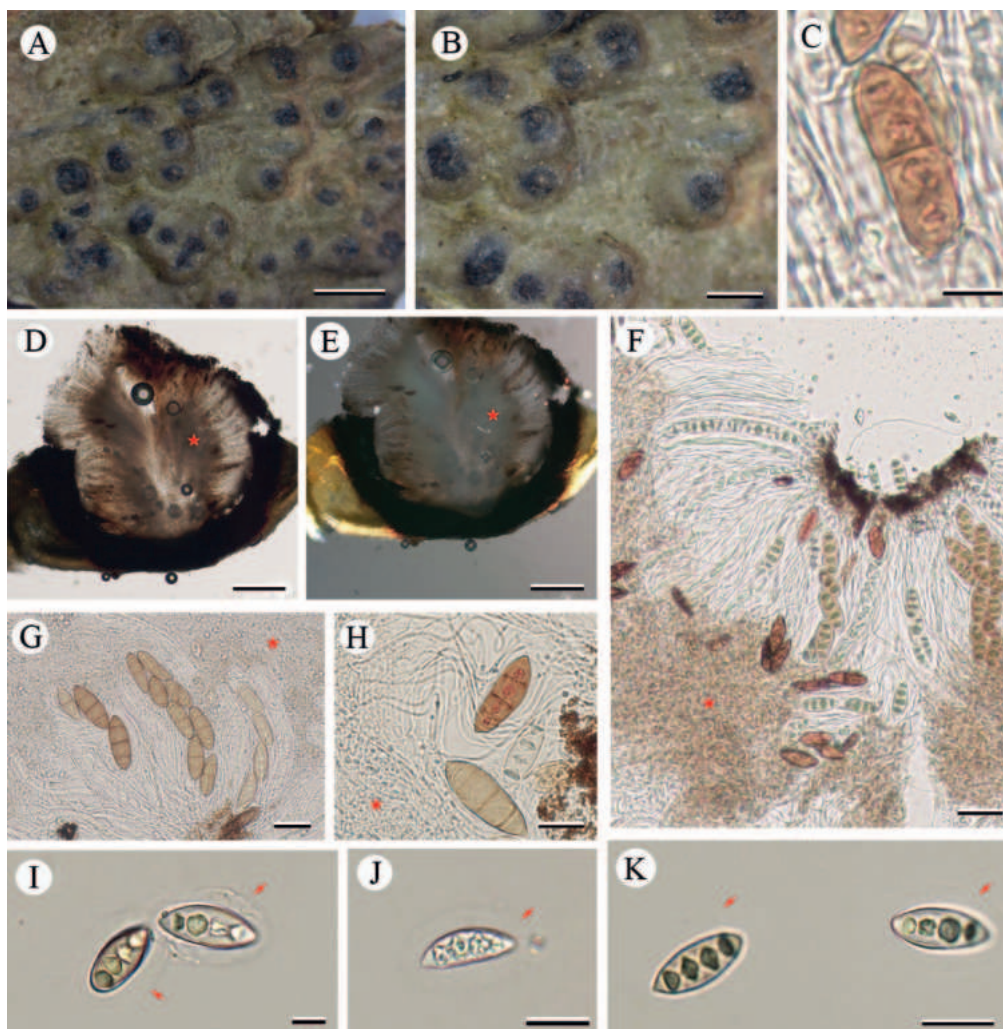
Fungal Names: FN 571675

Fig. 2

**Diagnosis.** The new species can be distinguished from the most similar species *Pyrenula thailandica* Aptroot by the hamathecium densely inspersed with minute granules and colourless oil droplets.

**Type.** CHINA. Hainan Province: Changjiang County, Bawangling Nature Reserve, Yajia, 19°05'07"N, 109°07'25"E, alt. 444 m, on bark, 10 December 2017, X.H. Wu HN17058 (LCUF:holotype: HN17058; GenBank OR578591 for ITS and OR578572 for LSU).

**Description.** *Thallus* corticolous, crustose, brown, surface dull, uneven, corticate with pseudocyphellae, UV-. ASCOMATA perithecioid, emergent, dispersed,



**Figure 2.** *Pyrenula inspersa* (LCUF HN17058) **A** thallus with apothecia **B** apothecia and pseudocyphellae **C**, **F–H** ascospores at different developmental stages, over-mature ascospores with orange-oil can be seen in **C**, **F** and **H** **D** section of apothecium **E** section visualised with polarised light showing cortex of apothecium with crystals, red stars in **D–H** show the inspersed in hamathecium **I–K** young ascospores, red arrows show gelatinous halo. Scale bars: 2 mm (**A**); 1 mm (**B**); 10  $\mu$ m (**C**, **I**); 200  $\mu$ m (**D**, **E**); 50  $\mu$ m (**F**, **H**); 35  $\mu$ m (**G**); 20  $\mu$ m (**J**, **K**).

aggregated occasionally when crowded, hemispherical, 1–1.5 mm diam., with crystals, KOH-. **Ostioles** apical. **Hamathecium** heavily inspersioned with minute granules and colourless oil droplets (close-up in Suppl. material 2), IKI-. **Ascospores** 8 per ascus, irregularly biserial, with gelatinous halo before becoming old, 3-septate, 28.5–50 × 10–20 µm; middle lumina diamond-shaped, end lumina triangular, with a thick layer of endospore in the spore tips; hyaline when young, brown when mature, over-mature ascospores with orange oil.

**Chemistry.** Thallus K-, C-, KC-, UV-, hamathecium IKI-.

**Ecology and distribution.** The new species is currently only known from the tropical regions of southern China on bark.

**Etymology.** The specific epithet *inspersa* refers to the inspersioned hamathecium.

**Note.** This new species is similar to *Pyrenula thailandica*, *P. bahiana* and *P. concastroma* in having 3-septate ascospores with red or orange oil when over-mature. It differs from *P. thailandica* by an inspersioned hamathecium and larger ascomata, which are in the latter species 0.6–1.1 mm wide (Aptroot 2012; Aptroot et al. 2012, 2013; Ingle et al. 2018). This new species differs from *P. bahiana* by larger ascospores, which are in the latter species 26–33(–35) × 10–13(–15) µm (Malme 1929; Aptroot 2012; Aptroot et al. 2013; Ingle et al. 2018). *Pyrenula concastroma* differs from the new species by the mostly aggregated ascomata with fused walls, but separate ostioles (Aptroot 2012; Schumm and Aptroot 2021). Although *P. quassicola* and *P. pyrenuloides* are phylogenetically close to this new species, they can be distinguished easily by the morphology. *P. quassicola* has smaller ascomata (0.3–0.7 mm), smaller ascospores (28–35 (–40) × 12–16 µm) containing colourless oil when over-mature and not inspersioned, IKI+ (orange) hamathecium (Harris 1989). *P. pyrenuloides* has smaller ascomata (0.5–1.0 mm), larger ascospores (50–62 × 18–24 µm) containing no oil when over-mature and not inspersioned, IKI+ (orange) hamathecium (Harris 1989).

## 2. *Pyrenula thailandicoides* M.Z. Dou & Z.F. Jia, sp. nov.

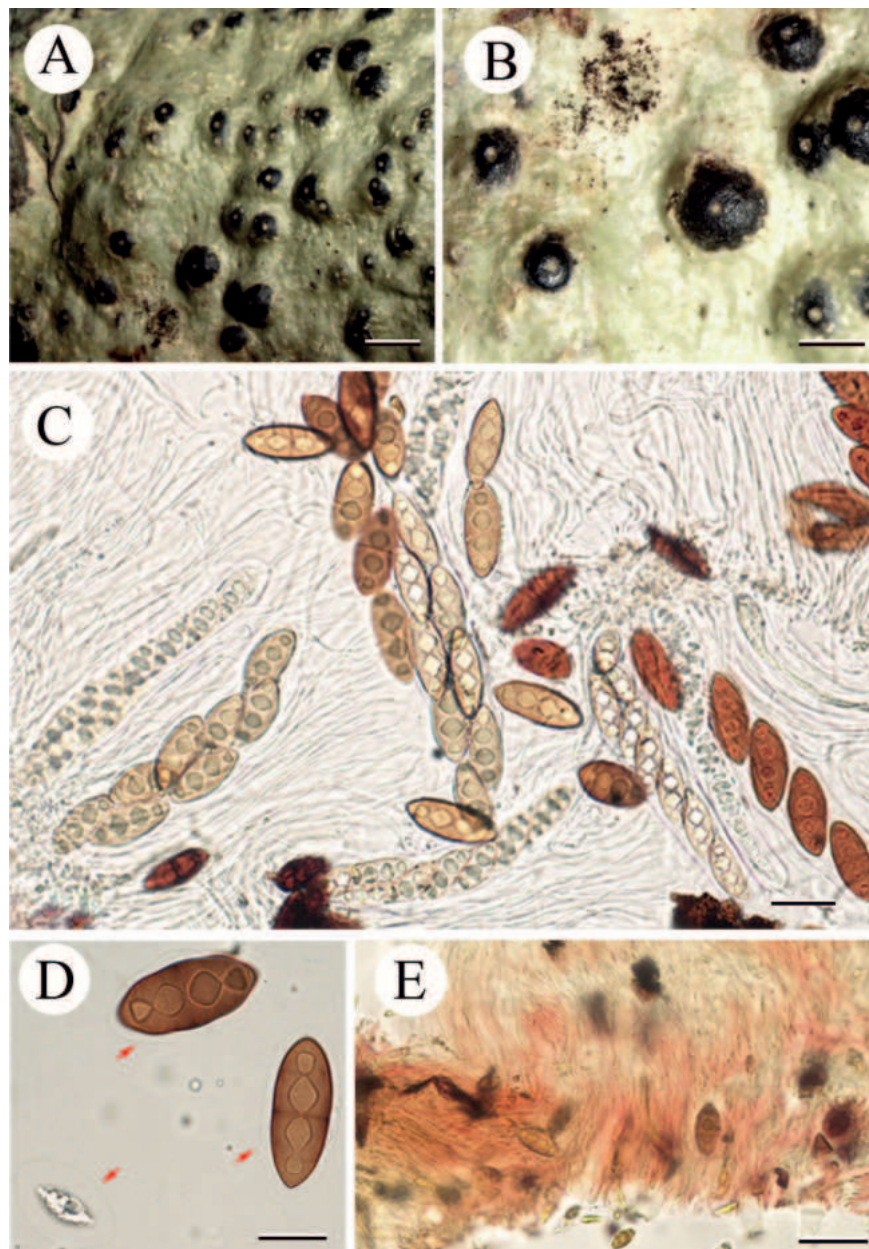
Fungal Names: FN 571676

Fig. 3

**Diagnosis.** The new species can be distinguished from the most closely-related species *Pyrenula thailandica* by the IKI+ red hamathecium and an unidentified lichen substance.

**Type.** CHINA. Yunnan Province: Mengla County, Xishuangbanna Tropic Botanical Garden, Chinese Academy of Sciences, Rainforest Valley, 21°54'51"N, 101°11'28"E, alt. 626 m, on bark, 26 January 2018, X.H. Wu YN18212 (LCUF: holotype: YN18212; GenBank OR578589 for ITS and OR578570 for LSU).

**Description.** **Thallus** corticolous, crustose, olive-green, corticate with few pseudocyphellae, UV-. **ASCOMATA** perithecioid, emergent, dispersed, conical, 0.8–1.6 mm diam., with crystals, KOH-. **Ostioles** apical, white, 0.25–0.45 mm. **Hamathecium** not inspersioned (close-up in Suppl. material 3), IKI+/I+ red (Fig. 2 and Suppl. material 4). **Ascospores** 8 per ascus, irregularly biserial, with gelatinous halo before becoming old, 3-septate, (30–)35–55 × (12–)15–23 µm; middle lumina diamond-shaped, end lumina triangular, with a thick layer of endospores in the spore tips; hyaline when young, reddish-brown when mature, over-mature ascospores with red oil.



**Figure 3.** *Pyrenula thailandicoides* (LCUF YN18212) **A, B** thallus with apothecia **C, D** ascospores at different developmental stages, over-mature ascospores with red-oil can be seen in **C**, red arrows in **D** show gelatinous halo **E** IKI+ red hamathecium. Scale bars: 2 mm (**A**); 1 mm (**B**); 30 µm (**C**); 20 µm (**D**); 50 µm (**E**).

**Chemistry.** Thallus K+ orange–brown, C-, KC+ yellow, UV-, hamathecium IKI+ red, TLC showed an unidentified substance at Rf four of solvent C (Suppl. material 5).

**Ecology and distribution.** The new species is currently only known from the tropical and subtropical regions of southern China on bark.

**Etymology.** The specific epithet *thailandicoides* refers to the similarity to *Pyrenula thailandica*.

**Additional specimens examined.** CHINA. Yunnan Province: Mengla County, Xishuangbanna Tropic Botanical Garden, Chinese Academy of Sciences, 21°55'37"N, 101°15'27"E, alt. 555 m, on bark, 25 January 2018, X. Zhao YN18015 (LCUF; YN18015; GenBank OR578590 for ITS and OR578571 for LSU). CHINA. Fujian Province: Longyan City, Dongxiao National Forest Park, Frog Stone,

24°58'07"N, 117°01'14"E, alt. 679 m, on bark, 12 July 2022, Z.G. Ma FJ220208 (LCUF; GenBank OR578593 for ITS).

**Notes.** This new species is similar to *Pyrenula thailandica*, *P. bahiana* and *P. concastroma* in having 3-septate ascospores with red or orange oil when over-mature. The colour reaction of hamathecium of *Pyrenula* species in IKI is negative (such as *Pyrenula thailandica* and *P. bahiana*) or IKI+ red/orangish (such as *P. concastroma*) or IKI+ blue (such as *P. massariospora*). This new species differs from *P. thailandica* by its IKI+ red hamathecium and an unidentified lichen substance (Aptroot 2012; Aptroot et al. 2012, 2013; Ingle et al. 2018). This new species differs from *P. bahiana* by its IKI+ red hamathecium, an unidentified lichen substance and larger ascospores, the latter 26–33(–35) × 10–13(–15) µm (Malme 1929; Aptroot 2012; Aptroot et al. 2013; Ingle et al. 2018). *P. concastroma* differs from the new species by the mostly aggregated ascomata with fused walls, but separate ostioles (Aptroot 2012; Schumm and Aptroot 2021).

### 3. *Pyrenula apiculata* M.Z. Dou & Z.F. Jia, sp. nov.

Fungal Names: FN 571678

Fig. 4

**Diagnosis.** The new species can be distinguished from the most similar species *Pyrenula bahiana* by the absence of endospore layers in the spore tips and the absence of pseudocyphellae.

**Type.** CHINA. Yunnan Province: Mengla County, Xishuangbanna Tropic Botanical Garden, Chinese Academy of Sciences, Green Stone Forest, Buttress Roots, 21°54'39"N, 101°17'05"E, alt. 672 m, on bark, 26 January 2018, X. Zhao YN18172 (LCUF: holotype: YN18172; GenBank OR578592 for ITS and OR578573 for LSU).

**Description.** *Thallus* corticolous, crustose, olive-green, corticate without pseudocyphellae, UV-. *Ascomata* perithecioid, emergent, dispersed, conical, flattened, 0.3–0.5 mm diam., with crystals, the sides partly covered by the thallus, KOH-. *Ostioles* apical, black. *Hamathecium* not interspersed, IKI-. *Ascospores* 8 per ascus, uniseriate, with gelatinous halo before becoming old, 3-septate, 18–34 × 10–15 µm; middle lumina triangular to round, end lumina triangular, without layer of endospore in the spore tips; hyaline when young, reddish-brown when mature, over-mature ascospores with red oil.

**Chemistry.** Thallus K-, C-, KC-, UV-, hamathecium IKI-.

**Ecology and distribution.** The new species is currently only known from the tropical region of southern China on bark.

**Etymology.** The specific epithet *apiculata* refers to the pointed bulge of the end locules of ascospores.

**Additional specimens examined.** CHINA. Yunnan Province: Mengla County, Xishuangbanna Tropic Botanical Garden, Chinese Academy of Sciences, Green Stone Forest, Buttress Roots, 21°54'39"N, 101°17'05"E, alt. 672 m, on bark, 26 January 2018, X. Zhao YN18173 (LCUF, GenBank for ITS and for LSU), same locality, YN18174; CHINA.

**Notes.** This new species is similar to *Pyrenula thailandica*, *P. bahiana* and *P. concastroma* in having 3-septate ascospores with red or orange oil when

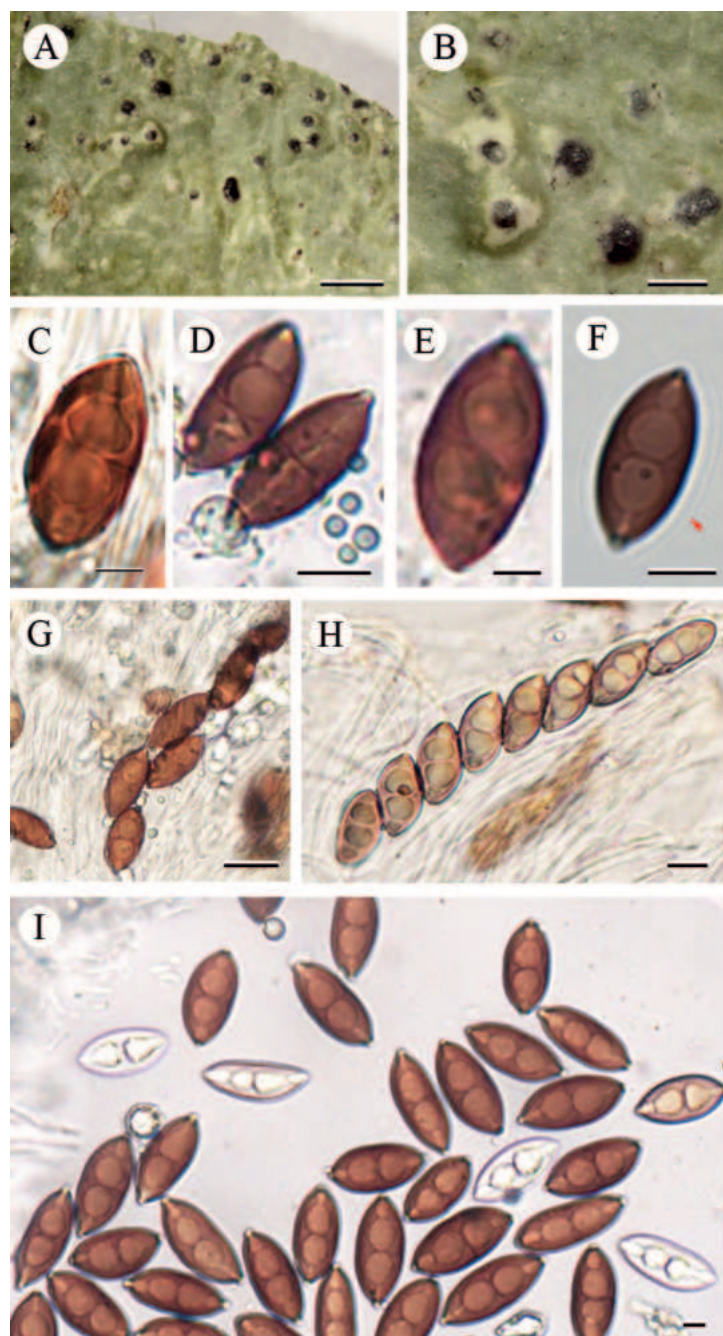


**Figure 4.** *Pyrenula apiculata* (LCUF YN18172) **A, B** thallus with apothecia **C–E** over-mature ascospores with red oil **F–I** ascospores at different developmental stages, red arrow in **F** shows gelatinous sheath. Scale bars: 2 mm (**A**); 1 mm (**B**); 5  $\mu$ m (**C, E, I**); 10  $\mu$ m (**D, F, H**); 20  $\mu$ m (**G**).

over-mature. It differs from *P. thailandica* by the absence of pseudocyphellae, the absence of endospore layers in the spore tips and reddish-brown and smaller ascospores, which measure in the latter (30–)35–51  $\times$  (10–)14–20  $\mu$ m (Aptroot 2012; Aptroot et al. 2012, 2013; Ingle et al. 2018). This new species differs from *P. bahiana* by the reddish-brown ascospores when mature, absence of endospore layers in the spore tips and absence of pseudocyphellae (Aptroot 2012; Aptroot et al. 2013; Ingle et al. 2018). *P. concastroma* differs from the new species by the mostly aggregated ascomata with fused walls, but separate ostioles (Aptroot 2012; Schumm and Aptroot 2021).

### Key to *Pyrenula* with red or orange oil in over-mature ascospores

- 1 Ascospores transversely septate ..... 2
  - Ascospores submuriform to muriform ..... 8
- 2 Ascospores 5-septate, 22–34 × 8–14 µm .....
  - ..... ***Pyrenula sexlocularis* (Nyl.) Müll. Arg.**
  - Ascospores 3-septate ..... 3
- 3 Ascomata mostly aggregated, with fused walls, but with separate ostioles, ascospores 31–40 × 15–16 µm ..... ***Pyrenula concastroma* R.C. Harris**
  - Ascomata mostly simple, only aggregated by chance when crowded ..... 4
- 4 Hamathecium interspersed, ascospores 28.5–50 × 10–20 µm, ascomata ca. 1–1.5 mm diam ..... ***Pyrenula inspersa* M.Z. Dou & Z.F. Jia**
  - Hamathecium not interspersed ..... 5
- 5 Ascospores < 35 µm long ..... 6
  - Ascospores > 35 µm long ..... 7
- 6 Terminal locules directly against the exospore wall; ascospores 18–34 × 10–15 µm; ascomata ca. 0.3–0.5 mm diam .....
  - ..... ***Pyrenula apiculata* M.Z. Dou & Z.F. Jia**
  - Terminal locules separated from the exospore wall by endospore thickening; ascospores 26–33(–35) × 10–13(–15) µm; ascomata ca. 0.4–0.6 mm diam ..... ***Pyrenula bahiana* Malme**
- 7 Hamathecium IKI–; no substances detected by TLC; ascospores (30–)35–51 × (10–)14–20 µm; ascomata ca. 0.6–1.1 mm diam .....
  - ..... ***Pyrenula thailandica* Aptroot**
  - Hamathecium IKI+ red; TLC showed an unidentified substance at R<sub>f</sub> four of solvent C; ascospores (30–)35–55 × (12–)15–23 µm; ascomata ca. 0.8–1.6 mm diam ..... ***Pyrenula thailandicoides* M.Z. Dou & Z.F. Jia**
- 8 Ascospores submuriform, the sections usually simple, the rest bicellular, 22–40 × 10–17 µm ..... ***Pyrenula seminuda* (Müll. Arg.) Sipman & Aptroot**
  - Ascospores muriform ..... 9
- 9 Ascospores 25–35 × 12–13 µm, with 8 rows of 3–4 lumina per row .....
  - ..... ***Pyrenula breutelii* (Müll. Arg.) Aptroot**
  - Ascospores 35–45 × 14–16 µm, with 8 rows of 1–3 lumina per row .....
    - ..... ***Pyrenula macularis* (Zahlbr.) R.C. Harris**

### Acknowledgements

We sincerely thank Fangluan Gao (Fujian Agriculture and Forestry University) and Xinmei Qin (Guangxi Institute of Botany, Guangxi Zhuang Autonomous Region and Chinese Academy of Sciences) for the generous help in analysing the data.

### Additional information

#### Conflict of interest

The authors have declared that no competing interests exist.

#### Ethical statement

No ethical statement was reported.

## Funding

This study was supported by the National Natural Science Foundation of China (32300005); Shandong Provincial Natural Science Foundation, China (ZR2023MC105 and ZR2023QC245); Doctoral Initiation Fund of Liaocheng University (318051813) and Research Fund of Liaocheng University (318012011).

## Author contributions

Data curation: MD, JL, SL. Formal analysis: MD. Funding acquisition: MD. Methodology: JL, MD, SL. Project administration: MD. Software: SL, MD. Validation: ZJ, AA. Visualization: MD. Writing – original draft: MD. Writing – review and editing: MD, ZJ.

## Author ORCIDs

Jiechen Li  <https://orcid.org/0009-0001-8819-8407>

André Aptroot  <https://orcid.org/0000-0001-7949-2594>

## Data availability

All of the data that support the findings of this study are available in the main text or Supplementary Information.

## References

- Acharius E (1814) *Synopsis methodica lichenum. Litteris et sumptibus Svanborg et soc., Lund*, 392 pp.
- Aptroot A (2012) A world key to the species of *Anthracothecium* and *Pyrenula*. *Lichenologist* 44(1): 5–53. <https://doi.org/10.1017/S0024282911000624>
- Aptroot A (2021) World key to the species of Pyrenulaceae and Trypetheliaceae. *Archive for lichenology* 29: 1–91.
- Aptroot A, Schumm F, Cáceres MES (2012) Six new species of *Pyrenula* from the tropics. *Lichenologist* 44(5): 611–618. <https://doi.org/10.1017/S0024282912000254>
- Aptroot A, Sipman HJM, Cáceres MES (2013) Twenty-one new species of *Pyrenula* from South America, with a note on over-mature ascospores. *Lichenologist* 45(2): 169–198. <https://doi.org/10.1017/S0024282912000734>
- Aptroot A, Sipman HJM, Mercado Diaz JA, Mendonça CO, Feuerstein SC, Cunha-Dias IPR, Pereira TA, Cáceres MES (2018) Eight new species of Pyrenulaceae from the Neotropics, with a key to 3-septate *Pyrgillus* species. *Lichenologist* 50(1): 77–87. <https://doi.org/10.1017/S0024282917000573>
- Dou MZ, Wu XH, Li M, Zhao X, Jia ZF (2018) *Gyalecta caudiospora* sp. Nov. from China. *Mycotaxon* 133(4): 721–727. <https://doi.org/10.5248/133.721>
- Fu JM, Wang ZL, Wang CX, Zhang LL (2018) New records of six *Pyrenula* species from China. *Mycotaxon* 133(3): 473–480. <https://doi.org/10.5248/133.473>
- Fu JM, Aptroot A, Wang ZL, Zhang LL (2019) Four *Pyrenula* species new to China. *Mycotaxon* 134(1): 155–160. <https://doi.org/10.5248/134.155>
- Gardes M, Bruns TD (1993) ITS primers with enhanced specificity for Basidiomycetes – application to the identification of mycorrhiza and rusts. *Molecular Ecology* 2(2): 113–118. <https://doi.org/10.1111/j.1365-294X.1993.tb00005.x>
- Geiser DM, Gueidan C, Miadlikowska J, Lutzoni F, Kauff F, Hofstetter V, Fraker E, Schoch C, Tibell L, Untereiner WA, Aptroot A (2006) Eurotiomycetes: Eurotiomycetidae and Chaetothyriomycetidae. *Mycologia* 98(6): 1054–1065. <https://doi.org/10.1080/15572536.2006.11832633>

- Gueidan C, Aptroot A, Cáceres MES, Binh NQ (2016) Molecular phylogeny of the tropical lichen family Pyrenulaceae: Contribution from dried herbarium specimens and FTA card samples. *Mycological Progress* 15(1): 1–21. <https://doi.org/10.1007/s11557-015-1154-8>
- Harris RC (1989) A sketch of the family Pyrenulaceae in Eastern North America. *Memoirs of the New York Botanical Garden* 49: 74–107.
- Ingle KK, Uppadhyay V, Nayaka S, Trivedi S, Sahoo D (2018) New records and an updated key of *Pyrenula* from India. *Cryptogam Biodiversity and Assessment*: 37–46. <https://doi.org/10.21756/cab.esp7>
- Jia ZF, Wei JC (2016) *Flora Lichenum Sinicorum* (Vol. 13). – Ostropales (I) – Graphidaceae 1. Science Press, Beijing, 210 pp.
- Katoh K, Standley DM (2013) MAFFT multiple sequence alignment software version 7: Improvements in performance and usability. *Molecular Biology and Evolution* 30(4): 772–780. <https://doi.org/10.1093/molbev/mst010>
- Lanfear R, Frandsen PB, Wright AM, Senfeld T, Calcott B (2017) PartitionFinder 2: New methods for selecting partitioned models of evolution for molecular and morphological phylogenetic analyses. *Molecular Biology and Evolution* 34(3): 772–773. <https://doi.org/10.1093/molbev/msw260>
- Lücking R, Álvaro-Alba WR, Moncada B, Marín-Canchala NL, Tunjano SS, Cárdenas-López D (2023) Lichens from the Colombian Amazon: 666 taxa including 28 new species and 157 new country records document an extraordinary diversity. *The Bryologist* 126(2): 242–303. <https://doi.org/10.1639/0007-2745-126.2.242>
- Lutzoni F, Pagel M, Reeb V (2001) Major fungal lineages are derived from lichen symbiotic ancestors. *Nature* 411(6840): 937–940. <https://doi.org/10.1038/35082053>
- Malme GOA (1929) *Pyrenulae* et *Anthracothecia* Herbarii Regnelliani. *Arkiv för Botanik* 22A(11): 1–40.
- Mangold A, Martín MP, Lücking R, Lumbsch HT (2008) Molecular phylogeny suggests synonymy of Thelotremaaceae within Graphidaceae (Ascomycota: Ostropales). *Taxon* 57(2): 476–486. <https://doi.org/10.1017/S0024282908007366>
- Mason-Gamer R, Kellogg E (1996) Testing for phylogenetic conflict among molecular datasets in the tribe Triticeae (Graminae). *Systematic Biology* 45(4): 524–545. <https://doi.org/10.1093/sysbio/45.4.524>
- Mendonça CO, Aptroot A, Cáceres MES (2016) Six new species of the lichen genus *Pyrenula* (Pyrenulaceae) from northeast Brazil. *Phytotaxa* 286(3): 169–176. <https://doi.org/10.11646/phytotaxa.286.3.4>
- Miranda-González R, Bungartz F, Lücking R, Gaya E, de Oliveira Mendonça C, Viñas-Portilla C, da Silva Cáceres ME, de los Angeles Herrera-Campos M (2022) Phylogeny of the *Pyrenula ochraceoflava* group (Pyrenulaceae) reveals near-cryptic diversification and the inclusion of the *Mazaediothecium album* aggregate. *The Bryologist* 125(4): 541–557. <https://doi.org/10.1639/0007-2745-125.4.541>
- Mishra GK, Nayaka S, Upreti DK, Bajpai R (2022) *Pyrenula awasthii* sp. nov., containing lichexanthone and anthraquinone from India. *Cryptogam Biodiversity and Assessment* 6(1): 14–16.
- Orange A, James PW, White FJ (2010) *Microchemical Methods for the Identification of Lichens*. British Lichen Society, London, 101 pp.
- Rambaut A, Suchard MA, Xie D, Drummond AJ (2014) Tracer v1.6. <http://beast.bio.ed.ac.uk/Tracer>
- Ronquist F, Teslenko M, van der Mark P, Ayres DL, Darling A, Höhna S, Larget B, Liu L, Suchard MA, Huelsenbeck JP (2012) MrBayes 3.2: Efficient Bayesian phylogenetic

- inference and model choice across a large model space. *Systematic Biology* 61(3): 539–542. <https://doi.org/10.1093/sysbio/sys029>
- Schumm F, Aptroot A (2021) Atlas of Pyrenulaceae and Trypetheliaceae (Vol 3): Lichenized Ascomycota. Books on Demand, 524 pp.
- Soto-Medina EA, Aptroot A, Lücking R (2023) New species of lichen for Colombia tropical dry forest. *Cryptogamie, Mycologie* 44(7): 103–107. <https://doi.org/10.5252/cryptogamie-mycologie2023v44a7>
- Stamatakis A (2014) RAxML version 8: A tool for phylogenetic analysis and post-analysis of large phylogenies. *Bioinformatics* 30(9): 1312–1313. <https://doi.org/10.1093/bioinformatics/btu033>
- Vilgalys R, Hester M (1990) Rapid genetic identification and mapping of enzymatically amplified ribosomal DNA from several *Cryptococcus* species. *Journal of Bacteriology* 172(8): 4238–4246. <https://doi.org/10.1128/jb.172.8.4238-4246.1990>
- Wang ZL, Yan SK, Tang R, Sun MJ, Zhang LL (2018) New records of *Lepraria* and *Pyrenula* from China. *Mycotaxon* 133(1): 89–96. <https://doi.org/10.5248/133.89>
- Weerakoon G, Aptroot A, Lumbsch HT, Wolseley PA, Wijeyaratne SC, Gueidan C (2012) New molecular data on Pyrenulaceae from Sri Lanka reveal two well-supported groups within this family. *Lichenologist* 44(5): 639–647. <https://doi.org/10.1017/S0024282912000333>
- Wei JC (2020) The Enumeration of Lichenized Fungi in China. China Forestry Publishing House, Beijing, 606 pp.
- White T, Bruns T, Lee S, Taylor J (1990) Amplification and direct sequencing of fungal ribosomal RNA genes for phylogenetics. In: Innis MA, Gelfand DH, Sninsky JJ, White TJ (Eds) PCR Protocols: A Guide to Methods and Applications. Academic Press, New York, 315–322. <https://doi.org/10.1016/B978-0-12-372180-8.50042-1>
- Xie CM, Zhao ZT, Cheng PF, Zhang LL (2021) Additional species of *Pyrenula* (Pyrenulaceae) from China. *Herzogia* 34(1): 93–100. <https://doi.org/10.13158/heia.34.1.2021.93>
- Zhang D, Gao FL, Jakovli I, Zou H, Wang GT (2020) Phylosuite: An integrated and scalable desktop platform for streamlined molecular sequence data management and evolutionary phylogenetics studies. *Molecular Ecology Resources* 20(1): 348–355. <https://doi.org/10.1111/1755-0998.13096>
- Zhang Q, Qin XM, Lu YB, Li PW, Huang XY (2023) A comprehensive alignment-filtering methodology improves phylogeny particularly by filtering overly divergent segments. *bioRxiv*. <https://doi.org/10.1101/2023.12.26.573321>

## Supplementary material 1

### ML tree showing the internal phylogeny of the family Pyrenulaceae, based on a two-gene dataset (ITS and nuLSU) and 121 taxa

Authors: Mingzhu Dou, Shengnan Liu, Jiechen Li, André Aptroot, Zefeng Jia

Data type: pdf

Explanation note: *Cyphellophora europaea* and *Endocarpon pusillum* are the out-group taxa. Only significant values (higher than 70% BS) are shown.

Copyright notice: This dataset is made available under the OpeOn.0 Database License (<http://opendatacommons.org/licenses/odbl/1.0/>). The Open Database License (ODbL) is a license agreement intended to allow users to freely share, modify, and use this Dataset while maintaining this same freedom for others, provided that the original source and author(s) are credited.

Link: <https://doi.org/10.3897/mycokeys.102.113619.suppl1>

## Supplementary material 2

### Section of the ascomata of *Pyrenula inspersa* (LCUF HN17058) showing hamathecium with inspersion

Authors: Mingzhu Dou, Shengnan Liu, Jiechen Li, André Aptroot, Zefeng Jia

Data type: jpg

Copyright notice: This dataset is made available under the Open Database License (<http://opendatacommons.org/licenses/odbl/1.0/>). The Open Database License (ODbL) is a license agreement intended to allow users to freely share, modify, and use this Dataset while maintaining this same freedom for others, provided that the original source and author(s) are credited.

Link: <https://doi.org/10.3897/mycokeys.102.113619.suppl2>

## Supplementary material 3

### Section of the ascomata of *Pyrenula thailandicoides* (LCUF YN18212) showing hamathecium without inspersion

Authors: Mingzhu Dou, Shengnan Liu, Jiechen Li, André Aptroot, Zefeng Jia

Data type: jpg

Copyright notice: This dataset is made available under the Open Database License (<http://opendatacommons.org/licenses/odbl/1.0/>). The Open Database License (ODbL) is a license agreement intended to allow users to freely share, modify, and use this Dataset while maintaining this same freedom for others, provided that the original source and author(s) are credited.

Link: <https://doi.org/10.3897/mycokeys.102.113619.suppl3>

## Supplementary material 4

### The colour reaction of hamathecium of *Pyrenula thailandicoides* (LCUF YN18212) just in I

Authors: Mingzhu Dou, Shengnan Liu, Jiechen Li, André Aptroot, Zefeng Jia

Data type: tif

Copyright notice: This dataset is made available under the Open Database License (<http://opendatacommons.org/licenses/odbl/1.0/>). The Open Database License (ODbL) is a license agreement intended to allow users to freely share, modify, and use this Dataset while maintaining this same freedom for others, provided that the original source and author(s) are credited.

Link: <https://doi.org/10.3897/mycokeys.102.113619.suppl4>

## Supplementary material 5

### TLC test of the new species *Pyrenula thailandicoides* using C solvent systems

Authors: Mingzhu Dou, Shengnan Liu, Jiechen Li, André Aptroot, Zefeng Jia

Data type: pdf

Copyright notice: This dataset is made available under the Open Database License (<http://opendatacommons.org/licenses/odbl/1.0/>). The Open Database License (ODbL) is a license agreement intended to allow users to freely share, modify, and use this Dataset while maintaining this same freedom for others, provided that the original source and author(s) are credited.

Link: <https://doi.org/10.3897/mycokeys.102.113619.suppl5>

## Supplementary material 6

### TLC test of the new species *Pyrenula thailandicoides* using B solvent systems

Authors: Mingzhu Dou, Shengnan Liu, Jiechen Li, André Aptroot, Zefeng Jia

Data type: pdf

Copyright notice: This dataset is made available under the Open Database License (<http://opendatacommons.org/licenses/odbl/1.0/>). The Open Database License (ODbL) is a license agreement intended to allow users to freely share, modify, and use this Dataset while maintaining this same freedom for others, provided that the original source and author(s) are credited.

Link: <https://doi.org/10.3897/mycokeys.102.113619.suppl6>



# Additional four species of *Tatraea* (Leotiomycetes, Helotiales) in Yunnan Province, China

Cui-Jin-Yi Li<sup>1,2,3,4</sup>, Kandawatte Wedaralalage Thilini Chethana<sup>2,4</sup>,  
Prapassorn Damrongkool Eungwanichayapant<sup>2</sup>, De-Qun Zhou<sup>1,5</sup>, Qi Zhao<sup>1,3</sup>

1 Key Laboratory for Plant Diversity and Biogeography of East Asia, Yunnan Key Laboratory of Fungal Diversity and Green Development, Kunming Institute of Botany, Chinese Academy of Sciences, Kunming, Yunnan 650201, China

2 School of Science, Mae Fah Luang University, Chiang Rai, 57100, Thailand

3 Institute of Applied Fungi, Southwest Forestry University, Kunming, Yunnan 650224, China

4 Center of Excellence in Fungal Research, Mae Fah Luang University, Chiang Rai, 57100, Thailand

5 Institute of Fanjing Mountain National Park, Tongren University, Tongren, Guizhou 554300, China

Corresponding author: Qi Zhao (zhaoqi@mail.kib.ac.cn)

## Abstract

During the investigations of discomycetes in Yunnan, China, five species of *Tatraea* were discovered on decayed, decorticated oak trees or unidentified wood. All species have typical disc-like, large fruiting bodies with grey, brown or greyish-green colors. The ITS sequence analysis showed that they belong to *Tatraea* (Helotiaceae, Helotiales) and the LSU and ITS combination revealed a different topology within the genus. Four species, *T. clepsydriformis*, *T. griseoturcoisina*, *T. yunnanensis* and *T. yuxiensis* were established as new species, and *T. aseptata* was collected and described on oak woods. The pairwise homoplasy index (PHI) test results indicated that there is no significant genetic recombination ( $\Phi_w = 1.0$ ) between all related species pairs. All the species described here are supported by descriptions, illustrations and multi-gene analyses.

**Key words:** Four new species, Helotiaceae, phylogeny, saprobic fungi, taxonomy



Academic editor: Xinlei Fan  
Received: 12 September 2023  
Accepted: 27 October 2023  
Published: 14 February 2024

Citation: Li C-J-Y, Thilini Chethana KW, Eungwanichayapant PD, Zhou D-Q, Zhao Q (2024) Additional four species of *Tatraea* (Leotiomycetes, Helotiales) in Yunnan Province, China. MycoKeys 102: 127–154. <https://doi.org/10.3897/mycokeys.102.112565>

Copyright: © Cui-Jin-Yi Li et al.  
This is an open access article distributed under terms of the Creative Commons Attribution License (Attribution 4.0 International – CC BY 4.0).

## Introduction

*Tatraea* Svrček belongs to Helotiaceae, Helotiales, Leotiomycetes (Wijayawardene et al. 2022) and is characterized by large, brown or grey cupulate apothecia with a stipe, distinct dark-colored subhymenium, hyaline medullary excipulum, light-brown colored ectal excipulum, large asci and ascospores (Velenovský 1934; Baral et al. 1999). The type species, *Tatraea dumbirensis* (Velen.) Svrček was initially recognized as *Helotium dumbirensis* in Leotiaceae based on the materials collected in the Nizke Tatra Mountains, Slovakia (Velenovský 1934). In 1985, Svrček re-observed and measured ascospores, and synonymized the species with *Rutstroemia macrospora* (Peck) Kanouse (Velenovský 1934). However, Spooner (1987, 1988) transferred both *H. dumbirensis* and *R. macrospora* to Sclerotiniaceae and synonymized them into *Ciboria peckiana* (Cooke) Korf and *Ciboria dumbirensis*, respectively, based on their morphological characteristics. After that, Svrček (1993) erected *Tatraea* based on

the distinct characters between the materials from Europe and *C. peckiana*. Baral et al. (1999) also accepted the genus *Tatraea* and transferred *Tatraea macrospora* (Peck) Baral back. However, Baral et al. (1999) did not observe any isodiametric cells in hypothecium, a character significant of Sclerotiniaceae. Recent research showed *Tatraea* belonging to Helotiaceae, and the third species was added by a subsequent study (Vasilyeva 2010). To date, there are three species accepted in *Tatraea* (Index Fungorum 2023).

To date, members of *Tatraea* have been only found as saprobes on the rotting and permanently moist, decorticated trunks of beech wood (*Fagus sylvatica*), rarely occurring on *Fraxinus excelsior* or *Betula* and have been reported in Austria, China, Croatia, Denmark, France, Germany, Great Britain, Italy, Slovakia, Spain, Sweden and Switzerland (Svrček 1993; Baral et al. 1999, 2013a, 2013b; Holec et al. 2015). The significance of fungi in forest ecosystems was reviewed by Niego et al. (2023a), highlighting their diverse functional contributions. This emphasizes the critical need to integrate fungal contributions into ecological conservation policies. Additionally, fungi hold significant value, encompassing not only the economic worth of wild and cultivated mushrooms but also the augmented value derived from fungal products and their involvement in various production processes. Furthermore, fungal involvement in ecosystem processes like carbon sequestration and recreational foraging also increases their traded value. In their study, Niego et al. (2023b) provided estimates to support more effective ecological conservation policies for fungal resources, highlighting the importance of studying and conserving these organisms. Decay fungi are able to produce enzymes that degrade components of wood, such as lignin, cellulose and xylans (Bucher et al. 2004) and are known as lignicolous fungi. Different lignicolous fungi prefer dead wood at different stages of decaying, for example, *Tatraea* mainly grows and decomposes the intermediate and late stages of wood decay (DS4) (Svrček 1993; Baral et al. 1999, 2013a; Heilmann-Clausen 2001; Holec et al. 2015; Dvořák 2017; Ujházy et al. 2018; Kunca et al. 2022). Due to the high density of managed forests, their low understory vegetation diversity compared to that of primary forests as well as the lack of late-stage decayed wood, members of *Tatraea* were rarely discovered in managed forests. Thus *T. dumbirensis* was considered an indicator of the primary forest and forest continuity, but also rarely collected in beech-dominated managed forests (Dvořák 2017; Ujházy et al. 2018). In China, only one species (*Tatraea aseptata* H.L. Su & Q. Zhao) was discovered in the protected primary forests, and other species were mainly found in the Center of Europe (Baral et al. 1999). *Tatraea* species are mostly found in old, natural primary montane forests (Baral et al. 1999). These species may have specialized adaptations to the undisturbed, virgin primary forests, contributing to overall biodiversity. Hence, they might not thrive or even survive in disturbed or secondary forests. These findings stress the importance of accurate management of primary forests to conserve their fungal diversity as well as the fungal gene pool (Baral et al. 1999). Furthermore, the rarity of these *Tatraea* species also highlights the importance of conducting studies on rare Leotiomycetes fungi to conserve them before they become extinct.

We have been conducting comprehensive studies on discomycetes, encompassing investigations into taxonomy, species diversity and evolutionary research, among other aspects (Ekanayaka et al. 2017, 2018, 2019; Lestari et al. 2022, 2023; Phutthacharoen et al. 2022). In this study, the authors aim to

investigate the diversity of discomycetes in Yunnan Province, China. During our exploration, we discovered and collected the rare *Tatraea* species. In this study, we identified four new species of *Tatraea* on decayed and decorticated wood with detailed morphological descriptions and illustrations as recommended by Chethana et al. (2021). In previous studies, the classification of *Tatraea* mainly relied on morphological evidence, and only ITS sequences were available for phylogenetic analysis. Here, we provide additional gene regions and complete morphologies for future taxonomic and evolutionary research.

## Materials and methods

### Sample collection and morphological studies

Specimens were collected from decayed wood in Yunnan Province, China, during field investigations conducted from June, 2021 to October, 2022. All samples were obtained from highly humid natural broadleaf forests and protected areas rarely accessed by humans. During the collection period, the temperature of the collection site was basically in the range of 17 °C to 27 °C, and the temperature of Jingdong County, Puer City was 14 °C to 16 °C due to the influence of high altitude. The fruiting bodies were found on the surface of extremely wet decaying wood following rainfall events. The specimens with their substrates were gently wrapped in a single layer of tissue, rotated and pinched ends tightly with a hollow center to prevent squeezing the specimen. The specimens dried naturally in air, re-wrapped in a hard-paper boxes containing a small amount of silica gel and rehydrated before being observed in the laboratory.

Fresh apothecia were photographed in the field by a Canon EOS M100 camera (Canon Co. LTD, Japan). The dried and partially fresh apothecia were captured using a Canon EOS 70D(W) digital camera attached to a C-PSN stereomicroscope (Nikon Corporation Tokyo, Japan). The dried apothecia were sectioned by hand using razor blades and photographed by a charge-coupled device SC 2000C attached to a Nikon ECLIPSE Ni-U compound microscope (Nikon Corporation Tokyo, Japan). Vertical sections were used to observe the excipulum and hymenium. Asci, ascospores and paraphyses were observed by mounting squashed mature apothecia in water. Melzer's reagent checked the blue iodine reaction of the ascus apex.

All measurements were carried out using Tarosoft (R) Image Framework program (IFW) and modified in Adobe Photoshop 2020 (Adobe system, USA).  $Q$  value indicates the length to width ratio of ascospores,  $n$  indicates the number of measured structures, and  $Q_m$  indicates the average of  $Q$  value. The size of apothecia was defined as large (greater than 3.5 mm wide), moderate (greater than 2.5 mm and less than 3.5 mm wide) and small (less than 2.5 mm wide) based on mean and extreme values. The length of stipes was defined as long (longer than 1.1 mm), moderate (greater than 0.4 mm and less than 1.1 mm) and short (shorter than 0.4 mm). The colors of apothecia were determined following Kornerup and Wanscher (1967). The dried specimens were deposited at the Herbarium of Cryptogams, Kunming Institute of Botany Academia Sinica (KUN-HKAS). Facesoffungi numbers were obtained as in Jayasiri et al. (2015), and Index Fungorum numbers were obtained as in Index Fungorum (2023). Furthermore, details of all the species described in this study were uploaded to the Discomycetes website (<https://discomycetes.org/>, Lestari et al. 2023).

## DNA extraction, PCR amplification, and sequencing

Two to three mature fruit bodies were carefully selected and thoroughly cleaned using sterilized water and 75% alcoholic solution. Subsequently, several layers of epidermal cells were meticulously removed using sterilized surgical blades. Following this step, approximately 1 mm<sup>3</sup> of tissue was meticulously collected from both the receptacles and stipes using new sterile surgical blades. The collected tissue was then transferred into a sterile 1.5 mL centrifuge tube. Total genomic DNA was extracted using the Trilief™ Plant Genomic DNA Kit (Tsingke Biological Technology Co., LTD, Beijing, China). The total reaction volume for the Polymerase Chain Reaction (PCR) was 25 µl, containing 12.5 µl of 2 × Power Taq PCR MasterMix, 7.5 µl of sterile deionized water, 1 µl of each primer (100 µM stock), and 3 µl of DNA template. The amplifications were performed in a TC-type gene amplifier (LifeE-CO) (Hangzhou Bori Technology Co., LTD, Hangzhou City, Zhejiang Province, China). The primers used in this study are shown in Table 1. The conditions of PCR for each gene are as follows: for the ITS, LSU, mtSSU and *RPB1*, initial denaturation at 94 °C for 3 min, 35 cycles of denaturation at 94 °C for 30 s, 40 s of annealing at 53 °C, 1 min elongation at 72 °C, followed by a final extension for 10 min at 72 °C; for the *RPB2* initial denaturation at 94 °C for 5 min, 35 cycles of denaturation at 94 °C for 1 min, 1 min of annealing at 56 °C for *RPB2*, 1 min elongation at 72 °C, followed by a final extension for 10 min at 72 °C. The PCR products were verified by 1% agarose gel electrophoresis followed by staining with TS-GelRed Ver.2 10,000 × in Water (Tsingke Biological Technology Co., LTD, Beijing, China). Products were sequenced at Tsingke biological technology Co., LTD, Beijing, China.

## Sequence assembly and alignment

Sequences were assembled in ContigExpress (Invitrogen, USA), and then checked and edited in BioEdit 7.2.5.0 (Hall 1999). The homologous sequences were selected based on the results of the BLASTn search performed against the GenBank database available at NCBI. All new and related sequences used in this study were derived from GenBank and used for phylogenetic analyses. Two species in *Chlorociboria* (Chlorociboriaceae, Helotiales) were selected as the outgroup taxa.

**Table 1.** Primers used for the PCR amplifications in this study.

Locus	Primers	Nucleotide sequence (5'-3')	Reference
ITS	ITS1-F (F)	5'-TCCGTAGGTGAACCTGCGG-3'	(White et al. 1990)
	ITS4 (R)	5'-TCCTCCGCTTATTGATATGC-3'	
LSU	LR0R (F)	5'-ACCCGCTGAACTTAAGC-3'	(Vilgalys and Hester 1990)
	LR5 (R)	5'-TCCTGAGGGAACTTCG-3'	
mtSSU	mrSSU1 (F)	5'-AGCAGTGAGGAATATTGGTC-3'	(Zoller et al. 1999)
	mrSSU3R (R)	5'-ATGTGGCACGTCTATAGCCC-3'	
<i>RPB1</i>	<i>RPB1</i> -Af (F)	5'-GARTGYCCDGGDCAYTTYGG-3'	(Stiller and Hall 1997)
	<i>RPB1</i> -Cr (R)	5'-CCNGCDATNCRTRTCCATRTA-3'	
<i>RPB2</i>	fRPB2-5F (F)	5'-GAYGAYMGWGATCAYTTYGG-3'	(Liu et al. 1999)
	fRPB2-7cR (R)	5'-CCCATWGCYTGCTTMCCCAT-3'	

The datasets were aligned in MAFFT v. 7 (Katoh et al. 2019) with G-INS-i as the iterative refinement and default parameters were applied except for the gap penalty, which was changed to 1.00, and improved manually in BioEdit v. 7.2.5.0. Then, datasets were trimmed in TrimAl v. 1.3 using the gappyout option (Capella-Gutiérrez et al. 2009). The multiple loci association matrixes were concatenated to a combined dataset in SequenceMatrix 1.7.8. (Vaidya et al. 2011). Due to the lack of sequence data for protein genes, the phylogenetic tree was constructed using the ITS gene and the combined LSU and ITS gene regions (Figs 1, 2). The combined ITS, LSU, mtSSU, *RPB1* and *RPB2* dataset was used to analyze the recombination level within phylogenetically and closely related species (Fig. 3). The ALTER (Alignment Transformation EnviRonment) online tool was used to convert from “.fasta” to “.nexus” format. The newly generated sequences in this study were deposited in GenBank (Table 2), and the combined alignment was deposited at the TreeBASE (submission ID: 30884).

### Phylogenetic analyses

Maximum likelihood (ML) analysis was performed in RAxML-HPC2 on XSEDE (8.2.12) on the CIPRES Science Gateway platform (<http://www.phylo.org/portal2>) using the GTR model with 1,000 bootstrap replications. Bayesian inference (BI) analysis was performed using MrBayes v. 3.1.2. The Markov Chain Monte Carlo sampling (MCMC) was used to evaluate the posterior probabilities (PP). The general time-reversible model with a discrete gamma distribution coupled with a proportion of an invariant (GTR+I+G) was selected for nLSU and ITS as the best model using MrModeltest v.2.3 (Nylander et al. 2004). Four simultaneous Markov Chains were run for 2,000,000 generations, with trees sampling at every 100<sup>th</sup> generation. The 25% of the trees representing the burn-in phase were discarded, and the remaining trees were used to calculate the posterior probability. The finalized phylogenetic tree was visualized in Figtree v.1.4.0 (Rambaut 2012) and edited in Adobe Illustrator 2020 and Adobe Photoshop 2020 (<https://www.adobe.com/>). Splitstree4 4.17.1 was used to determine the recombination level between phylogenetically and closely related but ambiguous species based on the PHI (pairwise homoplasy index) value (Taylor et al. 2000; Silvestro and Michalak 2012). The relationships between the two species were shown in splits graphs with the Log-Det transformation option. The relationship between *T. macrospora* and *T. yunnanensis* was visualized by constructing a split graph (Fig. 3A) from ITS. The relationship between the other two pairs (*T. yuxiensis* and *T. aseptata*, and *T. griseoturcoisina* and *T. clepsydriiformis*) were visualized by constructing splits graphs, Fig. 3B and Fig. 3C, respectively, from 5-locus concatenated dataset. A pairwise homoplasy index below a 0.05 threshold ( $\Phi_w < 0.05$ ) indicates the presence of significant recombination between the two species (Chethana et al. 2017).

## Results

### Phylogenetic analyses

The dataset for the phylogenetic analysis based on the ITS gene consists of 69 taxa, represented by 81 isolates, including two outgroup taxa, *Chlorociboria aeruginosa*



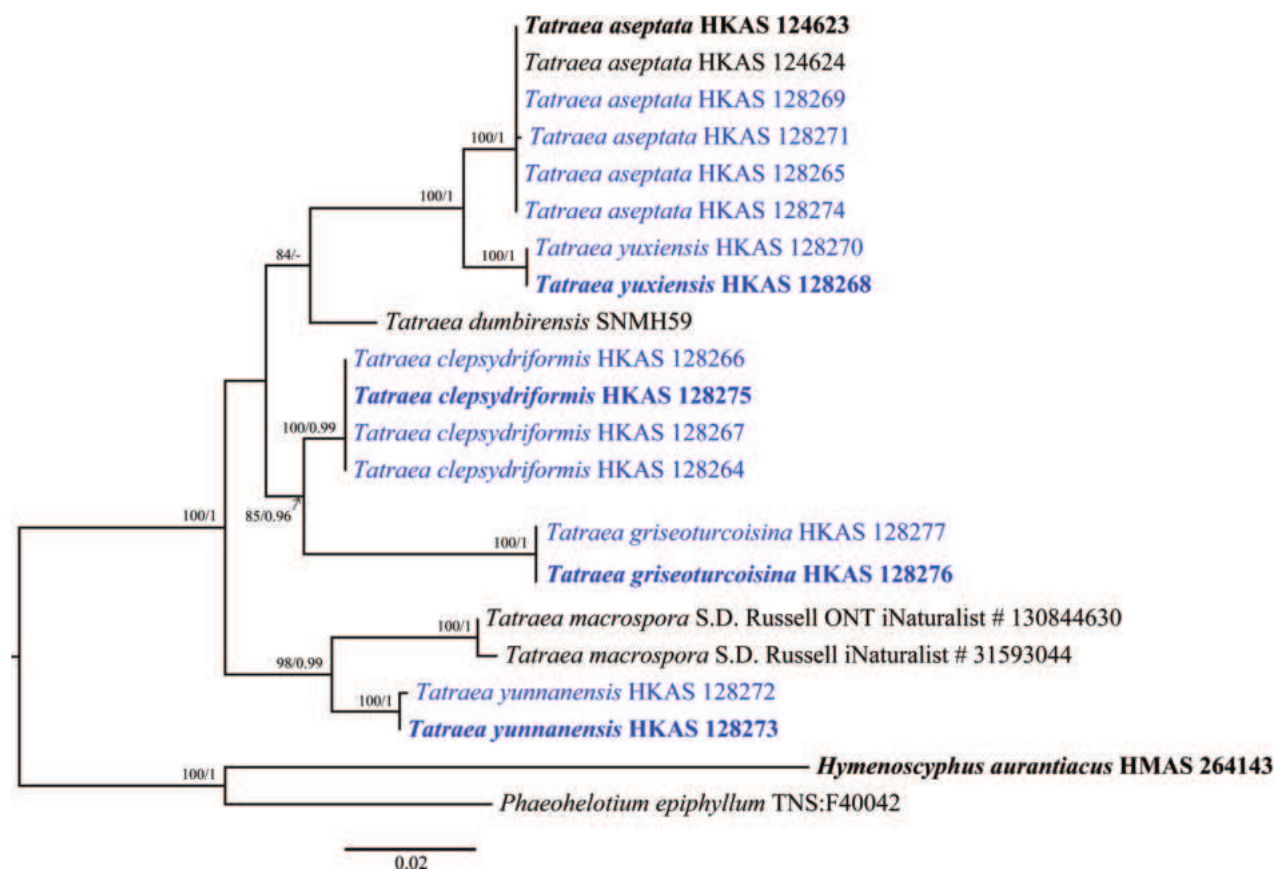


**Figure 2.** Maximum likelihood tree based on a combined dataset of LSU and ITS sequences for the genus *Tatraea*. The ML bootstrap proportions (ML-BP) equal to or higher than 70% and Bayesian posterior proportions (BI-PP) equal to or higher than 0.90 are shown near the branches on the phylogenetic tree. Newly generated isolates of the current study are shown in blue and ex-types are shown in bold.

(TNS:F13596) and *Chlorociboria aeruginascens* (TNS:F36241). The dataset contains 550 total characters with gaps. The combined alignment contains 239 constant characters, 54 variable and parsimony uninformative characters and 254 parsimony-informative characters. The RAxML analysis of the ITS gene dataset yielded the best-scoring tree with a final likelihood value of -8336.600892 (Fig. 1). The maximum likelihood matrix comprises 366 distinct alignment patterns with 8.85% undetermined characters or gaps. Estimated base frequencies are as follows: A = 0.219317, C = 0.265186, G = 0.257196, T = 0.258302; substitution rates AC = 1.749614, AG = 2.352229, AT = 1.537478, CG = 0.647334, CT = 5.060114, GT = 1.000000; gamma distribution shape parameter  $\alpha$  = 0.360268. The LSU and ITS concatenated dataset consists of 9 taxa, represented by 21 isolates, including two outgroup taxa, *Hymenoscyphus aurantiacus* (HMAS 264143) and *Phaeohelotium epiphyllum* (TNS:F40042). The concatenated dataset contains 1744 aligned nucleotide sites, including 1256 bp for the LSU region and 488 bp for the ITS region with gaps. The combined alignment contains 1471 constant characters, 89 variable and parsimony uninformative characters and 184 parsimony-informative characters. The RAxML analysis of the combined dataset (LSU and ITS) yielded the best-scoring tree with a final likelihood value of -4243.290550 (Fig. 2). The dataset comprises 259 distinct alignment patterns with 31.66% undetermined characters or gaps. Estimated base frequencies are as follows: A = 0.227902, C = 0.244223, G = 0.295968, T = 0.231906; substitution rates AC = 0.961500, AG =

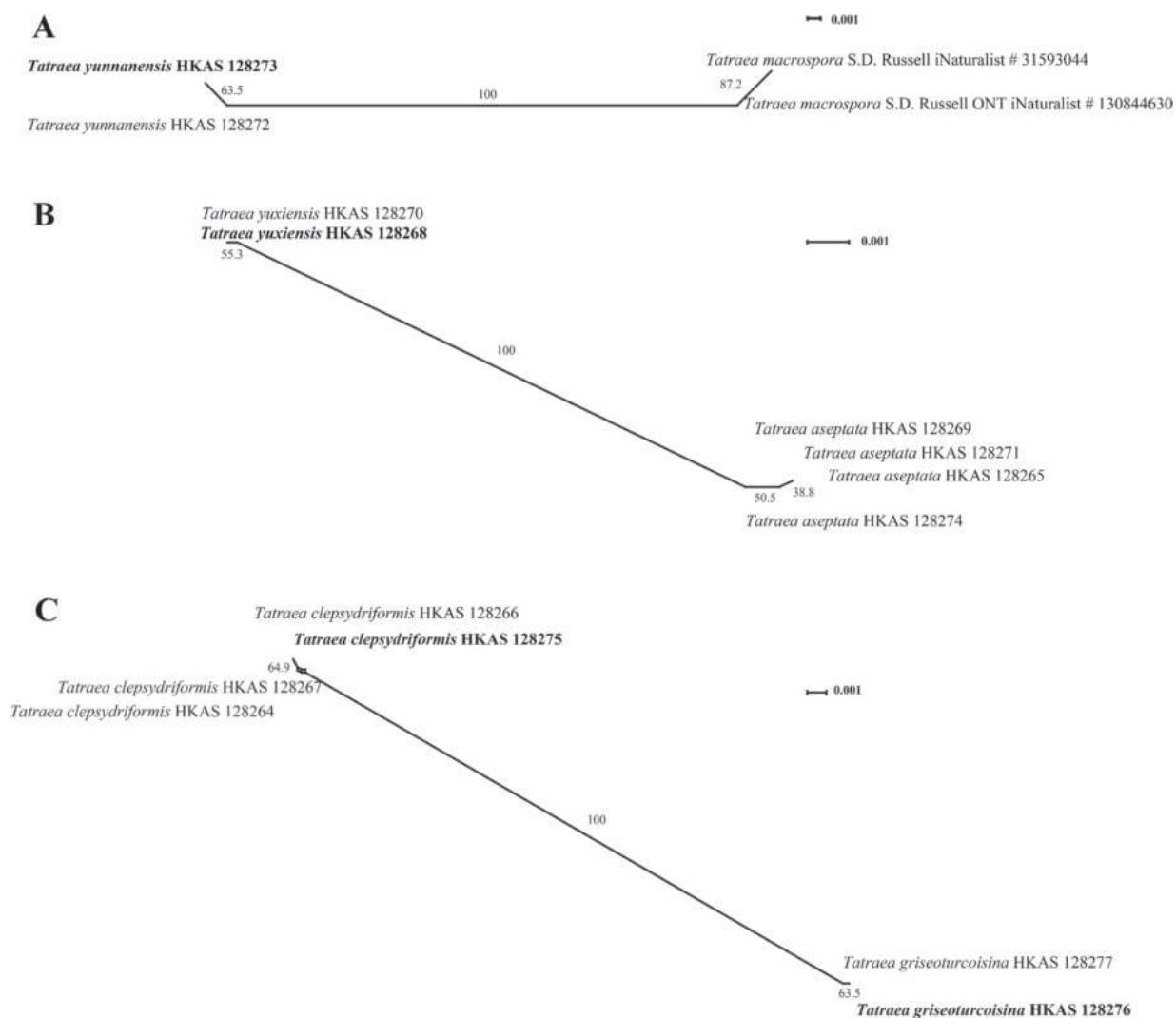


**Figure 3.** The results of the pairwise homoplasies (PHI) test for the closely related species in *Tatraea* using LogDet transformation. A. PHI test for *Tatraea yunnanensis* vs. *Tatraea macrospora*. B. PHI test for *Tatraea yuxiensis* vs. *Tatraea aseptata*. C. PHI test for *Tatraea clepsydriformis* vs. *Tatraea griseoturcoisina*. PHI test results ( $\Phi_w < 0.05$ ) indicate significant recombination within the dataset.

2.058057, AT = 0.608426, CG = 0.460988, CT = 7.662978, GT = 1.000000; gamma distribution shape parameter  $\alpha = 0.183205$ . Species in *Hymenoscyphus* showed different topologies in ML and BI analyses, but the support values for the nodes are less. Despite the different taxon sampling, the topological structure of the phylogenetic tree shown in Fig. 1 is similar to that of Johnston et al. (2019). In the ML and Bayes analyses, *Tatraea* formed a monophyletic clade within Helotiaceae with 67% ML bootstrap support and 0.98 Bayesian probability in the ITS phylogeny (Fig. 1). Some nodes in Clade II and Clade III have low support values (Fig. 1). In Clade I, our collections of *Tatraea aseptata* clustered with the type species and formed a sub-clade sister to *T. yuxiensis* with 98% ML support and 1.00 Bayesian probability support. However, this clade comprising *T. aseptata* and *T. yuxiensis* separated from *T. dumbirensis* with 74% ML bootstrap support and 0.57 Bayesian probability. Collections of *T. clepsydriformis* and *T. griseoturcoisina* formed two individual clades in Fig. 1 with 50% ML bootstrap support and 0.80 Bayesian probability, and 52% ML bootstrap support and 0.92 Bayesian probability, respectively. However, these two species clustered as a separate sub-clade with 85%

**Table 2.** Detailed information and corresponding GenBank accession numbers of the taxa used in the phylogenetic analyses of this study. “†” Denotes type species. Newly generated sequences are shown in bold. “-”: indicates sequence data is not available.

Taxon name	Voucher	Gene accession No.				
		ITS	LSU	mtSSU	<i>RPB1</i>	<i>RPB2</i>
<i>Bryoscyphus rhytidadelphii</i>	H.B. 7214	OM808923	-	-	-	-
<i>Chlorociboria aeruginosa</i>	TNS-F-13596	LC425047	-	-	-	-
<i>C. aeruginascens</i>	TNS-F-36241	LC425045	-	-	-	-
<i>Cyathicula coronata</i>	CBS:197.62	MH858141	-	-	-	-
<i>Cy. culmicola</i>	F-171,707	FJ005119	-	-	-	-
<i>Cy. culmicola</i>	F-112,249	FJ005121	-	-	-	-
<i>Dicephalospora albolutea</i> †	HMAS 279693	MK425601	-	-	-	-
<i>D. chiangraiensis</i> †	MFLU 21-0018	MZ241817	-	-	-	-
<i>D. dentata</i>	3093	KP204263	-	-	-	-
<i>D. huangshanica</i>	MFLU 18-1828	MK584979	-	-	-	-
<i>D. irregularis</i> †	CM 31	ON511117	-	-	-	-
<i>D. rufocornea</i>	MFLU 18-1827	MK584978	-	-	-	-
<i>D. sessilis</i> †	MFLU 18-1823	NR_163779	-	-	-	-
<i>D. shennongjiana</i> †	HMAS 279698	MK425606	-	-	-	-
<i>Glarea lozoyensis</i> †	ATCC 20868	NR_137138	-	-	-	-
<i>Gloeotinia granigena</i>	1931. S	Z81432	-	-	-	-
<i>Helicodendron microsporum</i> †	CBS:100.149	NR_137974	-	-	-	-
<i>Hymenoscyphus albidoides</i> †	HMAS 264140	NR_154903	-	-	-	-
<i>H. aurantiacus</i> †	HMAS 264143	NR_154907	NG_059509	-	-	-
<i>H. brevicellulus</i>	HMAS 264015	JX977149	-	-	-	-
<i>H. calyculus</i>	HMAS 264146	KJ472291	-	-	-	-
<i>H. caudatus</i>	FeF217	MZ492984	-	-	-	-
<i>H. cf. calyculus</i>	MFLU 16-1865	MK584966	-	-	-	-
<i>H. fraxineus</i> †	ZT Myc 2022	NR_111479	-	-	-	-
<i>H. fructigenus</i>	CBS:186.47	MH856211	-	-	-	-
<i>H. fucatus</i>	1149-1	MW959791	-	-	-	-
<i>H. ginkgonis</i> †	KUS F51352	NR_119669	-	-	-	-
<i>H. kiko</i> †	ICMP:19613	NR_137110	-	-	-	-
<i>H. lepismoides</i> †	H.B. 9832	KM199777	-	-	-	-
<i>H. linearis</i> †	Chic_18	KM114535	-	-	-	-
<i>H. macrodiscus</i> †	HMAS 264158	NR_154908	-	-	-	-
<i>H. menthae</i>	P6291	MH063781	-	-	-	-
<i>H. microcaudatus</i> †	HMAS 264020	JX977156	-	-	-	-
<i>H. microserotinus</i> †	HMAS 68520	NR_132814	-	-	-	-
<i>H. occultus</i> †	CBS:139.469	NR_147434	-	-	-	-
<i>H. ohakune</i> †	ICMP:19601	NR_137109	-	-	-	-
<i>H. pusillus</i> †	HMC 21525	MH476516	-	-	-	-
<i>H. repandus</i>	420526MF0293	MG712335	-	-	-	-
<i>H. scutula</i>	CBS:101.66	MH858736	-	-	-	-
<i>H. seminis-alni</i>	H.B. 4974	KM114536	-	-	-	-
<i>H. serotinus</i>	H.B. 8023	KM114541	-	-	-	-
<i>H. subpalescens</i>	HMAS 264022	JX977154	-	-	-	-
<i>H. subsymmetricus</i> †	HMAS 264021	JX977153	-	-	-	-
<i>H. tetrasporus</i> †	490	KJ472302	-	-	-	-
<i>H. trichosporus</i>	H.B. 6456	KM114538	-	-	-	-

Taxon name	Voucher	Gene accession No.				
		ITS	LSU	mtSSU	<i>RPB1</i>	<i>RPB2</i>
<i>H. waikaia</i> <sup>†</sup>	PDD:102886	NR_137111	–	–	–	–
<i>Hymenotorrendiella andina</i>	PRJ SA193	KJ606682	–	–	–	–
<i>Hy. brevisetosa</i>	ICMP:18823	JN225946	–	–	–	–
<i>Hy. cannibalensis</i>	ICMP:18818	JN225947	–	–	–	–
<i>Hy. clelandii</i>	D1492	OK346623	–	–	–	–
<i>Hy. communis</i> <sup>†</sup>	CPC:32835	NR_170836	–	–	–	–
<i>Hy. dingleyae</i>	PDD:112191	MK039692	–	–	–	–
<i>Hy. eucalypti</i>	AH7636	KF588379	–	–	–	–
<i>Hy. indonesiana</i>	CPC:11049	DQ195787	–	–	–	–
<i>Hy. madsenii</i>	PRJ:D672	AY755336	–	–	–	–
<i>Neocrinula lambertiae</i> <sup>†</sup>	CBS:143.423	NR_156388	–	–	–	–
<i>N. xanthorrhoeae</i> <sup>†</sup>	CPC:29474	NR_154252	–	–	–	–
<i>Phaeohelotium epiphyllum</i>	TNS:F40042	AB926061	AB926130			
<i>Roesleria subterranea</i>	TNS:F38701	AB628057	–	–	–	–
<i>Symphyosirinia clematidis</i>	H.B. 7075	OM808922	–	–	–	–
<i>Tatraea dumbirensis</i>	SNMH59	MK907417	–	–	–	–
<i>T. macrospora</i>	S.D. Russell ONT iNaturalist # 130844630	OP643029	–	–	–	–
<i>T. macrospora</i>	S.D. Russell iNaturalist # 31593044	OM473784	–	–	–	–
<i>T. aseptata</i>	HKAS 124624	OP538031	–	–	–	–
<i>T. aseptata</i> <sup>†</sup>	HKAS 124623	OP538030	–	–	–	–
<b><i>T. aseptata</i></b>	HKAS 128269	<b>OQ921780</b>	<b>OR214956</b>	–	<b>OR703635</b>	–
<b><i>T. aseptata</i></b>	HKAS 128274	<b>OQ921783</b>	<b>OR214952</b>	<b>OR237204</b>	<b>OR703633</b>	<b>OR735340</b>
<b><i>T. aseptata</i></b>	HKAS 128271	<b>OQ921782</b>	<b>OR220038</b>	<b>OR237210</b>	<b>OR703636</b>	<b>OR735342</b>
<b><i>T. aseptata</i></b>	HKAS 128265	<b>OQ921777</b>	<b>OR214955</b>	<b>OR237207</b>	<b>OR703634</b>	<b>OR735341</b>
<b><i>T. clepsydriformis</i></b>	HKAS 128266	<b>OQ520277</b>	<b>OR214945</b>	<b>OR271555</b>	<b>OR703642</b>	<b>OR735348</b>
<b><i>T. clepsydriformis</i></b> <sup>†</sup>	HKAS 128275	<b>OQ520268</b>	<b>OR214946</b>	<b>OR237205</b>	<b>OR703641</b>	<b>OR735347</b>
<b><i>T. clepsydriformis</i></b>	HKAS 128264	<b>OQ921768</b>	<b>OR214949</b>	<b>OR237203</b>	<b>OR703643</b>	–
<b><i>T. clepsydriformis</i></b>	HKAS 128267	<b>OQ921773</b>	<b>OR214951</b>	<b>OR271554</b>	<b>OR703644</b>	<b>OR735349</b>
<b><i>T. griseoturcoisina</i></b> <sup>†</sup>	HKAS 128276	<b>OQ520299</b>	<b>OR214959</b>	<b>OR237211</b>	<b>OR703646</b>	<b>OR735351</b>
<b><i>T. griseoturcoisina</i></b>	HKAS 128277	<b>OQ520298</b>	<b>OR214965</b>	<b>OR237207</b>	<b>OR703645</b>	<b>OR735350</b>
<b><i>T. yunnanensis</i></b>	HKAS 128272	<b>OQ546436</b>	<b>OR220043</b>	<b>OR237209</b>	<b>OR703639</b>	<b>OR735345</b>
<b><i>T. yunnanensis</i></b> <sup>†</sup>	HKAS 128273	<b>OQ520294</b>	<b>OR220044</b>	<b>OR237212</b>	<b>OR703640</b>	<b>OR735346</b>
<b><i>T. yuxiensis</i></b> <sup>†</sup>	HKAS 128268	<b>OQ546437</b>	<b>OR220042</b>	<b>OR237202</b>	<b>OR703637</b>	<b>OR735343</b>
<b><i>T. yuxiensis</i></b>	HKAS 128270	<b>OQ546435</b>	<b>OR220039</b>	<b>OR237208</b>	<b>OR703638</b>	<b>OR735344</b>

ML support and 0.96 Bayesian probability support in the ITS and LSU combined phylogeny (Fig. 2). *Tatraea yunnanensis* clustered with *T. macrospora* with 98% ML bootstrap support and 0.99 Bayesian probability support in the LSU and ITS phylogeny (Fig. 2). A pairwise homoplasy index below 0.05 typically indicated the presence of significant recombination among the groups. In our analysis, the pairwise homoplasy index (PHI or  $\Phi_w$ ) for three pairs of species (*T. macrospora* vs. *T. yunnanensis*, *T. yuxiensis* vs. *T. aseptata* and *T. griseoturcoisina* vs. *T. clepsydriformis*) were 1.0, 1.0 and 0.4185, respectively. These results indicated no significant recombination among these pairs.

## Taxonomy

### *Tatraea aseptata* H.L. Su & Q. Zhao

Index Fungorum: IF559987

Facesoffungi Number: FoF12892

Fig. 4

**Type material. Holotype.** HKAS 124623.

**Description.** Saprobic on the decayed branches of oak trees. **Sexual morph:** Apothecia 2.5–4.7 mm wide ( $\bar{x} = 3.3 \pm 0.5$  mm,  $n = 27$ ) when fresh, 1–2.4 mm wide  $\times$  0.6–1.2 mm high ( $\bar{x} = 1.6 \pm 0.3 \times 0.9 \pm 0.1$  mm,  $n = 28$ ) when dry, scattered or gregarious, superficial, discoid with glabrous, short stipe. Disc flat and circular, light brown (7D5–7D6) in wet habitat, slightly dark alabaster grey (5B2) in slightly dried habitat when fresh, edge undulating and slightly curl inward towards the disc, dark brown (8F5–8F6) to dull green (30E4) or greyish green (30E5) when dry, sometimes orange white to pale greenish white (29A2) or dull yellow (3B4) to greyish yellow (3B5–3B6) near center. Margins white when immature and fresh, concolorous to the disc when mature and fresh, white to pale yellow or concolorous to the receptacles when dry. Receptacle smooth and brown (6D7–6D8) when fresh, yellowish brown (5E5–5E6), flank darker when dry, rough and fine pustules on the surface. Stipe 280–725  $\mu\text{m}$  wide  $\times$  340–735  $\mu\text{m}$  long ( $\bar{x} = 500 \pm 148 \times 540 \pm 125$   $\mu\text{m}$ ,  $n = 11$ ), short, broad at upside part, narrower at lower part, golden brown (5D7) when fresh, light brown when dry, finely granular pustules, ridged at maturity. Hymenium 142–190  $\mu\text{m}$  ( $\bar{x} = 160 \pm 14$   $\mu\text{m}$ ,  $n = 15$ ), hyaline. Subhymenium 35–52  $\mu\text{m}$  ( $\bar{x} = 44 \pm 4$   $\mu\text{m}$ ,  $n = 25$ ), dense brown hyphae forming a *textura intricata*, hyphae 3.4–4.3  $\mu\text{m}$  ( $\bar{x} = 3.8 \pm 0.3$   $\mu\text{m}$ ,  $n = 25$ ) diam., gather with excipulum at the margin. Medullary excipulum 120–145  $\mu\text{m}$  ( $\bar{x} = 133 \pm 7$   $\mu\text{m}$ ,  $n = 15$ ), thick, well-developed, comprised of thin-walled, septate, pale brown and slightly loose hyphae of *textura intricata*, hyphae 4.3–7.4  $\mu\text{m}$  ( $\bar{x} = 6.0 \pm 0.8$   $\mu\text{m}$ ,  $n = 25$ ) diam., hyaline, becoming dense and well-organized, parallel near to the ectal excipulum, non-gelatinous. Ectal excipulum visible, different from the medullary excipulum, the inner layers generally consists of 3–4 layers *textura globulosa* to *textura angularis* cells, 30–48  $\mu\text{m}$  ( $\bar{x} = 38 \pm 4$   $\mu\text{m}$ ,  $n = 35$ ) thick, moderately thick-walled, cells 8.4–16.5  $\mu\text{m}$  ( $\bar{x} = 13.0 \pm 1.9$   $\mu\text{m}$ ,  $n = 50$ ) diam., wall 0.63–1.54  $\mu\text{m}$  ( $\bar{x} = 1.01 \pm 0.18$   $\mu\text{m}$ ,  $n = 70$ ) thick; the outer layers partially uneven proliferous to 8–12 layers, stack into triangles to trapezoids, 50–89  $\mu\text{m}$  ( $\bar{x} = 69 \pm 9$   $\mu\text{m}$ ,  $n = 60$ ) thick (including the inner layers), cells 3–11  $\mu\text{m}$  ( $\bar{x} = 8 \pm 1.7$   $\mu\text{m}$ ,  $n = 75$ ) diam., wall 0.6–1.7  $\mu\text{m}$  ( $\bar{x} = 0.95 \pm 0.21$   $\mu\text{m}$ ,  $n = 65$ ) thick; cells from the outer to the inner layers gradually increase in diameter, brown to colorless; terminal cells of 3–4 layers at flank stretch to 13.1–15.3  $\mu\text{m}$  long  $\times$  2.6–3.8  $\mu\text{m}$  wide ( $\bar{x} = 14.1 \pm 0.8 \times 3.3 \pm 0.5$  mm,  $n = 10$ ), straight, ends narrow and slightly sharp, thin-walled, brown. Paraphyses 1.9–3.7  $\mu\text{m}$  ( $\bar{x} = 2.6 \pm 0.4$   $\mu\text{m}$ ,  $n = 50$ ) wide, hyaline, filiform, rounded apex, 0–2-septate, unbranched, with conspicuous lipid bodies, scarcely extending beyond the asci. Asci (132–)136.7–157.8(–172)  $\times$  (12.5–)13.2–16.0(–17.3)  $\mu\text{m}$  ( $\bar{x} = 148.2 \pm 7.8 \times 14.5 \pm 1.0$   $\mu\text{m}$ ,  $n = 40$ ), unitunicate, 8-spored, almost filling the whole asci, clavate, slightly curved, apically rounded with an amyloid apical pore in Melzer's reagent, an incrassated



**Figure 4.** *Tatraea aseptata* (HKAS 128275) **a–c** Fresh ascomata on the wood **d–g** dried ascomata on the wood **h** vertical section of an ascoma **i–j** excipulum **k** paraphyses **l–p** asci (**o–p** asci in Meltzer’s reagent) **q–v** ascospores. Scale bars: 1.5 mm (**d**); 400  $\mu$ m (**e**); 800  $\mu$ m (**f–g**); 1000  $\mu$ m (**h**); 200  $\mu$ m (**i**); 100  $\mu$ m (**j**); 70  $\mu$ m (**k–p**); 15  $\mu$ m (**q–v**).

wall at apex, 7.4–11.1  $\mu\text{m}$  wide  $\times$  3.7–6.1  $\mu\text{m}$  high ( $\bar{x}$  = 9.0  $\pm$  0.7  $\times$  4.8  $\pm$  0.5  $\mu\text{m}$ , n = 40), slightly constricted downward, tapering to obconical or short subtruncated base, sometimes not obvious, croziers present. Ascospore (21.8–)24.6–31.6(–33.7)  $\times$  (7.6–)7.8–10.0(–10.8)  $\mu\text{m}$  ( $\bar{x}$  = 27.4  $\pm$  2.3  $\times$  8.8  $\pm$  0.7  $\mu\text{m}$ , n = 80), Q = (2.3–)2.5–3.7(–4.0), Qm = 3.1  $\pm$  0.3, overlapping uniseriate, slightly asymmetrical, reniform with a large guttule and several multiple granules, obtusely rounded at the apex, slightly pointed at the base, hyaline, thin-walled, smooth and aseptate. **Asexual morph:** Undetermined.

**Material examined.** CHINA, Yunnan Province, Puer City, Jingdong County, altitude 2455 m, on the decayed oak tree twig, 23 August 2022, Cuijinyi Li, LCJY-1221 (HKAS 128274); *ibid.*, Ailao Mountain, altitude 2520 m, on mossy, decaying unknown wood, 9 June 2022, Cuijinyi Li, LCJY-743 (HKAS 128271); *ibid.*, Kunming City, Panlong District, altitude 1920 m, on the decayed oak tree twig, 25 May 2022, Cuijinyi Li, LCJY-477 (HKAS 128265); *ibid.*, Yuxi City, Xiping County, altitude 1920 m, on soft decayed unknown wood, 5 June 2022, Cuijinyi Li, LCJY-601 (HKAS 128269).

**Notes.** Our collections are clustered with *T. aseptata* H.L. Su & Q. Zhao with 100% ML bootstrap support and 1.0 Bayesian probability. Fruiting bodies are mostly founded on decayed oak tree branches and share similar characteristics with *T. aseptata* by having fresh apothecia of similar size, brown receptacles when dry and the same reniform ascospores. In contrast, our collection also showed differences in their outer ectal excipulum comprising 8–12 layers of uneven proliferous cells with no hairs, thinner medullary excipulum and shorter asci (136.7–157.8  $\mu\text{m}$  vs. 150–185  $\mu\text{m}$ ).

***Tatraea clepsydriiformis* C.J.Y. Li & Q. Zhao, sp. nov.**

Index Fungorum: IF901178

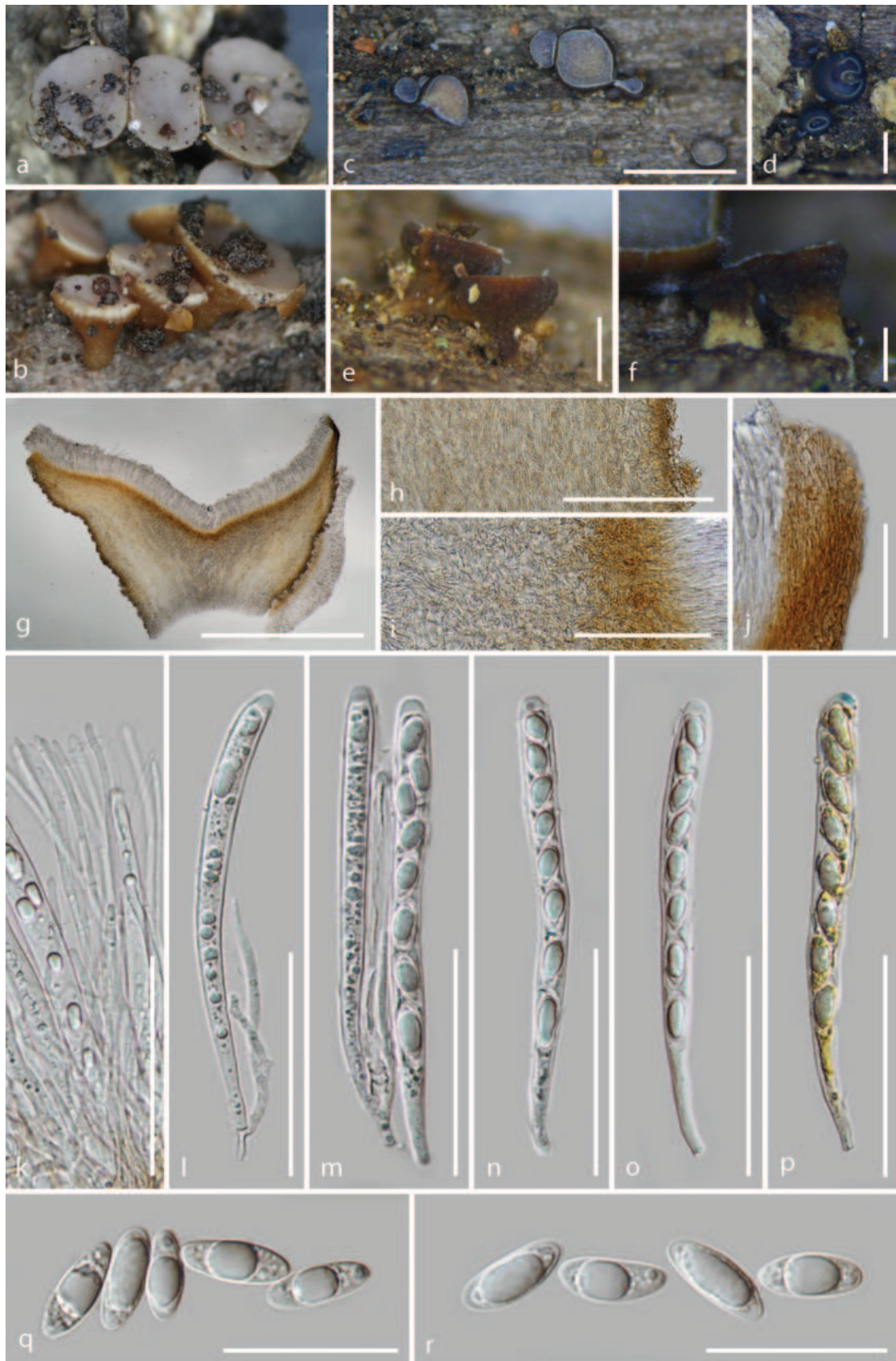
Facesoffungi Number: Fo15190

Fig. 5

**Etymology.** The specific epithet refers to the hourglass shape apothecia.

**Holotype.** HKAS 128275.

**Description.** Saprobiic on the decayed branches of oak tree. **Sexual morph:** Apothecia 1.3–3.5 mm wide ( $\bar{x}$  = 2.5  $\pm$  0.7 mm, n = 13) when fresh, 0.9–1.3 mm wide  $\times$  0.6–0.9 mm high ( $\bar{x}$  = 1.1  $\pm$  0.15  $\times$  0.7  $\pm$  0.12 mm, n = 13) when dry, gregarious, superficial, hourglass shape or cupulate, glabrous, with a wide stipe. Disc flat and circular, pale grey (5C1) when fresh, edge slightly curl inward towards the disc, melon yellow (5A6) to apricot yellow (5B6) or pale orange (5A2) near the center, darken to concolorous as receptacle near the edge when dry, or dark blue (20E7) when immature. Margins concolorous to the disc when fresh, white, smooth or dentate when dry. Receptacle slightly rough and dark yellowish brown (5D8) when fresh, slightly rough, light brown (6D8) to hazel brown (6E8) when mature and dry, sometimes edge with white narrow-band, smooth and dark blackish blue (20F8) when immature and dry. Stipe 360–596  $\mu\text{m}$  wide  $\times$  463–571  $\mu\text{m}$  long ( $\bar{x}$  = 470  $\pm$  85  $\times$  515  $\pm$  47  $\mu\text{m}$ , n = 13), short and broad, concolorous to the receptacle or pale yellow when fresh, concolorous to dried receptacle when mature, butter yellow (4A5) when immature, slightly rough on surface. Hymenium



**Figure 5.** *Tatraea clepsydriformis* (HKAS 128275, holotype) **a–b** fresh ascomata on the wood **c–f** dried ascomata on the wood **g** vertical section of an ascoma **h–j** excipulum **k** paraphyses **l–p** asci (**o–p** asci in Meltzer's reagent) **q–r** ascospores. Scale bars: 2 mm (**c**); 600  $\mu$ m (**d**); 700  $\mu$ m (**e**); 250  $\mu$ m (**f**); 800  $\mu$ m (**g**); 150  $\mu$ m (**h**, **j**); 100  $\mu$ m (**i**); 60  $\mu$ m (**k–p**); 40  $\mu$ m (**q–r**).

122–155  $\mu\text{m}$  ( $\bar{x} = 135 \pm 12 \mu\text{m}$ ,  $n = 30$ ), hyaline. Subhymenium (24–)36–60(–65)  $\mu\text{m}$  ( $\bar{x} = 44 \pm 8 \mu\text{m}$ ,  $n = 37$ ), dense golden brown (5D7) hyphae, forming *textura intricata*, hyphae 2.2–2.9  $\mu\text{m}$  ( $\bar{x} = 2.6 \pm 0.2 \mu\text{m}$ ,  $n = 25$ ) wide. Medullary excipulum 335–535  $\mu\text{m}$  ( $\bar{x} = 415 \pm 51 \mu\text{m}$ ,  $n = 15$ ) thick, well-developed, comprised of thin-walled, septate, branched, pale brown and slightly loose hyphae of *textura intricata* in center, hyphae 3.3–5.1  $\mu\text{m}$  ( $\bar{x} = 4.2 \pm 0.5 \mu\text{m}$ ,  $n = 45$ ) diam., hyaline, near the ectal excipulum becoming well-organized parallel, non-gelatinous. Ectal excipulum 29–80  $\mu\text{m}$  ( $\bar{x} = 50 \pm 14 \mu\text{m}$ ,  $n = 48$ ) thick, comprised of 3–5 layers, large cells inside and several outer layers of smaller cells of *textura angularis*, 4.9–15.3  $\mu\text{m}$  ( $\bar{x} = 8.9 \pm 2.4 \mu\text{m}$ ,  $n = 64$ ) diam., wall moderately thick, 0.5–1.1  $\mu\text{m}$  ( $\bar{x} = 0.7 \pm 0.1 \mu\text{m}$ ,  $n = 52$ ) thick, pale brown to pale yellow from the outer inward the inner layers; proliferous cells not observed; terminal cells at margin inconspicuous elongated. Paraphyses 2.1–3.4  $\mu\text{m}$  ( $\bar{x} = 2.6 \pm 0.3 \mu\text{m}$ ,  $n = 45$ ) wide, hyaline, straight and filiform, apically round, 1–3-septate, unbranched, no conspicuous contents, scarcely extending beyond the asci. Asci (104.0–)112.4–135.8  $\times$  8.2–12.2  $\mu\text{m}$  ( $\bar{x} = 121.5 \pm 5.7 \times 10.1 \pm 0.9 \mu\text{m}$ ,  $n = 40$ ), unitunicate, 8-spored, cylindrical or subclavate, apically rounded with an amyloid apical pore in Melzer's reagent, apical wall incrassated, 5.0–8.5  $\mu\text{m}$  wide  $\times$  2.0–3.7(–4.4)  $\mu\text{m}$  high ( $\bar{x} = 6.8 \pm 0.7 \times 3.1 \pm 0.5 \mu\text{m}$ ,  $n = 40$ ), slightly constricted downward when immature, tapering to a cylindrical and aporhynchous, subtruncated base, croziers present. Ascospore (12.9–)14.0–17.9  $\times$  5.1–6.8  $\mu\text{m}$  ( $\bar{x} = 15.2 \pm 0.9 \times 5.7 \pm 0.4 \mu\text{m}$ ,  $n = 65$ ),  $Q = 2.1$ –3.2,  $Q_m = 2.7 \pm 0.1$ , overlapping uniseriate, ellipsoidal with a large guttule, obtusely rounded at both ends, slightly pointed at the base, hyaline, almost symmetrical, thin-walled, smooth and aseptate.

**Asexual morph:** Undetermined.

**Material examined.** CHINA, Yunnan Province, Puer City, Jingdong County, altitude 2455 m, on the decayed oak tree twig, 23 August 2022, Cuijinyi Li, LCJY-1226 (HKAS 128275, holotype); *ibid.*, Kunming City, Panlong District, altitude 1920 m, on the decayed oak tree twig with ant nests, 29 May 2022, Cuijinyi Li, LCJY-497 (HKAS 128266, paratype); *ibid.*, Yeya Lake, altitude 1900 m, on the decayed oak tree twig with ant nests, 3 July 2021, Cuijinyi Li, LCJY-127 (HKAS 128264, paratype); *ibid.*, Sanjian Mountain, altitude 1950 m, on decayed wood, 18 December 2021, Cuijinyi Li, LCJY-392 (HKAS 128267, paratype).

**Notes.** The distinctive characteristics of *T. clepsydriformis* are moderate-sized apothecia (2.5 mm wide when fresh), with fresh brown receptacles and stipes, light brown to hazel brown at dry condition, stipes concolorous to receptacles, pale yellow, proliferous cells of ectal excipulum not observed, aporhynchous asci and small, ellipsoidal ascospores without septa.

Phylogenetically, our collections clustered with *T. griseoturcoisina* with 85% ML bootstrap support and 0.96 Bayesian probability in the combined LSU and ITS phylogeny (Fig. 2). Morphologically, both species have small ascospores shown in Suppl. material 1 (shorter than 23  $\mu\text{m}$ ). *Tatraea clepsydriformis* are distinguished from other species by their shorter asci and smaller ascospores except for *T. griseoturcoisina* (Suppl. material 1). *Tatraea clepsydriformis* differs from *T. griseoturcoisina* by having brown receptacles, a broader medullary excipulum (335–535  $\mu\text{m}$  vs. 164–308  $\mu\text{m}$ ) and shorter ascospores (15.2  $\times$  5.7  $\mu\text{m}$  vs. 17.1  $\times$  5.4  $\mu\text{m}$ ).

***Tatraea griseoturcoisina* C.J.Y. Li & Q. Zhao, sp. nov.**

Index Fungorum: IF901179

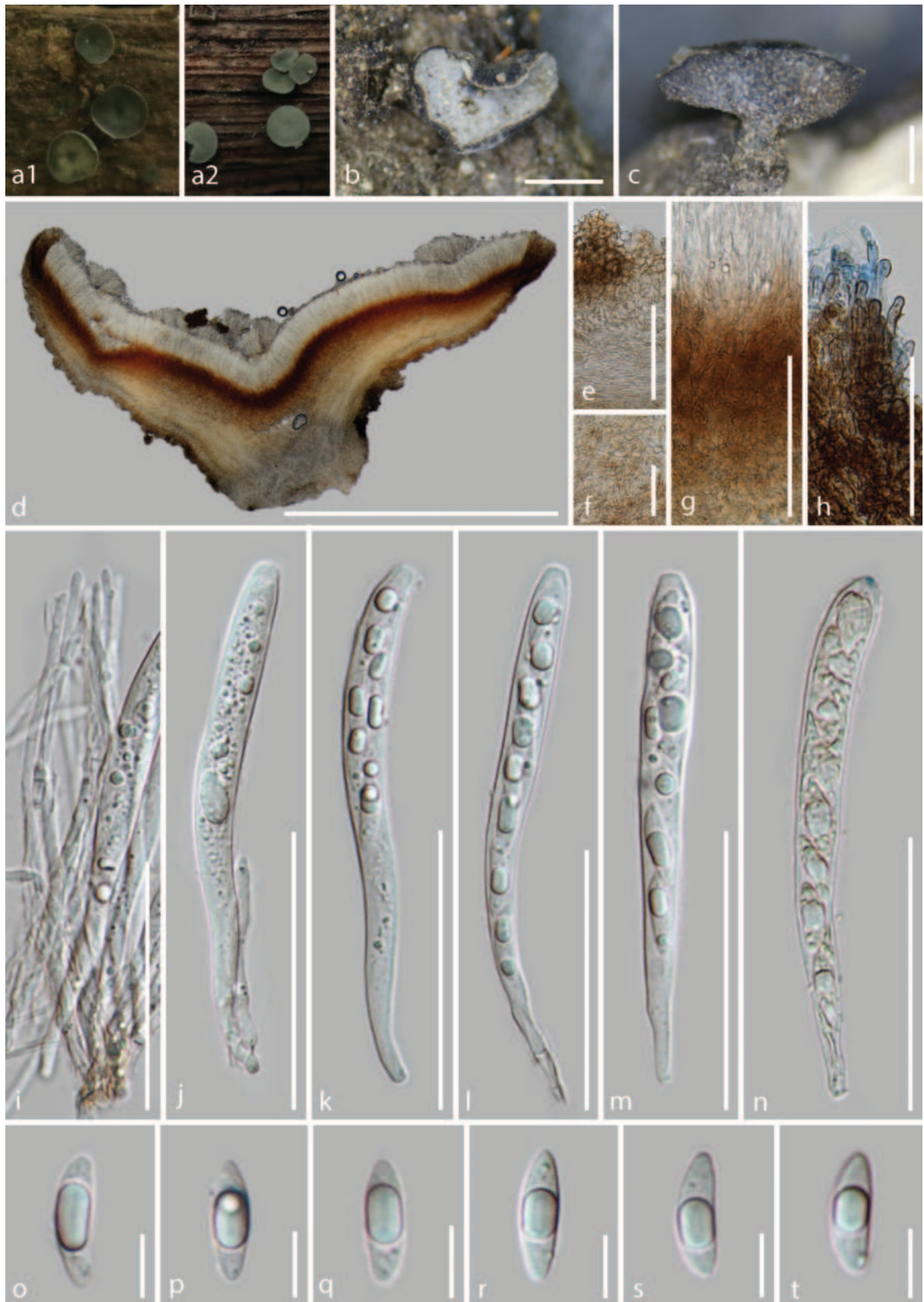
Facesoffungi Number: Fo15191

Fig. 6

**Etymology.** The specific epithet refers to the greyish turquoise color of the disc.

**Holotype.** HKAS 128276.

**Description.** Saprobic on decayed branches. **Sexual morph:** Apothecia 2.5–4.0 mm wide ( $\bar{x} = 3.1 \pm 0.4$  mm,  $n = 27$ ) when fresh, 1.0–2.1 mm wide  $\times$  0.6–0.8 mm high ( $\bar{x} = 1.6 \pm 0.3 \times 0.7 \pm 0.1$  mm,  $n = 20$ ) when dry, scattered or gregarious, superficial, discoid with thin and short stipitate, glabrous. Disc flat and circular, greyish turquoise (24E5) when fresh in wet habitat, slightly concave in the center, edge slightly curved upwards, deep green (28E8) with greyish green (28D5) to dark greyish green (28F7) when fresh in slightly dried habitat, edge slightly fold inward towards the discs, yellowish white (1A2) to snow white (1A1) when dry. Margins concolorous to the discs when fresh in wet habitat, white when dry or living in the dried habitat. Receptacle not observed when fresh, rough and finely pustules, dark brown to nearly black when dry, with some slightly dark and irregular veins on the surface. Stipe 330–360  $\mu\text{m}$  wide  $\times$  220–440  $\mu\text{m}$  long ( $\bar{x} = 350 \pm 89 \times 330 \pm 8$   $\mu\text{m}$ ,  $n = 5$ ), short and thin, rough and finely pustules, concolorous to the receptacle. Hymenium 103–138  $\mu\text{m}$  ( $\bar{x} = 117 \pm 8$   $\mu\text{m}$ ,  $n = 25$ ), hyaline. Subhymenium 43–66  $\mu\text{m}$  ( $\bar{x} = 53 \pm 6$   $\mu\text{m}$ ,  $n = 15$ ), dense brownish-orange (6C8) hyphae of *textura intricata*, hyphae 1.3–2.9(–3.9)  $\mu\text{m}$  ( $\bar{x} = 2.2 \pm 0.5$   $\mu\text{m}$ ,  $n = 50$ ) diam., appear with excipulum at the margin, non-gelatinous. Medullary excipulum 164–308  $\mu\text{m}$  ( $\bar{x} = 238 \pm 33$   $\mu\text{m}$ ,  $n = 15$ ) thick, well-developed, comprised of thin-walled, septate, pale brown to pale yellow cells of *textura intricata*, hyphae 2.6–5.2  $\mu\text{m}$  ( $\bar{x} = 3.9 \pm 0.5$   $\mu\text{m}$ ,  $n = 30$ ) diam., hyaline, slightly loose in the center, becoming well-organized, parallel and strongly dense near the ectal excipulum, narrow hyphae 1.3–3.2  $\mu\text{m}$  ( $\bar{x} = 2.3 \pm 0.4$   $\mu\text{m}$ ,  $n = 30$ ) diam., non-gelatinous. Ectal excipulum well-differentiated from the medullary part, the inner layers generally consists of 5–6 layers *textura angularis* cells, 27–68  $\mu\text{m}$  ( $\bar{x} = 42 \pm 9$   $\mu\text{m}$ ,  $n = 37$ ) thick, cells 6.6–14.4  $\mu\text{m}$  ( $\bar{x} = 10.2 \pm 2.4$   $\mu\text{m}$ ,  $n = 100$ ) diam., wall moderately thick 0.41–0.84  $\mu\text{m}$  ( $\bar{x} = 0.6 \pm 0.1$   $\mu\text{m}$ ,  $n = 50$ ); the outer layers partially uneven proliferous to some gradually smaller brown cells, stack into short and broad triangles to trapezoids, 20–46(–63)  $\mu\text{m}$  ( $\bar{x} = 31 \pm 12$   $\mu\text{m}$ ,  $n = 20$ ) thick (excluding the inner layers), cells 4.5–10.2  $\mu\text{m}$  ( $\bar{x} = 7.8 \pm 1.6$   $\mu\text{m}$ ,  $n = 80$ ) diam., wall moderate; cells from the outer inward the inner layers gradually increase in diameter, brown to pale yellow; terminal cells at the margin stretch to elongated *textura prismatica* cells 10–13  $\mu\text{m} \times$  3.3–4.1  $\mu\text{m}$  with rounded ends, wall moderately thick, brown, non-gelatinous. Paraphyses 1.7–2.7  $\mu\text{m}$  ( $\bar{x} = 2.3 \pm 0.2$   $\mu\text{m}$ ,  $n = 35$ ), hyaline, filiform, rounded apex, 2-septate at the middle, unbranched, conspicuous contents not observed, scarcely extending beyond the asci. Asci (91–)109–122  $\times$  8.2–11.5  $\mu\text{m}$  ( $\bar{x} = 113 \pm 5 \times 9.5 \pm 0.7$   $\mu\text{m}$ ,  $n = 25$ ), unitunicate, 8-spored, almost filling the whole asci, clavate, rounded apex with an amyloid apical pore in Melzer's reagent, wall incrassated at the apex, 5.5–6.8  $\mu\text{m}$  wide  $\times$  2.3–4.2  $\mu\text{m}$  high ( $\bar{x} = 6.0 \pm 0.5 \times 3.2 \pm 0.4$   $\mu\text{m}$ ,  $n = 25$ ), slightly constricted downward when developing, tapering to a cylindrical and aporhynchous subtruncate base, croziers present. Ascospore 14.6–20.4(–22.5)  $\times$  4.9–6.2  $\mu\text{m}$  ( $\bar{x} = 17.1$



**Figure 6.** *Tatraea griseoturcoisina* (HKAS 128276, holotype) **a** fresh ascomata on the wood **d–g** dried ascomata on the wood **d** vertical section of an ascoma **e–h** excipulum **i** paraphyses **j–n** asci (**o–n** asci in Meltzer's reagent) **o–t** ascospores. Scale bars: 900 µm (**b**); 600 µm (**c**); 1000 µm (**d**); 80 µm (**e**, **g**); 40 µm (**f**); 60 µm (**h–n**); 10 µm (**o–t**).

$\pm 1.7 \times 5.4 \pm 0.4 \mu\text{m}$ ,  $n = 60$ ),  $Q = 2.4\text{--}3.7(-4.2)$ ,  $Q_m = 3.1 \pm 0.1$ , overlapping uniseriate, slightly narrow ellipsoidal with a large guttule, ends rounded at the base, slightly pointed at the apex, slightly curved on the lateral view, hyaline, thin-walled, smooth and aseptate. **Asexual morph:** Undetermined.

**Material examined.** CHINA, Yunnan Province, Xishuangbanna City, Menghai County, altitude 1660 m, on decayed oak tree branches in a managed plantation, 8 September 2022, Cuijinyi Li, LCJY-1402 (HKAS 128276, holotype); *ibid.*, Menghai County, altitude 1500 m, on decayed oak tree branches in a managed plantation, 8 September 2022, Cuijinyi Li, 22-9-8-5 (HKAS 128277, paratype).

**Notes.** The distinctive characteristics of *Tatraea griseoturcoisina* are greyish-green apothecia, with yellowish-white to snow white discs when dry, narrow hyphae of medullary excipulum, short aporhynchous asci and slightly narrow ellipsoidal ascospores without septa.

Phylogenetically, *T. griseoturcoisina* grouped with *T. clepsydriformis* with 85% ML bootstrap support and 0.96 Bayesian probability in the combined LSU and ITS phylogeny (Fig. 2). A pairwise homoplasy index (PHI) test was conducted using a five-gene dataset (ITS, LSU, mtSSU, RPB1 and RPB2) to assess the recombination level between clades of *T. griseoturcoisina* and *T. clepsydriformis*. The results revealed that there were no significant recombination events observed between these two groups ( $\Phi_w > 0.05$ ), indicating that they are genetically isolated and thus supporting them as distinct species (Fig. 3). *Tatraea griseoturcoisina* is distinct from all other species based on its unique macro-characteristics of greyish-green apothecia, dried discs and receptacles. Micro-characteristics of *T. griseoturcoisina* resemble *T. clepsydriformis* by having narrow hyphae of medullary excipulum, short asci and smaller ellipsoidal ascospores, but it is distinct from *T. clepsydriformis* by having a thinner medullary excipulum ( $164\text{--}308 \mu\text{m}$  vs.  $335\text{--}535 \mu\text{m}$ ), longer ( $17.1 \times 5.4 \mu\text{m}$  vs.  $15.2 \times 5.7 \mu\text{m}$ ) and curved ascospores. *Tatraea griseoturcoisina* can be distinguished from the other five species (*T. aseptata*, *T. dumbirensis*, *T. macrospora*, *T. yunnanensis* and *T. yuxiensis*) based on its short asci ( $109\text{--}122 \mu\text{m}$ ) and ascospores ( $14.6\text{--}20.4 \mu\text{m}$ ) (see Suppl. material 1).

***Tatraea yunnanensis* C.J.Y. Li & Q. Zhao, sp. nov.**

Index Fungorum: IF901180

Facesoffungi Number: Fo15192

Fig. 7

**Etymology.** The specific epithet refers to the locality from where the type species was collected.

**Holotype.** HKAS 128273.

**Description.** Saprobic on the decayed wood. **Sexual morph:** Apothecia  $3.8\text{--}5.0 \text{ mm wide} \times 2.5\text{--}4.1 \text{ mm high}$  ( $\bar{x} = 4.8 \pm 0.8 \times 3.7 \pm 0.8 \text{ mm}$ ,  $n = 10$ ) when dry, scattered, superficial when fresh, short stipitate, glabrous. Disc circular, flat or slightly concave when fresh, yellowish white (4A2) to orange white (5A2), edge strongly curl inward towards the disc when dry, pastel green (29A4-30A4) to light green (29A5), dull green (29E4) near the edge. Margins concolorous to the disc when fresh, white or concolorous to the disc when dry. Receptacle rough and pale greyish orange (5B3) with loose, finely yellowish brown (5E8) pustules

when fresh, rough and light brown (5E4) with finely dark pustules and irregular patches when dry, center of vertical section appears white powder, outwardly yellowish waxy materials. Stipe 0.5 mm wide × 1.1 mm long, concolorous to the receptacle, dense finely granular pustules. Hymenium 173–213  $\mu\text{m}$  ( $\bar{x} = 192 \pm 10 \mu\text{m}$ ,  $n = 20$ ) thick, hyaline. Subhymenium 51.5–68.5  $\mu\text{m}$  ( $\bar{x} = 60.5 \pm 5.0 \mu\text{m}$ ,  $n = 27$ ) thick, slightly indistinguishable from the medullary excipulum, comprised of dense and unordered brown (5D4) hyphae of *textura intricata*, hyphae 2.2–5.4  $\mu\text{m}$  ( $\bar{x} = 3.9 \pm 0.9 \mu\text{m}$ ,  $n = 20$ ) diam., with excipulum at the margin. Medullary excipulum 435–560  $\mu\text{m}$  ( $\bar{x} = 518 \pm 48 \mu\text{m}$ ,  $n = 10$ ) thick, well-developed, comprised of thin-walled, septate, branched, hyaline and lose hyphae of *textura intricata* in the center, partially cells of hyphae becoming swollen, hyphae 3.6–7.8(–8.9)  $\mu\text{m}$  ( $\bar{x} = 5.3 \pm 0.9 \mu\text{m}$ ,  $n = 77$ ) diam., becoming well-organized, parallel near to the ectal excipulum, hyphae narrower, non-gelatinous. Ectal excipulum of the inner layers usually comprised of 3–5 layers of *textura angularis* to *textura prismatica* cells oriented vertically to the receptacle, brown to hyaline from the outside to inside, 37–65  $\mu\text{m}$  ( $\bar{x} = 49.5 \pm 8.8 \mu\text{m}$ ,  $n = 70$ ) thick, cells 8.4–16.5  $\mu\text{m}$  ( $\bar{x} = 13.0 \pm 1.1 \mu\text{m}$ ,  $n = 50$ ) diam., wall moderately thick 0.56–0.9  $\mu\text{m}$  ( $\bar{x} = 0.72 \pm 0.11 \mu\text{m}$ ,  $n = 84$ ) thick; the outer layers uneven dense proliferous 2–10 layers of *textura angularis* to *textura prismatica* cells, 20–74  $\mu\text{m}$  ( $\bar{x} = 49 \pm 12 \mu\text{m}$ ,  $n = 43$ ) thick (out of the inner layers), usually parallel to receptacle, forming an inverted arched or irregular shaped, not obvious change in *textura angularis* cells on diameter, slightly larger on *textura prismatica* cells, brown; terminal cells at the margin, indistinctly elongated. Paraphyses 1.5–2.8  $\mu\text{m}$  ( $\bar{x} = 2.1 \pm 0.4 \mu\text{m}$ ,  $n = 80$ ) wide, hyaline, filiform, rounded apex, 3–4-septate, sometimes branched at mid and base, with conspicuous contents and fine oil drops, scarcely extending beyond the asci. Asci (163.8–)170.9–197.4 × 10.1–15.5  $\mu\text{m}$  ( $\bar{x} = 180.5 \pm 7.2 \times 12.6 \pm 1.4 \mu\text{m}$ ,  $n = 50$ ), unitunicate, 8-spored, almost filling in some short asci, cylindric or subclavate, rounded apex with an amyloid apical pore in Melzer's reagent, apical wall incrassated, 6.4–9.3(–10.3) × 2.7–5.1(–6.0) ( $\bar{x} = 7.8 \pm 0.8 \times 3.8 \pm 0.7 \mu\text{m}$ ,  $n = 40$ ), thicken when immature, tapering to subtruncated base, croziers present. Ascospore 32.5–42.4 × 4.8–7.1  $\mu\text{m}$  ( $\bar{x} = 36.3 \pm 2.6 \times 6.5 \pm 0.4 \mu\text{m}$ ,  $n = 50$ ),  $Q = 4.4\text{--}6.5(–7.2)$ ,  $Q_m = 5.6 \pm 0.4$ , uniseriate or overlapping uniseriate, elongated to narrow fusiform with 1–2 guttules to multiple granules, hyaline, slightly curved, bluntly rounded at the base, slightly pointed at the apex, thin-walled, smooth and aseptate. **Asexual morph:** Undetermined.

**Material examined.** CHINA, Yunnan Province, Puer City, Jingdong County, altitude 1455 m, on the decayed wood, 23 August 2022, Cuijinyi Li, LCJY-1218 (HKAS 128273, holotype); *ibid.*, Tengchong City, altitude 1714 m, on decayed wood, 16 August 2022, Cuijinyi Li, LCJY-1119-2 (HKAS 128272, paratype).

**Notes.** The distinctive characteristics of *T. yunnanensis* are large (4.8 mm wide), brown apothecia with pastel green to light green discs and short stipes, thick medullary excipulum comprising 2–10 layers of inverted proliferous cells, arched or irregular shaped, pleurorhynchous asci with J+ pores, filiform, 3-septate paraphyses and elongated fusiform ascospores without septa.

Phylogenetically, our collections clustered sister to *T. macrospora* with 98% ML bootstrap support and 1.0 Bayesian probability in the combined LSU and ITS phylogeny (Fig. 2). It was shown that the two species do not have any genetic recombination ( $\Phi_w = 1.0$ ) based on the pairwise homoplasy index (PHI) value (Fig. 3). *Tatraea yunnanensis* resembles *T. macrospora* in having cupulate



**Figure 7.** *Tatraea yunnanensis* (HKAS 128273, holotype) **a–b** fresh ascomata on the wood **c** dried ascomata on the wood **d** vertical section of an ascoma **e–g** excipulum **h** paraphyses **i–m** asci (**m** asci in Meltzer's reagent) **n–s** ascospores. Scale bars: 3.5 mm (**c**); 1200  $\mu$ m (**d**); 300  $\mu$ m (**e**); 50  $\mu$ m (**f**); 100  $\mu$ m (**g**); 80  $\mu$ m (**h–m**); 20  $\mu$ m (**n–s**).

apothecia, yellowish-white to orange-white discs when fresh and large ascospores. In contrast, our species differ from *T. macrospora* by having longer ascospores (32.5–42.4  $\mu\text{m}$  vs. 22–40  $\mu\text{m}$ ) with 3–8-septate ascospores (Baral et al. 1999). For *T. macrospora*, the morphological descriptions provided in previous studies are incomplete and lack details on the apothecial size and color, stalk and spores.

***Tatraea yuxiensis* C.J.Y. Li & Q. Zhao, sp. nov.**

Index Fungorum: IF901187

Facesoffungi Number: Fo15193

Fig. 8

**Etymology.** The specific epithet refers to the locality from where the type species was collected.

**Holotype.** HKAS 128268.

**Description.** Saprobic on the decayed wood. **Sexual morph:** Apothecia 2.3–4.2 mm wide ( $\bar{x} = 3.0 \pm 0.6$  mm,  $n = 15$ ) when fresh, 1.2–2.0(–2.5) mm wide  $\times$  0.47–0.72 mm high ( $\bar{x} = 1.6 \pm 0.3 \times 0.58 \pm 0.09$  mm,  $n = 18$ ) when dry, scattered or gregarious, disk-like with short stipitate, glabrous, developing on the surface of the substrate. Disc flat and circular, slightly convex at the center and downward at the edge when fresh, edge slightly curls inward towards the center, edge of large ascoma somewhat undulating, orange grey (5B2) to brownish grey (5C2) when fresh, dark brownish black or deep green (1D8) to olive (1E8) when dry. Margins concolorous to the disc when fresh, white to pale yellow or concolorous to the receptacles when dry. Receptacle dark brownish black or dark ochraceous-brown when dry, slightly rough and finely pustules when mature. Stipe 270–480(–650)  $\mu\text{m}$  wide  $\times$  190–400  $\mu\text{m}$  long ( $\bar{x} = 400 \pm 86 \times 320 \pm 76$   $\mu\text{m}$ ,  $n = 18$ ), short, regular cylindrical, concolorous to the receptacle or nearly black, almost smooth on the surface. Hymenium 173–227  $\mu\text{m}$  ( $\bar{x} = 210 \pm 17$   $\mu\text{m}$ ,  $n = 15$ ), hyaline. Subhymenium not obvious. Medullary excipulum 273–330  $\mu\text{m}$  ( $\bar{x} = 307 \pm 22$   $\mu\text{m}$ ,  $n = 15$ ) thick, well-developed, comprised of thin-walled, septate, pale brown and slightly loose hyphae of *textura intricata*, hyphae (3.5–)4.2–8.7  $\mu\text{m}$  ( $\bar{x} = 6.2 \pm 1.5$   $\mu\text{m}$ ,  $n = 70$ ) diam., hyaline, becoming dense near to the hymenium, darkening, dense and well-organized parallel near to the ectal excipulum, non-gelatinous. Ectal excipulum of the inner layers generally comprised of 3–6 layers vertically oriented *textura angularis* cells, 34–62(–77)  $\mu\text{m}$  ( $\bar{x} = 49 \pm 10$   $\mu\text{m}$ ,  $n = 60$ ) thick, pale brown to hyaline toward inwards, cells of inner layers 10.5–18.5(–20.4)  $\mu\text{m}$  ( $\bar{x} = 14.0 \pm 2.6$   $\mu\text{m}$ ,  $n = 100$ ) diam., wall (0.49–)0.65–1.09(–1.3)  $\mu\text{m}$  ( $\bar{x} = 0.87 \pm 0.15$   $\mu\text{m}$ ,  $n = 100$ ) thick; proliferate 3–4 layers irregular-shaped and minimal *textura angularis* or *textura prismatica* cells, 4.0–8.4  $\mu\text{m}$  ( $\bar{x} = 6.3 \pm 1.3$   $\mu\text{m}$ ,  $n = 100$ ) diam., wall 0.59–0.94  $\mu\text{m}$  ( $\bar{x} = 0.77 \pm 0.12$   $\mu\text{m}$ ,  $n = 70$ ) thick; terminal cells at margin obviously elongated to 17–33  $\mu\text{m} \times$  3.6–5.9  $\mu\text{m}$ , slightly curved and soft, apex rounded and sometimes swollen, thin-walled, pale brown or hyaline. Paraphyses 1.9–3.3  $\mu\text{m}$  ( $\bar{x} = 2.6 \pm 0.5$   $\mu\text{m}$ ,  $n = 70$ ) wide, hyaline, filiform, rounded apex, 1–2-septate, unbranched, with conspicuous contents in Melzer's reagent, scarcely extending beyond the asci. Asci (159.6–)167.4–190.7(–200.0)  $\times$  11.3–15.8  $\mu\text{m}$  ( $\bar{x} = 177.5 \pm 8.7 \times 13.1 \pm 1.2$   $\mu\text{m}$ ,  $n = 30$ ), unitunicate, 8-spored, cylindrical or subclavate, apical-



**Figure 8.** *Tatraea yuxiensis* (HKAS 128268, holotype) **a** fresh ascomata on the wood **b–e** dried ascomata on the wood **f** vertical section of an ascoma **g–i** excipulum **j–k** paraphyses **l–o** asci (**o–p** asci in Meltzer's reagent) **p–v** ascospores. Scale bars: 1.5 mm (**b**); 700  $\mu$ m (**d–c**); 400  $\mu$ m (**e**); 800  $\mu$ m (**f–g**); 1000  $\mu$ m (**h**); 200  $\mu$ m (**i**); 100  $\mu$ m (**j**); 70  $\mu$ m (**k–p**); 15  $\mu$ m (**q–v**).

ly rounded with an amyloid apical pore in Melzer's reagent, thickened wall at apex,  $7.2\text{--}11.5 \times 3.0\text{--}5.7$  ( $\bar{x} = 9.2 \pm 1.5 \times 4.2 \pm 0.7$   $\mu\text{m}$ ,  $n = 40$ ), tapering to a pleurorhynchous subtruncate base, croziers present. Ascospore ( $24.1\text{--}26.2\text{--}34.9\text{--}36.5$ )  $\times$  ( $6.3\text{--}7.0\text{--}8.9\text{--}9.5$ )  $\mu\text{m}$  ( $\bar{x} = 30.0 \pm 2.8 \times 7.9 \pm 0.6$   $\mu\text{m}$ ,  $n = 100$ ),  $Q = (2.8\text{--}3.2\text{--}4.6\text{--}5.2)$ ,  $Q_m = 3.8 \pm 0.2$ , uniseriate, elongated ellipsoidal with a large guttule, slightly curved and asymmetrical on the lateral view, ends rounded, hyaline, thin-walled, smooth, aseptate, appearing 1-septate when germinating. **Asexual morph:** Undetermined.

**Material examined.** CHINA, Yunnan Province, Yuxi City, Xinping County, altitude 2090 m, on soft decayed unknown wood in managed plantation, 5 June 2022, Cuijinyi Li, LCJY-633 (HKAS 128268, holotype); *ibid.*, altitude 2340 m, on decayed unknown wood, 6 June 2022, Cuijinyi Li, LCJY-634 (HKAS 128270, paratype).

**Notes.** The distinctive characteristics of *T. yuxiensis* are orange-grey to brownish-grey discs when fresh, dark brownish-black or dark ochraceous-brown when dry, short and regular cylindrical stipe, 3–4 layers of proliferous minimal cells, pleurorhynchous asci and elongated ellipsoidal and laterally asymmetrical ascospores.

Morphologically, *T. yuxiensis* resembles *T. aseptata* with their similar-sized and disk-like apothecia with a short stipe, filiform paraphyses, cylindrical asci and ellipsoidal ascospores. In contrast to *T. aseptata*, *T. yuxiensis* has darker receptacles, regular cylindrical stipes, inconspicuous subhymenium, thicker medullary excipulum ( $273\text{--}330$   $\mu\text{m}$  vs.  $120\text{--}145$   $\mu\text{m}$ ) with larger terminal cells ( $17\text{--}33$   $\mu\text{m} \times 3.6\text{--}5.9$   $\mu\text{m}$  vs.  $13.1\text{--}15.3$   $\mu\text{m} \times 2.6\text{--}3.8$   $\mu\text{m}$ ) that almost appear as 3–4 layers of proliferous minimal cells and ascospores with higher length-width ratio (3.8 vs. 2.97). Furthermore, our collections of *T. aseptata* (HKAS 128265, HKAS 128269, HKAS 128271, HKAS 128274) have shorter asci ( $136.7\text{--}157.8$   $\mu\text{m}$  vs.  $167.4\text{--}190.7$   $\mu\text{m}$ ) and 8–12 layers of proliferous cells, compared to *T. yuxiensis*.

Phylogenetically, *T. yuxiensis* clustered sister to *T. aseptata* with 100% ML bootstrap support and 1.0 Bayesian probability in the combined LSU and ITS phylogeny (Fig. 2). The pairwise homoplasy index (PHI) indicated no significant genetic recombination ( $\Phi_w = 1.0$ ) between *T. yuxiensis* and *T. aseptata* and confirmed that they are different species (Fig. 3).

## Discussion

*Tatraea* was initially collected a 100 years ago from the Nizke Tatra Mountains in Europe and was subsequently found in several countries (Velenovský 1934; Baral et al. 1999). In Britain and Croatia, *T. dumbirensis* is listed on the Red List as a threatened species (Ujházy et al. 2018). *Tatraea macrospora* appeared in some countries, but no official records were found. Therefore, the accuracy of species identification could not be confirmed. Since the study in 1999, there have been no new species reports in *Tatraea* from other continents. All collections in this study were collected from Yunnan, China, of which most were collected from protected natural forests and from areas comprising mainly oak trees. Some species are found in plantations that have been protected and nursed for many years, however, the host is too decayed to identify. In most cases, the decayed oak wood is still the main nutrient provider in forests. After the addition of our collections (*T. clepsydriformis* and *T. griseoturcoisina*), the

description of *Tatraea* should be extended from long asci and large ascospores to include slightly shorter asci and smaller spores, as well as the initial greyish turquoise color of the apothecia.

In the past, the type species, *T. dumbirensis* was incorrectly recognized to be a member of the Leotiaceae or Sclerotiniaceae (Velenovský 1934; Baral et al. 1999). The exclusion from the Sclerotiniaceae was due to the absence of darkening and sclerotia formation in the cultures (Baral et al. 1999). In the present taxonomic study, *Tatraea* was included in Helotiaceae, and we also agreed on this treatment based on the ITS analysis in our study (Vasilyeva 2010). The genus-level placements of each species in *Tatraea* changed after adding data from other genera into the analysis. Previously, *T. clepsydriformis* and *T. griseoturcoisina* clustered into separate clades, later clustered into a single main clade as sister sub-clades after adding more taxa, and their micro-morphological characteristics were more similar. In the phylogenetic analyses, the taxonomic status of species is provisional due to the lack of genetic information for the type species. To assess the significant recombination levels of related species, we performed five gene analyses individually and for the combined dataset, both of which provided evidence for them being different species. The dilemma for conducting research is the paucity of available molecular information for the known species. More informative loci were provided in this study, including mitochondrial genes and protein genes, hence, future taxonomy, phylogeny research and evolutionary studies in Helotiaceae can be benefited from this study. Additionally, some species with similar morphological characteristics to *Tatraea*, such as *Ciboria fusispora*, are currently unable to transfer due to a lack of evidence and fresh samples. Therefore, more research with more fresh specimens is essential to facilitate the classification of these species.

## Acknowledgements

Cui-Jin-Yi Li thanks Mae Fah Luang University for the award of partial scholarship. And Cui-Jin-Yi Li also would like to thank Dr. Shaun Pennycook for his valuable assistance with the Latin binomial.

## Additional information

### Conflict of interest

The authors have declared that no competing interests exist.

### Ethical statement

No ethical statement was reported.

## Funding

This study is supported by the Second Tibetan Plateau Scientific Expedition and Research (STEP) Program (Grant No. 2019QZKK0503); The Survey of Wildlife Resources in Key Areas of Tibet (ZL202203601); Major science and technology projects and key R&D plans/programs, Yunnan Province (202202AE090001); Natural Science Foundation of Guizhou Province (Gran No. Qian Ke Zhong Yin Di [2021]4031, Qian Ke He Zhi Cheng [2021] Generally 200); The open research project of “Cross-Cooperative Team” of the Germplasm Bank of Wild Species, Kunming Institute of Botany, Chinese Academy

of Sciences (Grant No. 292019312511043); Science and Technology Service Network Initiative of the Chinese Academy of Sciences (KFJ-ST5-QYZD-171); The Biodiversity Survey and Assessment Project of the Ministry of Ecology and Environment, PR China (2019HJ2096001006).

### Author contributions

Supervision: PDE, KWTC, QZ. Writing - original draft: CJYL. Writing - review and editing: QZ, KWTC, DQZ.

### Author ORCIDs

Cui-Jin-Yi Li  <https://orcid.org/0000-0002-2805-7071>

Kandawatte Wedaralalage Thilini Chethana  <https://orcid.org/0000-0002-5816-9269>

Prapassorn Damrongkool Eungwanichayapant  <https://orcid.org/0000-0001-8005-4137>

De-Qun Zhou  <https://orcid.org/0009-0009-3459-3186>

Qi Zhao  <https://orcid.org/0000-0001-8169-0573>

### Data availability

All of the data that support the findings of this study are available in the main text or Supplementary Information.

### References

- Baral H-O, Bemmam M (2013a) *Hymenoscyphus serotinus* and *H. lepismoides* sp. nov., two lignicolous species with a high host specificity. *Ascomycete.Org : Revue Internationale pour la Taxinomie des Ascomycota* 5(4): 109–128.
- Baral H-O, Galan-Marquez R, Krisai-Greilhuber I, Matočec N, Palmer JT (1999) *Tatraea dumbirensis*, new records of a rare leotialean discomycete in Europe. *Österreichische Zeitschrift für Pilzkunde* 8: 71–82.
- Baral H-O, Marson G, Bogale M, Untereiner WA (2013b) *Xerombrophila crystallifera*, a new genus and species in the Helotiales. *Mycological Progress* 12(3): 475–488. <https://doi.org/10.1007/s11557-012-0854-6>
- Bucher VVC, Hyde KD, Pointing SB, Reddy CA (2004) Production of wood decay enzymes, mass loss and lignin solubilization in wood by marine ascomycetes and their anamorphs. *Fungal Diversity* 15: 1–14.
- Capella-Gutiérrez S, Silla-Martínez JM, Gabaldón T (2009) trimAl: A tool for automated alignment trimming in large-scale phylogenetic analyses. *Bioinformatics* 25(15): 1972–1973. <https://doi.org/10.1093/bioinformatics/btp348>
- Chethana KWT, Zhou Y, Zhang W, Liu M, Xing QK, Li XH, Yan JY, Hyde KD (2017) *Coniella vitis* sp. nov. is the common pathogen of white rot in Chinese vineyards. *Plant Disease* 101(12): 2123–2136. <https://doi.org/10.1094/PDIS-12-16-1741-RE>
- Chethana KWT, Manawasinghe S, Hurdeal VG, Bhunjun CS, Appadoo MA, Gentekaki E, Raspé O, Promputtha I, Hyde KD (2021) What are fungal species and how to delineate them? *Fungal Diversity* 109(1): 1–25. <https://doi.org/10.1007/s13225-021-00483-9>
- Dvořák D, Vašutová M, Hofmeister J, Beran M, Hošek J, Běťák J, Burel J, Deckerová H (2017) Macrofungal diversity patterns in central European forests affirm the key importance of oldgrowth forests. *Fungal Ecology* 27: 145–154. <https://doi.org/10.1016/j.funeco.2016.12.003>
- Ekanayaka AH, Ariyawansa HA, Hyde KD, Jones EBG, Daranagama DA, Phillips AJL, Hongsanan S, Jayasiri SC, Zhao Q (2017) Discomycetes: The apothecial represen-

- tatives of the phylum Ascomycota. *Fungal Diversity* 87(1): 237–298. <https://doi.org/10.1007/s13225-017-0389-x>
- Ekanayaka AH, Hyde KD, Jones EG, Zhao Q (2018) Taxonomy and phylogeny of operculate discomycetes: Pezizomycetes. *Fungal Diversity* 90(1): 161–243. <https://doi.org/10.1007/s13225-018-0402-z>
- Ekanayaka AH, Hyde KD, Gentekaki E, McKenzie EHC, Zhao Q, Bulgakov TS, Camporesi E (2019) Preliminary classification of Leotiomycetes. *Mycosphere* 10(1): 310–489. <https://doi.org/10.5943/mycosphere/10/1/7>
- Hall T (1999) BioEdit: A user-friendly biological sequence alignment editor and analysis program for Windows 95/98/NT. *Nucleic Acids Symposium Series* 41: 95–98.
- Heilmann-Clausen J (2001) A gradient analysis of communities of macrofungi and slime moulds on decaying beech logs. *Mycological Research* 105(5): 575–596. <https://doi.org/10.1017/S0953756201003665>
- Holec J, Kříž M, Pouzar Z, Šandová M (2015) Boubínský prales virgin forest, a Central European refugium of boreal-montane and old-growth forest fungi. *Czech Mycology* 67(2): 157–226. <https://doi.org/10.33585/cmy.67204>
- Index Fungorum (2023) Index Fungorum. <http://www.indexfungorum.org/> [Accessed on July 13, 2023]
- Jayasiri SC, Hyde KD, Ariyawansa HA, Bhat J, Buyck B, Cai L, Dai YC, Abd-Elsalam KA, Ertz D, Hidayat I, Jeewon R, Jones EBG, Bahkali AH, Karunarathna SC, Liu JK, Luangsa-ard JJ, Lumbsch HT, Maharachchikumbura SSN, McKenzie EHC, Moncalvo J-M, Ghobad-Nejhad M, Nilsson H, Pang K-L, Pereira OL, Phillips AJL, Raspé O, Rollins AW, Romero AI, Etayo J, Selçuk F, Stephenson SL, Suetrong S, Taylor JE, Tsui CKM, Vizzini A, Abdel-Wahab MA, Wen TC, Boonmee S, Dai DQ, Daranagama DA, Dissanayake AJ, Ekanayaka AH, Fryar SC, Hongsanan S, Jayawardena RS, Li WJ, Perera RH, Phookamsak R, de Silva NI, Thambugala KM, Tian Q, Wijayawardene NN, Zhao RL, Zhao Q, Kang JC, Prompttha I (2015) The Faces of Fungi database: Fungal names linked with morphology, phylogeny and human impacts. *Fungal Diversity* 74(1): 3–18. <https://doi.org/10.1007/s13225-015-0351-8>
- Johnston PR, Quijada L, Smith CA, Baral H-O, Hosoya T, Baschien C, Pärtel K, Zhuang WY, Haelewaters D, Park D, Carl S, López-Giráldez F, Wang Z, Townsend JP (2019) A multigene phylogeny toward a new phylogenetic classification of Leotiomycetes. *IMA Fungus* 10(1): 1–22. <https://doi.org/10.1186/s43008-019-0002-x>
- Katoh K, Rozewicki J, Yamada K (2019) MAFFT online service: Multiple sequence alignment, interactive sequence choice and visualization. *Briefings in Bioinformatics* 20(4): 1160–1166. <https://doi.org/10.1093/bib/bbx108>
- Kornerup A, Wanscher JH (1967) *Methuen handbook of colour*.
- Kunca V, Peiger M, Tomka P, Vampola P (2022) Old-growth forest fungi—New localities and habitat and host preferences in Slovakia (I). *Czech Mycology* 74(1): 33–55. <https://doi.org/10.33585/cmy.74103>
- Lestari AS, Chethana KWT (2022) Morpho-phylogenetic insights reveal *Bisporella montana* as *Calycina montana* comb. nov. (Pezizellaceae, Helotiales). *Phytotaxa* 558(2): 185–202. <https://doi.org/10.11646/phytotaxa.558.2.3>
- Lestari AS, Ekanayaka AH, Chethana KWT (2023) Phytopathogenic discomycetes, their economic impacts and control applications. *Current Research in Environmental & Applied Mycology* 13(1): 299–346. <https://doi.org/10.5943/cream/13/1/13> [Journal of Fungal Biology]

- Liu Y, Wheelen S, Hall B (1999) Phylogenetic relationships among ascomycetes: Evidence from an RNA polymerase II subunit. *Molecular Biology and Evolution* 16(12): 1799–1808. <https://doi.org/10.1093/oxfordjournals.molbev.a026092>
- Niego AGT, Rapior S, Thongklang N, Raspé O, Hyde KD, Mortimer P (2023a) Reviewing the contributions of macrofungi to forest ecosystem processes and services. *Fungal Biology Reviews* 44: 100. <https://doi.org/10.1016/j.fbr.2022.11.002>
- Niego AGT, Lambert C, Mortimer P, Thongklang N, Rapior S, Grosse M, Schrey H, Charria-Girón E, Walker A, Hyde KD, Stadler M (2023b) The contribution of fungi to the global economy. *Fungal Diversity* 121(1): 95–137. <https://doi.org/10.1007/s13225-023-00520-9>
- Nylander JAA, Ronquist F, Huelsenbeck JP, Nieves-Aldrey J (2004) Bayesian phylogenetic analysis of combined data. *Systematic Biology* 53(1): 47–67. <https://doi.org/10.1080/10635150490264699>
- Phutthacharoen K, Chethana KT, Lestari AS, Stadler M, Hyde KD (2022) Three new species of *Dicephalospora* (Helotiaceae, Helotiales) from Thailand. *Diversity* 14(8): 645. <https://doi.org/10.3390/d14080645>
- Rambaut A (2012) Figtree 1.4.0. <http://tree.bio.ed.ac.uk/software/figtree/>
- Silvestro D, Michalak I (2012) raxmlGUI: A graphical front-end for RAxML. *Organisms, Diversity & Evolution* 12(4): 335–337. <https://doi.org/10.1007/s13127-011-0056-0>
- Spooner BM (1987) Helotiales of Australasia. *Bibliotheca Mycologica* 116: 1–711.
- Spooner BM (1988) On *Helotium dumbirensis* (Helotiales) and a collection from Britain. *Transactions of the British Mycological Society* 91(3): 515–517. [https://doi.org/10.1016/S0007-1536\(88\)80129-3](https://doi.org/10.1016/S0007-1536(88)80129-3)
- Stiller JW, Hall BD (1997) The origin of red algae: Implications for plastid evolution. *Proceedings of the National Academy of Sciences of the United States of America* 94(9): 4520–4525. <https://doi.org/10.1073/pnas.94.9.4520>
- Svrček M (1993) New or less known Discomycetes. XXIII. *Czech Mycology* 38: 197–202.
- Taylor JW, Jacobson DJ, Kroken S, Kasuga T, Geiser DM, Hibbett DS, Fisher MC (2000) Phylogenetic species recognition and species concepts in fungi. *Fungal Genetics and Biology* 31(1): 21–32. <https://doi.org/10.1006/fgbi.2000.1228>
- Ujházy K, Ujházyová M, Bučinová K, Čiliak M, Glejdura S, Mihál I (2018) Response of fungal and plant communities to management-induced overstorey changes in montane forests of the Western Carpathians. *European Journal of Forest Research* 137(2): 169–183. <https://doi.org/10.1007/s10342-017-1096-6>
- Vaidya G, Lohman DJ, Meier R (2011) SequenceMatrix: Concatenation software for the fast assembly of multi-gene datasets with character set and codon information. *Cladistics* 27(2): 171–180. <https://doi.org/10.1111/j.1096-0031.2010.00329.x>
- Vasilyeva LN (2010) Ascomycetes: Sordariomycetidae, Dothideomycetidae, Erysiphomycetidae, Rhytismomycetidae. *Fungi of Ussuri River Valley*, 1.
- Velenovský J (1934) *Monographia Discomycetum Bohemiae*. Czechoslovakia, Prague 1: 1–436.
- Vilgalys R, Hester M (1990) Rapid genetic identification and mapping of enzymatically amplified ribosomal DNA from several *Cryptococcus* species. *Journal of Bacteriology* 172(8): 4238–4246. <https://doi.org/10.1128/jb.172.8.4238-4246.1990>
- White TJ, Bruns T, Lee SJWT, Taylor J (1990) Amplification and direct sequencing of fungal ribosomal RNA genes for phylogenetics. *PCR Protocols: A Guide to Methods and Applications* 18: 315–322. <https://doi.org/10.1016/B978-0-12-372180-8.50042-1>
- Wijayawardene NN, Hyde KD, Dai DQ, Sánchez-García M, Goto BT, Saxena RK, Erdoğdu M, Selçuk F, Rajeshkumar KC, Aptroot A, Błaszczowski J, Boonyuen N, da Silva GA,

de Souza FA, Dong W, Ertz D, Haelewaters D, Jones EBG, Karunarathna SC, Kirk PM, Kukwa M, Kumla J, Leontyev DV, Lumbsch HT, Maharachchikumbura SSN, Marguno F, Martínez-Rodríguez P, Mešić A, Monteiro JS, Oehl F, Pawłowska J, Pem D, Pfliegler WP, Phillips AJL, Pošta A, He MQ, Li JX, Raza M, Sruthi OP, Suetrong S, Suwannarach N, Tedersoo L, Thiyagaraja V, Tibpromma S, Tkalčec Z, Tokarev YS, Wanasinghe DN, Wijesundara DSA, Wimalaseana SDMK, Madrid H, Zhang GQ, Gao Y, Sánchez-Castro I, Tang LZ, Stadler M, Yurkov A, Thines M (2022) Outline of Fungi and fungus-like taxa–2021. *Mycosphere* 13(1): 53–453. <https://doi.org/10.5943/mycosphere/13/1/2>

Zoller S, Scheidegger C, Sperisen C (1999) PCR primers for the amplification of mitochondrial small subunit ribosomal DNA of lichen-forming ascomycetes. *Lichenologist* 31(5): 511–516. <https://doi.org/10.1006/lich.1999.0220>

## Supplementary material 1

### Main differences between *Tatraea*

Author: Cui-Jin-Yi Li

Data type: docx

Copyright notice: This dataset is made available under the Open Database License (<http://opendatacommons.org/licenses/odbl/1.0/>). The Open Database License (ODbL) is a license agreement intended to allow users to freely share, modify, and use this Dataset while maintaining this same freedom for others, provided that the original source and author(s) are credited.

Link: <https://doi.org/10.3897/mycokeys.102.112565.suppl1>

# Phylogeny of the genus *Loxospora* s.l. (Sarrameanales, Lecanoromycetes, Ascomycota), with *Chicitaea* gen. nov. and five new combinations in *Chicitaea* and *Loxospora*

Łucja Ptach-Styn<sup>1</sup>, Beata Guzow-Krzemińska<sup>1</sup>, James C. Lendemer<sup>2</sup>, Tor Tønsberg<sup>3</sup>, Martin Kukwa<sup>1</sup>

<sup>1</sup> Department of Plant Taxonomy and Nature Conservation, Faculty of Biology, University of Gdańsk, Wita Stwosza 59, PL-80-308 Gdańsk, Poland

<sup>2</sup> Department of Botany, Research and Collections, CEC 3140, The New York State Museum, 222 Madison Ave., Albany NY 12230, USA

<sup>3</sup> Department of Natural History, University Museum, University of Bergen, Allegt. 41, 7800, 5020 Bergen, Norway

Corresponding authors: Beata Guzow-Krzemińska (beata.guzow-krzeminska@ug.edu.pl); Martin Kukwa (martin.kukwa@ug.edu.pl)

## Abstract

*Loxospora* is a genus of crustose lichens containing 13 accepted species that can be separated into two groups, based on differences in secondary chemistry that correlate with differences in characters of the sexual reproductive structures (asci and ascospores). Molecular phylogenetic analyses recovered these groups as monophyletic and support their recognition as distinct genera that differ in phenotypic characters. Species containing 2'-O-methylperlatolic acid are transferred to the new genus, *Chicitaea* Guzow-Krzem., Kukwa & Lendemer and four new combinations are proposed: *C. assateaguensis* (Lendemer) Guzow-Krzem., Kukwa & Lendemer, *C. confusa* (Lendemer) Guzow-Krzem., Kukwa & Lendemer, *C. cristinae* (Guzow-Krzem., Łubek, Kubiak & Kukwa) Guzow-Krzem., Kukwa & Lendemer and *C. lecanoriformis* (Lumbsch, A.W. Archer & Elix) Guzow-Krzem., Kukwa & Lendemer. The remaining species produce thamnolic acid and represent *Loxospora* s.str. Haplotype analyses recovered sequences of *L. elatina* in two distinct groups, one corresponding to *L. elatina* s.str. and one to *Pertusaria chloropolia*, the latter being resurrected from synonymy of *L. elatina* and, thus, requiring the combination, *L. chloropolia* (Erichsen) Ptach-Styn, Guzow-Krzem., Tønsberg & Kukwa. Sequences of *L. ochrophaea* were found to be intermixed within the otherwise monophyletic *L. elatina* s.str. These two taxa, which differ in contrasting reproductive mode and overall geographic distributions, are maintained as distinct, pending further studies with additional molecular loci. Lectotypes are selected for *Lecanora elatina*, *Pertusaria chloropolia* and *P. chloropolia* f. *cana*. The latter is a synonym of *Loxospora chloropolia*. New primers for the amplification of mtSSU are also presented.

**Key words:** Lichenised fungi, mtSSU, nuITS, phylogeny, RPB1, Sarrameanaceae, secondary metabolites, sorediate lichens, sterile lichens, taxonomy



Academic editor: Thorsten Lumbsch  
Received: 23 November 2023  
Accepted: 22 January 2024  
Published: 19 February 2024

Citation: Ptach-Styn Ł, Guzow-Krzemińska B, Lendemer JC, Tønsberg T, Kukwa M (2024) Phylogeny of the genus *Loxospora* s.l. (Sarrameanales, Lecanoromycetes, Ascomycota), with *Chicitaea* gen. nov. and five new combinations in *Chicitaea* and *Loxospora*. MycoKeys 102: 155–181. <https://doi.org/10.3897/mycokeys.102.116196>

Copyright: © Łucja Ptach-Styn et al.  
This is an open access article distributed under terms of the Creative Commons Attribution License (Attribution 4.0 International – CC BY 4.0).

## Introduction

Lichens are specialised fungi that associate in symbiotic relationships with photoautotrophic partners, termed photobionts, which are mainly represented by green microalgae or cyanobacteria (Büdel and Scheidegger 2008). Numerous

lichenised fungi have developed special vegetative diaspores (usually isidia and soredia), which allow the co-dispersal of symbiotic partners and maintenance of the symbiosis (Poelt 1970; Werth and Scheidegger 2012; Sanders 2014; Onuþ-Brännström et al. 2018). Lichen species that produce specialised vegetative diaspores are frequently sterile, rarely producing sexual reproductive structures and ascospores (Poelt 1970). This complicates, especially in the case of taxa with crustose thalli, the determination of their systematic position and can render identification difficult due to the scarcity of diagnostic morphological characters (e.g. Ekman and Tønsberg (2002); Kukwa and Pérez-Ortega (2010); Hodgkinson and Lendemer (2012, 2013); Guzow-Krzemińska et al. (2017, 2018, 2019); Malíček et al. (2018); Orange (2020); Kukwa et al. (2023)).

Some species that produce lichenised vegetative diaspores are morphologically (except for the development of such diaspores) and chemically almost identical to the taxa that lack those structures and such cases are referred to as species pairs (Poelt 1970; Crespo and Pérez-Ortega 2009). Molecular phylogenetic studies of such pairs and of species with lichenised vegetative diaspores generally, however, suggest that the situation is more complex and nuanced than binary pairs of species that either lack vegetative diaspores and are sexually reproducing or produce vegetative diaspores and are only infrequently sexually reproducing. In some cases, neither species delimited by the presence or absence of vegetative diaspores was found to be monophyletic and, instead, representatives of each were intermingled suggesting that independent lineages do not correspond to reproductive mode (e.g. Lohtander et al. (1998); Buschbom and Mueller (2006); Myllys et al. (2011); Tehler et al. (2013); Ertz et al. (2018)). In other cases, such pairs of species have been recovered as reciprocally monophyletic and sister (e.g. Miadlikowska et al. (2011); Lendemer and Harris (2014); Yakovchenko et al. (2017); Ohmura (2020)). Further, there are recent examples where next generation sequence data have provided support for species pair delimitations that lacked support from analyses of traditionally used loci that are typically more conserved and fewer in number (e.g. Grewe et al. (2018)).

The genus *Loxospora* A. Massal. was described by Massalongo (1852) and, at present, includes thirteen accepted species (Kalb and Hafellner 1992; Kantvilas 2000; Lumbsch et al. 2007; Lendemer 2013; Lücking et al. 2017; Guzow-Krzemińska et al. 2018). *Loxospora* species have been reported from many regions globally (e.g. Kalb and Hafellner (1992); Kantvilas (2000); Lumbsch et al. (2007); Papong et al. (2009); Kelly et al. (2011); Lendemer (2013); Hafellner and Türk (2016); Berger et al. (2018); Guzow-Krzemińska et al. (2018); Wirth et al. (2018); Marthinsen et al. (2019); Urbanavichus et al. (2020); Westberg et al. (2021)). The genus is classified at present in Sarrameanales B.P. Hodk. & Lendemer in Lecanoromycetes O.E. Erikss. & Winka (Lücking et al. 2017). Previous molecular phylogenetic studies have recovered *Loxospora* to form a well-supported clade, with members divided into two distinct clades (Lumbsch et al. 2007; Lendemer 2013; Guzow-Krzemińska et al. 2018). The species in one clade are characterised by asci having uniformly amyloid apical dome, septate, fusiform to ellipsoidal ascospores and the production of thamnolic acid as the main secondary metabolite (Hafellner 1984; Kantvilas 2000; Guzow-Krzemińska et al. 2018). This clade corresponds to *Loxospora* s.str. and contains the type species, *L. elatina* (Ach.) A. Massal. (Massalongo 1852; Galloway 2007). The second clade comprises four species producing 2'-O-methylperlatolic acid

(Lumbsch et al. 2007; Lendemer 2013; Guzow-Krzemińska et al. 2018). Ascomata are known only in one of those species, *L. lecanoriformis* Lumbsch, A.W. Archer & Elix and, in that taxon, the asci lack an amyloid apical dome and have simple ascospores (Lumbsch et al. 2007; Papong et al. 2009). The chemical and anatomical characters, especially the ascus apical dome amyloidy, combined with the monophyletic resolution as distinct from *Loxospora* s.str., suggest that this latter group merits recognition at the genus level.

In summer 2021, while performing field lichen studies in northern Poland, we collected specimens resembling *Loxospora elatina* growing on bark of *Alnus glutinosa* in black alder forest. They contained thamnolic acid as the main secondary metabolite; however, the thallus was continuous to areolate, in contrast to the tuberculate thalli typically found in *L. elatina* (e.g. Stenroos et al. (2016)). Molecular analyses showed that these specimens and some other samples published by Kelly et al. (2011) formed a group distinct from samples of *L. elatina* with typical tuberculate thalli. Recognising the need to re-evaluate the delimitation of *L. elatina* based on this material, we analysed additional sequences and specimens of other *Loxospora* species to confirm the relationships amongst currently recognised species, especially *L. ochrophaea* (Tuck.) R.C.Harris, which has been presumed to be the strictly sexual, esorediate counterpart to *L. elatina* (Brodo et al. 2001; Guzow-Krzemińska et al. 2018). Based on these analyses, we recognise the material of *L. elatina* with continuous to areolate thalli as distinct and introduce a new combination for it, discuss the status of *L. elatina* s.str. and *L. ochrophaea* (Tuck.) R.C. Harris and introduce the genus *Chicitea* for the clade of *Loxospora* species producing 2'-*O*-methylperlatolic acid, which necessitates four new combinations.

## Materials and methods

### Taxon sampling

Lichen material was studied from BG, BM, BILAS, E, HBG, H-ACH, NY, O, UGDA and herb. Maliček. Morphology was examined using a Nikon SMZ 800N stereomicroscope. Secondary lichen metabolites were studied by thin layer chromatography (TLC) (Culberson and Kristinsson 1970; Orange et al. 2001). For reference of squamatic acid and thamnolic acid, we used extracts from *Cladonia glauca* Flörke and *C. digitata* (L.) Baumg., respectively.

### DNA extraction, PCR amplification and DNA sequencing

Small pieces of thalli (approx. 2 mm<sup>2</sup>) were put into Eppendorf tubes. Then DNA was extracted using a GeneMATRIX Plant & Fungi DNA Purification Kit (EURX) or a modified CTAB method (Guzow-Krzemińska and Węgrzyn 2000). Sequences of three molecular markers were amplified: nuITS rDNA using ITS1F (Gardes and Bruns 1993) or ITS5 (White et al. 1990) and ITS4 (White et al. 1990) primers, RPB1 using g-RPB1-A for (Stiller and Hall 1997) and f-RPB1-C rev (Matheny et al. 2002) primers and mtSSU using mrSSU1 (Zoller et al. 1999) and mrSSU3R (Zoller et al. 1999) primers. Due to difficulties in mtSSU amplification, new primers were designed by one of the authors (Beata Guzow-Krzemińska; primers here referred to as "Lox\_mtSSU620\_For": 5'-TTTACCTATATGTCTTGACCAA-3'

and “Lox\_mtSSU620\_Rev”: 5'-CTCTTATCATATTCCAATATAATG-3'). PCR settings for each set of primers are shown in Suppl. material 1. Electrophoresis was performed on a 1% agarose gel to determine whether amplification of target molecular markers was successful. PCR products were purified using Clean-Up Concentrator (A&A Biotechnology). Sequencing was performed by MacroGen (The Netherlands). All newly-generated sequences were deposited in GenBank and their GenBank Acc. Numbers are presented in Table 1.

### Sequence alignments and phylogenetic analyses

The newly-obtained sequences were trimmed using the Chromas programme (<http://technelysium.com.au/wp/>). All sequences were analysed using BLASTn search (Altschul et al. 1990). Independent alignments of nuITS, mtSSU rDNA and RPB1 markers were prepared using Seaview software (Galtier et al. 1996; Gouy et al. 2010) employing muscle option and guidance2 software implemented on an online website (Sela et al. 2015; <https://guidance.tau.ac.il/>). Single locus alignments consisted of 68 nuITS rDNA sequences with 548 sites, 47 mtSSU rDNA sequences with 635 sites and 13 RPB1 sequences with 562 sites. Then, datasets were concatenated into one matrix which consisted of 83 terminals with 1745 positions. The concatenated dataset was subjected to IQ-TREE analysis to find best-fitting nucleotide substitution models for each partition (Nguyen et al. 2015; Chernomor et al. 2016; Kalyaanamoorthy et al. 2017; Hoang et al. 2018). The model selection was restricted to models implemented in MrBayes and the following nucleotide substitution models for the three predefined subsets were selected: HKY+F+I for mtSSU rDNA, K2P+F+G4 for nuITS and K2P+F+I for RPB1. The search for the Maximum Likelihood tree was performed in IQ-TREE and followed with 1000 bootstrap replicates (Nguyen et al. 2015; Chernomor et al. 2016; Kalyaanamoorthy et al. 2017; Hoang et al. 2018).

The Bayesian analysis was conducted using MrBayes 3.2.7a (Huelsenbeck and Ronquist 2001; Ronquist and Huelsenbeck 2003) on the CIPRES Science Gateway (Miller et al. 2010). The analyses were conducted by running 10,000,000 generations. The chain was sampled every 1000<sup>th</sup> generation. Posterior probabilities (PP) were determined by calculating a majority-rule consensus tree after discarding the initial 25% trees of each chain as the burn-in. All trees were visualised in FigTree v.1.4. (Rambaut 2009) and further modified in Inkscape (<https://inkscape.org/>). Bootstrap support (BS values  $\geq 75$ ) and PP values (values  $\geq 0.95$ ) are given near the branches on the phylogenetic tree.

Sequences obtained from GenBank and used in phylogenetic analyses are listed in Suppl. material 2.

### Preparation of haplotype networks

Moreover, independent alignments of each marker for specimens of *L. elatina*, *L. ochrophaea* and *L. chloropolia* were prepared using Seaview software (Galtier et al. 1996; Gouy et al. 2010) employing muscle option and followed with manual correction. The final nuITS rDNA alignment consisted of 46 sequences with 443 sites, while RPB1 alignment consisted of 11 sequences with 723 sites. Haplotype analyses were performed using PopART software (<https://popart.maths.otago.ac.nz>) employing TCS network option (Clement et al. 2002). Moreover,

**Table 1.** Specimen data and the GenBank accession numbers of newly-obtained sequences of the taxa used in the phylogenetic analyses. A dash provides information about lack of DNA sequence. For sequences obtained from GenBank, see Suppl. material 2.

Species	Origin	Collection and herbarium	GenBank accession numbers		
			nuITS	mtSSU	RPB1
<i>Chicitaea confusa</i> 3	U.S.A. North Carolina. Carteret Co.	Lendemer 35738 (NY-1885635)	PP080079	PP080125	–
<i>Chicitaea confusa</i> 4	U.S.A. North Carolina. Jones Co.	Lendemer 35691 (NY-1885682)	PP080080	PP080126	–
<i>Chicitaea confusa</i> 5	U.S.A. North Carolina. Carteret Co.	Lendemer 35485 (NY-1885425)	PP080081	PP080127	–
<i>Chicitaea aff. confusa</i> 6	U.S.A. North Carolina. Jones Co.	Lendemer 35655 (NY-1885717)	PP080082	PP080128	–
<i>Chicitaea confusa</i> 7	U.S.A. North Carolina. Craven Co.	Lendemer 35418 (NY-1885382)	PP080083	PP080129	–
<i>Chicitaea confusa</i> 8	U.S.A. North Carolina. Dare Co.	Lendemer 36747 (NY-1885847)	PP080084	–	–
<i>Chicitaea confusa</i> 9	U.S.A. North Carolina. Tyrrell Co.	Lendemer 36584 (NY-1886010)	PP080085	–	–
<i>Chicitaea confusa</i> 10	U.S.A. North Carolina. Washington Co.	Lendemer 36398 (NY-1886197)	PP080086	–	–
<i>Chicitaea cristinae</i> 10	Poland. Carpathians, Bieszczady	Szymczyk s.n. (UGDA L-60232)	PP080087	PP080130	–
<i>Loxospora chloropolia</i> 5	Poland. Wybrzeże Słowińskie	Ptach-Styn, Kukwa Lox. 1 (UGDA L-60093)	PP080088	–	PP083715
<i>Loxospora chloropolia</i> 6	Poland. Wybrzeże Słowińskie	Ptach-Styn, Kukwa Lox. 2 (UGDA L-60094)	PP080089	–	PP083716
<i>Loxospora chloropolia</i> 7	Poland. Wybrzeże Słowińskie	Ptach-Styn, Kukwa Lox. 3 (UGDA L-60095)	PP080090	–	PP083717
<i>Loxospora chloropolia</i> 8	Poland. Wybrzeże Słowińskie	Ptach-Styn, Kukwa Lox. 4 (UGDA L-60096)	PP080091	–	PP083718
<i>Loxospora chloropolia</i> 9	Poland. Wybrzeże Słowińskie	Ptach-Styn, Kukwa Lox. 5 (UGDA L-60097)	PP080092	–	–
<i>Loxospora chloropolia</i> 10	Poland. Wybrzeże Słowińskie	Ptach-Styn, Kukwa Lox. 6 (UGDA L-60098)	PP080093	–	PP083720
<i>Loxospora chloropolia</i> 11	Poland. Wybrzeże Słowińskie	Ptach et al. B1 (UGDA L-47764)	PP080094	PP080131	PP083721
<i>Loxospora chloropolia</i> 12	Poland. Wybrzeże Słowińskie	Ptach et al. B2 (UGDA L-47765)	PP080095	PP080132	PP083714
<i>Loxospora chloropolia</i> 13	Poland. Wybrzeże Słowińskie	Ptach et al. B3 (UGDA L-47766)	PP080096	PP080133	–
<i>Loxospora cismonica</i> 2	U.S.A. Tennessee. Blount Co.	Lendemer 44526 (NY-2438341)	PP080097	–	–
<i>Loxospora cismonica</i> 3	Canada. New Brunswick. Charlotte Co.	Harris 61785 (NY-2712391)	PP080098	PP080134	–
<i>Loxospora cismonica</i> 4	Romania. Carpathians	Malíček 14899, Steinová (herb. Malíček)	–	PP080135	–
<i>Loxospora elatina</i> 6	Poland. Carpathians, Bieszczady	Szymczyk s.n. (UGDA L-47757)	PP080099	PP080136	–
<i>Loxospora elatina</i> 7	Poland. Carpathians, Bieszczady	Szymczyk s.n. (UGDA L-47759)	PP080100	PP080137	–
<i>Loxospora elatina</i> 8	Poland. Carpathians, Bieszczady	Szymczyk s.n. (UGDA L-47760)	PP080101	PP080138	–
<i>Loxospora elatina</i> 9	Poland. Carpathians, Bieszczady	Szymczyk s.n. (UGDA L-47761)	PP080102	PP080139	–
<i>Loxospora elatina</i> 10	Poland. Carpathians, Bieszczady	Szymczyk s.n. (UGDA L-47762)	PP080103	PP080140	–
<i>Loxospora elatina</i> 11	Poland. Białowiecki National Park	Szymczyk 883 (UGDA L-47745)	PP080104	–	–
<i>Loxospora elatina</i> 12	Poland. Białowiecki National Park	Szymczyk 1076 (UGDA L-47746)	PP080105	PP080141	–
<i>Loxospora elatina</i> 13	Poland. Białowiecki National Park	Szymczyk 1085 (UGDA L-47747)	PP080106	–	–
<i>Loxospora elatina</i> 14	Poland. Białowiecki National Park	Szymczyk 1208 (UGDA L-47748)	PP080107	–	–
<i>Loxospora elatina</i> 15	Poland. Białowiecki National Park	Szymczyk 1255 (UGDA L-47750)	PP080108	–	–
<i>Loxospora elatina</i> 16	Poland. Białowiecki National Park	Szymczyk 1295 (UGDA L-47751)	PP080109	PP080142	–
<i>Loxospora elatina</i> 17	Poland. Równina Bielska	Szymczyk 1405 (UGDA L-47752)	PP080120	–	–
<i>Loxospora elatina</i> 18	Poland. Równina Bielska	Szymczyk 1464 (UGDA L-47755)	PP080121	–	–
<i>Loxospora elatina</i> 19	Estonia. Pärnu Co.	Kukwa 20481 (UGDA L-34378)	–	PP080147	–
<i>Loxospora elatina</i> 20	U.S.A. Maine. Washington Co.	Harris 60661 (NY-1818725)	PP080119	–	–
<i>Loxospora elatina</i> 21	U.S.A. Michigan. Cheboygan Co.	Lendemer 45025 (NY-2439450)	PP080117	–	–
<i>Loxospora elatina</i> 22	U.S.A. New York. Greene Co.	Lendemer 52960 (NY-3217196)	PP080114	–	–
<i>Loxospora elatina</i> 23	U.S.A. North Carolina. Haywood Co.	Lendemer 53286 (NY-3218018)	PP080115	–	–
<i>Loxospora elatina</i> 24	U.S.A. North Carolina. Macon Co.	Lendemer 46493 (NY-2795153)	–	PP080145	–
<i>Loxospora elatina</i> 25	U.S.A. Tennessee. Sevier Co.	Tripp 5040 (NY-2358356)	PP080110	PP080143	–
<i>Loxospora elatina</i> 26	Canada. Newfoundland	McCarthy 4138 (NBM)	PP080122	–	PP083719
<i>Loxospora elatina</i> 27	Canada. Newfoundland	McCarthy 4139 (NBM)	PP080123	–	–
<i>Loxospora elatina</i> 28	Russia. Caucasus Mts	Malíček et al. 10346 (herb. Malíček)	–	PP080146	–
<i>Loxospora elatina</i> 29	Czechia. Southern Bohemia	Malíček 14726 (herb. Malíček)	–	PP080148	–
<i>Loxospora elatina</i> 30	Czechia. Silesia	Malíček et al. 8916 (herb. Malíček)	–	PP080149	–
<i>Loxospora elatina</i> 31	Russia. Caucasus Mts	Malíček et al. 10515 (herb. Malíček)	–	PP080150	–
<i>Loxospora ochrophaea</i> 3	U.S.A. Maine. Washington Co.	Harris 60662 (NY-1818726)	PP080116	–	–
<i>Loxospora ochrophaea</i> 4	U.S.A. North Carolina. Yancey Co.	Kraus 44 (NY-2607571)	PP080124	–	–
<i>Loxospora ochrophaea</i> 5	U.S.A. North Carolina. Haywood Co.	Lendemer 45473 (NY-2440690)	PP080111	–	–
<i>Loxospora ochrophaea</i> 6	U.S.A. Tennessee. Sevier Co.	Lendemer 47245 (NY-2795450)	PP080112	PP080144	–
<i>Loxospora ochrophaea</i> 7	U.S.A. Tennessee. Sevier Co.	Lendemer 46150 (NY-2606798)	PP080113	PP091207	–
<i>Loxospora ochrophaea</i> 8	U.S.A. Tennessee. Sevier Co.	Lendemer 45684 (NY-2441234)	PP080118	–	–

variable sites that distinguish these taxa were identified. Similar analyses were done for specimens of *L. assateaguensis*, *L. confusa* and *L. lecanoriformis*. The final alignment of nuITS rDNA consisted of 11 sequences with 534 sites, while mtSSU rDNA alignment consisted of eight sequences and 613 sites.

## Results and discussion

The representatives of the genus *Loxospora* s.l. are split into two highly-supported major clades (Fig. 1). The larger clade corresponds to *Loxospora* s.str. (type: *L. elatina*), all containing thamnolic acid as the main secondary lichen substance and having asci with a uniformly amyloid apical dome and ascospores that are septate, fusiform to ellipsoidal and somewhat curved or twisted (Tønsberg 1992; Brodo et al. 2001; Sanderson et al. 2008). This clade is divided into two subclades. The smaller one consists of representatives of *L. cismonica* (Beltr.) Hafellner, while the larger subclade consists of two poorly-supported lineages, which might be the result of uneven coverage of sequences for each species in this subclade (see Table 1, Suppl. material 2). However, the phylogenetic analyses, based only on nuITS (not shown here) and the nuITS haplotype network analysis (Fig. 2), recovered these two groups as different and with high confidence. In the nuITS rDNA haplotype network analysis, these groups differ from each other in 21 nucleotide positions and the variability within the groups is up to three substitutions. Moreover, RPB1 haplotype network analysis also supports distinction of these two groups as they differ in 10 positions (Fig. 3), while the mtSSU rDNA marker showed very low variation (data not shown). The larger group includes sequences of specimens with at least partly tuberculate thalli with soralia, which are often fusing (i.e. corresponding to *L. elatina* s.str.) and thalli that uniformly lack soralia, but are typically fertile (i.e. corresponding to *L. ochrophaea*). The smaller group consists of sequences of samples in which the thalli are continuous to slightly cracked-areolate, but never tuberculate and soralia are usually discrete, rarely fusing and, if so, then only in older parts of the thallus.

The specimens whose sequences were recovered in this latter group correspond morphologically to the type material of *Pertusaria chloropolia* Erichsen ( $\equiv$  *Lecanora chloropolia* (Erichsen) Almb.), not to the type of *Lecanora elatina* Ach. (basionym of *Loxospora elatina*). *Pertusaria chloropolia* was synonymised with *Loxospora elatina* by Laundon (1963), a treatment followed subsequently by Hafellner and Türk (2016) and Westberg et al. (2021). All of the existing herbarium specimens corresponding to the type of *Pertusaria chloropolia* and presented in this present paper were initially identified as *L. elatina* and filed under that name in herbaria. However, as the molecular data show, this material corresponds to a phenotypically distinct monophyletic group for which the name *P. chloropolia* is available. The name is resurrected from synonymy and a new combination is proposed below. The revised circumscriptions of both *Loxospora chloropolia* and *L. elatina* are presented below and lectotypes are selected for both names. Moreover, in addition to morphology, their nuITS rDNA and RPB1 sequences differ in numerous positions of which several may be used as diagnostic characters to distinguish these taxa (Tables 2, 3).

The smaller clade of *Loxospora* s.l. is represented by *L. assateaguensis* Lendemer, *L. confusa* Lendemer, *L. cristinae* Guzow-Krzem., Łubek, Kubiak &

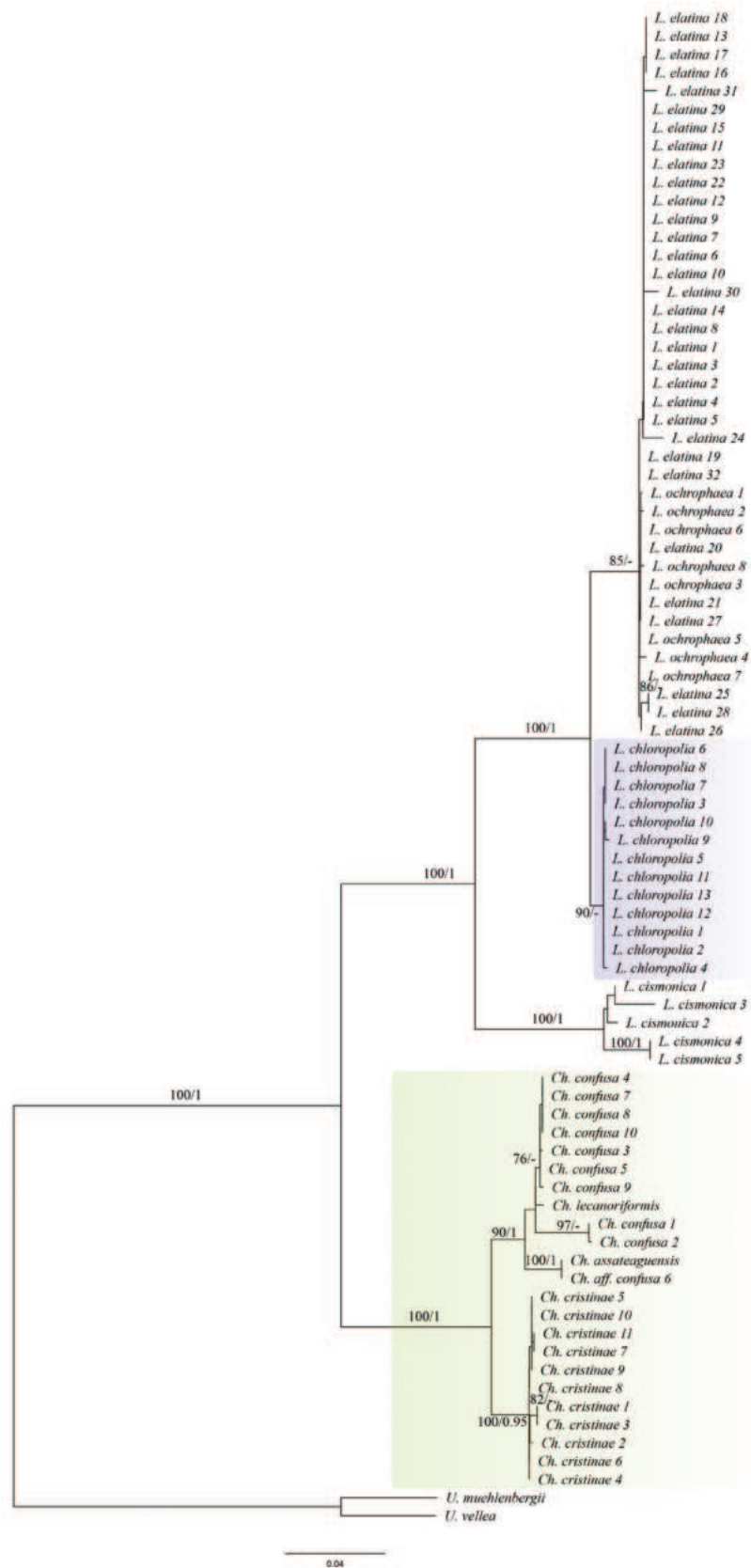


**Figure 1.** IQ-tree based on a combined nuITS rDNA, mtSSU and RPB1 dataset for *Loxospora* s.l. The names of species are followed with sample number (see Table 1, Suppl. material 2). Bootstrap supports from IQ-tree analysis  $\geq 70$  (first value) and posterior probabilities from BA  $\geq 0.95$  (second value) are indicated near the branches. *Umbilicaria* spp. were used as outgroup. *Loxospora chloropolia* clade is marked with blue box and *Chicitea* gen. nov. is marked with green box.

Kukwa and *L. lecanoriformis* (Fig. 1). All these species produce 2'-*O*-methylp-erlatolic acid and it has been repeatedly suggested that they represent a group distinct from the thamnolic acid producing species of *Loxospora* s. str. which likely merits recognition as a distinct genus (Lumbsch et al. 2007; Lendemer 2013; Guzow-Krzemińska et al. 2018). While apothecia are known only in *L. lecanoriformis*, in that species, the asci lack an amyloid apical dome, unlike in *Loxospora* s.str. and the ascospores are simple, ellipsoidal, straight or slightly bent (Lumbsch et al. 2007; Papong et al. 2009). Due to the consistent differences from *Loxospora* s.str. in secondary lichen substances, the differences in ascus amyloidy and the strongly-supported monophyly of this group in molecular phylogenetic analyses, we recognise it as a distinct genus under the name *Chicitaea* below. Four new combinations are proposed for the species currently known to belong to this clade. *Chicitaea cristinae* was recovered as monophyletic and sister to the rest of the species, which form a well-supported clade, but with poorly resolved relationships between *Ch. confusa* and *Ch. lecanoriformis*. The fertile *Ch. lecanoriformis*, known from Australia and Thailand (Lumbsch et al. 2007; Papong et al. 2009), is nested within a subclade of sequences of *Ch. confusa*, an isidioid species which occurs in North America and is not known to occur in the Southern Hemisphere or Australasia (Lendemer 2013). Due to the lack of nuITS rDNA sequence for *Ch. lecanoriformis* and very low variation found in mtSSU sequences (Fig. 4), the relationship between these species cannot be resolved. Nevertheless, both species clearly differ morphologically and have disjunctive distributions (Lumbsch et al. 2007; Papong et al. 2009; Lendemer 2013). *Chicitaea confusa* seems to be paraphyletic and may represent two cryptic species (Fig. 1). This conclusion is also supported by the haplotype analyses of mtSSU and nuITS sequences (Figs 4, 5) which also show that two specimens (*Ch. confusa* 1 and 2) significantly differ from all the newly-sequenced representatives of *Ch. confusa*, but more material is needed to solve this problem. The sequences of one specimen, initially determined as *Ch. confusa* (*Ch. aff. confusa* 6; Figs 1, 4, 5), is identical in mtSSU and nuITS sequences with *Ch. assateaguensis*. This suggests that *Ch. assateaguensis* can represent a cryptic species, even though, as stated by Lendemer (2013), the species differed from *Ch. confusa*, but more material is necessary before final conclusions.

*Loxospora elatina* s.str. and *L. ochrophaea* are morphologically similar in terms of thallus and apothecia and both produce thamnolic acid often with elatinic acid and trace amounts of squamatic acid (Tønberg 1992; Brodo et al. 2001; Sanderson et al. 2008). The only difference between *L. elatina* s.str. and *L. ochrophaea* is the consistent presence of soralia in *L. elatina* (apothecia are very rare) and the absence of soralia in *L. ochrophaea* which is, instead, consistently fertile and routinely produces apothecia (Kalb and Hafellner 1992; Tønberg 1992; Brodo et al. 2001; Sanderson et al. 2008). From a phenotypic perspective, these two taxa can be considered a species pair (cf. Poelt (1970); Crespo and Pérez-Ortega (2009)).

Although both species are frequently found on the acidic bark of trees and both are distributed in the Northern Hemisphere, their distributions are divergent and not entirely sympatric. *Loxospora elatina* is widely distributed in boreal and northern temperate areas of the Northern Hemisphere with oceanic climates (e.g. Sanderson et al. (2008); Urbanavichus (2010); Stenroos et al. (2016)).

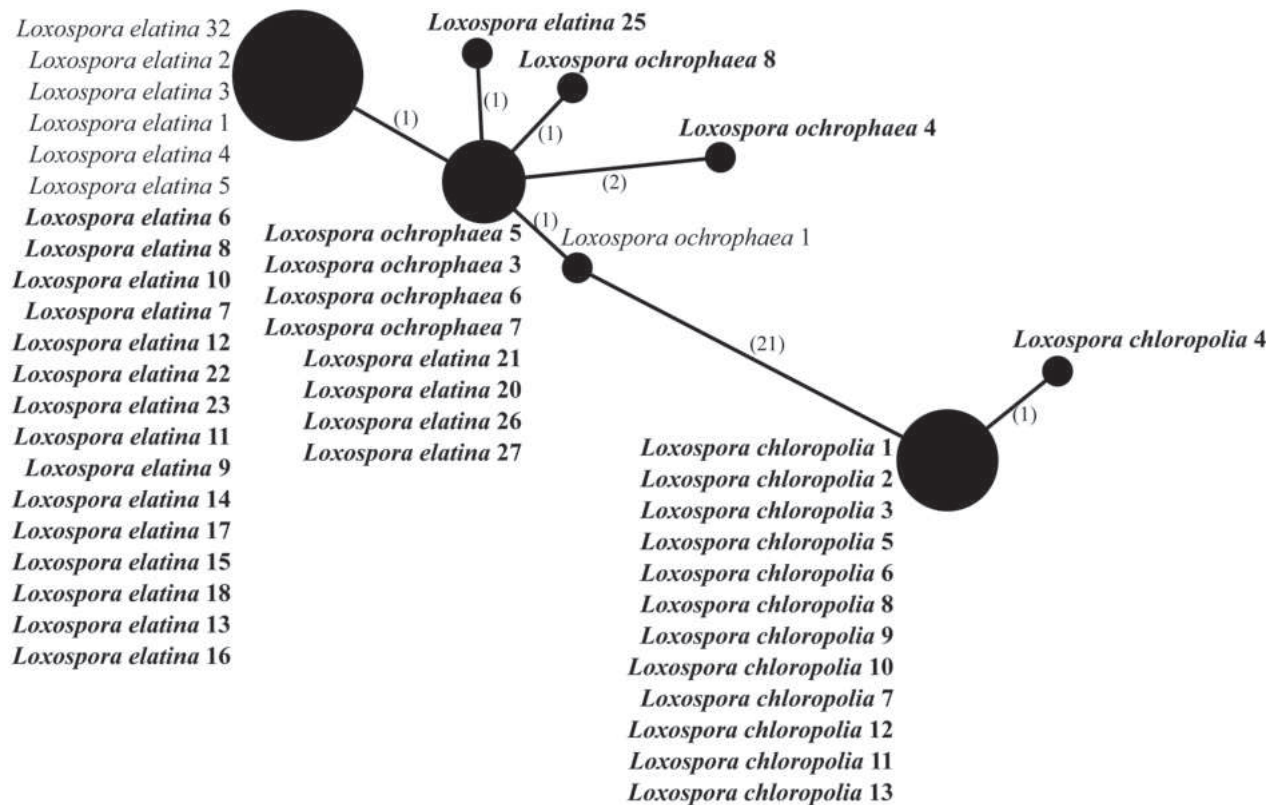


**Figure 2.** Haplotype network showing relationships between nuITS rDNA sequences from *Loxospora chloropolia*, *L. elatina* and *L. ochrophaea*. The names of species are followed with sample numbers (see Table 1, Suppl. material 2). Newly-sequenced samples are marked in bold. Mutational changes are presented as numbers in brackets near lines between haplotypes.

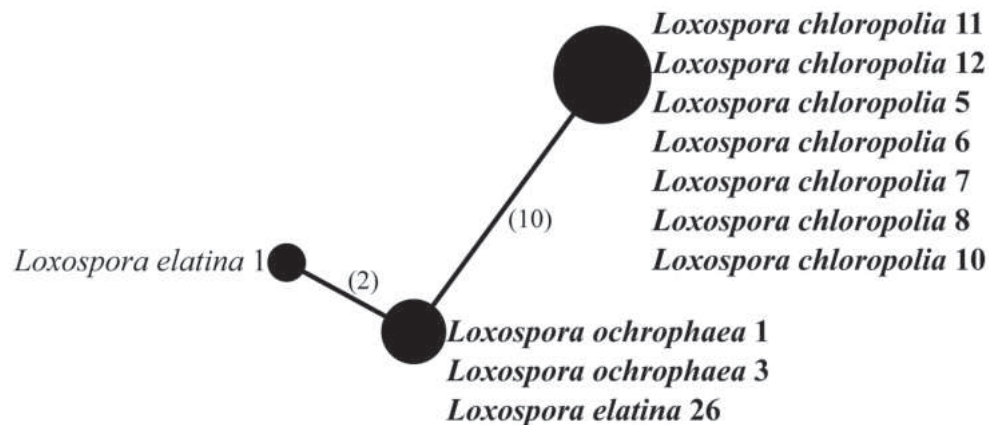


**Figure 3.** Haplotype network showing relationships between RPB1 sequences from *Loxospora chloropolia*, *L. elatina* and *L. ochrophaea*. The names of species are followed with sample numbers (see Table 1, Suppl. material 2). Newly-sequenced samples are marked in bold. Mutational changes are presented as numbers in brackets near lines between haplotypes.

In contrast, *L. ochrophaea* has a narrower, disjunct distribution between the Appalachian-Great Lakes regions of eastern North America and north-eastern Asia (Japan and the Russian Far East) (e.g. Tuckerman (1848); Brodo et al. (2001); Urbanavichus (2010); Ohmura and Kashiwadani (2018)). Indeed, the distributions of these two taxa follow the predictions of the species pair hypothesis, wherein the species with vegetative diaspores has a much larger range compared to that of the strictly sexual species that lacks vegetative diaspores (Poelt 1970; Mattsson and Lumbsch 1989).

**Table 2.** Variable positions in the alignment of nuITS rDNA marker of *Loxospora chloropolia*, *L. elatina* and *L. ochrophaea*. Variable characters are marked in bold, while diagnostic nucleotide position characters to distinguish *L. chloropolia* from both *L. elatina* and *L. ochrophaea* are marked with a gray background, including indels.

Sequence	Position in alignment																																														
	11	15	16	17	19	20	27	34	35	37	38	42	43	44	45	46	52	68	79	107	311	321	332	334	340	341	342	347	371	387	389	393	401	405	412	416	417	419	420	432	435	439	441				
<i>L. chloropolia</i> 1	C	C	C	T	T	T	C	T	A	T	A	-	-	-	T	C	C	G	A	T	C	G	G	C	T	G	G	G	T	G	T	G	T	A	T	T	T	T	T	G	T	-	G	G	G		
<i>L. chloropolia</i> 2	C	C	C	T	T	T	C	T	A	T	A	-	-	-	T	C	C	G	A	T	C	G	G	C	T	G	G	T	G	T	G	T	A	T	T	T	T	T	T	G	T	-	G	G	G		
<i>L. chloropolia</i> 3	C	C	C	T	T	T	C	T	A	T	A	-	-	-	T	C	C	G	A	T	C	G	G	C	T	G	G	T	G	T	G	T	A	C	T	T	T	T	T	G	T	-	G	G	G		
<i>L. chloropolia</i> 5	C	C	C	T	T	T	C	T	A	T	A	-	-	-	T	C	C	G	A	T	C	G	G	C	T	G	G	T	G	T	G	T	A	Y	T	T	T	T	T	G	T	-	G	G	G		
<i>L. chloropolia</i> 6	C	C	C	T	T	T	C	T	A	T	A	-	-	-	T	C	C	G	A	T	C	G	G	C	T	G	G	T	G	T	G	T	A	C	T	T	T	T	T	G	T	-	G	G	G		
<i>L. chloropolia</i> 8	C	C	C	T	T	T	C	T	A	T	A	-	-	-	T	C	C	G	A	T	C	G	G	C	T	G	G	T	G	T	G	T	A	C	T	T	T	T	T	G	T	-	G	G	G		
<i>L. chloropolia</i> 9	C	C	C	T	T	T	C	T	A	T	A	-	-	-	T	C	C	G	A	T	C	G	G	C	T	G	G	T	G	T	G	T	A	C	T	T	T	T	T	G	T	-	G	G	G		
<i>L. chloropolia</i> 10	C	C	C	T	T	T	C	T	A	T	A	-	-	-	T	C	C	G	A	T	C	G	G	C	T	G	G	T	G	T	G	T	A	T	T	T	T	T	T	G	T	-	G	G	G		
<i>L. chloropolia</i> 7	C	C	C	T	T	T	C	T	A	T	A	-	-	-	T	C	C	G	A	T	C	G	G	C	T	G	G	T	G	T	G	T	A	C	T	T	T	T	T	G	T	-	G	G	G		
<i>L. chloropolia</i> 4	C	C	C	T	T	T	C	T	A	T	A	-	-	-	T	C	C	G	A	T	C	G	G	C	T	G	G	T	G	T	G	T	A	C	T	T	T	T	T	G	T	-	G	A	G		
<i>L. chloropolia</i> 12	C	C	C	T	T	T	C	T	A	T	-	-	-	-	T	C	C	G	A	T	C	G	G	C	T	G	G	T	G	T	G	T	A	T	T	T	T	T	T	G	T	-	G	G	G		
<i>L. chloropolia</i> 11	C	C	C	T	T	T	C	T	A	T	-	-	-	-	T	C	C	G	A	T	C	G	G	C	T	G	G	T	G	T	G	T	A	T	T	T	T	T	T	G	T	-	G	G	G		
<i>L. chloropolia</i> 13	C	C	C	T	T	T	C	T	A	T	-	-	-	-	T	C	C	G	A	T	C	G	G	C	T	G	G	T	G	T	G	T	A	T	T	T	T	T	T	G	T	-	G	G	G		
<i>L. ochrophaea</i> 1	-	C	C	G	A	A	T	C	G	C	A	T	C	T	T	T	T	T	G	A	C	T	A	A	T	C	A	T	C	A	G	C	T	G	T	C	T	C	T	G	T	-	G	G	G		
<i>L. ochrophaea</i> 5	-	C	C	G	A	A	T	C	G	C	A	T	C	T	T	T	T	T	G	A	C	T	A	A	T	C	A	T	C	A	G	C	C	T	G	T	C	T	C	T	G	T	-	G	G	G	
<i>L. ochrophaea</i> 3	-	C	C	G	A	A	T	C	G	C	-	T	C	T	T	T	T	T	G	A	C	T	A	A	T	C	A	T	C	A	G	C	C	C	C	T	C	T	C	T	G	T	-	G	G	G	
<i>L. ochrophaea</i> 6	-	C	Y	G	A	A	T	C	G	C	A	T	C	T	T	T	T	T	G	A	C	T	A	A	T	C	A	T	C	A	G	C	C	C	C	T	C	T	C	T	G	T	-	G	G	G	
<i>L. ochrophaea</i> 7	-	Y	C	G	A	A	T	C	G	C	A	T	C	T	T	T	T	T	G	A	C	T	A	A	T	C	A	T	C	A	G	C	C	C	C	T	C	T	C	T	G	T	-	G	G	G	
<i>L. ochrophaea</i> 8	-	C	C	G	A	A	T	C	G	C	A	T	C	T	T	T	T	T	G	A	C	T	A	A	T	C	A	T	C	A	G	C	C	C	C	T	C	T	C	T	G	T	-	G	G	G	
<i>L. ochrophaea</i> 4	-	C	C	G	A	A	T	C	G	C	A	T	C	T	T	T	T	T	G	<b>G</b>	C	T	A	A	T	C	A	T	C	A	G	C	C	C	C	T	C	T	<b>C</b>	C	T	<b>C</b>	G	G	G	G	
<i>L. elatina</i> 2	-	C	C	G	A	A	T	C	G	C	A	T	C	T	T	T	T	T	G	A	C	T	A	A	T	C	A	T	C	A	G	C	C	C	C	T	C	A	C	T	G	T	-	G	G	G	
<i>L. elatina</i> 3	-	C	C	G	A	A	T	C	G	C	A	T	C	T	T	T	T	T	G	A	C	T	A	A	T	C	A	T	C	A	G	C	C	C	C	T	C	A	C	T	G	T	-	G	G	G	
<i>L. elatina</i> 1	-	C	C	G	A	A	T	C	G	C	A	T	C	T	T	T	T	T	G	A	C	T	A	A	T	C	A	T	C	A	G	C	C	C	C	T	C	A	C	T	G	T	-	G	G	G	
<i>L. elatina</i> 4	-	C	C	G	A	A	T	C	G	C	A	T	C	T	T	T	T	T	G	A	C	T	A	A	T	C	A	T	C	A	G	C	C	C	C	T	C	A	C	T	G	T	-	G	G	G	
<i>L. elatina</i> 5	-	C	C	G	A	A	T	C	G	C	A	T	C	T	T	T	T	T	G	A	C	T	A	A	T	C	A	T	C	A	G	C	C	C	C	T	C	A	C	T	G	T	-	G	G	G	
<i>L. elatina</i> 6	-	C	C	G	A	A	T	C	G	C	-	T	C	T	T	T	T	T	G	A	C	T	A	A	T	C	A	T	C	A	G	C	C	C	C	C	T	C	A	C	T	G	T	-	G	G	G
<i>L. elatina</i> 8	-	C	C	G	A	A	T	C	G	C	-	T	C	T	T	T	T	T	G	A	C	T	A	A	T	C	A	T	C	A	G	C	C	C	C	T	C	A	C	T	G	T	-	G	G	G	
<i>L. elatina</i> 10	-	C	C	G	A	A	T	C	G	C	-	T	C	T	T	T	T	T	G	A	C	T	A	A	T	C	A	T	C	A	G	C	C	C	C	T	C	A	C	T	G	T	-	G	G	G	
<i>L. elatina</i> 7	-	C	C	G	A	A	T	C	G	C	-	T	C	T	T	T	T	T	G	A	C	T	A	A	T	C	A	T	C	A	G	C	C	C	C	T	C	A	C	T	G	T	-	G	G	G	
<i>L. elatina</i> 12	-	C	C	G	A	A	T	C	G	C	-	T	C	T	T	T	T	T	G	A	C	T	A	A	T	C	A	T	C	A	G	C	C	C	C	T	C	A	C	T	G	T	-	G	G	G	
<i>L. elatina</i> 22	-	C	C	G	A	A	T	C	G	C	-	T	C	T	T	T	T	T	G	A	C	T	A	A	T	C	A	T	C	A	G	C	C	C	C	T	C	A	C	T	G	T	-	G	G	G	
<i>L. elatina</i> 23	-	C	C	G	A	A	T	C	G	C	-	T	C	T	T	T	T	T	G	A	C	T	A	A	T	C	A	T	C	A	G	C	C	C	C	T	C	A	C	T	G	T	-	G	G	G	
<i>L. elatina</i> 11	-	C	C	G	A	A	T	C	G	C	-	T	C	T	T	T	T	T	G	A	C	T	A	A	T	C	A	T	C	A	G	C	C	C	C	T	C	A	C	T	G	T	-	G	G	G	
<i>L. elatina</i> 9	-	C	C	G	A	A	T	C	G	C	-	T	C	T	T	T	T	T	G	A	C	T	A	A	T	C	A	T	C	A	G	C	C	C	C	T	C	A	C	T	G	T	-	G	G	G	

Sequence	Position in alignment																																												
	11	15	16	17	19	20	27	34	35	37	38	42	43	44	45	46	52	68	79	107	311	321	332	334	340	341	342	347	371	387	389	393	401	405	412	416	417	419	420	432	435	439	441		
<i>L. elatina</i> 21	-	C	C	G	A	A	T	C	G	C	<b>A</b>	T	C	T	T	T	T	T	G	A	C	T	A	A	A	T	C	A	G	C	C	C	G	T	C	<b>T</b>	C	T	G	T	-	G	G	G	G
<i>L. elatina</i> 20	-	C	C	G	A	A	T	C	G	C	-	T	C	T	T	T	T	T	G	A	C	T	A	A	T	C	A	G	C	C	C	G	T	C	<b>T</b>	C	T	G	T	-	G	G	G	G	G
<i>L. elatina</i> 14	-	C	C	G	A	A	T	C	G	C	-	T	C	T	T	T	T	T	G	A	C	T	A	A	T	C	A	G	C	C	C	G	T	C	<b>A</b>	C	T	G	T	-	G	G	G	G	G
<i>L. elatina</i> 17	-	C	C	G	A	A	T	C	G	C	-	T	C	T	T	T	T	T	G	A	C	T	A	A	T	C	A	G	C	C	C	G	T	C	<b>A</b>	C	T	G	T	-	G	G	G	G	G
<i>L. elatina</i> 15	-	C	C	G	A	A	T	C	G	C	-	T	C	T	T	T	T	T	G	A	C	T	A	A	T	C	A	G	C	C	C	G	T	C	<b>A</b>	C	T	G	T	-	G	G	-	G	G
<i>L. elatina</i> 18	-	C	C	G	A	A	T	C	G	C	-	T	C	T	T	T	T	T	G	A	C	T	A	A	T	C	A	G	C	C	C	G	T	C	<b>A</b>	C	T	G	T	-	G	G	-	G	G
<i>L. elatina</i> 13	-	C	C	G	A	A	T	C	G	C	-	T	C	T	T	T	T	T	G	A	C	T	A	A	T	C	A	G	C	C	C	G	T	C	<b>A</b>	C	T	G	T	-	G	G	-	G	G
<i>L. elatina</i> 16	-	C	C	G	A	A	T	C	G	C	-	T	C	T	T	T	T	T	G	A	C	T	A	A	T	C	A	G	C	C	C	G	T	C	<b>A</b>	C	T	G	T	-	G	G	-	G	G
<i>L. elatina</i> 26	-	C	C	G	A	A	T	C	G	C	<b>A</b>	T	C	T	T	T	T	T	G	A	C	T	A	A	T	C	A	G	C	C	C	G	T	C	<b>T</b>	C	T	G	T	-	G	G	-	G	G
<i>L. elatina</i> 27	-	C	C	G	A	A	T	C	G	C	<b>A</b>	T	C	T	T	T	T	T	G	A	C	T	A	A	T	C	A	G	C	C	C	G	T	C	<b>T</b>	C	T	G	T	-	G	G	-	G	G
<i>L. elatina</i> 25	-	C	Y	G	A	A	T	C	G	C	<b>A</b>	T	C	T	T	T	T	T	S	A	C	T	A	A	T	C	A	K	C	C	C	G	T	C	<b>T</b>	C	T	S	Y	-	G	<b>C</b>	G	G	
<i>L. elatina</i> 32	-	C	C	G	A	A	T	C	G	C	<b>A</b>	T	C	T	T	T	T	T	G	A	C	T	A	A	T	C	A	G	C	C	C	G	T	C	<b>A</b>	C	T	G	T	-	G	G	-	G	G

**Table 3.** Variable positions in the alignment of RPB1 marker of *Loxospora chloropolia*, *L. elatina* and *L. ochrophaea*. Variable characters are marked in bold, while diagnostic nucleotide position characters to distinguish *L. chloropolia* from both *L. elatina* and *L. ochrophaea* are marked with a gray background.

Sequence	Position in alignment																															
	73	82	106	201	282	291	315	342	344	355	357	414	439	441	472	475	507	513	519	527	540	603	687	700	706	711	723					
<i>L. ochrophaea</i> 1	G	G	T	T	G	T	T	G	A	G	C	A	G	G	A	A	G	G	A	A	A	T	T	A	C	A	C	A	C			
<i>L. ochrophaea</i> 2	G	G	T	T	G	T	T	G	A	G	C	A	G	G	A	A	G	G	A	A	A	T	T	A	G	A	C	C				
<i>L. elatina</i> 1	?	?	?	T	G	T	<b>C</b>	G	R	G	C	A	G	G	A	A	G	G	A	<b>G</b>	A	T	T	N	C	A	C					
<i>L. elatina</i> 26	G	G	T	T	<b>K</b>	T	T	R	A	S	C	A	D	G	R	M	G	G	A	A	A	T	T	A	C	A	C					
<i>L. chloropolia</i> 11	<b>A</b>	<b>A</b>	<b>C</b>	<b>C</b>	G	<b>C</b>	T	G	A	G	<b>T</b>	<b>C</b>	G	<b>A</b>	A	A	<b>A</b>	<b>T</b>	<b>G</b>	A	<b>G</b>	<b>C</b>	<b>C</b>	A	C	<b>G</b>	<b>T</b>					
<i>L. chloropolia</i> 12	<b>A</b>	<b>A</b>	<b>C</b>	<b>C</b>	G	<b>C</b>	T	G	A	G	<b>T</b>	<b>C</b>	G	<b>A</b>	A	A	<b>A</b>	<b>T</b>	<b>G</b>	A	<b>G</b>	<b>C</b>	<b>C</b>	A	C	<b>G</b>	<b>T</b>					
<i>L. chloropolia</i> 5	<b>A</b>	<b>A</b>	<b>C</b>	<b>C</b>	G	<b>C</b>	T	G	A	G	<b>T</b>	<b>C</b>	G	<b>A</b>	A	A	<b>A</b>	<b>T</b>	<b>G</b>	A	<b>G</b>	<b>C</b>	<b>C</b>	A	C	<b>G</b>	<b>T</b>					
<i>L. chloropolia</i> 6	<b>A</b>	<b>A</b>	<b>C</b>	<b>C</b>	G	<b>C</b>	T	G	A	G	<b>T</b>	<b>C</b>	G	<b>A</b>	A	A	<b>A</b>	<b>T</b>	<b>G</b>	A	<b>G</b>	<b>C</b>	<b>C</b>	A	C	<b>G</b>	<b>T</b>					
<i>L. chloropolia</i> 7	<b>A</b>	<b>A</b>	<b>C</b>	<b>C</b>	G	<b>C</b>	T	G	A	G	<b>T</b>	<b>C</b>	G	<b>A</b>	A	A	<b>A</b>	<b>T</b>	<b>G</b>	A	<b>G</b>	<b>C</b>	<b>C</b>	A	C	<b>G</b>	<b>T</b>					
<i>L. chloropolia</i> 8	<b>A</b>	<b>A</b>	<b>C</b>	<b>C</b>	G	<b>C</b>	T	G	A	G	<b>T</b>	<b>C</b>	G	<b>A</b>	A	A	<b>A</b>	<b>T</b>	<b>G</b>	A	<b>G</b>	<b>C</b>	<b>C</b>	A	C	<b>G</b>	<b>T</b>					
<i>L. chloropolia</i> 10	<b>A</b>	<b>A</b>	<b>C</b>	<b>C</b>	G	<b>C</b>	T	G	A	G	<b>T</b>	<b>C</b>	R	<b>A</b>	A	A	<b>A</b>	<b>T</b>	<b>G</b>	A	<b>G</b>	<b>C</b>	<b>C</b>	?	?	?	?					

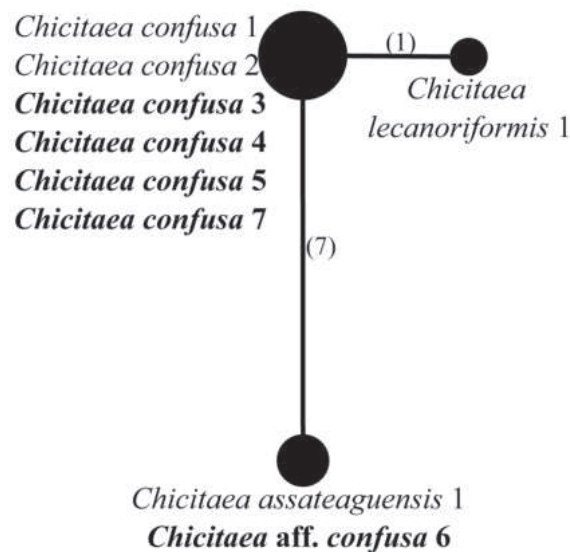


**Figure 4.** Haplotype network showing relationships between mtSSU rDNA sequences from *Chicitaea assateaguensis*, *Ch. confusa* and *Ch. lecanoriformis*. The names of species are followed with sample numbers (see Table 1, Suppl. material 2). Newly-sequenced samples are marked in bold. Mutational changes are presented as numbers in brackets near lines between haplotypes.

In our analyses, sequences of *Loxospora elatina* s.str. were intermingled with *L. ochrophaea* within the same clade (Fig. 1). Six different nuITS haplotypes were found in these species which differed up to three nucleotide substitutions between each other (Fig. 2). The most common haplotype was found in 20 specimens of *L. elatina* collected in Poland, Switzerland and two geographically distant locations in Appalachian eastern North America (sample *L. elatina* 22 is from New York, U.S.A. and sample *L. elatina* 23 is from North Carolina, U.S.A.; Table 1). Moreover, in the nuITS haplotype network, four samples of *L. elatina* and four samples of *L. ochrophaea* share the same haplotype (Fig. 2). While these samples were all collected in eastern North America, they include samples of each species that were collected at very distant locations (e.g. sample *L. ochrophaea* 3 is from coastal Maine, U.S.A., while samples *L. ochrophaea* 5, 6 and 7 are from Appalachian North Carolina and Tennessee, U.S.A.; sample *L. elatina* 20 is from coastal Maine, U.S.A, sample *L. elatina* 21 is from the Great Lakes of Michigan, U.S.A., while samples *L. elatina* 26 and *L. elatina* 27 are from Newfoundland, Canada; Table 1). Interestingly, a sample of each species was collected in close proximity at the same locality (samples *L. ochrophaea* 3 and *L. elatina* 20, both from the same location on Roque Island in Maine, U.S.A.; Table 1). Given their phenotypic similarity and the lack of resolution using nuITS rDNA, the molecular barcoding marker for fungi, it is possible that *L. elatina* and *L. ochrophaea* may represent variants of a single species. On the other hand, it is also possible that our data were insufficient to distinguish between two closely-related species and more detailed study would allow to find differences between them. Recently, in the case of *Usnea antarctica* Du Rietz and *U. aurantiacoatra* (Jacq.) Bory, RAD-seq and comparative genomics supported recognition of a species pair that had previously been proposed to be synonyms (Grewe et al. 2018). Given that the species have strongly divergent distributions and that they are morphologically distinct when they co-occur, we refrain from synonymising them at this time.

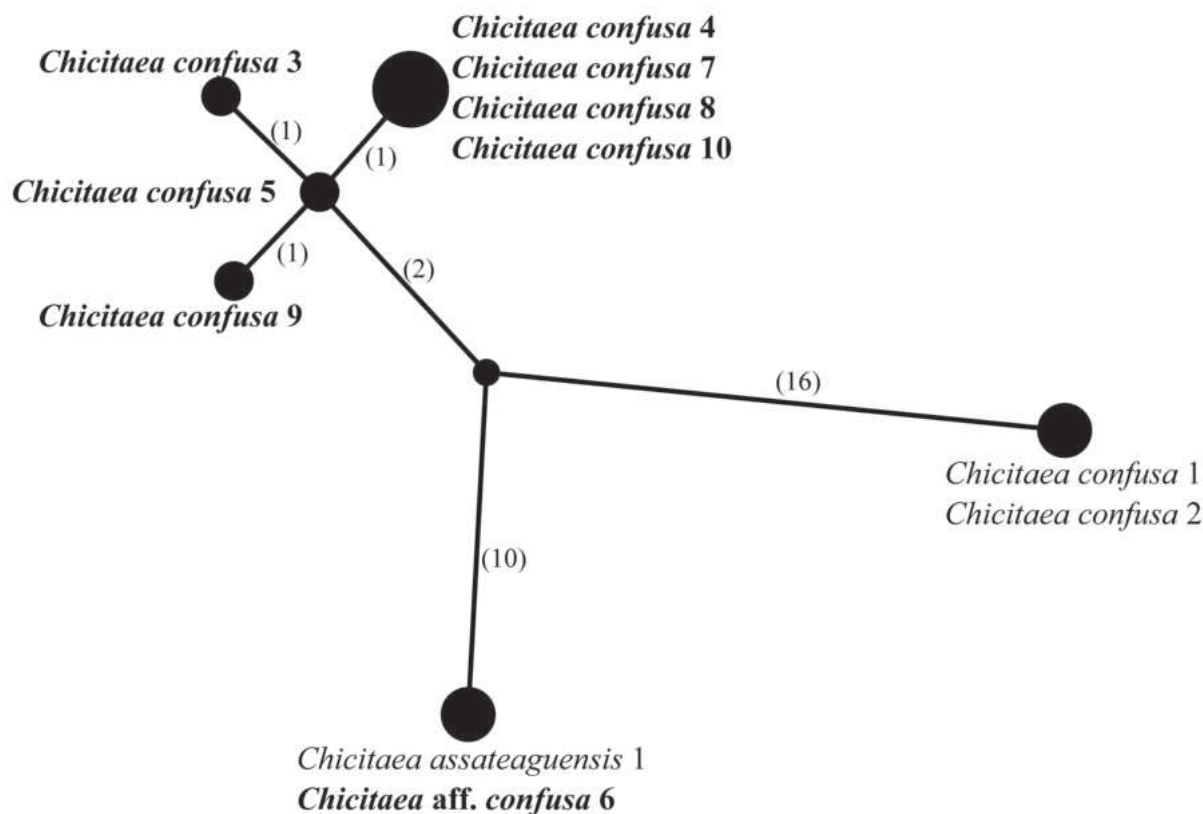


**Figure 5.** Haplotype network showing relationships between nuITS rDNA sequences from *Chicitaea assateaguensis* and *Ch. confusa*. The names of species are followed with sample numbers (see Table 1, Suppl. material 2). Newly-sequenced samples are marked in bold. Mutational changes are presented as numbers in brackets near lines between haplotypes.

## Taxonomy

### *Chicitaea* Guzow-Krzem., Kukwa & Lendemer, gen. nov.

MycoBank No: 851779

**Diagnosis.** Differs from *Loxospora* s.str. in the presence of 2'-*O*-methylperlatolic acid (vs. thamnolic acid), asci without an amyloid apical dome (vs. asci with a uniformly amyloid apical dome) and simple, broadly ellipsoid, straight or slightly bent ascospores (known only in the type species; vs. transversely septate ascospores).

**Generic type.** *Chicitaea lecanoriformis* (Lumbsch, A.W. Archer & Elix) Guzow-Krzem., Kukwa & Lendemer.

**Etymology.** The generic epithet honours Chicita F. Culberson (1931–2023), Senior Research Scientist at Duke University, U.S.A., for her foundational, pioneering and lifelong contributions to the fields of lichen chemistry and lichen taxonomy. In addition to establishing standardised protocols to study lichen secondary chemistry that have been routinely used by workers worldwide for more than half a century, she was an influence for generations of lichenologists with whom she generously shared her knowledge and experience.

**Description.** Thallus corticolous, pale grey-green to olive-grey, thin or thick, surface smooth to verrucose, sorediate, isidate or without vegetative propagules. Apothecia known in one species, lecanorine, up to 1.5 mm diam., sessile, concave.

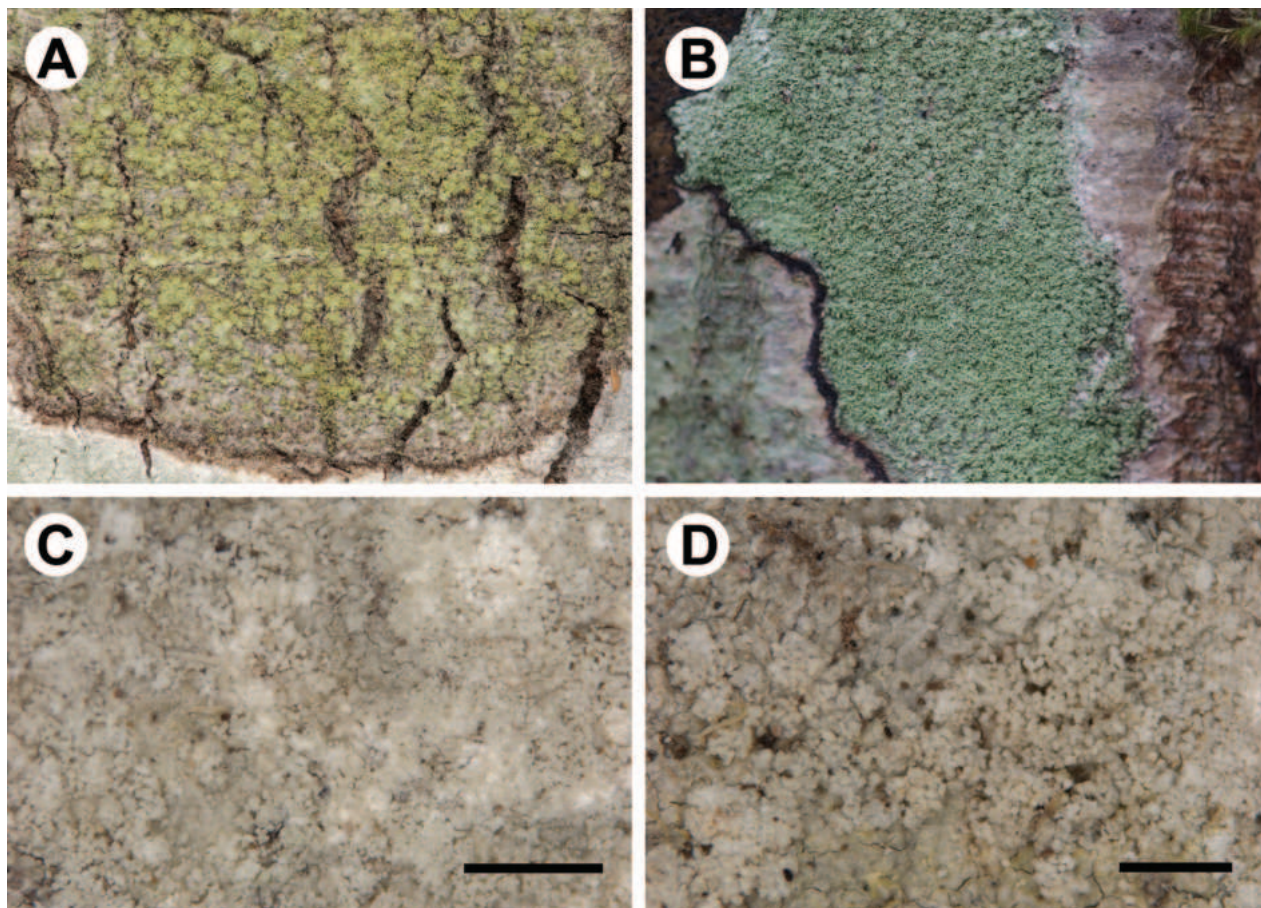


**Figure 6.** Morphology of two species of *Chicitaeta* **A** Thallus of *Ch. confusa* on tree trunk (taken by J. Hollinger in the field) **B** thallus of *Ch. cristinae* on tree trunk (taken by D. Kubiak in the field) **C, D** Thalli of *Ch. cristinae* showing soralia (paratypes of *L. cristinae* **C** UGDA L-22396 **D** UGDA L-20385). Scale bars: 1 mm (**C, D**).

Thalline margin present, scabrid when young, later entire, dentate, persistent, often flexuose. Disc dark reddish-brown to black, epruinose. Hymenium colourless, interspersed with infrequent oil droplets. Paraphyses simple, unbranched. Hypothecium colourless or pale yellow-brown. Asci claviform to obovate, I-, KI+ slightly blue-green, damaged asci amyloid. Ascospores 6–8 per ascus, broadly ellipsoid, straight or slightly bent, with a single thin wall. Pycnidia found in one species, immersed, visible as minute black dots. Conidia bacilliform.

**Chemistry.** 2'-O-methylperlatolic acid (major) and perlatolic acid (minor or trace; reported only from *Chicitaeta lecanoriformis*). Spot tests: cortex K-, C-, KC-, P-, UV-; medulla and soralia K-, C-, KC-, P-, UV+ white.

For morphology of *Chicitaeta* species, see Lumbsch et al. (2007), Papong et al. (2009), Lendemer (2013), Guzow-Krzemińska et al. (2018) and Fig. 6.

***Chicitaeta assateaguensis* (Lendemer) Guzow-Krzem., Kukwa & Lendemer, comb. nov.**

MycoBank No: 851780

*Loxospora assateaguensis* Lendemer, J. North Carolina Acad. Sci. 129(3): 74 (2013). Basionym.

***Chicitea confusa* (Lendemer) Guzew-Krzem., Kukwa & Lendemer, comb. nov.**

MycoBank No: 851781

*Loxospora confusa* Lendemer, J. North Carolina Acad. Sci. 129(3): 77 (2013).  
Basionym.

***Chicitea cristinae* (Guzew-Krzem., Łubek, Kubiak & Kukwa) Guzew-Krzem.,  
Kukwa & Lendemer, comb. nov.**

MycoBank No: 851782

*Loxospora cristinae* Guzew-Krzem., Łubek, Kubiak & Kukwa, in Guzew-Krzemińska, Łubek, Kubiak, Ossowska & Kukwa, Phytotaxa 348(3): 216 (2018).  
Basionym.

***Chicitea lecanoriformis* (Lumbsch, A.W. Archer & Elix) Guzew-Krzem.,  
Kukwa & Lendemer, comb. nov.**

MycoBank No: 851783

*Loxospora lecanoriformis* Lumbsch, A.W. Archer & Elix, Lichenologist 39(6): 514  
(2007). Basionym.

***Loxospora* A. Massal.**

Ric. Auton. Lich. Crost.: 137 (1852).

**Notes.** Three species, *L. cyamidia* (Stirt.) Kantvilas, *L. septata* (Sipman & Aptroot) Kantvilas and *L. solenospora* (Müll. Arg.) Kantvilas (syn. *Sarrameana tasmanica* Vězda & Kantvilas), from the Southern Hemisphere have not been sequenced so far. However, they have ascospores similar in shape to other *Loxospora* spp. (although, in *L. cyamidia* and *L. solenospora*, they are rarely septate), asci with an amyloid apical dome and contain thamnolic acid (although *L. solenospora* may sometimes contain additionally gyrophoric acid or only the latter substance) (Kantvilas 2000, 2004). Given the morphological and chemical similarities to the type species *L. elatina* and other members of *Loxospora* s.str., they are treated here as belonging to this genus. *Loxospora isidiata* Kalb (described from the Philippines) and *L. ochrophaeoides* Kalb & Hafellner (described from Madeira), introduced by Kalb and Hafellner (1992) and *L. glaucomiza* (Nyl.) Kalb & Staiger (described from Japan) treated by Staiger and Kalb (1995) are also treated as belonging to *Loxospora* s.str. due to the production of thamnolic acid.

The name *Loxospora pustulata* (Brodo & W.L. Culb.) Egan was applied to a common and widespread pustulose-sorediate crustose species with thamnolic acid that occurs throughout eastern North America (Brodo and Culberson 1986; Lendemer and Noell 2018). The discovery of fertile material led to its being transferred to the genus *Lepra* Scop. as *L. pustulata* (Brodo & W.L. Culb.) Lendemer & R.C. Harris (Lendemer and Harris 2017).

***Loxospora chloropolia* (Erichsen) Ptach-Styn, Guzow-Krzem., Tønsberg & Kukwa, comb. nov.**

MycoBank No: 851745

Fig. 7

*Pertusaria chloropolia* Erichsen, in Zahlbr., Rabenh. Krypt.-Fl. Ed. 2, 9(5[1]): 645 (1935[1936]). Basionym. Type. [SWITZERLAND. Jura Mts:] Mont de Baulmes, 1100 m elev., [on *Abies*] 1934, Meylan (lectotype: HBG!, selected here; MycoBank No: MBT 10017691).

*Pertusaria chloropolia* f. *cana* Erichsen, in Zahlbr., Rabenh. Krypt.-Fl. Ed. 2, 9(5[1]): 646 (1935[1936]). Syn. nov. Type. [UKRAINE. Carpathians:] Lopušanka, 500 m elev., [corticolous] 1931, Nádvořník (lectotype: HBG!, selected here; MycoBank No: MBT 10017692).

**Typifications.** The type specimen of *Pertusaria chloropolia* consists of thin, continuous thallus with discrete soralia forming from flat parts of thalli or from slightly convex areoles and contains thamnolic acid (detected by I. M. Brodo). In the type specimen of *P. chloropolia* f. *cana*, soralia are partly damaged, but, similarly to the type of *P. chloropolia*, the type consists of thin, continuous thallus with discrete soralia and contains thamnolic acid (detected by I. M. Brodo). In the protologue of *P. chloropolia* f. *cana*, the type locality was cited as 'Tschechoslowakei: Karpatorußland, Lopusanka' (Erichsen 1935), but to our knowledge, it is now located in western Ukraine. The name 'Lopusanka' is a spelling error as, on the label, it is 'Lopušanka'.

Erichsen (1935) cited only one locality for both names. However, the lectotypes are selected, because it is not known if, at the time of describing both taxa, C. F. E. Erichsen used only one element upon which the validating descriptions were based (Art. 9.3; Turland et al. (2018); see also McNeill (2014)).

**Description.** Thallus crustose, grey, matt or more often shiny, thin, continuous, slightly folded, cracked to cracked areolate. Areoles flat or rarely convex, not constricted at the base. Soralia whitish to greenish-grey, flat or more often convex, rounded or irregular, mostly discrete and separated, bursting from flat parts of thallus or from areoles, sometimes crowded and the neighbouring soralia more or less fused, but still the boundaries often visible between them or, very rarely, soralia fused into irregular patches in older parts of thallus. Soredia up to 50 µm in diam., often in consoredia up to 100 µm wide. Apothecia very rare, single, up to 1.2 mm in diam. Thalline margin present, esorediate or partly to completely sorediate. Excipulum proporium not evident. Disc reddish-brown, thinly white pruinose. Hymenium up to 100 µm high. Epihymenium straw-brown (K+ pale reddish-brown), with dense granules dissolving in K. Paraphyses not capitate, sometimes anastomosing. Asci 8-spored, with uniformly KI+ blue apical dome. Ascospores 0–3(–5)-septate, spiralled in asci, hyaline, fusiform, curved, 35–48 × 5–7 µm. Pycnidia not known. Photobiont chlorococcoid, cells up to 12 µm in diam.

**Chemistry.** Thamnolic acid (major), elatinic acid (minor, trace or absent) and squamatic acid (trace or absent). Spot tests: cortex, apothecial section, soralia and medulla K+ lemon-yellow, Pd+ yellow to orange, UV–.

**Notes.** *Loxospora chloropolia* differs from *L. elatina* in having a thin, continuous to cracked-areolate thallus with mostly regular soralia, which are discrete

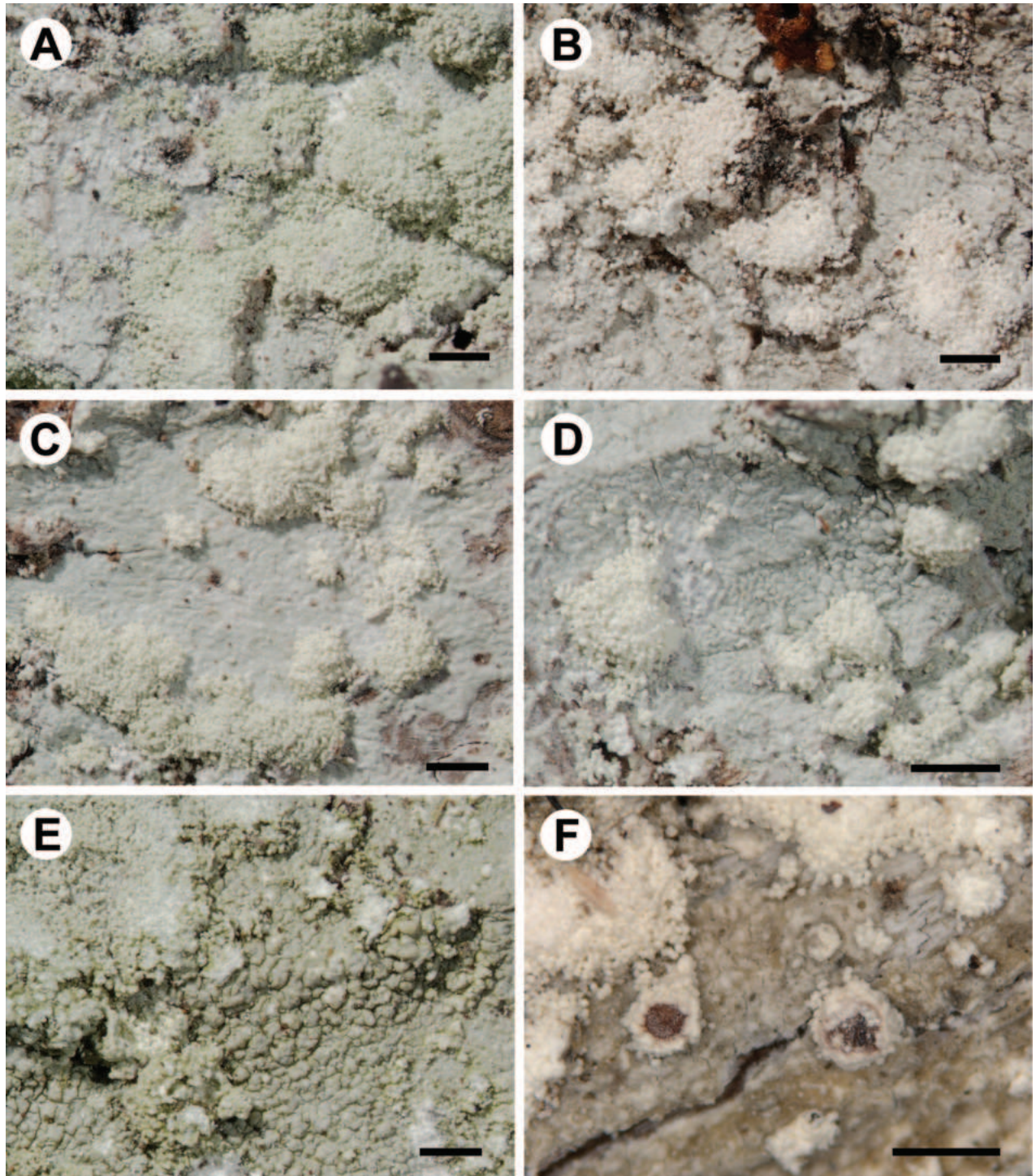


**Figure 7.** Morphology of *Loxospora chloropolia* (for details of specimens, see Table 1, Suppl. material 3) **A–C** smooth to folded thalli with mostly discrete soralia (**A** UGDA L-60095 **B** UGDA L-31983 **C** UGDA L-54253) **D, E** thalli with folded to areolate areas (**D** UGDA L-60093 **E** UGDA L-60096) **F** apothecia with sorediate margins (Ellis L456, E 01043201). Scale bars: 1 mm.

at least in young parts of thalli (Fig. 7). Areoles in the central parts of larger thalli may become convex (in few specimens; Fig. 7E), but are never tuberculate or isidia-like as in *L. elatina* (Fig. 8). Soralia develop by breaking the cortex and are mostly regular, discrete and convex, rarely flat. Sometimes the neighbouring soralia are fused; however it is still possible to detect the boundaries

between individual soralia in most cases. *Loxospora elatina*, in contrast, has thalli which are, in most cases, tuberculate (sometimes only locally) or with areoles that resemble coarse isidia (Fig. 8). Tuberculate areoles are grouped or dispersed and constricted at the base. Soralia develop from the top of the tuberculate or pustulate areoles and are never regular as in *L. chloropolia* and, in most thalli, form granular-sorediate patches covering large areas (sometimes almost the entire thallus is covered with soredia; Fig. 8D). Moreover, these species differ in several nucleotide positions in both nuITS rDNA and RPB1 markers (Tables 2, 3).

*Loxospora chloropolia* can be confused with sorediate species of *Chicitaeta*, but they contain 2'-*O*-methylperlatolic acid and the thallus is K negative (Lendemmer 2013; Guzow-Krzemińska et al. 2018). *Lecanora norvegica* Tønsberg is another similar species, which occurs on similar substrates, but it contains atranorin and protocetraric acid (Tønsberg 1992; Kukwa and Kubiak 2007).

**Habitat and distribution.** The species is corticolous and grows in deciduous or mixed forests on bark of *Abies alba*, *Acer pseudoplatanus*, *Alnus glutinosa*, *Betula* spp., *Corylus avellana*, *Fagus sylvatica*, *Juniperus communis*, *Larix decidua*, *Picea abies*, *Pinus sylvestris*, *Populus tremula*, *Quercus* spp., *Sorbus aucuparia* and *Tilia cordata*. So far, it is known from Czechia, Great Britain, Latvia, Norway, Poland, Sweden, Switzerland (type locality) and Ukraine.

**Specimens examined.** See Suppl. material 3.

### ***Loxospora elatina* (Ach.) A. Massal.**

Fig. 8

Ric. Auton. Lich. Crost.: 138 (1852). – *Lecanora elatina* Ach., Lich. Univ.: 387 (1810).

**Type.** Lusatia, [corticolous], Mosig? (lectotype: H-ACH 1199A!, selected here; MycoBank No: MBT 10017693).

**Typification.** In the protologue of *Lecanora elatina*, Acharius (1810) cited the locality as “Habitat in cortice *Pini Abietis* Silesiae. Mosig”. The type collection in H-ACH consists of four pieces of bark covered with thalli of *Loxospora elatina*. Three (H-ACH 1199A, 1199B and 1199C) are annotated “Lusatia” with a very faint pencil note next to H-ACH 1199A deciphered as possibly “Mosig” (this note probably not added by Acharius himself as the handwriting in pencil differs from all notes made in ink). The fourth specimen, H-ACH 1199D is annotated “Germania. Schrader”. According to the label added in modern times and attached to the type collection, Lusatia was part of Silesia, therefore, the three specimens annotated “Lusatia” can be considered original material; however, it is impossible to verify whether all three were collected by Mosig. Nevertheless, the largest sample (H-ACH 1199A) is fertile and apothecia were mentioned in the diagnosis, therefore it is selected as lectotype. The Acharius collection in BM also contains a specimen of *Lecanora elatina*, however without any locality details; therefore, it cannot be considered as an isolectotype.

**Description.** Thallus crustose, grey, matt, thin (at the margin) or more usually thick, continuous or cracked, slightly folded at least the margins, later areolate-verrucose to tuberculate (sometimes only part of the thallus tuberculate).

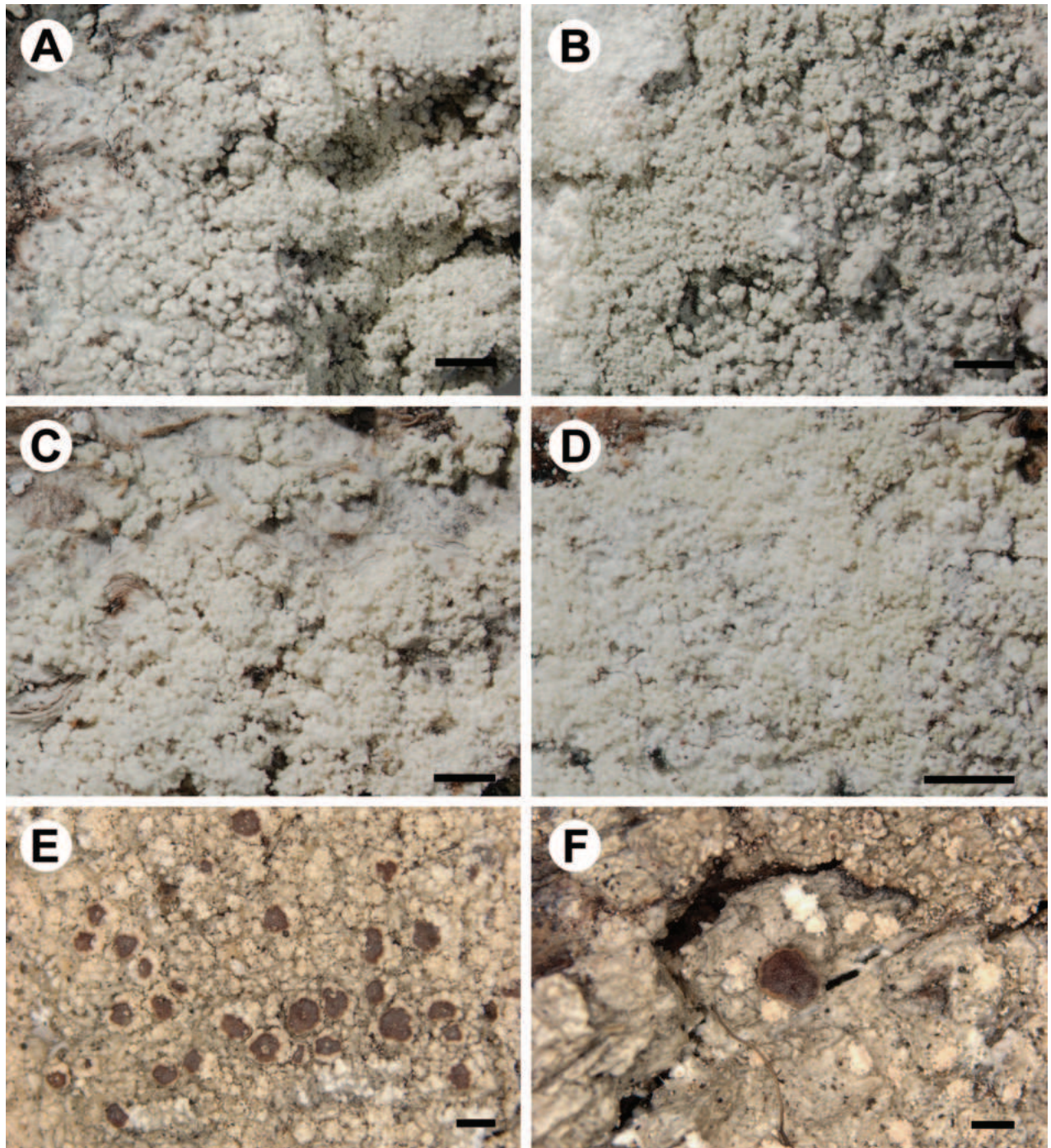


**Figure 8.** Morphology of *Loxospora elatina* (for details of specimens, see Table 1, Suppl. material 3) **A, B** thalli with tuberculate areoles and irregular and partly fused soralia (**A** UGDA L-47757 **B** UGDA L- 47762) **C** thallus with soralia bursting from areoles and later fused (UGDA L-47761) **D** soralia covering most parts of the thallus (UGDA L-47760) **E, F** apothecia with sorediate or esorediate margins (O L-97759). Scale bars: 1 mm.

Areoles usually strongly convex, tuberculate and constricted at the base or resembling coarse isidia, sometimes pustulate, dispersed or aggregated. Soralia whitish to greenish-grey, flat or more often convex, rounded or more often irregular, bursting from the top of areoles, often fused and tending to coalesce locally on the thallus or covering most parts of the thallus, sometimes developing from irregular cracks of the thallus. Soredia up to 60  $\mu\text{m}$  in diam., often

in consoredia up to 120 µm wide. Apothecia rare, up to 1.2 mm in diam., single or grouped up to five apothecia. Thalline margin present in young apothecia, smooth to flexuose, verrucose or dentate, sometimes with small soralia, later excluded. Excipulum proprium thin, flesh-coloured to white grey in surface view, orange-brown in section, smooth or more often flexuose, up to 100 µm wide in section. Disc reddish-brown, thinly white pruinose. Hymenium up to 125 µm high. Epihymenium straw-brown (K+ pale reddish-brown), with dense granules dissolving in K. Paraphyses not capitate, sometimes anastomosing. Asci 8-spored, with uniformly KI+ blue apical dome. Ascospores 0–5-septate, spiralled in asci, hyaline, fusiform, curved, 35–53(–64) × 4.5–6.5(–7) µm. Pycnidia not known. Photobiont chlorococcoid, cells up to 12 µm in diam.

**Chemistry.** Thamnic acid (major), elatinic acid (minor, trace or absent) and squamatic acid (trace or absent). Spot tests: cortex, apothecial section, soralia and medulla K+ lemon-yellow, Pd+ yellow to orange, UV–.

**Notes.** *Loxospora elatina* is similar to *L. chloropolia*; for differences, see under that species. The name (often as *Haematomma elatinum* (Ach.) A. Massal.) was often used in the past for the non-sorediate specimens currently referred to as *L. ochrophaea*. Both species, as mentioned above, are indeed morphologically (except for the production of soralia) and chemically almost identical and may represent the same species.

*Loxospora ochrophaeoides*, when described, was compared with *L. ochrophaea* and characterised as differing only in the presence of semi-globose soralia (Kalb and Hafellner 1992). Whether this taxon is distinct or synonymous with *L. elatina* or *L. chloropolia*, needs further studies using molecular techniques.

Some specimens of *L. elatina* were found to be determined as *Ochrolechia androgyna* (Hoffm.) Arnold, but that species and the recently segregated *O. bahusiensis* H. Magn. and *O. mahuensis* Räsänen differ in the production of gyrophoric acid and simple, larger ascospores (Tønsberg 1992; Kukwa 2011).

**Habitat and distribution.** The species is corticolous or lignicolous and grows on bark of various coniferous and deciduous tree in forests. The species was reported from many countries in the Northern Hemisphere; however, as some records may belong to *L. chloropolia*, its distribution needs revision. In the course of this study, we examined specimens from Austria, Czechia, Estonia, Finland, Latvia, Lithuania, Poland, Slovakia, United Kingdom, Ukraine and USA.

**Specimens of *Loxospora elatina* and *L. ochrophaea* examined.** See Suppl. material 3.

## Acknowledgements

The authors express gratitude to Curators of BG, BILAS, E, H, O Herbaria and Dr. Jiří Maliček for the loan of *Loxospora* spp. specimens, Professor Teuvo Ahti for a discussion of the Acharius collection of *Lecanora elatina* and Professor H. Thorsten Lumbsch for the information on the sequences of *Loxospora lecanoriformis*. Our friends, Dr. Adam Flakus and Dr. Emilia A. Ossowska are thanked for their help with taking pictures of species of *Loxospora* s.l. and Dr. Rafał Szymczyk, for sending us several fresh collections of *Loxospora*. Jason Hollinger and Dr. Dariusz Kubiak are thanked for allowing us to use pictures of two *Chicitea* species. Author Lendemer's contribution is part of US NSF DEB Award #2115190.

## Additional information

### Conflict of interest

The authors have declared that no competing interests exist.

### Ethical statement

No ethical statement was reported.

### Funding

No funding was reported.

### Author contributions

Łucja Ptach-Styn: conceptualization, molecular and phylogenetic analyses, identification of secondary metabolites, manuscript writing and editing; Beata Guzow-Krzemińska: conceptualization, molecular and phylogenetic analyses, manuscript writing and editing; James Lendemer: conceptualization, identification of specimens, manuscript writing and editing; Tor Tønsberg: identification of secondary metabolites, manuscript writing and editing; Martin Kukwa: conceptualization, identification of secondary metabolites and revision of specimens, manuscript writing and editing.

### Author ORCIDs

Łucja Ptach-Styn  <https://orcid.org/0000-0003-2027-1636>

Beata Guzow-Krzemińska  <https://orcid.org/0000-0003-0805-7987>

James C. Lendemer  <https://orcid.org/0000-0003-1186-0711>

Martin Kukwa  <https://orcid.org/0000-0003-1560-909X>

### Data availability

All of the data that support the findings of this study are available in the main text or Supplementary Information.

## References

- Acharius E (1810) *Lichenographia Universalis*. J. F. Danckwerts, Göttingen, 1–696. [+ Tab. XIV]
- Altschul SF, Gish W, Miller W, Myers EW, Lipman DJ (1990) Basic local alignment search tool. *Journal of Molecular Biology* 215(3): 403–410. [https://doi.org/10.1016/S0022-2836\(05\)80360-2](https://doi.org/10.1016/S0022-2836(05)80360-2)
- Berger F, Breuss O, Maliček J, Türk R (2018) Lichens in the primeval forest areas ‘Großer Urwald’ and ‘Kleiner Urwald’ (Rothwald, ‘Dürrenstein Wilderness Area’, Lower Austria, Austria). *Herzogia* 31(1): 716–731. <https://doi.org/10.13158/hea.31.1.2018.716>
- Brodo IM, Culberson WL (1986) *Haematomma pustulatum*, sp. nov. (Ascomycotina, Haematommataceae): A common, widespread, sterile lichen of eastern North America. *The Bryologist* 89(3): 203–205. <https://doi.org/10.2307/3243284>
- Brodo IM, Sharnoff SL, Sharnoff S (2001) *Lichens of North America*. Yale University Press, New Haven & London, 1–795. <https://doi.org/10.29173/bluejay5827>
- Büdel B, Scheidegger C (2008) Thallus morphology and anatomy. In: Nash III TH (Ed.) *Lichen Biology*. 2<sup>nd</sup> Ed. Cambridge University Press, Cambridge, 40–68. <https://doi.org/10.1017/CBO9780511790478.005>

- Buschbom J, Mueller GM (2006) Testing “species pair” hypotheses: Evolutionary processes in the lichen-forming species complex *Porpidia flavocoerulescens* and *Porpidia melinodes*. *Molecular Biology and Evolution* 23(3): 574–586. <https://doi.org/10.1093/molbev/msj063>
- Chernomor O, von Haeseler A, Minh BQ (2016) Terrace aware data structure for phylogenomic inference from supermatrices. *Systematic Biology* 65(6): 997–1008. <https://doi.org/10.1093/sysbio/syw037>
- Clement M, Snell Q, Walke P, Posada D, Crandall K (2002) TCS: estimating gene genealogies. 16<sup>th</sup> International Parallel and Distributed Processing Symposium 2: 184. <https://doi.org/10.1109/IPDPS.2002.1016585>
- Crespo A, Pérez-Ortega S (2009) Cryptic species and species pairs in lichens: A discussion on the relationship between molecular phylogenies and morphological characters. *Anales del Jardín Botánico de Madrid* 66(1): 71–81. <https://doi.org/10.3989/ajbm.2225>
- Culberson CF, Kristinsson H (1970) A standardized method for the identification of lichen products. *Journal of Chromatography A* 46: 85–93. [https://doi.org/10.1016/S0021-9673\(00\)83967-9](https://doi.org/10.1016/S0021-9673(00)83967-9)
- Ekman S, Tønsberg T (2002) Most species of *Lepraria* and *Leproloma* form a monophyletic group closely related to *Stereocaulon*. *Mycological Research* 106(11): 1262–1276. <https://doi.org/10.1017/S0953756202006718>
- Erichsen CFE (1935) [1936] Pertusariaceae. In: Zahlbruckner A (Ed.) *Dr. L. Rabenhorsts Kryptogamenflora von Deutschland, Österreich und der Schweiz*. Leipzig, Akademische Verlagsgesellschaft 9(5)[1]: 321–701.
- Ertz D, Guzow-Krzemińska B, Thor G, Łubek A, Kukwa M (2018) Photobiont switching causes changes in the reproduction strategy and phenotypic dimorphism in the Arthoniomycetes. *Scientific Reports* 8(1): 4952. <https://doi.org/10.1038/s41598-018-23219-3>
- Galloway DJ (2007) *Flora of New Zealand. Lichens. Revised Second Edition Including Lichen-Forming and Lichenicolous Fungi. Vol. 1.* Manaaki Whenua Press, Lincoln, Vol. 1, [i–cxxx +] 1–1006.
- Galtier N, Gouy M, Gautier C (1996) SEAVIEW and PHYLO\_WIN: Two graphic tools for sequence alignment and molecular phylogeny. *Bioinformatics (Oxford, England)* 12(6): 543–548. <https://doi.org/10.1093/bioinformatics/12.6.543>
- Gardes M, Bruns TD (1993) ITS primers with enhanced specificity for basidiomycetes – application to the identification of mycorrhizae and rusts. *Molecular Ecology* 2(2): 113–118. <https://doi.org/10.1111/j.1365-294X.1993.tb00005.x>
- Gouy M, Guindon S, Gascuel O (2010) SeaView version 4: A multiplatform graphical user interface for sequence alignment and phylogenetic tree building. *Molecular Biology and Evolution* 27(2): 221–224. <https://doi.org/10.1093/molbev/msp259>
- Grewe F, Lagostina E, Wu H, Printzen C, Lumbsch HT (2018) Population genomic analyses of RAD sequences resolves the phylogenetic relationship of the lichen-forming fungal species *Usnea antarctica* and *Usnea aurantiacoatra*. *MycKeys* 43: 91–113. <https://doi.org/10.3897/mycokeys.43.29093>
- Guzow-Krzemińska B, Węgrzyn G (2000) Potential use of restriction analysis of PCR-amplified DNA fragments in taxonomy of lichens. *Mycotaxon* 76: 305–313.
- Guzow-Krzemińska B, Malíček J, Tønsberg T, Oset M, Łubek A, Kukwa M (2017) *Lecanora stanislai*, a new, sterile, usnic acid containing lichen species from Eurasia and North America. *Phytotaxa* 329(3): 201–211. <https://doi.org/10.11646/phytotaxa.329.3.1>

- Guzow-Krzemińska B, Łubek A, Kubiak D, Ossowska E, Kukwa M (2018) Phylogenetic approaches reveal a new sterile lichen in the genus *Loxospora* (Sarrameanales, Ascomycota) in Poland. *Phytotaxa* 348(3): 211–220. <https://doi.org/10.11646/phytotaxa.348.3.4>
- Guzow-Krzemińska B, Sérusiaux E, van den Boom PPG, Brand AM, Launis A, Łubek A, Kukwa M (2019) Understanding the evolution of phenotypical characters in the *Micarea prasina* group (Pilocarpaceae) and descriptions of six new species within the group. *MycKeys* 57: 1–30. <https://doi.org/10.3897/mycokeys.57.33267>
- Hafellner J (1984) Studien in Richtung einer natürllicheren Gliederung der Sammelfamilien Lecanoraceae und Lecideaceae. Beiheft zur Nova Hedwigia 79: 241–371.
- Hafellner J, Türk R (2016) Die lichenisierten Pilze Österreichs – eine neue Checkliste der bisher nachgewiesenen Taxa mit Angaben zu Verbreitung und Substratökologie. *Stapfia* 104(1): 1–216.
- Hoang DT, Chernomor O, Von Haeseler A, Minh BQ, Vinh LS (2018) UFBoot2: Improving the ultrafast bootstrap approximation. *Molecular Biology and Evolution* 35(2): 518–522. <https://doi.org/10.1093/molbev/msx281>
- Hodkinson BP, Lendemer JC (2012) Phylogeny and taxonomy of an enigmatic sterile lichen. *Systematic Botany* 37(4): 835–844. <https://doi.org/10.1600/036364412X656536>
- Hodkinson BP, Lendemer JC (2013) Next-generation sequencing reveals sterile crustose lichen phylogeny. *Mycosphere: Journal of Fungal Biology* 4(6): 1028–1039. <https://doi.org/10.5943/mycosphere/4/6/1>
- Huelsenbeck JP, Ronquist F (2001) MRBAYES: Bayesian inference of phylogeny. *Bioinformatics (Oxford, England)* 17(8): 754–755. <https://doi.org/10.1093/bioinformatics/17.8.754>
- Kalb K, Hafellner J (1992) Bemerkenswerte Flechten und lichenicole Pilze von der Insel Madeira. *Herzogia* 9: 45–102. <https://doi.org/10.1127/herzogia/9/1992/45>
- Kalyaanamoorthy S, Minh B, Wong T, von Haeseler A, Jermiin LS (2017) ModelFinder: Fast model selection for accurate phylogenetic estimates. *Nature Methods* 14(6): 587–589. <https://doi.org/10.1038/nmeth.4285>
- Kantvilas G (2000) Additions from the Southern Hemisphere to the lichen genus *Loxospora*. *Herzogia* 14: 35–38. <https://doi.org/10.1127/herzogia/14/2000/35>
- Kantvilas G (2004) Sarrameanaceae. In: McCarthy PM, Mallett K (Eds) *Flora of Australia*. Volume 56A, Lichens 4. CSIRO Publishing, Melbourne, 74–77.
- Kelly LJ, Hollingsworth PM, Coppins BJ, Ellis CJ, Harrold P, Tosh J, Yahr R (2011) DNA barcoding of lichenized fungi demonstrates high identification success in a floristic context. *The New Phytologist* 191(1): 288–300. <https://doi.org/10.1111/j.1469-8137.2011.03677.x>
- Kukwa M (2011) The lichen genus *Ochrolechia* in Europe. *Fundacja Rozwoju Uniwersytetu Gdańskiego, Gdańsk*, 1–309.
- Kukwa M, Kubiak D (2007) Six sorediate crustose lichens new to Poland. *Mycotaxon* 102: 155–164.
- Kukwa M, Pérez-Ortega S (2010) A second species of *Botryolepraria* from the Neotropics and the phylogenetic placement of the genus within Ascomycota. *Mycological Progress* 9(3): 345–351. <https://doi.org/10.1007/s11557-009-0642-0>
- Kukwa M, Kosecka M, Jabłońska A, Flakus A, Rodriguez-Flakus P, Guzow-Krzemińska B (2023) *Pseudolepraria*, a new leprose genus revealed in Ramalinaceae (Ascomycota, Lecanoromycetes, Lecanorales) to accommodate *Lepraria stephaniana*. *MycKeys* 96: 97–112. <https://doi.org/10.3897/mycokeys.96.98029>
- Laundon JR (1963) The taxonomy of sterile crustaceous lichens in the British Isles. 2. Corticolous and lignicolous species. *Lichenologist (London, England)* 2(2): 101–151. <https://doi.org/10.1017/S002428296300013X>

- Lendemer JC (2013) Two new sterile species of *Loxospora* (Sarrameanaceae: Lichenized Ascomycetes) from the Mid-Atlantic Coastal Plane. *Journal of the North Carolina Academy of Science* 129(3): 71–81. <https://doi.org/10.7572/2167-5880-129.3.71>
- Lendemer JC, Harris RC (2014) Studies in lichens and lichenicolous fungi – No. 18: Resolution of three names introduced by Degelius and Magnusson based on material from the Great Smoky Mountains. *Castanea* 79(2): 106–117. <https://doi.org/10.2179/14-006>
- Lendemer JC, Harris RC (2017) Nomenclatural changes for North American members of the *Variolaria*-group necessitated by the recognition of *Lepra* (Pertusariales). *The Bryologist* 120(2): 182–189. <https://doi.org/10.1639/0007-2745-120.2.182>
- Lendemer JC, Noell N (2018) *Delmarva Lichens: An illustrated manual*. *Memoirs of the Torrey Botanical Society* 28: 1–386.
- Lohtander K, Myllys L, Sundin R, Källersjö M, Tehler A (1998) The species pair concept in the lichen *Dendrographa leucophaea* (Arthoniales): Analyses based on ITS sequences. *The Bryologist* 101(3): 404–411. [https://doi.org/10.1639/0007-2745\(1998\)101\[404:TSPCIT\]2.0.CO;2](https://doi.org/10.1639/0007-2745(1998)101[404:TSPCIT]2.0.CO;2)
- Lücking R, Hodkinson BP, Leavitt SD (2017 [2016]) The 2016 classification of lichenized fungi in the Ascomycota and Basidiomycota – Approaching one thousand genera. *The Bryologist* 119(4): 361–416. <https://doi.org/10.1639/0007-2745-119.4.361>
- Lumbsch HT, Archer AW, Elix JA (2007) A new species of *Loxospora* (lichenized Ascomycota: Sarrameanaceae) from Australia. *Lichenologist* (London, England) 39(6): 509–517. <https://doi.org/10.1017/S0024282907007153>
- Malíček J, Palice Z, Vondrák J, Lúbek A, Kukwa M (2018) *Bacidia albogranulosa* (Ramalinaceae, lichenized Ascomycota), a new sorediate lichen from European old-growth forests. *MycKeys* 44: 51–62. <https://doi.org/10.3897/mycokeys.44.30199>
- Marthinsen G, Rui S, Timdal E (2019) OLICH: A reference library of DNA barcodes for Nordic lichens. *Biodiversity Data Journal* 7: e36252. <https://doi.org/10.3897/BDJ.7.e36252>
- Massalongo AB (1852) *Ricerche sull'autonomia dei licheni crostosi e materiali pella loro naturale ordinazione*. Tipografia di Frizierio, Verona, 1–207.
- Matheny PB, Liu YJ, Ammirati JF, Hall BD (2002) Using RPB1 sequences to improve phylogenetic inference among mushrooms (*Inocybe*, Agaricales). *American Journal of Botany* 89(4): 688–698. <https://doi.org/10.3732/ajb.89.4.688>
- Mattsson J-E, Lumbsch HT (1989) The use of the species pair concept in lichen taxonomy. *Taxon* 38(2): 238–241. <https://doi.org/10.2307/1220840>
- McNeill J (2014) Holotype specimens and type citations: General issues. *Taxon* 63(5): 1112–1113. <https://doi.org/10.12705/635.7>
- Miadlikowska J, Schoch CL, Kageyama SA, Molnar K, Lutzoni F, McCune B (2011) *Hypogymnia* phylogeny, including *Cavernularia*, reveals biogeographic structure. *The Bryologist* 114(2): 392–400. <https://doi.org/10.1639/0007-2745-114.2.392>
- Miller MA, Pfeiffer W, Schwartz T (2010) Creating the CIPRES Science Gateway for inference of large phylogenetic trees in Proceedings of the Gateway Computing Environments Workshop (GCE), 14 Nov. 2010, New Orleans, LA, 1–8. <https://doi.org/10.1109/GCE.2010.5676129>
- Myllys L, Lohtander K, Tehler A (2011)  $\beta$ -Tubulin, ITS and group I intron sequences challenge the species pair concept in *Physcia aipolia* and *P. caesia*. *Mycologia* 93(2): 335–343. <https://doi.org/10.1080/00275514.2001.12063165>
- Nguyen LT, Schmidt HA, Von Haeseler A, Minh BQ (2015) IQ-TREE: A fast and effective stochastic algorithm for estimating maximum-likelihood phylogenies. *Molecular Biology and Evolution* 32(1): 268–274. <https://doi.org/10.1093/molbev/msu300>

- Ohmura Y (2020) *Usnea nipparensis* and *U. sinensis* form a 'species pair' presuming morphological, chemical and molecular phylogenetic data. *Plant and Fungal Systematics* 65(2): 265–271. <https://doi.org/10.35535/pfsyst-2020-0023>
- Ohmura Y, Kashiwadani H (2018) Checklist of lichens and allied fungi of Japan. National Museum of Nature and Science Monographs 49: 1–140.
- Onuț-Brännström I, Benjamin M, Scofield DG, Heiðmarsson S, Andersson MGI, Lindström ES, Johannesson H (2018) Sharing of photobionts in sympatric populations of *Thamnolia* and *Cetraria* lichens: Evidence from high-throughput sequencing. *Scientific Reports* 8(1): 4406. <https://doi.org/10.1038/s41598-018-22470-y>
- Orange A (2020) *Lithocalla* (Ascomycota, Lecanorales), a new genus of leprose lichens containing usnic acid. *Lichenologist* (London, England) 52(6): 425–435. <https://doi.org/10.1017/S0024282920000419>
- Orange A, James PW, White FJ (2001) Microchemical methods for the identification of lichens. British Lichen Society, London, 1–101.
- Papong K, Boonpragob K, Lumbsch HT (2009) Additional lichen records from Thailand 1. *Loxospora lecaniformis* (Sarrameanaceae). *Australasian Lichenology* 65: 50–51.
- Poelt J (1970) Das Konzept der Artenpaare bei den Flechten. *Vortrage aus dem Gesamtgebiet der Botanik, N.F.* 4: 187–198.
- Rambaut A (2009) FigTree v1.4., A Graphical Viewer of Phylogenetic Trees. <http://tree.bio.ed.ac.uk/software/figtree/>
- Ronquist F, Huelsenbeck JP (2003) MrBayes 3: Bayesian phylogenetic inference under mixed models. *Bioinformatics* (Oxford, England) 19(12): 1572–1574. <https://doi.org/10.1093/bioinformatics/btg180>
- Sanders WB (2014) Complete life cycle of the lichen fungus *Calopadia puiggarii* (Pilocarpaceae, Ascomycetes) documented in situ: Propagule dispersal, establishment of symbiosis, thallus development, and formation of sexual and asexual reproductive structures. *American Journal of Botany* 101(11): 1836–1848. <https://doi.org/10.3732/ajb.1400272>
- Sanderson NA, Brightman BJ, Brightman F (2008) *Loxospora* Massal. (1952). In: Smith CW, Aptroot A, Coppins BJ, Fletcher A, Gilbert OL, James PW, Wolseley PA (Eds) *The Lichens of Great Britain and Ireland*. British Lichen Society, London, 564.
- Sela I, Ashkenazy H, Katoh K, Pupko T (2015) GUIDANCE2: Accurate detection of unreliable alignment regions accounting for the uncertainty of multiple parameters. *Nucleic Acids Research* 43(W1): W7–W14. <https://doi.org/10.1093/nar/gkv318>
- Staiger B, Kalb K (1995) *Haematomma*-studien. I. Die Flechtengattung *Haematomma*. *Bibliotheca Lichenologica* 59: 1–198.
- Stenroos S, Velmala S, Pykälä J, Ahti T (2016) Lichens of Finland. *Norrinia* 30: 1–896.
- Stiller JW, Hall BD (1997) The origin of red algae: Implications for plastid evolution. *Proceedings of the National Academy of Sciences of the United States of America* 94(9): 4520–4525. <https://doi.org/10.1073/pnas.94.9.4520>
- Tehler A, Ertz D, Irestedt M (2013) The genus *Dirina* (Roccellaceae, Arthoniales) revisited. *Lichenologist* (London, England) 45(4): 427–476. <https://doi.org/10.1017/S0024282913000121>
- Tønsberg T (1992) The sorediate and isidiate, corticolous, crustose lichens in Norway. *Sommerfeltia* 14(1): 1–331. <https://doi.org/10.2478/som-1992-0002>
- Tuckerman E (1848) A synopsis of the lichens of New England, the Northern United States and British America. *Proceedings of the American Academy of Arts and Sciences* 1: 195–285. <https://doi.org/10.5962/bhl.title.51533>

- Turland NJ, Wiersema JH, Barrie FR, Greuter W, Hawksworth DL, Herendeen PS, Knapp S, Kusber W-H, Li D-Z, Marhold K, May TW, McNeill J, Monro AM, Prado J, Price MJ, Smith GF [Eds] (2018) International Code of Nomenclature for algae, fungi, and plants (Shenzhen Code) adopted by the Nineteenth International Botanical Congress Shenzhen, China, July 2017. *Regnum Vegetabile* 159, 254 pp. <https://doi.org/10.12705/Code.2018>
- Urbanavichus G (2010) A checklist of the lichen flora of Russia. Nauka, St. Petersburg, 1–194.
- Urbanavichus G, Vondrák J, Urbanavichene I, Palice Z, Maliček J (2020) Lichens and allied non-lichenized fungi of virgin forests in the Caucasus State Nature Biosphere Reserve (Western Caucasus, Russia). *Herzogia* 33(1): 90–138. <https://doi.org/10.13158/hea.33.1.2020.90>
- Werth S, Scheidegger C (2012) Congruent genetic structure in the lichen-forming fungus *Lobaria pulmonaria* and its green-algal photobiont. *Molecular Plant-Microbe Interactions* 25(2): 220–230. <https://doi.org/10.1094/MPMI-03-11-0081>
- Westberg M, Moberg R, Myrdal M, Nordin A, Ekman S (2021) Santesson's Checklist of Fennoscandian Lichen-Forming and Lichenicolous Fungi. Uppsala University, Museum of Evolution, Uppsala, 1–933.
- White TJ, Bruns T, Lee S, Taylor J (1990) Amplification and direct sequencing of fungal ribosomal RNA genes for phylogenetics. In: Innes MA, Gelfand DH, Sninsky JJ, White TJ (Eds) *PCR Protocols: A Guide to Methods and Applications*. Academic Press, Elsevier, 315–322. <https://doi.org/10.1016/B978-0-12-372180-8.50042-1>
- Wirth V, Tønsberg T, Feif A, Stevenson D (2018) *Loxospora cristinae* found in Germany. *Herzogia* 31(2): 995–999. <https://doi.org/10.13158/hea.31.2.2018.995>
- Yakovchenko LS, Vondrák J, Ohmura Y, Korchikov ES, Vondrákova OS, Davydov EA (2017) *Candelariella blastidiata* sp. nov. (Ascomycota, Candelariaceae) from Eurasia and North America, and a key for grey thalli *Candelariella*. *Lichenologist* (London, England) 49(2): 117–126. <https://doi.org/10.1017/S0024282917000020>
- Zoller S, Scheidegger C, Sperisen C (1999) PCR primers for the amplification of mitochondrial small subunit ribosomal DNA of lichen-forming ascomycetes. *Lichenologist* (London, England) 31(5): 511–516. <https://doi.org/10.1006/lich.1999.0220>

## Supplementary material 1

### Conditions for each set of primers used in PCR

Authors: Łucja Ptach-Styn, Beata Guzow-Krzemińska, James C. Lendemer, Tor Tønsberg, Martin Kukwa

Data type: docx

Copyright notice: This dataset is made available under the Open Database License (<http://opendatacommons.org/licenses/odbl/1.0/>). The Open Database License (ODbL) is a license agreement intended to allow users to freely share, modify, and use this Dataset while maintaining this same freedom for others, provided that the original source and author(s) are credited.

Link: <https://doi.org/10.3897/mycokeys.102.116196.suppl1>

## Supplementary material 2

### Sequences obtained from GenBank and used in phylogenetic analyses

Authors: Łucja Ptach-Styn, Beata Guzow-Krzemińska, James C. Lendemer, Tor Tønnsberg, Martin Kukwa

Data type: xlsx

Explanation note: Samples marked with an asterisk in herbarium column were revised by authors.

Copyright notice: This dataset is made available under the Open Database License (<http://opendatacommons.org/licenses/odbl/1.0/>). The Open Database License (ODbL) is a license agreement intended to allow users to freely share, modify, and use this Dataset while maintaining this same freedom for others, provided that the original source and author(s) are credited.

Link: <https://doi.org/10.3897/mycokeys.102.116196.suppl2>

## Supplementary material 3

### Specimens of *Loxospora chloropolia*, *L. elatina* and *L. ochrophaea* revised for this study

Authors: Łucja Ptach-Styn, Beata Guzow-Krzemińska, James C. Lendemer, Tor Tønnsberg, Martin Kukwa

Data type: xlsx

Copyright notice: This dataset is made available under the Open Database License (<http://opendatacommons.org/licenses/odbl/1.0/>). The Open Database License (ODbL) is a license agreement intended to allow users to freely share, modify, and use this Dataset while maintaining this same freedom for others, provided that the original source and author(s) are credited.

Link: <https://doi.org/10.3897/mycokeys.102.116196.suppl3>



# Three novel species of *Aquapteridospora* (Distoseptisporales, Aquapteridosporaceae) from freshwater habitats in Tibetan Plateau, China

Rong-Ju Xu<sup>1,3,4</sup>, Jun-Fu Li<sup>5</sup>, De-Qun Zhou<sup>1,6</sup>, Saranyaphat Boonmee<sup>3,4</sup>, Qi Zhao<sup>1</sup>, Ya-Ya Chen<sup>2</sup>

1 Key Laboratory for Plant Diversity and Biogeography of East Asia, Yunnan Key Laboratory of Fungal Diversity and Green Development, Kunming Institute of Botany, Chinese Academy of Sciences, Kunming, Yunnan 650201, China

2 Guizhou Provincial Institute of Crop Germplasm Resources, Guiyang 550006, China

3 School of Science, Mae Fah Luang University, Chiang Rai 57100, Thailand

4 Center of Excellence in Fungal Research, Mae Fah Luang University, Chiang Rai 57100, Thailand

5 Department of Economic Plants and Biotechnology, Yunnan Key Laboratory for Wild Plant Resources, Centre for Mountain Futures (CMF), Kunming Institute of Botany, Kunming, Yunnan 650201, China

6 Institute of Fanjing Mountain National Park, Tongren University, Guizhou 554300, China

Corresponding author: Ya-Ya Chen (wmlove@163.com), Qi Zhao (zhaoqi@mail.kib.ac.cn)

## Abstract

During an investigation of lignicolous freshwater fungi in the Tibetan Plateau, three *Aquapteridospora* taxa were collected from freshwater habitats in Xizang, China. The new species possess polyblastic, sympodial, denticles conidiogenous cells and fusiform, septate, with or without sheath conidia, that fit within the generic concept of *Aquapteridospora*, and multi-gene phylogeny placed these species within *Aquapteridospora*. Detailed morphological observations clearly demarcate three of these from extant species and are hence described as new taxa. The multi-gene phylogeny of the combined LSU, *TEF1-α*, and ITS sequence data to infer phylogenetic relationships and discuss phylogenetic affinities with morphologically similar species. Based on morphological characteristics and phylogenetic analyses, three new species viz. *A. linzhiensis*, *A. yadongensis*, and *A. submersa* are introduced. Details of asexual morphs are described, and justifications for establishing these new species are also provided in this study.

**Key words:** 3 new taxa, freshwater fungi, morphology, phylogeny, Sordariomycetes, taxonomy



Academic editor: S. C. Karunarathna

Received: 18 September 2023

Accepted: 17 October 2023

Published: 23 February 2024

Citation: Xu R-J, Li J-F, Zhou D-Q, Boonmee S, Zhao Q, Chen Y-Y (2024) Three novel species of *Aquapteridospora* (Distoseptisporales, Aquapteridosporaceae) from freshwater habitats in Tibetan Plateau, China. MycoKeys 102: 183–200. <https://doi.org/10.3897/mycokeys.102.112905>

Copyright: © Rong-Ju Xu et al.

This is an open access article distributed under terms of the Creative Commons Attribution License (Attribution 4.0 International – CC BY 4.0).

## Introduction

Freshwater ascomycetes are the ecological groups that occur saprobially on submerged or partially submerged plant substrates in aquatic habitats (Shearer 1993). Lignicolous freshwater fungi represent a highly diverse taxonomic group with a substantial population. These fungi play a pivotal role in the transfer of nutrients and the flow of energy between trophic levels in the food chain. They achieve this by breaking down complex organic compounds into simpler inorganic materials derived from dead flora and fauna (Krauss et al. 2011; Sridhar et al. 2013; Wurzbacher et al. 2014; Tsui et al. 2016). Recent research showed

that lignicolous freshwater fungi comprise a diverse taxonomic assemblage, with more than 3,870 species listed (Calabon et al. 2022). Among them, most are in the classes Dothideomycetes and Sordariomycetes (Hyde et al. 2016; Maharachchikumbura et al. 2016; Luo et al. 2019; Dong et al. 2020; Calabon et al. 2022; Wijayawardene et al. 2022). Sordariomycetes is a prominent class within Ascomycota, encompassing a wide variety of fungi (Luo et al. 2019; Calabon et al. 2022; Yang et al. 2023). In freshwater environments, Sordariomycetes stands out as a significant fungal group, playing a pivotal role in ecosystems. This class is renowned for its production of bioactive compounds (e.g., penicillins, tetracyclines, macrolides, aminoglycosides, and cephalosporins) (Poch et al. 1992; Jones et al. 2014; Wright et al. 2014; Calabon et al. 2023).

*Aquapteridospora* was initially introduced and classified within the Diaporthomycetidae genera *incertae sedis*, based on morphological and phylogenetic analyses by Yang et al. (2015). *Aquapteridospora*, with *A. lignicola* as the type species, is characterized by polyblastic, sympodial, denticles conidiogenous cells and fusiform, with pale to dark brown central cells and subhyaline end cells, with or without sheath conidia. Furthermore, Hyde et al. (2021a) introduced the family Aquapteridosporaceae to accommodate *Aquapteridospora* and placed this family in order Distoseptisporales based on divergence estimates, morphological characters, and phylogenetic analyses.

*Aquapteridospora* is a hyphomycetous genus that are commonly found in freshwater habitats, but only a few terrestrial species, such as *A. bambusinum* ( $\equiv$  *Pleurophragmium bambusinum*) was collected from dead culms of bamboo (Yang et al. 2015; Dai et al. 2017; Luo et al. 2019; Bao et al. 2021; Dong et al. 2021; Ma et al. 2022; Peng et al. 2022). These fungi play an important role in the decomposition of organics and nutrient cycling in aquatic environments (Hyde et al. 2016; Luo et al. 2018). In recent years, an increasing number of species in *Aquapteridospora* have been described and documented, including *A. aquatica*, *A. bambusinum*, *A. fusiformis*, *A. hyalina*, *A. jiangxiensis* and *A. lignicola* (Yang et al. 2015; Luo et al. 2019; Bao et al. 2021; Dong et al. 2021; Ma et al. 2022; Peng et al. 2022).

During an investigation of freshwater fungal diversity on the Tibetan Plateau, six collections possessing morphological characteristics that fit within the genus *Aquapteridospora* were collected. In particular, their morphological characteristics revealed that these collections were morphologically different from the other species in *Aquapteridospora*. In addition, phylogenetic analyses of a combined LSU, *TEF1*- $\alpha$  and ITS sequence data show that our new collections belong to distinct clades, which are distinct from other species in *Aquapteridospora*. Therefore, three new species *viz.* *Aquapteridospora linzhiensis*, *A. submersa* and *A. yadongensis* are introduced, as well as details of asexual morphs being described, and justifications for establishing these new species are provided in this study.

## Materials and methods

### Collection, morphological examination and isolation

Submerged decaying wood samples were collected from freshwater habitats in southeast Xizang, China. Fresh specimens were studied following the methods of Senanayake et al. (2020). Microscopic structures were examined by using a

stereomicroscope (SteREO Discovery.V12, Carl Zeiss Microscopy GmbH, Germany), photographed by using a Nikon ECLIPSE 80i compound microscope fitted with a Nikon DS-Ri2 digital camera, and measured by using the Tarosoft (R) Image Frame Work program. Illustrated figures were processed by using Adobe Photoshop CS6 version 10.0 software (Adobe Systems, San Jose, CA, USA).

Single spore isolation was performed on potato dextrose agar (PDA) plates following the methods described in Senanayake et al. (2020). Fungal herbarium specimens and axenic living cultures were deposited in the Herbarium of Cryptogams of the Kunming Institute of Botany, Chinese Academy of Sciences (KUN-HKAS) and Kunming Institute of Botany Culture Collection (KUNCC), Kunming, China. Faceoffungi and Index Fungorum numbers of novel species were registered (Jayasiri et al. 2015, <http://www.indexfungorum.org/Names/Names.asp>).

### **DNA extraction, PCR amplification, and sequencing**

Fresh mycelia were scraped off from colonies on PDA plates and transferred to a 1.5-ml microcentrifuge tube using a sterilized lancet for genomic DNA extraction. The TOLOBIO Plant Genomic DNA Extraction Kit, Shanghai Co. Ltd. P.R. China was used to extract fungal genomic DNA, following the protocols in the manufacturer's instructions. The DNA polymerase chain reaction (PCR) amplifications were performed by using primer pairs as follows: ITS5/ITS4 for internal transcribed spacer rDNA region and covered 5.8S ribosomal (ITS); LR0R/LR5 for the nuclear ribosomal large subunit 28S rDNA gene (LSU), and *TEF1*-983F/*TEF1*-2218R for *TEF1- $\alpha$*  (Vilgalys and Hester 1990; White et al. 1990). DNA template was carried out in 25  $\mu$ L reaction volume containing 21  $\mu$ L of 1  $\times$  Power Taq PCR Master Mix, 1  $\mu$ L of each primer (10  $\mu$ L stock) and 2  $\mu$ L of genomic DNA template. Amplifications were carried out by using the BioTeke GT9612 thermocycler (Beijing City, China). The PCR amplification conditions for ITS and LSU consisted of initial denaturation at 98  $^{\circ}$ C for 3 minutes, followed by 35 cycles of denaturation at 98  $^{\circ}$ C for 20 seconds, annealing at 53  $^{\circ}$ C for 10 seconds, extension at 72  $^{\circ}$ C for 20 seconds, final extension at 72  $^{\circ}$ C for 5 minutes; the PCR amplification conditions for *TEF1- $\alpha$*  consisted of initial denaturation at 98  $^{\circ}$ C for 3 minutes, followed by 35 cycles of denaturation at 98  $^{\circ}$ C for 20 seconds, annealing at 64  $^{\circ}$ C for 10 seconds, extension at 72  $^{\circ}$ C for 20 seconds, final extension at 72  $^{\circ}$ C for 5 minutes. PCR products were visualized by using 1% agarose gel electrophoresis stained with ethidium bromide and distinct bands were checked in Gel documentation system (Compact Desktop UV Transilluminator analyzer GL-3120). The PCR products were sequenced by Tsingke Company, Beijing, P.R. China.

### **Phylogenetic analyses**

The sequences were uploaded in GenBank database (<http://www.ncbi.nlm.nih.gov/blast/>) to search for similar taxa. Sequences generated from the LSU, *TEF1- $\alpha$*  and ITS gene regions were carefully verified before further analyses. The new sequences were submitted to GenBank, and the strain information used in this paper was provided in Table 1. Multiple sequence alignments were aligned with MAFFT v.7 (Kato and Standley 2016) <http://mafft.cbrc.jp/alignment/server/index.html>] and dataset was trimmed by TrimAlv.1.3 using the gappout

**Table 1.** Strains used for phylogenetic analyses and their corresponding GenBank numbers. The newly generated sequences are in cells with light grey shading and the type strain are in bold font.

Species	Voucher number	GenBank accession number			Reference
		LSU	ITS	TEF1- $\alpha$	
<i>Aquapteridospora aquatic</i>	<b>MFLUCC 17-2371</b>	<b>MW287767</b>	<b>MW286493</b>	/	Dong et al. (2021)
<i>A. bambusinum</i>	<b>MFLUCC 12-0850</b>	<b>KU863149</b>	<b>KU940161</b>	<b>KU940213</b>	Dai et al. (2017)
<i>A. bambusinum</i>	MFLUCC_21_0027	MZ412526	MZ412514	MZ442688	Bao et al. (2021)
<i>A. hyalina</i>	<b>GZCC 22-0072</b>	<b>ON527945</b>	<b>ON527937</b>	<b>ON533681</b>	Ma et al. (2022)
<i>A. hyalina</i>	GZCC 22-0073	ON527948	ON527940	ON533684	Ma et al. (2022)
<i>A. jiangxiensis</i>	<b>JAUCC 3008</b>	<b>MZ871502</b>	<b>MZ871501</b>	<b>MZ855767</b>	Peng et al. (2022)
<i>A. fusiformis</i>	<b>MFLUCC 18-1606</b>	<b>MK849798</b>	<b>MK828652</b>	<b>MN194056</b>	Luo et al. (2019)
<i>A. lignicola</i>	<b>MFLUCC 15-0377</b>	<b>KU221018</b>	<b>MZ868774</b>	<b>MZ892980</b>	Yang et al. (2015)
<i>A. linzhienis</i>	<b>KUNCC 10420</b>	<b>OQ970576</b>	<b>OP626343</b>	<b>OR597592</b>	This study
<i>A. linzhienis</i>	KUNCC 10444	OQ970575	OQ847781	OR597591	This study
<i>A. submersa</i>	<b>KUNCC 10446</b>	<b>OQ970579</b>	<b>OQ847783</b>	<b>OR597595</b>	This study
<i>A. submersa</i>	KUNCC 10449	OQ970580	OQ970557	OR597596	This study
<i>A. yadongensis</i>	<b>KUNCC 10445</b>	<b>OQ970577</b>	<b>OQ847782</b>	<b>OR597593</b>	This study
<i>A. yadongensis</i>	KUNCC 10448	OQ970578	OQ970556	OR597594	This study
<i>Distoseptispora atroviridis</i>	<b>GZCC 20-0511</b>	<b>MZ868763</b>	<b>MZ868772</b>	<b>MZ892978</b>	Yang et al. (2021)
<i>D. bambusae</i>	<b>MFLUCC 20-0091</b>	<b>MT232718</b>	<b>MT232713</b>	<b>MT232880</b>	Sun et al. (2020)
<i>D. euseptata</i>	MFLU 20-0568	MW081545	MW081540	MW084994	Li et al. (2021)
<i>D. fusiformis</i>	<b>GZCC 20-0512</b>	<b>MZ868764</b>	<b>MZ868773</b>	<b>MZ892979</b>	Yang et al. (2021)
<i>D. guizhouensis</i>	<b>GZCC 21-0666</b>	<b>MZ474869</b>	<b>MZ474868</b>	<b>MZ501610</b>	Hyde et al. (2021b)
<i>D. hyalina</i>	<b>MFLUCC 17-2128</b>	<b>MZ868760</b>	<b>MZ868769</b>	<b>MZ892976</b>	Yang et al. (2021)
<i>D. multiseptata</i>	MFLU 17-0856	MF077555	MF077544	MF135652	Yang et al. (2018)
<i>D. rayongensis</i>	<b>MFLUCC 18-0415</b>	<b>MH457137</b>	<b>MH457172</b>	<b>MH463253</b>	Hyde et al. (2020)
<i>D. rayongensis</i>	MFLUCC 18-0417	MH457138	MH457173	MH463254	Hyde et al. (2020)
<i>D. rostrata</i>	<b>MFLUCC 16-0969</b>	<b>MG979766</b>	<b>MG979758</b>	<b>MG988424</b>	Luo et al. (2018)
<i>D. saprophytica</i>	<b>MFLUCC 18-1238</b>	<b>MW287780</b>	<b>MW286506</b>	<b>MW396651</b>	Dong et al. (2021)
<i>D. verrucosa</i>	<b>GZCC 20-0434</b>	<b>MZ868762</b>	<b>MZ868771</b>	<b>MZ892977</b>	Yang et al. (2021)
<i>D. xishuangbannaensis</i>	<b>KUMCC 17-0290</b>	<b>MH260293</b>	<b>MH275061</b>	<b>MH412768</b>	Tibpromma et al. (2018)
<i>D. yunnansis</i>	<b>MFLUCC 20-0153</b>	<b>MW081546</b>	<b>MW081541</b>	<b>MW084995</b>	Li et al. (2021)
<i>Pseudostanjehughesia aquitropica</i>	<b>MFLUCC 16-0569</b>	<b>MF077559</b>	<b>MF077548</b>	<b>MF135655</b>	Yang et al. (2018)
<i>P. lignicola</i>	<b>MFLUCC 15-0352</b>	<b>MK849787</b>	<b>MK828643</b>	<b>MN194047</b>	Luo et al. (2019)
<i>Sporidesmium dulongense</i>	<b>MFLUCC 17-0116</b>	<b>MH795817</b>	<b>MH795812</b>	<b>MH801191</b>	Luo et al. (2019)
<i>S. lageniforme</i>	<b>DLUCC 0880</b>	<b>MK849782</b>	<b>MK828640</b>	<b>MN194044</b>	Luo et al. (2019)
<i>S. pyriformatum</i>	<b>MFLUCC 15-0620</b>	<b>KX710141</b>	<b>KX710146</b>	<b>MF135662</b>	Hyde et al. (2016)
<i>S. thailandense</i>	MFLUCC 15-0617	MF077561	MF077550	MF135657	Yang et al. (2018)
<i>S. thailandense</i>	<b>MFLUCC 15-0964</b>	<b>MF374370</b>	<b>MF374361</b>	<b>MF370957</b>	Zhang et al. (2017)
<i>Myrmecridium aquaticum</i>	<b>MFLUCC 15-0366</b>	<b>MK849804</b>	/	/	Luo et al. (2019)
<i>M. aquaticum</i>	S-1158	MK849803	MK828656	MN194061	Luo et al. (2019)
<i>M. banksiae</i>	<b>CBS 132536</b>	<b>JX069855</b>	<b>JX069871</b>	/	Crous et al. (2012)
<i>M. schulzeri</i>	CBS 100.54	EU041826	EU041769	/	Arzanlou et al. (2007)

option (<http://phylemon.bioinfo.cipf.es/utilities.html>) (Capella-Gutierrez et al. 2009). A combined sequence dataset was performed with the SquenceMatrix v.1.7.8 (Vaidya et al. 2011).

Maximum likelihood (ML) analysis was performed by RAxML-HPC2 v.8.2.12 (Stamatakis 2014) in the CIPRES Science Gateway web server (<http://www.phylo.org/portal2>) by using 1,000 rapid bootstrap replicates and the GTRGAMMA+I model. Bootstrap support values for ML equal to or greater than 75% were given above the nodes in the phylogenetic tree (Fig. 1). The model of evolution for the Bayesian inference (BI) analysis was performed by using MrModeltest v2.3 (Nylander 2004). GTR+I+G was selected as the best-fitting model for LSU, *TEF1*- $\alpha$  and ITS dataset. The Markov chain Monte Carlo sampling (BMCMC) was carried out to assess posterior probabilities (PP) by using MrBayes v.3.2.7 (Ronquist et al. 2012). Six simultaneous Markov chains were run for random trees for 1,000,000 generations, and trees were sampled every 200<sup>th</sup> generation. Bayesian posterior probabilities (PP) equal to or greater than 0.95 were given above the nodes in the phylogenetic tree (Fig. 1). Phylograms were visualized by using FigTree v1.4.0 (Rambaut 2012) and rearranged in Adobe Photoshop

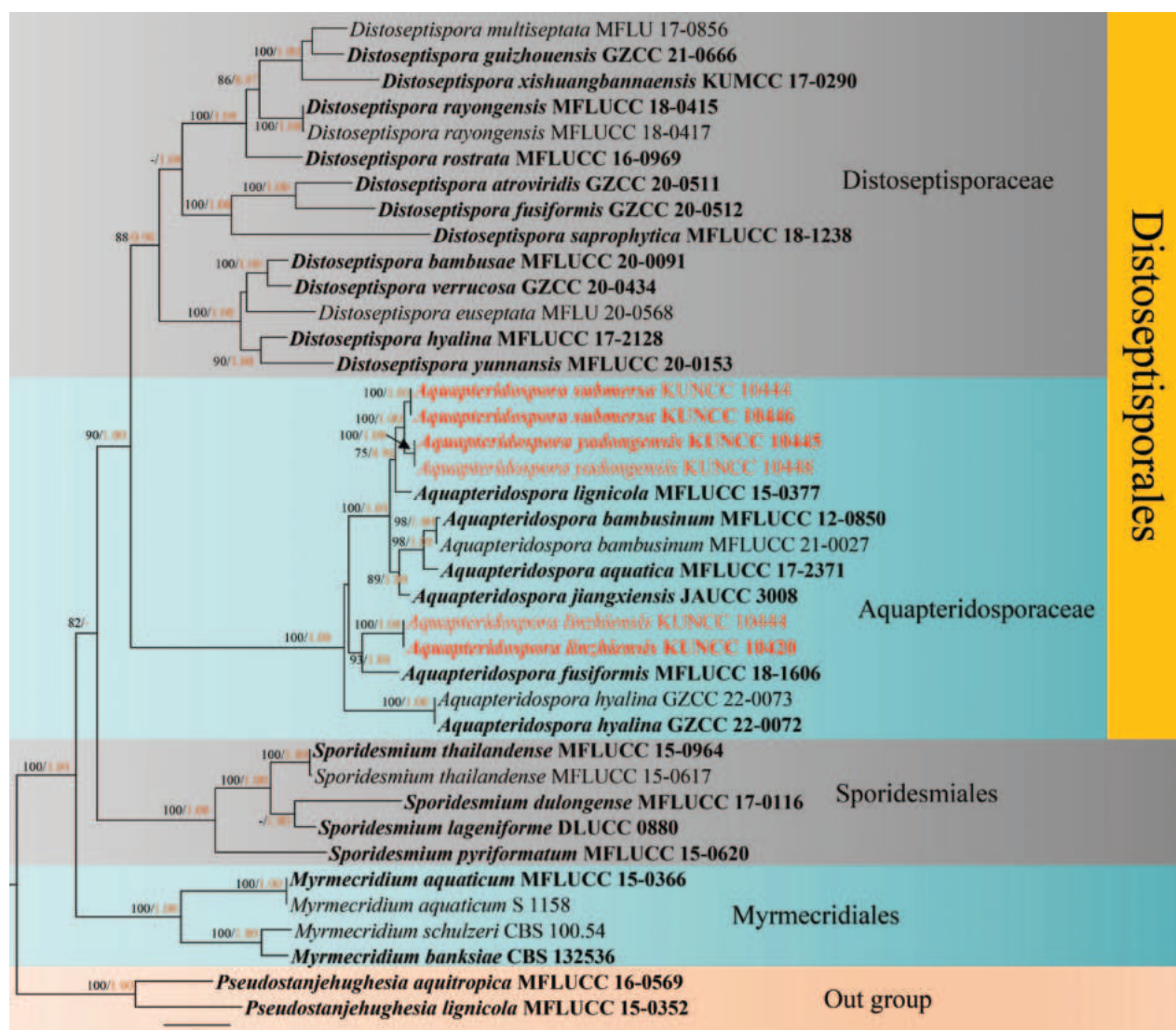


**Figure 1.** Maximum likelihood (ML) tree is based on combined LSU, *TEF1*- $\alpha$  and ITS sequence data. ML bootstrap support values equal to or greater than 70% and Bayesian posterior probabilities (PP) equal to or greater than 0.95 given above the nodes, shown as "ML/PP". The tree is rooted with *Pseudostanjehughesia aquitropica* (MFLUCC 16-0569) and *P. lignicola* (MFLUCC 15-0352). New species are indicated in red and type strains are in bold.

CS6 software (Adobe Systems, USA). The new sequences were deposited in GenBank (Table 1), and the final alignments and phylogenetic tree were registered in TreeBASE under the submission ID: 30133 (<http://www.treebase.org/>).

## Results

### Phylogenetic analyses

The concatenated sequence dataset of LSU, *TEF1*- $\alpha$  and ITS, comprised 39 strains with *Pseudostanjehughesia aquitropica* (MFLUCC 16-0569) and *P. lignicola* (MFLUCC 15-0352) as the outgroup taxa (Fig. 1). The datasets contained 2,168 characters including gaps after alignments (LSU: 1–763 bp,  $\alpha$  = 764–1,660 bp, ITS: 1,661–2,168 bp). The RAxML analysis of the combined datasets yielded a best scoring tree with a final ML optimization likelihood value of -15404.143090. The aligned sequences matrix comprised 849 distinct alignment patterns with 6.45% of undetermined characters or gaps. Estimated base frequencies were as follows: A = 0.229844, C = 0.282249, G = 0.282387, T = 0.205520, with substitution rates AC = 0.921073, AG = 2.039438, AT = 1.172967, CG = 0.817703, CT = 5.518393, GT = 1.000000; gamma distribution shape parameter  $\alpha$  = 0.0010000000. The tree topologies of combined sequence data obtained from ML and BI analyses were not significantly different (Fig. 1).

The phylogenetic analyses showed that our six strains nested within the genus *Aquapteridospora* represent three species. Two strains of *A. linzhienensis* (KUNCC 10420 and KUNCC 10444) formed a well resolved subclade sister to *A. fusiformis* (93% ML/1.00 PP support); while strains of *A. yadongensis* (KUNCC 10445 and KUNCC 10448) formed a distinct subclade sister to *A. submersa* (KUNCC 10446 and KUNCC 10449) with a high support (100% ML/1.00 PP) and clustered with *A. lignicola* (MFLUCC 15-10377) with a significant support (75% ML/0.96 PP) (Fig. 1).

### Taxonomy

#### *Aquapteridospora linzhienensis* R.J. Xu, Q. Zhao & Boonmee, sp. nov.

Index Fungorum: IF901109

Facesoffungi Number: FoF14348

Fig. 2

**Etymology.** Referring to the location “Linzi City, China” where the holotype of this fungus was collected.

**Holotype.** HKAS 128991.

**Description.** *Saprobic* on decaying wood submerged in freshwater. **Sexual morph:** Undetermined. **Asexual morph: Colonies** on the natural substrate effuse, hairy, pale brown to brown, scattered or in small groups. **Mycelium** mostly superficial, consisting of branched, septate, smooth, pale brown to brown hyphae. **Conidiophores** 113–210  $\times$  4–6  $\mu$ m ( $\bar{x}$  = 162  $\times$  4  $\mu$ m, n = 15), macronematous, mononematous, solitary or 2–3 group, erect, straight or slightly flexuous, simple, unbranched, smooth, cylindrical, 6–12-septate, brown at the base, pale brown towards apex. **Conidiogenous cells** polyblastic, monoblastic, terminal,



**Figure 2.** *Aquapteridospora linzhiensis* (HKAS 128991, holotype) **a** colonies on the substratum **b–e** conidiophores, conidigenous cells with conidia **f, g** conidiogenous cells with developmental conidia **h–k** conidia **l, m** culture on PDA. Scale bars: 50  $\mu\text{m}$  (**b–e**); 20  $\mu\text{m}$  (**f, g**); 10  $\mu\text{m}$  (**h–k**).

becoming intercalary, cylindrical, pale brown, integrated, with several sympodial proliferations, conspicuous denticles, bearing tiny, protuberant, circular scars. **Conidia** 10–14 × 5–6 μm ( $\bar{x}$  = 12 × 6 μm, n = 25), solitary or acropleurogenous, fusiform or elliptical, smooth, 2-septate, truncate at base, dark brown in central cells and subhyaline at end cells, guttulate. Conidial secession schizolytic.

**Culture characteristics.** Conidia were germinated on PDA within 48 hours. Germ tubes produced from each end. Colonies grown on PDA, circular, flat, superficial, dark brown from above, reverse-side brown in the centre, with greyish white near the edge.

**Material examined.** CHINA, Xizang, Linzhi City, Motuo County, on submerged decaying wood, 1675 msl, 29°10'56"N, 95°8'53"E, 11 July 2022, R.J. Xu, XK-33–3 (HKAS 128991, holotype), ex-type living culture (KUNCC 10420). Xizang, Linzhi City, Motuo County, Gelin Village, on submerged decaying wood, 1143 msl, 29°1'43"N, 94°48'5.7"E, 12 July 2022, R.J. Xu, XK-32, (HKAS 128990), living culture (KUNCC 10444).

**Notes.** Phylogenetic analyses show that *Aquapteridospora linzhiensis* (KUNCC 10420 and KUNCC 10444) clustered into a distinct subclade and sister to *A. fusiformis* (MFLUCC 18-1606) with bootstrap support (93% ML/1.00 PP, Fig. 1). However, *A. linzhiensis* differs from *A. fusiformis* in having obvious, guttulate conidia and less septate on maturity (2-septate vs. 3–4-septate) (Luo et al. 2019). Additionally, comparisons of ITS sequences demonstrate a 6.7% (39/586 bp, excluding gaps) difference between *A. linzhiensis* and *A. fusiformis* Jeewon and Hyde (2016). Therefore, *A. linzhiensis* was identified as a new species supported with both morphological and phylogenetic evidences.

### ***Aquapteridospora yadongensis* R.J. Xu, Q. Zhao & Boonmee, sp. nov.**

Index Fungorum: IF901110

Facesoffungi Number: FoF14349

Fig. 3

**Etymology.** Referring to the location “Yadong County, China” where the holotype of this fungus was collected.

**Holotype.** HKAS 128992.

**Description.** **Saprobic** on decaying wood submerged in freshwater. **Sexual morph:** Undetermined. **Asexual morph:** **Colonies** on the natural substrate effuse, hairy, pale brown to brown, scattered or in small groups, usually retiform. **Mycelium** mostly superficial, consisting of branched, septate, smooth, pale brown to brown hyphae. **Conidiophores** 440–856 × 4–6 μm ( $\bar{x}$  = 581 × 5 μm, n = 20), macronematous, mononematous, solitary, erect, straight or slightly flexuous, unbranched, smooth, cylindrical, multi-septate, tapering towards apex, brown to pale brown, slightly constricted at some septa. **Conidiogenous cells** polyblastic, monoblastic, terminal, becoming intercalary, cylindrical, pale brown, integrated, denticles, bearing tiny, protuberant, circular scars. **Conidia** 14–20 × 4–7 μm ( $\bar{x}$  = 17 × 5 μm, n = 30), acropleurogenous, fusiform, smooth, 3-septate, rounded at apex, truncate at base, dark brown in central cells and light at end cells. Conidial secession schizolytic.

**Culture characteristics.** Conidia were germinated on PDA within 48 hours. Germ tubes produced from each end. Colonies grown on PDA, regular concentric

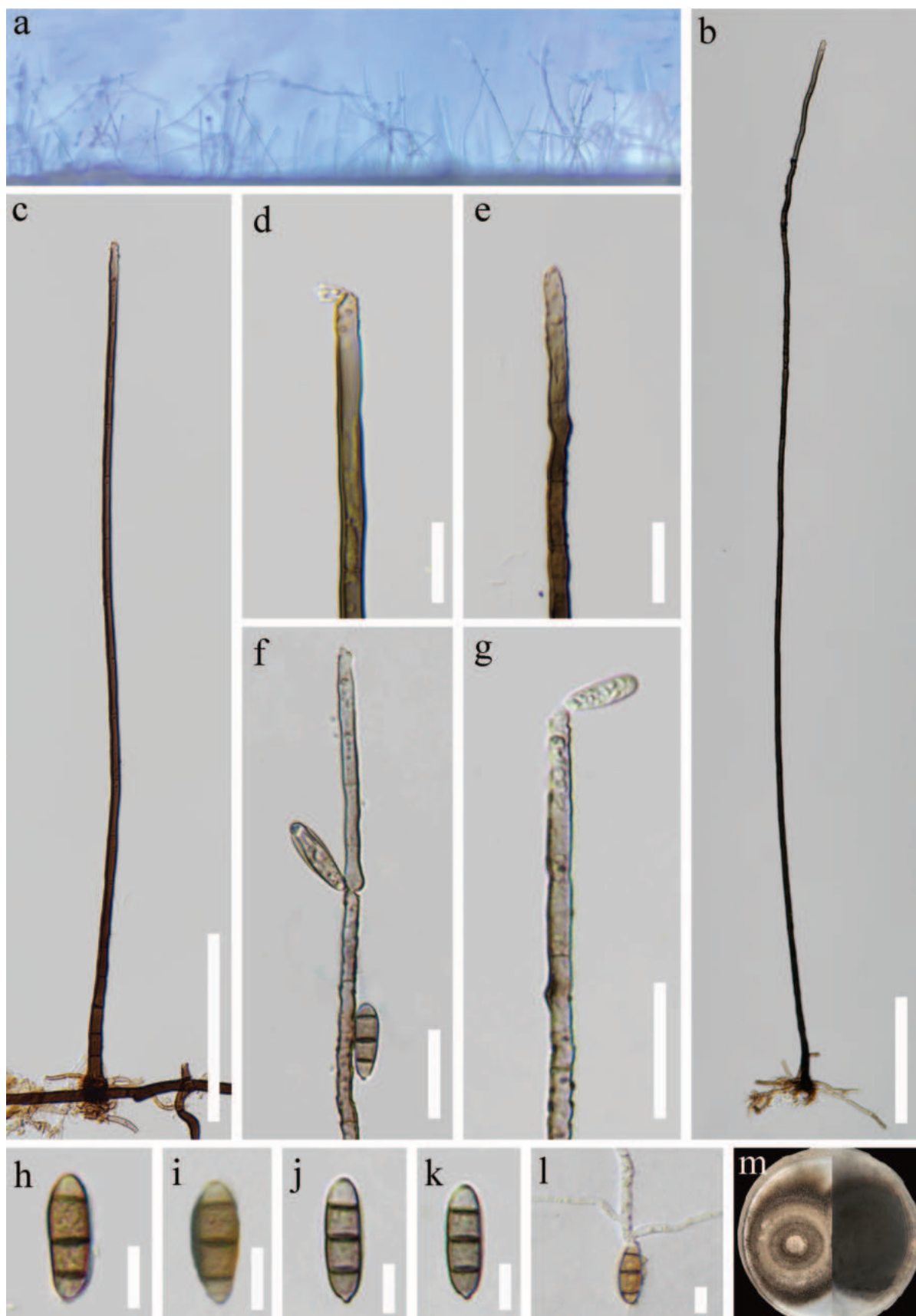


**Figure 3.** *Aquapteridospora yadongensis* (HKAS 128992, holotype) **a** colonies on the substratum **b, c** conidiophore and conidiogenous cell **d-g** conidiogenous cells with developmental conidia **h-k** conidia **l** germinating conidium **m** culture on PDA. Scale bars: 100  $\mu\text{m}$  (**b, c**); 20  $\mu\text{m}$  (**d, g**); 10  $\mu\text{m}$  (**h-l**).

circles, flat, superficial, with dense mycelium at around, grey brown from above, dark brown from below.

**Material examined.** CHINA, Xizang, Shigatse City, Yadong County, on submerged decaying wood, 3061 msl, 27°21'11"N, 88°58'10"E, 01 July 2022, R.J. Xu, LTS-20 (HKAS 128992, holotype), ex-type living culture (KUNCC 10445). Xizang, Shigatse City, Dingjie County, on submerged decaying wood, 3042 msl, 27°53'8.7"N, 87°27'36"E, 05 July 2022, L.T. Shun, LTS-20-1, (HKAS 128993), living culture (KUNCC 10448).

**Notes.** *Aquapteridospora yadongensis* possess its conidial characteristics that fit with *Aquapteridospora* (Yang et al. 2015). In phylogenetic analyses, *A. yadongensis* formed a distinct lineage close to *A. submersa* with high bootstrap support (100% ML/1.00 PP, Fig. 1). A comparison of ITS nucleotide shows that *A. yadongensis* (KUNCC 10445) differs from *A. submersa* (KUNCC 10446) in 10/572 bp (1.8%, excluding gap), a comparison of *TEF1- $\alpha$*  nucleotide shows that *A. yadongensis* (KUNCC 10445) differs from *A. submersa* (KUNCC 10446) in 8/821 bp (0.8%, excluding gap) (Jeewon and Hyde 2016). In addition, *A. yadongensis* differs from *A. submersa* in having narrower conidiophores (4–6 vs. 5–12  $\mu\text{m}$ ), while conidia of *A. submersa* have slightly constricted septa; the culture of *A. yadongensis* have regular concentric circles differing from *A. submersa* having pale mycelium in the centre. Furthermore, *A. yadongensis* differs from *A. lignicola* in having long conidiophores (440–856 vs. 70–200  $\mu\text{m}$ ) and conidia without a conspicuous sheath (Yang et al. 2015).

***Aquapteridospora submersa* R.J. Xu, Q. Zhao & Boonmee, sp. nov.**

Index Fungorum: IF901111

Facesoffungi Number: FoF14350

Fig. 4

**Etymology.** Referring to the fungus's habitat "decaying wood submerged in freshwater habitats".

**Holotype.** HKAS 128980.

**Description.** **Saprobic** on decaying wood submerged in freshwater. **Sexual morph:** Undetermined. **Asexual morph: Colonies** on the natural substrate effuse, glistening, pale brown to brown, scattered or in small groups. **Mycelium** mostly superficial, consisting of branched, septate, smooth, pale brown to brown hyphae. **Conidiophores** 376–708  $\times$  5–12  $\mu\text{m}$  ( $\bar{x}$  = 451  $\times$  7  $\mu\text{m}$ ,  $n$  = 20), macronematous, mononematous, solitary, erect, straight or slightly flexuous, unbranched, smooth, cylindrical, multi-septate, tapering towards apex, brown to pale brown. **Conidiogenous cells** polyblastic, monoblastic, terminal, becoming intercalary, cylindrical, pale brown, integrated, with several sympodial proliferations, conspicuous denticles, bearing tiny, protuberant, circular scars. **Conidia** 19–22  $\times$  6–8  $\mu\text{m}$  ( $\bar{x}$  = 21  $\times$  7  $\mu\text{m}$ ,  $n$  = 20), solitary or acropleurogenous, fusiform, smooth, 2–3-septate, rounded at apex, truncate at base, slightly constricted at septa, hyaline when young, sub-hyaline to pale brown when mature, two big guttulate when young. Conidial secession schizolytic.

**Culture characteristics.** Conidia were germinated on PDA within 48 hours. Germ tubes produced from each end. Colonies grown on PDA, circular, flat,

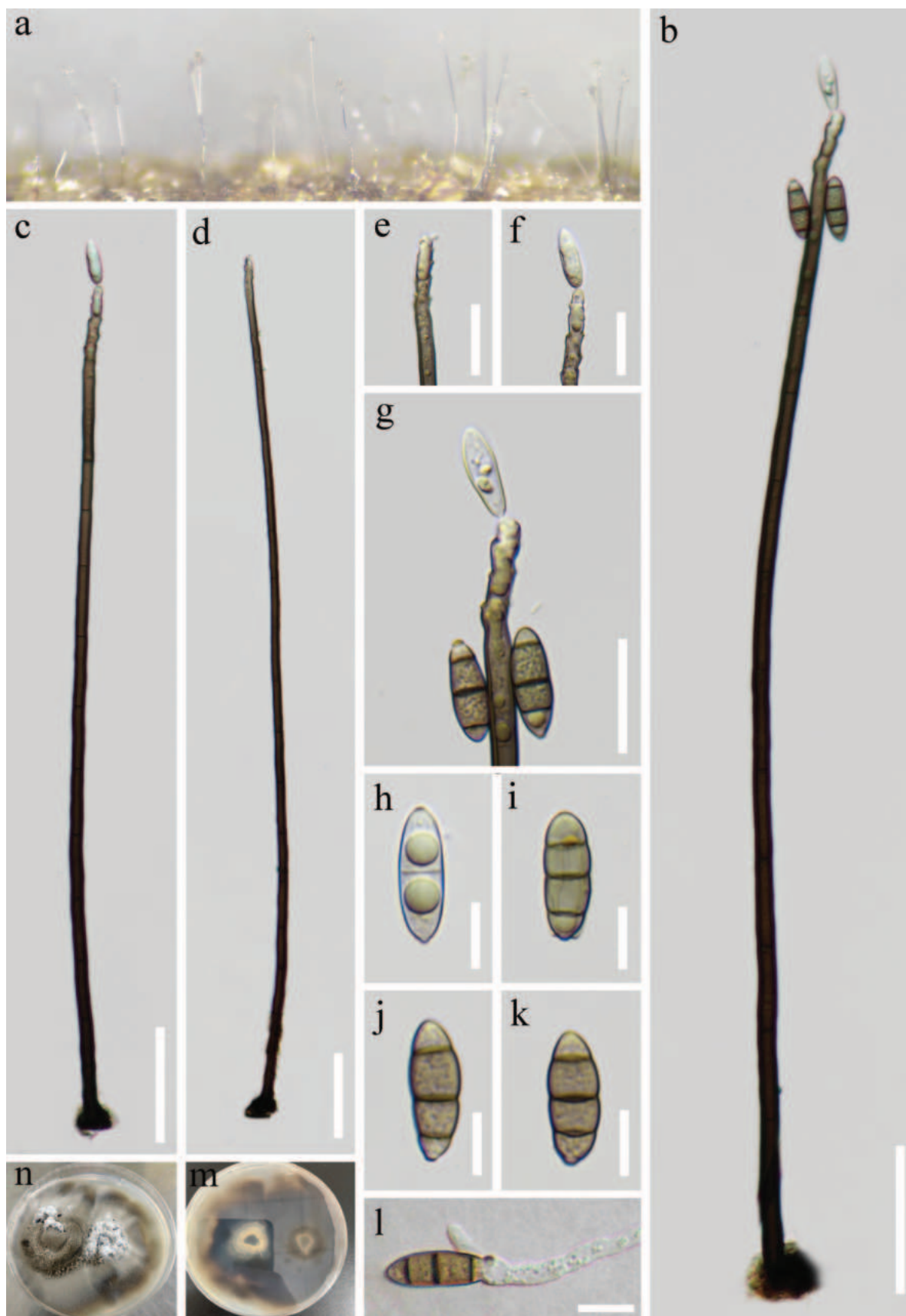


**Figure 4.** *Aquapteridospora submersa* (HKAS 128980, holotype) **a** colonies on the substratum **b–d** conidiophores, conidiogenous cells with conidia **e–g** conidiogenous cells with developmental conidia **h–k** conidia **l** germinating conidium **m, n** culture on PDA. Scale bars: 50  $\mu\text{m}$  (**b–d**); 20  $\mu\text{m}$  (**e–g**); 10  $\mu\text{m}$  (**h–l**).

superficial, raised, with dense, pale mycelium in the centre. Grey brown from above, dark brown from below.

**Material examined.** CHINA, Xizang, Linzhi City, Motuo County, on submerged decaying wood, 677 msl, 29°19'43"N, 95°21'19"E, 13 July 2022, R.J. Xu, LJJN-15 (HKAS 128980, holotype), ex-type living culture (KUNCC 10446). Xizang, Linzhi City, Motuo County, Gelin Village, on submerged decaying wood, 677 msl, 29°19'43"N, 95°21'19"E, 12 July 2022, R.J. Xu, LJJN-15-5, (HKAS 128981), living culture (KUNCC 10444).

**Notes.** Phylogenetic analyses show that *Aquapteridospora submersa* (KUNCC 10446, KUNCC 10444), formed a sister grouped with *A. yadongensis* (KUNCC 10445 and KUNCC 10488) and was close to *A. lignicola* (MFLUCC 15-0377) with 75% ML/0.96 PP, Fig. 1. However, the comparison of conidial characteristics and nucleotides shows that *A. submersa* differs from *A. yadongensis* (see the notes of *A. yadongensis*). Indeed, *A. submersa* differs from *A. lignicola* in having long conidiophores (376–708 vs. 70–200 µm) and conidia without a conspicuous sheath (Yang et al. 2015). *Aquapteridospora submersa* is introduced here as a new species.

## Discussion

Species of *Aquapteridospora* are morphologically unique in the taxonomic characteristics, especially in the features of the conidiophores and conidia (Table 2). In most species, the conidia are fusiform and pigmented, featuring brown to dark brown central cells and subhyaline end cells. However, some species exhibit conidia with a distinct sheath, such as *A. aquatica*, *A. jiangxiensis* and *A. lignicola* (Yang et al. 2015; Dong et al. 2021; Peng et al. 2022). Additionally, a few species are characterized by hyaline to sub-hyaline conidia, as observed in *A. hyalina* (Ma et al. 2022). In addition, the length of conidiophores in species of *Aquapteridospora* varies significantly. Most species have conidiophores ranging in length from 70 to 305 µm, as observed in species like *A. aquatica*, *A. fusiformis*, *A. hyaline*, *A. jiangxiensis*, *A. lignicola* and *A. linzhiensis* (Yang et al. 2015; Luo et al. 2019; Dong et al. 2021; Ma et al. 2022; Peng et al. 2022), a few species exhibit conidiophores exceeding 400 µm in length, with the longest reaching 856 µm. This is the case for species such as *A. bambusinum*, *A. yadongensis* and *A. submersa* (Bao et al. 2021, this study).

Molecular phylogenetic analyses play a crucial role in elucidating the classification of hyphomycetous fungi (Dhanasekaran et al. 2006; Tekpinar and Kalmer 2019). *Pleurophragmium bambusinum* was initially described by Dai et al. (2017), and was previously assigned to Sordariomycetes *incertae sedis* based on its morphological characteristics. According to the phylogenetic analysis conducted by Dong et al. (2021), *P. bambusinum* was found to cluster within the *Aquapteridospora* clade with (100% ML/1.00 PP) support. However, their studies did not synonymize *P. bambusinum* under *Aquapteridospora* due to the ellipsoidal and conidia without a sheath, which indicate that it does not fit within the characteristics of *Aquapteridospora* species. Subsequently, Bao et al. (2021) transferred *P. bambusinum* to *Aquapteridospora* and synonymized *A. bambusinum* instead of *P. bambusinum*, based on both phylogeny and morphology.

**Table 2.** Synopsis of known species in *Aquapteridospora*.

Species	Conidiophores (µm)	Conidiogenous cells (µm)	Conidia (µm)	Host	Habitat	Distribution	Reference
<i>Aquapteridospora aquatic</i>	125–215 × 3–5	10–85 × 4–5.5, Polyblastic, terminal, intercalary, denticles	19–27.5 × 5–7.5, acropleurogenous, solitary, olivaceous or brown in the middle cells, fusiform, 3-septate, gelatinous, thin sheath	Unidentified, submerged wood	Freshwater	Thailand	Dong et al. (2021)
<i>A. bambusinum</i>	615–715 × 9–13	Polyblastic, sympodial, denticulate, integrated, terminal	15–18 × 5.5–7, acrogenous, solitary, pale brown to dark brown, ellipsoid to fusiform, 3-septate, straight	Unidentified, submerged wood	Freshwater	Thailand	Bao et al. (2021)
<i>A. fusiformis</i>	(88–) 134–188 × 5–7	Polyblastic, terminal, intercalary, sympodial proliferations	14–18 × 5–7, solitary, brown to dark brown in central cells and subhyaline at end cells, fusiform, 3–4-septate,	Unidentified, submerged wood	Freshwater	China	Luo et al. (2019)
<i>A. hyalina</i>	68–130 × 4.5–6.5	25–62 × 4–6.5, polyblastic, monoblastic, denticles	17–28 × 4–6, acropleurogenous, solitary, sub-hyaline to pale brown, fusiform, 1–3-septate,	Unidentified, submerged wood	Freshwater	China	Ma et al. (2022)
<i>A. jiangxiensis</i>	78–305 × 4–7	20–68 × 4–6, integrated, terminal, intercalary	20–25 × 6–7.5, acrogenous or lateral, dark brown to black, fusiform to subclavate, 3-septate, sometimes with a sheath	Unidentified, submerged wood	Freshwater	China	Peng et al. (2022)
<i>A. lignicola</i>	70–200 × 4–7	14.5–30 × 4.5–7.5, polyblastic, terminal, intercalary	15–24 × 6–8, solitary, acropleurogenous, with pale to dark brown central cells and subhyaline end cells, fusiform, 3-septate, with a conspicuous sheath	Unidentified, submerged wood	Freshwater	Thailand	Yang et al. (2015)
<i>A. linzhiensis</i>	113–210 × 4–6	Polyblastic, terminal, intercalary, denticles	10–14 × 5–6, solitary or acropleurogenous, dark brown in central cells and subhyaline at end cells, fusiform or elliptical, 2-septate, guttulate	Unidentified, submerged wood	Freshwater	China	This study
<i>A. yadongensis</i>	440–856 × 4–6	Polyblastic, monoblastic, terminal, intercalary, denticles	14–20 × 4–7, acropleurogenous, dark brown in central cells and subhyaline at end cells, fusiform, 3-septate	Unidentified, submerged wood	Freshwater	China	This study
<i>A. submersa</i>	376–708 × 5–12	Polyblastic, monoblastic, terminal, intercalary, denticles	19–22 × 6–8, solitary or acropleurogenous, hyaline when young, sub-hyaline to pale brown when mature, fusiform, 2–3-septate, two big guttulate when young	Unidentified, submerged wood	Freshwater	China	This study

The Tibetan Plateau is renowned for its distinctive biological diversity and extensive array of aquatic habitats, encompassing lakes, rivers, and wetlands, which provide sustenance for various fungal communities (Yao et al. 2019). While freshwater fungi play a crucial role in the ecosystem, they have remained understudied in this region, primarily due to the limited number of researchers focusing on freshwater fungi in the Tibetan Plateau. During our investigation into freshwater fungal diversity on the Tibetan Plateau, we introduced three new species within the genus *Aquapteridospora*, supported by both phylogenetic analysis and morphology. The discovery of these new species revealed the abundant fungal diversity in Tibetan Plateau and more scientific studies in this region are expected in the future.

### Additional information

#### Conflict of interest

The authors have declared that no competing interests exist.

#### Ethical statement

No ethical statement was reported.

## Funding

This study is supported by the Survey of Wildlife Resources in Key Areas of Tibet (ZL202203601), the Second Tibetan Plateau Scientific Expedition and Research (STEP) Program (Grant No. 2019QZKK0503); Major science and technology projects and key R&D plans/programs, Yunnan Province (202202AE090001), the Biodiversity Survey and Assessment Project of the Ministry of Ecology and Environment, P.R. China (2019HJ2096001006). The authors appreciate the support given by Thesis Writing Grant of Mae Fah Luang University, Thailand, to Rong Ju Xu.

## Author contributions

Funding acquisition: QZ. Writing - original draft: RJX. Writing - review and editing: SB, JFL, DQZ.

## Author ORCIDs

Rong-Ju Xu  <https://orcid.org/0000-0002-3968-8442>

Jun-Fu Li  <https://orcid.org/0009-0008-6088-2072>

De-Qun Zhou  <https://orcid.org/0009-0009-3459-3186>

Saranyaphat Boonmee  <https://orcid.org/0000-0001-5202-2955>

Qi Zhao  <https://orcid.org/0000-0001-8169-0573>

Ya-Ya Chen  <https://orcid.org/0000-0002-8293-168X>

## Data availability

All of the data that support the findings of this study are available in the main text.

## References

- Arzanlou M, Groenewald JZ, Gams W, Braun U, Shin H-D, Crous PW (2007) Phylogenetic and morphotaxonomic revision of *Ramichloridium* and allied genera. *Studies in Mycology* 58: 57–93. <https://doi.org/10.3114/sim.2007.58.03>
- Bao DF, Hyde KD, McKenzie EHC, Jeewon R, Su HY, Nalumpang S, Luo ZL (2021) Biodiversity of lignicolous freshwater hyphomycetes from china and thailand and description of sixteen species. *Journal of Fungi* 7(8): 669. <https://doi.org/10.3390/jof7080669>
- Calabon MS, Hyde KD, Jones EBG, Luo ZL, Dong W, Hurdeal VG, Gentekaki E, Rossi W, Leonardi M, Thiyagaraja V, Lestari AS, Shen HW, Bao DF, Boonyuen N, Zeng M (2022) Freshwater fungal numbers. *Fungal Diversity* 114(1): 3–235. <https://doi.org/10.1007/s13225-022-00503-2>
- Calabon MS, Hyde KD, Jones EBG, Bao DF, Bhunjun CS, Phukhamsakda C, Shen HW, Gentekaki E, Al Sharie AH, Barros J, Chandrasiri KSU, Hu DM, Hurdeal VG, Rossi W, Valle LG, Zhang H, Figueroa M, Raja HA, Seena S, Song HY, Dong W, El-Elimat T, Leonardi M, Li Y, Li YJ, Luo ZL, Ritter CD, Strongman DB, Wei MJ, Balasuriya A (2023) Freshwater fungal biology. *Mycosphere* 14(1): 195–413. <https://doi.org/10.5943/mycosphere/14/1/4>
- Capella-Gutierrez S, Silla-Martinez JM, Gabaldon T (2009) trimAl: A tool for automated alignment trimming in large-scale phylogenetic analyses. *Bioinformatics* 25(15): 1972–1973. <https://doi.org/10.1093/bioinformatics/btp348>
- Crous PW, Summerell BA, Shivas RG, Burgess TI, Decock CA, Dreyer LL, Granke LL, Guest DI, Hardy GESTJ, Hausbeck MK, Hüberli D, Jung T, Koukol O, Lennox CL, Liew ECY, Lombard L, McTaggart AR, Pryke JS, Roets F, Saude C, Shuttleworth LA, Stukely MJC, Vánky K, Webster BJ, Windstam ST, Groenewald JZ (2012) *Fungal Planet description*

- tion sheets: 107–127. *Persoonia - Molecular Phylogeny and Evolution of Fungi* 28: 138–182. <https://doi.org/10.3767/003158512X652633>
- Dai DQ, Phookamsak R, Wijayawardene NN, Li WJ, Bhat DJ, Xu JC, Taylor JE, Hyde KD, Chukeatirote E (2017) Bambusicolous fungi. *Fungal Diversity* 82(1): 1–105. <https://doi.org/10.1007/s13225-016-0367-8>
- Dhanasekaran V, Jeewon R, Hyde KD (2006) Molecular taxonomy, origins and evolution of freshwater ascomycetes. *Fungal Diversity* 23: 351–390.
- Dong W, Wang B, Hyde KD, McKenzie EHC, Raja HA, Tanaka K, Abdel-Wahab MA, Abdel-Aziz FA, Doilom M, Phookamsak R, Hongsanan S, Wanasinghe DN, Yu XD, Wang GN, Yang H, Yang J, Thambugala KM, Tian Q, Luo ZL, Yang JB, Miller AN, Fournier J, Boonmee S, Hu DM, Nalumpang S, Zhang H (2020) Freshwater Dothideomycetes. *Fungal Diversity* 105(1): 319–575. <https://doi.org/10.1007/s13225-020-00463-5>
- Dong W, Hyde HD, Jeewon R, Doilom M, Yu XD, Wang GN, Liu NG, Hu DM, Nalumpang S, Zhang H (2021) Towards a natural classification of annulatasceae-like taxa II: Introducing five new genera and eighteen new species from freshwater. *Mycosphere* 12(1): 1–88. <https://doi.org/10.5943/mycosphere/12/1/1>
- Hyde KD, Fryar S, Tian Q, Bahkali AH, Xu J (2016) Lignicolous freshwater fungi along a north–south latitudinal gradient in the Asian/Australian region; can we predict the impact of global warming on biodiversity and function? *Fungal Ecology* 19: 190–200. <https://doi.org/10.1016/j.funeco.2015.07.002>
- Hyde KD, Jeewon R, Chen Y-J, Bhunjun CS, Calabon MS, Jiang H-B, Lin C-G, Norphanphoun C, Sysouphanthong P, Pem D, Tibpromma S, Zhang Q, Doilom M, Jayawardena RS, Liu J-K, Maharachchikumbura SSN, Phukhamsakda C, Phookamsak R, Al-Sadi AM, Thongklang N, Wang Y, Gafforov Y, Gareth Jones EB, Lumyong S (2020) The numbers of fungi: Is the descriptive curve flattening? *Fungal Diversity* 103(1): 219–271. <https://doi.org/10.1007/s13225-020-00458-2>
- Hyde KD, Bao DF, Hongsanan S, Chethana KWT, Yang J, Suwannarach N (2021a) Evolution of freshwater Diaporthomycetidae (Sordariomycetes) provides evidence for five new orders and six new families. *Fungal Diversity* 107(1): 71–105. <https://doi.org/10.1007/s13225-021-00469-7>
- Hyde KD, Suwannarach N, Jayawardena RS, Manawasinghe IS, Liao CF, Doilom M, Cai L, Zhao P, Buyck B, Phukhamsakda C, Su WX, Fu YP, Li Y, Zhao RL, He MQ, Li JX, Tibpromma S, Lu L, Tang X, Kang JC, Ren GC, Gui H, Hofstetter V, Ryoo R, Antonín V, Hurdeal VG, Gentekaki E, Zhang JY, Lu YZ, Senanayake IC, Yu FM, Zhao Q, Bao DF (2021b) *Mycosphere notes* 325–344 – Novel species and records of fungal taxa from around the world. *Mycosphere* 12(1): 1101–1156. <https://doi.org/10.5943/mycosphere/12/1/14>
- Jayasiri SC, Hyde KD, Ariyawansa HA, Bhat J, Buyck B, Cai L, Dai Y-C, Abd-Elsalam KA, Ertz D, Hidayat I, Jeewon R, Jones EBG, Bahkali AH, Karunarathna SC, Liu J-K, Luangsa-ard JJ, Lumbsch HT, Maharachchikumbura SSN, McKenzie EHC, Moncalvo J-M, Ghobad-Nejhad M, Nilsson H, Pang K-L, Pereira OL, Phillips AJL, Raspé O, Rollins AW, Romero AI, Etayo J, Selçuk F, Stephenson SL, Suetrong S, Taylor JE, Tsui CKM, Vizzini A, Abdel-Wahab MA, Wen T-C, Boonmee S, Dai DQ, Daranagama DA, Dissanayake AJ, Ekanayaka AH, Fryar SC, Hongsanan S, Jayawardena RS, Li W-J, Perera RH, Phookamsak R, de Silva NI, Thambugala KM, Tian Q, Wijayawardene NN, Zhao R-L, Zhao Q, Kang J-C, Promputtha I (2015) The Faces of Fungi database: Fungal names linked with morphology, phylogeny and human impacts. *Fungal Diversity* 74(1): 3–18. <https://doi.org/10.1007/s13225-015-0351-8>

- Jeewon R, Hyde KD (2016) Establishing species boundaries and new taxa among fungi: Recommendations to resolve taxonomic ambiguities. *Mycosphere* 7(11): 1669–1677. <https://doi.org/10.5943/mycosphere/7/11/4>
- Jones EBG, Southworth D, Libkind D, Marvanová L (2014) Fresh water Basidiomycota. In: Jones EBG, Hyde KD, Pang KL (Eds) *Freshwater fungi and fungal-like organisms*. De Gruyter, Berlin, 73–108. <https://doi.org/10.1515/9783110333480.73>
- Katoh K, Standley DM (2016) A simple method to control over-alignment in the MAFFT multiple sequence alignment program. *Bioinformatics* 32(13): 1933–1942. <https://doi.org/10.1093/bioinformatics/btw108>
- Krauss G-J, Solé M, Krauss G, Schlosser D, Wesenberg D, Bärlocher F (2011) Fungi in freshwaters: Ecology, physiology and biochemical potential. *FEMS Microbiology Reviews* 35(4): 620–651. <https://doi.org/10.1111/j.1574-6976.2011.00266.x>
- Li WL, Liu ZP, Zhang T, Dissanayake AJ, Luo ZL, Su HY, Liu JK (2021) Additions to *Distoseptispora* (Distoseptisporaceae) associated with submerged decaying wood in China. *Phytotaxa* 520(1): 75–86. <https://doi.org/10.11646/phytotaxa.520.1.5>
- Luo ZL, Hyde KD, Liu JK, Bhat DJ, Bao DF, Li WL, Su HY (2018) Lignicolous freshwater fungi from China II: Novel *Distoseptispora* (Distoseptisporaceae) species from northwestern Yunnan Province and a suggested unified method for studying lignicolous freshwater fungi. *Mycosphere* 9(3): 444–461. <https://doi.org/10.5943/mycosphere/9/3/2>
- Luo ZL, Hyde KD, Liu JK, Maharachchikumbura SSN, Jeewon R, Bao D-F, Bhat DJ, Lin C-G, Li W-L, Yang J, Liu N-G, Lu Y-Z, Jayawardena RS, Li J-F, Su H-Y (2019) Freshwater Sordariomycetes. *Fungal Diversity* 99(1): 451–660. <https://doi.org/10.1007/s13225-019-00438-1>
- Ma J, Zhang JY, Xiao XJ, Xiao YP, Tang X, Boonmee S, Kang JC, Lu YZ (2022) Multi-gene phylogenetic analyses revealed five new species and two new records of Distoseptisporales from China. *Journal of Fungi* 8(11): 1202. <https://doi.org/10.3390/jof8111202>
- Maharachchikumbura SSN, Hyde KD, Jones EBG, McKenzie EHC, Bhat JD, Dayarathne MC, Huang S-K, Norphanphoun C, Senanayake IC, Perera RH, Shang Q-J, Xiao Y, D'souza MJ, Hongsanan S, Jayawardena RS, Daranagama DA, Konta S, Goonasekara ID, Zhuang W-Y, Jeewon R, Phillips AJL, Abdel-Wahab MA, Al-Sadi AM, Bahkali AH, Boonmee S, Boonyuen N, Cheewangkoon R, Dissanayake AJ, Kang J, Li Q-R, Liu JK, Liu XZ, Liu Z-Y, Luangsa-ard JJ, Pang K-L, Phookamsak R, Promputtha I, Suetrong S, Stadler M, Wen T, Wijayawardene NN (2016) Families of Sordariomycetes. *Fungal Diversity* 79(1): 1–317. <https://doi.org/10.1007/s13225-016-0369-6>
- Nylander JAA (2004) MrModeltest v2, Program distributed by the author, Evolutionary Biology Centre, Uppsala University.
- Peng SQ, Liu YL, Huang JE, Li XH, Yan XY, Song HY, Gao Y, Zhai ZJ, Liu YQ, Hu DM (2022) *Aquapteridospora jiangxiensis*, a new aquatic hyphomycetous fungus from a freshwater habitat in China. *Archives of Microbiology* 204(7): 378. <https://doi.org/10.1007/s00203-022-02942-6>
- Poch GK, Gloer JB, Shearer CA (1992) New bioactive metabolites from a freshwater isolate of the fungus *Kirschsteiniothelia* sp. *Journal of Natural Products* 55(8): 1093–1099. <https://doi.org/10.1021/np50086a010>
- Rambaut A (2012) FigTree v1. 4. University of Edinburgh, Edinburgh, UK.
- Ronquist F, Teslenko M, Van Der Mark P, Ayres DL, Darling A, Höhna S, Larget B, Liu L, Suchard MA, Huelsenbeck JP (2012) MrBayes 3.2: Efficient Bayesian phylogenetic inference and model choice across a large model space. *Systematic Biology* 61(3): 539–542. <https://doi.org/10.1093/sysbio/sys029>

- Senanayake I, Rathnayaka A, Marasinghe D, Calabon M, Gentekaki E, Lee H, Hurdeal V, Pem D, Dissanayake L, Wijesinghe S, Bundhun D, Nguyen T, Goonasekara I, Abeywickrama P, Bhunjun C, Jayawardena R, Wanasinghe D, Jeewon R, Bhat D (2020) Morphological approaches in studying fungi: Collection, examination, isolation, sporulation and preservation. *Mycosphere* 11(1): 2678–2754. <https://doi.org/10.5943/mycosphere/11/1/20>
- Shearer CA (1993) The freshwater ascomycetes. *Nova Hedwigia* 56: 1–33.
- Sridhar KR, Karamchand KS, Seena S (2013) Fungal assemblage and leaf litter decomposition in riparian tree holes and in a coastal stream of the south-west India. *Mycology*. *Mycology* 4(2): 118–124. <https://doi.org/10.1080/21501203.2013.825657>
- Stamatakis A (2014) RAxML version 8: A tool for phylogenetic analysis and post-analysis of large phylogenies. *Bioinformatics* 30(9): 1312–1313. <https://doi.org/10.1093/bioinformatics/btu033>
- Sun YR, Goonasekara ID, Thambugala KM, Jayawardena RS, Wang Y, Hyde KD (2020) *Distoseptispora bambusae* sp. nov. (Distoseptisporaceae) on bamboo from China and Thailand. *Biodiversity Data Journal* 8: e53678. <https://doi.org/10.3897/BDJ.8.e53678>
- Tekpinar AD, Kalmer A (2019) Utility of various molecular markers in fungal identification and phylogeny. *Nova Hedwigia* 109(1–2): 187–224. [https://doi.org/10.1127/nova\\_hedwigia/2019/0528](https://doi.org/10.1127/nova_hedwigia/2019/0528)
- Tibpromma S, Hyde KD, McKenzie EHC, Bhat DJ, Phillips AJL, Wanasinghe DN, Samarakoon MC, Jayawardena RS, Dissanayake AJ, Tennakoon DS, Doilom M, Phookamsak R, Tang AMC, Xu J, Mortimer PE, Promputtha I, Maharachchikumbura SSN, Khan S, Karunarathna SC (2018) Fungal diversity notes 840–928: Micro-fungi associated with Pandanaceae. *Fungal Diversity* 93(1): 1–160. <https://doi.org/10.1007/s13225-018-0408-6>
- Tsui CKM, Baschien C, Goh T-K (2016) Biology and ecology of freshwater fungi. In: Li DW (Ed.) *Biology of Microfungi*. *Fungal Biology*. Springer, Cham, 285–313. [https://doi.org/10.1007/978-3-319-29137-6\\_13](https://doi.org/10.1007/978-3-319-29137-6_13)
- Vaidya G, Lohman DJ, Meier R (2011) SequenceMatrix: Concatenation software for the fast assembly of multi-gene datasets with character set and codon information. *Cladistics* 27(2): 171–180. <https://doi.org/10.1111/j.1096-0031.2010.00329.x>
- Vilgalys R, Hester M (1990) Rapid genetic identification and mapping of enzymatically amplified ribosomal DNA from several *Cryptococcus* species. *Journal of Bacteriology* 172(8): 4238–4246. <https://doi.org/10.1128/jb.172.8.4238-4246.1990>
- White TJ, Bruns T, Lee S, Taylor J (1990) Amplification and direct sequencing of fungal ribosomal RNA genes for phylogenetics. *PCR protocols: a guide to methods and applications* 18: 315–322. <https://doi.org/10.1016/B978-0-12-372180-8.50042-1>
- Wijayawardene N, Hyde K, Dai D, Sánchez-García M, Goto B, Saxena R, Erdoğdu M, Selçuk F, Rajeshkumar K, Aptroot A, Błaszczowski J, Boonyuen N, da Silva G, de Souza F, Dong W, Ertz D, Haelewaters D, Jones E, Karunarathna S, Kirk P, Kukwa M, Kumla J, Leontyev D, Lumbsch H, Maharachchikumbura S, Marguno F, Martínez-Rodríguez P, Mešić A, Monteiro J, Oehl F, Pawłowska J, Pem D, Pfliegler W, Phillips A, Pošta A, He M, Li J, Raza M, Sruthi O, Suetrong S, Suwannarach N, Tedersoo L, Thiyagaraja V, Tibpromma S, Tkalčec Z, Tokarev Y, Wanasinghe D, Wijesundara D, Wimalaseana S, Madrid H, Zhang G, Gao Y, Sánchez-Castro I, Tang L, Stadler M, Yurkov A, Thines M (2022) Outline of Fungi and fungus-like taxa – 2021. *Mycosphere* 13(1): 53–453. <https://doi.org/10.5943/mycosphere/13/1/2>
- Wright PM, Seiple IB, Myers AG (2014) The evolving role of chemical synthesis in antibacterial drug discovery. *Angewandte Chemie International Edition* 53(34): 8840–8869. <https://doi.org/10.1002/anie.201310843>

- Wurzbacher C, Rösler S, Rychła A, Grossart H-P (2014) Importance of saprotrophic freshwater fungi for pollen degradation. *PLoS ONE* 9(4): e94643. <https://doi.org/10.1371/journal.pone.0094643>
- Yang J, Maharachchikumbura SSN, Hyde KD, Bhat DJ, McKenzie EC, Bahkali AH, Gareth Jones EB, Liu Z-Y (2015) *Aquapteridospora lignicola* gen. et sp. nov., a new Hyphomycetous taxon (Sordariomycetes) from wood submerged in a freshwater stream. *Cryptogamie, Mycologie* 36(4): 469–478. <https://doi.org/10.7872/crym/v36.iss4.2015.469>
- Yang J, Maharachchikumbura SSN, Liu J-K, Hyde KD, Gareth Jones EB, Al-Sadi AM, Liu Z-Y (2018) *Pseudostanjehughesia aquitropica* gen. et sp. nov. and *Sporidesmium* sensu lato species from freshwater habitats. *Mycological Progress* 17(5): 591–616. <https://doi.org/10.1007/s11557-017-1339-4>
- Yang J, Liu LL, Gareth Jones EB, Li WL, Hyde KD, Liu ZY (2021) Morphological variety in *Distoseptispora* and introduction of six novel species. *Journal of Fungi* 7(11): 945. <https://doi.org/10.3390/jof7110945>
- Yang J, Liu LL, Jones EBG, Hyde KD, Liu ZY, Bao DF, Liu NG, Li WL, Shen HW, Yu XD, Liu JK (2023) Freshwater fungi from karst landscapes in China and Thailand. *Fungal Diversity* 119(1): 1–212. <https://doi.org/10.1007/s13225-023-00514-7>
- Yao TD, Wu GJ, Xu BQ, Wang WC, Gao J, An BS (2019) Asian Water Tower Change and Its Impacts. *Bulletin of the Chinese Academy of Sciences* 34: 1203–1209. <https://doi.org/10.16418/j.issn.1000-3045.2019.11.003>
- Zhang H, Dong W, Hyde KD, Maharachchikumbura SSN, Hongsanan S, Jayarama Bhat D, Al-Sadi AM, Zhang D (2017) Towards a natural classification of Annulatasceae-like taxa: Introducing Atractosporales ord. nov. and six new families. *Fungal Diversity* 85(1): 75–110. <https://doi.org/10.1007/s13225-017-0387-z>

# Diversity, pathogenicity and two new species of pestalotioid fungi (Amphisphaeriales) associated with Chinese Yew in Guangxi, China

Yifeng Wang<sup>1</sup>, Kin-Ming Tsui<sup>2,3</sup>, Shimei Chen<sup>1</sup>, Chongjuan You<sup>1</sup>

<sup>1</sup> Beijing Key Laboratory for Forest Pest Control, Beijing Forestry University, Beijing 100083, China

<sup>2</sup> National Centre for Infectious Diseases, Tan Tock Seng Hospital, Singapore 308433, Singapore

<sup>3</sup> Faculty of Medicine, University of British Columbia, Vancouver, V6T 1Z3, Canada

Corresponding author: Chongjuan You (chongjuanyou@bjfu.edu.cn)

## Abstract

Chinese yew, *Taxus chinensis* var. *mairei* is an endangered shrub native to south-eastern China and is widely known for its medicinal value. The increased cultivation of Chinese yew has increased the incidence of various fungal diseases. In this study, Pestalotioid fungi associated with needle spot of Chinese yew were isolated from Guangxi Province. Based on morphological examinations and multi-locus (ITS, *tub2*, *tef-1a*) phylogenies, these isolates were identified to five species, including two new species, *Pestalotiopsis taxicola* and *P. multicolor*, two potential novel *Neopestalotiopsis* species, *Neopestalotiopsis* sp. 3 and *Neopestalotiopsis* sp. 4, with a known *Pestalotiopsis* species (*Pestalotiopsis trachycarpicola*), firstly recorded from Chinese yew. These two new *Pestalotiopsis* species were morphologically and phylogenetically distinct from the extant Pestalotioid species in Chinese yew. Pathogenicity and culture characteristic tests of these five Pestalotioid species were also performed in this study. The pathogenicity test results revealed that *Neopestalotiopsis* sp. 3 can cause diseases in Chinese yew needles. These results have indicated that the diversity of Pestalotioid species associated with Chinese yew was greater than previously determined and provided helpful information for Chinese yew disease diagnosis and management.

**Key words:** *Neopestalotiopsis*, *Pestalotiopsis*, phylogeny, taxonomy, two new species



Academic editor: Nattawut Boonyuen

Received: 5 October 2023

Accepted: 27 January 2024

Published: 27 February 2024

**Citation:** Wang Y, Tsui K-M, Chen S, You C (2024) Diversity, pathogenicity and two new species of pestalotioid fungi (Amphisphaeriales) associated with Chinese Yew in Guangxi, China. MycoKeys 102: 201–224. <https://doi.org/10.3897/mycokeys.102.113696>

**Copyright:** © Yifeng Wang et al.

This is an open access article distributed under terms of the Creative Commons Attribution License (Attribution 4.0 International – CC BY 4.0).

## Introduction

The Chinese yew (*Taxus chinensis* var. *mairei* (Lemée et Lév.) Cheng et L.K. Fu) is an evergreen tall tree unique to south-eastern China and is widely known as a significant variety of medicinal plants because it contains taxol (paclitaxel) which is a natural antitumour drug with unique physiological functions in the bark, branches and leaves (Pyo et al. 2004; Li et al. 2008; Wu et al. 2013). Chinese yew has been listed on the IUCN Red List as an endangered species and has been under first-class protection in China, as it grows slowly and has poor regeneration ability, making it unable to meet strong medical demands (Ru 2006; Liu et al. 2019). Many natural reserves and conservation parks have been established to protect the Chinese yew. It has been widely cultivated in 17 provinces of China over the past few decades (Gao 2006; Zhang et al. 2018; Li et al. 2021a).

The expansion of Chinese yew cultivation in recent years has led to the emergence of various diseases that pose a significant threat to the Chinese yew industry (Zhang et al. 2018). Many fungal pathogens have been reported to cause Chinese yew diseases during their growth, such as needle spot caused by *Neopestalotiopsis clavispora* and *Pestalotiopsis affinis* (Chen et al. 2002; Wang et al. 2019), needle blight caused by *Pestalotiopsis microspora* (Li 2017), anthracnose disease caused by *Colletotrichum gloeosporioides* (Fan et al. 2006) and wilt disease caused by *Phoma* sp., while *Fusarium oxysporum* is responsible for root rot (Qian et al. 2015). Needle diseases caused by Pestalotioid fungal species (e.g. *N. clavispora*, *P. affinis* and *P. microspora*) are a serious threat to Chinese yew in Fujian and Yunnan Provinces, China (Chen et al. 2002; Li 2017; Wang et al. 2019). Up to 40% of the Chinese yew are severely affected in the field (Wang et al. 2019). The needles of Chinese yew became brown and reddish-brown from the leaf margin to the main vein, with irregular or round spots. Eventually, the spots coalesced and the needles withered and abscised (Li 2017; Wang et al. 2019). Jeon and Cheon (2014) reported that *P. microspora* also caused leaf blight in Japanese yew (*Taxus cuspidata* Sieb. & Zucc.) in South Korea. This disease developed on needles, particularly under high humidity, producing brown or tan spots that coalesce to form large lesions (Jeon and Cheon 2014).

Pestalotioid fungi (*Pestalotiopsis*-like fungi) represent an important fungal group that commonly occur as plant pathogens, endophytes and saprophytes in a wide range of hosts (Maharachchikumbura et al. 2014; Reddy et al. 2016; Ran et al. 2017; Freitas et al. 2019; Yang et al. 2021; Xiong et al. 2022). This group, which comprise *Neopestalotiopsis*, *Pestalotiopsis* and *Pseudopestalotiopsis*, belongs to the order Amphisphaeriales (Jiang et al. 2022; Zhang et al. 2022). The two genera *Neopestalotiopsis* and *Pseudopestalotiopsis* were segregated from *Pestalotiopsis* by Maharachchikumbura et al. (2014) based on multigene phylogenetic analysis and morphological differences (conidiogenous cells and colour intensities of the median conidial cell). *Pestalotiopsis* is characterised by lightly pigmented concolorous median cells, whereas *Neopestalotiopsis* species are characterised by versicolorous median cells and indistinct conidiophores and *Pseudopestalotiopsis* by darkly coloured concolorous median conidial cells (Maharachchikumbura et al. 2014). Many *Pestalotiopsis* species have been isolated from *Taxus* spp. as endophytes rich in secondary metabolites. For example, *Pestalotiopsis versicolor* has been isolated from healthy leaves of *Taxus cuspidata* and is an excellent alternative source of paclitaxel supply (Kumaran et al. 2010). Furthermore, *P. microspora*, which causes Chinese yew leaf blight, is an endophyte of the Himalayan yew (*Taxus wallichiana*), which produces taxol (Strobel et al. 1996).

During a survey of diseases in Chinese yew, moderate-to-severe incidences of needle spot and stem canker diseases were observed in some planting areas in Guangxi Province in 2020, and several Pestalotioid fungi were isolated from the diseased Chinese yew. The objectives of our study were to: (i) identify the Pestalotioid fungi recovered from symptomatic Chinese yew using morphological features and molecular data analyses; (ii) evaluate the pathogenicity of different fungal species on detached Chinese yew; and (iii) evaluate the effects of temperature, light duration and carbon source on the mycelial growth rate of different fungal species.

## Materials and methods

### Sample collections and Fungal Isolation

In May 2020, twenty symptomatic Chinese yew specimens were collected from the Guangxi Province. Small sections (5 × 5 mm) were cut from the margins of the infected needles and stems, surface-sterilised in 75% ethanol for 30 s, sterilised in 3% (vol/vol) sodium hypochlorite for 1 min, followed by three rinses in sterile distilled water and finally dried on sterilised filter paper (Rubini et al. 2005; Li et al. 2021b). The sections were plated on PDA plates and incubated at 25 °C. The isolates were aseptically transferred to fresh PDA and purified using a single-spore culture. The holotype specimens in this study are deposited in the Museum of Beijing Forestry University (Herbarium Code: BJFC). The pure fungal cultures in this study are deposited in China Forestry Culture Collection Center (Acronym: CFCC).

### Morphological and culture characterisation

The colony characteristics (colour and texture) of each isolate on PDA were observed after 7 d incubation at 25 °C and the morphological characters of conidiophores, conidiogenous cells and conidia of each isolate on PDA were observed after 14 d incubation at 25 °C (Li et al. 2021b). The size was determined by measuring the length and width of 50 randomly chosen conidia using an Olympus SZX2-FOF Light microscope (Tokyo, Japan) according to the method described by Shu et al. (2020). Descriptions, nomenclature and illustrations of taxonomic novelties have been deposited in MycoBank (<https://www.mycobank.org/>).

### DNA extraction and PCR amplification

Genomic DNA was extracted from 7 day-old colonies grown on PDA using the cetyltrimethylammonium bromide (CTAB) method (Doyle and Doyle 1990). Three loci were amplified: the internal transcribed spacer region of ribosomal DNA (ITS) with primers ITS1/ITS4 (White et al. 1990); beta-tubulin (*tub2*) with primers Bt2a/Bt2b (Glass and Donaldson 1995) and the translation elongation factor 1-alpha gene (*tef-1a*) with EF1-688F/EF1-1251R (Alves et al. 2008). The PCR mixture consisted of 10 µl TopTaq Master Mix, 7 µl nuclease-free H<sub>2</sub>O, 1 µl of each primer and 1 µl DNA samples were made up to the final volume of 20 µl. Primer sequences and reaction conditions were shown in Suppl. material 1. The PCR products were sent for sequencing at Beijing Tsingke Biotech Company, Ltd., Beijing, China. The DNA sequences have been deposited in GenBank (Suppl. material 2).

### Sequence alignment and phylogenetic analyses

The taxa used in the analyses were obtained from the sequence data of *Pestalotiopsis* and *Neopestalotiopsis* downloaded from GenBank (Suppl. material 2). Sequence alignments were performed using MAFFT v.7 ([mafft.cbrc.jp/alignment/server](http://mafft.cbrc.jp/alignment/server)) (Kato and Standley 2013). Phylogenetic analyses, based on a combined dataset of ITS, *tub2* and *tef-1a* sequence data, were performed with Maximum Parsimony (MP), Maximum Likelihood (ML) and Bayesian Inference (BI). MP analysis was performed with PAUP 4.0b using a heuristic search algorithm (1,000 random-addition sequences) with tree bisection and reconnection

(TBR) branch swapping. MaxTrees were set to 5,000, branches of zero length were collapsed and all equally parsimonious trees were saved (Swofford 2003). ML analysis was performed using RAxML-HPC BlackBox v. 8.2.12, with 1000 rapid bootstrap replicate runs using the GTRGAMMA model of nucleotide evolution (Stamatakis 2014). For BI analysis, the best-fit evolutionary models for each partitioned locus were deduced on the AIC (ITS: GTR+I+G, *tub2*: HKY+I+G and *tef-1α*: TrN+I+G) which were estimated in MrModelTest v. 2.3. The BI analysis was performed using MrBayes v.3.1.2, with a Markov Chain Monte Carlo (MCMC) algorithm running from random trees for 1,000,000 generations. The resulting trees were edited using FigTree v.1.4.2 (Rambaut 2016) and Adobe Illustrator CS5.

### Culture characteristics

Five Pestalotioid species were selected to evaluate the effects of temperature, light duration and carbon source on mycelial growth. Mycelial plugs of each species were taken from the colony margins of 3-day-old cultures and transferred to fresh plates (20 ml of culture medium, pH 6). The effects of temperature were tested in the range 19 to 31 °C with a 3 °C gradient on PDA and incubated in dark. To monitor the effects of light duration, the isolates were tested under three diel light cycles (24 h dark, 12 h light/12 h dark and 24 h light per day) on PDA and incubated at 25 °C. The effects of the carbon source were tested using sucrose, maltose and dextrose with the same carbon content. Three replicates were used for the temperature and light duration tests and two replicates were used for the carbon test. The colony diameters were measured daily.

### Pathogenicity testing

Healthy needles were collected from five-year old and healthy Chinese yew grown in a greenhouse. The needles were washed with tap water, submerged in 70% ethanol for 2 min and rinsed twice with sterile water (Li et al. 2021b). Clean dry needles were placed on Petri dishes with moist filter paper underneath. Puncture wounds were made in the middle of each needle using a sterilised needle. The wounded needles were inoculated with mycelial PDA plugs (3 mm in diameter) and spore suspensions (18 µl, 10<sup>6</sup> conidia/ml) of five Pestalotioid isolates, respectively. Three replicates were used for the mycelial PDA plug test and 10 replicates were used for the spore suspension test. Lesion length was recorded daily.

## Results

### Field observations and fungal isolation

A field survey was conducted from April to October 2020 in a forest farm in northern Guangxi, China, where more than 500 Chinese yew trees were maintained. Needle spot disease in Chinese yew causes serious damage, with an incidence of 58–70% in plants. The spots on the needles were initially small, brown to black and oval to irregular. Subsequently, they gradually expand and finally coalesce, forming large black spots. In severe cases, lesions can develop in large portions of a single needle. Over time, the heavily infected leaves dried and died. Lesions were also visible on the stems and the spots on the stems darkened and became necrotic (Fig. 1).

Thirty-six isolates were obtained from the diseased needles and stems of Chinese yew and 18 isolates of Pestalotioid fungi were identified based on their culture characteristics and conidial morphology. Eight isolates were grouped into *Neopestalotiopsis* species with versicolorous median cells and ten isolates were identified as *Pestalotiopsis* with lightly pigmented concolorous median cells. Colonies of most Pestalotioid stains were initially whitish and later greyish or yellow on PDA. Conidia varied from 14.5 to 25.0  $\mu\text{m}$  mean length and 3.5 to 8.0  $\mu\text{m}$  mean width. The apical appendages showed the largest variation in size, with a mean length of 5.0 to 23.0  $\mu\text{m}$ . The number of apical appendages varied between two and four, with three being the most common. Basal appendages were hyaline, straight or slightly curved and varied from 1.0 to 5.0  $\mu\text{m}$  mean length.

### Phylogenetic analyses

The phylogenetic tree (*Pestalotiopsis*), based on the concatenated sequences of ITS, *tub2* and *tef-1a*, comprised 121 ingroups and one outgroup, *Pseudopestalotiopsis cocos* (CBS 272.29). A total of 1,496 characters including gaps (401 for ITS, 313 for *tub2* and 860 for *tef-1a*) were included in the phylogenetic analysis. Similar tree topologies were obtained using the MP, ML and BI methods and the best-scoring MP tree obtained from a heuristic search with 1000 random taxon additions is presented (Fig. 2). The phylogenetic tree placed the six *Pestalotiopsis* isolates into three well-supported monophyletic clades, representing two novel and one known species. Two of our isolates (CFCC59981 and CFCC59982), described as *Pestalotiopsis multicolor*, formed monophyletic groups with high support values (100% MP and ML, 1.00 BI). Two isolates (CFCC59976 and CFCC59978), identified as *Pestalotiopsis taxicola*, constituted an independent and strongly-supported subclade (100% MP and ML, 1.00 BI), sharing close affinity with *Pestalotiopsis unicolor* and *Pestalotiopsis jiangxiensis*. Two strains (BJFUCC42 and BJFUCC42-2) clustered with *Pestalotiopsis trachycarpicola* and were, therefore, described as known species.

The phylogenetic tree (*Neopestalotiopsis*), based on the concatenated gene sequences of ITS, *tub2* and *tef-1a*, comprised 95 ingroups and one outgroup, *Pestalotiopsis diversiseta* (MFLUCC 12-0287). A total of 1,386 characters including gaps (411 for ITS, 393 for *tub2* and 582 for *tef-1a*) were included in

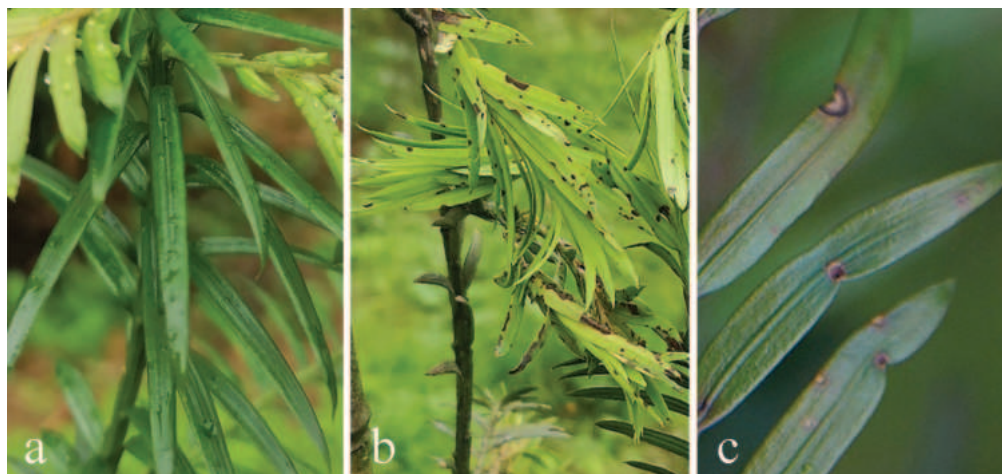


**Figure 1.** **a** healthy Chinese yew needles **b, c** chinese yew needles with spots.

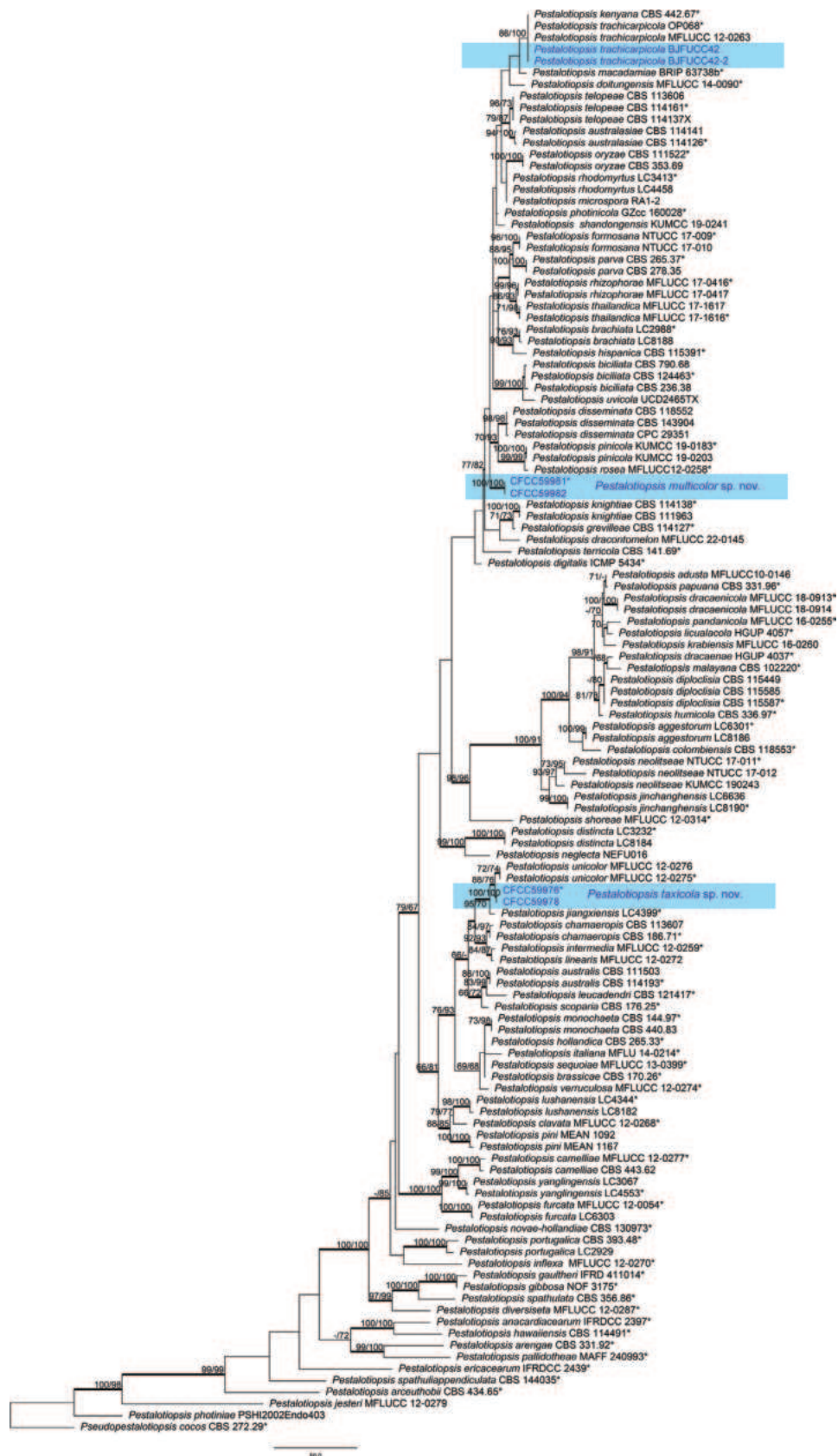


Figure 2. A phylogenetic tree of *Pestalotiopsis* generated from MP analysis, based on combined ITS, *tub2* and *tef-1a* sequence data. Maximum Parsimony and Maximum Likelihood bootstrap values  $\geq 65\%$  are given at the nodes. The branches with Bayesian Inference posterior probabilities  $\geq 0.90$  are bold. Strains from this study are marked in blue. Ex-type strains are labelled with \*.

the phylogenetic analysis. Similar tree topologies were obtained using the MP, ML and BI methods and the best-scoring MP tree obtained from a heuristic search with 1000 random taxon additions is presented (Fig. 3). Two of our isolates (CFCC59989 and CFCC59990) clustered together and nested in a clade containing two different *Neopestalotiopsis* sp. 2 isolates (CFCC 54340 and ZX22B). In contrast, two isolates (CFCC59985 and CFCC59986), grouped *Neopestalotiopsis rhapsidis* (Fig. 3).



**Figure 3.** A phylogenetic tree of *Neopestalotiopsis* generated from MP analysis, based on combined ITS, *tub2* and *tef-1a* sequence data. Maximum Parsimony and Maximum Likelihood bootstrap values  $\geq 65\%$  are given at the nodes. The branches with Bayesian Inference posterior probabilities  $\geq 0.90$  are bold. Strains from this study are marked in blue. Ex-type strains are labelled with \*.

## Taxonomy

### *Pestalotiopsis trachycarpicola* Yan M. Zhang & K.D. Hyde, 2012

Fig. 4

**Conidiogenesis.** Conidiophores reduced to conidiogenous cells, indistinct. Conidiogenous cells were discrete, ampulliform, thin-walled, hyaline, smooth. Conidia fusiform to clavate, straight or slightly curved, olivaceous to brown, 4-septate,  $18.5\text{--}25 \times 4\text{--}6 \mu\text{m}$ , with apical and basal appendages. Basal cell obconic, hyaline, thin-walled, smooth,  $3\text{--}5 \mu\text{m}$ ; the three median cells dolioform, versicolor, pale brown to brown with septa darker than the rest of the cells,  $11.5\text{--}13.5 \mu\text{m}$ , the second cell from base  $3.5\text{--}6 \mu\text{m}$ ; the third cell  $3.5\text{--}4.5 \mu\text{m}$ ; the fourth cell  $3.5\text{--}5 \mu\text{m}$ ; apical cell  $2.5\text{--}4 \mu\text{m}$ , cylindrical, hyaline; 2–4 tubular apical appendages, arising from the apex of the apical cell each at different point, filiform,  $5\text{--}15 \mu\text{m}$ ; basal appendage present most of the time, single, tubular, unbranched,  $3.5\text{--}4.5 \mu\text{m}$  (Fig. 4c–e). Sexual morph not observed.

**Culture characteristics.** Colonies on PDA reaching 90 mm diameter after seven days at  $25 \text{ }^\circ\text{C}$ , with an undulate and radial edge, with dense aerial mycelium on surface, white to faint yellow on front, pale honey-coloured on the reverse side (Fig. 4a). *Conidiomata acervular* in culture on PDA, globose,  $100\text{--}500 \mu\text{m}$  in diameter, solitary or aggregated in clusters, exuding black conidial masses (Fig. 4b).

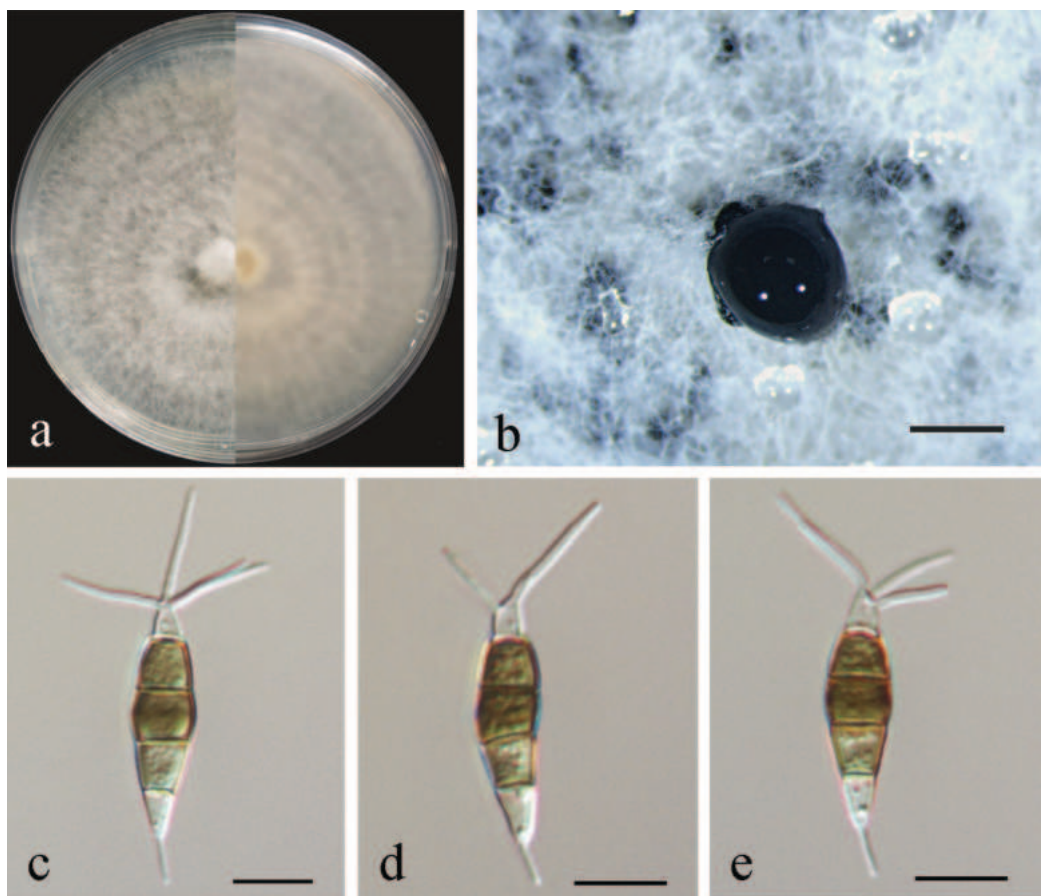


**Figure 4.** *Pestalotiopsis trachycarpicola* (BJFUCC42) **a** culture on PDA **b** conidiomata formed on PDA **c–e** conidia. Scale bars:  $500 \mu\text{m}$  (**b**);  $10 \mu\text{m}$  (**c–e**).

**Material examined.** CHINA, Guangxi Province, from diseased needles of Chinese yew, May 2020, Y. F. Wang (BJFC-S1955); living cultures BJFUCC42, BJFUCC42-2.

**Notes.** *Pestalotiopsis trachycarpicola* was originally described from leaves of *Trachycarpus fortunei* in Kunming Botany Garden, Kunming, Yunnan Province, China (Zhang et al. 2012). In the present study, the two isolates clustered with *P. trachycarpicola* and *P. kenyana* with high support values (MP/ML = 86/100). *P. kenyana* (CBS 442.67, ex-type) and *P. trachycarpicola* (OP068, ex-type MFLUCC 12-0263) were demonstrated to be the same species, as there was no genetic distance between the two samples (Suppl. material 3). Morphologically, our new collections resembled *P. trachycarpicola* in colour and size of the conidiogenous cells, conidia and appendages (Zhang et al. 2012). Therefore, we reported the two isolates as a new host record of *P. trachycarpicola* from yews.

***Pestalotiopsis taxicola* Y. F. Wang & C. J. You, sp. nov.**

MycoBank No: 847791

Fig. 5

**Etymology.** Named after the host species, *Taxus chinensis*.

**Holotype.** BJFC-S1954.

**Conidiogenesis.** Conidiophores reduced to conidiogenous cells, indistinct. Conidiogenous cells were discrete, ampulliform, thin-walled, hyaline, smooth. Conidia fusiform to clavate, straight or slightly curved, olivaceous to brown, 4-septate, 16.5–21 × 4–6 µm, with apical and basal appendages. Basal cell obconic, hyaline, thin-walled, smooth, 2.5–4 µm; the three median cells dolioform, versicolor, pale brown to brown with septa darker than the rest of the cells, 10.5–12 µm, the second cell from base 3–4 µm; the third cell 3.5–4 µm; the fourth cell 3.5–4 µm; apical cell 2.5–4 µm, cylindrical, hyaline; 3 tubular apical appendages, arising from the apex of the apical cell each at a different point, filiform, 9.5–15 µm; basal appendage present most of the time, single, tubular, unbranched, 2–5 µm (Fig. 5c–e). Sexual morph not observed.

**Culture characteristics.** Colonies on PDA reaching 90 mm diameter after seven days at 25 °C, with an undulate and radial edge, with dense aerial mycelium on surface, initially yellow in the centre, becoming white at the margin, with white appressed mycelia radiating outwards (Fig. 5a). *Conidiomata acervular* in culture on PDA, globose, 200–700 µm in diameter, solitary or aggregated in clusters, exuding black conidial masses (Fig. 5b).

**Material examined.** CHINA, Guangxi Province, from diseased needles of Chinese yew, May 2020, Y. F. Wang (BJFC-S1954, holotype); ex-type living culture CFCC59976, living cultures CFCC59978, CFCC59979 and CFCC59980.

**Notes.** *Pestalotiopsis taxicola* was phylogenetically placed in a clade encompassing *P. unicolor*, but as a unique lineage with high support (MP/ML = 100/100) (Fig. 2). Compared with *P. unicolor* (MFLUCC 12-0276, ex-type) and *P. taxicola* (CFCC59976, ex-type), there were one nucleotide difference in the ITS region and nine nucleotide differences in the *tef-1a* region. Morphologically, *P. taxicola* had smaller conidia (16.5–21 × 4–6 µm) than *P. unicolor* (20–24.5 × 4–6 µm). In addition, *P. taxicola* had only one basal appendage, whereas *P. unicolor* had 1–2 basal appendages (Maharachchikumbura et al. 2012). Therefore, the four isolates were designated as a new species.

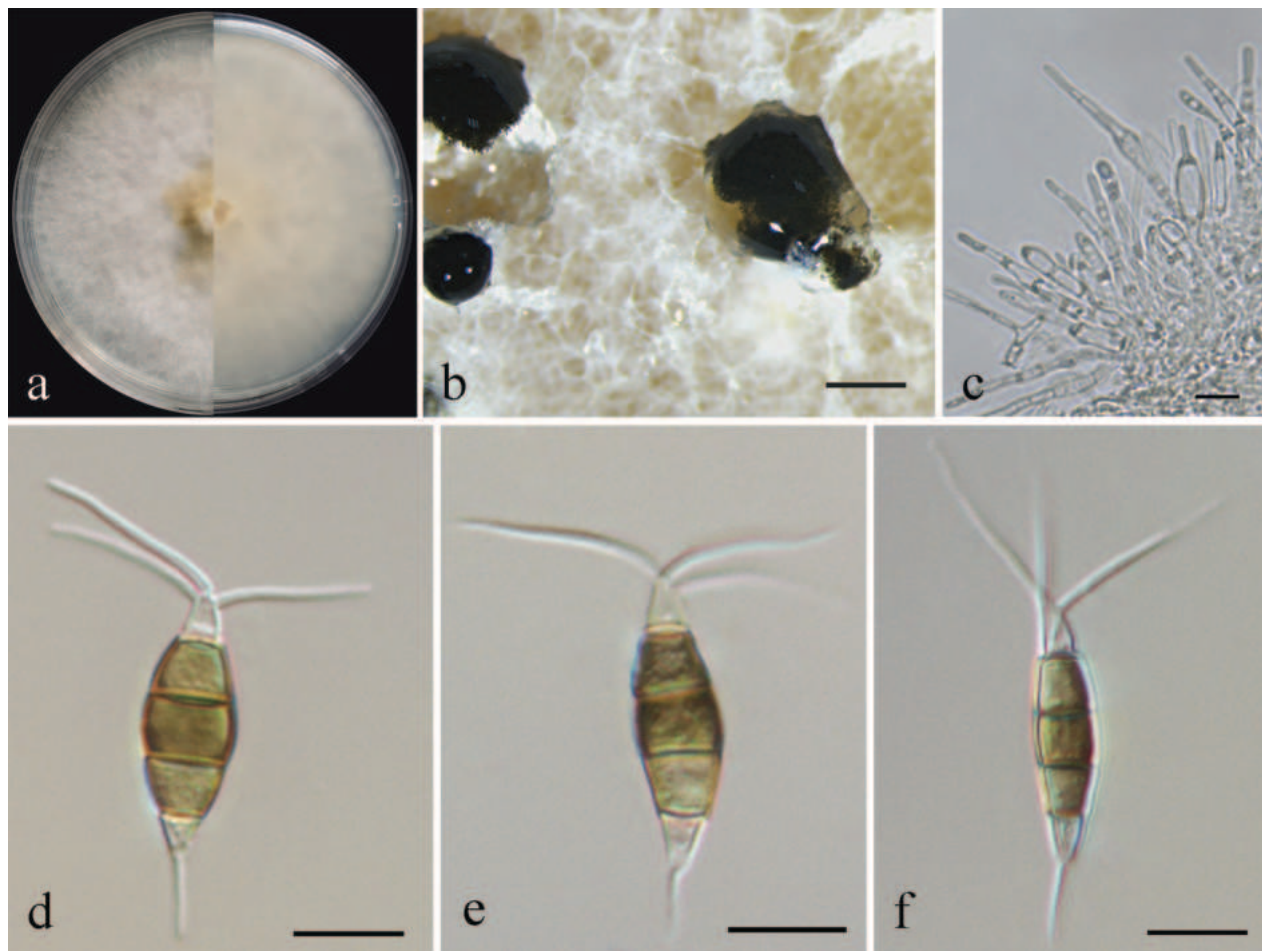


**Figure 5.** *Pestalotiopsis taxicola* (CFCC59976) **a** culture on PDA **b** conidiomata formed on PDA **c** conidiogenous cells **d–f** conidia. Scale bars: 500 µm (**b**); 10 µm (**c–f**).

***Pestalotiopsis multicolor* Y. F. Wang & C. J. You, sp. nov.**

MycoBank No: 847792

Fig. 6

**Etymology.** In reference to the multicoloured median cells.

**Holotype.** BJFC-S1956.

**Conidiogenesis.** Conidiophores reduced to conidiogenous cells, short, subcylindrical and hyaline. Conidiogenous cells were discrete, ampulliform, thin-walled, hyaline, smooth. Conidia fusiform to clavate, straight or slightly curved, olivaceous to brown, 4-septate,  $14.5\text{--}20 \times 3.5\text{--}5.5 \mu\text{m}$ , with apical and basal appendages. Basal cell obconic, hyaline, thin-walled, smooth,  $2\text{--}4.5 \mu\text{m}$ ; the three median cells dolioform, versicolor, pale brown to brown with septa darker than the rest of the cells,  $9.5\text{--}13 \mu\text{m}$ , the second cell from base  $2.5\text{--}4.5 \mu\text{m}$ ; the third cell  $3\text{--}4.5 \mu\text{m}$ ; the fourth cell  $3\text{--}4 \mu\text{m}$ ; apical cell  $2.5\text{--}3.5 \mu\text{m}$ , cylindrical, hyaline; 2–3 (mostly 3) tubular apical appendages, arising from the apex of the apical cell each at a different point, filiform,  $8\text{--}16 \mu\text{m}$ ; basal appendage present most of the time, single, tubular, unbranched,  $2.5\text{--}4.5 \mu\text{m}$  (Fig. 6c–e). Sexual morph not observed.

**Culture characteristics.** Colonies on PDA reaching 90 mm diameter after seven days at 25 °C, with an undulate and radial edge, white aerial mycelium on surface flat or raised (Fig. 6a). *Conidiomata acervular* in culture on PDA, glo-

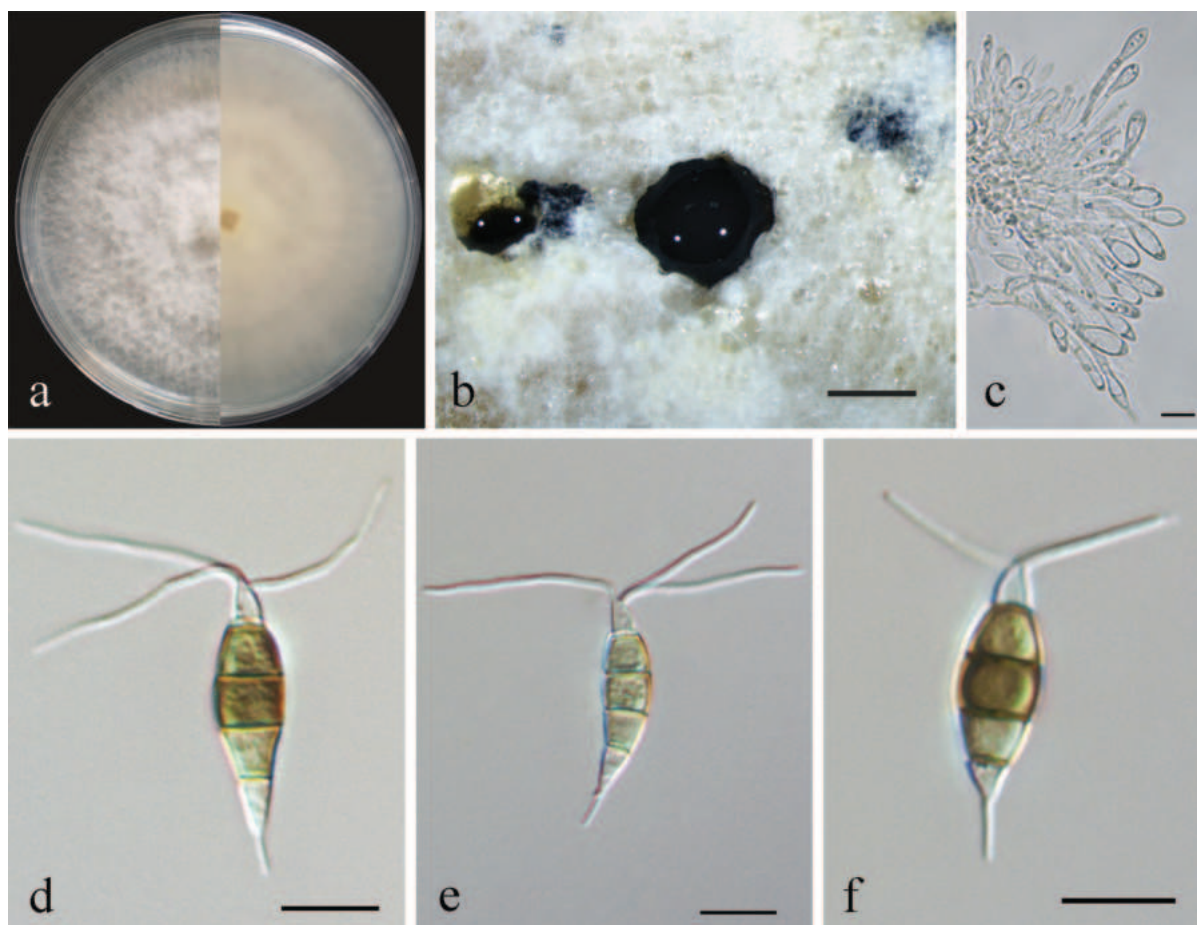


**Figure 6.** *Pestalotiopsis multicolor* (CFCC59981) **a** culture on PDA **b** conidiomata form on PDA **c** conidiogenous cells **d–f** conidia. Scale bars: 500 µm (**b**); 10 µm (**c–f**).

bose, 200–800 µm in diameter, solitary or aggregated in clusters, exuding black conidial masses (Fig. 5b).

**Material examined.** CHINA, Guangxi Province, from diseased needles of Chinese yew, May 2020, Y. F. Wang (BJFC-S1956, holotype); ex-type living culture CFCC59981, living cultures CFCC59982, CFCC59983, and CFCC59984.

**Notes.** The two isolates (CFCC59981 and CFCC59982) formed a distinct lineage with high support values (MP/ML = 100/100) in the phylogenetic tree. The morphology of the two isolates was distinctive within the *Pestalotiopsis* genus because the conidia were far smaller than those of any other species. In addition, the colour of median cells in our new collections changed from light concolorous to versicolorous. Therefore, four isolates in the present study were designated as a new species.

### ***Neopestalotiopsis* sp. 3**

Fig. 7

**Conidiogenesis.** Conidiophores reduced to conidiogenous cells, hyaline, smooth. Conidiogenous cells were discrete, ampulliform, thin-walled, hyaline to light brown, smooth. Conidia fusiform to clavate, straight or slightly curved, olivaceous to brown, 4-septate, 15.5–19 × 6–7.5 µm, with apical and basal appendages. Bas-

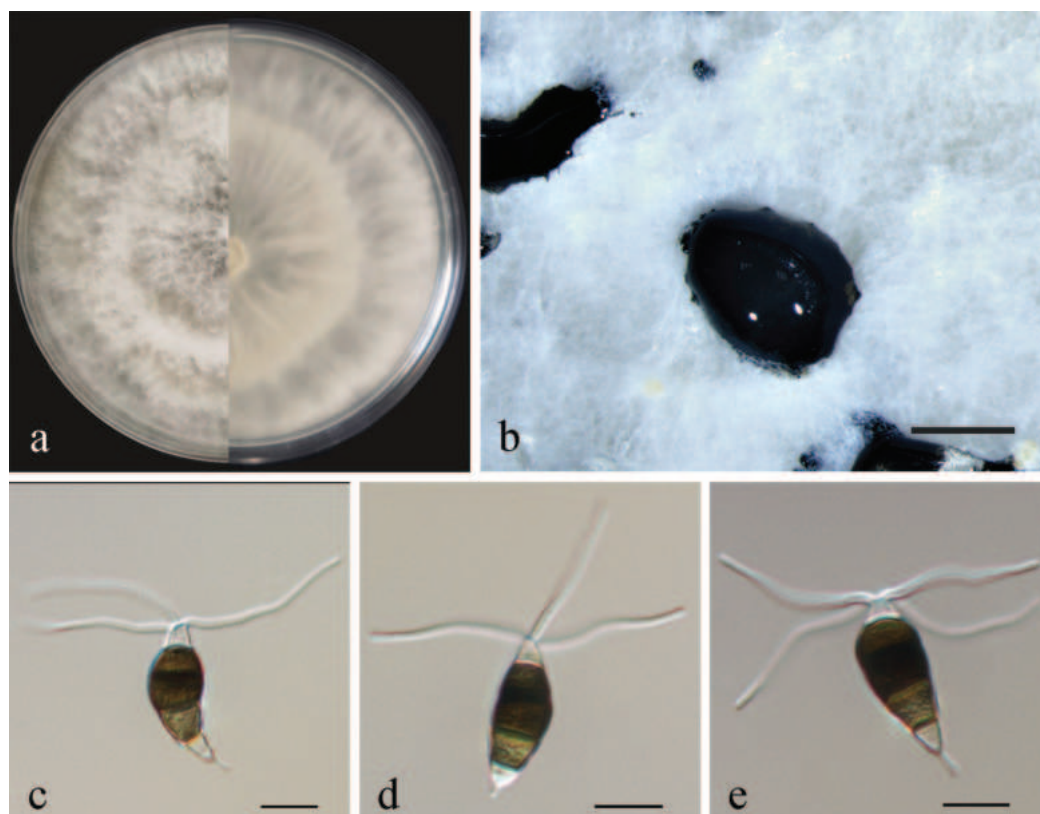


**Figure 7.** *Neopestalotiopsis* sp. 3 (CFCC59985) **a** culture on PDA **b** conidiomata form on PDA **c–e** conidia. Scale bars: 500  $\mu$ m (**b**); 10  $\mu$ m (**c–e**).

al cell obconic, hyaline, thin-walled, smooth, 2–4  $\mu$ m; the three median cells 10.5–12  $\mu$ m, dolioform, versicolor, pale brown to brown with septa darker than the rest of the cells, the second cell from base 2.5–4.5  $\mu$ m; the third cell 3.5–4.5  $\mu$ m; the fourth cell 3–4  $\mu$ m; apical cell 1.5–3  $\mu$ m, cylindrical, hyaline; 3–4 (mostly 3) tubular apical appendages, arising from the apex of the apical cell each at a different point, filiform, 16–23  $\mu$ m; basal appendage present most of the time, single, tubular, unbranched, 1–2.5  $\mu$ m (Fig. 7c–e). Sexual morph not observed.

**Culture characteristics.** Colonies on PDA reaching 90 mm diameter after seven days at 25 °C, white aerial mycelium on surface, flat or raised, radiating outwards with an undulate and radial edge (Fig. 7a). *Conidiomata acervular* in culture on PDA, globose, 80–800  $\mu$ m diameter, solitary or aggregated in clusters, exuding black conidial masses (Fig. 7b).

**Material examined.** CHINA, Guangxi Province, from diseased shoots of Chinese yew, May 2020, Y. F. Wang (BJFC-S1957); living cultures CFCC59985, CFCC59986, CFCC59987, CFCC59988.

**Notes.** *Neopestalotiopsis* sp. 3 (CFCC59985 and CFCC59986) was phylogenetically close to *N. rhapsidis* (Yang et al. 2021) (Fig. 3) but differed in conidial size (15.5–19  $\times$  6–7.5  $\mu$ m in *Neopestalotiopsis* sp. 3 vs. 22–25.5  $\times$  4–6  $\mu$ m in *N. rhapsidis*). Furthermore, *Neopestalotiopsis* sp. 3 had longer apical appendages (16–23  $\mu$ m vs. 11–16  $\mu$ m) and shorter basal appendage (1–2.5  $\mu$ m vs. 2–5.5  $\mu$ m) than *N. rhapsidis*. Compared with *N. rhapsidis* (GUCC 21501, ex-type) and *Neopestalotiopsis* sp. 3, there were eleven nucleotide differences in the ITS region, four nucleotide differences in the *tef-1a* region and six nucleotide differences in the *tub2* region. In the genus *Neopestalotiopsis*, the interspe-

cific relationship remains unclear (Li et al. 2021b), as some clades were not unanimously strongly supported, meaning the genus will be largely revised in the near future. Many taxa are likely to be synonymised in future publications. Therefore, CFCC59985 and CFCC59986 were not proposed as a new species.

#### ***Neopestalotiopsis* sp. 4**

Fig. 8

**Conidiogenesis.** Conidiophores reduced to conidiogenous cells, hyaline, smooth. Conidiogenous cells were discrete, ampulliform, thin-walled, hyaline to light brown, smooth. Conidia fusiform to clavate, straight or slightly curved, olivaceous to brown, 4-septate,  $15.5\text{--}18.5 \times 6\text{--}8 \mu\text{m}$ , with apical and basal appendages. Basal cell obconic, hyaline, thin-walled, smooth,  $2.5\text{--}4 \mu\text{m}$ ; the three median cells  $10.5\text{--}12 \mu\text{m}$ , dolioform, versicolor, pale brown to brown with septa darker than the rest of the cells, the second cell from base  $3\text{--}3.5 \mu\text{m}$ ; the third cell  $3\text{--}4.5 \mu\text{m}$ ; the fourth cell  $3\text{--}5.5 \mu\text{m}$ ; apical cell  $1\text{--}2.5 \mu\text{m}$ , cylindrical, hyaline; 3–4 (mostly 3) tubular apical appendages, arising from the apex of the apical cell each at a different point, filiform,  $9.5\text{--}15.5 \mu\text{m}$ ; basal appendage present most of the time, single, tubular, unbranched,  $1.5\text{--}4.5 \mu\text{m}$  (Fig. 8c–e). Sexual morph not observed.

**Culture characteristics.** Colonies on PDA reaching 90 mm diameter after seven days at  $25 \text{ }^\circ\text{C}$ , radiating outwards with an undulate and radial edge, white aerial mycelium was flat on the centres of the colony, while raised sharply in the outer ring (Fig. 8a). *Conidiomata acervular* in culture on PDA, globose,  $100\text{--}900 \mu\text{m}$  diameter, solitary or aggregated in clusters, exuding black conidial masses (Fig. 8b).

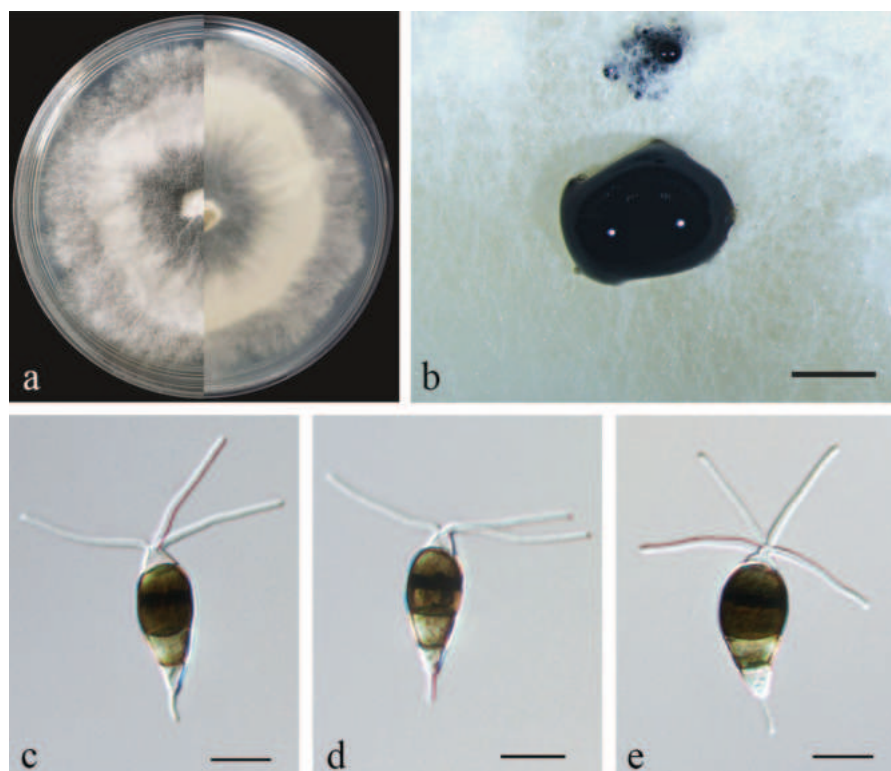


**Figure 8.** *Neopestalotiopsis* sp. 4 (CFCC59989) **a** culture on PDA **b** conidiomata form on PDA **c–e** conidia. Scale bars:  $500 \mu\text{m}$  (**b**);  $10 \mu\text{m}$  (**c–e**).

**Material examined.** CHINA, Gungxi Province, from diseased branches of Chinese yew, May 2020, Y. F. Wang (BJFC-S1958); living cultures CFCC59989, CFCC59990, CFCC59991 and CFCC59992.

**Notes.** *Neopestalotiopsis* sp. 4 (CFCC59989 and CFCC59990) was phylogenetically placed in a clade encompassing two *Neopestalotiopsis* sp. 2 isolates (CFCC54340 and ZX22B) from Yaan City, Sichuan Province (Jiang et al. 2021) (Fig. 3). Morphologically, *Neopestalotiopsis* sp. 4 had shorter conidia and longer apical appendages ( $15.5\text{--}18.5 \times 6\text{--}8 \mu\text{m}$ ,  $9.5\text{--}15.5 \mu\text{m}$ ) than CFCC54340 and ZX22B ( $22\text{--}25.2 \times 6.2\text{--}7.7 \mu\text{m}$ ,  $5\text{--}10 \mu\text{m}$ ). In addition, *Neopestalotiopsis* sp. 4 had more tubular apical appendages (3–4, mostly 3) than *Neopestalotiopsis* sp. 2 (2, seldom 3). Compared with *Neopestalotiopsis* sp. 2 (ZX22B) and *Neopestalotiopsis* sp. 4, there were six nucleotide differences in the ITS region, five nucleotide differences in the *tef-1a* region and three nucleotide differences in the *tub2* region. The taxonomy of the genera and species in this group remains unclear (Li et al. 2021b), as some clades were not unanimously strongly supported, meaning the genus will be largely revised in near future. Many taxa are likely to be synonymised in future publications. Therefore, CFCC59989 and CFCC59990 were not proposed as a new species.

### Culture characteristics

The effects of temperature on the growth of the five Pestalotioid species were shown in Fig. 9. When grown on PDA in the dark, all isolates grew at a temperature range of 19 to 31 °C, with optimum growth between 22 °C and 28 °C. The growth rate was drastically reduced below 22 °C and started to decline above 28 °C. The regression analysis showed the optimum temperatures for *P. trachycarpicola*, *P. taxicola*, *P. multicolor*, *Neopestalotiopsis* sp. 3 and *Neopestalotiopsis* sp. 4 were 25 °C, 24–26 °C, 22–25 °C, 25–28 °C and 25 °C, respectively. Within four days, the diameter of the majority of the isolates was approximately 90 mm, which is the diameter of the PDA plate.

Light duration had no effect on the mycelial growth of the two Pestalotioid species (*P. trachycarpicola* and *P. multicolor*) and the best growth of the three Pestalotioid fungi (*P. taxicola*, *P. multicolor* and *Neopestalotiopsis* sp. 4) was observed under continuous light (Suppl. material 4). The growth rate was highest for *P. taxicola* in 24 h light, which reached 66.4 mm diameter after four days. The growth rate was lowest for *P. trachycarpicola* in 12 h light/12 h dark, which reached only 55.5 mm in diameter after four days.

Five Pestalotioid species grew on all three tested carbon sources (Suppl. material 5). Maltose utilisation was the least efficient and the medium with dextrose showed comparatively high growth of the three tested fungi (*P. trachycarpicola*, *P. multicolor* and *Neopestalotiopsis* sp. 3). For *P. taxicola*, the utilisation of dextrose appeared to be higher than that of sucrose.

### Pathogenicity assay

The pathogenicity of two *Neopestalotiopsis* isolates (*Neopestalotiopsis* sp. 3 and *Neopestalotiopsis* sp. 4) and three *Pestalotiopsis* isolates (*P. trachycarpicola*, *P. taxicola* and *P. multicolor*) was tested by inoculating detached healthy needles according to Keith et al. (2003). Dark brown lesions and a

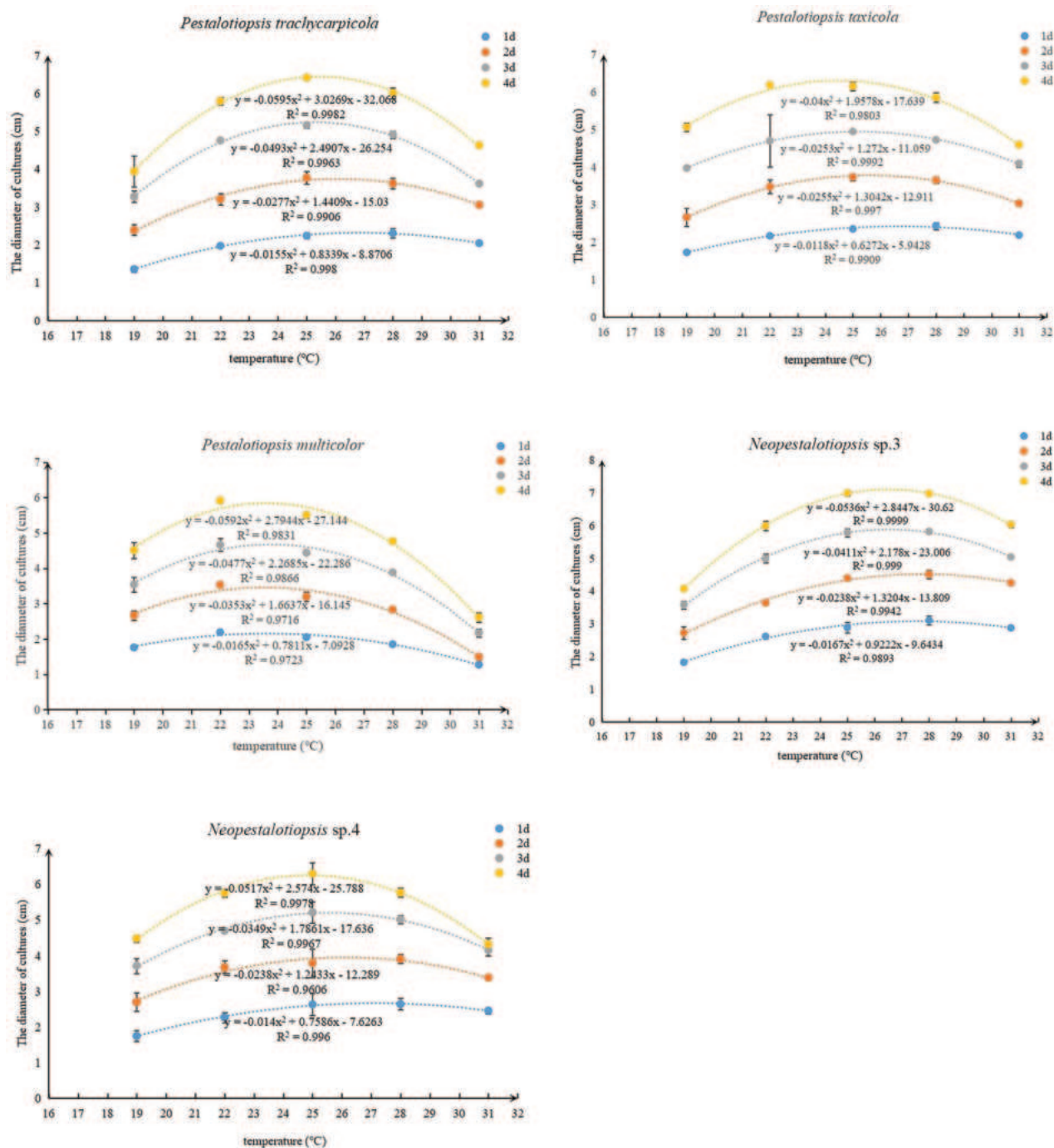
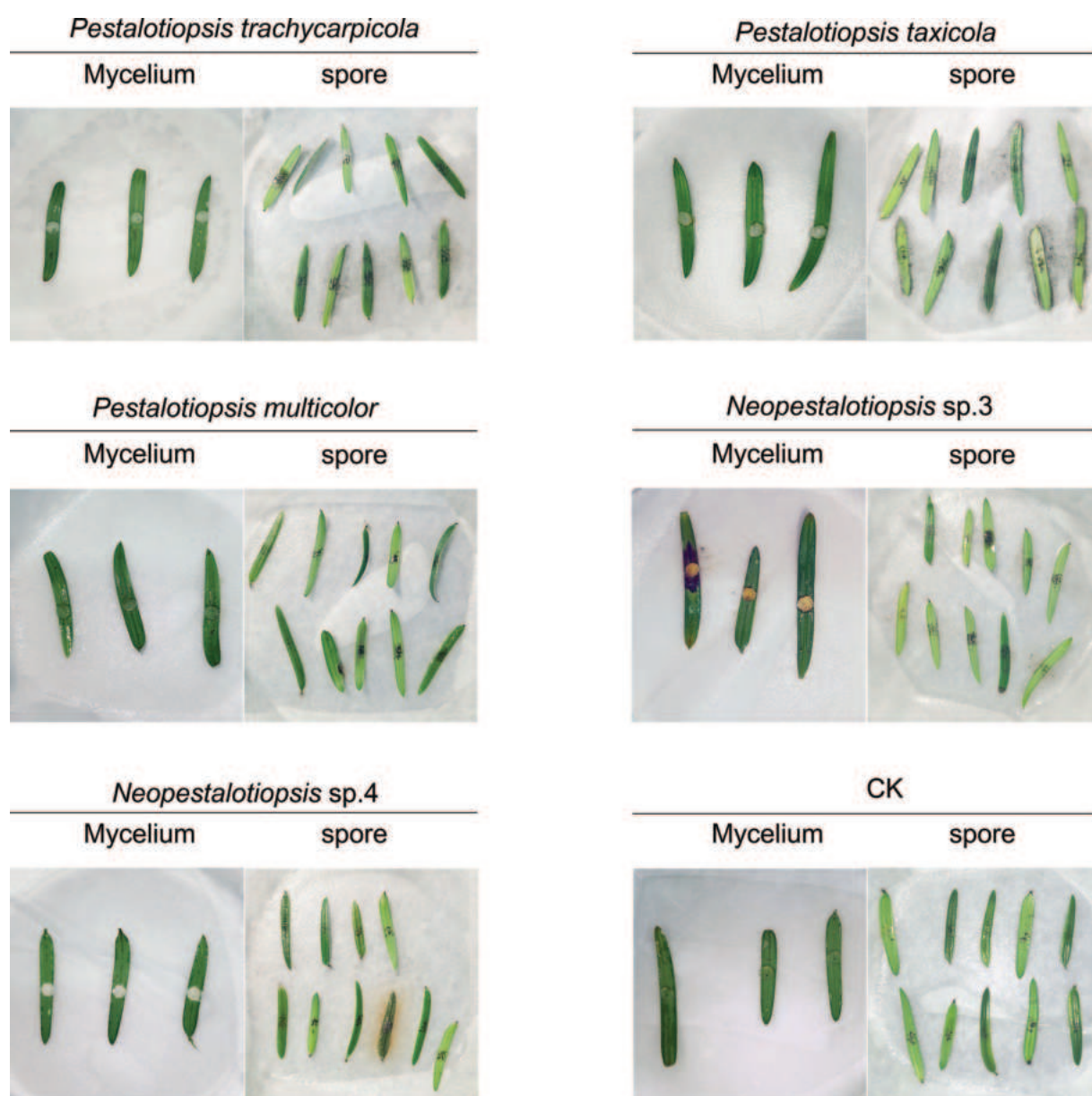


Figure 9. Effects of temperature on growth of isolates.

necrotic zone, which resembled the symptoms that occurred in the field, were observed on the needles 20 days after inoculation with mycelium plugs of *Neopestalotiopsis* sp. 3, which did not occur in the control inoculated with agar media or with the other four *Pestalotioid* species (Fig. 10). *Neopestalotiopsis* sp. 3 was re-isolated from the infected needles and was confirmed to be the same as the inoculated pathogen through morphological and phylogenetic analyses. However, none of the five isolates produced typical symptoms in the wounded needles inoculated with the spore suspension (Fig. 10). The results revealed that only *Neopestalotiopsis* sp. 3 is pathogenic to Chinese yew needles.

## Discussion

Cultivation of Chinese yew in some regions (e.g. Guangxi) has resulted in an increase in yew diseases, including new needle spot diseases, which have caused great losses in production. However, very little is known about the pathogens and the presence and prevalence of needle diseases in Chinese yew (Wang et al. 2019). During the investigation of Pestalotioid fungi isolated from diseased Chinese yew in the Guangxi Province of China, *Neopestalotiopsis* sp. 3 was found to cause needle spots on Chinese yew. Two new species of *Pestalotiopsis* were identified in association with symptomatic Chinese yew, namely, *P. taxicola* and *P. multicolor* and one known species, *P. trachycarpicola*, was identified, based on morphology and multi-locus phylogeny. The results indicated that the diversity of Pestalotioid species associated with Chinese yew was greater than previously determined.



**Figure 10.** Lesions of the Chinese yew needles after 20 days. CK is the blank control. The black spots in the mid-region of the needles are puncture wounds made by sterilised needles.

In the present study, the two species were distinct from other Pestalotioid species found in Chinese yew (Chen et al. 2002; Ding et al. 2009; Liu et al. 2010; Ismail et al. 2013; Li 2017; Subban et al. 2019; Qi et al. 2022; Sun et al. 2023). Morphologically, the conidia of *P. taxicola* and *P. multicolor* are smaller ( $16.5\text{--}21 \times 4\text{--}6 \mu\text{m}$  and  $14.5\text{--}20 \times 3.5\text{--}5.5 \mu\text{m}$ , respectively). Phylogenetically, the two novel species in the present study were distantly related to four known Pestalotioid species, with the exception of *P. affinis*, which was known only from its morphological descriptions; there were no DNA-based sequence data to compare the phylogenetic relationship with our novel species (Chaiwan et al. 2020).

Pestalotioid fungi represent a diverse group of more than 593 taxa (<http://www.indexfungorum.org/>). However, the taxonomy of the genera and species in this group remains unclear (Maharachchikumbura et al. 2014). In recent years, multi-gene phylogenetic analyses (Combined ITS, *tub2* and *tef-1a* sequence data) have been increasingly utilised to distinguish taxa in the group (Maharachchikumbura et al. 2012). In this study, the low statistical support for some species in the phylogenetic tree of *Neopestalotiopsis* may be due to the absence of *tub2* and *tef-1a* data in some taxa (Yang et al. 2021). The interspecific relationships in the genus *Neopestalotiopsis* are ambiguous (Li et al. 2021b), as some clades are not unambiguously strongly supported, indicating that the relationships amongst different species should be revised and re-evaluated. We decided against describing *Neopestalotiopsis* sp. 3 and sp. 4 as novel species in the genus. These two potentially novel species may be synonymised with existing species during revision and/or monography. Additional examination of archived specimens and sequence data is required for a better resolution and circumscription of *Neopestalotiopsis*.

In the present study, *P. trachycarpicola* was isolated from diseased needles. This is the first report of *P. trachycarpicola* isolated from yews in China. Under the trial conditions, no symptom development occurred in any of the inoculated needles, suggesting that *P. trachycarpicola* may behave as an endophyte in Chinese yew. *P. trachycarpicola* was first described in *Trachycarpus fortunei* in the Yunnan Province of China, causing leaf spot (Zhang et al. 2012) and has already been isolated from a wide range of hosts and locations worldwide (Fan et al. 2021; Khalilabad and Fotouhifar 2022; Araujo et al. 2023; Lan et al. 2023). For example, this fungus has been identified as the causal agent of leaf spots on *Sorghum bicolor* and *Panax notoginseng* in China (Fan et al. 2021; Lan et al. 2023), *Codiaeum variegatum* in Iran (Khalilabad and Fotouhifar 2022) and blueberry in Brazil (Araujo et al. 2023).

In the present study, various *Neopestalotiopsis* and *Pestalotiopsis* species were isolated from infected Chinese yew samples with similar symptoms. Moreover, pathogenicity tests showed that only *Neopestalotiopsis* sp. 3 was pathogenic to Chinese yew, causing dark brown lesions on wounded needles, suggesting that *Neopestalotiopsis* sp. 3 is responsible for needle-spot disease in Chinese yew. The four other Pestalotioid fungi that do not produce typical disease symptoms may be due to their relatively low virulence or endophytes (Reddy et al. 2016; Ma et al. 2019). Alternatively, the development of needle spots disease is the result of more than one biotic or abiotic factor. Different studies have indicated that some *Neopestalotiopsis* and *Pestalotiopsis* species have been isolated from healthy and dead tissues and reported as endophytic fungi. Several *Pestalotiopsis* species have been isolated as endophytes, but have been reported as pathogens in various hosts and in different regions (Moslemi and Taylor 2015; Nozawa et al. 2019; Wang et al. 2019; Chen et al.

2021; Jiang et al. 2021). This suggests that some species may have interchangeable lifestyles such as endophytes, pathogens and saprobes within the same host. Understanding the external factors that influence fungal lifestyles can have major implications for plant health (Sun et al. 2023). Furthermore, the inoculation of wounded needles with mycelial plugs and spore suspensions of *Neopestalotiopsis* sp. 3 was found to be ineffective against disease infection and development. In future studies, the inoculum form and field conditions, such as relative humidity and temperature, should be considered. Furthermore, *Neopestalotiopsis* sp. 3 grew faster than other Pestalotioid species on all three carbon sources tested ( $p < 0.01$ ), possibly contributing to its greater virulence than the others, but its growth on dextrose was not significantly different from that on the other two carbon sources (sucrose and maltose). In the present study, our results showed that temperature affected mycelial growth and *Neopestalotiopsis* sp. 3 grew well at 25–28 °C. The average monthly temperature between May and September is 25.6 °C and 26.8 °C, respectively, at our study site (<http://www.weather.com.cn/>). This is consistent with the most severe epidemic incidence and events observed during field surveillance and observation. Therefore, the culture characteristics of pathogenic fungi can be utilised to forecast and model disease spread.

In conclusion, the present study illustrates the diversity of Pestalotioid species associated with needle spot disease in Chinese yew. Understanding the taxonomy, biology and pathogenicity of Pestalotioid species associated with the Chinese yew will provide a foundation for monitoring disease development and provide information for management strategies for these pathogens.

## Additional information

### Conflict of interest

The authors have declared that no competing interests exist.

### Ethical statement

No ethical statement was reported.

### Funding

This work was supported by National Key R&D Program of China (No. 2021YFC2600400), The Fundamental Research Funds for the Central Universities, China (No. 2021ZY12) and National Natural Science Foundation of China (No. 31770683).

### Author contributions

All authors contributed extensively to the work presented in this paper. Conceptualisation: You CJ; Investigation: Wang YF; Data analysis: Chen SM; Writing-original draft: Wang YF; Writing & editing: You CJ & Tsui KM.

### Author ORCIDs

Yifeng Wang  <https://orcid.org/0009-0006-6533-6615>

Kin-Ming Tsui  <https://orcid.org/0000-0001-5129-1037>

Shimei Chen  <https://orcid.org/0009-0000-9862-9453>

Chongjuan You  <https://orcid.org/0000-0001-6130-5703>

## Data availability

All of the data that support the findings of this study are available in the main text or Supplementary Information.

## References

- Alves A, Crous PW, Correia A, Phillips AJL (2008) Morphological and molecular data reveal cryptic speciation in *Lasiodiplodia theobromae*. *Fungal Diversity* 28: 1–13. <https://doi.org/10.1002/yea.1554>
- Araujo L, Ferreira Pinto FAM, de Andrade CCL, Mituti T, Falkenbach BR, Gomes LB, Duarte V (2023) *Pestalotiopsis trachycarpicola* causes leaf spot disease on blueberry in Santa Catarina, Brazil. *Australasian Plant Disease Notes, Australasian Plant Pathology Society* 18(1): 14. <https://doi.org/10.1007/s13314-023-00500-7>
- Chaiwan N, Wanasinghe DN, Mapook A, Jayawardena RS, Norphanphoun C, Hyde KD (2020) Novel species of *Pestalotiopsis* fungi on *Dracaena* from Thailand. *Mycology* 11(04): 306–315. <https://doi.org/10.1080/21501203.2020.1801873>
- Chen Y, Wei G, Chen W (2002) New species of *Pestalotiopsis*. *Mycosystema* 21(03): 316–323.
- Chen Y, Wan Y, Zeng L, Meng Q, Yuan L, Tong H (2021) Characterization of *Pestalotiopsis chamaeropsis* causing gray blight disease on tea leaves (*Camellia sinensis*) in Chongqing, China. *Canadian Journal of Plant Pathology* 43(3): 413–420. <https://doi.org/10.1080/07060661.2020.1816582>
- Ding G, Zheng Z, Liu S, Zhang H, Guo L, Che Y (2009) Photinides A-F, cytotoxic benzofuranone-derived  $\gamma$ -Lactones from the plant endophytic fungus *Pestalotiopsis photiniae*. *Journal of Natural Products* 72(5): 942–945. <https://doi.org/10.1021/np900084d>
- Doyle JJ, Doyle JL (1990) Isolation of plant DNA from fresh tissue. *Focus (San Francisco, Calif.)* 12: 13–15.
- Fan X, Zhu J, Zhou X, Meng X, Lin Z, Guo W (2006) The identification and biological characteristics of the anthracnose pathogen of Southern Chinese yew. *Journal-Fujian College Forestry* 26(2): 117–122.
- Fan J, Qiu HB, Long HJ, Zhao W, Xiang XL, Hu AL (2021) First report of leaf spot on sorghum caused by *Pestalotiopsis trachycarpicola* in China. *Journal of Plant Pathology* 103(3): 1043–1044. <https://doi.org/10.1007/s42161-021-00853-x>
- Freitas EFS, Silva MD, Barros MVP, Kasuya MCM (2019) *Neopestalotiopsis hadrolaeliae* sp. nov., a new endophytic species from the roots of the endangered orchid *Hadrolaelia jongheana* in Brazil. *Phytotaxa* 416(3): 211–220. <https://doi.org/10.11646/phytotaxa.416.3.2>
- Gao ZW (2006) Research on *Taxus chinensis* var. *Mairei*. China Forestry Publishing House, China, 143 pp.
- Glass NL, Donaldson GC (1995) Development of primer sets designed for use with the PCR to amplify conserved genes from filamentous ascomycetes. *Applied and Environmental Microbiology* 61(4): 1323–1330. <https://doi.org/10.1128/aem.61.4.1323-1330.1995>
- Ismail AM, Cirvilleri G, Polizzi G (2013) Characterisation and pathogenicity of *Pestalotiopsis uvicola* and *Pestalotiopsis clavisporea* causing grey leaf spot of mango (*Mangifera indica* L.) in Italy. *European Journal of Plant Pathology* 135(4): 619–625. <https://doi.org/10.1007/s10658-012-0117-z>
- Jeon YH, Cheon W (2014) First report of leaf blight of Japanese yew caused by *Pestalotiopsis microspora* in Korea. *Plant Disease* 98(05): 691–691. <https://doi.org/10.1094/PDIS-08-13-0821-PDN>

- Jiang N, Fan X, Tian C (2021) Identification and characterization of leaf-inhabiting fungi from *Castanea* plantations in China. *Journal of Fungi* 7(1): 64. <https://doi.org/10.3390/jof7010064>
- Jiang N, Voglmayr H, Xue H, Piao CG, Li Y (2022) Morphology and phylogeny of *Pestalotiopsis* (Sporocadaceae, Amphisphaeriales) from Fagaceae leaves in China. *Microbiology Spectrum* 10(6): e03272–e22. <https://doi.org/10.1128/spectrum.03272-22>
- Katoh K, Standley DM (2013) MAFFT multiple sequence alignment software version 7: Improvements in performance and usability. *Molecular Biology and Evolution* 30(4): 772–780. <https://doi.org/10.1093/molbev/mst010>
- Keith RC, Keith LM, Hernandez-Guzman G, Uppalapati SR, Bender CL (2003) Alginate gene expression by *Pseudomonas syringae* pv. tomato DC3000 in host and non-host plants. *Microbiology (Reading, England)* 149(5): 1127–1138. <https://doi.org/10.1099/mic.0.26109-0>
- Khalilabad AA, Fotouhifar KB (2022) Morphological and molecular characterization of a novel *Pestalotiopsis trachycarpicola*, causing Garden Croton leaf spot in Iran. *Mycologia Iranica* 9(1): 59–66.
- Kumaran RS, Kim HJ, Hur BK (2010) Taxol promising fungal endophyte, *Pestalotiopsis* species isolated from *Taxus cuspidata*. *Journal of Bioscience and Bioengineering* 110(5): 541–546. <https://doi.org/10.1016/j.jbiosc.2010.06.007>
- Lan CZ, Lin X, Dai YL, Gan L, Liu XF, Ruan HC, Yang XJ (2023) First report of leaf blight on *Panax notoginseng* caused by *Pestalotiopsis trachycarpicola* in China. *Journal of Plant Pathology* 105(1): 321–321. <https://doi.org/10.1007/s42161-022-01236-6>
- Li Y (2017) Identification of the leaf spot pathogen on Chinese yew and screening of fungicides to *Pestalotiopsis microspora*. PhD Thesis, Fujian Agriculture and Forestry University, Fujian, China.
- Li C, Huo C, Zhang M, Shi Q (2008) Chemistry of Chinese yew, *Taxus chinensis* var. *mairei*. *Biochemical Systematics and Ecology* 36(4): 266–282. <https://doi.org/10.1016/j.bse.2007.08.002>
- Li K, Zhang G, Zhang Y, Griffith MP (2021a) A noteworthy case of rewilding Chinese yew from a garden population in eastern China. *PeerJ* 9: e12341. <https://doi.org/10.7717/peerj.12341>
- Li L, Yang Q, Li H (2021b) Morphology, phylogeny, and pathogenicity of Pestalotioid species on *Camellia oleifera* in China. *Journal of Fungi (Basel, Switzerland)* 7(12): 1080. <https://doi.org/10.3390/jof7121080>
- Liu AR, Chen SC, Wu SY, Xu T, Guo LD, Jeewon R, Wei JG (2010) Cultural studies coupled with DNA based sequence analyses and its implication on pigmentation as a phylogenetic marker in *Pestalotiopsis* taxonomy. *Molecular Phylogenetics and Evolution* 57(2): 528–535. <https://doi.org/10.1016/j.ympev.2010.07.017>
- Liu L, Wang Z, Huang L, Wang T, Su Y (2019) Chloroplast population genetics reveals low levels of genetic variation and conformation to the central-marginal hypothesis in *Taxus wallichiana* var. *mairei*, an endangered conifer endemic to China. *Ecology and Evolution* 9(20): 11944–11956. <https://doi.org/10.1002/ece3.5703>
- Ma XY, Maharachchikumbura SSN, Chen BW, Hyde KD, McKenzie EHC, Chomnunti P, Kang JC (2019) Endophytic pestalotioid taxa in *Dendrobium* orchids. *Phytotaxa* 419(3): 268–286. <https://doi.org/10.11646/phytotaxa.419.3.2>
- Maharachchikumbura SSN, Guo LD, Cai L, Chukeatirote E, Wu WP, Sun X, Crous PW, Bhat DJ, McKenzie EHC, Bahkali A, Hyde KD (2012) A multi-locus backbone tree for *Pestalotiopsis*, with a polyphasic characterization of 14 new species. *Fungal Diversity* 56(1): 95–129. <https://doi.org/10.1007/s13225-012-0198-1>

- Maharachchikumbura SSN, Hyde KD, Groenewald JZ, Xu J, Crous PW (2014) *Pestalotiopsis* revisited. *Studies in Mycology* 79(1): 121–186. <https://doi.org/10.1016/j.simyco.2014.09.005>
- Moslemi A, Taylor PWJ (2015) *Pestalotiopsis chamaeropsis* causing leaf spot disease of round leaf mint-bush (*Prostanthera rotundifolia*) in Australia. *Australasian Plant Disease Notes, Australasian Plant Pathology Society* 10(1): 1–5. <https://doi.org/10.1007/s13314-015-0179-9>
- Nozawa S, Seto Y, Watanabe K (2019) First report of leaf blight caused by *Pestalotiopsis chamaeropsis* and *Neopestalotiopsis* sp. in Japanese andromeda. *Journal of General Plant Pathology* 85(6): 449–452. <https://doi.org/10.1007/s10327-019-00868-4>
- Pyo SH, Park HB, Song BK, Han BH, Kim JH (2004) A large-scale purification of paclitaxel from cell cultures of *Taxus chinensis*. *Process Biochemistry (Barking, London, England)* 39(12): 1985–1991. <https://doi.org/10.1016/j.procbio.2003.09.028>
- Qi XL, He J, Ju Y, Huang L (2022) First report of leaf spot on *Elaeagnus pungens* caused by *Neopestalotiopsis clavisporea* in China. *Plant Disease* 107(7): 2251. <https://doi.org/10.1094/PDIS-10-22-2457-PDN>
- Qian TM, Rong L, Zhu TH (2015) Identification of the pathogen isolated from root rot of *Taxus chinensis* var. *mairei* and screening of its antagonistic *Bacillus*. *Plant Protection* 41(06): 60–66.
- Rambaut A (2016) FigTree v1.4.3. Institute of Evolutionary Biology, University of Edinburgh, UK. <http://tree.bio.ed.ac.uk/software/figtree>
- Ran SF, Maharachchikumbura SSN, Ren YL, Liu H, Chen KR, Wang YX, Wang Y (2017) Two new records in Pestalotiopsidaceae associated with Orchidaceae disease in Guangxi Province, China. *Mycosphere* 8(01): 121–130. <https://doi.org/10.5943/mycosphere/8/1/11>
- Reddy MS, Murali TS, Suryanarayanan TS, Rajulu MG, Thirunavukkarasu N (2016) *Pestalotiopsis* species occur as generalist endophytes in trees of Western Ghats forests of southern India. *Fungal Ecology* 24: 70–75. <https://doi.org/10.1016/j.funeco.2016.09.002>
- Ru WM (2006) Study on the ecology of endangering plant *Taxus chinensis* var. *mairei*. PhD Thesis, Shanxi University, Shanxi, China.
- Rubini MR, Silva-Ribeiro RT, Pomella AW, Maki CS, Araújo WL, Dos Santos DR, Azevedo JL (2005) Diversity of endophytic fungal community of cacao (*Theobroma cacao* L.) and biological control of *Crinipellis pernicioso*, causal agent of Witches' Broom Disease. *International Journal of Biological Sciences* 1: 24–33. <https://doi.org/10.7150/ijbs.1.24>
- Shu J, Yu Z, Sun W, Zhao J, Li Q, Tang L, Guo T, Huang S, Mo J, Hsiang T, Luo S (2020) Identification and characterization of pestalotioid fungi causing leaf spots on mango in southern China. *Plant Disease* 104(4): 1207–1213. <https://doi.org/10.1094/PDIS-03-19-0438-RE>
- Stamatakis A (2014) RAxML version 8: A tool for phylogenetic analysis and post-analysis of large phylogenies. *Bioinformatics* 30(9): 1312–1313. <https://doi.org/10.1093/bioinformatics/btu033>
- Strobel G, Yang X, Sears J, Kramer R, Sidhu RS, Hess WM (1996) Taxol from *Pestalotiopsis microspora*, an endophytic fungus of *Taxus wallichiana*. *Microbiology (Reading, England)* 142(2): 435–440. <https://doi.org/10.1099/13500872-142-2-435>
- Subban K, Subramani R, Srinivasan VPM, Johnpaul M, Chelliah J (2019) Salicylic acid as an effective elicitor for improved taxol production in endophytic fungus *Pestalotiopsis microspora*. *PLOS ONE* 14(2): e0212736. <https://doi.org/10.1371/journal.pone.0212736>
- Sun YR, Jayawardena RS, Sun JE, Wang Y (2023) Pestalotioid species associated with medicinal plants in southwest China and Thailand. *Microbiology Spectrum* 11(1): e03987–e22. <https://doi.org/10.1128/spectrum.03987-22>

- Swofford D (2003) PAUP\* - Phylogenetic analysis using parsimony (\*and other methods). Version 4. Sinauer Associates, Sunderland, Massachusetts, USA.
- Wang R, Chen S, Zheng B, Liu P, Li B, Weng Q, Chen Q (2019) Occurrence of leaf spot disease caused by *Neopestalotiopsis clavispora* on *Taxus chinensis* in China. *Forest Pathology* 49(5): e12540. <https://doi.org/10.1111/efp.12540>
- White TJ, Bruns T, Lee S, Taylor J (1990) Amplification and direct sequencing of fungal ribosomal RNA genes for phylogenetics. *PCR-Protocols: A guide to methods and applications* 18: 315–322. <https://doi.org/10.1016/B978-0-12-372180-8.50042-1>
- Wu L, Han T, Li W, Jia M, Xue L, Rahman K, Qin L (2013) Geographic and tissue influences on endophytic fungal communities of *Taxus chinensis* var. *mairei* in China. *Current Microbiology* 66(1): 40–48. <https://doi.org/10.1007/s00284-012-0235-z>
- Xiong Y, Manawasinghe I, Maharachchikumbura SSN, Dong ZY, Xiang MM, Li L (2022) Pestalotioid species associated with palm species from Southern China. *Current Research in Environmental & Applied Mycology* 12(1): 285–321. <https://doi.org/10.5943/cream/12/1/18>
- Yang Q, Zeng XY, Yuan J, Zhang Q, He YK, Wang Y (2021) Two new species of *Neopestalotiopsis* from southern China. *Biodiversity Data Journal* 9: e70446. <https://doi.org/10.3897/BDJ.9.e70446>
- Zhang Y, Maharachchikumbura SS, Mckenzie EH, Hyde KD (2012) A novel species of *Pestalotiopsis* causing leaf spots of *Trachycarpus fortunei*. *Cryptogamie. Mycologie* 33(3): 311–318. <https://doi.org/10.7872/crym.v33.iss3.2012.311>
- Zhang GF, Li Q, Hou XR (2018) Structural diversity of naturally regenerating Chinese yew (*Taxus wallichiana* var. *mairei*) populations in ex situ conservation. *Nordic Journal of Botany* 36(4): njb–01717. <https://doi.org/10.1111/njb.01717>
- Zhang Z, Liu R, Liu S, Mu T, Zhang X, Xia J (2022) Morphological and phylogenetic analyses reveal two new species of Sporocadaceae from Hainan, China. *MycKeys* 88: 171–192. <https://doi.org/10.3897/mycokeys.88.82229>

## Supplementary material 1

### PCR primer and PCR reaction conditions

Authors: Yifeng Wang, Kin-Ming Tsui, Shimei Chen, Chongjuan You

Data type: xlsx

Explanation note: **table S1**. PCR primer and PCR reaction conditions.

Copyright notice: This dataset is made available under the Open Database License (<http://opendatacommons.org/licenses/odbl/1.0/>). The Open Database License (ODbL) is a license agreement intended to allow users to freely share, modify, and use this Dataset while maintaining this same freedom for others, provided that the original source and author(s) are credited.

Link: <https://doi.org/10.3897/mycokeys.102.113696.suppl1>

## Supplementary material 2

### Specimen information and GenBank accession numbers

Authors: Yifeng Wang, Kin-Ming Tsui, Shimei Chen, Chongjuan You

Data type: xlsx

Explanation note: **table S2**. Isolates and GenBank accession numbers of sequences used in this study (the isolates from this study are marked in red).

Copyright notice: This dataset is made available under the Open Database License (<http://opendatacommons.org/licenses/odbl/1.0/>). The Open Database License (ODbL) is a license agreement intended to allow users to freely share, modify, and use this Dataset while maintaining this same freedom for others, provided that the original source and author(s) are credited.

Link: <https://doi.org/10.3897/mycokeys.102.113696.suppl2>

## Supplementary material 3

### Evolutionary divergence between sequences

Authors: Yifeng Wang, Kin-Ming Tsui, Shimei Chen, Chongjuan You

Data type: xls

Explanation note: **table S3**. Estimates of Evolutionary Divergence between Sequences.

Copyright notice: This dataset is made available under the Open Database License (<http://opendatacommons.org/licenses/odbl/1.0/>). The Open Database License (ODbL) is a license agreement intended to allow users to freely share, modify, and use this Dataset while maintaining this same freedom for others, provided that the original source and author(s) are credited.

Link: <https://doi.org/10.3897/mycokeys.102.113696.suppl3>

## Supplementary material 4

### Effects of light on growth of isolates

Authors: Yifeng Wang, Kin-Ming Tsui, Shimei Chen, Chongjuan You

Data type: jpg

Explanation note: **fig. S1**. Effects of light on growth of isolates.

Copyright notice: This dataset is made available under the Open Database License (<http://opendatacommons.org/licenses/odbl/1.0/>). The Open Database License (ODbL) is a license agreement intended to allow users to freely share, modify, and use this Dataset while maintaining this same freedom for others, provided that the original source and author(s) are credited.

Link: <https://doi.org/10.3897/mycokeys.102.113696.suppl4>

## Supplementary material 5

### Effects of carbon sources on growth of isolates

Authors: Yifeng Wang, Kin-Ming Tsui, Shimei Chen, Chongjuan You

Data type: jpg

Explanation note: **fig. S2**. Effects of carbon sources on growth of isolates.

Copyright notice: This dataset is made available under the Open Database License (<http://opendatacommons.org/licenses/odbl/1.0/>). The Open Database License (ODbL) is a license agreement intended to allow users to freely share, modify, and use this Dataset while maintaining this same freedom for others, provided that the original source and author(s) are credited.

Link: <https://doi.org/10.3897/mycokeys.102.113696.suppl5>

## Supplementary material 6

### Nucleotide differences between the isolates in this study

Authors: Yifeng Wang, Kin-Ming Tsui, Shimei Chen, Chongjuan You

Data type: pdf

Explanation note: documentation S1: Nucleotide differences between the isolates in this study.

Copyright notice: This dataset is made available under the Open Database License (<http://opendatacommons.org/licenses/odbl/1.0/>). The Open Database License (ODbL) is a license agreement intended to allow users to freely share, modify, and use this Dataset while maintaining this same freedom for others, provided that the original source and author(s) are credited.

Link: <https://doi.org/10.3897/mycokeys.102.113696.suppl6>

## Supplementary material 7

### Sequence data of the isolates in this study

Authors: Yifeng Wang, Kin-Ming Tsui, Shimei Chen, Chongjuan You

Data type: zip

Explanation note: zip package S1: Sequence data of the isolates in this study.

Copyright notice: This dataset is made available under the Open Database License (<http://opendatacommons.org/licenses/odbl/1.0/>). The Open Database License (ODbL) is a license agreement intended to allow users to freely share, modify, and use this Dataset while maintaining this same freedom for others, provided that the original source and author(s) are credited.

Link: <https://doi.org/10.3897/mycokeys.102.113696.suppl7>

# Two new species of *Diaporthe* (Diaporthaceae, Diaporthales) associated with *Camellia oleifera* leaf spot disease in Hainan Province, China

Hong Y. Liu<sup>1,2\*</sup>, Dun Luo<sup>3\*</sup>, Han L. Huang<sup>3</sup>, Qin Yang<sup>1,2</sup>

<sup>1</sup> Forestry Biotechnology Hunan Key Laboratory, Central South University of Forestry and Technology, Changsha 410004, China

<sup>2</sup> The Key Laboratory for Non-Wood Forest Cultivation and Conservation of the Ministry of Education, Central South University of Forestry and Technology, Changsha 410004, China

<sup>3</sup> Guangxi State-owned Bobai Forest Farm, Yulin 537600, China

Corresponding author: Qin Yang (T20192466@csuft.edu.cn)

## Abstract

Tea-oil tree (*Camellia oleifera* Abel.) is an important edible oil woody plant with a planting area over 3,800,000 hectares in southern China. Species of *Diaporthe* inhabit a wide range of plant hosts as plant pathogens, endophytes and saprobes. Here, we conducted an extensive field survey in Hainan Province to identify and characterise *Diaporthe* species associated with tea-oil leaf spots. As a result, eight isolates of *Diaporthe* were obtained from symptomatic *C. oleifera* leaves. These isolates were studied, based on morphological and phylogenetic analyses of partial ITS, *cal*, *his3*, *tef1* and *tub2* gene regions. Two new *Diaporthe* species (*D. hainanensis* and *D. pseudofoliicola*) were proposed and described herein.

**Key words:** DNA phylogeny, systematics, taxonomy, tea-oil tree, two new taxa



Academic editor: Thorsten Lumbsch

Received: 28 September 2023

Accepted: 25 January 2024

Published: 27 February 2024

**Citation:** Liu HY, Luo D, Huang HL, Yang Q (2024) Two new species of *Diaporthe* (Diaporthaceae, Diaporthales) associated with *Camellia oleifera* leaf spot disease in Hainan Province, China. MycoKeys 102: 225–243. <https://doi.org/10.3897/mycokeys.102.113412>

**Copyright:** © Hong Y. Liu et al.

This is an open access article distributed under terms of the Creative Commons Attribution License (Attribution 4.0 International – CC BY 4.0).

## Introduction

Tea-oil tree, *Camellia oleifera* Abel., is a unique woody edible oil species in China, mainly distributed in the Qinling-Huaihe River area. It has a long history of cultivation and utilisation for more than 2300 years since ancient China (Zhuang 2008). Camellia oil, obtained from *C. oleifera* seeds, is rich in unsaturated fatty acids and unique flavours and has become a rising high-quality edible vegetable oil in China. The edible of tea-oil is also conducive to preventing cardiovascular sclerosis, anti-tumour, lowering blood lipid, protecting liver and enhancing human immunity (Wang et al. 2007). According to the Three-year Action Plan for Accelerating the Development of oil tea Industry, Hainan Province is listed as a key development area of oil tea and the total area of oil tea planting in the Province is planned to reach 16,667 hm<sup>2</sup> by 2025. The development of *C. oleifera* industry is of great significance for the economic development of Hainan Province and the poverty alleviation of local farmers.

\* These authors contributed equally to this work and should be considered as co-first authors.

The expanding cultivation of *C. oleifera* over the last several decades has attracted increasing attention from plant pathologists to infectious diseases on this crop. Therein, diseases caused by *Diaporthe* species have become the emerging Camellia leaf diseases in southern China (Zhou and Hou 2019; Yang et al. 2021). During July and August of 2022, new leaf spots were detected on tea-oil tree with irregular, brownish-grey lesions, often associated with leaf margins. Infected leaves cultured on medium had dark pycnidia producing ellipsoid guttulate conidia, similar to that of *Diaporthe* species (Yang et al. 2021). The asexual morph is characterised by ostiolate conidiomata, with cylindrical phialides producing three types (alpha, beta and gamma conidia) of hyaline, aseptate conidia (Udayanga et al. 2011; Gomes et al. 2013).

Species identification criteria in *Diaporthe* has mainly relied on host association, morphology and culture characteristics (Mostert et al. 2001; Santos and Phillips 2009; Udayanga et al. 2011), which resulted in the description of over 200 species. Some species of *Diaporthe* were reported to colonise a single host plant, while other species were found to be associated with different host plants (Santos and Phillips 2009; Diogo et al. 2010; Santos et al. 2011; Gomes et al. 2013). In addition, considerable variability of the phenotypic characters was found to be present within a species (Rehner and Uecker 1994; Mostert et al. 2001; Udayanga et al. 2011). During the past decade, a polyphasic approach, based on multi-locus DNA data, morphological, phytopathological and phylogenetical analyses, has been employed for species boundaries in the genus *Diaporthe* (Huang et al. 2015; Gao et al. 2016, 2017; Guarnaccia and Crous 2017, 2018; Guarnaccia et al. 2018; Yang et al. 2018, 2020, 2021; Cao et al. 2022; Bai et al. 2023; Zhu et al. 2023).

The classification of *Diaporthe* has been on-going; however, little is known about species able to infect *C. oleifera*. Thus, the objective of the present study was to identify the prevalence of *Diaporthe* spp. associated with tea-oil tree leaf spot in the major plantations in Hainan Province, based on morphological and phylogenetic features.

## Materials and methods

### Fungal isolation

Leaves of *C. oleifera* with typical symptoms of leaf spots were collected from the main tea-oil camellia production fields in Hainan Province. Small sections (3 × 3 mm) were cut from the margins of infected tissues and surface-sterilised in 75% ethanol for 30 s, then sterilised in 5% sodium hypochlorite for 1 min, followed by three rinses with sterilised water and finally dried on sterilised filter paper (Yang et al. 2021). The sections were then plated on to PDA plates and incubated at 25 °C. Fungal growth was examined daily for up to 7 d. Isolates were then transferred aseptically to fresh PDA and purified by single-spore culturing (Fan et al. 2015). All fungal isolates were placed on PDA slants and stored at 4 °C. Specimens and axenic cultures are maintained in the Central South University of Forestry and Technology (CSUFT) in Changsha, Hunan Province.

## Morphological and cultural characterisation

Agar plugs (6 mm diam.) were taken from the edge of actively growing cultures on PDA and transferred on to the centre of 9 cm diam. Petri dishes containing 2% tap water agar supplemented with sterile pine needles (PNA; Smith et al. (1996)) and potato dextrose agar (PDA) and incubated at 25 °C under a 12 h near-ultraviolet light/12 h dark cycle to induce sporulation as described in recent studies (Gomes et al. 2013; Lombard et al. 2014). Colony characters and pigment production on PNA and PDA were noted after 10 d. Colony colours were rated according to Rayner (1970). Cultures were examined periodically for the development of ascomata and conidiomata. The morphological characteristics were examined by mounting fungal structures in clear lactic acid and 30 measurements at 1000× magnification were determined for each isolate using a Leica compound microscope (DM 2500) with interference contrast (DIC) optics. Descriptions, nomenclature and illustrations of taxonomic novelties are deposited in MycoBank (Crous et al. 2004a).

## DNA extraction, PCR amplification and sequencing

Genomic DNA was extracted from colonies grown on cellophane-covered PDA using a CTAB (cetyltrimethylammonium bromide) method (Doyle and Doyle 1990). DNA was estimated by electrophoresis in 1% agarose gel and the quality was measured using the NanoDrop 2000 (Thermo Scientific, Waltham, MA, USA), following the user manual (Desjardins et al. 2009). PCR amplifications were performed in a DNA Engine Peltier Thermal Cycler (PTC-200; Bio-Rad Laboratories, Hercules, CA, USA). The primer set ITS1/ITS4 (White et al. 1990) was used to amplify the ITS region. The primer pair CAL228F/CAL737R (Carbone and Kohn 1999) was used to amplify the calmodulin gene (*cal*) and the primers CYLH4F (Crous et al. 2004b) and H3-1b (Glass and Donaldson 1995) were used to amplify part of the histone H3 (*his3*) gene. The primer pair EF1-728F/EF1-986R (Carbone and Kohn 1999) was used to amplify a partial fragment of the translation elongation factor 1- $\alpha$  gene (*tef1*). The primer set T1 (O'Donnell and Cigelnik 1997) and Bt2b (Glass and Donaldson 1995) was used to amplify the beta-tubulin gene (*tub2*); the additional combination of Bt2a/Bt2b (Glass and Donaldson 1995) was used in case of amplification failure of the T1/Bt2b primer pair. The PCR amplifications of the genomic DNA with the phylogenetic markers were undertaken using the same primer pairs and conditions as in Yang et al. (2018). PCR amplification products were assayed via electrophoresis in 2% agarose gels. DNA sequencing was performed using an ABI PRISM 3730XL DNA Analyzer with a BigDye Terminator Kit v.3.1 (Invitrogen, USA) at the Shanghai Invitrogen Biological Technology Company Limited (Beijing, China).

## Phylogenetic analyses

The quality of the amplified nucleotide sequences was checked and combined using SeqMan v.7.1.0 and reference sequences were retrieved from the National Center for Biotechnology Information (NCBI), based on recent publications on the genus *Diaporthe* (Guarnaccia et al. 2018; Yang et al. 2018, 2020, 2021; Cao et al. 2022). Sequences were aligned using MAFFT v.6 (Katoh and Toh

2010) and corrected manually using Bioedit 7.0.9.0 (Hall 1999). The best-fit nucleotide substitution models for each gene were selected using jModelTest v.2.1.7 (Darriba et al. 2012) under the Akaike Information Criterion.

The phylogenetic analyses of the combined gene regions were performed using Maximum Likelihood (ML) and Bayesian Inference (BI) methods. ML was conducted using PhyML v.3.0 (Guindon et al. 2010), with 1000 bootstrap replicates, while BI was performed using a Markov Chain Monte Carlo (MCMC) algorithm in MrBayes v.3.0 (Ronquist and Huelsenbeck 2003). Two MCMC chains, started from random trees for 1,000,000 generations and trees, were sampled every 100<sup>th</sup> generation, resulting in a total of 10,000 trees. The first 25% of trees were discarded as burn-in of each analysis. Branches with significant Bayesian Posterior Probabilities (BPP) were estimated in the remaining 7500 trees. Phylogenetic trees were viewed with FigTree v.1.3.1 (Rambaut and Drummond 2010) and processed by Adobe Illustrator CS5. The nucleotide sequence data of the new taxa were deposited in GenBank (Table 1). The multilocus sequence alignments were deposited in TreeBASE ([www.treebase.org](http://www.treebase.org)) as accession S30780.

**Table 1.** Isolates and GenBank accession numbers used in the phylogenetic analyses of *Diaporthe*.

Species	Isolate	GenBank accession numbers				
		ITS	<i>cal</i>	<i>his3</i>	<i>tef1</i>	<i>tub2</i>
<i>Diaporthe acaciigena</i>	CBS 129521	KC343005	KC343247	KC343489	KC343731	KC343973
<i>Diaporthe acericola</i>	MFLUCC 17-0956	KY964224	KY964137	NA	KY964180	KY964074
<i>Diaporthe acerigena</i>	CFCC 52554	MH121489	MH121413	MH121449	MH121531	NA
<i>Diaporthe acuta</i>	PSCG 047	MK626957	MK691125	MK726161	MK654802	MK691225
<i>Diaporthe acutispora</i>	LC6161	KX986764	KX999274	KX999235	KX999155	KX999195
<i>Diaporthe aestuarium</i>	BRIP 59930a	OM918686	NA	NA	OM960595	OM960613
<i>Diaporthe alangii</i>	CFCC 52556	MH121491	MH121415	MH121451	MH121533	MH121573
<i>Diaporthe albosinensis</i>	CFCC 53066	MK432659	MK442979	MK443004	MK578133	MK578059
<i>Diaporthe alleghaniensis</i>	CBS 495.72	KC343007	KC343249	KC343491	KC343733	KC343975
<i>Diaporthe ambigua</i>	CBS 114015	KC343010	KC343252	KC343494	KC343736	KC343978
<i>Diaporthe ampelina</i>	STE-U 2660	AF230751	AY745026	NA	AY745056	JX275452
<i>Diaporthe amygdali</i>	CBS 126679	MH864208	KC343264	KC343506	KC343748	KC343990
<i>Diaporthe amygdali</i> syn. <i>D. chongqingensis</i>	PSCG 435	MK626916	MK691209	MK726257	MK654866	MK691321
<i>Diaporthe amygdali</i> syn. <i>D. fusicola</i>	CGMCC 3.17087	KF576281	KF576233	NA	KF576256	KF576305
<i>Diaporthe amygdali</i> syn. <i>D. garethjonesii</i>	MFLUCC 12-0542a	KT459423	KT459470	NA	KT459457	KT459441
<i>Diaporthe amygdali</i> syn. <i>D. kadsurae</i>	CFCC 52586	MH121521	MH121439	MH121479	MH121563	MH121600
<i>Diaporthe amygdali</i> syn. <i>D. mediterranea</i>	SAUCC194.111	MT822639	MT855718	MT855606	MT855836	MT855951
<i>Diaporthe amygdali</i> syn. <i>D. ovoicicola</i>	CGMCC 3.17093	KF576265	KF576223	NA	KF576240	KF576289
<i>Diaporthe amygdali</i> syn. <i>D. sterilis</i>	CBS 136969	KJ160579	KJ160548	MF418350	KJ160611	KJ160528
<i>Diaporthe amygdali</i> syn. <i>D. ternstroemiae</i>	CGMCC 3.15183	KC153098	NA	NA	KC153089	NA
<i>Diaporthe anacardii</i>	CBS 720.97	KC343024	KC343266	KC343508	KC343750	KC343992
<i>Diaporthe angelicae</i>	CBS 111592	KC343027	KC343269	KC343511	KC343753	KC343995
<i>Diaporthe annellsiae</i>	BRIP 59731a	OM918687	NA	NA	OM960596	OM960614
<i>Diaporthe apiculata</i>	CFCC 53068	MK432651	MK442973	MK442998	MK578127	MK578054
<i>Diaporthe aquatica</i>	IFRDCC 3051	JQ797437	NA	NA	NA	NA
<i>Diaporthe arctii</i>	DP0482	KJ590736	KJ612133	KJ659218	KJ590776	KJ610891
<i>Diaporthe arecae</i>	CBS 161.64	KC343032	KC343274	KC343516	KC343758	KC344000

Species	Isolate	GenBank accession numbers				
		ITS	<i>cal</i>	<i>his3</i>	<i>tef1</i>	<i>tub2</i>
<i>Diaporthe arengae</i>	CBS 114979	KC343034	KC343276	KC343518	KC343760	KC344002
<i>Diaporthe aseana</i>	MFLUCC 12-0299a	KT459414	KT459464	NA	KT459448	KT459432
<i>Diaporthe asheicola</i>	CBS 136967	KJ160562	KJ160542	NA	KJ160594	KJ160518
<i>Diaporthe aspalathi</i>	CBS 117169	KC343036	KC343278	KC343520	KC343762	KC344004
<i>Diaporthe australafricana</i>	CBS 111886	KC343038	KC343280	KC343522	KC343764	KC344006
<i>Diaporthe australiana</i>	CBS 146457	MN708222	NA	NA	MN696522	MN696530
<i>Diaporthe australpacificae</i>	BRIP 60163d	OM918688	NA	NA	OM960597	OM960615
<i>Diaporthe baccae</i>	CBS 136972	KJ160565	MG281695	MF418264	KJ160597	MF418509
<i>Diaporthe batatas</i>	CBS 122.21	KC343040	KC343282	KC343524	KC343766	KC344008
<i>Diaporthe bauhiniae</i>	CFCC 53071	MK432648	MK442970	MK442995	MK578124	MK578051
<i>Diaporthe beasleyi</i>	BRIP 59326a	OM918689	NA	NA	OM960598	OM960616
<i>Diaporthe beilharziae</i>	BRIP 54792	JX862529	NA	NA	JX862535	KF170921
<i>Diaporthe benedicti</i>	SBen914	KM669929	KM669862	NA	KM669785	NA
<i>Diaporthe betulae</i>	CFCC 50469	KT732950	KT732997	KT732999	KT733016	KT733020
<i>Diaporthe betulicola</i>	CFCC 51128	KX024653	KX024659	KX024661	KX024655	KX024657
<i>Diaporthe betulina</i>	CFCC 52560	MH121495	MH121419	MH121455	MH121537	MH121577
<i>Diaporthe biconispora</i>	ZJUD62	KJ490597	NA	KJ490539	KJ490476	KJ490418
<i>Diaporthe biguttulata</i>	ZJUD47	KJ490582	NA	KJ490524	KJ490461	KJ490403
	CFCC 52584	MH121519	MH121437	MH121477	MH121561	MH121598
<i>Diaporthe bohemiae</i>	CBS 143347	MG281015	MG281710	MG281361	MG281536	MG281188
<i>Diaporthe bounty</i>	BRIP 59361a	OM918690	NA	NA	OM960599	OM960617
<i>Diaporthe brasiliensis</i>	CBS 133183	KC343042	KC343284	KC343526	KC343768	KC344010
<i>Diaporthe breyniae</i>	CBS 148910	ON400846	ON409189	ON409187	ON409188	ON409186
<i>Diaporthe brumptoniae</i>	BRIP 59403a	OM918702	NA	NA	OM960611	OM960629
<i>Diaporthe caatingaensis</i>	URM7486	KY085927	KY115597	KY115605	KY115603	KY115600
<i>Diaporthe camelliae-sinensis</i>	SAUCC194.92	MT822620	MT855699	MT855588	MT855932	MT855817
<i>Diaporthe camelliae-oleiferae</i>	HNZZ027	MZ509555	MZ504685	MZ504696	MZ504707	MZ504718
<i>Diaporthe canthii</i>	CPC 19740	JX069864	KC843174	NA	KC843120	KC843230
<i>Diaporthe carrae</i>	BRIP 59932a	OM918691	NA	NA	OM960600	OM960618
<i>Diaporthe caryae</i>	CFCC 52563	MH121498	MH121422	MH121458	MH121540	MH121580
<i>Diaporthe cassines</i>	CPC 21916	KF777155	NA	NA	KF777244	NA
<i>Diaporthe caulivora</i>	CBS 127268	MH864501	KC343287	KC343529	KC343771	KC344013
<i>Diaporthe celticola</i>	CFCC 53074	MK573948	MK574587	MK574603	MK574623	MK574643
<i>Diaporthe cercidis</i>	CFCC 52565	MH121500	MH121424	MH121460	MH121542	MH121582
<i>Diaporthe chamaeropsis</i>	CBS 454.81	KC343048	KC343290	KC343532	KC343774	KC344016
<i>Diaporthe charlesworthii</i>	BRIP 54884m	KJ197288	NA	NA	KJ197250	KJ197268
<i>Diaporthe chiangmaiensis</i>	MFLU 18-1305	OK393702	NA	NA	OL439482	OK490918
<i>Diaporthe chrysalidocarpi</i>	SAUCC194.35	MT822563	MT855646	MT855532	MT855760	MT855876
<i>Diaporthe cichorii</i>	MFLUCC 17-1023	KY964220	KY964133	NA	KY964176	KY964104
<i>Diaporthe cinnamomi</i>	CFCC 52569	MH121504	NA	MH121464	MH121546	MH121586
<i>Diaporthe cissampeli</i>	CPC 27302	KX228273	NA	KX228366	NA	KX228384
<i>Diaporthe citri</i>	AR3405	KC843311	KC843157	KJ420881	KC843071	KC843187
<i>Diaporthe chensiensis</i>	CFCC 52567	MH121502	MH121426	MH121462	MH121544	MH121584
<i>Diaporthe citriasiana</i>	CGMCC 3.15224	JQ954645	KC357491	KJ490515	JQ954663	KC357459
<i>Diaporthe citrichinensis</i>	CGMCC 3.15225	JQ954648	KC357494	KJ420880	JQ954666	KJ490396
<i>Diaporthe collariana</i>	MFLU 17-2770	MG806115	MG783042	NA	MG783040	MG783041
<i>Diaporthe compactum</i>	LC3083	KP267854	NA	KP293508	KP267928	KP293434

Species	Isolate	GenBank accession numbers				
		ITS	<i>cal</i>	<i>his3</i>	<i>tef1</i>	<i>tub2</i>
<i>Diaporthe conica</i>	CFCC 52571	MH121506	MH121428	MH121466	MH121548	MH121588
<i>Diaporthe convolvuli</i>	CBS 124654	KC343054	KC343296	KC343538	KC343780	KC344022
<i>Diaporthe coryli</i>	CFCC 53083	MK432661	MK442981	MK443006	MK578135	MK578061
<i>Diaporthe crotalariae</i>	CBS 162.33	MH855395	JX197439	KC343540	GQ250307	KC344024
<i>Diaporthe crousii</i>	CAA 823	MK792311	MK883835	MK871450	MK828081	MK837932
<i>Diaporthe cucurbitae</i>	DAOM 42078	KM453210	NA	KM453212	KM453211	KP118848
<i>Diaporthe cuppatea</i>	CBS 117499	MH863021	KC343299	KC343541	KC343783	KC344025
<i>Diaporthe cynaroidis</i>	CBS 122676	KC343058	KC343300	KC343542	KC343784	KC344026
<i>Diaporthe cytosporella</i>	FAU461	KC843307	KC843141	MF418283	KC843116	KC843221
<i>Diaporthe diospyricola</i>	CPC 21169	KF777156	NA	NA	NA	NA
<i>Diaporthe discoidispora</i>	ZJUD89	KJ490624	NA	KJ490566	KJ490503	KJ490445
<i>Diaporthe dorycnii</i>	MFLUCC 17-1015	KY964215	NA	NA	KY964171	KY964099
<i>Diaporthe drenthii</i>	CBS 146453	MN708229	NA	NA	MN696526	MN696537
<i>Diaporthe durionigena</i>	VTCC 930005	MN453530	NA	NA	MT276157	MT276159
<i>Diaporthe elaeagni-glabrae</i>	LC4802	KX986779	KX999281	KX999251	KX999171	KX999212
<i>Diaporthe endophytica</i>	CBS 133811	KC343065	KC343307	KC343549	KC343791	KC344033
<i>Diaporthe eres</i>	AR5193	KJ210529	KJ434999	KJ420850	KJ210550	KJ420799
<i>Diaporthe etinsideae</i>	BRIP 64096a	OM918692	NA	NA	OM960601	OM960619
<i>Diaporthe eucalyptorum</i>	CBS 132525	MH305525	NA	NA	NA	NA
<i>Diaporthe foeniculacea</i>	CBS 111553	KC343101	KC343343	KC343585	KC343827	KC344069
<i>Diaporthe fraxini-angustifoliae</i>	BRIP 54781	JX862528	NA	NA	JX862534	KF170920
<i>Diaporthe fraxinicola</i>	CFCC 52582	MH121517	MH121435	NA	MH121559	NA
<i>Diaporthe fructicola</i>	MAFF 246408	LC342734	LC342738	LC342737	LC342735	LC342736
<i>Diaporthe fulvicolor</i>	PSCG 051	MK626859	MK691132	MK726163	MK654806	MK691236
<i>Diaporthe ganjae</i>	CBS 180.91	KC343112	KC343354	KC343596	KC343838	KC344080
<i>Diaporthe ganzhouensis</i>	CFCC 53087	MK432665	MK442985	MK443010	MK578139	MK578065
<i>Diaporthe goulteri</i>	BRIP 55657a	KJ197290	NA	NA	KJ197252	KJ197270
<i>Diaporthe gossiae</i>	BRIP 59730a	OM918693	NA	NA	OM960602	OM960620
<i>Diaporthe grandiflori</i>	SAUCC194.84	MT822612	MT855691	MT855580	MT855809	MT855924
<i>Diaporthe griceae</i>	BRIP 67014a	OM918694	NA	NA	OM960603	OM960621
<i>Diaporthe guangxiensis</i>	JZB320087	MK335765	MK736720	NA	MK500161	MK523560
<i>Diaporthe gulyae</i>	BRIP 54025	JF431299	NA	NA	JN645803	KJ197271
<i>Diaporthe guttulata</i>	CGMCC 3.20100	MT385950	MW022470	MW022491	MT424685	MT424705
<b><i>Diaporthe hainanensis</i></b>	<b>HNCM049</b>	<b>OR647684</b>	<b>NA</b>	<b>OR671936</b>	<b>OR671944</b>	<b>OR671952</b>
	<b>HNCM050</b>	<b>OR647685</b>	<b>NA</b>	<b>OR671937</b>	<b>OR671945</b>	<b>OR671953</b>
	<b>HNCM051</b>	<b>OR647686</b>	<b>NA</b>	<b>OR671938</b>	<b>OR671946</b>	<b>OR671954</b>
	<b>HNCM052</b>	<b>OR647687</b>	<b>NA</b>	<b>OR671939</b>	<b>OR671947</b>	<b>OR671955</b>
<i>Diaporthe helianthi</i>	CBS 592.81	KC343115	KC343357	KC343599	KC343841	KC344083
<i>Diaporthe heliconiae</i>	SAUCC194.77	MT822605	MT855684	MT855573	MT855802	MT855917
<i>Diaporthe heterophyllae</i>	CPC 26215	MG600222	MG600218	MG600220	MG600224	MG600226
<i>Diaporthe heterostemmatis</i>	SAUCC194.85	MT822613	MT855692	MT855581	MT855810	MT855925
<i>Diaporthe hickoriae</i>	CBS 145.26	KC343118	KC343360	KC343620	KC343844	KC344086
<i>Diaporthe hispaniae</i>	CBS 143351	MG281123	MG281820	MG281471	MG281644	MG281296
<i>Diaporthe hongkongensis</i>	CBS 115448	KC343119	KC343361	KC343603	KC343845	KC344087
<i>Diaporthe howardiae</i>	BRIP 59697a	OM918695	NA	NA	OM960604	OM960622
<i>Diaporthe hubeiensis</i>	JZB320123	MK335809	MK500235	NA	MK523570	MK500148
<i>Diaporthe hunanensis</i>	HNZZ023	MZ509550	MZ504680	MZ504691	MZ504702	MZ504713

Species	Isolate	GenBank accession numbers				
		ITS	<i>cal</i>	<i>his3</i>	<i>tef1</i>	<i>tub2</i>
<i>Diaporthe incompleta</i>	LC6754	KX986794	KX999289	KX999265	KX999186	KX999226
<i>Diaporthe inconspicua</i>	CBS 133813	KC343123	KC343365	KC343607	KC343849	KC344091
<i>Diaporthe infecunda</i>	CBS 133812	KC343126	KC343368	KC343610	KC343852	KC344094
<i>Diaporthe irregularis</i>	CGMCC 3.20092	MT385951	MT424721	NA	MT424686	MT424706
<i>Diaporthe isoberliniae</i>	CPC 22549	KJ869190	NA	NA	NA	KJ869245
<i>Diaporthe juglandicola</i>	CFCC 51134	KU985101	KX024616	KX024622	KX024628	KX024634
<i>Diaporthe kochmanii</i>	BRIP 54033	JF431295	NA	NA	JN645809	NA
<i>Diaporthe kongii</i>	BRIP 54031	JF431301	NA	NA	JN645797	KJ197272
<i>Diaporthe krabiensis</i>	MFLUCC 17-2481	MN047100	NA	NA	MN433215	MN431495
<i>Diaporthe lenispora</i>	CGMCC 3.20101	MT385952	MW022472	MW022493	MT424687	MT424707
<i>Diaporthe litchicola</i>	BRIP 54900	JX862533	NA	NA	JX862539	KF170925
<i>Diaporthe litchii</i>	SAUCC194.22	MT822550	MT855635	MT855519	MT855747	MT855863
<i>Diaporthe lithocarp</i>	CGMCC 3.15175	KC135104	KF576235	NA	KC153095	KF576311
<i>Diaporthe longicolla</i>	FAU599	KJ590728	KJ612124	KJ659188	KJ590767	KJ610883
<i>Diaporthe longispora</i>	CBS 194.36	MH855769	KC343377	KC343619	KC343861	KC344103
<i>Diaporthe lovellaceae</i>	BRIP 60163a	OM918696	NA	NA	OM960605	OM960623
<i>Diaporthe lusitanicae</i>	CBS 123212	MH863279	KC343378	KC343620	KC343862	KC344104
<i>Diaporthe lutescens</i>	SAUCC194.36	MT822564	MT855647	MT855533	MT855761	MT855877
<i>Diaporthe macadamiae</i>	CBS 146455	MN708230	NA	NA	MN696528	MN696539
<i>Diaporthe macintoshii</i>	BRIP 55064a	KJ197289	NA	NA	KJ197251	KJ197269
<i>Diaporthe malorum</i>	CAA 734	KY435638	KY435658	KY435648	KY435627	KY435668
<i>Diaporthe marina</i>	MFLU 17-2622	MN047102	NA	NA	NA	NA
<i>Diaporthe masirevicii</i>	BRIP 54256	KJ197276	NA	NA	KJ197238	KJ197256
<i>Diaporthe mayteni</i>	CBS 133185	KC343139	KC343381	KC343623	KC343865	KC344107
<i>Diaporthe maytenicola</i>	CPC 21896	KF777157	NA	NA	NA	KF777250
<i>Diaporthe mclennaniae</i>	BRIP 60072a	OM918697	NA	NA	OM960606	OM960624
<i>Diaporthe melastomatis</i>	SAUCC194.55	MT822583	MT855664	MT855551	MT855780	MT855896
<i>Diaporthe melonis</i>	CBS 435.87	KC343141	KC343383	KC343625	KC343867	KC344109
<i>Diaporthe middletonii</i>	BRIP 54884e	KJ197286	NA	NA	KJ197248	KJ197266
<i>Diaporthe minima</i>	CGMCC 3.20097	MT385953	MT424722	MW022496	MT424688	MT424708
<i>Diaporthe minusculata</i>	CGMCC 3.20098	MT385957	MW022475	MW022499	MT424692	MT424712
<i>Diaporthe miriciae</i>	BRIP 54736j	KJ197282	NA	NA	KJ197244	KJ197262
<i>Diaporthe monetii</i>	MF-Ha18-048	MW008493	MZ671938	MZ671964	MW008515	MW008504
<i>Diaporthe morinia</i>	BRIP 60190a	OM918698	NA	NA	OM960607	OM960625
<i>Diaporthe multigutullata</i>	CFCC 53095	MK432645	MK442967	MK442992	MK578121	MK578048
<i>Diaporthe musigena</i>	CBS 129519	KC343143	KC343385	KC343267	KC343869	KC344111
<i>Diaporthe myracrodruonis</i>	URM 7972	MK205289	MK205290	NA	MK213408	MK205291
<i>Diaporthe neoarctii</i>	CBS 109490	KC343145	KC343387	KC343629	KC343871	KC344113
<i>Diaporthe neoraonikayaporum</i>	MFLUCC 14-1136	KU712449	KU749356	NA	KU749369	KU743988
<i>Diaporthe norfolkensis</i>	BRIP 59718a	OM918699	NA	NA	OM960608	OM960626
<i>Diaporthe nothofagi</i>	BRIP 54801	JX862530	NA	NA	JX862536	KF170922
<i>Diaporthe novem</i>	CBS 127269	KC343155	KC343397	KC343639	KC343881	KC344123
<i>Diaporthe ocoteae</i>	CPC 26217	KX228293	NA	NA	NA	KX228388
<i>Diaporthe oraccinii</i>	LC3166	KP267863	NA	KP293517	KP267937	KP293443
<i>Diaporthe ovalispora</i>	ZJUD93	KJ490628	NA	KJ490570	KJ490507	KJ490449
<i>Diaporthe oxe</i>	CBS 133186	KC343164	KC343406	KC343648	KC343890	KC344132
<i>Diaporthe padina</i>	CFCC 52590	MH121525	MH121443	MH121483	MH121567	MH121604

Species	Isolate	GenBank accession numbers				
		ITS	<i>cal</i>	<i>his3</i>	<i>tef1</i>	<i>tub2</i>
<i>Diaporthe pandanicola</i>	MFLUCC 17-0607	MG646974	NA	NA	NA	MG646930
<i>Diaporthe paranensis</i>	CBS 133184	KC343171	KC343413	KC343655	KC343897	KC344139
<i>Diaporthe parapterocarpi</i>	CPC 22729	KJ869138	NA	NA	NA	KJ869248
<i>Diaporthe parvae</i>	PSCG 035	MK626920	MK691169	MK726211	MK654859	MK691249
<i>Diaporthe pascoei</i>	BRIP 54847	JX862538	NA	NA	JX862538	KF170924
<i>Diaporthe passiflorae</i>	CPC 19183	JX069860	KY435644	KY435654	KY435623	KY435674
<i>Diaporthe passifloricola</i>	CPC 27480	KX228292	NA	KX228367	NA	KX228387
<i>Diaporthe penetrитеum</i>	LC3215	KP267879	NA	KP293532	KP267953	NA
<i>Diaporthe perijuncta</i>	CBS 109745	KC343172	KC343414	KC343656	KC343898	KC344140
<i>Diaporthe perseae</i>	CBS 151.73	KC343173	KC343415	KC343657	KC343899	KC343141
<i>Diaporthe pescicola</i>	MFLUCC 16-0105	KU557555	KU557603	NA	KU557623	KU557579
<i>Diaporthe phaseolorum</i>	AR4203	KJ590738	KJ612135	KJ659220	KJ590739	KJ610893
<i>Diaporthe platzii</i>	BRIP 60353a	OM918700	NA	NA	OM960609	OM960627
<i>Diaporthe phillipsii</i>	CAA 817	MK792305	MK883831	MK871445	MK828076	MN000351
<i>Diaporthe podocarpi-macrophylli</i>	LC6155	KX986774	KX999278	KX999246	KX999167	KX999207
<i>Diaporthe pometiae</i>	SAUCC194.72	MT822600	MT855679	MT855568	MT855797	MT855912
<i>Diaporthe pseudoalnea</i>	CFCC 54190	MZ727037	MZ753468	MZ781302	MZ816343	MZ753487
<b><i>Diaporthe pseudofoliicola</i></b>	<b>HNCM045</b>	<b>OR647680</b>	<b>NA</b>	<b>OR671932</b>	<b>OR671940</b>	<b>OR671948</b>
	<b>HNCM046</b>	<b>OR647681</b>	<b>NA</b>	<b>OR671933</b>	<b>OR671941</b>	<b>OR671949</b>
	<b>HNCM047</b>	<b>OR647682</b>	<b>NA</b>	<b>OR671934</b>	<b>OR671942</b>	<b>OR671950</b>
	<b>HNCM048</b>	<b>OR647683</b>	<b>NA</b>	<b>OR671935</b>	<b>OR671943</b>	<b>OR671951</b>
<i>Diaporthe pseudomangiferae</i>	CBS 101339	KC343181	KC343423	KC343665	KC343907	KC344149
<i>Diaporthe pseudophoenicicola</i>	CBS 176.77	KC343183	KC343425	KC343667	KC343909	KC344151
<i>Diaporthe psoraleae</i>	CPC 21634	KF777158	NA	NA	KF777245	KF777251
<i>Diaporthe psoraleae-pinnatae</i>	CPC 21638	KF777159	NA	NA	NA	KF777252
<i>Diaporthe pterocarpi</i>	CPC 22729	JQ619899	JX197451	NA	JX275416	JX275460
<i>Diaporthe pterocarpicola</i>	MFLUCC 10-0580a	JQ619887	JX197433	NA	JX275403	JX275441
<i>Diaporthe pungensis</i>	SAUCC194.112	MT822640	MT855719	MT855607	MT855837	MT855952
<i>Diaporthe pyracanthae</i>	CAA483	KY435635	KY435656	KY435645	KY435625	KY435666
<i>Diaporthe racemosae</i>	CPC 26646	MG600223	MG600219	MG600221	MG600225	MG600227
<i>Diaporthe raonikayaporum</i>	CBS 133182	KC343188	KC343430	KC343672	KC343914	KC344156
<i>Diaporthe ravennica</i>	MFLUCC 16-0997	NA	NA	NA	MT394670	NA
<i>Diaporthe rhodomirti</i>	CFCC 53101	MK432643	MK442965	MK442990	MK578119	MK578046
<i>Diaporthe rhusicola</i>	CPC 18191	JF951146	KC843124	NA	KC843100	KC843205
<i>Diaporthe rosae</i>	MFLUCC 17-2658	MG828894	MG829273	NA	NA	MG843878
<i>Diaporthe rosiphthora</i>	COAD 2914	MT311197	MT313691	NA	MT313693	NA
<i>Diaporthe rossmaniae</i>	CAA 762	MK792290	MK883822	MK871432	MK828063	MK837914
<i>Diaporthe rostrata</i>	CFCC 50062	KP208847	KP208849	KP208851	KP208853	KP208855
<i>Diaporthe rudis</i>	AR3422	KC843331	KC843146	NA	KC843090	KC843177
<i>Diaporthe saccarata</i>	CBS 116311	KC343190	KC343432	KC343674	KC343916	KC344158
<i>Diaporthe sackstonii</i>	BRIP 54669b	KJ197287	NA	NA	KJ197249	KJ197267
<i>Diaporthe salicicola</i>	BRIP 54825	JX862531	NA	NA	JX862537	KF170923
<i>Diaporthe sambucusii</i>	CFCC 51986	KY852495	KY852499	KY852503	KY852507	KY852511
<i>Diaporthe schimae</i>	CFCC 53103	MK442640	MK442962	MK442987	MK578116	MK578043
<i>Diaporthe schini</i>	CBS 133181	KC343191	KC343433	KC343675	KC343917	KC344159
<i>Diaporthe schisandrae</i>	CFCC 51988	KY852497	KY852501	KY852505	KY852509	KY852513

Species	Isolate	GenBank accession numbers				
		ITS	<i>cal</i>	<i>his3</i>	<i>tef1</i>	<i>tub2</i>
<i>Diaporthe schoeni</i>	MFLU 15-1279	KY964226	KY964139	NA	KY964182	KY964109
<i>Diaporthe sclerotiooides</i>	CBS 296.67	MH858974	KC343435	KC343677	KC343919	KC344161
<i>Diaporthe searlei</i>	BRIP 66528	MN708231	NA	NA	NA	MN696540
<i>Diaporthe sennae</i>	CFCC 51636	KY203724	KY228875	NA	KY228885	KY228891
<i>Diaporthe sennicola</i>	CFCC 51634	KY203722	KY228873	KY228879	KY228883	KY228889
<i>Diaporthe serafiniae</i>	BRIP 55665a	KJ197274	NA	NA	KJ197236	KJ197254
<i>Diaporthe shaanxiensis</i>	CFCC 53106	MK432654	MK442976	MK443001	MK578130	NA
<i>Diaporthe shawiae</i>	BRIP 64534a	OM918701	NA	NA	OM960610	OM960628
<i>Diaporthe siamensis</i>	MFLUCC 10-0573a	JQ619879	JX197423	NA	JX275393	JX275429
<i>Diaporthe silvicola</i>	CFCC 54191	MZ727041	MZ753472	MZ753481	MZ816347	MZ753491
<i>Diaporthe sojae</i>	FAU635	KJ590719	KJ612116	KJ659208	KJ590762	KJ610875
<i>Diaporthe spinosa</i>	PSCG 383	MK626849	MK691129	MK726156	MK654811	MK691234
<i>Diaporthe stictica</i>	CBS 370.54	KC343212	KC343454	KC343696	KC343938	KC344180
<i>Diaporthe subclavata</i>	ZJUD95	KJ490630	NA	KJ490572	KJ490509	KJ490451
<i>Diaporthe subcylindrospora</i>	KUMCC 17-0151	MG746629	NA	NA	MG746630	MG746631
<i>Diaporthe subellipicola</i>	KUMCC 17-0153	MG746632	NA	NA	MG746633	MG746634
<i>Diaporthe subordinaria</i>	CBS 464.90	KC343214	KC343456	KC343698	KC343940	KC344182
<i>Diaporthe taoicola</i>	MFLUCC 16-0117	KU557567	NA	NA	KU557635	KU557591
<i>Diaporthe tectonae</i>	MFLUCC 12-0777	KU712430	KU749345	NA	KU749359	KU743977
<i>Diaporthe tectonendophytica</i>	MFLUCC 13-0471	KU712439	KU749354	NA	KU749367	KU743986
<i>Diaporthe tectonigena</i>	MFLUCC 12-0767	KX986782	KX999284	KX999254	KX999174	KX999214
<i>Diaporthe terebinthifolii</i>	CBS 133180	KC343216	KC343458	KC343700	KC343942	KC344184
<i>Diaporthe thunbergii</i>	MFLUCC 10-0576a	JQ619893	JX197440	NA	JX275409	JX275449
<i>Diaporthe thunbergiicola</i>	MFLUCC 12-0033	KP715097	NA	NA	KP715098	NA
<i>Diaporthe tibetensis</i>	CFCC 51999	MF279843	MF279888	MF279828	MF279858	MF279873
<i>Diaporthe tulliensis</i>	BRIP 62248a	KR936130	NA	NA	KR936133	KR936132
<i>Diaporthe trevorowii</i>	BRIP 70737a	OM918703	NA	NA	OM960612	OM960630
<i>Diaporthe ueckerae</i>	FAU656	KJ590726	KJ612122	KJ659215	KJ590747	KJ610881
<i>Diaporthe ukurunduensis</i>	CFCC 52592	MH121527	MH121445	MH121485	MH121569	NA
<i>Diaporthe undulata</i>	LC6624	KX986798	NA	KX999269	KX999190	KX999230
<i>Diaporthe unshuiensis</i>	CFCC 52594	MH121529	MH121447	MH121487	MH121571	MH121606
	CFCC 52595	MH121530	MH121448	MH121488	MH121572	MH121607
<i>Diaporthe vaccinii</i>	CBS 160.32	KC343228	KC343470	KC343712	KC343954	KC343196
<i>Diaporthe vangoghii</i>	MF-Ha18-045	MW008491	MZ671936	MZ671962	MW008513	MW008502
<i>Diaporthe vangeriae</i>	CBS 137985	KJ869137	NA	NA	NA	KJ869247
<i>Diaporthe vawdreyi</i>	BRIP 57887a	KR936126	NA	NA	KR936129	KR936128
<i>Diaporthe velutina</i>	LC4421	KX986790	NA	KX999261	KX999182	KX999223
<i>Diaporthe verniciicola</i>	CFCC 53109	MK573944	MK574583	MK574599	MK574619	MK574639
<i>Diaporthe viniferae</i>	JZB320071	MK341551	MK500119	NA	MK500107	MK500112
<i>Diaporthe virgiliae</i>	CMW 40748	KP247556	NA	NA	NA	KP247575
<i>Diaporthe xishuangbanica</i>	LC6707	KX986783	NA	KX999255	KX999175	KX999216
<i>Diaporthe xunwuensis</i>	CFCC 53085	MK432663	MK442983	MK443008	MK578137	MK578063
<i>Diaporthe yunnanensis</i>	LC6168	KX986796	KX999290	KX999267	KX999188	KX999228
<i>Diaporthe zaobaisu</i>	PSCG 031	MK626922	NA	MK726207	MK654855	MK691245
<i>Diaporthe corylina</i>	CBS 121124	KC343004	KC343246	KC343488	KC343730	KC343972

Note: NA, not applicable. Strains in this study are marked in bold.

## Results

### Phylogenetic analyses

The five-gene sequence dataset (ITS, *cal*, *his3*, *tef1* and *tub2*) was analysed to infer the interspecific relationships within *Diaporthe*. The dataset consisted of 259 sequences including the outgroup taxon, *Diaporthella corylina* (CBS 121124). A total of 2909 characters including gaps (528 for ITS, 608 for *cal*, 563 for *his3*, 646 for *tef1* and 564 for *tub2*) were included in the phylogenetic analysis. The best nucleotide substitution model for ITS, *his3* and *tub2* was TrN+I+G, while HKY+I+G was selected for both *cal* and *tef1*. The topologies resulting from ML and BI analyses of the concatenated dataset were congruent (Fig. 1). According to the phylogenetic tree, *D. hainanensis* and *D. pseudofoliicola* are new to science, based on the distinct and well-supported molecular phylogenetic placement with their closest described relatives. Phylogenetically, *D. pseudofoliicola* clustered together with *D. longicolla* and *D. unshiuensis*. *Diaporthe hainanensis* clustered together with *D. cercidis* and *D. guangxiensis*.

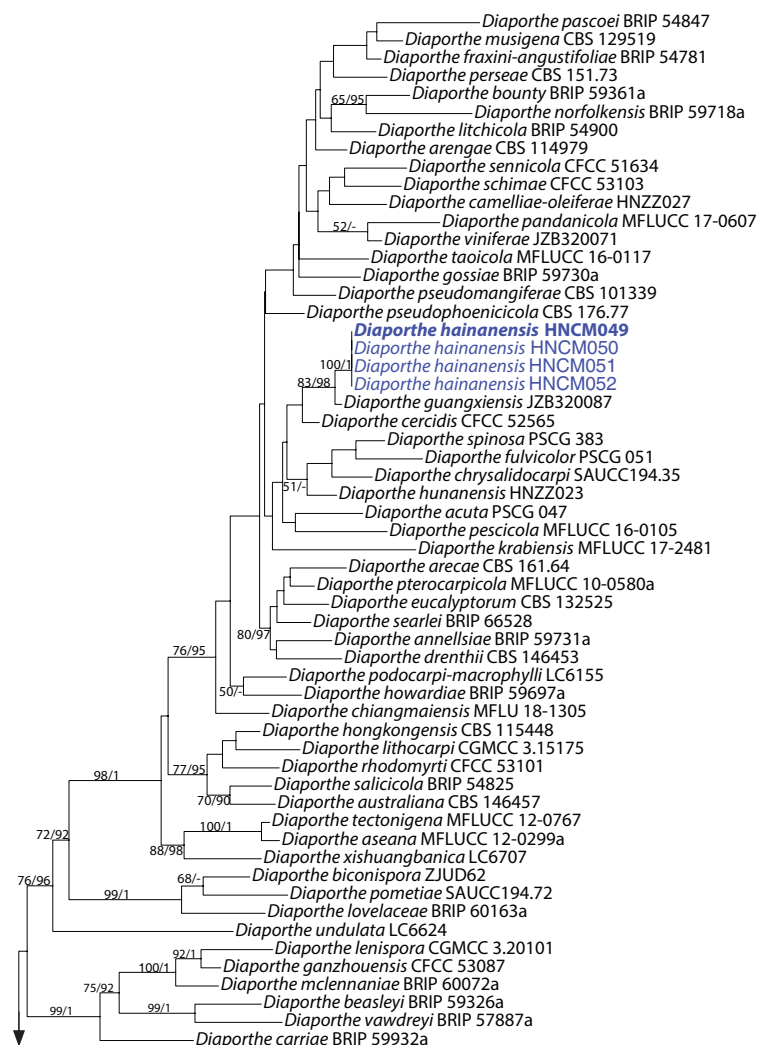


**Figure 1.** Phylogram of *Diaporthe* resulting from a Maximum Likelihood analysis, based on combined ITS, *cal*, *his3*, *tef1* and *tub2*. Numbers above the branches indicate ML bootstraps (left, ML BS  $\geq$  50%) and Bayesian Posterior Probabilities (right, BPP  $\geq$  0.9). The tree is rooted with *Diaporthella corylina*. Isolates in the current study are in blue. “-” indicates ML BS < 50% or BI PP < 0.9.

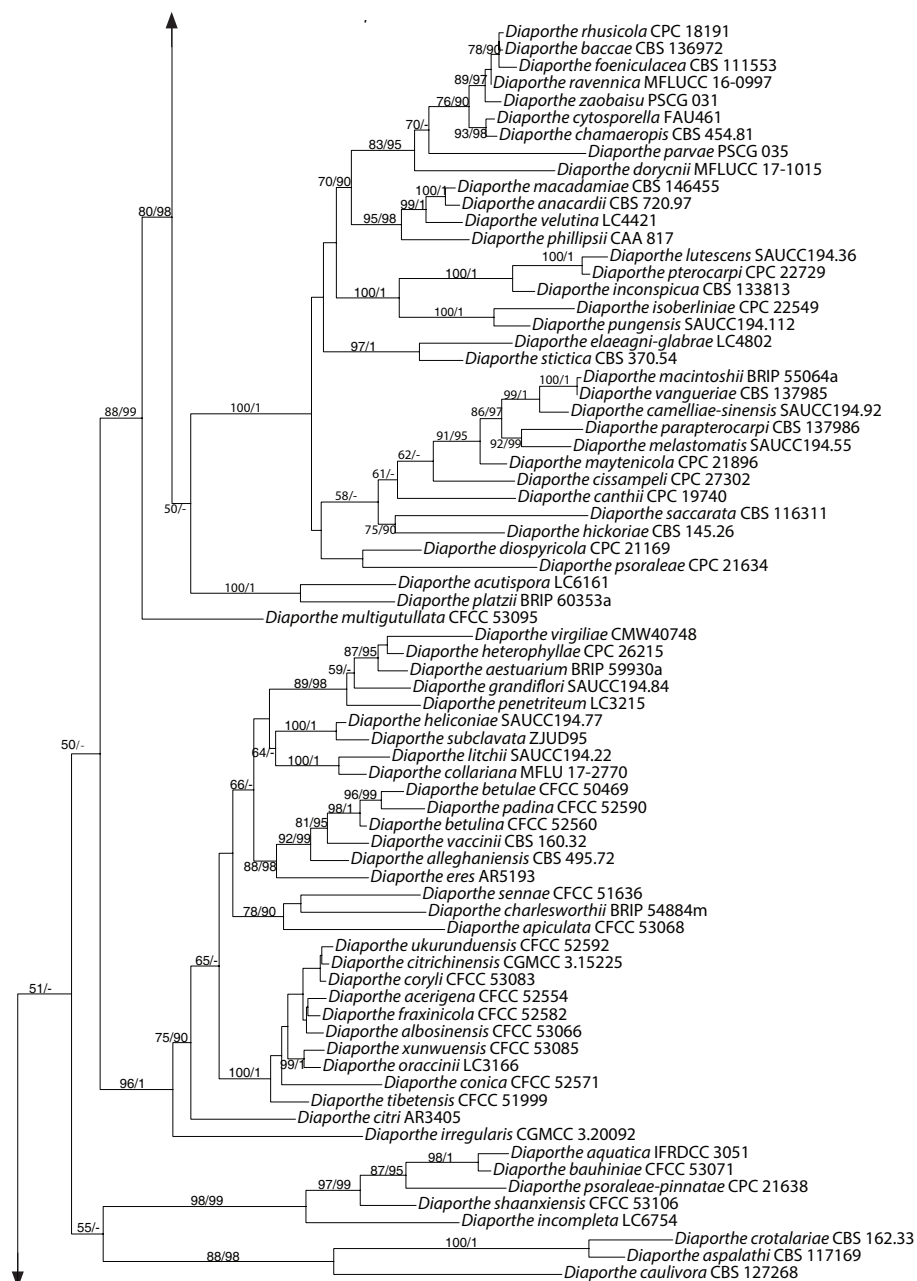


Figure 1. Continued.

## Taxonomy

### *Diaporthe hainanensis* Q. Yang, sp. nov.

Mycobank No: 848328

Fig. 2

**Diagnosis.** Distinguished from *D. cercidis* in narrower alpha conidia; from *D. guangxiensis* in shorter beta conidia.

**Etymology.** In reference to the Hainan Province, from where the fungus was first collected.

**Description. Asexual morph:** Conidiomata on PNA pycnidial, globose or rostrated, black, erumpent in tissue, erumpent at maturity, 450–600 µm diam., often with pale yellowish conidial drops exuding from the ostioles. **Conidiophores**

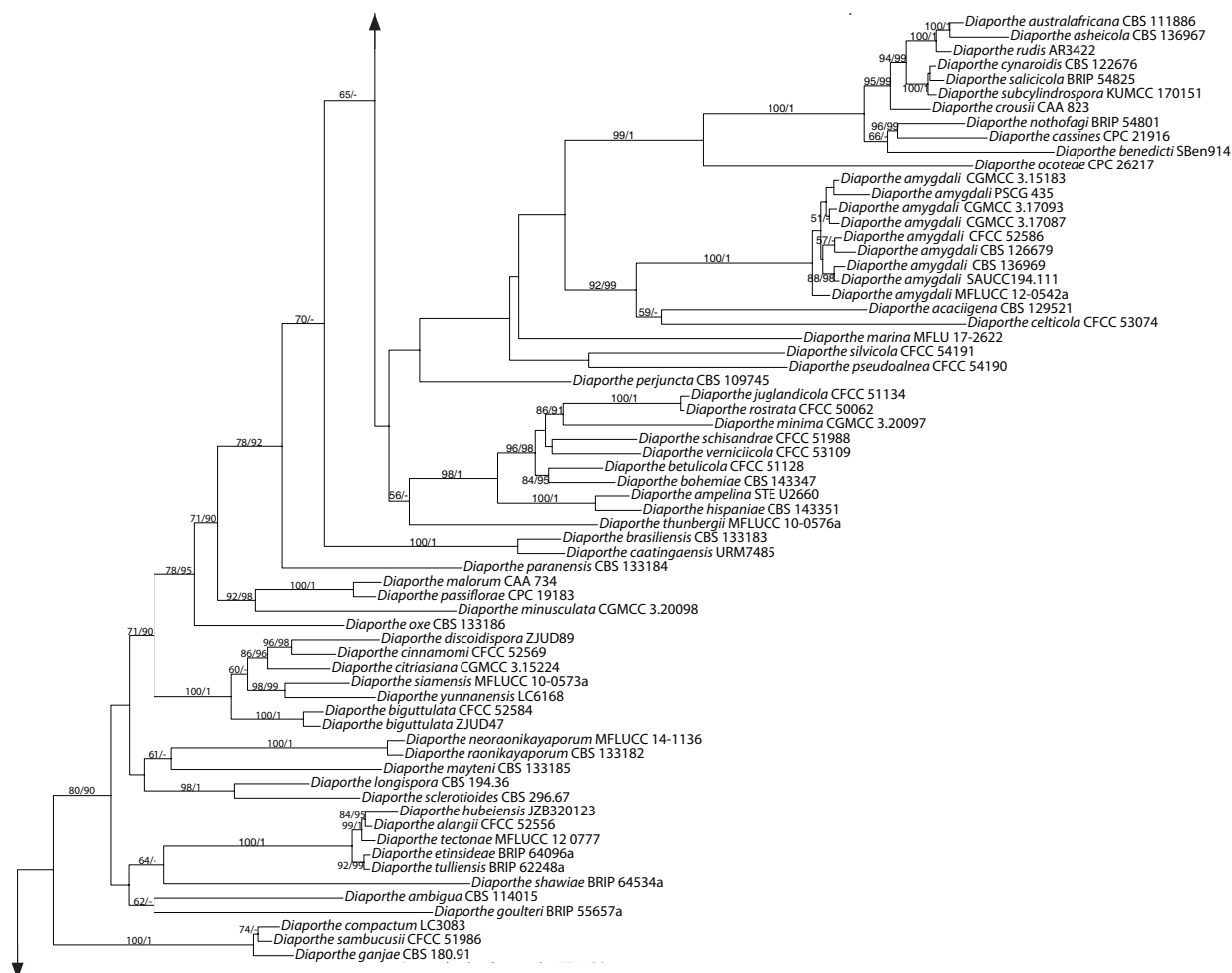


Figure 1. Continued.

reduced to conidiogenous cells. **Conidiogenous cells** (10.5–)14.5–20(–21.5) × 1.4–1.8 μm (n = 30), aseptate, cylindrical, phialidic, straight or slightly curved. **Alpha conidia** (5.5–)7–8(–8.5) × 2.1–2.9 μm (n = 30), aseptate, hyaline, ellipsoidal, biguttulate. **Beta conidia** (21.5–)23–25 × 1.1 μm (n = 30), hyaline, aseptate, filiform, sinuous at one end, eguttulate.

**Culture characters.** Culture incubated on PNA at 25 °C, originally white, fluffy aerial mycelium, becoming pale yellow with age, with visible solitary conidiomata pine needles after 15 days.

**Specimens examined.** CHINA. Hainan Province: Chengmai County, on leaves of *Camellia oleifera*, 19°34'10"N, 110°18'09"E, 25 July 2022, Q. Yang (holotype CSUFT055; ex-type living culture: HNCM049; other living cultures: HNCM050, HNCM051 and HNCM052).

**Notes.** Four isolates representing *D. hainanensis* cluster in a well-supported clade (ML/Bi = 100/1) and appear most closely related to *D. cercidis* on *Cercis chinensis* and *D. guangxiensis* on *Macadamia* sp. *Diaporthe hainanensis* can be distinguished from *D. cercidis*, based on ITS, *his3*, *tef1* and *tub2* loci (13/458 in ITS, 5/455 in *his3*, 33/341 in *tef1* and 5/401 in *tub2*); from *D. guangxiensis*, based on ITS, *tef1* and *tub2* loci (5/457 in ITS, 2/339 in *tef1* and 16/403 in *tub2*). Morphologically, *D. hainanensis* differs from *D. cercidis* in narrower alpha conidia (2.1–2.9 μm vs. 3–3.5 μm) (Yang et al. 2018); from *D. guangxiensis* in shorter beta conidia (23–25 μm vs. 20–32 μm) (Manawasinghe et al. 2019).

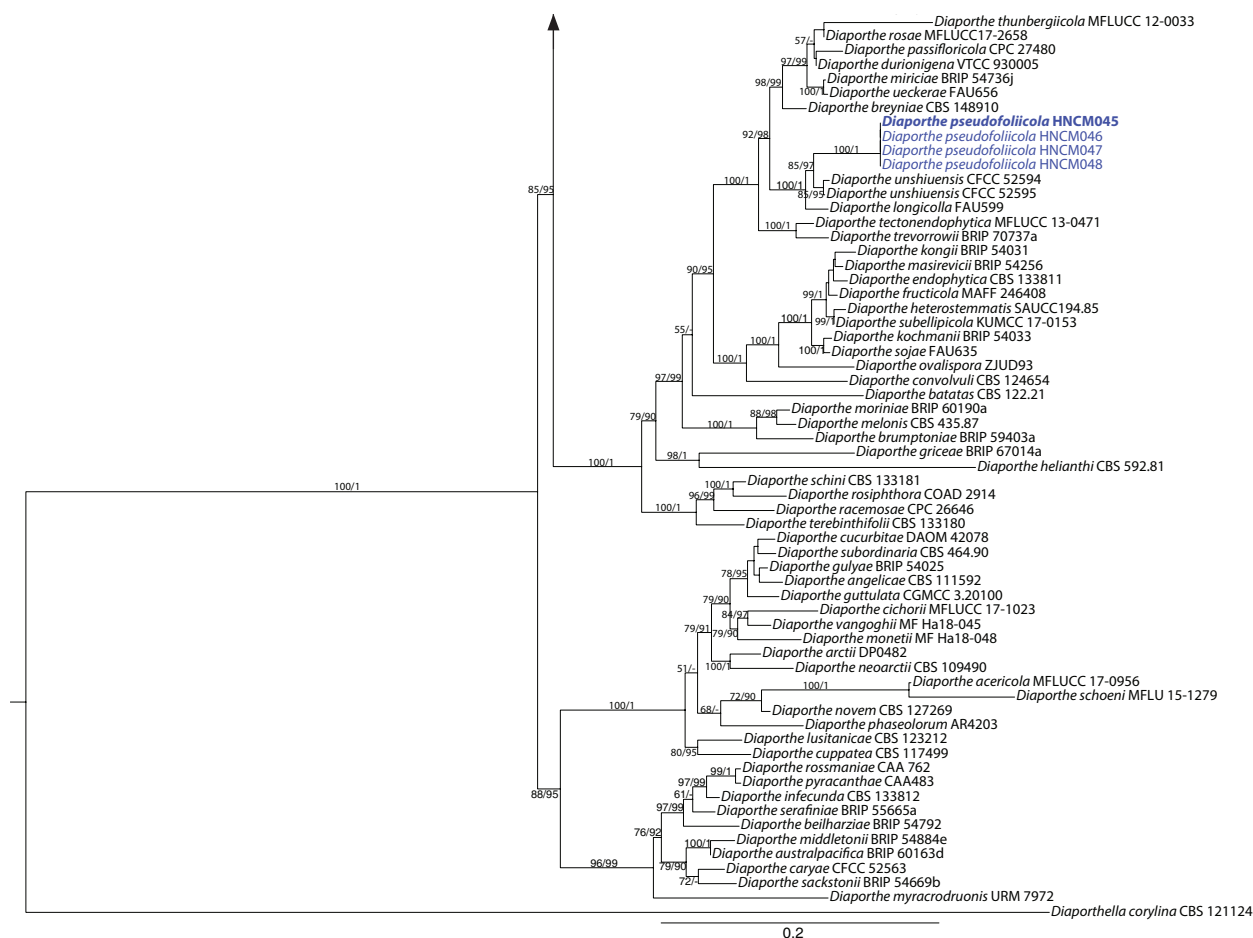


Figure 1. Continued.

***Diaporthe pseudofoliicola* Q. Yang, sp. nov.**

MycoBank No: 848327

Fig. 3

**Diagnosis.** Distinguished from *D. longicolla* in having smaller alpha conidia; from *D. unshiuensis* in having narrower conidiophores.

**Etymology.** The epithet “*pseudofoliicola*” refers to its habitat similar to *Diaporthe foliicola*.

**Description. Asexual morph:** Conidiomata on PDA pycnidial, 190–330 µm in diam., superficial, scattered on PDA, dark brown to black, globose, solitary or clustered in groups of 1–3 pycnidia. Pale yellow conidial drops exuding from ostioles. **Conidiophores** reduced to conidiogenous cells. **Conidiogenous cells** (10.5–)12.5–18(–22) × 1.3–1.5 µm (n = 30), phialidic, aseptate, cylindrical, straight, densely aggregated, terminal, slightly tapered towards the apex. **Alpha conidia** 5–6.5(–7) × 2.3–3.0 µm (n = 30), aseptate, hyaline, ellipsoidal to fusiform, biguttulate, both ends obtuse. **Beta conidia** (27.5–)30–33(–35.5) × 1.2–1.4 µm (n = 30), hyaline, aseptate, filiform, sinuous at one end, eguttulate.

**Culture characters.** Culture incubated on PDA at 25 °C, originally flat with white fluffy aerial mycelium, becoming pale brown due to pigment formation, with yellowish-cream conidial drops exuding from the ostioles after 20 days.

**Specimens examined.** CHINA. Hainan Province: Chengmai County, on leaves of *Camellia oleifera*, 110°15'16"E, 19°23'20"N, 25 July 2022, Q. Yang (holotype)

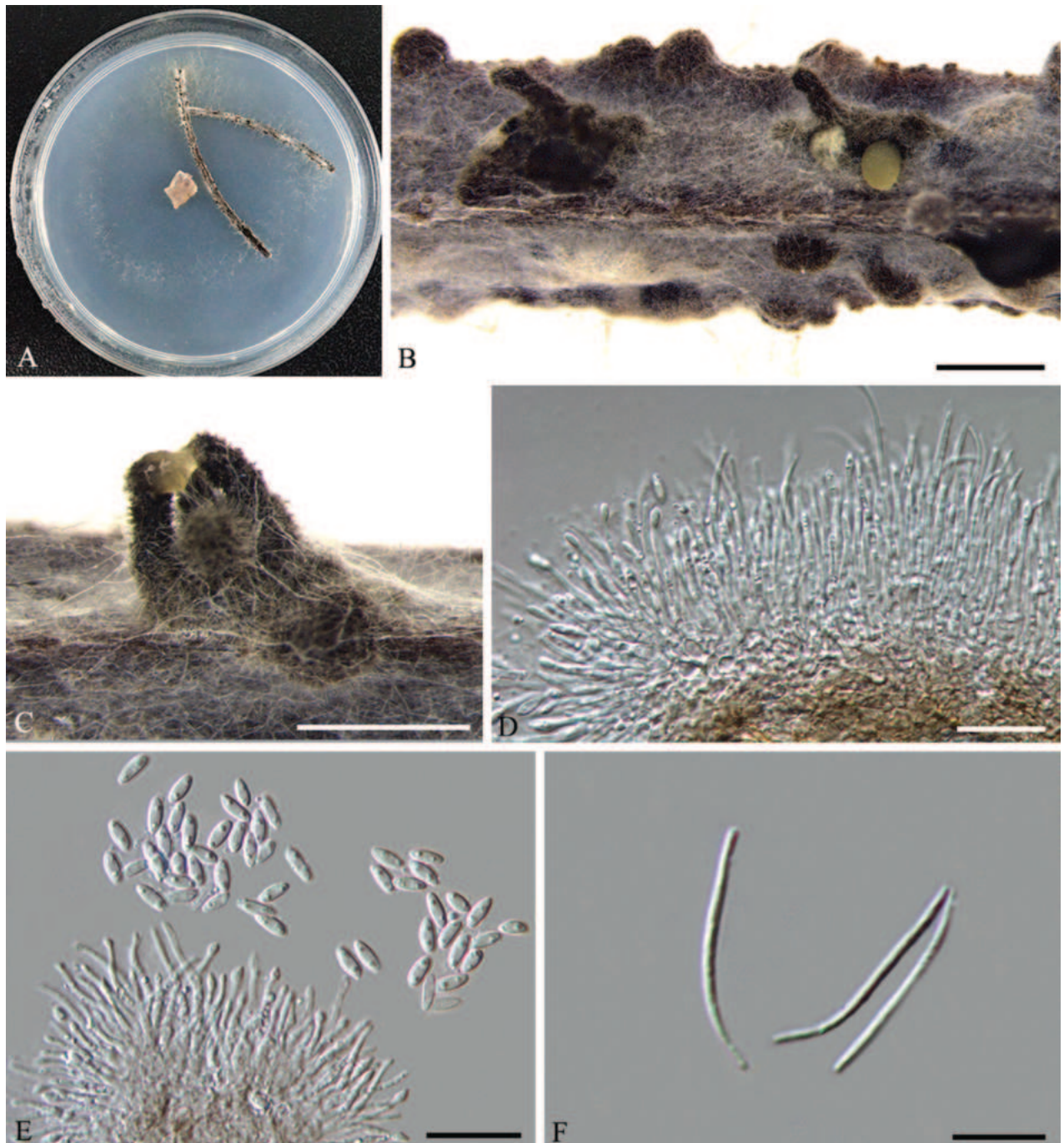


**Figure 2.** *Diaporthe hainanensis* (HNCM049) **A** culture on PNA **B, C** conidiomata **D** conidiogenous cells **E** alpha conidia **F** beta conidia. Scale bars: 500 µm (**B, C**); 10 µm (**C, F**), 20 µm (**E**).

CSUFT050; ex-type living culture: HNCM045; other living cultures: HNCM046, HNCM047 and HNCM048).

**Notes.** Four isolates representing *D. pseudofoliicola* cluster in a well-supported clade (ML/BI = 100/1) and appear most closely related to *D. longicolla* on *Glycine max* and *D. unshiuensis* on *Citrus unshiu*. *Diaporthe pseudofoliicola* can be distinguished from *D. longicolla*, based on ITS, *tef1* and *tub2* loci (9/462 in ITS, 16/318 in *tef1* and 4/444 in *tub2*); from *D. unshiuensis*, based on *his3* and *tef1* loci (51/457 in *his3* and 17/318 in *tef1*). Morphologically, *D. pseudofoliicola* differs from *D. longicolla* in having smaller alpha conidia

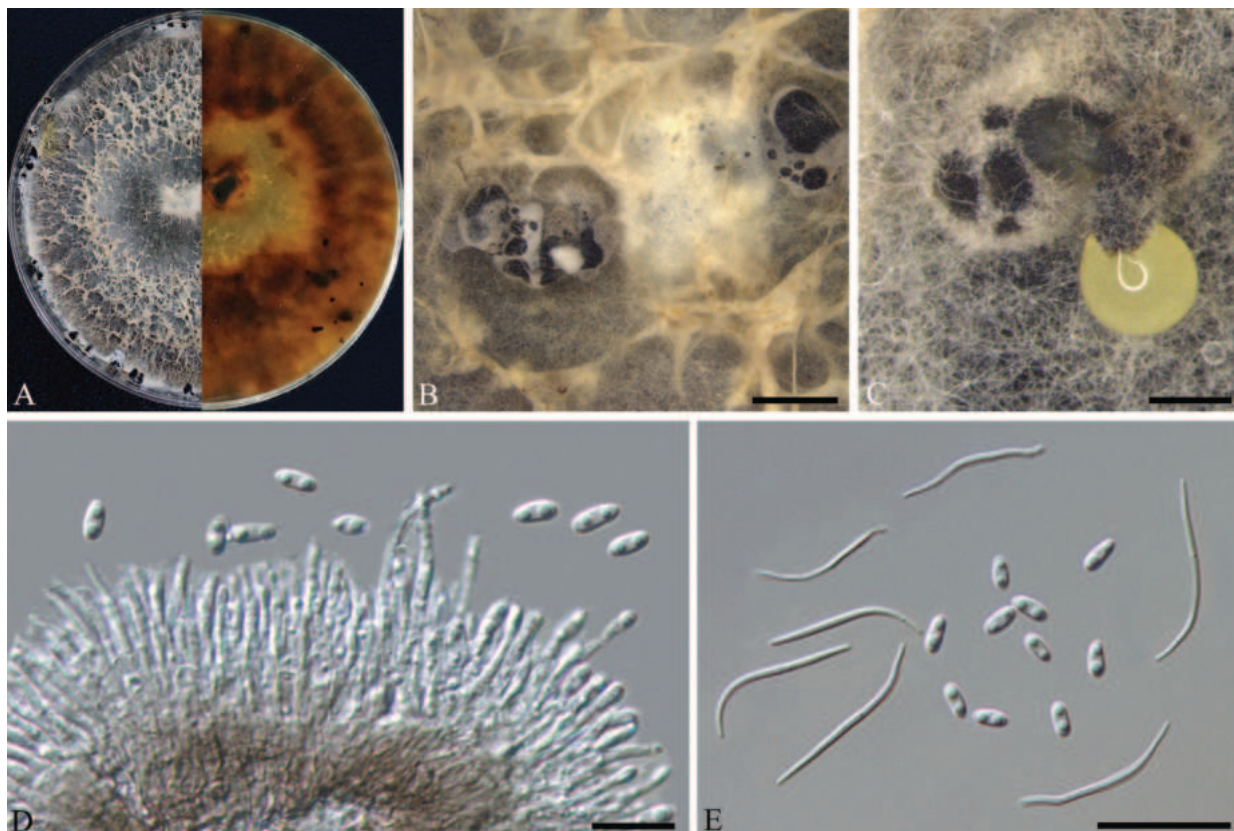


**Figure 3.** *Diaporthe pseudofoliicola* (HNCM045) **A** culture on PDA **B, C** conidiomata **D** conidiogenous cells **E** alpha and beta conidia. Scale bars: 200  $\mu\text{m}$  (**B, C**), 10  $\mu\text{m}$  (**D**), 20  $\mu\text{m}$  (**E**).

(5–6.5  $\times$  2.3–3.0  $\mu\text{m}$  vs. 6.9–7.2  $\times$  1.6–2.8  $\mu\text{m}$ ) (Santos et al. 2011); from *D. unshiuensis* in having narrower conidiophores (1.3–1.5  $\mu\text{m}$  vs. 1.4–2.6  $\mu\text{m}$ ) (Huang et al. 2015).

## Discussion

In this study, an important oil-tea tree species, *Camellia oleifera* was investigated and *Camellia* leaf disease was found as a common disease in plantations in Hainan Province. Identification of our collections was conducted, based on isolates from symptomatic leaves of *C. oleifera* using five combined loci (ITS, *cal*, *his3*, *tef1* and *tub2*), as well as morphological characters. Two new *Diaporthe* species were described, i.e. *D. hainanensis* and *D. pseudofoliicola*.

According to the USDA Fungal-host interaction database, there are six records of *Diaporthe* species associated with *C. oleifera* (<https://nt.ars-grin.gov/fungaldatabases>; accessed on 18 Sep 2023). These records are related to the following six *Diaporthe* species: *D. eres*, *D. camelliae-oleiferae*, *D. hubeiensis*, *D. hunanensis*, *D. huangshanensis* and *D. sojiae* (Zhou and Hou 2019; Yang et al. 2021). *Diaporthe eres*, the type species of the genus, was described by Nitschke (1870) on *Ulmus* sp. collected in Germany, which has a widespread distribution and a broad host range as pathogens, endophytes or saprobes (Udayanga et al. 2014). *Diaporthe eres* differs from *D. pseudofoliicola* and *D. hainanensis* in having wider alpha conidia (3–4  $\mu\text{m}$  in *D. eres* vs. 2.3–3.0  $\mu\text{m}$  in *D. pseudofoliicola* vs. 2.1–2.9  $\mu\text{m}$  in *D. hainanensis*) (Gomes et al. 2013); *D. huangshanensis* differs from *D. pseudofoliicola* in having shorter beta co-

nidia (19.5–30  $\mu\text{m}$  vs. 30–33  $\mu\text{m}$ ); from *D. hainanensis* in having wider alpha conidia (2.7–4.5  $\mu\text{m}$  vs. 2.1–2.9  $\mu\text{m}$ ) (Zhou and Hou 2019). Yang et al. (2021) recorded four *Diaporthe* species, *D. camelliae-oleiferae*, *D. hubeiensis*, *D. hunanensis* and *D. sojiae*, which were isolated from *Camellia oleifera* in Hunan Province and which can be distinguished from *D. pseudofoliicola* and *D. hainanensis*, based on DNA sequence data (Fig. 1).

As the species concept of *Diaporthe* has been greatly improved by using molecular data (Huang et al. 2015; Gao et al. 2016, 2017; Guarnaccia and Crous 2017; Guarnaccia et al. 2018; Yang et al. 2018, 2020, 2021; Manawasinghe et al. 2019; Guo et al. 2020; Jiang et al. 2021; Cao et al. 2022; Bai et al. 2023; Zhu et al. 2023), many new species have been discovered and reported in recent years. In this study, the *Diaporthe* isolates from *C. oleifera* were identified, based on sequence analysis and morphological characteristics. Future studies should focus on pathogenicity, epidemiology and fungicide sensitivity of the important plant fungal pathogen to develop effective management of *C. oleifera* disease and on the pathogenic molecular mechanism.

## Additional information

### Conflict of interest

The authors have declared that no competing interests exist.

### Ethical statement

No ethical statement was reported.

### Funding

This study is financed by the Guilin Scientific Research [2022ZC] No. 27, the introduction of talent research start-up fund project of CSUFT (Project No.: 2019YJ025) and the Changsha Natural Science Foundation project (kq2202284).

### Author contributions

Hong Y. Liu conceived and designed the study; Dun Luo and Han L. Huang conducted the experiments; Qin Yang wrote the manuscript and revised.

### Data availability

All of the data that support the findings of this study are available in the main text.

## References

- Bai Y, Lin L, Pan M, Fan XL (2023) Studies of *Diaporthe* (Diaporthaceae, Diaporthales) species associated with plant cankers in Beijing, China, with three new species described. *MycKeys* 98: 59–86. <https://doi.org/10.3897/mycokeys.98.104156>
- Cao L, Luo D, Lin W, Yang Q, Deng XJ (2022) Four new species of *Diaporthe* (Diaporthaceae, Diaporthales) from forest plants in China. *MycKeys* 91: 25–47. <https://doi.org/10.3897/mycokeys.91.84970>
- Carbone I, Kohn LM (1999) A method for designing primer sets for speciation studies in filamentous ascomycetes. *Mycologia* 3(3): 553–556. <https://doi.org/10.1080/00275514.1999.12061051>

- Crous PW, Gams W, Stalpers JA, Robert V, Stegehuis G (2004a) MycoBank: An online initiative to launch mycology into the 21<sup>st</sup> century. *Studies in Mycology* 50: 19–22.
- Crous PW, Groenewald JZ, Risède JM, Simoneau P, Hywel-Jones NL (2004b) *Calonectria* species and their *Cylindrocladium* anamorphs: Species with sphaeropedunculate vesicles. *Studies in Mycology* 50: 415–430.
- Darriba D, Taboada GL, Doallo R, Posada D (2012) jModelTest 2: More models, new heuristics and parallel computing. *Nature Methods* 9(8): 772. <https://doi.org/10.1038/nmeth.2109>
- Desjardins P, Hansen JB, Allen M (2009) Microvolume protein concentration determination using the NanoDrop 2000c spectrophotometer. *Journal of Visualized Experiments* 33(33): 1–3. <https://doi.org/10.3791/1610>
- Diogo E, Santos JM, Phillips AJ (2010) Phylogeny, morphology and pathogenicity of *Diaporthe* and *Phomopsis* species on almond in Portugal. *Fungal Diversity* 44(1): 107–115. <https://doi.org/10.1007/s13225-010-0057-x>
- Doyle JJ, Doyle JL (1990) Isolation of plant DNA from fresh tissue. *Focus (San Francisco, Calif.)* 12: 13–15.
- Fan XL, Hyde KD, Udayanga D, Wu XY, Tian CM (2015) *Diaporthe rostrata*, a novel ascomycete from *Juglans mandshurica* associated with walnut dieback. *Mycological Progress* 14(10): 1–8. <https://doi.org/10.1007/s11557-015-1104-5>
- Gao YH, Liu F, Cai L (2016) Unravelling *Diaporthe* species associated with *Camellia*. *Systematics and Biodiversity* 14(1): 102–117. <https://doi.org/10.1080/14772000.2015.1101027>
- Gao YH, Liu F, Duan W, Crous PW, Cai L (2017) *Diaporthe* is paraphyletic. *IMA Fungus* 8(1): 153–187. <https://doi.org/10.5598/imafungus.2017.08.01.11>
- Glass NL, Donaldson GC (1995) Development of primer sets designed for use with the PCR to amplify conserved genes from filamentous ascomycetes. *Applied and Environmental Microbiology* 61(4): 1323–1330. <https://doi.org/10.1128/aem.61.4.1323-1330.1995>
- Gomes RR, Glienke C, Videira SIR, Lombard L, Groenewald JZ, Crous PW (2013) *Diaporthe*: A genus of endophytic, saprobic and plant pathogenic fungi. *Persoonia* 31(1): 1–41. <https://doi.org/10.3767/003158513X666844>
- Guarnaccia V, Crous PW (2017) Emerging citrus diseases in Europe caused by species of *Diaporthe*. *IMA Fungus* 8(2): 317–334. <https://doi.org/10.5598/imafungus.2017.08.02.07>
- Guarnaccia V, Crous PW (2018) Species of *Diaporthe* on *Camellia* and *Citrus* in the Azores Islands. *Phytopathologia Mediterranea* 57: 307–319. [https://doi.org/10.14601/Phytopathol\\_Mediterr-23254](https://doi.org/10.14601/Phytopathol_Mediterr-23254)
- Guarnaccia V, Groenewald JZ, Woodhall J, Armengol J, Cinelli T, Eichmeier A, Ezra D, Fontaine F, Gramaje D, Gutierrez-Aguirregabiria A, Kaliterna J, Kiss L, Larignon P, Luque J, Mugnai L, Naor V, Raposo R, Sándor E, Váczy KZ, Crous PW (2018) *Diaporthe* diversity and pathogenicity revealed from a broad survey of grapevine diseases in Europe. *Persoonia* 40(1): 135–153. <https://doi.org/10.3767/persoonia.2018.40.06>
- Guindon S, Dufayard JF, Lefort V, Anisimova M, Hordijk W, Gascuel O (2010) New algorithms and methods to estimate maximum-likelihood phylogenies: Assessing the performance of PhyML 3.0. *Systematic Biology* 59(3): 307–321. <https://doi.org/10.1093/sysbio/syq010>
- Guo YS, Crous PW, Bai Q, Fu M, Yang MM, Wang XH, Du YM, Hong N, Xu WX, Wang GP (2020) High diversity of *Diaporthe* species associated with pear shoot canker in China. *Persoonia* 45(1): 132–162. <https://doi.org/10.3767/persoonia.2020.45.05>

- Hall T (1999) BioEdit: A user-friendly biological sequence alignment editor and analysis program for Windows 95/98/NT. *Nucleic Acids Symposium Series* 41: 95–98.
- Huang F, Udayanga D, Wang X, Hou X, Mei X, Fu Y, Hyde KD, Li HY (2015) Endophytic *Diaporthe* associated with *Citrus*: A phylogenetic reassessment with seven new species from China. *Fungal Biology* 119(5): 331–347. <https://doi.org/10.1016/j.funbio.2015.02.006>
- Jiang N, Voglmayr H, Piao CG, Li Y (2021) Two new species of *Diaporthe* (Diaporthaceae, Diaporthales) associated with tree cankers in the Netherlands. *MycKeys* 85: 31–56. <https://doi.org/10.3897/mycokeys.85.73107>
- Katoh K, Toh H (2010) Parallelization of the MAFFT multiple sequence alignment program. *Bioinformatics (Oxford, England)* 26(15): 1899–1900. <https://doi.org/10.1093/bioinformatics/btq224>
- Lombard L, Van Leeuwen GCM, Guarnaccia V, Polizzi G, Van Rijswijk PC, Karin Rosendahl KC, Gabler J, Crous PW (2014) *Diaporthe* species associated with *Vaccinium*, with specific reference to Europe. *Phytopathologia Mediterranea* 53: 287–299. [https://doi.org/10.14601/Phytopathol\\_Mediterr-14034](https://doi.org/10.14601/Phytopathol_Mediterr-14034)
- Manawasinghe IS, Dissanayake AJ, Li X, Liu M, Wanasinghe DN, Xu J, Zhao W, Zhang W, Zhou Y, Hyde KD, Brooks S, Yan J (2019) High genetic diversity and species complexity of *Diaporthe* associated with grapevine dieback in China. *Frontiers in Microbiology* 10: 1936. <https://doi.org/10.3389/fmicb.2019.01936>
- Mostert L, Crous PW, Kang JC, Phillips AJ (2001) Species of *Phomopsis* and a *Libertella* sp. occurring on grapevines with specific reference to South Africa: Morphological, cultural, molecular and pathological characterization. *Mycologia* 93(1): 146–167. <https://doi.org/10.1080/00275514.2001.12061286>
- Nitschke T (1870) *Pyrenomyces Germanici* 2: 245. Breslau. Eduard Trewendt, Germany.
- O'Donnell K, Cigelnik E (1997) Two divergent intragenomic rDNA ITS2 types within a monophyletic lineage of the fungus *Fusarium* are nonorthologous. *Molecular Phylogenetics and Evolution* 7(1): 103–116. <https://doi.org/10.1006/mpev.1996.0376>
- Rambaut A, Drummond A (2010) FigTree v.1.3.1. Institute of Evolutionary Biology, University of Edinburgh, Edinburgh, UK.
- Rayner RW (1970) A mycological colour chart. Commonwealth Mycological Institute, Kew, UK.
- Rehner SA, Uecker FA (1994) Nuclear ribosomal internal transcribed spacer phylogeny and host diversity in the coelomycete *Phomopsis*. *Canadian Journal of Botany* 72(11): 1666–1674. <https://doi.org/10.1139/b94-204>
- Ronquist F, Huelsenbeck JP (2003) MrBayes 3: Bayesian phylogenetic inference under mixed models. *Bioinformatics (Oxford, England)* 19(12): 1572–1574. <https://doi.org/10.1093/bioinformatics/btg180>
- Santos JM, Phillips AJL (2009) Resolving the complex of *Diaporthe* (*Phomopsis*) species occurring on *Foeniculum vulgare* in Portugal. *Fungal Diversity* 34: 111–125.
- Santos JM, Vrandečić K, Ćosić J, Duvnjak T, Phillips AJL (2011) Resolving the *Diaporthe* species occurring on soybean in Croatia. *Persoonia* 27(1): 9–19. <https://doi.org/10.3767/003158511X603719>
- Smith H, Wingfeld MJ, Coutinho TA, Crous PW (1996) *Sphaeropsis sapinea* and *Botryosphaeria dothidea* endophytic in *Pinus* spp. and *Eucalyptus* spp. in South Africa. *South African Journal of Botany* 62(2): 86–88. [https://doi.org/10.1016/S0254-6299\(15\)30596-2](https://doi.org/10.1016/S0254-6299(15)30596-2)
- Udayanga D, Castlebury LA, Rossman AY, Chukeatirote E, Hyde KD (2014) Insights into the genus *Diaporthe*: Phylogenetic species delimitation in the *D. eres* species complex. *Fungal Diversity* 67(1): 203–229. <https://doi.org/10.1007/s13225-014-0297-2>

- Udayanga D, Liu X, McKenzie EH, Chukeatirote E, Bahkali AH, Hyde KD (2011) The genus *Phomopsis*: Biology, applications, species concepts and names of common phytopathogens. *Fungal Diversity* 50(1): 189–225. <https://doi.org/10.1007/s13225-011-0126-9>
- Wang WJ, Chen CG, Cheng J (2007) The medicinal active role of tea oil in health care. *Food and Nutrition in China* 9: 48–51. <https://doi.org/10.1002/mnfr.200700032>
- White TJ, Bruns T, Lee S, Taylor J (1990) Amplification and direct sequencing of fungal ribosomal RNA genes for phylogenetics. *PCR Protocols: A Guide to Methods and Applications* 18: 315–322. <https://doi.org/10.1016/B978-0-12-372180-8.50042-1>
- Yang Q, Fan XL, Guarnaccia V, Tian CM (2018) High diversity of *Diaporthe* species associated with dieback diseases in China, with twelve new species described. *MycKeys* 39: 97–149. <https://doi.org/10.3897/mycokeys.39.26914>
- Yang Q, Jiang N, Tian CM (2020) Three new *Diaporthe* species from Shaanxi Province, China. *MycKeys* 67: 1–18. <https://doi.org/10.3897/mycokeys.67.49483>
- Yang Q, Tang J, Zhou GY (2021) Characterization of *Diaporthe* species on *Camellia oleifera* in Hunan Province, with descriptions of two new species. *MycKeys* 84: 15–33. <https://doi.org/10.3897/mycokeys.84.71701>
- Zhou H, Hou CL (2019) Three new species of *Diaporthe* from China based on morphological characters and DNA sequence data analyses. *Phytotaxa* 422(2): 157–174. <https://doi.org/10.11646/phytotaxa.422.2.3>
- Zhu YQ, Ma CY, Xue H, Piao CG, Li Y, Jiang N (2023) Two new species of *Diaporthe* (Diaporthaceae, Diaporthales) in China. *MycKeys* 95: 209–228. <https://doi.org/10.3897/mycokeys.95.98969>
- Zhuang RL (2008) *Camellia oleifera*. 2<sup>nd</sup> ed. China Forestry Press, Beijing.



# Two new species and one new combination of *Ophiocordyceps* (Hypocreales, Ophiocordycipitaceae) in Guizhou

Xing-Can Peng<sup>1,2,3,4,5\*</sup>, Ting-Chi Wen<sup>2,3,6,7\*</sup>, De-Ping Wei<sup>2,3</sup>, Yu-Hong Liao<sup>8,9</sup>, Yi Wang<sup>2,3,7</sup>, Xian Zhang<sup>2,3,4,5</sup>, Gui-Ying Wang<sup>2,3,7</sup>, Yun Zhou<sup>2,3,7</sup>, Khanobporn Tangtrakulwanich<sup>5</sup>, Jian-Dong Liang<sup>1,6</sup>

1 Basic Medical School, Guizhou University of Traditional Chinese Medicine, Guiyang 550002, China

2 National Key Laboratory of Green Pesticide, Key Laboratory of Green Pesticide and Agricultural Bioengineering, Ministry of Education, Guizhou University, Guiyang 550025, Guizhou, China

3 Engineering Research Center of Southwest Bio-Pharmaceutical Resources, Ministry of Education, Guizhou University, Guiyang 550025, Guizhou, China

4 Center of Excellence in Fungal Research, Mae Fah Luang University, Chiang Rai 57100, Thailand

5 School of Science, Mae Fah Luang University, Chiang Rai 57100, Thailand

6 Guizhou Key Laboratory of Edible Fungi Breeding, Guiyang 550006, China

7 School of Pharmacy, Guizhou University, Guiyang 550025, Guizhou, China

8 Shenzhen Ainiang Biotechnology Co., Ltd., Shenzhen 518118, China

9 Shenzhen Longgang Buji Middle School, Shenzhen 518112, China

Corresponding author: Jian-Dong Liang (jdl@gzzy.edu.cn)



Academic editor: Marc Stadler

Received: 27 September 2023

Accepted: 27 January 2024

Published: 29 February 2024

Citation: Peng X-C, Wen T-C, Wei D-P, Liao Y-H, Wang Y, Zhang X, Wang G-Y, Zhou Y, Tangtrakulwanich K, Liang J-D (2024) Two new species and one new combination of *Ophiocordyceps* (Hypocreales, Ophiocordycipitaceae) in Guizhou. MycoKeys 102: 245–266. <https://doi.org/10.3897/mycokeys.102.113351>

Copyright: © Xing-Can Peng et al. This is an open access article distributed under terms of the Creative Commons Attribution License (Attribution 4.0 International – CC BY 4.0).

## Abstract

*Ophiocordyceps* is the largest genus in Ophiocordycipitaceae and has a broad distribution with high diversity in subtropical and tropical regions. In this study, two new species, pathogenic on lepidopteran larvae are introduced, based on morphological observation and molecular phylogeny. *Ophiocordyceps fenggangensis* **sp. nov.** is characterised by having fibrous, stalked stroma with a sterile tip, immersed perithecia, cylindrical asci and filiform ascospores disarticulating into secondary spores. *Ophiocordyceps liangii* **sp. nov.** has the characteristics of fibrous, brown, stipitate, filiform stroma, superficial perithecia, cylindrical asci and cylindrical-filiform, non-disarticulating ascospores. A new combination *Ophiocordyceps musicaudata* (syn. *Cordyceps musicaudata*) is established employing molecular analysis and morphological characteristics. *Ophiocordyceps musicaudata* is characterised by wiry, stipitate, solitary, paired to multiple stromata, yellowish, branched fertile part, brown stipe, immersed perithecia, cylindrical asci and cylindrical-filiform, non-disarticulating ascospores.

**Key words:** Entomopathogenic fungi, morphology, phylogenetic, two new taxa

## Introduction

Hypocreales is a fungal order enriched in arthropod-pathogens, which are taxonomically placed in Clavicipitaceae, Cordycipitaceae, Ophiocordycipitaceae and Polycephalomycetaceae (Luangsa-Ard et al. 2018; Wei et al. 2021a; Xiao et al. 2023). Entomopathogens in these four families can infect many orders of insects and arachnids (Luangsa-Ard et al. 2018; Wei et al. 2022). Hypocrealean entomopathogens can infect various developmental stages of the

\* These authors contributed equally to this work.

insect, from larva, pupa to nymph and adults (Luangsa-Ard et al. 2018). For example, *Ophiocordyceps acicularis* is a parasite on larvae of Coleoptera (Sung et al. 2007), *Cordyceps morakotii* on pupa of Hymenoptera (Tasanathai et al. 2016), *Cordyceps cocoonihabita* on cocoons of Lepidoptera (Wang et al. 2020), *Ophiocordyceps asiana* on adults of Hemiptera (Khao-ngam et al. 2021), *Ophiocordyceps dipterigena* on adults of Diptera (Quandt et al. 2014) and *Simplicillium yunnanense* on the Araneae (Wang et al. 2020).

Ophiocordycipitaceae contains more than 500 species and about three out of five species are distributed in its type genus *Ophiocordyceps*. *Ophiocordyceps* was established by Petch (1931) to accommodate four species with non-disarticulating ascospores, as well as clavate asci with thickened apices: *Ophiocordyceps blattae*, *O. unilateralis*, *O. rhizoidea* and *O. peltata*. Subsequently, an increasing number of species were transferred from *Cordyceps* into *Ophiocordyceps* (Sung et al. 2007; Quandt et al. 2014). *Ophiocordyceps* are characterised by dark, fibrous, wiry, pliant stromata, superficial to completely immersed perithecia, cylindrical asci with thickened cap, fusiform to filiform ascospores disarticulating or non-disarticulating (Sung et al. 2007; Xiao et al. 2019). The asexual genera associated with *Ophiocordyceps* are *Hirsutella*, *Hymenostilbe*, *Paraisaria*, *Stilbella* and *Syngliocladium* (Sung et al. 2007; Quandt et al. 2014; Yang et al. 2021). By employing multigene phylogeny, Quandt et al. (2014) updated the generic composition of Ophiocordycipitaceae and accepted *Drechmeria*, *Harposporium*, *Ophiocordyceps*, *Polycephalomyces*, *Purpureocillium* and *Tolypocladium* in this family; meanwhile, twelve genera including *Cordycepioideus*, *Didymobotryopsis*, *Didymobotrys*, *Hirsutella*, *Hymenostilbe*, *Mahevia*, *Paraisaria*, *Sorosporella*, *Syngliocladium*, *Synnematium*, *Trichosterigma* and *Troglobiomyces* were rejected in favour of *Ophiocordyceps*, following the principle of “one fungus one name”. Mongkolsamrit et al. (2019) resurrected the genus *Paraisaria* in Ophiocordycipitaceae. Crous et al. (2020) and Araújo et al. (2022) established *Hantamomyces* and *Torrubiellomyces*, respectively. Xiao et al. (2023) transferred *Polycephalomyces*, *Perennicordyceps* and *Pleurocordyceps* from Ophiocordycipitaceae to a new family, Polycephalomycetaceae, based on biphasic analyses. Therefore, Ophiocordycipitaceae currently contains eight genera, namely *Drechmeria*, *Hantamomyces*, *Harposporium*, *Ophiocordyceps*, *Paraisaria*, *Purpureocillium*, *Tolypocladium* and *Torrubiellomyces*.

In this study, we collected three entomopathogenic fungi from lepidoptera larvae found in disturbed forests in Guizhou Province, China. These specimens have typical characters of *Ophiocordyceps* in terms of the macro- and micro-morphologies. This study attempts to reveal their taxonomic placements, based on morphological characteristics and molecular analysis of the combined LSU, ITS, SSU, *tef1-a*, *rpb1* and *rpb2* dataset.

## Materials and methods

### Collection, isolation and morphological study

Specimens were scanned from the ground of disturbed forests in Guizhou Province, China. Three species were found to infect lepidopteran larvae and their stromata protruded from the ground. Amongst them, the hosts of specimen HKAS 125848 were found completely immersed into soil. The host of specimen

GACP SY22072880 was found semi-immersed into soil. The specimen HKAS 125845 was found on leaf litter. Macro-morphological characteristics of fresh collections were documented with a camera (Canon 6D) and locations were recorded with Biotracks in the field. The specimens were collected into a plastic box and transported to the laboratory for subsequent studies. The culture of the specimens was obtained by transferring a small mass of mycelium inside the body of the host into potato dextrose agar (PDA) using a sterile inoculation needle and incubated at 25 °C (Wei et al. 2021b). A Leica stereomicroscope (Leica S9E) was used to examine and section the fruiting bodies. Sections of fertile head were mounted on glass slides with a drop of ultrapure water and covered with a cover slip. A Leica compound microscope (Leica DM2500) was used to photograph and measure perithecia, asci, peridium, apical cap, ascospores and secondary ascospores. The fruiting bodies were dried with allochroic silica gel and deposited in the Herbarium of Cryptogams, Kunming Institute of Botany of the Chinese Academy of Sciences (**KUN-HKAS**), the cultures being deposited in the Herbarium of Guizhou University (**GACP**).

### DNA extraction, PCR amplification and sequencing

DNA was extracted from mycelium inside the body of insect hosts and from fresh mycelium on PDA medium using DNA extraction kit (Fungal gDNA Isolation Kit, Biomiga, CA, USA), following the protocol of the manufacturer. The obtained total genomic DNA was stored at -20 °C. Six loci including the partial large subunit rRNA gene (LSU), internal transcribed spacer including the 5.8S rDNA gene (ITS), the partial small subunit rRNA gene (SSU), the translation elongation factor 1-alpha gene (*tef1-a*), the partial RNA polymerase II largest subunit (*rpb1*) and the partial RNA polymerase II second largest subunit (*rpb2*) were amplified and sequenced. The primers LROR/LR5 were used for LSU (Vilgalys and Hester 1990), ITS5/ITS4 for ITS (White et al. 1990), NS1/NS4 for SSU (White et al. 1990), EF1-983F/EF1-2218R for *tef1-a* (Rehner and Buckley 2005), CRPB1A/RPB1Cr for *rpb1* (Castlebury et al. 2004) and fRPB2-5f/fRPB2-7cR for *rpb2* (Castlebury et al. 2004). The Polymerase Chain Reaction (PCR) was performed in a 50 µl volumes consisting of 22 µl PCR mixture (2× *Taq* PCR StarMix with Loading Dye, GenStar) which contains *Taq* DNA polymerase, dNTPs, Mg<sup>2+</sup>, a reaction buffer and stabiliser, 20 µl of double distilled water, 2 µl of each primer and 4 µl of DNA template. Amplifications were carried out using a BioRAD T100 Thermal Cycler (Singapore) with the following conditions: (1) initialisation at 94 °C for 3 min, for ITS (2) 33 cycles of denaturation at 94 °C for 30 sec, annealing at 51 °C for 50 sec and extension at 72 °C for 45 sec; for SSU and LSU (2) 33 cycles of denaturation at 94 °C for 30 sec, annealing at 50 °C for 30 sec and extension at 72 °C for 2 min; for *tef1-a* (2) 33 cycles of denaturation at 94 °C for 30 sec, annealing at 58 °C for 50 sec and extension at 72 °C for 1 min; for *rpb1* and *rpb2* (2) 33 cycles of denaturation at 94 °C for 30 sec, annealing at 51 °C for 40 sec and extension at 72 °C for 1 min 20 sec and followed by (3) final extension at 72 °C for 10 min. The PCR products were sent to Tsingke Biological Technology in Chongqing, China, for sequencing using the above primers. The generated sequences were edited manually for excluding ambiguous region with BioEdit v.7.0.5.3 (Hall et al. 2011). The accession numbers and hosts are listed in Table 1.

**Table 1.** GenBank accession numbers of the taxa used in the phylogenetic analyses, the newly- generated sequences are in bold,<sup>T</sup> Represents type strain, type specimens or neotype.

Current name	Voucher	host	LSU	ITS	SSU	<i>tef1</i> - $\alpha$	<i>rpb1</i>	<i>rpb2</i>	References
<i>Cordyceps militaris</i>	OSC 93623	Lepidoptera	AY184966	JN049825	AY184977	DQ522332	DQ522377	AY545732	Kepler et al. 2012
	YFCC 6587		MN576818		MN576762	MN576988	MN576878	MN576932	Wang et al. 2020
<i>Drechmeria balanoides</i>	CBS 250.82 <sup>T</sup>		AF339539		AF339588	DQ522342		DQ522442	Sung et al. 2007
<i>D. gunnii</i>	OSC 76404	Lepidoptera	AF339522	JN049822	AF339572	AY489616	AY489650	DQ522426	Luangsa-Ard et al. 2018
<i>D. panacis</i>	CBS 142798 <sup>T</sup>	Apiales	MF588897	MF588878	MF588890	MF614144			Yeh et al. 2021
<i>D. zeospora</i>	CBS 335.80 <sup>T</sup>		AF339540	MH861269	AF339589	EF469062	EF469091	EF469109	Vu et al. 2019
<i>Harposporium anguillulae</i>	ARSEF 5593		AY636081						Chaverri et al. 2005
<i>Har. cycloides</i>	ARSEF 5599		AY636083						Chaverri et al. 2005
<i>Har. harposporiferum</i>	ARSEF 5472 <sup>T</sup>		NG_060621		AF339569				Sung et al. 2001
<i>Har. helicoides</i>	ARSEF 5354	Nematode	AF339527		AF339577				Sung et al. 2001
<i>Hirsutella citrifomis</i>	ARSEF1 035	Hemiptera	KM652105	KM652153	KM652064	KM651989	KM652030		Simmons et al. 2015
	ARSEF 1446	Hemiptera	KM652106	KM652154	KM652065	KM651990	KM652031		Simmons et al. 2015
<i>Hir. fusiformis</i>	ARSEF 5474	Coleoptera	KM652110		KM652067	KM651993	KM652033		Simmons et al. 2015
<i>Hir. gigantea</i>	ARSEF 30	Hymenoptera	JX566977			JX566980	KM652034		Simmons et al. 2015
<i>Hir. kuankuoshuiensis</i>	GZUIFR-2012KKS3-1	Lepidoptera	KY415582	KY415575		KY415590	KY945360		Qu et al. 2021
<i>Hir. radiata</i>	ARSEF 1369	Diptera	KM652119		KM652076	KM652002	KM652042		Simmons et al. 2015
<i>Hir. shennongjiaensis</i>	GZUIFR-Snj121022 <sup>T</sup>	Dermaptera	KY945357	KT390721			KY945364		Zou et al. 2016
<i>Ophiocordyceps acicularis</i>	OSC 110987	Coleoptera	EF468805		EF468950	EF468744	EF468852		Sung et al. 2007
<i>O. agriotidis</i>	ARSEF 5692	Coleoptera	DQ518754	JN049819	DQ522540	DQ522322	DQ522368	DQ522418	Kepler et al. 2012
<i>O. alboperitheciata</i>	YHH 16755 <sup>T</sup>	Lepidoptera	MT222278			MT222279	MT222280	MT222281	Fan et al. 2021
<i>O. appendiculata</i>	NBRC 106959	Coleoptera	JN941412	JN943325	JN941729	AB968578	JN992463	AB968540	Ban et al. 2015
<i>O. araracuarensis</i>	HUA 186135	Hemiptera	KC610769	KP200891	KC610788	KC610738	KF658665	KC610716	Sanjuan et al. 2015
<i>O. asiatica</i>	BCC 86435	Blattodea	MH753676	MH754723			MK214106	MK214092	Tasanathai et al. 2019
<i>O. bidoupensis</i>	YHH 20036 <sup>T</sup>	Coleoptera			OK571396	OK556893	OK556897	OK556899	Zou et al. 2022
<i>O. brunneiperitheciata</i>	TBRC 8100	Lepidoptera	MF614658			MF614643		MF614685	Luangsa-Ard et al. 2018
	BCC 49312	Lepidoptera	MF614660			MF614642		MF614686	Luangsa-Ard et al. 2018
<i>O. coccidiicola</i>	NBRC 100682		AB968419	AB968404	AB968391	AB968583		AB968545	Ban et al. 2015
<i>O. communis</i>	BCC 1874	Blattodea	MH753679	MH754725		MK284267	MK214109	MK214095	Tasanathai et al. 2019
<i>O. crinalis</i>	GDGM 17327	Lepidoptera	KF226254		KF226253	KF226256	KF226255		Wang et al. 2014
<i>O. delicatula</i>	ARSEF 14442 <sup>T</sup>	Hemiptera			MZ198251	MZ246828	MZ246829		Clifton et al. 2021
<i>O. elongata</i>	OSC 110989	Lepidoptera	EF468808			EF468748	EF468856		Sung et al. 2007
<i>O. entomorrhiza</i>	KEW 53484	Lepidoptera	EF468809	JN049850	EF468954	EF468749	EF468857	EF468911	Quandt et al. 2014
<i>Ophiocordyceps fenggangensis</i>	HKAS 125848 <sup>T</sup>	Lepidoptera	<b>OR527542</b>	<b>OR527535</b>		<b>OR526346</b>	<b>OR526351</b>		<b>This study</b>
	GACP FG21042850	Lepidoptera	<b>OR527541</b>	<b>OR527534</b>	<b>OR527538</b>	<b>OR526345</b>	<b>OR526350</b>	<b>OR526353</b>	<b>This study</b>
<i>O. flabellata</i>	YFCC 8795 <sup>T</sup>	Hymenoptera	OL310724		OL310721	OL322688	OL322687	OL322695	Tang et al. 2023b
<i>O. formosana</i>	TNM F13893	Coleoptera			KJ878908	KJ878956	KJ878988	KJ878943	Quandt et al. 2014
<i>O. fusiformis</i>	BCC 93025 <sup>T</sup>	Blattodea	MZ675422	MZ676743		MZ707849	MZ707855	MZ707805	Tasanathai et al. 2022

Current name	Voucher	host	LSU	ITS	SSU	<i>tef1</i> - $\alpha$	<i>rpb1</i>	<i>rpb2</i>	References
<i>O. gracillima</i>	HUA 186132	Coleoptera	KC610768	KF937353		KC610744	KF658666		Sanjuan et al. 2015
<b><i>Ophiocordyceps liangii</i></b>	<b>HKAS 125845<sup>T</sup></b>	<b>Lepidoptera</b>	<b>OR527543</b>	<b>OR527536</b>	<b>OR527539</b>	<b>OR526347</b>			<b>This study</b>
	<b>GACP LB22071253</b>	<b>Lepidoptera</b>	<b>OR527544</b>	<b>OR527537</b>	<b>OR527540</b>	<b>OR526348</b>		<b>OR526354</b>	<b>This study</b>
<i>O. macroacicularis</i>	NBRC 105888	Lepidoptera	AB968417	AB968401	AB968389	AB968575		AB968537	Ban et al. 2015
<i>O. melolonthae</i>	OSC 110993	Coleoptera	DQ518762		DQ522548	DQ522331	DQ522376		Spatafora et al. 2007
<i>O. monacidis</i>	MF74	Hymenoptera	KX713605		KX713647		KX713712		Araújo et al. 2018
<i>O. mosingoensis</i>	BCC 30904	Blattodea	MH753686	MH754732		MK284273	MK214115	MK214100	Tasanathai et al. 2019
<i>O. multiperitheciata</i>	BCC 22861	Lepidoptera	MF614656			MF614640	MF614670	MF614683	Araújo et al. 2018
<b><i>Ophiocordyceps musicaudata</i></b>	<b>GACP SY22072879</b>	<b>Lepidoptera</b>	<b>OR527545</b>			<b>OR526349</b>	<b>OR526352</b>		<b>This study</b>
<i>O. naomipierceae</i>	DAWKSAN <sup>T</sup>	Hymenoptera	KX713589		KX713664		KX713701		Araújo et al. 2018
<i>O. nigra</i>	TNS 16250	Coleoptera			KJ878942	KJ878987	KJ879021		Quandt et al. 2014
<i>O. nigrella</i>	EFCC 9247	Lepidoptera	EF468818	JN049853	EF468963	EF468758	EF468866	EF468920	Sung et al. 2007
<i>O. nooreniae</i>	BRIP 55363 <sup>T</sup>	Hymenoptera	KX673810		KX673811	KX673812		KX673809	Crous et al. 2016
<i>O. ovatospora</i>	YHH 2206001 <sup>T</sup>	Blattodea	OP295113	OP295105	OP295110	OP313801	OP313803	OP313805	Tang et al. 2022
<i>O. pseudocommunis</i>	BCC 16757	Blattodea	MH753687	MH754733		MK284274	MK214117	MK214101	Tasanathai et al. 2019
<i>O. pseudorhizoidea</i>	BCC 86431	Blattodea	MH753674	MH754721		MK284262	MK751469	MK214090	Tasanathai et al. 2019
<i>O. purpureostromata</i>	TNS F18430	Coleoptera	KJ878897		KJ878931	KJ878977	KJ879011		Quandt et al. 2014
<i>O. ravenelii</i>	OSC 110995	Coleoptera	DQ518764		DQ522550	DQ522334	DQ522379	DQ522430	Spatafora et al. 2007
<i>O. robertsii</i>	KEW 27083	Lepidoptera	EF468826			EF468766			Sung et al. 2007
<i>O. sinensis</i>	EFCC 7287	Lepidoptera	EF468827	JN049854	EF468971	EF468767	EF468874	EF468924	Sung et al. 2007
<i>O. spataforae</i>	OSC 128575	Hemiptera	EF469079	JN049845	EF469126	EF469064	EF469093	EF469110	Sung et al. 2007
<i>O. unilateralis</i>	OSC 128574	Hymenoptera	DQ518768		DQ522554	DQ522339	DQ522385	DQ522436	Spatafora et al. 2007
<i>Parasaria amazonica</i>	HUA 186143	Orthoptera	KJ917571		KJ917562	KM411989	KP212902	KM411982	Sanjuan et al. 2015
<i>Par. blattarioides</i>	HUA 186093	Blattodea	KJ917570		KJ917559	KM411992	KP212910		Sanjuan et al. 2015
	HUA 186108	Blattodea	KJ917569		KJ917558		KP212912	KM411984	Sanjuan et al. 2015
<i>Par. coenomyiae</i>	NBRC 108993 <sup>T</sup>	Diptera	AB968412	AB968396	AB968384	AB968570		AB968532	Ban et al. 2015
<i>Par. gracilioides</i>	HUA 186092	Coleoptera	KJ130992		KJ917555		KP212915		Araújo et al. 2018
<i>Par. gracilis</i>	EFCC 3101	Lepidoptera	EF468810		EF468955	EF468750	EF468858	EF468913	Araújo et al. 2018
<i>Par. heteropoda</i>	EFCC 10125	Hemiptera	EF468812	JN049852	EF468957	EF468752	EF468860	EF468914	Sung et al. 2007
<i>Par. orthopterorum</i>	TBRC 9710	Orthoptera	MK332582	MH754743		MK214081	MK214085		Mongkolsamrit et al. 2019
<i>Par. phuwiangensis</i>	BBH 43491	Coleoptera	MK192058	MH188542			MH211351		Mongkolsamrit et al. 2019
<i>Par. tettigonia</i>	GZUH CS14062709 <sup>T</sup>	Orthoptera		KT345954	KT345955	KT375440	KT375441		Wen et al. 2016
<i>Par. yodhathaii</i>	TBRC 8502	Coleoptera	MH201168	MH188540		MH211354	MH211350		Mongkolsamrit et al. 2019
<i>Pur. lavendulum</i>	FMR 10376	Soil	FR775489			FR775516	FR775512		Perdomo et al. 2013
<i>Pur. lilacinum</i>	CBS 431.87	Tylenchida	EF468844	AY624188		EF468791	EF468897	EF468940	Kepler et al. 2012
<i>Pur. takamizusanense</i>	NHJ 3582	Hemiptera	EU369034		EU369097	EU369015			Johnson et al. 2009
<i>Tolypocladium bacillisporum</i>	C53 <sup>T</sup>	Eurotiales	LC684523	LC684523	LC684523	LC684526			Yamamoto et al. 2022
<i>Tol. cylindrosporium</i>	ARSEF 2920 <sup>T</sup>	Soil	MH871712	MG228381		MG228390	MG228384	MG228387	Vu et al. 2019
<i>Tol. inflatum</i>	OSC 71235	Coleoptera	EF469077	JN049844	EF469124	EF469061	EF469090	EF469108	Kepler et al. 2012
<i>Tol. ophioglossoides</i>	NBRC 106332	Eurotiales	JN941409	JN943322	JN941732		JN992466		Schoch et al. 2012

Current name	Voucher	host	LSU	ITS	SSU	<i>tef1</i> - $\alpha$	<i>rpb1</i>	<i>rpb2</i>	References
<i>Tol. paradoxum</i>	NBRC 100945		JN941410	JN943323	JN941731	AB968599	JN992465	AB968560	Ban et al. 2015
<i>Torrubiellomyces zombiae</i>	NY04434801 <sup>T</sup>	Hypocreales	ON493602		ON493543	ON513396	ON513398	ON513402	Araújo et al. 2022
	Polyceph	Hypocreales				ON513394			Araújo et al. 2022

Abbreviations: **ARSEF**: Agricultural Research Service Entomopathogenic Fungus Collection, USDA, USA; **BBH**: BIOTEC Bangkok Herbarium, Thailand; **BCC**: BIOTEC Culture Collection, Klong Luang, Thailand; **BRIP**: Queensland Plant Pathology Herbarium, Australia; **C**: Medical Mycology Research Center, Chiba University, Japan; **CBS**: Centraalbureau voor Schimmelcultures, Utrecht, the Netherlands; **EFCC**: Entomopathogenic Fungal Culture Collection, Chuncheon, Korea; **FMR**: Culture Collection, Facultad de Medicina i Ciències de la Salut, Reus, Spain; **GDGM**: the Fungal Herbarium of Guangdong Institute of Microbiology, China; **GZUH/GACP**: Herbarium of Guizhou University, China; **GZUIFR**: Institute of Fungal Resources of Guizhou University, China; **HKAS**: Kunming Institute of Botany, Academia Sinica, China; **HUA**: Herbarium Antioquia University, Medellín, COL; **KEW**: mycology collection of Royal Botanical Garden, Surrey, UK; **NBRC**: Biological Resource Center, the National Institute of Technology and Evaluation, Japan; **NHJ**: Nigel Hywel-Jones personal collection, Thailand; **NY**: The New York Botanical Garden Herbarium, US; **OSC**: Oregon State University Herbarium, Corvallis, Oregon, USA; **TBRC**: Thailand Bioresources Research Center, Thailand; **YFCC**: Yunnan Fungal Culture Collection of Yunnan University, China; **YHH**: Yunnan Herbal Herbarium, China.

## Sequence alignment and phylogenetic analyses

The taxa used for phylogenetic analyses were selected, based on BLAST search results and related references (Sung et al. 2007; Quandt et al. 2014; Sanjuan et al. 2015; Araújo et al. 2018; Luangsa-Ard et al. 2018). Each locus was independently aligned with the representative sequences using MAFFT v.7 (Katoh and Standley 2013; Katoh et al. 2019). Uninformative gaps and ambiguous regions were removed using Trimal v.1.2 (Capella-Gutiérrez et al. 2009). Trimmed alignments were combined with SequenceMatrix 1.8 (Vaidya et al. 2011). The final combined dataset was deposited on TreeBASE (accession URL: <http://purl.org/phylo/treebase/phyloids/study/TB2:S30990>) and used for Maximum Likelihood analysis and Bayesian analysis. AliView (Larsson 2014) was used to convert format with NEXUS file for Bayesian Inference analysis and FASTA file for Maximum Likelihood analysis. Two strains of *Cordyceps militaris* (BCC 56302 and YFCC 6587) were selected as outgroup taxa.

Maximum Likelihood (ML) analysis was performed using IQ-TREE 1.6.12 with branch support being estimated from 5000 ultrafast bootstraps (<http://iqtree.cibiv.univie.ac.at/>, accessed on 04 Sep 2023, Minh et al. (2020)). MrModelTest v. 2.3 (Nylander 2004) as implemented in MrMTgui v.1.0. (Nuin 2007) was used to determine the best-fit evolution model for Bayesian Inference analyses under the Akaike Information Criterion (AIC). The best-fit substitution model GTR+I+G was decided for LSU, ITS, SSU, *tef1*- $\alpha$  and *rpb2* and HKY+I+G for *rpb1*. MrBayes on XSEDE (3.2.7a) in the CIPRES Science Gateway was utilised to perform Bayesian analysis using Markov Chain Monte Carlo sampling (MCMC). Six simultaneous Markov chains were run for 100,000,000 generations and trees were sampled every 1000 generations. The first 20% of the trees were discarded, as they represented the burn-in phase of the analyses, while the remaining trees were used for calculating posterior probabilities (PP) in the majority rule consensus tree. Bayesian Inference trees convergence was declared when the average standard deviation reached 0.01. The trees were viewed with FigTree v.1.4.0 programme (Rambaut 2016) and edited with Adobe illustrator CS6.

## Results

### Phylogenetic analyses

Phylogenetic analyses were constructed with combined 6-locus sequences data representing 73 taxa of Ophiocordycipitaceae. The concatenated LSU-ITS-SSU-*tef1*- $\alpha$ -*rpb1*-*rpb2* data matrix was subjected to Maximum Likelihood

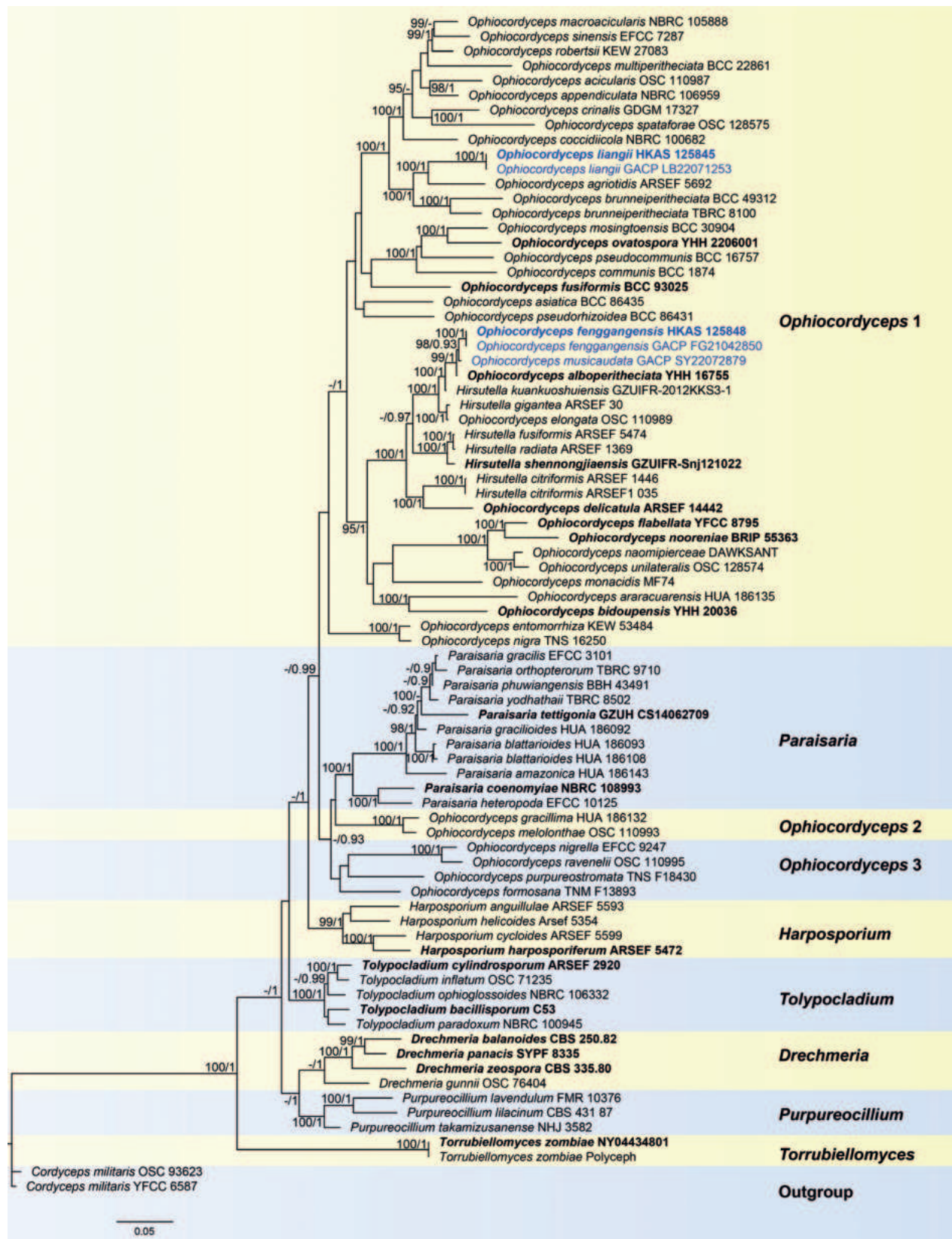


Figure 1. Phylogram generated from Maximum Likelihood analysis, based on combined LSU, ITS, SSU, *tef1-a*, *rpb1* and *rpb2* sequence data. ML bootstrap values equal to or greater than 95% and the PP equal to or greater than 0.90 are given above each node. The newly-generated sequences are indicated in blue. Type strain, type specimens or neotype are denoted in black bold.

(ML) and Bayesian Inference (BI) analyses. Trees were rooted to *Cordyceps militaris* in Cordycipitaceae. The alignment contains 4831 characters, including gaps (834 bp for LSU, 506 bp for ITS, 1022 bp for SSU, 918 bp for *tef1-a*, 665 bp for *rpb1* and 886 bp for *rpb2*). The likelihood of the best scoring ML tree was -50301.608. The respective best-fit models determined by ModelFinder on IQ-TREE were GTR+F+I+G4 for LSU, TIM3+F+I+G4 for ITS, K2P+I+G4 for SSU, TIM2+F+I+G4 for TEF1- $\alpha$ , TN+F+I+G4 for RPB1 and RPB2.

In the phylogenetic analyses (Fig. 1), seven genera of Ophiocordycipitaceae are included and their names were labelled on the right side of the tree. The phylogenetic results indicated that the two new species *Ophiocordyceps fenggangensis*, *O. liangii* and one new combination *O. musicaudata* are distinct from other known species. *Ophiocordyceps fenggangensis* and *O. musicaudata* form a monophyletic clade close to *O. alboperitheciata* and *Hirsutella kuankuoshuiensis* with strong support (100% ML / 1.00 PP, Fig. 1). *Ophiocordyceps liangii* (HKAS 102546) sister to *O. agriotidis* with strong support (100% ML/1.00 PP, Fig. 1).

## Taxonomy

### *Ophiocordyceps fenggangensis* X. C. Peng & T. C. Wen, sp. nov.

Index Fungorum: IF901112

Facesoffungi Number: FoF14887

Fig. 2

**Etymology.** Named after the location where the type specimen was found, Fenggang County, Guizhou Province, China.

**Diagnosis.** Parasitic on a larva of Lepidoptera. Stroma arising from the junction between head and thorax of lepidopteran larva, with a sterile tip. Perithecia immersed, grey-white.

**Sexual morph. Stroma** solitary, unbranched, brown to grey-white, 102  $\times$  1–1.5 mm. **Fertile part** up to 24  $\times$  1.5 mm, cylindrical, attenuated toward the apex, grey-white when fresh, yellowish when dry, surface spinous due to the protruding ostioles, with a sterile tip (ca. 0.5 mm in length). **Stipe** cylindrical, brown to black, fibrous, 77.5  $\times$  1–1.2 mm. **Perithecia** 306–496  $\times$  134–223  $\mu\text{m}$  ( $\bar{x}$  = 388.4  $\times$  175.9  $\mu\text{m}$ ,  $\sigma$  = 57.35  $\times$  31.05,  $n$  = 15), immersed, ovoid to oblong-ovate. **Asci** 91–176  $\times$  2–8  $\mu\text{m}$  ( $\bar{x}$  = 136.5  $\times$  5.3  $\mu\text{m}$ ,  $\sigma$  = 38.22  $\times$  2.63,  $n$  = 20), cylindrical, hyaline, with thickened apex. **Apical cap** 2.5–5.0  $\times$  3.5–5.6  $\mu\text{m}$  ( $\bar{x}$  = 3.6  $\times$  4.7  $\mu\text{m}$ ,  $\sigma$  = 0.78  $\times$  0.48,  $n$  = 20), hyaline, hemispherical. **Ascospores** 0.3–0.7  $\mu\text{m}$  ( $\bar{x}$  = 0.4  $\mu\text{m}$ ,  $\sigma$  = 38.22  $\times$  2.63,  $n$  = 20) wide, filiform, hyaline, easily breaking into part-spores. **Secondary ascospores** 2.8–6.0  $\times$  0.3–0.7  $\mu\text{m}$  ( $\bar{x}$  = 4.0  $\times$  0.4  $\mu\text{m}$ ,  $\sigma$  = 0.89  $\times$  0.08,  $n$  = 20), cylindrical, smooth-walled. **Asexual morph:** undetermined.

**Culture characteristics.** Colonies on PDA, attaining a diameter of 28–32 mm within 39 d at 20 °C, dense, leathery, cream white, convex, undulate margin, reverse brown, radial striation, no sporulation observed.

**Material examined.** CHINA, Guizhou Province, Fenggang County, Yongan Town (28°05'30.83"N, 107°31'53.38"E, alt. 1149 m), on dead larva of Lepidoptera, 28 April 2021, Xing-Can Peng, FG21042850 (HKAS 125848 holotype, GACP FG21042850 ex-type living culture).

**Notes.** Multigene phylogenetic analysis showed that *Ophiocordyceps fenggangensis* forms a sister clade to *O. musicaudata* with a high support value (98%

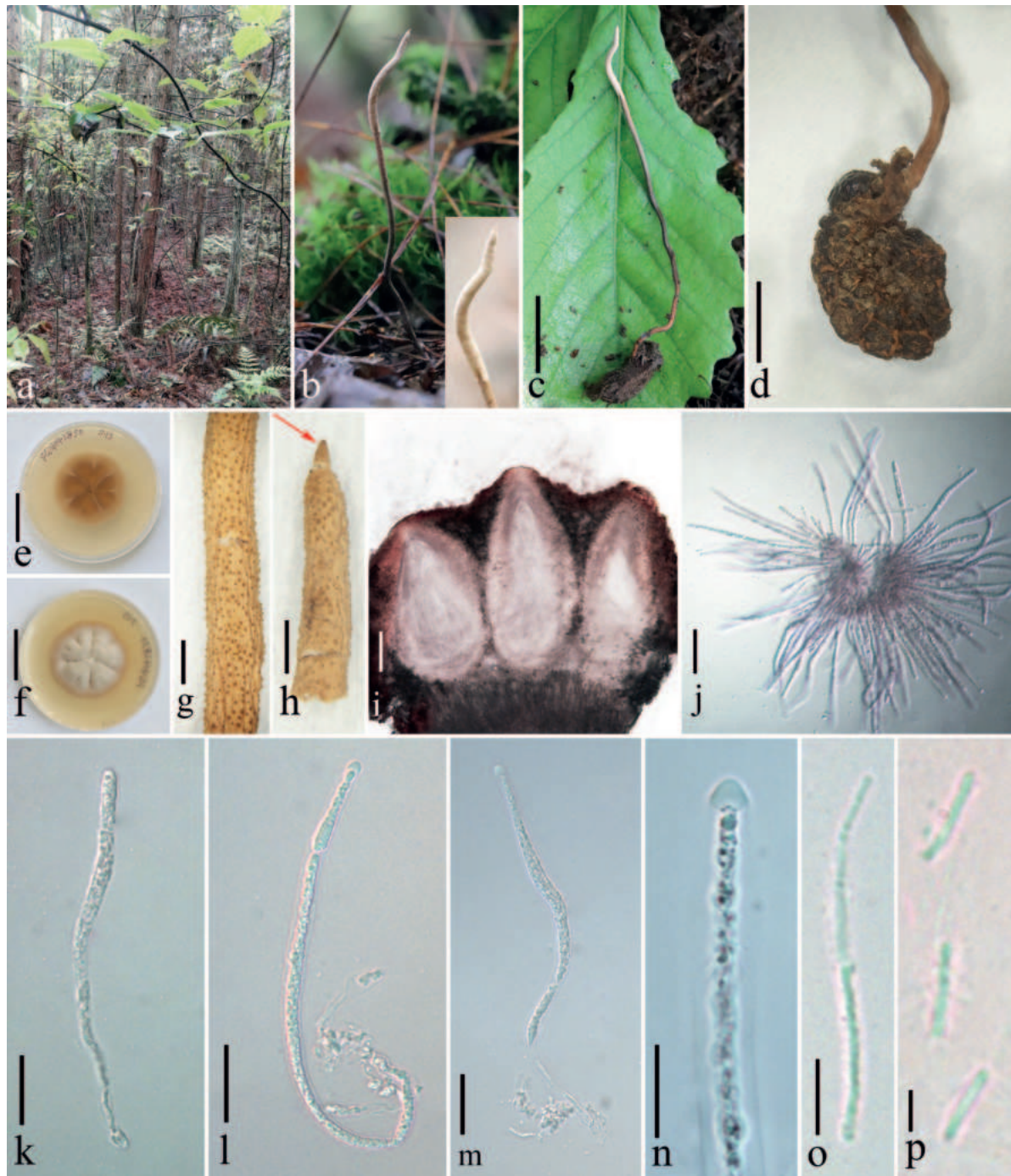


**Figure 2.** *Ophiocordyceps fenggangensis* (holotype HKAS 125848) **a** habitat **b** host imbedded into the soil with the stroma emerging from the ground **c** stroma arising from the larva of Lepidoptera **d** host **e, f** reverse and front view of the culture on PDA **g** part of fertile head **h** part of fertile head with sterile tip (arrow indicate) **i** perithecia **j–m** asci **n** ascus cap **o** part of ascospores **p** secondary ascospores. Scale bars: 2 cm (**c, e, f**); 5 mm (**d**); 1 mm (**g, h**); 100  $\mu$ m (**i, j**); 25  $\mu$ m (**k–m**); 10  $\mu$ m (**n**); 5  $\mu$ m (**o**); 2  $\mu$ m (**p**).

ML / 0.93 PP) and grouped with *O. alboperitheciata* and *Hirsutella kuankuoshuiensis* (Fig. 1). *Ophiocordyceps fenggangensis* GACP FG21042850 and *O. musicaudata* GACP SY22072879 have 8 bp differences of nucleotides (0 bp in LSU, 3 bp in *tef1-a* and 5 bp in *rpb1*). Morphologically, *Ophiocordyceps fenggangensis* is distinguished from *O. musicaudata* in having a solitary unbranched shorter stroma, longer perithecia, smaller asci, narrower ascospores and disarticulating

ascospores. *Ophiocordyceps alboperithecata* is distinct from *O. fenggangensis* by its superficial, white to nearly light brown fertile part and ovoid perithecia (Fan et al. 2021), whereas our new species has grey-white to yellowish fertile part and immersed, ovoid to oblong-ovate perithecia. Additionally, the stroma of *O. fenggangensis* is longer than that of *O. alboperithecata*. Perithecia and asci of *O. fenggangensis* are smaller than those of *O. alboperithecata*. *Hirsutella kuankuoshuiensis* was described only from its asexual morph which is characterised by clavate, narrow fusiform or botuliform conidia; and subulate or slender columnar phialides tapering gradually to a long narrow neck (Qu et al. 2021). BLAST search result showed that the ex-type strain (GACP FG21042850) matches *Hirsutella kuankuoshuiensis* GZUIFR-2012KKS3-1; however, they are different in 59 bp (including 1 gap) and 8 bp (including 1 gap) within ITS and *rpb1* sequences, respectively. The detailed comparisons of the morphologies between these four aforementioned species are shown in Table 2. Based on the morphological differences, we introduce this fungus as a new species of *Ophiocordyceps*.

***Ophiocordyceps liangii* X. C. Peng & T. C. Wen, sp. nov.**

Index Fungorum: IF901113

Facesoffungi Number: FoF14888

Fig. 3

**Etymology.** Named in honour of Prof. Zong-Qi Liang, who has made a significant contribution to the studies of Cordyceps sensu lato.

**Diagnosis.** Parasitic on lepidopteran larva. Stroma arising from the back and tail of host, no sterile tip. Perithecia superficial, dark brown.

**Sexual morph. Stroma** paired, flexuous, fibrous, filiform, tapering gradually towards the apex, unbranched, brown to dark brown, 11.3–18.8 × 0.2 cm. **Fertile part** cylindrical, dark brown, 5.4–6.1 × 0.2 cm. **Stipe** flexuous, brown, 5.1–13.5 × 0.1–0.2 cm. **Perithecia** 350–548 × 203.5–446 μm ( $\bar{x}$  = 430.5 × 296 μm,  $\sigma$  = 56.45 × 60.83, n = 25), superficial, brown, obovoid. **Asci** 122–271.5 × 3.5–13.5 μm ( $\bar{x}$  = 204.8 × 8.0 μm,  $\sigma$  = 38.22 × 2.63, n = 40), filiform, 8-spored, cylindrical, with thickened apices. **Apical cap** 1.7–4.5 × 4.0–6.6 μm ( $\bar{x}$  = 3.2 × 5.4 μm,  $\sigma$  = 0.56 × 0.59, n = 40), hyaline, conspicuous. **Ascospores** 67.5–270.5 × 1.5–4.0 μm ( $\bar{x}$  = 151.3 × 2.6 μm,  $\sigma$  = 36.31 × 0.61, n = 55), fusiform to filiform, aseptate, guttulate, non-disarticulating. **Asexual morph:** undetermined.

**Culture characters.** Colonies on PDA, attaining a diameter of 21–27 mm within 25 d at 25 °C, dense, leathery, pale yellow at centre, white at periphery, radially striate, with brown or translucent droplets, reverse black brown, producing brown pigment. Sporulation not observed.

**Material examined.** CHINA, Guizhou Province, Libo County, Xiaoqikong Scenic Area (25°15'15.68"N, 107°43'43.98"E, alt. 458 m), on dead larva of Lepidoptera, on leaf litter, 12 July 2022, Xing-Can Peng, LB22071253 (HKAS 125845 holotype, GACP LB22071253 ex-type culture).

**Notes.** Phylogenetic analyses revealed that *Ophiocordyceps liangii* is closely related to *O. agriotidis* and *O. brunneiperithecata* with high support (100% ML/1.00 PP, Fig. 1). *Ophiocordyceps liangii* differs from *O. brunneiperithecata* and *O. agriotidis* in having longer stroma, larger perithecia and asci (see Table 2). The comparison of the nucleotide sequences between *O. liangii* (GACP

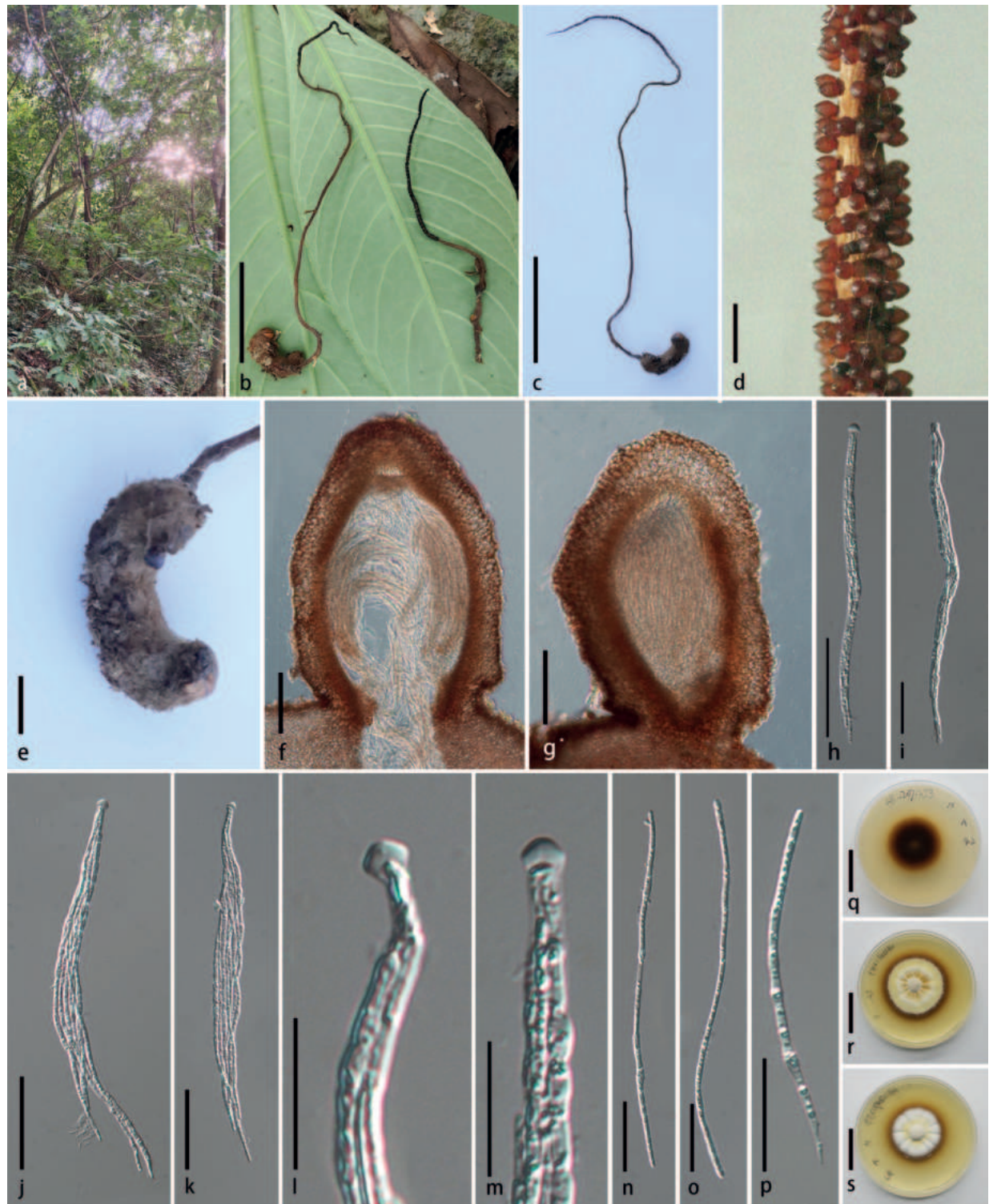


**Figure 3.** *Ophiocordyceps liangii* (holotype HKAS 125845) **a** habitat **b, c** stromata arising from host **d** superficial perithecia **e** host **f, g** section of perithecia **h-k** ascus **h-i** immature **j, k** mature **l, m** ascus cap **n-p** ascospores **q-s** reverse and front view of culture on PDA. Scale bars: 4 cm (**b, c**), 1 mm (**d**), 5 mm (**e**), 100  $\mu$ m (**f, g**), 50  $\mu$ m (**h-k**), 20  $\mu$ m (**l, m**), 30  $\mu$ m (**n-p**), 2 cm (**q-s**).

LB22071253) and *O. brunneiperitheciata* (TBRC 8100) showed 23 bp (including 3 gaps) differences in LSU, 102 bp in *tef1-a* and 88 bp in *rpb2* sequences. *Ophiocordyceps liangii* differs from *O. agriotidis* ARSEF 5692 by 3 bp in SSU, 70 bp (including 20 gaps) in ITS, 20 bp (including 1 gap) in LSU, 106 bp in *tef1-a* and 79 bp in *rpb2*. Henceforth, we describe this taxon as a new species in *Ophiocordyceps*.

***Ophiocordyceps musicaudata* (Z. Q. Liang & A. Y. Liu) X. C. Peng & T. C. Wen, comb. nov.**

Index Fungorum: IF901114

Facesoffungi Number: FoF14889

Fig. 4

*Cordyceps musicaudata* Z. Q. Liang & A. Y. Liu. Basionym.

**Diagnosis.** Parasitic on larvae of insect (Lasiocampidae, Lepidoptera). Stroma arising from body of the host, no sterile tip. Perithecia immersed, yellowish.

**Sexual morph. Stroma** solitary, paired to multiple, simple or branched, flexuous, cylindrical with acute or round ends, 13–14 × 0.1–0.2 cm. **Fertile part** cylindrical, yellowish, 2–4.3 × 0.1–0.2 cm. **Stipe** flexuous, brown, 10–12 × 0.1 cm. **Peridium** 15–49 μm ( $\bar{x}$  = 33 μm,  $\sigma$  = 8.41, n = 40) wide, composed of brown cells of *textura angularis*. **Perithecia** 260–492 × 144–314 μm ( $\bar{x}$  = 378 × 221 μm,  $\sigma$  = 37.29 × 1.57, n = 25), immersed, flask-shaped. **Asci** 123–264 × 5–13 μm ( $\bar{x}$  = 191 × 8.1 μm,  $\sigma$  = 58.76 × 48.94, n = 80), cylindrical, 8-spored, with inconspicuous thickened cap. **Ascospores** 114–298 × 1.5–4.0 μm ( $\bar{x}$  = 198 × 2.3 μm,  $\sigma$  = 46.03 × 0.48, n = 45), filiform, irregular multi-septate, non-disarticulating. **Asexual morph:** undetermined.

**Culture characteristics.** Colonies on PDA, attaining a diameter of 21–27 mm within 43 d at 25 °C, dense, velvety, off-white, wrinkled bulge, reverse brown. No sporulation observed.

**Epitype designated here.** CHINA, Guizhou Province, Suiyang County, Kuankuoshui National Nature Reserve (28°13'N, 107°09'E, alt. 1470–1507 m), on dead larva of Lepidoptera sp. buried in soil, 28 July 2022, Xing-Can Peng, SY22072880 (HKAS 131911 epitype); Ting-Chi Wen, SY22072879 (HKAS 131912, GACP SY22072879, live culture).

**Notes.** Liang et al. (1996) published a new species, *Cordyceps musicaudata* solely based on morphological observation. The type specimen (CGAC89-62301) was found on the insect (Lasiocampidae, Lepidoptera) in the Kuankuoshui National Nature Reserve, Guizhou Province, China. It is regrettable that the type specimen has been destroyed, thus its DNA and morphological observations could not be obtained. Liang et al. (1996) stated that the type specimen has characteristics of paired rat-tailed stromata, white to pale brown fertile part, brown stipe, immersed perithecia, cylindrical asci with thickened apices and filiform, multi-septate ascospores. In this study, we collected two fresh specimens from the same location to the type specimen. The fresh specimen shares similar morphology with the type specimen of *C. musicaudata* in the lepidopteran hosts, stipitate rat-tailed stromata with yellowish fertile part, immersed perithecia and filiform, multi-septate, intact ascospores. Phylogenetic analysis indicated that *C. musicaudata* has close affinity with *O. alboperitheciata* and *O. fenggangensis* with adequate support (99% ML / 1 PP, Fig. 1). The differences between *C. musicaudata* and *O. fenggangensis* have been mentioned in the notes of *O. fenggangensis*. The difference between *C. musicaudata* and *O. alboperitheciata* is the size and the arrangements of the perithecia. *Ophiocordyceps musicaudata* has smaller and immersed perithecia, whereas *O. alboperitheciata* has larger and superficial perithecia. The detailed comparisons of morphologies between our specimen and related species including species without molecular data are shown in Table 2 (*Cordyceps ochraceostromata*, *Ophiocordyceps alboperitheciata*, *O. dayiensis*, *O. emeiensis*, *O. fenggan-*



**Figure 4.** *Ophiocordyceps musicaudata* (HKAS 131911) **a** redrawn of Liang (2007) **b** habitat **c, d** stromata arising from host **e** fertile parts **f, g** reverse and front view of culture on PDA **h, i** perithecia **j–l** asci **m** ascus cap **n–p** ascospores, the arrows in the **n, p** indicating septate. Scale bars: 2 cm (**c, d**); 5 mm (**e**); 1 cm (**f, g**); 100  $\mu$ m (**h, i**); 50  $\mu$ m (**j–l, n–p**); 5  $\mu$ m (**m**).

*gensis*, *O. laojunshanensis*, *O. larvarum*, *O. zhangjiajiensis* and *O. paludosa*). Our specimen morphologically more matches *Cordyceps musicaudata* rather than other *Ophiocordyceps* species included in the Table 2. Therefore, we determined these specimens as *Cordyceps musicaudata* and move this species into the genus *Ophiocordyceps*, based on the phylogenetic affiliation of this new collection.

## Discussion

It has been observed that there are eight genera in Ophiocordycipitaceae that possess versatile lifestyles (Crous et al. 2020; Araújo et al. 2022; Xiao et al. 2023). *Drechmeria* typically live as endoparasites inside nematodes and lepidopteran larvae (Yu et al. 2018). *Hantamomyces* is a monotypic genus that was established by Crous et al. (2020), based on *H. aloidendri* found on the leaves of *Aloidendron dichotomum*. Most species of *Harposporium* parasitise free-living nematodes and rotifers; however, the taxonomic status of some species in this genus is still difficult to determine (Crous et al. 2023). *Paraisaria* accommodate 18 species that were established due to their distinctive features, such as the fleshy, robust solitary stroma, globose to ovoid fertile head and brighter colour. These characteristics are different from other Ophiocordycipitaceae species (Mongkolsamrit et al. 2019). *Purpureocillium* contains six species that are entomopathogenic fungi or pathogenic to humans (Luangsa-Ard et al. 2011). Species of *Tolypocladium* infect hosts crossing animals, plants and fungi, showing highly diverse lifestyles (Yu et al. 2021). *Torrubiellomyces* is a genus with only one species that is a mycoparasite. The species has superficial perithecia that grow directly on the host's surface (Araújo et al. 2022). Genera of Ophiocordycipitaceae are monophyletic with the exception of *Ophiocordyceps* which has been split into three clades due to erection of *Paraisaria* (Mongkolsamrit et al. 2019; Wei et al. 2021b; Wei et al. 2022). So far, there are 419 species in the *Ophiocordyceps*, including 98 unclarified *Hirsutella* species (until 28 Aug 2023). Amongst them, molecular data are not available for 194 species. In this study, 75 taxa representing 70 species of *Ophiocordyceps* are sampled and used for phylogenetic analysis. The topologies of the main clades are similar to previous studies (Wei et al. 2022; Xiao et al. 2023). Insertion of *Paraisaria* causes paraphyly of *Ophiocordyceps*; *Drechmeria* and *Purpureocillium* form a clade sister and *Harposporium* forms a clade sister with *Ophiocordyceps* s. s. and *Paraisaria* (Xiao et al. 2023). The sexual morphs of *Ophiocordyceps* species phenotypically share a darkly or brightly coloured, fibrous stromata often with aperithecial apices or lateral pads. Perithecia are superficial to completely immersed, ordinal or oblique in arrangement. Asci are cylindrical to filiform with thickened apex. Ascospores are cylindrical, multi-septate, disarticulating into secondary spores or not (Sung et al. 2007). However, they can be distinguished according to their associated host, arrangement of perithecia, size, shape, colour of fertile part and morphologies of ascospores and part-spores. Notably, combined molecular phylogenetic analysis provides further evidence of their interspecific relationship.

Most of the fungal species published before the 1990s relied on classical morphology to determine the taxonomic status. It is difficult to gain access to their molecular data and morphological illustration and other related information as well as their type specimens. These issues emphasise the importance of collecting fresh specimens and clarifying them with modern approaches. Such work has been conducted by Sung et al. (2007) who systematically classified *Cordyceps* and clavicipitaceous fungi through molecular phylogenetic analysis and revised most of the species of *Cordyceps* s. l. Henceforth, an increasing number of new species were described and the natural classification of hypocrealean entomopathogens were gradually elucidated, based

Table 2. Synopsis of *Ophiocordyceps* species discussed in the paper.

Species	Host	Stromata (mm)	Perithecia(µm)	Asci (µm)	Ascospores (µm)	Reference
<i>Ophiocordyceps liangii</i>	larvae of Lepidoptera	113–188 × 2, paired, cylindrical, unbranched, brown to dark brown	350–548 × 203.5–446, superficial, brown, obovoid	122–271.5 × 3.5–13.5, filiform, 8-spored, with thickened apices	67.5–270.5 × 1.5–4.0, filiform to spindle, non-disarticulating	This study
<i>Ophiocordyceps agriotidis</i>	larvae of Elateridae, Coleoptera	70 × 1, solitary, cylindrical, black brown to black	400–480 × 225–300, superficial to pseudo-immersed, ovoid	235–300 × 12, cylindrical, with an oblate apical cap	115–150 × 4.2–45, cylindrical, multi-septate, non-disarticulating	Liang (2007)
<i>Ophiocordyceps brunneiperitheciata</i>	Lepidopteran larvae	4–8 × 0.5–1, paired to multiple, simple, wiry to pliant or fibrous	350–400 × 180–200, superficial, brown to dark brown, ovoid	125–175 × 6–8, cylindrical, 8-spored, with thickened apices	110–160 × 3–4, filiform, multi-septate, non-disarticulating	Luangsa-Ard et al. (2018)
<i>Ophiocordyceps fenggangensis</i>	larvae of Lepidoptera	102 × 1–1.5, solitary, cylindrical, brown to off-white	306–496 × 134–223, immersed, off-white to yellowish, ovoid to oblong-ovate.	91–176 × 2–8, cylindrical, apex thickened	0.3–0.7 wide, filiform, hyaline, disarticulating, secondary ascospores 2.8–6.0 × 0.3–0.7, cylindrical	This study
<i>Ophiocordyceps alboperitheciata</i>	larva of Noctuidae, Lepidoptera	69–71 × 0.6–1.2, paired, cylindrical, unbranched, with a sterile tip, light brown to dark brown	410–550 × 230–320, superficial, white to pale brown, nearly ovoid	144–246 × 3.5–4.7, cylindrical, 8-spored, with a hemispheric apical cap	0.5–0.6 wide, multi-septate, non-disarticulating	Fan et al. (2021)
<i>Ophiocordyceps musicaudata</i>	larvae of Lasiocampidae, Lepidoptera	130–140 × 1–2, solitary or numerous, simple or branched, cylindrical, brown to yellowish	260–492 × 144–314, immersed, yellowish, flask-shaped.	123–264 × 5–13, filiform, cylindrical, 8-spored, usually without thickened apices	114–298 × 1.5–4.0, cylindrical, irregular multi-septate, non-disarticulating	This study
<i>Ophiocordyceps musicaudata</i>	larvae of Lasiocampidae, Lepidoptera	up to 165 in length, twin, unbranched, light brown to white	420 × 210, immersed, pseudo-oval	230 × 7.6, cylindrical, with short cylindrical apices	filiform, multi-septate	Liang et al. (1996)
<i>Ophiocordyceps larvarum</i>	larva of Lepidoptera	90 × 3.5, solitary, cylindrical, cinnamon light brown	340–380 × 160–200, pseudo-embedding, oblong	180–200 × 8.5, with a hemispheric ascus cap	4–9 × 2–2.5, columnar, septate	Liang et al. (2007)
<i>Cordyceps ochraceostromata</i>	larva of Lepidoptera	up to 60 in length, single or paired, cylindrical, pale ochraceous-reddish to brownish	350 × 200, immersed, ovoid	up to 7 in width, with thickened apices	disarticulating, secondary ascospores 7–10 × 1.5–2, truncated on both sides	Kobayasi and Shimizu (1980)
<i>Ophiocordyceps zhangjiajiensis</i>	pupa of Lepidoptera	100 × 2, single or paired, cylindrical, not ramified, leathery, brown to snuff-coloured	330–375 × 180–230, pseudo-embedding, ovoid	200 × 10, approximately fusiform, with thickened apices	disarticulating, secondary ascospores 15–23 × 3, cylindrical	Liang et al. (2002)
<i>Ophiocordyceps dayiensis</i>	larva of Lepidoptera	140 × 2, single, filiform, unbranched, brownish	430–480 × 210–270, immersed, narrowly ovoid	225–345 × 6–7.5, slender cylindrical, with very thin cap of ascus	300 × 1–1.8, filiform, multi-septate, non-disarticulating	Liang et al. (2003)
<i>Ophiocordyceps emelensis</i>	larva of Hepialidae, Lepidoptera	100–160 × 1.5–3, single or paired, branched, brown	320–460 × 220–320, superficial, brown to black, ellipsoid or ovoid	173–213 × 7.5–8, cylindrical, with hemisphaeris heads	45–60 × 1–1.5, filiform, multi-septate	Liang et al. (2007)
<i>Ophiocordyceps laojunshanensis</i>	Larvae of Hepialidae, Lepidoptera	47–93 × 1–3.9, simple, rarely 2 or 3, apex sterile acuminate, purplish to dark brown	200–300 × 200–350, globose, arranged loosely in irregular lateral cushions.	165–275 × 11.5–14.5, clavate	130.0–250 × 5–6, filiform, septate	Chen et al. (2011)
<i>Ophiocordyceps paludosa</i>	larvae of Lepidoptera	55–130 × 0.5–1.0, slender filiform, greyish-brown	800–855 × 375–410, superficial, greyish-brown to deep brown, flattened-ovoid	480–550 × 8–10, cylindrical	390–490 × 2.0–2.5, filiform, multi-septate, non-disarticulating	Mains (1940)

on more sufficient taxa sampling (Ban et al. 2009; Evans et al. 2011; Sanjuan et al. 2015; Simmons et al. 2015; Spatafora et al. 2015; Araújo et al. 2018; Khonsanit et al. 2019; Araújo et al. 2020; Mongkolsamrit et al. 2021; Yang et al. 2021; Araújo et al. 2022; Mongkolsamrit et al. 2022; Tang et al. 2022; Mongkolsamrit et al. 2023; Tang et al. 2023a, b). However, *Cordyceps musicaudata* has not been revised because there are no specimens available for study of its morphological and molecular data. We have conducted a study wherein fresh specimens were collected from the same location as the type of *Cordyceps musicaudata*. Our observations reveal that there are certain similarities between the fresh specimen and some species mentioned in Table 2, both at a macroscopic and microscopic level. However, we also observed noticeable differences between them. For example, the perithecia of *Ophiocordyceps larvarum* and *O. zhangjiayi* are pseudo-immersed; *O. emeiensis* and *O. paludosa* have superficial perithecia; the ascospores of *O. dayiensis* are slender; the stromata of *O. laojunshanensis* are short and the perithecia are globoid; and the ascospores of *Cordyceps ochraceostromata* disarticulate into secondary spores (see Table 2). Based on molecular analysis and updated morphological illustration, we identified the specimen as *Cordyceps musicaudata* and synonymised it as *O. musicaudata*. Moreover, two new species, *O. fenggangensis* and *O. liangii* are described from their sexual morphs and phylogenetic results support their novelty.

## Additional information

### Conflict of interest

The authors have declared that no competing interests exist.

### Ethical statement

No ethical statement was reported.

### Funding

This study was supported by the Science and Technology Foundation of Guizhou Province (No. [2022]025-8, No. GZU-SZBJMS001 & No. (2020-1Y391)).

### Author contributions

Investigation: YW, GYW. Resources: YZ, XZ, YHL. Writing – original draft: TCW, XCP. Writing – review and editing: DPW, JDL, KT.

### Author ORCIDs

Xing-Can Peng  <https://orcid.org/0000-0002-7271-7639>

Ting-Chi Wen  <https://orcid.org/0000-0003-1744-5869>

De-Ping Wei  <https://orcid.org/0000-0002-3740-0142>

Yi Wang  <https://orcid.org/0009-0006-5412-7893>

Xian Zhang  <https://orcid.org/0009-0008-0919-4303>

Khanobporn Tangtrakulwanich  <https://orcid.org/0009-0002-7081-618X>

Jian-Dong Liang  <https://orcid.org/0000-0002-3939-3900>

### Data availability

All of the data that support the findings of this study are available in the main text.

## References

- Araújo J, Evans HC, Kepler R, Hughes DP (2018) Zombie-ant fungi across continents: 15 new species and new combinations within *Ophiocordyceps*. I. Myrmecophilous hirsutelloid species. *Studies in Mycology* 90(1): 119–160. <https://doi.org/10.1016/j.simyco.2017.12.002>
- Araújo JP, Evans HC, Fernandes IO, Ishler MJ, Hughes DP (2020) Zombie-ant fungi cross continents: II. Myrmecophilous hymenostilboid species and a novel zombie lineage. *Mycologia* 112(6): 1138–1170. <https://doi.org/10.1080/00275514.2020.1822093>
- Araújo J, Lebert B, Vermeulen S, Brachmann A, Ohm R, Evans HC, Debekker C (2022) Masters of the manipulator: Two new hypocrealean genera, *Niveomyces* (Cordycipitaceae) and *Torrubiellomyces* (Ophiocordycipitaceae), parasitic on the zombie ant fungus *Ophiocordyceps camponoti-floridani*. *Persoonia* 49(1): 171–194. <https://doi.org/10.3767/persoonia.2022.49.05>
- Ban S, Sakane T, Toyama K, Nakagiri A (2009) Teleomorph–anamorph relationships and reclassification of *Cordyceps cuboidea* and its allied species. *Mycoscience* 50(4): 261–272. <https://doi.org/10.1007/S10267-008-0480-Y>
- Ban S, Sakane T, Nakagiri A (2015) Three new species of *Ophiocordyceps* and overview of anamorph types in the genus and the family Ophiocordycepsaceae. *Mycological Progress* 14(1): 1–12. <https://doi.org/10.1007/s11557-014-1017-8>
- Capella-Gutiérrez S, Silla-Martínez JM, Gabaldón T (2009) trimAl: A tool for automated alignment trimming in large-scale phylogenetic analyses. *Bioinformatics* 25(15): 1972–1973. <https://doi.org/10.1093/bioinformatics/btp348>
- Castlebury LA, Rossman AY, Song GH, Hyten AS, Spatafora JW (2004) Multigene phylogeny reveals new lineage for *Stachybotrys chartarum*, the indoor air fungus. *Mycological Research* 108(8): 864–872. <https://doi.org/10.1017/S0953756204000607>
- Chaverri P, Bischoff JF, Liu M, Hodge KT (2005) A new species of *Hypocrella*, *H. macrostroma*, and its phylogenetic relationships to other species with large stromata. *Mycological Research* 109(11): 1268–1275. <https://doi.org/10.1017/S0953756205003904>
- Chen JY, Cao YQ, Yang DR, Li MH (2011) A new species of *Ophiocordyceps* (Clavicipitales, Ascomycota) from southwestern China. *Mycotaxon* 115(1): 1–4. <https://doi.org/10.5248/115.1>
- Clifton EH, Castrillo LA, Hajek AE (2021) Discovery of two hypocrealean fungi infecting spotted lanternflies, *Lycorma delicatula*: *Metarhizium pemphigi* and a novel species, *Ophiocordyceps delicatula*. *Journal of Invertebrate Pathology* 186: e107689. <https://doi.org/10.1016/j.jip.2021.107689>
- Crous PW, Wingfield MJ, Burgess TI, Hardy GSJ, Crane C, Barrett S, Cano-Lira JF, Le Roux JJ, Thangavel R, Guarro J, Stchigel AM, Martín MP, Alfredo DS, Barber PA, Barreto PW, Baseia IG, Cano-Canals J, Cheewangkoon R, Ferreira RJ, Gené J, Lechat C, Moreno G, Roets F, Shivas RG, Sousa JO, Tan YP, Wiederhold NP, Abell SE, Accioly T, Albizu JL, Alves JL, Antonioli ZI, Aplin N, Araújo J, Arzanlou M, Bezerra JDP, Bouchara JP, Carlavilla JR, Castillo A, Castroagudín VL, Ceresini PC, Claridge GF, Coelho G, Coimbra VRM, Costa LA, da Cunha KC, da Silva SS, Daniel R, de Beer ZW, Dueñas M, Edwards J, Enwistle P, Fiuza PO, Fournier J, García D, Gibertoni TB, Giraud S, Guevara-Suarez M, Gusmão LFP, Haituk S, Heykoop M, Hirooka Y, Hofmann TA, Houbraken J, Hughes DP, Kautmanová I, Koppel O, Koukol O, Larsson E, Latha KPD, Lee DH, Lisboa DO, Lisboa WS, López-Villalba Á, Maciel JLN, Manimohan P, Manjón JL, Marinowitz S, Marney TS, Meijer M, Miller AN, Olariaga I, Paiva LM, Piepenbring M, Poveda-Molero JC, Raj KNA, Raja HA, Rougeron A, Salcedo I, Samadi R, Santos TAB, Scarlett K, Seifert

- KA, Shuttleworth LA, Silva GA, Silva M, Siqueira JPZ, Souza-Motta CM, Stephenson SL, Sutton DA, Tamakeaw N, Telleria MT, Valenzuela-Lopez N, Viljoen A, Visagie CM, Vizzini A, Wartchow F, Wingfield BD, Yurchenko E, Zamora JC, Groenewald JZ (2016) Fungal Planet description sheets: 469–557. *Persoonia*. *Persoonia* 37(1): 218–403. <https://doi.org/10.3767/003158516X694499>
- Crous PW, Cowan DA, Maggs-Kölling G, Yilmaz N, Larsson E, Angelini C, Brandrud TE, Dearnaley JDW, Dima B, Dovana F, Fechner N, García D, Gené J, Halling RE, Houbraken J, Leonard P, Luangsa-Ard JJ, Noisripoom W, Rea-Ireland AE, Ševčíková H, Smyth CW, Vizzini A, Adam JD, Adams GV, Alexandrova AV, Alizadeh A, Álvarez DE, Andjic V, Antonín V, Arenas F, Assabgui R, Ballarà J, Banwell A, Berraf-Tebbal A, Bhatt VK, Bonito G, Botha W, Burgess TI, Caboň M, Calvert J, Carvalhais LC, Courtecuisse R, Cullington P, Davoodian N, Decock CA, Dimitrov R, Di Piazza S, Drenth A, Dumez S, Eichmeier A, Etayo J, Fernández I, Fiard JP, Fournier J, Fuentes-Aponte S, Ghanbary MAT, Ghorbani G, Giraldo A, Glushakova AM, Gouliamova DE, Guarro J, Halleen F, Hampe F, Hernández-Restrepo M, Iturrieta-González I, Jeppson M, Kachalkin AV, Karimi O, Khalid AN, Khonsanit A, Kim JI, Kim K, Kiran M, Krisai-Greilhuber I, Kučera V, Kušan I, Langenhoven SD, Lebel T, Lebeuf R, Liimatainen K, Linde C, Lindner DL, Lombard L, Mahamedi AV, Matočec N, Maxwell A, May TW, McTaggart AR, Meijer M, Mešić A, Mileto AJ, Miller AN, Molia A, Mongkolsamrit S, Muñoz Cortés C, Muñoz-Mohedano J, Morte A, Morozova OV, Mostert L, Mostowfizadeh-Ghalamfarsa R, Nagy LG, Navarro-Ródenas A, Örstadius L, Overton BE, Papp V, Para R, Peintner U, Pham THU, Pordel A, Pošta A, Rodríguez A, Romberg M, Sandoval-Denis M, Seifert KA, Semwal KC, Sewall BJ, Shivas RG, Slovák M, Smith K, Spetik M, Spies CFJ, Syme K, Tasanathai K, Thorn RG, Tkalčec Z, Tomashevskaya MA, Torres-García D, Ullah Z, Visagie CM, Voitek A, Winton LM (2020) Fungal Planet description sheets: 1112–1181. *Persoonia* 45(1): 251–409. <https://doi.org/10.3767/persoonia.2020.45.10>
- Crous PW, Akulov A, Balashov S, Boers J, Braun U, Castillo J, Delgado M, Denman S, Erhard A, Gusella G, Jurjević Ž, Kruse J, Malloch DW, Osieck ER, Polizzi G, Schumacher RK, Slotweg E, Starink-Willemse M, van Iperen AL, Verkley GJM, Groenewald JZ (2023) New and Interesting Fungi. 6. *Fungal Systematics and Evolution* 11(1): 109–156. <https://doi.org/10.3114/fuse.2023.11.09>
- Evans HC, Elliot SL, Hughes DP (2011) Hidden diversity behind the zombie-ant fungus *Ophiocordyceps unilateralis*: Four new species described from carpenter ants in Minas Gerais, Brazil. *PLOS ONE* 6(3): e17024. <https://doi.org/10.1371/journal.pone.0017024>
- Fan Q, Wang Y-B, Zhang GD, Tang DX, Yu H (2021) Multigene phylogeny and morphology of *Ophiocordyceps alboperitheciata* sp. nov., a new entomopathogenic fungus attacking Lepidopteran larva from Yunnan, China. *Mycobiology* 49(2): 133–141. <https://doi.org/10.1080/12298093.2021.1903130>
- Hall T, Biosciences I, Carlsbad C (2011) BioEdit: An important software for molecular biology. *GERF Bulletin of Biosciences* 2: 60–61.
- Johnson D, Sung G-H, Hywel-Jones NL, Luangsa-Ard JJ, Bischoff JF, Kepler RM, Spatafora JW (2009) Systematics and evolution of the genus *Torrubiella* (Hypocreales, Ascomycota). *Mycological Research* 113(3): 279–289. <https://doi.org/10.1016/j.mycres.2008.09.008>
- Katoh K, Standley DM (2013) MAFFT multiple sequence alignment software version 7: Improvements in performance and usability. *Molecular Biology and Evolution* 30(4): 772–780. <https://doi.org/10.1093/molbev/mst010>

- Katoh K, Rozewicki J, Yamada KD (2019) MAFFT online service: Multiple sequence alignment, interactive sequence choice and visualization. *Briefings in Bioinformatics* 20(4): 1160–1166. <https://doi.org/10.1093/bib/bbx108>
- Kepler R, Sung G-H, Ban S, Nakagiri A, Chen M-J, Huang B, Li ZZ, Spatafora JW (2012) New teleomorph combinations in the entomopathogenic genus *Metacordyceps*. *Mycologia* 104(1): 182–197. <https://doi.org/10.3852/11-070>
- Khao-ngam S, Mongkolsamrit S, Rungjindamai N, Noisriboom W, Pooissarakul W, Duangthisan J, Himaman W, Luangsa-Ard JJ (2021) *Ophiocordyceps asiana* and *Ophiocordyceps tessaratomidarum* (Ophiocordycipitaceae, Hypocreales), two new species on stink bugs from Thailand. *Mycological Progress* 20(3): 341–353. <https://doi.org/10.1007/s11557-021-01684-x>
- Khonsanit A, Luangsa-Ard JJ, Thanakitpipattana D, Kobmoo N, Piasai O (2019) Cryptic species within *Ophiocordyceps myrmecophila* complex on formicine ants from Thailand. *Mycological Progress* 18(1–2): 147–161. <https://doi.org/10.1007/s11557-018-1412-7>
- Kobayasi Y, Shimizu D (1980) *Cordyceps* species from Japan 3. *Bulletin of the National Science Museum Series B* 6: 125–146.
- Larsson A (2014) AliView: A fast and lightweight alignment viewer and editor for large datasets. *Bioinformatics* 30(22): 3276–3278. <https://doi.org/10.1093/bioinformatics/btu531>
- Liang ZQ (2007) *Cordyceps*. *Flora fungorum sinicorum* (Vol. 32). Science Press, Beijing, 190 pp.
- Liang ZQ, Liu AY, Huang JZ, Jiao YC (1996) The genus *Cordyceps* from Kuankuoshui Preserve in Guizhou I. *Acta Mycologica Sinica* 15: 271–276.
- Liang ZQ, Liu AY, Huang JZ (2002) Some entomogenous fungi from Wuyishan and Zhangjiajie nature reserves I *Cordyceps*. *Mycosystema* 21: 162–166.
- Liang ZQ, Wang B, Kang JC (2003) Several rare entopathogenic fungi from the Western Sichuan mountains. *Fungal Diversity* 12: 129–134.
- Luangsa-Ard JJ, Houbraken J, van Doorn T, Hong S-B, Borman AM, Hywel-Jones NL, Samson RA (2011) *Purpureocillium*, a new genus for the medically important *Paezilomyces lilacinus*. *FEMS Microbiology Letters* 321(2): 141–149. <https://doi.org/10.1111/j.1574-6968.2011.02322.x>
- Luangsa-Ard JJ, Tasanathai K, Thanakitpipattana D, Khonsanit A, Stadler M (2018) Novel and interesting *Ophiocordyceps* spp. (Ophiocordycipitaceae, Hypocreales) with superficial perithecia from Thailand. *Studies in Mycology* 89(1): 125–142. <https://doi.org/10.1016/j.simyco.2018.02.001>
- Mains EB (1940) *Cordyceps* species from Michigan. *Papers of the Michigan Academy of Science* 25: 79–84.
- Minh BQ, Schmidt HA, Chernomor O, Schrempf D, Woodhams MD, Von Haeseler A, Lanfear R (2020) IQ-TREE 2: New models and efficient methods for phylogenetic inference in the genomic era. *Molecular Biology and Evolution* 37(5): 1530–1534. <https://doi.org/10.1093/molbev/msaa015>
- Mongkolsamrit S, Noisriboom W, Arnarnart N, Lamlerthton S, Himaman W, Jangsantear P, Samson RA, Luangsa-Ard JJ (2019) Resurrection of *Paraisaria* in the Ophiocordycipitaceae with three new species from Thailand. *Mycological Progress* 18(9): 1213–1230. <https://doi.org/10.1007/s11557-019-01518-x>
- Mongkolsamrit S, Noisriboom W, Pumiputikul S, Boonlarppradab C, Samson RA, Stadler M, Becker K, Luangsa-Ard JJ (2021) *Ophiocordyceps flavida* sp. nov. (Ophiocordycipitaceae), a new species from Thailand associated with *Pseudogibbellula formicarum*

- (Cordycipitaceae), and their bioactive secondary metabolites. *Mycological Progress* 20(4): 477–492. <https://doi.org/10.1007/s11557-021-01683-y>
- Mongkolsamrit S, Noisriboom W, Tasanathai K, Kobmoo N, Thanakitpipattana D, Khonsanit A, Petcharad B, Sakolrak B, Himaman W (2022) Comprehensive treatise of *Hevansia* and three new genera *Jenniferia*, *Parahevansia* and *Polystromomyces* on spiders in Cordycipitaceae from Thailand. *MycKeys* 91: 113–149. <https://doi.org/10.3897/mycokeys.91.83091>
- Mongkolsamrit S, Noisriboom W, Hasin S, Sinchu P, Jangsantear P, Luangsa-Ard JJ (2023) Multi-gene phylogeny and morphology of *Ophiocordyceps laotii* sp. nov. and a new record of *O. buquetii* (Ophiocordycipitaceae, Hypocreales) on ants from Thailand. *Mycological Progress* 22(1): 1–5. <https://doi.org/10.1007/s11557-022-01855-4>
- Nuin P (2007) MrMTgui. v 1.0. MrModelTest/ModelTest Graphical interface for Windows/Linux.
- Nylander JAA (2004) MrModeltest Version 2. Program distributed by the author. <https://github.com/nylander/MrModeltest2>
- Perdomo H, Cano J, Gené J, Garcia D, Hernández M, Guarro J (2013) Polyphasic analysis of *Purpureocillium lilacinum* isolates from different origins and proposal of the new species *Purpureocillium lavendulum*. *Mycologia* 105(1): 151–161. <https://doi.org/10.3852/11-190>
- Petch T (1931) Notes on entomogenous fungi. *Transactions of the British Mycological Society* 16(1): 55–75. [https://doi.org/10.1016/S0007-1536\(31\)80006-3](https://doi.org/10.1016/S0007-1536(31)80006-3)
- Qu JJ, Zou X, Cao W, Xu ZS, Liang ZQ (2021) Two new species of *Hirsutella* (Ophiocordycipitaceae, Sordariomycetes) that are parasitic on lepidopteran insects from China. *MycKeys* 82: 81–96. <https://doi.org/10.3897/mycokeys.82.66927>
- Quandt CA, Kepler RM, Gams W, Araújo JPM, Ban S, Evans HC, Hughes D, Humber R, Hywel-Jones N, Li ZZ, Luangsa-ard JJ, Rehner SA, Sanjuan T, Sato H, Shrestha B, Sung G-H, Yao Y-J, Zare R, Spatafora JW (2014) Phylogenetic-based nomenclatural proposals for Ophiocordycipitaceae (Hypocreales) with new combinations in *Tolypocladium*. *IMA Fungus* 5(1): 121–134. <https://doi.org/10.5598/imafungus.2014.05.01.12>
- Rambaut A (2016) FigTree version 1.4. 0. <http://tree.bio.ed.ac.uk/software/figtree> [Accessed 11 Sep. 2023]
- Rehner SA, Buckley E (2005) A *Beauveria* phylogeny inferred from nuclear ITS and *EF1- $\alpha$*  sequences: Evidence for cryptic diversification and links to *Cordyceps* teleomorphs. *Mycologia* 97(1): 84–98. <https://doi.org/10.3852/mycologia.97.1.84>
- Sanjuan TI, Franco-Molano AE, Kepler RM, Spatafora JW, Tabima J, Vasco-Palacios AM, Restrepo S (2015) Five new species of entomopathogenic fungi from the Amazon and evolution of neotropical *Ophiocordyceps*. *Fungal Biology* 119(10): 901–916. <https://doi.org/10.1016/j.funbio.2015.06.010>
- Schoch CL, Seifert KA, Huhndorf S, Robert V, Spouge JL, Levesque CA, Chen W, Consortium FB, List FBCA, Bolchacova E (2012) Nuclear ribosomal internal transcribed spacer (ITS) region as a universal DNA barcode marker for Fungi. *Proceedings of the National Academy of Sciences of the United States of America* 109(16): 6241–6246. <https://doi.org/10.1073/pnas.1117018109>
- Simmons DR, Kepler RM, Renner SA, Groden E (2015) Phylogeny of *Hirsutella* species (Ophiocordycipitaceae) from the USA: Remediating the paucity of *Hirsutella* sequence data. *IMA Fungus* 6(2): 345–356. <https://doi.org/10.5598/imafungus.2015.06.02.06>
- Spatafora JW, Sung GH, Sung JM, Hywel-Jones NL, White Jr JF (2007) Phylogenetic evidence for an animal pathogen origin of ergot and the grass endophytes. *Molecular Ecology* 16(8): 1701–1711. <https://doi.org/10.1111/j.1365-294X.2007.03225.x>

- Spatafora JW, Quandt CA, Kepler RM, Sung G-H, Shrestha B, Hywel-Jones NL, Luangsa-Ard JJ (2015) New 1F1N species combinations in Ophiocordycipitaceae (Hypocreales). *IMA Fungus* 6(2): 357–362. <https://doi.org/10.5598/imafungus.2015.06.02.07>
- Sung G-H, Spatafora JW, Zare R, Hodge KT, Gams W (2001) A revision of *Verticillium* sect. *Prostrata*. II. Phylogenetic analyses of SSU and LSU nuclear rDNA sequences from anamorphs and teleomorphs of the Clavicipitaceae. *Nova Hedwigia* 72(3–4): 311–328. <https://doi.org/10.1127/nova.hedwigia/72/2001/311>
- Sung G-H, Hywel-Jones NL, Sung J-M, Luangsa-Ard JJ, Shrestha B, Spatafora JW (2007) Phylogenetic classification of *Cordyceps* and the clavicipitaceous fungi. *Studies in Mycology* 57: 5–59. <https://doi.org/10.3114/sim.2007.57.01>
- Tang DX, Zhu J, Luo L, Hou D, Wang Z, Yang S, Yu H (2022) *Ophiocordyceps ovatospora* sp. nov. (Ophiocordycipitaceae, Hypocreales), pathogenic on termites from China. *Phytotaxa* 574(1): 105–117. <https://doi.org/10.11646/phytotaxa.574.1.8>
- Tang DX, Huang O, Zou W, Wang Y, Wang Y, Dong Q, Sun T, Yang G, Yu H (2023a) Six new species of zombie-ant fungi from Yunnan in China. *IMA Fungus* 14(1): 1–9. <https://doi.org/10.1186/s43008-023-00114-9>
- Tang DX, Xu Z, Wang Y, Wang Y, Tran N-L, Yu H (2023b) Multigene phylogeny and morphology reveal two novel zombie-ant fungi in *Ophiocordyceps* (Ophiocordycipitaceae, Hypocreales). *Mycological Progress* 22(4): 1–22. <https://doi.org/10.1007/s11557-023-01874-9>
- Tasanathai K, Thanakitpipattana D, Noisripoom W, Khonsanit A, Kumsao J, Luangsa-Ard JJ (2016) Two new *Cordyceps* species from a community forest in Thailand. *Mycological Progress* 15(3): 1–8. <https://doi.org/10.1007/s11557-016-1170-3>
- Tasanathai K, Noisripoom W, Chaitika T, Khonsanit A, Hasin S, Luangsa-Ard JJ (2019) Phylogenetic and morphological classification of *Ophiocordyceps* species on termites from Thailand. *MycKeys* 56: 101–129. <https://doi.org/10.3897/mycokeys.56.37636>
- Tasanathai K, Khonsanit A, Noisripoom W, Kobmoo N, Luangsa-Ard JJ (2022) Hidden species behind *Ophiocordyceps* (Ophiocordycipitaceae, Hypocreales) on termites: Four new species from Thailand. *Mycological Progress* 21(10): 1–86. <https://doi.org/10.1007/s11557-022-01837-6>
- Vaidya G, Lohman DJ, Meier R (2011) SequenceMatrix: Concatenation software for the fast assembly of multi-gene datasets with character set and codon information. *Cladistics* 27(2): 171–180. <https://doi.org/10.1111/j.1096-0031.2010.00329.x>
- Vilgalys R, Hester M (1990) Rapid genetic identification and mapping of enzymatically amplified ribosomal DNA from several *Cryptococcus* species. *Journal of Bacteriology* 172(8): 4238–4246. <https://doi.org/10.1128/jb.172.8.4238-4246.1990>
- Vu D, Groenewald M, De Vries M, Gehrman T, Stielow B, Eberhardt U, Al-Hatmi A, Groenewald JZ, Cardinali G, Houbraeken J, Boekhout T, Crous PW, Robert V, Verkley GJM (2019) Large-scale generation and analysis of filamentous fungal DNA barcodes boosts coverage for kingdom fungi and reveals thresholds for fungal species and higher taxon delimitation. *Studies in Mycology* 92(1): 135–154. <https://doi.org/10.1016/j.simyco.2018.05.001>
- Wang L, Li HH, Chen YQ, Zhang WM, Qu LH (2014) *Polycephalomyces lianzhouensis* sp. nov., a new species, co-occurs with *Ophiocordyceps crinalis*. *Mycological Progress* 13(4): 1089–1096. <https://doi.org/10.1007/s11557-014-0996-9>
- Wang YB, Wang Y, Fan Q, Duan DE, Zhang GD, Dai RQ, Dai YD, Zeng WB, Chen ZH, Li DD, Tang DX, Xu ZH, Sun T, Nguyen TT, Tran NL, Dao VM, Zhang CM, Huang LD, Liu YJ, Zhang XM, Yang DR, Sanjuan T, Liu XZ, Yang ZL, Yu H (2020) Multigene phylogeny of the family Cordycipitaceae (Hypocreales): New taxa and the new systematic position

- of the Chinese cordycipitoid fungus *Paecilomyces hepiali*. *Fungal Diversity* 103(1): 1–46. <https://doi.org/10.1007/s13225-020-00457-3>
- Wei DP, Wanasinghe DN, Gentekaki E, Thiyagaraja V, Lumyong S, Hyde KD (2021a) Morphological and phylogenetic appraisal of novel and extant taxa of Stictidaceae from Northern Thailand. *Journal of Fungi* 7(10): e880. <https://doi.org/10.3390/jof7100880>
- Wei DP, Wanasinghe DN, Xu JC, To-Anun C, Mortimer PE, Hyde KD, Elgorban AM, Madawala S, Suwannarach N, Karunarathna SC, Tibpromma S, Lumyong S (2021b) Three novel entomopathogenic fungi from China and Thailand. *Frontiers in Microbiology* 11: e608991. <https://doi.org/10.3389/fmicb.2020.608991>
- Wei DP, Gentekaki E, Wanasinghe DN, Tang SM, Hyde KD (2022) Diversity, molecular dating and ancestral characters state reconstruction of entomopathogenic fungi in Hypocreales. *Mycosphere* 13(1): 281–351. <https://doi.org/10.5943/mycosphere/si/1f/8>
- Wen TC, Xiao YP, Zha LS, Hyde KD, Kang JC (2016) Multigene phylogeny and morphology reveal a new species, *Ophiocordyceps tettigonia*, from Guizhou Province, China. *Phytotaxa* 280: 141–151. <https://doi.org/10.11646/phytotaxa.280.2.4>
- White TJ, Bruns T, Lee S, Taylor J (1990) Amplification and direct sequencing of fungal ribosomal RNA genes for phylogenetics. *PCR protocols: a guide to methods and applications* 18: 315–322. <https://doi.org/10.1016/B978-0-12-372180-8.50042-1>
- Xiao YP, Hongsanan S, Hyde KD, Brooks S, Xie N, Long FY, Wen TC (2019) Two new entomopathogenic species of *Ophiocordyceps* in Thailand. *MycKeys* 47: 53–74. <https://doi.org/10.3897/mycokeys.47.29898>
- Xiao YP, Wang YB, Hyde KD, Eleni G, Sun JZ, Yang Y, Meng J, Yu H, Wen TC (2023) Polycephalomycetaceae, a new family of clavicipitoid fungi segregates from Ophiocordycipitaceae. *Fungal Diversity* 120(1): 1–76. <https://doi.org/10.1007/s13225-023-00517-4>
- Yamamoto K, Sugawa G, Takeda K, Degawa Y (2022) *Tolypocladium bacillisporum* (Ophiocordycipitaceae): A new parasite of *Elaphomyces* from Japan. *Truffology* 5: 15–21.
- Yang Y, Xiao YP, Yu GJ, Wen TC, Deng CY, Meng J, Lu ZH (2021) *Ophiocordyceps saphrophoridarum* sp. nov., a new entomopathogenic species from Guizhou, China. *Biodiversity Data Journal* 9: e66115. <https://doi.org/10.3897/BDJ.9.e66115>
- Yeh YW, Huang Y-M, Hsieh C-M, Kirschner R (2021) *Pleurodesmospora acaricola* sp. nov. and a new record of *Pleurodesmospora coccorum* (Cordycipitaceae, Ascomycota) in Taiwan. *Taiwania* 66. <https://doi.org/10.6165/tai.2021.66.517>
- Yu Y, Hou SY, Sun ZL, Zhang MY, Zhang TY, Zhang YX (2018) *Drechmeria panacis* sp. nov., an endophyte isolated from *Panax notoginseng*. *International Journal of Systematic and Evolutionary Microbiology* 68(10): 3255–3259. <https://doi.org/10.1099/ijsem.0.002971>
- Yu FM, Chethana KWT, Wei DP, Liu JW, Zhao Q, Tang SM, Li L, Hyde KD (2021) Comprehensive review of *Tolypocladium* and description of a novel lineage from Southwest China. *Pathogens* 10(11): e1389. <https://doi.org/10.3390/pathogens10111389>
- Zou X, Zhou JX, Liang ZQ, Han YF (2016) *Hirsutella shennongjiaensis*, a new entomopathogenic species infecting earwig Dermaptera. *Mycosystem* 35: 1070–1079.
- Zou WQ, Tang DX, Xu ZH, Huang O, Wang YB, Tran NL, Yu H (2022) Multigene phylogeny and morphology reveal *Ophiocordyceps hydrangea* sp. nov. and *Ophiocordyceps bidouensis* sp. nov. (Ophiocordycipitaceae). *MycKeys* 92: 109–130. <https://doi.org/10.3897/mycokeys.92.86160>

# Morphological and molecular analyses reveal two new species of *Grifola* (Polyporales) from Yunnan, China

Song-Ming Tang<sup>1\*</sup>, De-Chao Chen<sup>1,2\*</sup>, Shuai Wang<sup>1,2</sup>, Xiao-Qu Wu<sup>1,2</sup>, Cheng-Ce Ao<sup>1,3</sup>, Er-Xian Li<sup>1</sup>, Hong-Mei Luo<sup>1</sup>, Shu-Hong Li<sup>1</sup>

<sup>1</sup> Biotechnology and Germplasm Resources Institute, Yunnan Academy of Agricultural Sciences, Kunming 650205, China

<sup>2</sup> School of Agriculture, Yunnan University, Kunming 650504, China

<sup>3</sup> College of Agriculture and Biological Science, Dali University, Dali 671003, China

Corresponding author: Shu-Hong Li (shuhongfungji@126.com)

## Abstract

Species of *Grifola* are famous edible mushrooms and are deeply loved by consumers around the world. Most species of this genus have been described and recorded in Oceania, Europe and South America, with only *Grifola frondosa* being recorded in Asia. In this study, two novel species of *Grifola* from southwestern China (Asia) are introduced. Macro and micromorphological characters are described. *Grifola edulis* **sp. nov.** present medium-size basidiomata with gray to gray-brown lobes upper surface, mostly tibiiform or narrowly clavate, rarely narrowly lageniform or ellipsoid chlamydospores, cuticle hyphae terminal segments slightly enlarged. *Grifola sinensis* **sp. nov.** has white to grayish white lobes upper surface, mostly ellipsoid, rarely narrowly utriform chlamydospores, and broadly ellipsoid to ellipsoid basidiospores (4.6–7.9 × 3.0–5.9 μm). The two new species are supported by phylogenetic analyses of combined nuclear rDNA internal transcribed spacer ITS1-5.8S-ITS2 rDNA (ITS) and β-tubulin (*TUBB*). Moreover, the genetic distance between *TUBB* sequences of those specimen from GenBank was 1.76–1.9%. Thus, the conspecificity relationship of our specimens remains uncertain, and further specimens are required to conclusively confirm its identity.

**Key words:** 2 new species, morphology, multi-gene phylogeny, Southeast Asia, taxonomy, Yunnan



Academic editor: María P. Martín

Received: 10 January 2024

Accepted: 12 February 2024

Published: 29 February 2024

**Citation:** Tang S-M, Chen D-C, Wang S, Wu X-Q, Ao C-C, Li E-X, Luo H-M, Li S-H (2024) Morphological and molecular analyses reveal two new species of *Grifola* (Polyporales) from Yunnan, China. MycoKeys 102: 267–284. <https://doi.org/10.3897/mycokeys.102.118518>

Copyright: © Song-Ming Tang et al.

This is an open access article distributed under terms of the CC0 Public Domain Dedication.

## Introduction

*Grifola* Gray (1821) was established based on the type species, *G. frondosa* (Dicks.) Gray (Gray 1821). *Grifola* species are characterized by their compound basidiomata developing on the ground from roots at the base of trees or stumps and causing white-rot (Gray 1821; Rajchenberg 2002; Ryvarden and Melo 2014). The genus presents monomitic or dimitic hyphal system with clamped generative hyphae, basidiospores ovoid to ellipsoid, inamyloid, and abundant chlamydospores in culture (Rugolo et al. 2023).

To date, six species of *Grifola* have been described worldwide, of which two reported from North Hemisphere (*G. frondosa* (Dicks.) Gray is widely distributed

\* These authors contributed equally as first authors to this work.

in Asia, North America and Europe (Rajchenberg 2002) and *G. amazonica* Ryvarden is only known from Brazil (Ryvarden 2004)), four species reported from South Hemisphere (*G. sordulenta* (Mont.) Singer from Argentina, Chile, New Zealand and Patagonia, *G. colensoi* (Berk.) G. Cunn. from Australia and New Zealand, *G. gargal* Singer from Argentina and Chile and *G. odorata* Hood, M. Rugolo & Rajchenb. from New Zealand) (Cunningham 1948; Singer 1962; Cunningham 1965; Singer 1969; Buchanan and Ryvarden 2000; Rajchenberg 2006; Rugolo et al. 2022; Rugolo et al. 2023).

*Grifola* species were formerly placed in several different genera, including *Boletus* (Dickson 1785), *Polyporus* (Hooker 1855), *Cautinia* (Maas Geesteranus 1967) and *Hydnum* (Bresadola 1925). In 1821, *Grifola* was erected with the introduction of six new species (Gray 1821), but later, only two species, *G. frondosa* and *G. platypora* Gray, have been accepted (Rugolo et al. 2023), four species have been recombined into different genera as synonyms, *Grifola varia* (Pers.) Gray as *Cerioporus varius* (Pers.) Zmitr. & Kovalenko (Zmitrovich and Kovalenko 2016), *Grifola lucida* (Curtis) Gray as *Ganoderma lucidum* (Curtis) P. Karst. synonyms (Karsten 1881), *Grifola cristata* (Schaeff.) Gray as *Laeticutis cristata* (Schaeff.) Audet synonyms (Audet 2010), *Grifola badia* (Pers.) Gray as *Picipes badius* (Oer.) Zmitr. & Kovalenko synonyms (Zmitrovich and Kovalenko 2016).

*Grifola frondosa* is an edible mushroom cultivated in different countries, known as “hen of the woods” or “maitake”. It is reported for producing anti-diabetic (n-hexane extract, glycoprotein, and ergosterol peroxide (Konno et al. 2013; Shen et al. 2015; He et al. 2016); anti-tumor (glycoprotein, water soluble extract (Shomori et al. 2009; Cui et al. 2013), anti-virus (protein, Gu et al. 2007) and antioxidant (protein and ergosterol, ergostra-4, 6, 8 (14), 22-tetraen-3-one, and 1-oleoyl-2-linoleoyl-3-palmitoylglycerol (Zhang et al. 2002)) compounds.

Recently, molecular phylogenetic approaches have increasingly been applied to investigate phylogenetic relationships among genera and species of Polyporales (Justo and Hibbett 2011; Justo et al. 2017). Through these studies, *Grifola* is strongly supported as Grifolaceae, with close relationship to the Polyporaceae (Justo and Hibbett 2011; Justo et al. 2017).

For the past 50 years, *Grifola* species have been described based only on morphological characteristics, until the advent of molecular phylogeny. Rugolo et al. (2023) provided molecular markers (ITS and *TUBB*), bringing more evidence for the classification of *Grifola* species.

During investigations on *Grifola* across southwestern China, several *Grifola* collections were made. Amongst them, two *Grifola* species from Yunnan, China, are newly described herein. In addition to the morphological descriptions and illustrations, molecular phylogenetic analyses based on the ITS1-5.8S-ITS2, and *TUBB* supported the two new species.

## Materials and methods

### Morphological studies

Macro-morphological characteristics and habitat descriptions were gathered from photographs and field notes. Color codes were assigned according to Kornerup and Wanscher's (1978). After recording the macromorphological characteristics, specimens were subjected to drying at 40 °C in a food dehydrator until all moisture

was eliminated. The dried specimens were then stored in sealed plastic bags. In the microscopic study, dried mushroom materials were sliced and placed in a 5% KOH solution and 1% Congo red for mounting. Microscopic features such as basidia, basidiospores, and cystidia were examined and photographed using a light microscope (Nikon Eclipse 80i) equipped for the purpose. In the descriptions of microscopic characters, measurements were conducted on 60–100 basidiospores and 20 basidia randomly selected. The notation [x/y/z] indicates x basidiospores measured from y basidiomata of z collections. Basidiospore dimensions are denoted as (a–) b–c (–d), where the range b–c represents 95% of the measured values, and “a” and “d” are extreme values. Q refers to the length/width ratio of individual basidiospores, while  $Q_m$  refers to the average Q value  $\pm$  standard deviation. Specimens of the two newly discovered *Grifola* species were stored at the herbarium of the Kunming Institute of Botany, Chinese Academy of Sciences (KUN-HKAS).

### DNA extraction, PCR amplification and sequencing

Genomic DNA extraction from dry specimens was performed using the Ezup Column Fungi Genomic DNA Extraction Kit (Genesand Biotech Co., Ltd, China, Beijing), following the manufacturer’s protocol. Subsequent steps included PCR amplification, purification of PCR products, and sequencing. The primers used for *TUBB* amplification were BTG3F and BTG5G (Shen et al. 2002). The ITS gene region was amplified using the primers ITS4 and ITS5, ITS2 and ITS3 (White and Hedenquist 1990).

### Sequence alignment and phylogenetic analyses

The sequences of *Grifola* species obtained in this study, along with sequences retrieved from GenBank (refer to Table 1), were aligned using MAFFT version 7 (Katoch and Standley 2013) and verified in BioEdit version 7.0.5 (Hall 2007). Consistent with previous phylogenetic investigations, *Polyporus umbellatus* (Pers.) Fr. and *P. squamosus* P.K. Buchanan & Ryvarden were employed as outgroup taxa (Shen et al. 2002).

Phylogenies and node support were initially deduced through Maximum Likelihood (ML) using RAxML-HPC2 version 8.2.12 (Stamatakis 2014). This process involved separate analyses of the three single-gene alignments, with 1,000 rapid bootstraps, and was executed on the Cipres portal (Miller et al. 2010). Since there was no identified conflict with substantial support (bootstrap support value (BS)  $\geq$  70%) among the topologies, the three single-gene alignments were concatenated using SequenceMatrix (Vaidya et al. 2011). For partitioned Maximum Likelihood (ML) the concatenated dataset was analyzed, following the previously mentioned procedure. In the case of Bayesian Inference (BI), the optimal substitution model for each character set was identified using the program MrModeltest 2.3 (Nylander et al. 2004) on the CIPRES platform. The selected models were K80+I for 5.8S, TIM1ef+G for ITS1+ITS2, JC+I+G for *TUBB* exon, F81+G for *TUBB* intron. Bayesian analysis was performed using MrBayes version 3.2.7a (Ronquist et al. 2011) as implemented on the Cipres portal (Miller et al. 2010); two runs of six chains each were conducted by setting generations to 800,000 and stoprul command with the stopval set to 0.01, and trees sampled every 200 generations. A clade was considered to be strongly supported if showing a BS  $\geq$  70% and a posterior probability (PP)  $\geq$  0.90. The alignment was submitted to Figshare (10.6084/m9.figshare.24923559).

**Table 1.** Names, specimen vouchers, origin, and corresponding GenBank accession numbers of the sequences used in this study. New taxa are in bold; “\*” following a species name indicates that the specimen is the type of that species and “N/A” refers to the unavailability of data.

Taxon	Voucher specimen	Origin	Host	GenBank accession no.		Reference
				ITS	TUBB	
<i>Grifola colensoi</i>	MEL 2320791	Australia	<i>Eucalyptus</i>	OP168968	N/A	Rugolo et al. 2023
	MEL 2106744	Australia	<i>Lophozonia Cunninghamsii</i>	OP168967	N/A	Rugolo et al. 2023
<b><i>G. edulis</i></b>	<b>HKAS 131996*</b>	<b>China</b>	<b><i>Lithocarpus corneus</i></b>	<b>PP079954</b>	<b>PP097725</b>	<b>This study</b>
	<b>HKAS 131997</b>	<b>China</b>	<b><i>Lithocarpus corneus</i></b>	<b>PP079955</b>	<b>PP097726</b>	<b>This study</b>
<i>G. gargal</i>	CIEFAPcc-700	Argentina	<i>Lophozonia obliqua</i>	OP168980	OP455971	Rugolo et al. 2023
	CIEFAPcc-327	Argentina	<i>Populus nigra</i>	OP168991	N/A	Rugolo et al. 2023
	HCFC 3143	Argentina	<i>Lophozonia alpina</i>	OP168989	OP455976	Rugolo et al. 2023
	SGO 092562*	Chile	N/A	N/A	OP455979	Rugolo et al. 2023
<i>G. odorata</i>	NZFRIM 1676*	New Zealand	<i>Podocarpus</i> sp.	OP168994	N/A	Rugolo et al. 2023
	PDD 86931	New Zealand	<i>Fuscospora solandri</i>	GU222266	OP455985	Rugolo et al. 2023
<b><i>G. sinensis</i></b>	<b>HKAS 131995*</b>	<b>China</b>	<b><i>Lithocarpus corneus</i></b>	<b>PP079956</b>	<b>PP097727</b>	<b>This study</b>
	<b>HKAS 131998</b>	<b>China</b>	<b><i>Lithocarpus corneus</i></b>	<b>PP079957</b>	<b>PP097728</b>	<b>This study</b>
	<b>HKAS 131994</b>	<b>China</b>	<b><i>Lithocarpus corneus</i></b>	<b>PP079958</b>	<b>PP097729</b>	<b>This study</b>
<i>G. sordulenta</i>	CIEFAPcc-699	Argentina	<i>Nothofagus dombeyi</i>	OP168974	N/A	Rugolo et al. 2023
	CIEFAPcc-280	Argentina	<i>Nothofagus dombeyi</i>	OP168973	OP455969	Rugolo et al. 2023
<i>G. frondosa</i>	WC493	Norway	<i>Quercus robur</i>	AY049128	AY049180	Shen et al. 2002
<i>Polyporus umbellatus</i>	Pen13513	China	N/A	KU189772	KU189862	Zhou et al. 2016
<i>P. squamosus</i>	Cui 10595	China	N/A	KU189778	KU189868	Zhou et al. 2016

## Results

### Phylogenetic analyses

A total of 10 newly generated sequences and 16 sequences from GenBank were used as ingroup. Four sequences of *Polyporus umbellatus* and *P. squamosus* retrieved from GenBank were used as outgroup. The alignments of the 5.8S, ITS1+ITS2, TUBB exon and TUBB intron sequences were 158, 396, 404, and 180 characters long after trimming, respectively. The combined data set had an aligned length of 1,138 characters, of which 721 characters were constant, 417 were variable but parsimony-uninformative, and 288 were parsimony-informative.

ML and BI analyses generated nearly identical tree topologies with little variation in statistical support. Therefore, only the ML tree is displayed (Fig. 1). Phylogenetic data together with thorough morphological analysis (see below) showed that the two newly described taxa in this study are significantly different from other known *Grifola* species.

### Taxonomy

#### ***Grifola edulis* S.M. Tang & S.H Li, sp. nov.**

MycoBank No: 851587

Figs 2–4, 10A, B

**Etymology.** The epithet “*edulis*” refers to the edibility of this species, locally considered a delicacy.

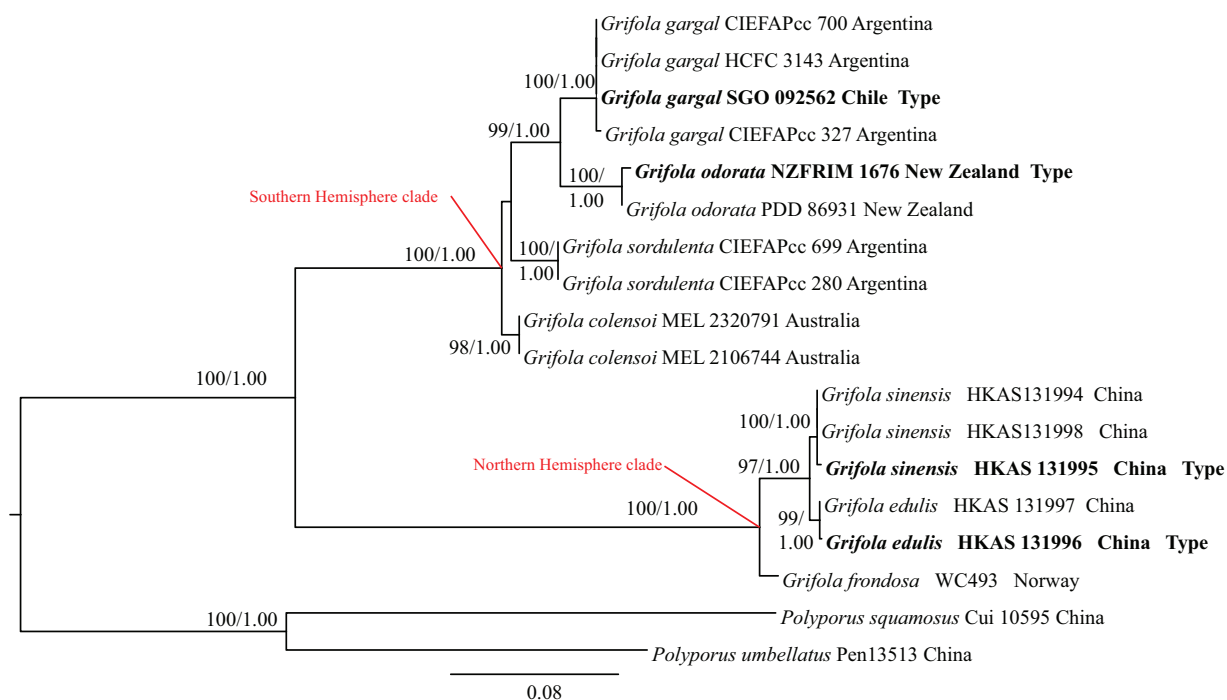


**Figure 1.** Strict consensus tree illustrating the phylogeny based on the combined 5.8S, ITS1+ITS2, *TUBB* exon and *TUBB* intron data set. Maximum likelihood bootstrap proportions equal to or higher than 70%, and Bayesian posterior probabilities equal to or higher than 0.90 are indicated at nodes. The two *Polyporus* species were used as the outgroup. Holotype specimens are in bold.

**Holotype.** CHINA. Yunnan province: Nujiang prefecture, Liuku town, elev. 2,300 m, 8 September 2019, Shu-Hong Li, L5366 (**holotype**:HKAS 131996!).

**Diagnosis.** Differs from other *Grifola* species in having variable and longer chlamydospores (13–) 22–94 (–115) × 7–12 μm, av. 49.8 ± 28.5 × 9.4 ± 1.4 μm, medium-sized basidiomata 12 × 10 × 18 cm, and growing at the base of *Lithocarpus corneus*.

**Description.** Basidiomata medium-sized, developing a fruiting structure composed of multiple flattened lobes that emanate from a central base, up to 12 × 10 × 18 cm. Lobes 5–7 cm wide, 8–10 cm long, upper surface gray to gray-brown, lower surface white. Thin cuticle. Context white, 0.5–1 mm. Pores are sizable and often have a convoluted, maze-like appearance, 2–4 per mm, tube layer 2–3 mm deep. Texture fleshy to cartilaginous, becoming hard and woody upon drying, emitting a pronounced almond scent when fresh or dry.

Skeletal hyphae with repent and abundant suberect, thin, aligned parallel longitudinal alone lobe, non-staining in IKI– and 5% NaOH solution, hyphae 5–7 μm wide, terminal slightly enlarged, hyphae 8–10 μm wide. Pores edge heteromorphous, more in number of parallel hyphae, thin-walled, colorless in 5% NaOH solution, 2–4 μm wide; pores trama regular, parallel, 80–120 μm wide, made up of thin-walled, cylindrical hyphae, 2–5 μm wide.

Basidia 17–29 × 5–7 μm, av. 24.6 ± 4.7 × 6.5 ± 0.5 μm, clavate, thin-walled, mostly 4-spored, rarely 2-spored; sterigmata 2–5 μm long. Basidiospores [100/2/2] (3.7–) 4.4–6.8 × 2.5–5.6 μm, av. 5.5 ± 0.5 × 4.1 ± 0.5 μm, Q = 1.1–1.8 (–2.2), Q<sub>m</sub> = 1.40 ± 0.18, broadly ellipsoid to ellipsoid, colorless in IKI– and 5% NaOH solution, thin-walled, irregular ornamented (Fig. 10); basidiospores scatter plot see Fig. 5.



**Figure 2.** Fresh basidiomata of *Grifola edulis* (holotype HKAS131996) **A** wild basidiomata **B–D** cultivated basidiomata **E** view of pores by stereoscope **F** side view of pore zone and context by stereoscope. Photographs by Song-Ming Tang. Scale bars: 1 cm (**A–D**); 1 mm (**E, F**).

Culture feature (Fig. 4). Colony regular, circular, greenish gray (1B2) to grayish yellow (1B3); reverse pale yellow (1A3). Dimitic hyphal system, generative hyphae rarely branched. Texture sub felty and farinaceous. Growth slow, 4 cm in 3 weeks, on Potato Dextrose Agar with Chloramphenicol and 24 °C. Mycelium with no distinctive odor, hyphae clamped, thin-walled, and colorless in 5% NaOH solution, 3–6  $\mu\text{m}$  wide. Chlamydospores terminal or intercalary, irregularly, thin-walled, mostly tibiiform or narrowly clavate, rarely narrowly lageniform or ellipsoid, (13–) 22–94 (–115)  $\times$  7–12  $\mu\text{m}$ , av.  $49.8 \pm 28.5 \times 9.4 \pm 1.4 \mu\text{m}$ ,  $Q = 1.4\text{--}8.3$  (–15.9),  $Q_m = 5.4 \pm 3.5$ , colorless in 5% NaOH solution.

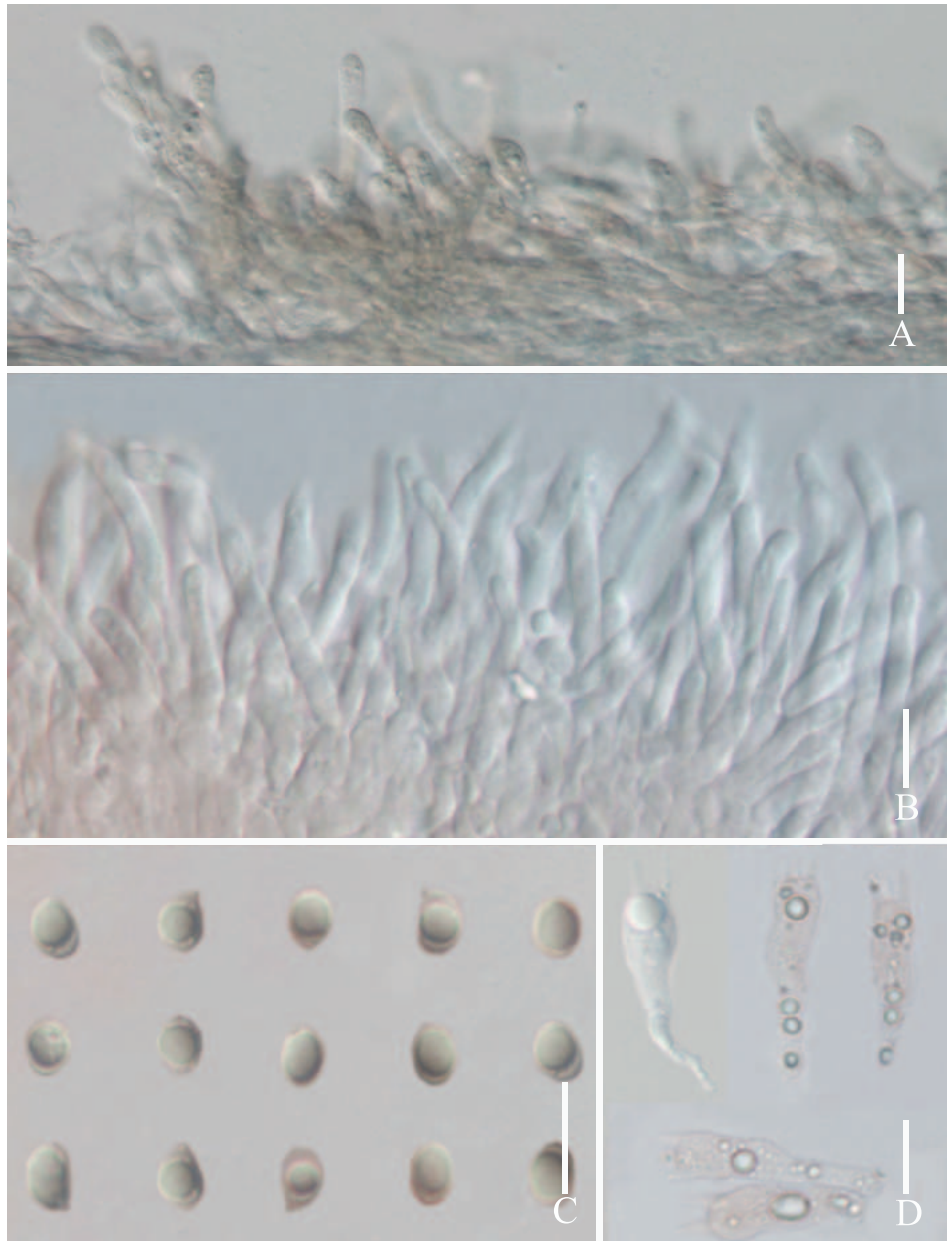


**Figure 3.** Micromorphological features of *Grifola edulis* (holotype HKAS131996) **A** cuticle hyphae **B** pore edge **C** basidiospores **D** basidia. Photographs by Song-Ming Tang. Scale bars: 10  $\mu$ m.

**Habitat and distribution.** *Grifola edulis* occurs in native forests in Yunnan, on *Lithocarpus corneus* at the base of trees, producing an aromatic white rot.

**Edibility.** This mushroom is highly appreciated by local communities.

**Additional material examined.** CHINA. Yunnan province: Lushui city, Laowo town, altitude 1,755 m, 12 August 2020, Shu-Hong Li, HKAS 131997.

**Notes.** *Grifola edulis* is close to *G. frondosa* and *G. amazonica*, until now the only species that have been described and recorded from the Northern Hemisphere (Shen et al. 2002; Rugolo et al. 2023). However, in *G. frondosa*, lobes' upper surface is gray to brown tomentose, basidiospores 5.5–6.5  $\times$  3.5–4.5  $\mu$ m, fruiting bodies occur from September to October, growing on *Quercus*, *Castanea*, *Fagus*, and *Carpinus* (Rugolo et al. 2023); *G. edulis* presents lobes' upper surface gray to gray brown, smooth, smaller basidiospores av. 5.5  $\pm$

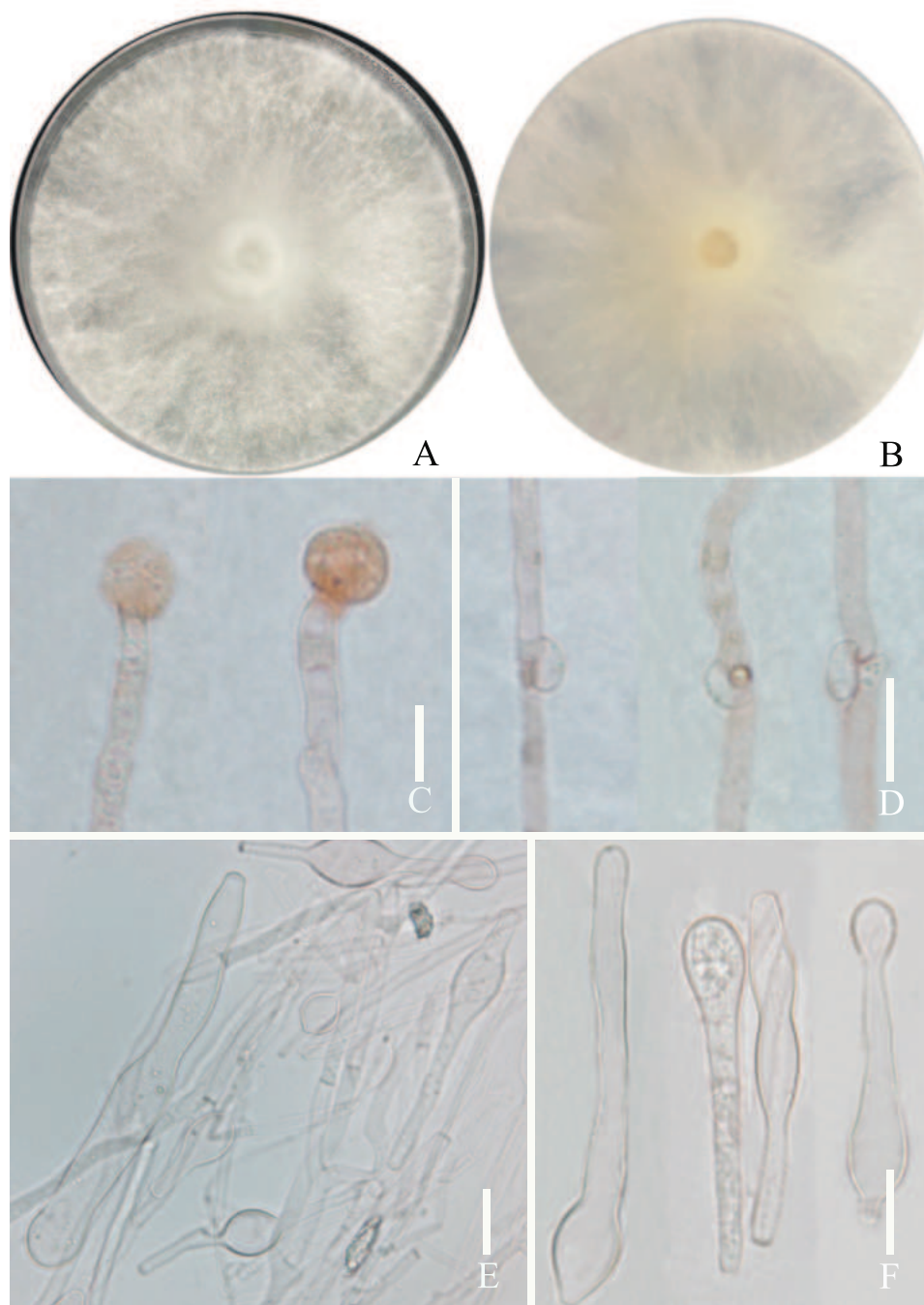


**Figure 4.** *Grifola edulis* culture characters (holotype HKAS131996) **A** colony obverse on PDA **B** colony in reverse **C** terminal chlamydospore **D** clamped generative hyphae **E–F** chlamydospores. Photographs by Song-Ming Tang. Scale bars: 10  $\mu$ m (**C–F**).

0.5  $\times$  4.1  $\pm$  0.5  $\mu$ m, and fruiting bodies occur from August to September, on *Lithocarpus corneus*. *Grifola amazonica* from Brazil, has lobes' upper surface evenly brown, glabrous to smooth, smaller basidiospores 4–4.5  $\times$  3–3.5  $\mu$ m, and pore surface pale grayish brown (Ryvarden 2004).

In our multi-locus phylogeny, *G. frondosa* and *G. sinensis* are sister to the clade of *G. edulis*. Specimen WC493 (from Norway) has the representative sequence for *G. frondosa*, given the original collection of *G. frondosa* in Europe (Britain). The *TUBB* genetic distances between *G. edulis* (holotype HKAS

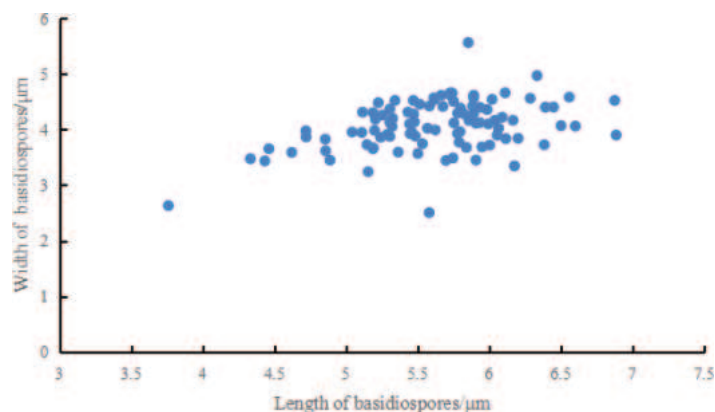


Figure 5. Basidiospores scatter plot of *Grifola edulis*.

131996) and other accessions in the latter clade were 4.50% (26/578) for *Grifola frondosa* (WC493), 1.21% (7/578) for *G. sinensis* (holotype HKAS 131995), thus classifying them as heterospecific.

***Grifola sinensis* S.M. Tang & S.H. Li, sp. nov.**

MycoBank No: 851588

Figs 6–8, 10C, D

**Etymology.** The epithet “sinensis” refers to the country China where this fungus was first discovered.

**Holotype.** CHINA. Yunnan province: Nujiang prefecture, Fugong city, elev. 2,230 m, 8 September 2019, Shu-Hong Li, L5453 (**holotype:** HKAS 131995!).

**Diagnosis.** Differs from other *Grifola* species in having a medium-sized basidiomata, with white to olive yellow lobes, smaller and irregular pore (2–4/mm), and ellipsoid to narrowly utriform chlamydo-spores.

**Description.** Basidiomata medium-sized, developing a fruiting structure composed of multiple flattened lobes that emanate from a central base, up to 10 × 12 × 15 cm. Lobes 4–7 cm wide, 7–10 cm long, lower and upper surface white (1A1) to grayish white (1A2) when young, changing to olive yellow (2C–D7) with age or when soaked. Thin cuticle. Context white, 1–2 mm thick. Pores often with a convoluted, maze-like appearance, 2–4 per mm, tubes 2–3 mm deep. Texture fleshy to cartilaginous, becoming hard and woody upon drying, and emitting a pronounced almond scent when fresh or dry.

Skeletal hyphae aligned parallel longitudinal along lobe, with repent and abundant suberect terminal segments, hyphae thin-walled, non-staining in IKI and 5% NaOH solution, 5–7 μm wide. Pores edge heteromorphous, hyphae thin-walled, colorless in 5% NaOH solution, 2–4 μm wide; trama of tubes regular, parallel, 120–190 μm wide, made up of thin-walled hyphae, 2–5 μm wide.

Basidia 15–28 (–32) × 5–8 μm, av. 23.0 ± 5.4 × 6.7 ± 0.7 μm, clavate, thin-walled, mostly 2-spored, rarely 4-spored; sterigmata 2–5 μm long. Basidiospores [68/2/2] 4.6–7.9 × 3.0–5.9 μm, av. 5.9 ± 0.6 × 4.2 ± 0.5 μm, Q = 1.1–1.6 (–1.8), Q<sub>m</sub> = 1.42 ± 0.15, broadly ellipsoid to ellipsoid, colorless in IKI and 5% NaOH solution, thin-walled, irregular ornamented (Fig. 10); basidiospores scatter plot, see Fig. 9.

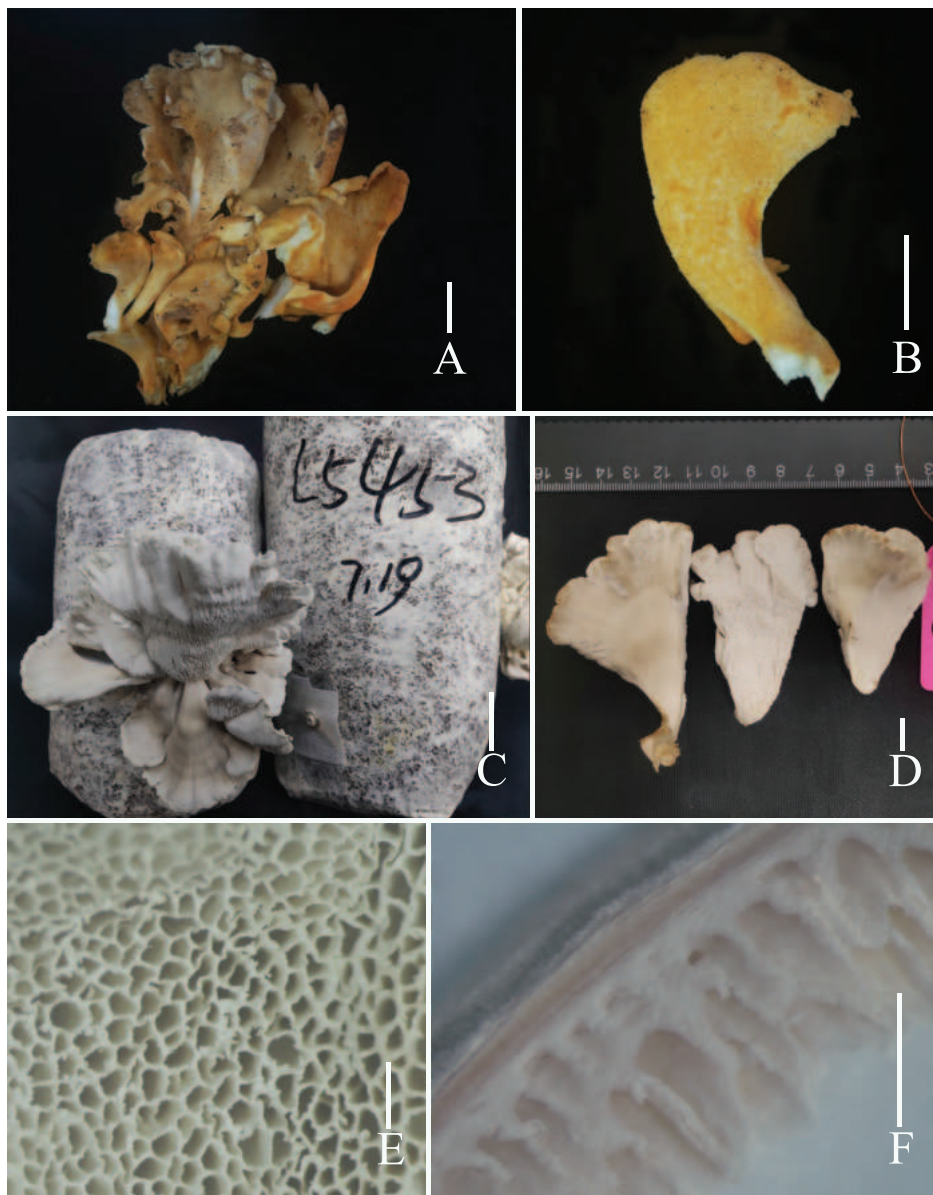


**Figure 6.** Fresh basidiomata of *Grifola sinensis* (holotype HKAS 131995) **A** view of wild basidiomata pilei **B** view of wild basidiomata pores **C, D** cultivated basidiomata **E** view of pores by stereoscope **F** side view of pore zone and context by stereoscope. Photographs by Song-Ming Tang. Scale bars: 1 cm (**A–D**); 1 mm (**E, F**).

Culture feature (Fig. 8). Colony regular, circular, greenish gray (1B2) to grayish yellow (1B3); reverse pale yellow (1A3). Dimitic hyphal system, generative hyphae rarely branched. Texture sub felty and farinaceous. Growth slow, 4 cm in 3 weeks on Potato Dextrose Agar with Chloramphenicol and 24 °C. Mycelium with no distinctive odor, generative hyphae clamped, thin-walled, and colorless in 5% NaOH solution, 3–5 µm wide. Presence of chlamydospores terminal or intercalary, mostly ellipsoid, rarely narrowly utriform, 9.6–16.1 (–21.9) × 7.4–11.9 µm, av. 13.4 ± 2.9 × 9.2 ± 1.2 µm, Q = 1.1–2.0 (–2.9), Q<sub>m</sub> = 1.5 ± 0.5, colorless in 5% NaOH solution, thin-walled. Generative hyphae hyaline, thin walled, clamped, 2.7–4.3 µm, av 3.6 ± 0.6 µm, hyphal endings arranged singly or in groups, with contents stained red in Congo solution.

**Habitat and distribution.** *Grifola sinensis* occurs in native forests in Yunnan, on *Lithocarpus corneus*, at the base of trees, causing an aromatic white rot.

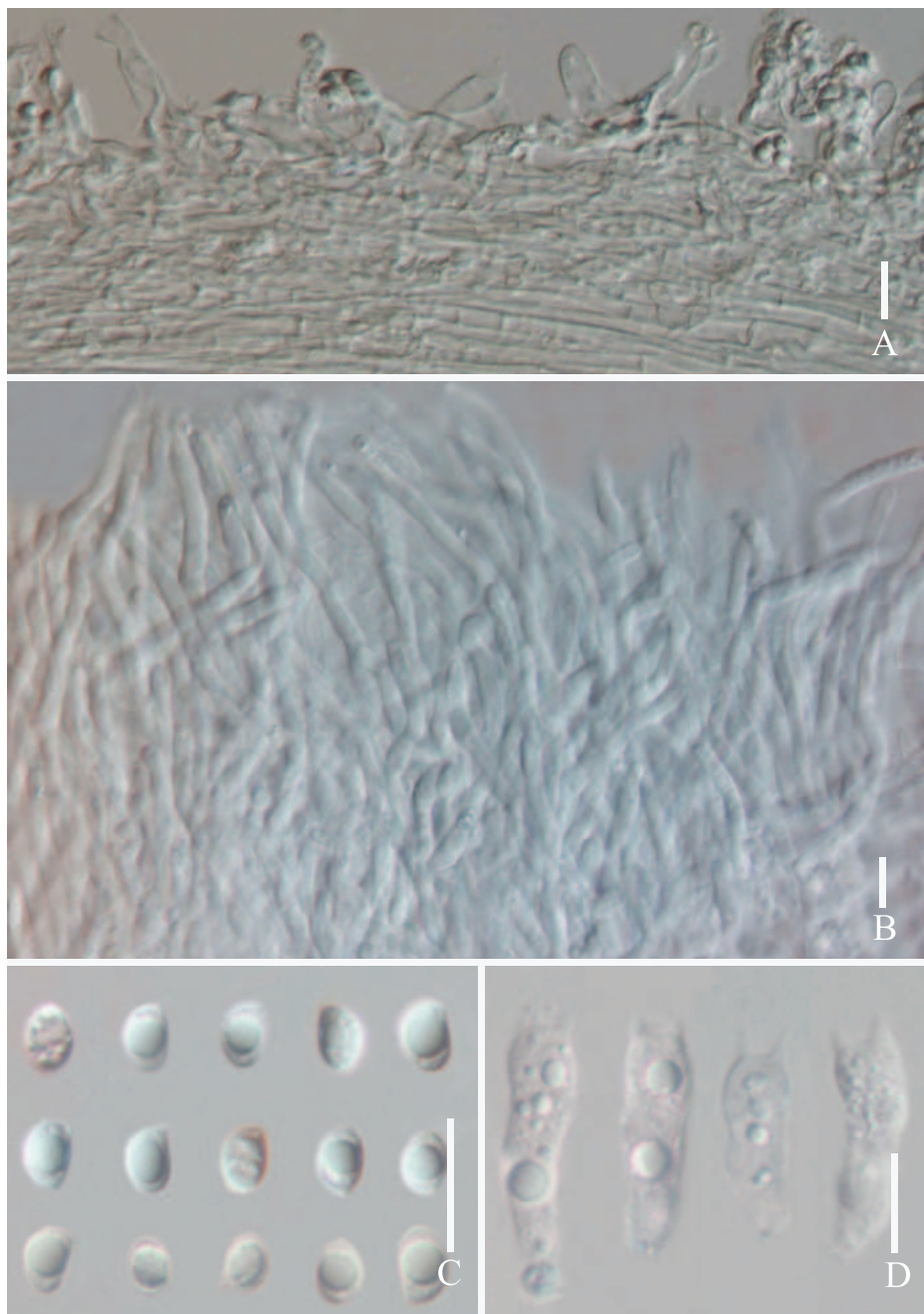


**Figure 7.** Micromorphological features of *Grifola sinensis* (holotype HKAS 131995) **A** cuticle hyphae **B** pore edge **C** basidiospores **D** basidia. Photographs by Song-Ming Tang. Scale bars: 10  $\mu$ m.

**Edibility.** This species is much appreciated by the locals in Yunnan, stir-frying it over high heat with green peppers; it has a robust almond essence that permeates through the palate, accompanied by a hearty, meat-like texture.

**Additional species examined.** CHINA. Yunnan Province, Nujiang prefecture, Fugong city, elev. 2,120 m, 5 September 2019, Shu-Hong Li, HKAS 131998; Nujiang prefecture, Bingzhongluo county, elev. 1,980 m 15 October 2023, Song-Ming Tang, HKAS 131994.

**Notes.** Morphologically, *G. sinensis* is similar to *G. amazonica* Ryvarden in having small irregular pores 2–4/mm. However, *G. amazonica* has evenly brown lobes, smaller basidiospores 4–4.5  $\times$  3–3.5  $\mu$ m, and basidia 12–14  $\times$

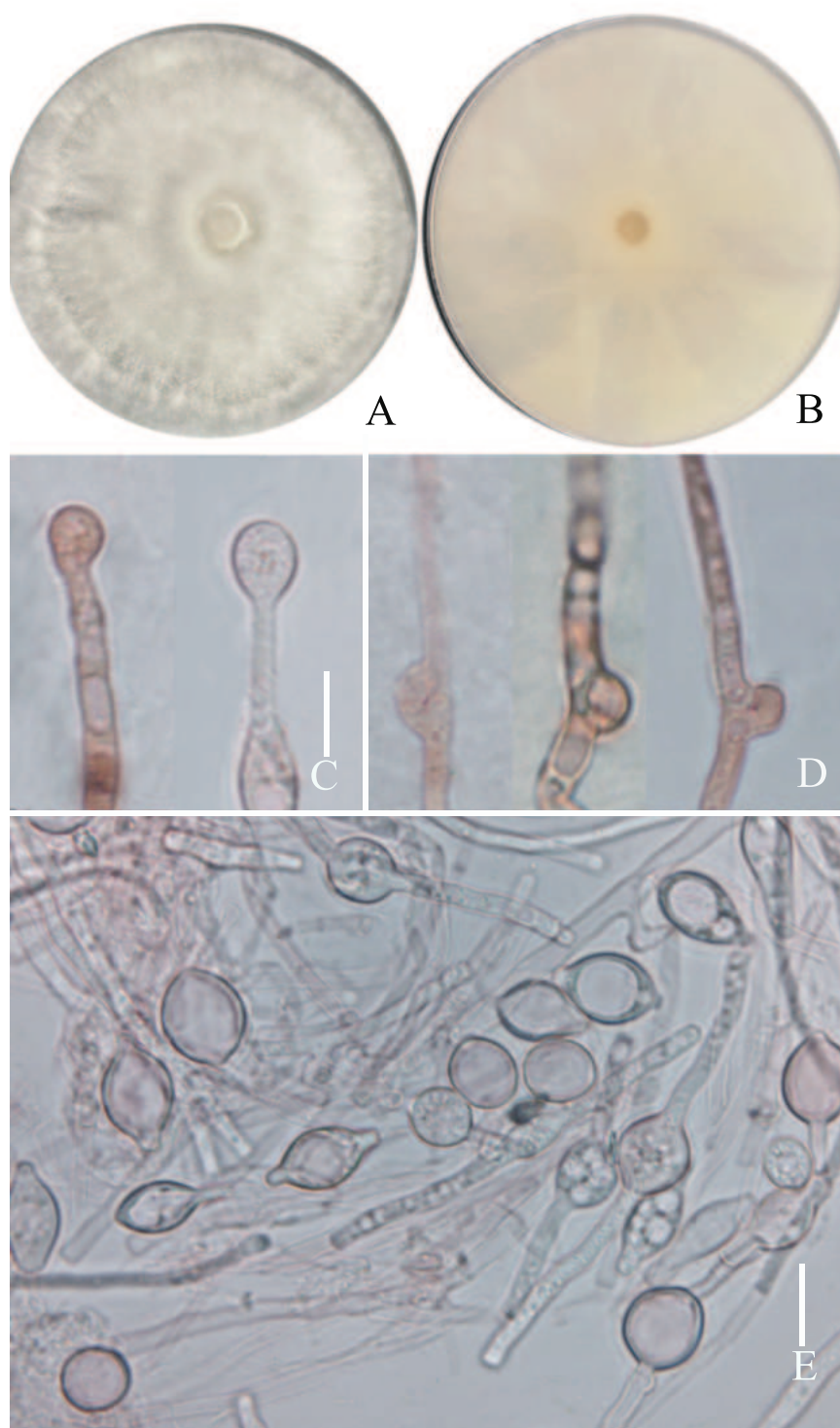


**Figure 8.** *Grifola sinensis* cultures characters (holotype HKAS 131995) **A** colony obverse on PDA **B** colony in reverse **C** terminal chlamydospore **D** clamped generative hyphae **E, F** chlamydospores. Photographs by Song-Ming Tang. Scale bars: 10  $\mu\text{m}$  (**C–F**).

3.5–4.5  $\mu\text{m}$ , grows on dead hardwood trees, and its distribution is in the North Hemisphere (Ryvarden 2004).

*Grifola gargal* Singer is close to *G. sinensis*, both having cream yellow pilei, and pores 1–2/mm. However, *G. gargal* has larger basidiospores, 7–8  $\times$  5–6  $\mu\text{m}$ , and monomitic hyphal system (Singer 1969; Rugolo et al. 2023).

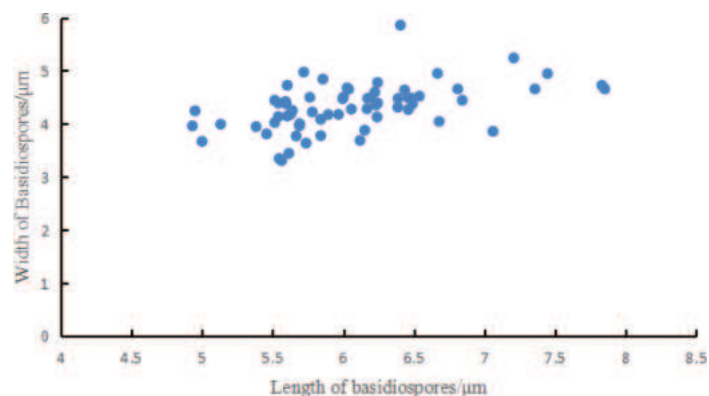


Figure 9. Basidiospores scatter plot of *Grifola sinensis*.



Figure 10. Characteristics of basidiospores ornamentations **A, B** *Grifola edulis* (HKAS 131996) **C, D** *Grifola sinensis* (HKAS 131995).

In our multi-locus phylogeny, *G. sinensis* is closely related to *G. frondosa* and *G. edulis*. However, *G. frondosa* has dark to pale gray pilei, larger basidiomata, up to 40–50 cm, and white pores. *Grifola edulis* has irregular, mostly tibiiform or narrowly clavate, rarely narrowly lageniform or ellipsoid and relatively larger chlamydospores, (13–) 22–94 (–115) × 7–12 μm, av.  $49.8 \pm 28.5 \times 9.4 \pm 1.4$  μm, gray to gray-brown pilei and cuticle hyphae terminal segments slightly enlarged (this study).

## Discussion

In this study, we combined sequences of four non-translated loci (5.8S, ITS1+ITS2, *TUBB* exon and *TUBB* intron) to carry out phylogenetic analyses of

**Table 2.** Synopsis of the species of *Grifola*.

Species	Basidiospores	Basidia	Pilei surface	Pores	Chlamydospores	Basidiomata size and hyphal system	Host	Reference
<i>G. amazonica</i>	Ellipsoid; 4–4.5 × 3–3.5 µm	12–14 × 3.5–4.5 µm	Deep purplish bay to dark brown	Pore surface pale grayish brown; pores 3–5 per mm; tubes concolorous, 5 mm deep	–	Up to 8 cm wide; dimitic hyphal system	On dead hardwood tree	Ryvarden L. 2004
<i>G. colensoi</i>	4–5 × 4–5 µm	–	Smoky brown, dark brown or purplish black	Pores large, irregular, usually rather elongated laterally, radially arranged	–	32 × 27 × 25 cm; dimitic hyphal system	<i>Fuscospora fusca</i> and <i>Eucalyptus</i>	Cunningham 1965; Rugolo et al. 2023
<i>G. edulis</i>	(3.7–) 4.4–6.8 × 2.5–5.6 µm; av. 5.5 ± 0.5 × 4.1 ± 0.5 µm	17–29 × 5–7 µm	Gray to gray-brown	Pore surface white; tubes 2–3 mm deep; pores 2–4 per mm	Mostly tibiiform or narrowly clavate, rarely narrowly lageniform or ellipsoid, (13–) 22–94 (–115) × 7–12 µm	12 × 10 × 18 cm; dimitic hyphal system	<i>Lithocarpus corneus</i>	This study
<i>G. gargal</i>	Ellipsoid; 7–8 × 5–6 µm	–	Cream yellow, light brown or gray	Pore surface white; tubes up to 5 mm deep; pores 1–2 per mm	–	Up to 30 cm wide; monomitic hyphal system	<i>Lophozonia obliqua</i> , <i>L. alpina</i> , <i>Weinmania</i> , <i>Amomyrtus</i> , and <i>Eucryphia</i>	Singer 1969; Rajchenberg 2002, 2006
<i>G. odorata</i>	Subglobose to broadly ellipsoid, 5.8–8.5 × 5–7 µm	30 × 8 µm	Gray, brown, light brown, or white	Pore surface white; pores 1–2 per mm	Subglobose, 10–11 × 7–8 µm	35 × 22 × 24 cm; monomitic hyphal system	<i>Metrosideros robusta</i> , <i>M. excelsa</i> , <i>Fuscospora solandri</i> , and <i>F. fusca</i>	Rugolo et al. 2023
<i>G. sinensis</i>	4.6–7.9 × 3.0–5.9 µm, av. 5.9 ± 0.6 × 4.2 ± 0.5 µm	15–28 (–32) × 5–8 µm	White to grayish white when young, changing to olive yellow with age or when soaked	Pore surface white to grayish white when young, changing to olive yellow with age or when soaked; tubes 2–3 mm deep, pores 2–4 per mm	Mostly ellipsoid, rarely narrowly utriform, 9.6–16.1 (–21.9) × 7.4–11.9 µm	10 × 12 × 15 cm; dimitic hyphal system	<i>Lithocarpus corneus</i>	This study
<i>G. sordulenta</i>	Ellipsoid to ovoid; 6–7 × 4–5 µm	–	Cream color, light cinnamon or grayish	Pore surface cream-color; pores 1–2 per mm	–	35 × 15 × 30 cm; monomitic hyphal system	<i>Nothofagus dombeyi</i>	Singer 1969; Rajchenberg 2002, 2006
<i>G. frondosa</i>	5.5–6.5 (–7) × 3.5–4.5 µm	–	Pale gray	Pore surface white; pores 2–4 per mm	–	Up to 40–50 cm wide; dimitic hyphal system	<i>Quercus</i> , <i>Castanea</i> , <i>Fagus</i> and <i>Carpinu</i>	Gray 1821; Rugolo et al. 2023

*Grifola* species, in order to investigate the phylogenetic relationships between the two new species we described and other *Grifola* species. At present, eight *Grifola* species have been described in the world, including this study two novel species, each species are given in the Table 2.

Chlamydospores size and shape are important characters for identifying species of *Grifola*, but ignored in previous studies, being Rugolo et al. (2023) the first to provide the description of *G. odorata* chlamydospores. Chlamydospores of *G. edulis* and *G. sinensis* clearly differ in size and shape, in *G. edulis* chlamydospores are irregular, mostly tibiiform or narrowly clavate, rarely narrowly lageniform or ellipsoid, (13–) 22–94 (–115) × 7–12 µm, av. 49.8 ± 28.5 × 9.4 ± 1.4 µm; in *G. sinensis* chlamydospores are mostly ellipsoid, rarely narrowly utriform, 9.6–16.1 (–21.9) × 7.4–11.9 µm, av. 13.4 ± 2.9 × 9.2 ± 1.2 µm, Q = 1.1–2.0 (–2.9).

The phylogenetic analysis conducted by Rugolo et al. (2023) revealed that *Grifola* taxa form two well clades, one from the northern Hemispheres and an-

other from the southern Hemisphere; our research also confirms this result. The North Hemisphere clade includes *G. frondosa*, as well as our collections of *G. edulis* and *G. sinensis*. Shen et al. (2002) studied the isolation of *G. frondosa* worldwide, and identified partition in different phylogenetic species. In this study, we designated specimen WC493 (from Norway) as *G. frondosa*, following the type specimen from Europe (Shen et al. 2002), and the three species are clearly separated in our phylogenetic tree (Fig. 1). The south Hemisphere clade comprises *G. sordulenta*, *G. colensoi*, *G. gargal* and *G. odorata*; species of *G. sordulenta* and *G. colensoi* form a sister clade, are characterized by dark brown or purplish black pilei, with no distinct odor (Rajchenberg 2006).

Previously, Asian *Grifola* isolates were all considered as of *G. frondosa* (Shen et al. 2002). Studies only based on morphology or molecular analyses were insufficiently informative. Combining morphological and phylogenetic analysis, we introduce two new species from Asia, very close to *G. frondosa* (WC493) (Fig. 1). Approximately four decades ago, maitake mushrooms were exclusively sourced from their natural habitat. *Grifola frondosa* commercial cultivation commenced in Japan, as documented by Takama et al. (1981). Since that time, Japan has emerged as the predominant global producer of maitake, contributing to 98% of the total worldwide production (Chang 1999). Subsequently, industrial cultivation of maitake in China also rapidly developed. In 2022, the annual maitake production in China reached approximately 50,000 tons (from the China Edible Fungi Association). As *Grifola frondosa*, *G. edulis* and *G. sinensis* form a clade, this implies that *G. edulis* and *G. sinensis* may also have potential cultivation value.

Species of *Grifola* host are variable, including genera *Eucalyptus*, *Lophozonia*, *Lithocarpus*, *Populus*, *Podocarpus*, *Fuscospora*, *Nothofagus*, and *Quercus*, most *Grifola* species have different hosts, rarely *Grifola* species only found under the same host (Cunningham 1948; Singer 1962; Cunningham 1965; Singer 1969; Buchanan and Ryvarden 2000; Rajchenberg 2006; Rugolo et al. 2023).

We use 750 mL plastic bottles to cultivate *G. edulis* and *G. sinensis* at room temperature of 20 °C–25 °C and air humidity of 70%–85%; the cultivated material is 80% sawdust, 18% wheat bran, 1% sugar and 1% gypsum, the biological conversion rate of *G. edulis* and *G. sinensis* is approximately 20%.

*Grifola edulis* and *G. sinensis* are widely distributed in the subtropical broad-leaved forests of Gongshan city in Yunnan, where the annual average temperature is 11–22 °C, and the elevation is between 1,170–5,128 m (Wang 2018). In China, Yunnan, there is a tropical to subtropical climate suitable for abundance of fungal resources, so certainly more *Grifola* species will be discovered in the future.

## Acknowledgements

We thank two anonymous reviewers for corrections and suggestions to improve our work.

## Additional information

### Conflict of interest

The authors have declared that no competing interests exist.

## Ethical statement

No ethical statement was reported.

## Funding

This work was supported by grants from Central guidance for local scientific and technological development funds (No. 202307AB110001) and the National Natural Science Foundation of China to Shu-Hong Li (No. 32060006, 31160010, 31560009, and 31960391) and edible fungi industry system of China (CARS-20).

## Author contributions

Investigation: SW, DCC. Methodology: CCA. Resources: EXL, XQW, HML. Supervision: SHL. Writing - original draft: SMT.

## Author ORCIDs

Song-Ming Tang  <https://orcid.org/0000-0002-6174-7314>

De-Chao Chen  <https://orcid.org/0009-0006-3626-1191>

Shuai Wang  <https://orcid.org/0009-0001-0157-6859>

Xiao-Qu Wu  <https://orcid.org/0009-0006-7980-2322>

Cheng-Ce Ao  <https://orcid.org/0000-0002-1569-3386>

Er-Xian Li  <https://orcid.org/0009-0008-4671-8698>

Hong-Mei Luo  <https://orcid.org/0009-0001-9976-4371>

Shu-Hong Li  <https://orcid.org/0000-0001-5806-9148>

## Data availability

All of the data that support the findings of this study are available in the main text.

## References

- Audet SA (2010) Essai de découpage systématique du genre *Scutigera* (Basidiomycota): *Albatrellopsis*, *Albatrellus*, *Polyporoletus*, *Scutigera* et description de six nouveaux genres. *Mycotaxon* 111(1): 431–464. <https://doi.org/10.5248/111.431>
- Bresadola G (1925) New species of fungi. *Mycologia* 17(2): 68–77. <https://doi.org/10.1080/00275514.1925.12020457>
- Buchanan PK, Ryvarden L (2000) An annotated checklist of polypore and polypore-like fungi recorded from New Zealand. *New Zealand Journal of Botany* 38(2): 265–323. <https://doi.org/10.1080/0028825X.2000.9512683>
- Chang ST (1999) World production of cultivated edible and medicinal mushroom in 1997 with emphasis on *Lentinus edodes* (Berk.) Sing. in China. *International Journal of Medicinal Mushrooms* 1(4): 291–300. <https://doi.org/10.1615/IntJMedMushr.v1.i4.10>
- Cui F, Zan X, Li Y, Yang Y, Sun W, Zhou Q, Yu S, Dong Y (2013) Purification and partial characterization of a novel anti-tumor glycoprotein from cultured mycelia of *Grifola frondosa*. *International Journal of Biological Macromolecules* 62: 684–690. <https://doi.org/10.1016/j.ijbiomac.2013.10.025>
- Cunningham GH (1948) New Zealand Polyporaceae. 3. The genus *Polyporus*. New Zealand Department of Scientific and Industrial Research, Plant Diseases Division. *Bulletin*, 74 pp.
- Cunningham GH (1965) Polyporaceae of New Zealand. *Bulletin of the New Zealand Department of Scientific and Industrial Research* 164: 1–304.

- Dickson J (1785) Fasciculus plantarum cryptogamicarum. Britanniae 1: 1–26.
- Gray SF (1821) A natural arrangement of British plants according to their relations to each other as pointed out by Jussieu, De Candolle, Brown, &c. Printed for Baldwin, Cradock and Joy, London, 824 pp. <https://doi.org/10.5962/bhl.title.43804>
- Gu CQ, Li JW, Chao F, Jin M, Wang XW, Shen ZQ (2007) Isolation, identification and function of a novel anti-HSV-1 protein from *Grifola frondosa*. *Antiviral Research* 75(3): 250–257. <https://doi.org/10.1016/j.antiviral.2007.03.011>
- Hall T (2007) BioEdit v7. <http://www.mbio.ncsu.edu/BioEdit/BioEdit.html>
- He XY, Du XZ, Zang XY, Dong LL, Gu ZJ, Cao LP, Chen D, Keyhani NO, Yao L, Qiu J, Guan X (2016) Extraction, identification and antimicrobial activity of a new furanone, grifolaone A, from *Grifola frondosa*. *Natural Product Research* 30(8): 941–947. <https://doi.org/10.1080/14786419.2015.1081197>
- Hooker JD (1855) The botany of the Antarctic Voyage II. *Flora Novae-Zelandiae* 2: 1–378.
- Justo A, Hibbett DS (2011) Phylogenetic classification of *Trametes* (Basidiomycota, Polyporales) based on a five-marker dataset. *Taxon* 60(6): 1567–1583. <https://doi.org/10.1002/tax.606003>
- Justo A, Miettinen O, Floudas D, Ortiz-Santana B, Sjökvist E, Lindner D, Nakasone K, Niemelä T, Larsson KH, Ryvarde L, Hibbett DS (2017) A revised family-level classification of the Polyporales (Basidiomycota). *Fungal Biology* 121(9): 798–824. <https://doi.org/10.1016/j.funbio.2017.05.010>
- Karsten PA (1881) Enumeratio Boletinearum et Polyporearum Fennicarum, systemate novo dispositarum. *Revue Mycologique Toulouse* 3: 16–19.
- Katoh K, Standley DM (2013) MAFFT multiple sequence alignment software version 7: Improvements in performance and usability. *Molecular Biology and Evolution* 30(4): 772–780. <https://doi.org/10.1093/molbev/mst010>
- Konno S, Alexander B, Zade J, Choudhury M (2013) Possible hypoglycemic action of SX-fraction targeting insulin signal transduction pathway. *International Journal of General Medicine*: 181–187. <https://doi.org/10.2147/IJGM.S41891>
- Kornerup A, Wanscher JH (1978) *Methuen handbook of colour*, 3<sup>rd</sup> edn. Eyre Methuen, London.
- Maas Geesteranus RA (1967) Studies in cup-fungi-I. *Persoonia Molecular Phylogeny and Evolution of Fungi* 4: 417–425.
- Miller MA, Pfeiffer W, Schwartz T (2010) Creating the CIPRES Science Gateway for inference of large phylogenetic trees. In: 2010 Gateway Computing Environments Workshop (GCE), New Orleans, LA, USA, 2010, 1–8. <https://doi.org/10.1109/GCE.2010.5676129>
- Nylander JA, Ronquist F, Huelsenbeck JP, Nieves-Aldrey J (2004) Bayesian phylogenetic analysis of combined data. *Systematic Biology* 53(1): 47–67. <https://doi.org/10.1080/10635150490264699>
- Rajchenberg M (2002) The genus *Grifola* (Aphyllorphorales, Basidiomycota) in Argentina revisited. *Boletín de la Sociedad Argentina de Botánica* 37: 19–27.
- Rajchenberg M (2006) Polypores (Basidiomycetes) from the Patagonian Andes Forests of Argentina. In *Bibliotheca Mycologica Band 201*, J Cramer Verlag, Stuttgart, 300 pp.
- Ronquist F, Huelsenbeck J, Teslenko M (2011) MrBayes version 3.2 manual: tutorials and model summaries. Distributed with the software. <http://brahms.biology.rochester.edu/software.html>
- Rugolo M, Mascoloti Spréa R, Dias MI, Pires TC, Añibarro-Ortega M, Barroetaveña C, Caleja C, Barros L (2022) Nutritional composition and bioactive properties of wild

- edible mushrooms from native *Nothofagus* Patagonian forests. *Foods* 11(21): 3516. <https://doi.org/10.3390/foods11213516>
- Rugolo M, Barroetaveña C, Barrett MD, Mata G, Hood IA, Rajchenberg M, Pildain MB (2023) Phylogenetic relationships and taxonomy of *Grifola* (Polyporales). *Mycological Progress* 22(1): 7. <https://doi.org/10.1007/s11557-022-01857-2>
- Ryvarden L (2004) Studies in neotropical polypores 20. Some new polypores from the Amazonas region. *Synopsis Fungorum* 18: 62–67.
- Ryvarden L, Melo I (2014) Poroid fungi of Europe. *Synopsis Fungorum* 31: 1–455.
- Shen Q, Geiser DM, Royse DJ (2002) Molecular phylogenetic analysis of *Grifola frondosa* (maitake) reveals a species partition separating eastern North American and Asian isolates. *Mycologia* 94(3): 472–482. <https://doi.org/10.1080/15572536.2003.11833212>
- Shen KP, Su CH, Lu TM, Lai MN, Ng LT (2015) Effects of *Grifola frondosa* non-polar bioactive components on high-fat diet fed and streptozotocin-induced hyperglycemic mice. *Pharmaceutical Biology* 53(5): 705–709. <https://doi.org/10.3109/13880209.2014.939290>
- Shomori K, Yamamoto M, Arifuku I, Teramachi K, Ito H (2009) Antitumor effects of a water-soluble extract from Maitake(*Grifola frondosa*) on human gastric cancer cell lines. *Oncology Reports* 22(3): 615–620. [https://doi.org/10.3892/or\\_00000480](https://doi.org/10.3892/or_00000480)
- Singer R (1962) Diagnoses fungorum novorum Agaricalium II. *Sydowia* 15: 45–83.
- Singer R (1969) Mycoflora Australis. *Nova Hedwigia* 29: 1–405.
- Stamatakis A (2014) RAxML version 8: A tool for phylogenetic analysis and post-analysis of large phylogenies. *Bioinformatics* 30(9): 1312–1313. <https://doi.org/10.1093/bioinformatics/btu033>
- Takama F, Ninomiya S, Yoda R, Ishii H, Muraki S (1981) Parenchyma cells, chemical components of maitake mushroom (*Grifola frondosa* S.F.gray) cultured artificially, and their changes by storage and boiling. *Mushroom* 11: 767–779.
- Vaidya G, Lohman DJ, Meier R (2011) SequenceMatrix: Concatenation software for the fast assembly of multi-gene datasets with character set and codon information. *Cladistics* 27(2): 171–180. <https://doi.org/10.1111/j.1096-0031.2010.00329.x>
- Wang SJ (2018) Spatiotemporal variability of temperature trends on the southeast Tibetan Plateau, China. *International Journal of Climatology* 38(4): 1953–1963. <https://doi.org/10.1002/joc.5308>
- White NC, Hedenquist JW (1990) Epithermal environments and styles of mineralization: Variations and their causes, and guidelines for exploration. *Journal of Geochemical Exploration* 36(1–3): 445–474. [https://doi.org/10.1016/0375-6742\(90\)90063-G](https://doi.org/10.1016/0375-6742(90)90063-G)
- Zhang Y, Mills GL, Nair MG (2002) Cyclooxygenase inhibitory and antioxidant compounds from the mycelia of the edible mushroom *Grifola frondosa*. *Journal of Agricultural and Food Chemistry* 50(26): 7581–7585. <https://doi.org/10.1021/jf0257648>
- Zhou JL, Zhu L, Chen H, Cui BK (2016) Taxonomy and phylogeny of *Polyporus* group *melanopus* (Polyporales, Basidiomycota) from China. *PLOS ONE* 11(8): e0159495. <https://doi.org/10.1371/journal.pone.0159495>
- Zmitrovich IV, Kovalenko AE (2016) Lentinoid and polyporoid fungi, two generic conglomerates containing important medicinal mushrooms in molecular perspective. *International Journal of Medicinal Mushrooms* 18(1): 23–38. <https://doi.org/10.1615/IntJMedMushrooms.v18.i1.40>

# Two novel species of arctic-alpine lichen-forming fungi (Ascomycota, Megasporaceae) from the Deosai Plains, Pakistan

Muhammad Usman<sup>1,2</sup>, Paul S. Dyer<sup>2</sup>, Matthias Brock<sup>2</sup>, Christopher M. Wade<sup>2</sup>, Abdul Nasir Khalid<sup>1</sup>

<sup>1</sup> Fungal Biology and Systematics Research Laboratory, Institute of Botany, University of the Punjab, Quaid-e-Azam Campus 54590, Lahore, Pakistan

<sup>2</sup> School of Life Sciences, University of Nottingham, Nottingham NG7 2RD, UK

Corresponding author: Muhammad Usman ([musmanmughal52@yahoo.com](mailto:musmanmughal52@yahoo.com))

## Abstract

Members of the lichen-forming fungal genus *Oxneriaria* are known to occur in cold polar and high altitudinal environments. Two new species, *Oxneriaria crittendenii* and *O. deosaiensis*, are now described from the high altitude Deosai Plains, Pakistan, based on phenotypic, multigene phylogenetic and chemical evidence. Phenotypically, *O. crittendenii* is characterised by orbicular light-brown thalli 1.5–5 cm across, spot tests (K, C, KC) negative, apothecia pruinose, hymenium initially blue then dark orange in response to Lugol's solution. *Oxneriaria deosaiensis* is characterised by irregular areolate grey thalli 1.5–2 cm across, K test (light brown), KC test (dark brown), apothecia epruinose, hymenium initially blue then dark blue in response to Lugol's solution. Both species share the same characters of thalli with black margins and polarilocular ascospores. The closest previously reported species, *O. pruinosa*, differs from *O. crittendenii* and *O. deosaiensis* in having non-lobate margins, thin thalline exciple (45–80 µm thick), short asci (55–80 × 25–42 µm) and K positive (yellow) and KC negative tests and divergent DNA sequence in the ITS, LSU and mt SSU regions. The newly-described *Oxneriaria* species add to growing evidence of the Deosai Plains as a region of important arctic-alpine biodiversity.

**Key words:** *Aspicilia*, Gilgit-Baltistan, Himalaya, Karakorum, Maximum Likelihood, Pertusariales, Skardu



Academic editor: Gerhard Rambold

Received: 26 September 2023

Accepted: 18 November 2023

Published: 1 March 2024

**Citation:** Usman M, Dyer PS, Brock M, Wade CM, Khalid AN (2024) Two novel species of arctic-alpine lichen-forming fungi (Ascomycota, Megasporaceae) from the Deosai Plains, Pakistan. MycoKeys 102: 285–299. <https://doi.org/10.3897/mycokeys.102.113310>

**Copyright:** © Muhammad Usman et al.

This is an open access article distributed under terms of the Creative Commons Attribution License (Attribution 4.0 International – CC BY 4.0).

## Introduction

The Deosai Plains are located between the Himalaya and Karakorum, two of the world's most famous mountain ranges, with an average elevation of over 4,000 m (Woods et al. 1997). They represent one of the most important high altitude alpine grasslands and summer pastures of the trans-Himalayan range in Pakistan. Three important river systems originate from the Deosai Plains, namely the Shatung, Bara Pani and Kala Pani, which combine to form the Shigar River, an important tributary of the Indus River (Hussain 2014). The Deosai Plains are characterised by an undulating topography with a range of edaphic conditions and ecological niches present that are subject to extreme cold conditions for long periods of the year. A diverse range of flora and fauna have been recorded, which are considered to be adapted for survival under such conditions (Woods et al. 1997; Usman et al.

2021). The highland arctic-alpine ecosystem includes herbaceous perennial grasses and sedges which dominate the vegetation of the plateau, forming dense moist grasslands in the valley plains, whilst dwarfed and stunted vegetation, flower fields, rocky outcrops and soil crusts are also present (Stewart 1961; Hussain et al. 2015).

Members of the lichen-forming genus *Oxneriaria* S.Y. Kondr. & Lőkös are distributed in cold polar and high-altitude localities of Eurasia and the Northern Hemisphere (Nordin et al. 2011; Haji-Moniri et al. 2017; Chesnokov et al. 2018; Halıcı et al. 2018). They are characterised by the presence of a radiating lichen thallus with a wrinkled or lobate peripheral zone, relatively small ascospores, production of substictic acid and positioning as a distinct branch on phylogenetic trees in the Megasperaceae. They grow on rocks and have been observed growing side by side with other taxa of the same and other genera (Haji-Moniri et al. 2017). The genus was first named by Haji-Moniri et al. (2017) who transferred over nine species that were previously included in the genus *Aspicilia*. A total of fourteen species have, so far, been described for the genus *Oxneriaria* (Haji-Moniri et al. 2017; Asghar et al. 2023; Iqbal et al. 2023; Zulfiqar et al. 2023).

Four species of the genus *Oxneriaria* have, so far, been described from Pakistan with a distance of 300 to 650 km from Deosai Plains, namely *O. iqbalii* R. Zulfiqar, H. S. Asghar, K. Habib & Khalid from Kohistan (350 km) and Swat (500 km), *O. kohistaniensis* R. Zulfiqar, K. Habib & Khalid from Kohistan (350 km), *O. pakistanica* M. S. Iqbal, Usman, K. Habib & Khalid from Darel (300 km) and *O. pruinosa* H. S. Asghar., Usman, K. Habib & Khalid from Chitral (650 km). These were all found at relatively high altitudes up to ca. 2,500 m (Asghar et al. 2023; Iqbal et al. 2023; Zulfiqar et al. 2023). During the period 2019 to 2020, several collections of lichens were made from the Deosai Plains and adjacent localities at altitudes above 4,000 m. From this collection, four samples were attributed to the genus *Oxneriaria*, which comprised two new species as will be described in this study.

## Materials and methods

### Sample collection

More than half of the Deosai Plains are situated between an elevation (elev.) of 4,000 and 4,500 m with an average daily temperature ranging from -20 °C (January-February) to 12 °C (July-August). Annual precipitation varies from 350 to 550 mm, mostly received during winter as snow (WAPDA 2012; Usman et al. 2021). Lichen collections were made from both rock and soil crusts during the period May 2019 to Sept 2020 from various locations in the Deosai Plains National Park, Gilgit Baltistan, Pakistan (see later for precise collection site details for particular specimens) at altitudes between 4,177 and 4,689 m. Samples were air dried before storage and examination.

### Morpho-anatomical and chemical studies

Methods for the examination of external morphology, macroscopic and microscopic characters and their measurements were followed and recorded according to the terminology of Ryan et al. (2002). All the measurements of anatomical structures were noted in water with an average of 25 ascospores per collection and 5 - 6 sections were prepared for the thallus, apothecia and

pycnidia. The algal partner was identified by following Friedl and Büdel (2008). For thallus chemical reactions, standard K (5% potassium hydroxide aqueous solution), C (commercial bleach), KC (commercial bleach after 5% potassium hydroxide aqueous solution) and ultra-violet (UV) tests were done. Solvents A (toluene/dioxane/ acetic acid as 180:45:5) and G (toluene/ ethyl acetate/ formic acid as 139:83:8) were used for the detection of secondary metabolites through thin layer chromatography (TLC) as described by Orange et al. (2010).

### Molecular and phylogenetic analyses

Nuclear DNA was extracted from apothecia present on thalli using a GF1 Plant DNA extraction kit according to the manufacturer's instruction (Vivantis, Selangor Darul Ehsan, Malaysia). Primers used for amplifications were ITS1F 5'-CCT GGT CAT TTA GAG GAA GT A A-3' and ITS4 5'-TCC TCC GCT CTA TTG ATA TGC-3' for the internal transcribed spacer (ITS1-5.8S-ITS2) region, while LROR 5'-ACC CGC TGA ACT TAA GC-3' and LR5 5'-TCC TGA GGG AAA CTT CG-3' were used for the nuclear large subunit (LSU) ribosomal RNA region (White et al. 1990; Gardes and Bruns 1993). For the mitochondrial (mt) small subunit (SSU) ribosomal RNA region, SSU1 5'-AGC AGT GAG GAA TAT TGG TC-3' and SSU3R 5'-ATG TGG CAC GTC TAT AGC CC-3' were used (Zoller et al. 1999). Polymerase chain reaction (PCR) conditions adapted from those of Gardes and Bruns (1993) were followed according to Zoller et al. (1999) and Usman and Khalid (2020). The PCR amplicons were purified using a QIAquick PCR Purification Kit (Qiagen, Valencia, CA, USA) and then sent for sequencing to TsingKe, China.

Forward and reverse sequences of the ITS, LSU and mt SSU regions were obtained in FASTA format and sequences were assembled using BIOEDIT v. 7.2.5 (Hall 1999). These were compared with related DNA sequences available online through BLAST at NCBI (<https://www.ncbi.nlm.nih.gov/guide>). The sequences used in the ITS, LSU and mt SSU dataset were retrieved from the NCBI database, based on similarity of 93% identity or greater, plus all published sequences from the genus *Oxneriaria* (Nordin et al. 2007; Nordin et al. 2011; Asghar et al. 2023; Iqbal et al. 2023; Zulfikar et al. 2023). Sequences of *Megaspora cretacea* Gasparyan, Zakeri & Aptroot were used as an outgroup in the ITS phylogenetic tree, while *Megaspora verrucosa* (Ach.) Arcadia & A. Nordin was used as outgroup in the LSU and mt SSU phylogenetic trees (Nordin et al. 2010; Sohrabi et al. 2013; Zakeri et al. 2016). Sequences used for the phylogenetic analyses are presented in Table 1 together with GenBank accession numbers, voucher numbers and country distribution. The final alignments of sequences were made in SEAVIEW software version 5.0.5 using the CLUSTAL W method (Gouy et al. 2010). Maximum Likelihood phylogenetic trees were inferred in RAXML-HPC2 using XSEDE (8.2.10) using the GTR+GAMMMA nucleotide substitution model and with 1000 bootstrap replicates. Phylogenetic analyses were undertaken using the CIPRES online portal (<https://www.phylo.org/>), with substitution model verified using jModelTest 2.1.6 and the Akaike Information Criterion (Akaike 1974; Darriba et al. 2012) to determine the best nucleotide substitution model. Phylogenetic trees were visualised using FigTree v. 1.4.2 (Rambaut 2012). Newly-generated sequences were deposited in GenBank (accession numbers OR037219–OR037226, OR037259–OR037262, Table 1). These were investigated further by DNA-based phylogenetic analyses and detailed morpho-anatomical and chemical studies as follows.

**Table 1.** Sequences used in the phylogenetic analyses. Novel sequences generated during this study are shown in bold. Note that sequences were not available for all regions for certain taxa.

Taxon name	Voucher number	GenBank accession			Country
		ITS	LSU	mt SSU	
<b><i>Oxneriaria crittendenii</i></b>	<b>LAH37193</b>	<b>OR037223</b>	<b>OR037219</b>	<b>OR037259</b>	<b>Pakistan</b>
<b><i>Oxneriaria crittendenii</i></b>	<b>LAH37194</b>	<b>OR037224</b>	<b>OR037220</b>	<b>OR037260</b>	<b>Pakistan</b>
<i>Oxneriaria dendroplaca</i>	UPS:Nordin 5952	HQ259259	HM060744	HM060706	Sweden
<i>Oxneriaria dendroplaca</i>	UPS:Nordin 6366	HQ259260	HM060758	–	Finland
<b><i>Oxneriaria deosaiensis</i></b>	<b>LAH37200</b>	<b>OR037225</b>	<b>OR037221</b>	<b>OR037261</b>	<b>Pakistan</b>
<b><i>Oxneriaria deosaiensis</i></b>	<b>LAH37416</b>	<b>OR037226</b>	<b>OR037222</b>	<b>OR037262</b>	<b>Pakistan</b>
<i>Oxneriaria iqbalii</i>	LAH37155	ON392710	–	–	Pakistan
<i>Oxneriaria iqbalii</i>	LAH37156	ON392709	ON392708	–	Pakistan
<i>Oxneriaria kohistaniensis</i>	LAH37152	ON392707	ON392711	–	Pakistan
<i>Oxneriaria kohistaniensis</i>	LAH37151	ON454505	–	–	Pakistan
<i>Oxneriaria mashiginensis</i>	Nordin 5790 (UPS)	EU057912	HM060732	HM060694	Sweden
<i>Oxneriaria mashiginensis</i>	UPS:Tibell 23557	HQ259266	–	–	Sweden
<i>Oxneriaria pakistanica</i>	LAH37495	OP114649	–	–	Pakistan
<i>Oxneriaria pakistanica</i>	LAH37501	OP627196	–	–	Pakistan
<i>Oxneriaria permutata</i>	Nordin 6027 (UPS)	EU057918	HM060747	HM060709	Sweden
<i>Oxneriaria permutata</i>	Nordin 6029 (UPS)	EU057919	–	–	Sweden
<i>Oxneriaria permutata</i>	Nordin 6039 (UPS)	EU057921	–	–	Sweden
<i>Oxneriaria permutata</i>	Nordin 5980 (UPS)	EU057930	–	–	Sweden
<i>Oxneriaria permutata</i>	Wheeler 4463	–	–	MW424810	Alaska, USA
<i>Oxneriaria pruinosa</i>	LAH37556	OP352770	–	–	Pakistan
<i>Oxneriaria pruinosa</i>	LAH37555	OP352771	–	–	Pakistan
<i>Oxneriaria rivulicola</i>	Nordin 5957 (UPS)	EU057922	HM060753	–	Sweden
<i>Oxneriaria rivulicola</i>	Nordin 5960 (UPS)	EU057923	–	–	Sweden
<i>Oxneriaria</i> sp	Nordin 6003 (UPS)	EU057931	–	–	Sweden
<i>Oxneriaria</i> sp	Nordin 6004 (UPS)	EU057932	–	–	Sweden
<i>Oxneriaria supertegens</i>	Owe-Larsson H-168a (UPS)	EU057935	–	–	Sweden
<i>Oxneriaria supertegens</i>	Owe-Larsson 9011 (UPS)	EU057937	–	–	Norway
<i>Oxneriaria supertegens</i>	Nordin 6023 (UPS)	EU057938	HM060751	–	Sweden
<i>Oxneriaria supertegens</i>	Owe-Larsson 9002 (UPS)	–	HM060742	HM060704	Norway
<i>Oxneriaria verruculosa</i>	Owe-Larsson 9007 (UPS)	EU057940	HM060741	HM060703	Norway
<i>Oxneriaria verruculosa</i>	Owe-Larsson 9003 (UPS)	EU057941	–	–	Norway
<i>Oxneriaria verruculosa</i>	Nordin 5942 (UPS)	EU057942	–	–	Sweden
<i>Oxneriaria virginea</i>	UPS:Nordin 6017a	HQ259270	–	–	Sweden
<i>Oxneriaria virginea</i>	UPS:Ebbestad SVL1-1	HQ259271	–	–	Svalbard
<i>Oxneriaria virginea</i>	Wheeler 7153 (hb. Wheeler)	–	–	MW424818	Montana, USA
<b>Outgroup</b>					
<i>Megaspora cretacea</i>	B 600200932	KX253974	–	–	Armenia
<i>Megaspora cretacea</i>	B 600199170	KX253975	–	–	Armenia
<i>Megaspora verrucosa</i>	St. Clair C54042 (BRY)	–	KC667062	–	Colorado, USA
<i>Megaspora verrucosa</i>	UPS:Nordin 6495	–	–	HM060687	Sweden

## Results

Out of almost 300 samples collected from the Deosai plains and its adjacent areas during the 2019 and 2020 surveys, four lichen thalli were putatively assigned to the genus *Oxneriaria* on the basis of gross morphological features (Figs 1, 2).

### Multigene phylogenetic analyses

DNA was extracted from the four different collections and used successfully in PCR to generate amplicons for the ITS, LSU and mt SSU regions, which ranged in size from 500–800, 900–950 and 900–960 base pairs, respectively. Sequence data of amplicons were aligned and used to construct separate ITS, LSU and mt SSU trees via Maximum Likelihood analyses to examine phylogenetic relationships. Distinct, well-supported clades were recovered from all datasets with minimal conflict, each taxon showing a unique position in all phylogenetic analyses with sequence divergence from other taxa. Clade names were provisionally assigned.

The ITS phylogenetic tree (Fig. 3) consisted of sequences from a total of 34 taxa including the outgroup clade A comprised of two sequences of *Megaspora cretacea* (KX253975, KX253974) and 32 sequences representing an *Oxneriaria* ingroup (Clade B), which could be further subdivided into two main clades C and D. Clade D consisted of a total of seven species of *Oxneriaria* including new, well-supported sequences named here *O. crittendenii* and *O. deosaiensis*, each represented by two of the four field collections. Within clade D, *Oxneriaria deosaiensis* formed a separate branch, sister to a clade which consisted of four species, namely *O. crittendenii*, *O. pakistanica*, *O. pruinosa* and *O. rivulicola* (H. Magn.) S. Y. Kondr. et L. Lőkös and showed 5%, 7.2%, 5.1% and 5% bp differences with *O. deosaiensis* in the sequences of ITS region, respectively, whilst *O. crittendenii* showed 6.1%, 5.3% and 5% bp differences with *O. pakistanica*, *O. pruinosa* and *O. rivulicola*, respectively. The closest species to *O. crittendenii* and *O. deosaiensis* was *O. pruinosa*, forming a separate branch.

The LSU phylogenetic tree (Fig. 4) similarly revealed that *O. crittendenii* and *O. deosaiensis* are positioned on well-supported branches and are monophyletic. The tree consisted of a total 15 available sequences of which 14 sequences represent an *Oxneriaria* ingroup (Clade B), while *Megaspora verrucosa* (Ach.) Arcadia & A. Nordin (KC667062) formed an outgroup (Clade A). Clade B could be further subdivided into Clades C and D. *Oxneriaria deosaiensis*, *O. crittendenii*, *O. dendroplaca* (H. Magn.) S. Y. Kondr. et L. Lőkös., *O. rivulicola* and *O. mashiginensis* (Zahlbr.) S. Y. Kondr. et L. Lőkös. were all positioned in the same clade (Clade D), where they each formed separate branches. Sequences of *O. deosaiensis* for the LSU region showed 1.2%, 1.5%, 1.2% and 2%, bp differences to *O. crittendenii*, *O. dendroplaca*, *O. rivulicola* and *O. mashiginensis*, respectively, whilst *Oxneriaria crittendenii* showed 1.5%, 1.4%, 1.5 and 2% bp differences with *O. rivulicola*, *O. dendroplaca* and *O. mashiginensis*, respectively.

The mt SSU phylogenetic tree (Fig. 5) consisted of a total 12 available sequences of which 11 sequences represented an *Oxneriaria* ingroup (Clade B), while *Megaspora verrucosa* (HM060087) was used as an outgroup (Clade A).

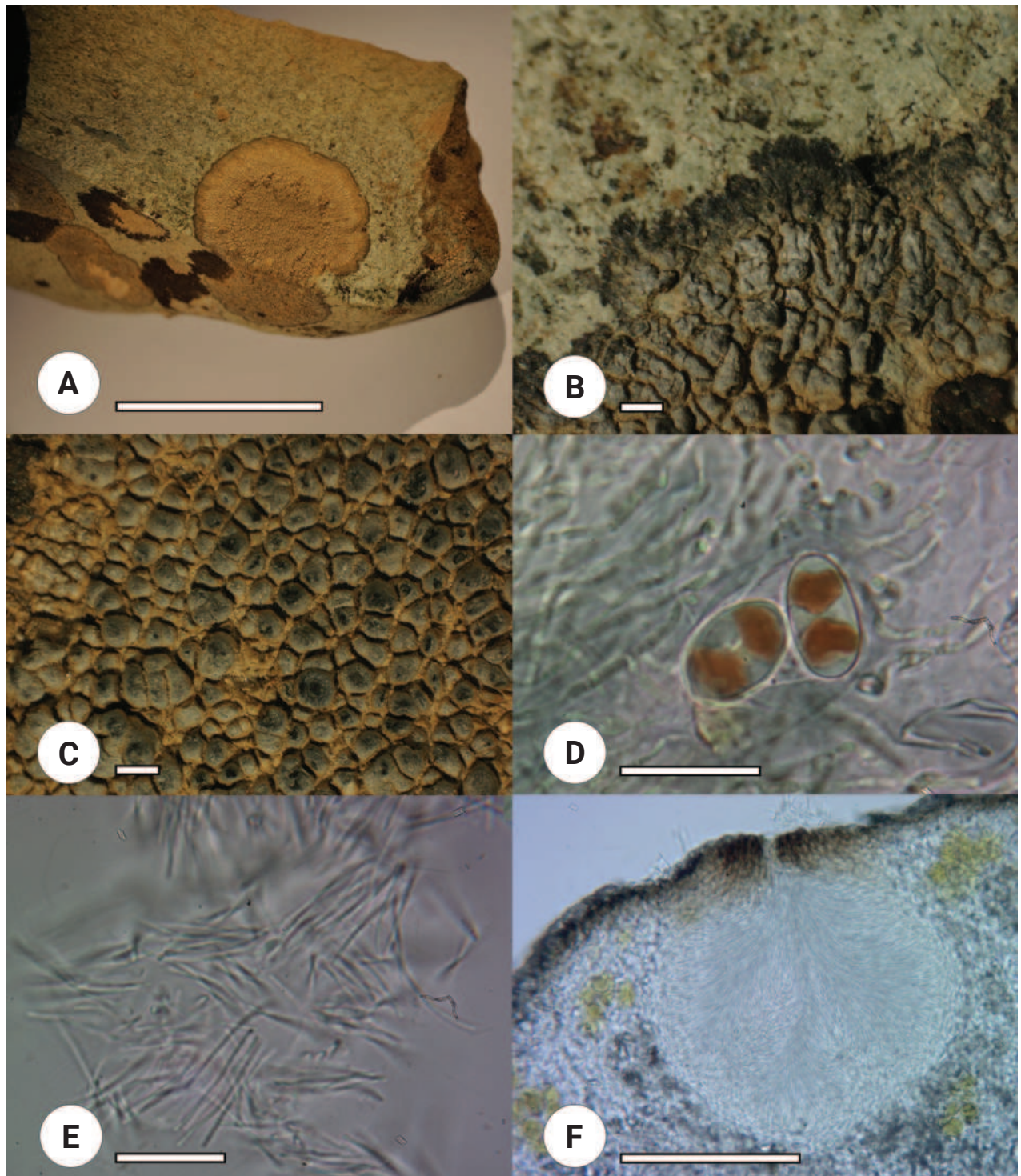


**Figure 1.** *Oxneriaria crittendenii* sp. nov. holotype (LAH37193) **A** thallus **B** margins **C** apothecia under stereomicroscope **D** ascospores in Lugol's solution **E** conidia **F** pycnidium. Photos by Muhammad Usman. Scale bars: 5 cm (**A**); 1 mm (**B**, **C**); 20 µm (**D**, **E**); 100 µm (**F**).

*Oxneriaria deosaiensis*, *O. crittendenii*, *O. dendroplaca* and *O. mashiginensis* formed a clade (Clade D) distinct from *O. verruculosa* forming clade C. Sequences of *O. deosaiensis* from the mt SSU region showed 1%, 2% and 2.5% bp differences with the sequences of closest species *O. crittendenii*, *O. dendro-*

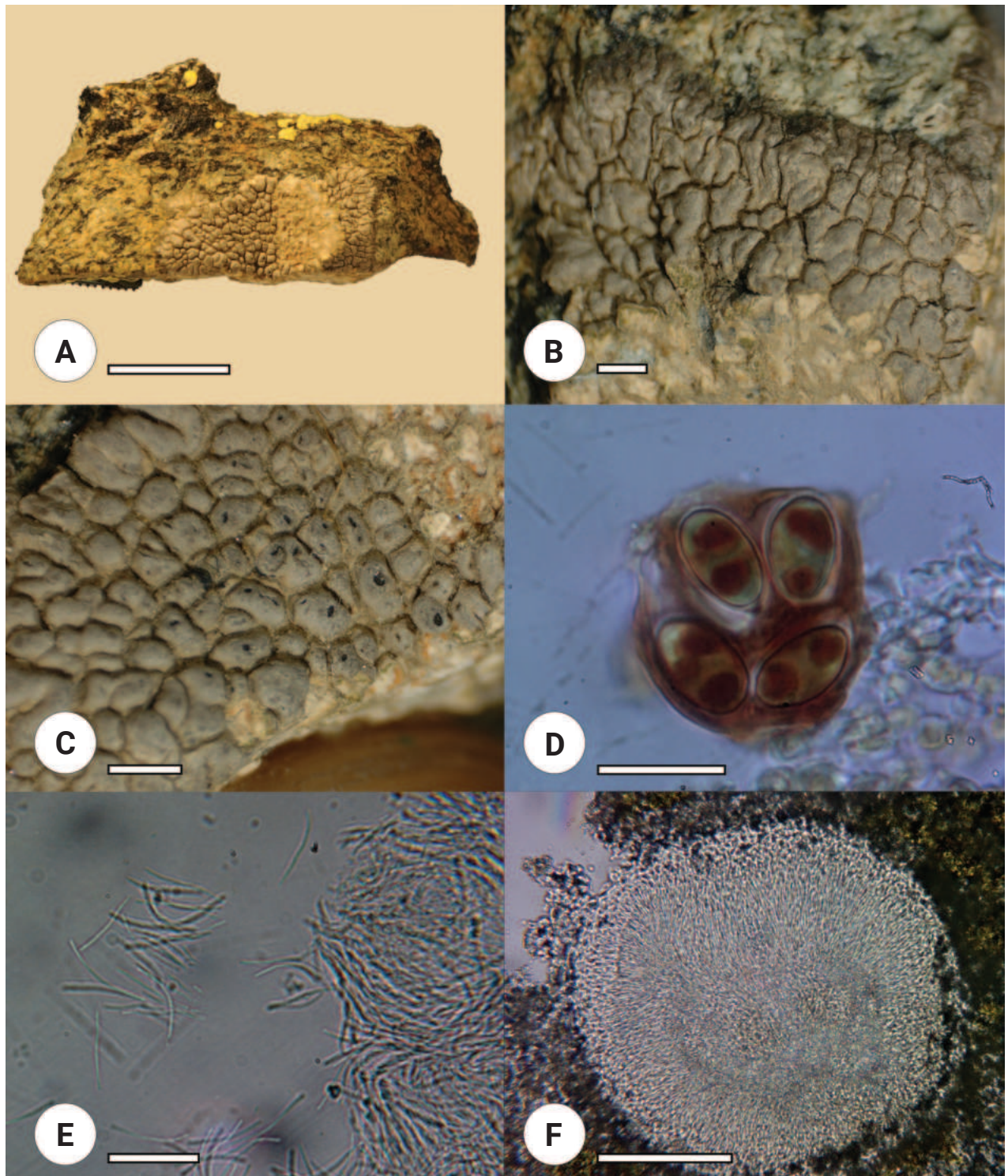


**Figure 2.** *Oxneriaria deosaiensis* sp. nov. holotype (LAH37200) **A** thallus **B** margins **C** apothecia under stereomicroscope **D** ascospores in Lugol's solution **E** conidia **F** pycnidium. Photos by Muhammad Usman. Scale bars: 1 cm (**A**); 1 mm (**B**, **C**); 20 µm (**D**); 30 µm (**E**); 100 µm (**F**).

*placa* and *O. mashiginensis*, respectively, whilst the *O. crittendenii* showed 2.1% and 2.4% bp differences with *O. dendroplaca* and *O. mashiginensis*, respectively. Thus, the mt SSU analysis again showed that sequences of *O. crittendenii* and *O. deosaiensis* are positioned on well-supported branches.

## Taxonomy

### *Oxneriaria crittendenii* Usman & Khalid

MycoBank No: 848889

Fig. 1

**Etymology.** The specific epithet “*crittendenii*” refers to the British lichenologist Prof. Peter D Crittenden in recognition for his outstanding contributions to lichenology.

**Holotype.** Pakistan. Gilgit Baltistan: Deosai Plains (35°0'45.73"N, 75°13'25.95"E, elev. 4,651 m) on rocks, 13 May 2019, M. Usman DEO117 (LAH, holotype; LAH37193). GenBank OR037223 [ITS], OR037219 [LSU], OR037259 [mt SSU].

**Diagnosis.** It differs from its closest species *O. pruinosa* by having lobate black margins (vs. non-lobate), orbicular thallus 1.5–5 cm (vs. irregular 3–8 cm), K test negative (vs. K positive yellow), distinct proper-exciple 17–40 µm wide (vs. indistinct) and polarilocular ellipsoid ascospores (vs. simple ellipsoid).

**Description.** Thallus crustose, epilithic, orbicular, 1.5–5 cm across, zonate, fine bullate to areolate in the centre to poorly areolate towards margin, in the centre areoles 0.5–1 mm diam. and a few areoles changing to squamules up to 1.8 mm in length, lobate at margins, determinate and radiate. **Hypothallus** distinct, shiny light brown. **Upper surface** grey with white powdery texture and black at margins. **Thallus** heteromerous, upper cortex 20–60 µm thick, globose to sub-globose hyaline paraplectenchymatous cells, 6–11 µm in diam. **Algal layer** discontinuous, 90–140 µm thick, photobiont *Trebouxia* sp, coccoid cells, globose to sub-globose 6–14 µm in diam. **Medulla** and **lower cortex** not differentiated and consisting of paraplectenchymatous, globose to sub-globose hyaline cells 25–45 µm in diam.

**Apothecia** without stipe, aspicilioid, one apothecium per areole, rounded, 600–950 µm in diam., pruinose with black disc 450–700 µm, dull and concave. **Proper exciple** 17–40 µm thick. **Thalline exciple** 140–190 µm thick. **Epihymenium** brown, 10–20 µm thick. **Hymenium** hyaline, 85–110 µm thick. **Hypothecium** hyaline, 35–55 µm thick. **Asci** clavate, 8-spored, 60–100 × 22–30 µm. **Ascospores** hyaline, ellipsoid, polarilocular, 13–18 × 7–11 µm. **Paraphyses** moniliform, septate, cylindrical cells 3–10 × 1–2.5 µm, with internally brown terminal cells. **Pycnidia** roccella type (Ryan et al. 2002), globose to pyriform, 115–200 × 85–200 µm dark brown ostiole, long filiform hyaline conidia, 17–24 × 1 µm.

**Ecology.** Saxicolous, calcareous, known only from Deosai Plains, Gilgit-Baltistan, occurring at elevations between 4,117 m and 4,651 m in extremely cold conditions.

**Chemical study:** K -ve, C -ve, KC -ve, UV +ve (light green), hymenium initially blue then turning dark orange after Lugol's solution. Substictic acid detected through TLC.

**Additional material examined.** PAKISTAN. GILGIT BALTISTAN: Deosai Plains, 35°7'22.48"N, 75°36'35.09"E, elev. 4,177 m, on rocks, 3 September 2020, M. Usman & M. Shafiq DEO129 (LAH, paratype; LAH37194; GenBank OR037224 [ITS], OR037220 [LSU], OR037260 [mt SSU].

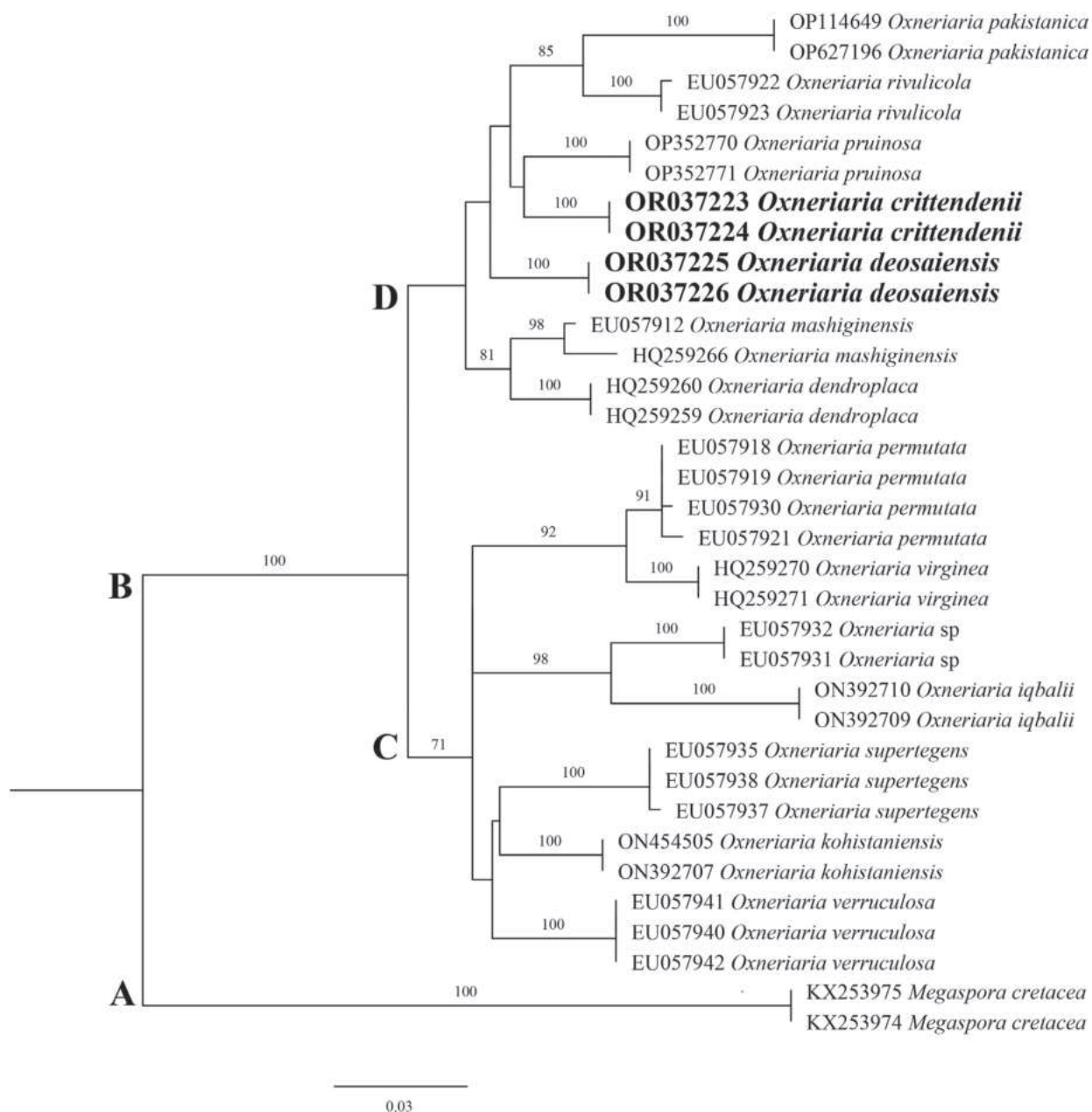


**Figure 3.** Phylogenetic tree of the genus *Oxneriaria* as generated by Maximum Likelihood (ML) analyses, based on ITS sequences. Bootstrap values > 70%, based on 1,000 replicates are shown at the branches. Novel sequences, generated during this study, are shown in bold.

***Oxneriaria deosaiensis* Khalid & Usman**

MycoBank No: 848890

Fig. 2

**Etymology.** The specific epithet “*deosaiensis*” refers to the Deosai Plains, the type locality.

**Holotype.** Pakistan. Gilgit Baltistan: Deosai Plains (35°0'10.06"N, 75°15'0.45"E, elev. 4,689 m) on soil, 13 May 2019, M. Usman DEO206 (LAH, holotype; LAH37200). GenBank OR037225 [ITS], OR037221 [LSU], OR037261 [mt SSU].

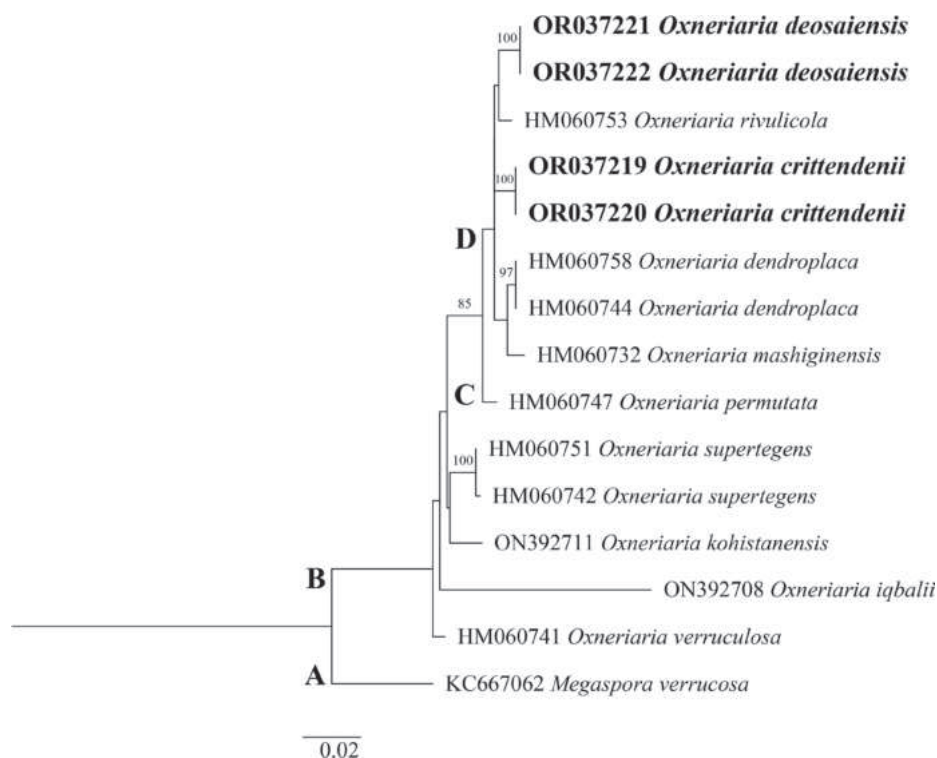


**Figure 4.** Phylogenetic tree of the genus *Oxneriaria* as generated by Maximum Likelihood (ML) analyses, based on LSU sequences. Bootstrap values > 70%, based on 1,000 replicates are shown at the branches. Novel sequences, generated during this study, are shown in bold.

**Diagnosis.** It differs from its closest species *O. pruinosa* by having lobate black margins (vs. non-lobate), K test positive light brown (vs. K positive yellow), KC test positive dark brown (vs. KC negative), apothecia epruinose (vs. densely pruinose), distinct proper-exciple 30–50  $\mu\text{m}$  wide (vs. indistinct) and polarilocular ellipsoid ascospores (vs. simple ellipsoid).

**Description.** Thallus crustose, epilithic, irregular, 1.5–2 cm across, zonate, areolate to poorly bullate up to 0.8 mm in diam. to lobate up to 1.5 mm at margins, determinate and radiate. **Hypothallus** light grey. **Upper surface** dull grey, black at margins. **Thallus** heteromerous, upper cortex 20–55  $\mu\text{m}$  thick, paraplectenchymatous hyaline cells 6–15  $\mu\text{m}$  in diam. **Algal layer** discontinuous, 50–90  $\mu\text{m}$  thick, photobiont *Trebouxia* sp, coccoid cells, globose to sub-globose, 13–21  $\mu\text{m}$  in diam. **Medulla** and **lower cortex** not differentiated and consisting of paraplectenchymatous, globose to sub-globose hyaline cells, 5–12  $\mu\text{m}$  diam.

**Apothecia** without stipe, aspicilioid, epruinose, one apothecium per areole, rounded, 520–700  $\mu\text{m}$  in diam., with black disc 350–550  $\mu\text{m}$  in diam., dull, concave. **Proper exciple**, 30–50  $\mu\text{m}$  thick. **Thalline exciple** 90–145  $\mu\text{m}$  thick. **Epihymenium** brown, 10–24  $\mu\text{m}$  thick. **Hymenium** hyaline, 90–160  $\mu\text{m}$  thick. **Hypothecium** hyaline, 50–90  $\mu\text{m}$  thick. **Asci** clavate, 8-spored, 75–110  $\times$  16–27  $\mu\text{m}$ . **Ascospores** hyaline, ellipsoid, polarilocular 11–18  $\times$  7–10  $\mu\text{m}$ . **Paraphyses** moniliform, septate, cylindrical cells 4–10  $\times$  1–2  $\mu\text{m}$ , with internally brown terminal cells. **Pycnidia** roccella type (Ryan et al. 2002), globose to pyriform, 230–320  $\times$  210–280  $\mu\text{m}$  dark brown ostiole, long filiform hyaline conidia, 19–35  $\times$  1  $\mu\text{m}$ .

**Ecology.** Saxicolous, Quartz, known only from Deosai Plains, Gilgit-Baltistan, occurring at elevations between 4,364 m and 4,689 m in extreme cold conditions.

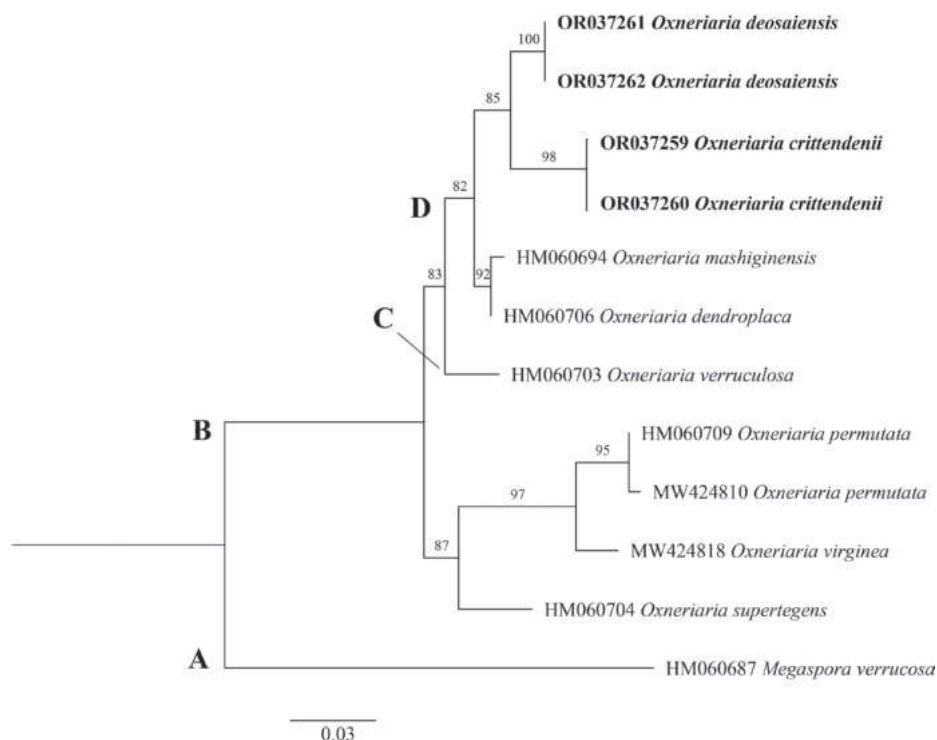


**Figure 5.** Phylogenetic tree of the genus *Oxneriaria* as generated by Maximum Likelihood (ML) analyses, based on mt SSU sequences. Bootstrap values > 70%, based on 1,000 replicates are shown at the branches. Novel sequences, generated during this study, are shown in bold.

**Chemical study.** K +ve (light brown), C -ve, KC +ve (dark brown), UV +ve (light green), hymenium initially blue then turning dark blue after Lugol's solution. Substictic acid and two unknown substances detected through TLC.

**Additional material examined.** PAKISTAN. GILGIT BALTISTAN: Deosai Plains, 35°6'28.58"N, 75°44'27.37"E, 4,364 m, on rocks, 15 May 2019, M. Usman & Kamran Habib DEO666 (LAH, paratype; LAH37416; GenBank OR037226 [ITS], OR037222 [LSU], OR037262 [mt SSU]).

## Discussion

The genus *Oxneriaria* was introduced by Haji-Moniri et al. (2017) and is characterised by the presence of radiating thalli with a wrinkled or lobate peripheral zone, relatively small ascospores, the possible presence of substictic acid and phylogenetic divergence from neighbouring taxa. Four species of the genus *Oxneriaria* have recently been described from Pakistan from relatively high altitude locations, namely *O. iqbalii* from Dassu and Miandam (at elev. 1,607 m and 1,800 m), *O. kohistaniensis* from Dassu and Razika Seo Valley (at elev. 1,607 m and 1,811 m), *O. pakistanica* from Darel Valley (at elev. 1,900 m and 2,000 m) and *O. pruinosa* from Chitral (at elev. 2,550 m) (Asghar et al. 2023; Iqbal et al. 2023; Zulfiqar et al. 2023). By contrast, the two proposed new species, *O. crittendenii* and *O. deosaiensis*, reported in the current study, were found occurring at very high altitude elevations between 4,117 m and 4,689 m in environments subject to periodic extremely cold conditions.

The two new proposed species share some morphological similarities to each other such as dull coloured grey to brown, areolate to bullate, heteromeric thalli with black lobate margins, a discontinuous algal layer, medulla consisting of paraplectenchymatous cells and concave black apothecia showing as light green in response to UV. However, the two species, *O. crittendenii* and *O. deosaiensis*, also exhibit differences from each other in thallus growth-pattern (orbicular vs. irregular), hypothallus appearance (shiny brown vs. light grey), algal layer (90–140 µm vs. 50–90 µm), size of algal cells (6–14 µm vs. 13–21 µm), size of lower cortex cells (25–45 µm vs. 5–12 µm), apothecia (pruinose 0.6–0.95 mm diam. vs. epruinose 0.52–0.7 mm diam.) and thalline exciple (140–190 µm vs. 90–145 µm thick) and hypothecium (35–55 µm vs. 50–90 µm thick), respectively. Additionally, in response to Lugol's solution, the hymenium of *O. crittendenii* turned dark orange, whilst that of *O. deosaiensis* turned dark blue.

The two new proposed species *O. crittendenii* and *O. deosaiensis* were found to be phylogenetically closely related to certain other *Oxneriaria* species, in particular *O. pakistanica*, *O. pruinosa* and *O. rivulicola*, although clear molecular differences were apparent in the ITS, LSU and mt SSU sequences. There were, in addition, some striking phenotypic characters showing the distinctive characteristics of the novel taxa along with the closest species and these are shown in Table 2.

In addition to the differences of Table 2, *O. crittendenii* and *O. deosaiensis* have polarilocular ellipsoid ascospores whilst *O. pakistanica*, *O. pruinosa* and *O. rivulicola* have simple ellipsoid ascospores. Chemically, *O. crittendenii* showed no change to K and KC tests, whilst the thalli of *O. deosaiensis* turned light brown and dark brown in response to K and KC tests, respectively. By contrast to these tests, *O. pakistanica* showed positive K (yellowish green) and KC (light green) tests, *O. pruinosa* showed K positive (yellow) and KC negative tests (Asghar et al. 2023; Iqbal et al. 2023), whilst *O. rivulicola* showed no change to K and KC tests (Magnusson 1923; Nordin et al. 2011).

**Table 2.** Comparison of closely-related species of *Oxneriaria* with novel taxa.

Characters	<i>O. crittendenii</i>	<i>O. deosaiensis</i>	<i>O. pakistanica</i>	<i>O. pruinosa</i>	<i>O. rivulicola</i>
<b>Margins</b>	lobate, determinate, black	lobate, determinate, black	areolate, indeterminate, whitish-grey	lobate, determinate, whitish-grey	Non-elongate areoles
<b>Hypothallus</b>	shiny light brown	light grey	light brown	light grey	light grey
<b>Upper Cortex</b>	20–60 µm thick	20–55 µm thick	10–25 µm thick	30–50 µm thick	25–40 µm thick
<b>Algal Layer (thick)</b>	90–140 µm	50–90 µm	30–50 µm	70–140 µm	30–50 µm
<b>Algal Cells (in diam.)</b>	6–14 µm	13–21 µm	10–15 µm	10–17 µm	7–15 µm
<b>Apothecia (in diam.)</b>	pruinose, 450–700 µm	epruinose, 520–700 µm	epruinose, up to 2 mm	densely pruinose, up to 1 mm	up to 2 mm
<b>Hypothecium (thick)</b>	35–55 µm	50–90 µm	90–170 µm	50–120 µm	80–100 µm
<b>Asci</b>	60–100 × 22–30 µm	75–110 × 16–27 µm.	60–80 × 30–40 µm	55–80 × 25–42 µm	70–85 × 20–24 µm
<b>Pycnidia</b>	roccella type	roccella type	absent	globose	globose
<b>Conidia</b>	17–24 × 1 µm	19–35 × 1 µm	absent	14–18 × 1 µm	30–37 × 1 µm
<b>References</b>	<b>This Study</b>	<b>This Study</b>	<b>Iqbal et al. (2023)</b>	<b>Asgar et al. (2023)</b>	<b>Magnusson (1923); Nordin et al. (2011)</b>

## Conclusions

In summary, as a result of all the distinct phenotypic and phylogenetic characters, we here propose the addition of two new species in the genus *Oxneriaria* from high altitudinal environments in Pakistan. Whilst these were found infrequently, the detection of the two new species *O. crittendenii* and *O. deosaiensis* add to reports of the discovery of other new species of lichen-forming fungi from the Deosai Plains in Pakistan (Usman et al. 2021, 2023), emphasising the importance of this region as a site of arctic-alpine biodiversity.

## Acknowledgements

The corresponding author (MU) thanks the Higher Education Commission of Pakistan for funding research work under the International Research Support Initiative Program (IRSIP) scheme. All the authors are grateful to Prof. Dr. Peter D Crittenden (School of Life Sciences, University of Nottingham, UK) and Prof. Dr. Pradeep Kumar Divakar (Departamento de Farmacología, Farmacognosia y Botánica Facultad de Farmacia, Universidad Complutense de Madrid Plaza de Ramón y Cajal, Madrid, Spain) for providing lichen herbarium specimens for thin layer chromatography.

## Additional information

### Conflict of interest

The authors have declared that no competing interests exist.

### Ethical statement

No ethical statement was reported.

### Funding

This research was supported by Higher Education Commission of Pakistan for funding research work under the International Research Support Initiative Program (IRSIP) scheme.

### Author contributions

Conceptualization: MU. Data curation: MU. Formal analysis: MU. Funding acquisition: ANK. Investigation: MU. Methodology: MU. Software: MU. Supervision: CMW, ANK, PSD, MB. Validation: ANK, MB, CMW, PSD. Visualization: CMW, ANK, MB, PSD. Writing - original draft: MU. Writing - review and editing: CMW, ANK, PSD, MB.

### Author ORCIDs

Muhammad Usman  <https://orcid.org/0000-0002-3490-058X>

Paul S. Dyer  <https://orcid.org/0000-0003-0237-026X>

Matthias Brock  <https://orcid.org/0000-0003-2774-1856>

Christopher M. Wade  <https://orcid.org/0000-0002-1269-9694>

Abdul Nasir Khalid  <https://orcid.org/0000-0002-5635-8031>

### Data availability

All of the data that support the findings of this study are available in the main text.

## References

- Akaike H (1974) A new look at the statistical model identification. *IEEE Transactions on Automatic Control* 19(6): 716–723. <https://doi.org/10.1109/TAC.1974.1100705>
- Asghar HS, Usman M, Habib K, Khalid AN (2023) [in review] Genus *Oxneriaria* (Megasporeaceae; lichenized Ascomycota) in Pakistan with the description of two new species. *Cryptogamie. Mycologie*.
- Chesnokov S, Konoreva L, Paukov A (2018) New species and records of saxicolous lichens from the Kodar Range (Trans-Baikal Territory, Russia). *Plant and Fungal Systematics* 63(1): 11–21. <https://doi.org/10.2478/pfs-2018-0003>
- Darriba D, Taboada GL, Doallo R, Posada D (2012) jModelTest 2: More models, new heuristics and parallel computing. *Nature Methods* 9(8): 772–772. <https://doi.org/10.1038/nmeth.2109>
- Friedl T, Büdel B (2008) Photobionts. In: Nash TH III (Ed.) *Lichen Biology*. Cambridge University Press, Cambridge, 7–26. <https://doi.org/10.1017/CBO9780511790478.003>
- Gardes M, Bruns TD (1993) ITS primers with enhanced specificity for basidiomycetes-application to the identification of mycorrhizae and rusts. *Molecular Ecology* 2(2): 113–118. <https://doi.org/10.1111/j.1365-294X.1993.tb00005.x>
- Gouy M, Guindon S, Gascuel O (2010) SeaView version 4: A multiplatform graphical user interface for sequence alignment and phylogenetic tree building. *Molecular Biology and Evolution* 27(2): 221–224. <https://doi.org/10.1093/molbev/msp259>
- Haji-Moniri M, Gromakova AB, Lőkös L, Kondratyuk SY (2017) New members of the Megasporeaceae (Pertusariales, lichenforming Ascomycota): *Megaspora iranica* spec. nova and *Oxneriaria* gen. nova. *Acta Botanica Hungarica* 59(3–4): 343–370. <https://doi.org/10.1556/034.59.2017.3-4.5>
- Halicı MG, Bartak M, Güllü M (2018) Identification of some lichenized fungi from James Ross Island (Antarctic Peninsula) using nrITS markers. *New Zealand Journal of Botany* 56(3): 276–290. <https://doi.org/10.1080/0028825X.2018.1478861>
- Hall TA (1999) BioEdit: A user-friendly biological sequence alignment editor and analysis program for Windows 95/98/NT. *Nucleic Acids Symposium Series* 41: 95–98.
- Hussain Z (2014) Vegetation analysis, grassland productivity and carrying capacity of Deosai national park, Gilgit-Baltistan. PhD Thesis, Pir Mehar Ali Shah Arid Agriculture University Rawalpindi, Pakistan.
- Hussain Z, Mirza SN, Ashraf MI, Nizami SM (2015) Grassland productivity and carrying capacity of Deosai National Park, Gilgit-Baltistan. *Pakistan Journal of Agricultural Research* 53: 437–452.
- Iqbal MS, Usman M, Habib K, Khalid AN (2023) *Oxneriaria pakistanica* sp. nov. (Megasporeaceae, Pertusariales, Ascomycota) from Darel Valley, Gilgit Baltistan, Pakistan. *Phytotaxa* 579(2): 125–131. <https://doi.org/10.11646/phytotaxa.579.2.6>
- Magnusson AH (1923) New or interesting Swedish Lichens I. *Botaniska Notiser* 1923: 401–416. <https://doi.org/10.25291/VR/1923-VLR-401>
- Nordin A, Tibell L, Owe-Larsson BR (2007) A preliminary phylogeny of *Aspicilia* in relation to morphological and secondary product variation. *Bibliotheca Lichenologica* 96: 247–266.
- Nordin A, Savič S, Tibell L (2010) Phylogeny and taxonomy of *Aspicilia* and Megasporeaceae. *Mycologia* 102(6): 1339–1349. <https://doi.org/10.3852/09-266>
- Nordin A, Björn OL, Tibell L (2011) Two new *Aspicilia* species from Fennoscandia and Russia. *Lichenologist* (London, England) 43(1): 27–37. <https://doi.org/10.1017/S0024282910000629>

- Orange A, James PW, White FJ (2010) Microchemical methods for the identification of lichens. British Lichen Society, London.
- Rambaut A (2012) FigTree v1.4.2. <http://tree.bio.ed.ac.uk/software/figtree> [Accessed 02 January 2023]
- Ryan BD, Bungartz F, Nash TH (2002) Morphology and anatomy of the lichen thallus. Lichen flora of the Greater Sonoran Desert Region. I. Lichens unlimited. Arizona State University, Tempe, 8–40.
- Sohrabi M, Rico SDLVJ, Halici MG, Shrestha G, Stenroos S (2013) *Teuvoa*, a new lichen genus in Megasperaceae (Ascomycota: Pertusariales), including *Teuvoa junipericola* sp. nov. Lichenologist (London, England) 45(3): 347–360. <https://doi.org/10.1017/S0024282913000108>
- Stewart RR (1961) The flora of Deosai plains. Pakistan Journal of Forestry 11: 225–295.
- Usman M, Khalid AN (2020) *Termitomyces acriumbonatus* sp. nov. (Lyophyllaceae, Agaricales) from Pakistan. Phytotaxa 477: 217–228. <https://doi.org/10.11646/phytotaxa.477.2.6>
- Usman M, Dyer PS, Khalid AN (2021) A novel arctic-alpine lichen from Deosai National Park, Gilgit Baltistan, Pakistan. The Bryologist 124(4): 484–493. <https://doi.org/10.1639/0007-2745-124.4.484>
- Usman M, Firdous Q, Dyer PS, Khalid AN (2023) A new species of the genus *Anamylopsora* (Baeomycetaceae; Ascomycota) from Deosai National Park, Gilgit-Baltistan, Pakistan. Lichenologist (London, England) 55(3–4): 125–132. <https://doi.org/10.1017/S002428292300018X>
- WAPDA (2012) Meteorological Data on Deosai Plains (Watersheds of Sadpara Dam Skardu). Unpublished Data recorded from Water & Power Development Authority, Government of Pakistan, Lahore.
- White TJ, Bruns T, Lee S, Taylor JW (1990) Amplification and direct sequencing of fungal ribosomal RNA genes for phylogenetics. In: Innis MA, Gelfand DH, Sninsky JJ, White TJ (Eds) PCR Protocols: A Guide to Methods and Applications. Academic Press Inc., New York, 315–322. <https://doi.org/10.1016/B978-0-12-372180-8.50042-1>
- Woods CA, Kilpatrick CW, Rafiq M, Shah M, Khan W (1997) Biodiversity and conservation of the Deosai Plateau, Northern Areas, Pakistan. In: Mufti SA, Woods CA, Hasan SA (Eds) Biodiversity of Pakistan. Pakistan Museum of Natural History, Islamabad, Pakistan, 33–61.
- Zakeri Z, Gasparyan A, Aptroot A (2016) A new corticolous *Megaspora* (Megasperaceae) species from Armenia. Willdenowia 46(2): 245–251. <https://doi.org/10.3372/wi.46.46205>
- Zoller S, Scheidegger C, Sperisen C (1999) PCR primers for the amplification of mitochondrial small subunit ribosomal DNA of lichen-forming ascomycetes. Lichenologist (London, England) 31(5): 511–516. <https://doi.org/10.1006/lich.1999.0220>
- Zulfiqar R, Asghar HS, Habib K, Khalid AN (2023) Two new species of the genus *Oxneriaria* (lichenized Ascomycota: Megasperaceae) from Pakistan. Plant Systematics and Evolution 309(1): 2. <https://doi.org/10.1007/s00606-022-01836-w>



# Two new species of Sordariomycetes (Chaetomiaceae and Nectriaceae) from China

Hai-Yan Wang<sup>1</sup>, Xin Li<sup>1</sup>, Chun-Bo Dong<sup>1</sup>, Yan-Wei Zhang<sup>2</sup>, Wan-Hao Chen<sup>3</sup>, Jian-Dong Liang<sup>3</sup>, Yan-Feng Han<sup>1</sup>

<sup>1</sup> Institute of Fungus Resources, Department of Ecology, College of Life Science, Guizhou University, Guiyang 550025 Guizhou, China

<sup>2</sup> School of Biological Sciences, Guizhou Education University, Guiyang 550018, China

<sup>3</sup> Center for Mycomedicine Research, Basic Medical School, Guizhou University of Traditional Chinese Medicine, Guiyang 550025, Guizhou, China

Corresponding author: Yan-Feng Han (swallow1128@126.com)

## Abstract

Rich and diverse fungal species occur in different habitats on the earth. Many new taxa are being reported and described in increasing numbers with the advent of molecular phylogenetics. However, there are still a number of unknown fungi that have not yet been discovered and described. During a survey of fungal diversity in different habitats in China, we identified and proposed two new species, based on the morphology and multi-gene phylogenetic analyses. Herein, we report the descriptions, illustrations and molecular phylogeny of the two new species, *Bisifusarium keratinophilum* **sp. nov.** and *Ovatospora sinensis* **sp. nov.**

**Key words:** Fungal taxonomy, mesophilic fungus, phylogeny, thermophilic fungus, two new taxa



Academic editor: Huzefa Raja

Received: 20 October 2023

Accepted: 11 December 2023

Published: 7 March 2024

**Citation:** Wang H-Y, Li X, Dong C-B, Zhang Y-W, Chen W-H, Liang J-D, Han Y-F (2024) Two new species of Sordariomycetes (Chaetomiaceae and Nectriaceae) from China. MycoKeys 102: 301–315. <https://doi.org/10.3897/mycokeys.102.114480>

**Copyright:** © Hai-Yan Wang et al.

This is an open access article distributed under terms of the Creative Commons Attribution License (Attribution 4.0 International – CC BY 4.0).

## Introduction

The species diversity of fungi on earth is extremely rich, with some studies suggesting that there are as many as 5.1 million species of fungi (Blackwell 2011), while others believe that there are 3.8 million species of fungi on the earth (Hawksworth and Lücking 2017). More recent estimates suggest 2.5 million fungal species (Niskanen et al. 2023). With the rapid increase in fungal DNA sequence data obtained, the species names and numbers of fungi are constantly updated (Wijayawardene et al. 2020). Fungi are one of the most diverse microbial communities on Earth and play a vital role in ecosystem processes and functions (Hyde et al. 2020). Meanwhile, fungi have an important influence on human life and production. On the one hand, they can produce a large number of biometabolites available to humans, such as various amino acids, enzymes, sugars, lipids, vitamins and antibiotics (Zhang et al. 2013; de Cassia Pereira et al. 2015; Pejin et al. 2019; Yokokawa et al. 2021; Arsenault et al. 2022; Mapook et al. 2022). On the other hand, they also infect humans, animals and plants and then cause great harm to human health and national economies (Fisher et al. 2012; Fisher et al. 2020; Zhang et al. 2023). At the same time, fungi widely exist

in various habitats, such as forests, grasslands, zoos, hospitals, agricultural land (Li et al. 2014; Shao et al. 2021; Yao et al. 2021; Liu et al. 2022).

Due to factors such as global climate change, urban growth and environmental pollution, there is an increasingly accelerated loss of natural habitats worldwide, which, in turn, leads to a decrease in species diversity and the abundance of non-human organisms (Driscoll et al. 2018; Kurth et al. 2021). At present, the threat to species and their extinction rates have risen to dangerous levels threatening biological diversity. Latest data from the International Union for Conservation of Nature (IUCN) has fuelled growing societal concern, indicating that 28% of all assessed species are threatened with extinction, which is a nerve-wrackingly high figure (Löbl et al. 2023). In times of a biodiversity crisis, the community structure and species diversity of fungi are also inevitably affected by various factors. In many habitats, it is suspected that species are disappearing before they are discovered (Wang et al. 2018; Löbl et al. 2023). Therefore, it is necessary to accelerate the intensity and speed of investigating. Study on the diversity of fungal species on the earth should be one of the important issues of modern biology (Löbl et al. 2023).

Fortunately, our team has discovered many new fungal species during the investigation of fungal diversity in different habitats in China (Li et al. 2022a, b; Ren et al. 2022; Zhang et al. 2023; Wang et al. 2023). In this study, based on the morphology and multi-gene phylogenetic analyses, two new species from zoo soils were identified and described, respectively.

## Materials and methods

### Sample collection and fungal isolation

Soil samples were collected from two zoos, Shandong Province, China. Samples from 3–10 cm below the soil surface were collected, and placed in Ziploc plastic bags and brought back to the laboratory. Then, the 2 g collected samples were placed into a sterile conical flask containing 20 ml sterile water and thoroughly shaken using a Vortex vibration meter. Next, the suspension was diluted to a concentration of  $10^{-3}$ . Subsequently, 1 ml of the diluted sample was added to a sterile Petri dish and mixed with Sabouraud's dextrose agar (SDA; peptone 10 g/l, dextrose 40 g/l, agar 20 g/l, 3.3 ml of 1% Bengal red aqueous solution) medium containing 50 mg/l penicillin and 50 mg/l streptomycin. After the plates were incubated at 25 °C and 45 °C for 1–2 weeks, single colonies were transferred from the plates to new potato dextrose agar (PDA, potato 200 g/l, dextrose 20 g/l, agar 20 g/l) plates.

### Morphological study

The target strains were transferred to plates of malt extract agar (MEA), oatmeal agar (OA) and potato dextrose agar (PDA) and were incubated at 25 °C and 45 °C. After seven days, their colony characteristics (the colony colours and diameters) on the surface and reverse of inoculated Petri dishes were observed and recorded and microscopic characteristics (fungal hyphae and conidiogenous structures) were examined and captured by making direct wet mounts with 25% lactic acid on PDA, with an optical microscope (DM4 B, Leica). The

ex-types of two new species were deposited in the China General Microbiological Culture Collection Center (CGMCC) and living cultures and dried holotypes were deposited in the Institute of Fungus Resources, Guizhou University (GZUIFR = GZAC). Taxonomic descriptions and nomenclature of two new species were recorded in MycoBank (<https://www.mycobank.org/>).

### DNA extraction, PCR amplification and sequencing

Total genomic DNA was extracted using the BioTeke Fungus Genomic DNA Extraction kit (DP2032, BioTeke) following the manufacturer's instruction. Primer combinations such as ITS1/ITS4 (White et al. 1990), LR0R/LR5 (Wang et al. 2022a), EF1-728F/EF2 (O'Donnell et al. 1998; Carbone and Kohn 1999), CAL-228F/CAL-2Rd (Carbone and Kohn 1999; Lombard et al. 2015), rpb2-5F2/rpb2-7CR (Sung et al. 2007; O'Donnell et al. 2007) and T1/TUB4Rd (O'Donnell and Cigelnik 1997; Woudenberg et al. 2009) were used for amplification of the internal transcribed spacers (ITS), the 28S nrRNA locus (LSU), translation elongation factor 1-alpha gene region (*tef1*), calmodulin gene (*cmdA*), RNA polymerase II second largest subunit gene (*rpb2*) and beta-tubulin gene (*tub2*), respectively. The PCR products were sent to Quintarabio (Wuhan, China) for purification and sequencing. The new sequences were submitted to GenBank (<https://www.ncbi.nlm.nih.gov/>) (Table 1).

**Table 1.** Strain and GenBank accession included in phylogenetic analyses.

Species	Strains	ITS	LSU	<i>tef1</i>	<i>cmdA</i>	<i>rpb2</i>	<i>tub2</i>	Reference
<i>Bisifusarium aseptatum</i>	LC13607	MW016390	MW016390	MW580430	MW566257	MW474376	MW533717	Wang et al. (2022b)
	LC13608	MW016391	MW016391	MW580431	MW566258	MW474377	MW533718	Wang et al. (2022b)
<i>Bisifusarium allantoides</i>	UBOCC-A-120035	MW654536	MW654511	MW811075	MW811017	MW811060	MW811090	Savary et al. (2021)
	UBOCC-A-120036T	MW654548	MW654523	MW811087	MW811029	MW811072	MW811102	Savary et al. (2021)
	UBOCC-A-120037	MW654549	MW654524	MW811088	MW811030	MW811073	MW811103	Savary et al. (2021)
<i>Bisifusarium biseptatum</i>	CBS 110311T	MW654547	MW654522	MW811086	MW811028	MW811071	MW811101	Savary et al. (2021)
<i>Bisifusarium dimerum</i>	MNHN-RF-05625T	MW654546	MW654521	MW811085	MW811027	–	MW811100	Savary et al. (2021)
	CBS 108944T	JQ434586	JQ434514	KR673912	KM231365	KM232363	EU926400	Lombard et al. (2015)
<i>Bisifusarium penicilloides</i>	UBOCC-A-120021T	MW654542	MW654517	MW811081	MW811023	MW811066	MW811096	Savary et al. (2021)
	UBOCC-A-120034	MW654541	MW654516	MW811080	MW811022	MW811065	MW811095	Savary et al. (2021)
	VTT-D-041022	MW654535	MW654510	MW811074	MW811016	MW811059	MW811089	Savary et al. (2021)
<i>Bisifusarium delphinoides</i>	CBS 120718T	EU926229	EU926229	EU926296	KM231363	–	EU926362	Lombard et al. (2015)
	CBS 110140	MW827603	–	EU926302	–	–	EU926368	Park et al. (2019)
	CBS 110310	EU926240	EU926240	EU926307	–	–	EU926373	Sun et al. (2017)
<i>Bisifusarium nectrioides</i>	CBS 176.31T	EU926245	EU926245	EU926312	KM231362	–	EU926378	Lombard et al. (2015)
<i>Bisifusarium penzigii</i>	CBS 116508	EU926256	EU926256	EU926323	–	–	EU926389	Sun et al. (2017)
<i>Bisifusarium domesticum</i>	CBS 102407	EU926221	EU926221	EU926288	–	–	EU926355	Sun et al. (2017)
	CBS 244.82	EU926220	EU926220	EU926287	–	–	EU926354	Sun et al. (2017)
<i>Bisifusarium lunatum</i>	CBS 632.76T	EU926224	EU926224	EU926291	KM231367	–	EU926357	Lombard et al. (2015)
<i>Bisifusarium tonghuanum</i>	CGMCC3.17369	KX790413	KX790414	KX790418	–	–	KX790417	Sun et al. (2017)
	CGMCC3.17370	KX790415	KX790416	KX790420	–	–	KX790419	Sun et al. (2017)
<i>Bisifusarium lovelliae</i>	BRIP 75047a	OQ629340	–	–	–	OQ626864	–	Tan et al. (2023)
<i>Bisifusarium keratinophilum</i>	CGMCC 3.23621T	OP693473	OP693469	OR168082	OR043998	OR168079	OR168085	This study
	GZUIFR 22.371	OP693474	OP693470	OR168083	OR043999	OR168080	OR168086	This study
	GZUIFR 22.372	OP693475	OP693471	OR168084	OR044000	OR168081	OR168087	This study

Species	Strains	ITS	LSU	<i>tef1</i>	<i>cmdA</i>	<i>rpb2</i>	<i>tub2</i>	Reference
<i>Longinectria lagenoides</i>	UBOCC-A-120039	MW654539	MW654514	MW811078	MW811020	MW811063	MW811093	Savary et al. (2021)
<i>Longinectria verticilliforme</i>	UBOCC-A-120043	MW654540	MW654515	MW811079	MW811021	MW811064	MW811094	Savary et al. (2021)
<i>Ovatospora amygdalispora</i>	CBS 672.82T	–	–	–	–	MZ342991	MZ343030	Wang et al. (2022a)
<i>Ovatospora angularis</i>	LC3973	KP336768	KP336817	–	–	KT149491	KP336866	Wang et al. (2022a)
<i>Ovatospora unipora</i>	CBS 109.83T	KX976689	KX976787	–	–	KX976902	KX977037	Wang et al. (2016)
<i>Ovatospora brasiliensis</i>	CBS 140.50	KX976683	KX976781	–	–	KX976896	KX977031	Wang et al. (2016)
<i>Ovatospora medusarum</i>	CBS 148.67T	KX976684	KX976782	–	–	KX976897	KX977032	Wang et al. (2016)
<i>Ovatospora mollicella</i>	CBS 583.83T	KX976685	KX976783	–	–	KX976898	KX977033	Wang et al. (2016)
<i>Ovatospora pseudomollicella</i>	CBS 251.75T	KX976686	KX976784	–	–	KX976899	KX977034	Wang et al. (2016)
<i>Ovatospora senegalensis</i>	CBS 728.84T	KX976687	KX976785	–	–	KX976900	KX977035	Wang et al. (2016)
<i>Trichocladium asperum</i>	CBS 903.85T	LT993632	LT993632	–	–	LT993551	LT993713	Wang et al. (2022a)
<i>Trichocladium acropullum</i>	CBS 114580T	LT993626	LT993626	–	–	LT993545	LT993707	Wang et al. (2022a)
<i>Trichocladium amorphum</i>	CBS 127763T	LT993628	LT993628	–	–	LT993547	LT993709	Wang et al. (2022a)
<i>Trichocladium antarcticum</i>	CBS 123565T	LT993629	LT993629	–	–	LT993548	LT993710	Wang et al. (2022a)
<i>Trichocladium beniowskiae</i>	CBS 757.74T	LT993635	LT993635	–	–	LT993554	LT993716	Wang et al. (2022a)
<i>Trichocladium gilmaniellae</i>	CBS 388.75T	LT993638	LT993638	–	–	LT993557	LT993719	Wang et al. (2022a)
<i>Thermochaetoides dissita</i>	CBS 180.67T	–	MK919319	–	–	MK919375	MK919433	Wang et al. (2022a)
<i>Thermochaetoides thermophila</i>	CBS 144.50T	–	MK919314	–	–	KM655436	MK919428	Wang et al. (2022a)
<b><i>Ovatospora sinensis</i></b>	<b>CGMCC40675T</b>	<b>OR016676</b>	<b>OR016679</b>	–	–	<b>OR043992</b>	<b>OR043995</b>	<b>This study</b>
	<b>GZUIFR 23.002</b>	<b>OR016677</b>	<b>OR016680</b>	–	–	<b>OR043993</b>	<b>OR043996</b>	<b>This study</b>
	<b>GZUIFR 23.003</b>	<b>OR016678</b>	<b>OR016681</b>	–	–	<b>OR043994</b>	<b>OR043997</b>	<b>This study</b>
<i>Triangularia verruculosa</i>	CBS 148.77	MK926874	MK926874	–	–	MK876836	MK926974	Wang et al. (2022a)
<i>Triangularia allahabadensis</i>	CBS 724.68T	MK926865	MK926865	–	–	MK876827	MK926965	Wang et al. (2022a)

Note: T=Ex-type; New isolates are in bold; The line “–” represents the absence of GenBank record; BRIP: Queensland Plant Pathology Herbarium, Australia; CBS: CBS-KNAW Fungal Biodiversity Centre, Utrecht, The Netherlands; CGMCC: The China General Microbiological Culture Collection Centre; GZUIFR: The Institute of Fungus Resources, Guizhou University, China; LC: Lei Cai’s personal culture collection, Beijing, China; MNHN: Museum National d’Histoire Naturelle culture collection, France; UBOCC: Université de Bretagne Occidentale Culture Collection, France; VTT: Culture Collection, Finland; *cmdA*: calm-odulin; ITS: the internal transcribed spacer region and intervening 5.8S nrRNA; LSU: 28S large subunit; *rpb2*: RNA polymerase II second largest subunit; *tef1*: translation elongation factor 1-alpha; *tub2*:  $\beta$ -tubulin.

## Phylogenetic analysis

In this study, the relevant sequences were obtained from GenBank (Table1). The sequence set was aligned and trimmed in MEGA v.6.06 (Tamura et al. 2013). We performed single gene and multi-gene phylogenetic analysis using ITS, LSU, *tef1*, *cmdA*, *rpb2* and *tub2* gene and found that the topology structures of the single-gene and multi-gene phylogenetic trees were consistent in PhyloSuite v.1.16. Therefore, multi-gene phylogenetic analysis was chosen in this study. The concatenation of loci and phylogenetic analysis were processed, using the “Concatenate Sequence” function in PhyloSuite v.1.16 (Zhang et al. 2020). The Maximum Likelihood (ML) and the Bayesian Inference (BI) methods were used for the phylogenetic construction of each loci dataset. The ML analysis was conducted in IQ-TREE v.1.6.11 (Nguyen et al. 2015) with 1000 bootstrap tests using the ultrafast algorithm (Minh et al. 2013). The BI analysis was performed in MrBayes v.3.2 (Ronquist et al. 2012) and Markov chain Monte Carlo (MCMC) simulations were used for 2,000,000 generations with a sampling frequency of every 100 generations. The phylogenetic trees were visualised using FigTree version 1.4.3 and subsequently edited in Adobe Photoshop.

## Results

### Phylogenetic analysis

The ITS regions of all isolates were sequenced and BLASTn searched in NCBI. Our isolates were identified as two genera, *Bisifusarium* L. Lombard, Crous & W. Gams and *Ovatospora* X. Wei Wang, Samson & Crous, respectively. The ITS sequences of the isolated strains were less than 97% similarity to the closest strains in GenBank and were considered as the potential new species.

To further determine the phylogenetic position of these isolated strains, we performed a multi-locus phylogenetic analysis, based on ITS, LSU, *tef1*, *cmdA*, *rpb2* and *tub2* gene. The phylogenetic trees (Figs 1, 3) using ML and BI analyses were consistent and strongly supported in most branches. The ML analysis for the combined dataset provided the best scoring tree. The best-fit evolutionary models for ML analysis and BI analysis are shown in Table 2.

In this study, three isolates of the genus *Bisifusarium* clustered in a well-separated clade with a high support value (BI/ML 1/100) (Fig. 1). Three isolates of the genus *Ovatospora* clustered together with a high support value (BI/ML

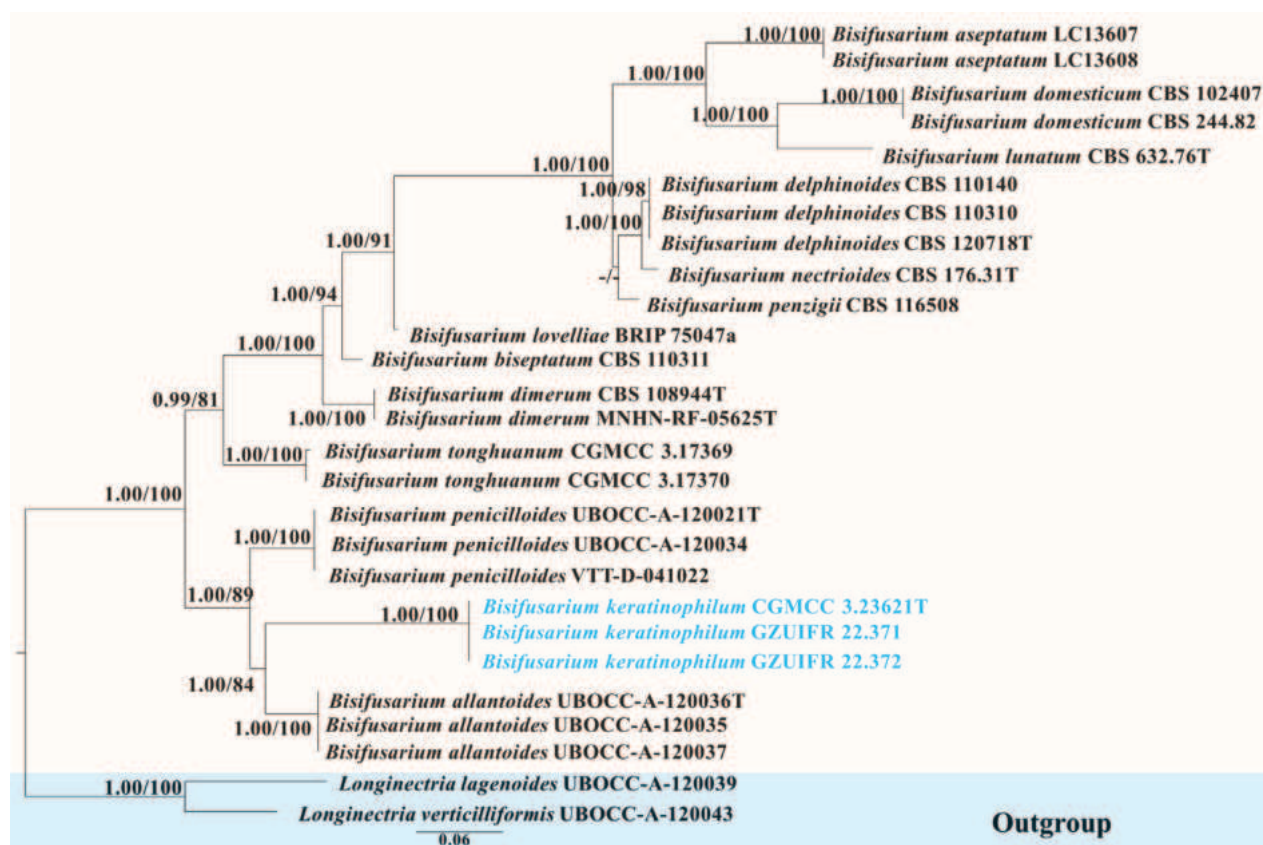


**Figure 1.** Phylogenetic tree of the genus *Bisifusarium* constructed from the dataset of ITS, LSU, *tef1*, *cmdA*, *rpb2* and *tub2*. Notes: Statistical support values (BI/ML) were shown at nodes. ML bootstrap values  $\geq 75\%$  and posterior probabilities  $\geq 0.90$  are shown above the internal branches. ‘-’ indicates the absence of statistical support ( $< 75\%$  for bootstrap proportions from ML analysis;  $< 0.90$  for posterior probabilities from Bayesian analysis). Three new strains are shown in blue font. BRIP: Queensland Plant Pathology Herbarium, Australia; CBS: CBS-KNAW Fungal Biodiversity Centre, Utrecht, The Netherlands; CG-MCC: The China General Microbiological Culture Collection Centre; GZUIFR: The Institute of Fungus Resources, Guizhou University, China; LC: Lei Cai’s personal culture collection, Beijing, China; MNHN: Museum National d’Histoire Naturelle culture collection, France; UBOCC: Université de Bretagne Occidentale Culture Collection, France; VTT: Culture Collection, Finland.

**Table 2.** The best-fit evolutionary models.

Genus		ITS	LSU	<i>tef1</i>	<i>cmdA</i>	<i>rpb2</i>	<i>tub2</i>
<i>Bisifusarium</i>	ML analysis	TIM2e+I+G4	K2P	TNe+R2	TIM3e+I+G4	TIM3e+I+G4	TIM3e+I+G4
	BI analysis	SYM+I+G4	K2P	K2P+G4	SYM+I+G4	SYM+I+G4	SYM+I+G4
<i>Ovatospora</i>	ML analysis	GTR+F+G4	TIM3+F+I			TIM3+F+G4	HKY+F+I+G4
	BI analysis	GTR+F+G4	GTR+F+I			GTR+F+I+G4	HKY+F+I+G4

1/100) (Fig. 3). Therefore, *Bisifusarium keratinophilum* H.Y. Wang, X. Li & Y.F. Han, sp. nov. and *Ovatospora sinensis* H.Y. Wang & Y.F. Han, sp. nov. are proposed according to the phylogenetic analysis.

## Taxonomy

**Sordariomycetes** O.E. Erikss. & Winka

**Hypocreales** Lindau

**Nectriaceae** Tul. & C. Tul.

***Bisifusarium*** L. Lombard, Crous & W. Gams

***Bisifusarium keratinophilum*** H.Y. Wang, X. Li & Y.F. Han, sp. nov.

MycoBank No: 849504

Fig. 2

**Etymology.** Referring to degradation properties of chicken feathers.

**Type.** CHINA: Shandong Province, Jinan City, Jinan Zoo (36°42'14"N, 116°58'55"E), soil, July 2021, Xin Li & Yan-Feng Han, ex-type CGMCC 3.23621 = GZUIFR 22.370, dried holotype GZAC 22.370.

**Description.** Culture characteristics: Colonies growing on MEA, OA and PDA after 7 days of incubation at 25 °C. On MEA, reaching up 20–25 mm diam., thick villiform, cream (RAL9001) at the centre, oyster white (RAL1013) at the edge, mostly regular in the margin, reverse light ivory (RAL 1015); On OA, reaching up 25–35 mm diam.; pure white (RAL9010), thin, villiform, mostly regular in the margin, reverse tele grey 4 (RAL7047); On PDA, reaching up 25–30 mm diam.; cream (RAL9001), thin, short villiform, mostly regular in the margin, reverse cream (RAL9001).

On PDA medium, **Hyphae** septate, hyaline, smooth, thick-walled, 1.5–3.5 µm wide. **Conidiophores** arising from hyphae, solitary, smooth, mostly clavate, 5–25 × 1–2.5 µm. Phialidic pegs arising from hyphae. **Monophialides** laterally on hyphae or phialidic pegs, cylindrical, erect. **Polyphialides** absent. **Macroconidia** produced by monophialidic conidiophores, mostly 0-1 septate, rarely 2-septate, mostly crescent, rarely clavate, 12–23.0 × 2.0–3.5 µm (av. 16 × 2.5 µm, n = 50). **Microconidia** produced by later phialidic pegs, monocelled, cymbiform, 6.0–9.5 × 1.5–2.5 µm (av. 7.5 × 2.0 µm, n = 50).

**Additional materials examined.** CHINA: Shandong Province, Jinan City, Jinan Zoo (36°42'14"N, 116°58'55"E), soil, July 2021, living cultures GZUIFR 22.371, GZUIFR 22.372.

**Notes.** Phylogenetically, our three strains (CGMCC 3.23621, GZUIFR 22.371 and GZUIFR 22.372) of *Bisifusarium keratinophilum* H.Y. Wang, X. Li & Y.F. Han sp. nov. clustered in a single separate clade with a high support value (BI/ML 1/100). Although it was closely related to *B. allantoides* O. Savary, M. Coton, E.

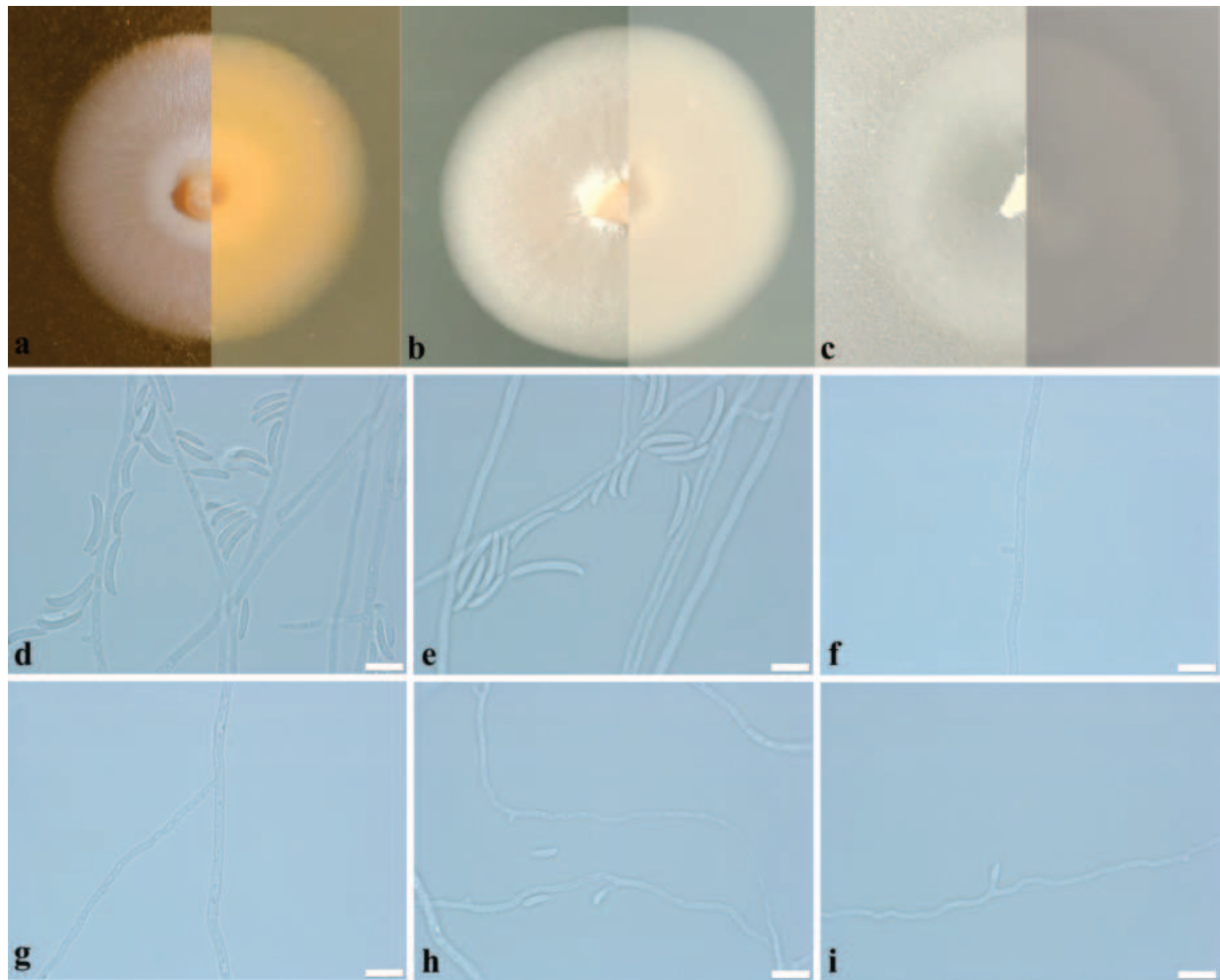


**Figure 2.** Morphological characteristics of *Bisifusarium keratinophilum* sp. nov. **a–c** front and reverse of colony on MEA, OA and PDA after 7 days at 25 °C **d, e** conidiophores and macroconidia **f** phialidic pegs **g** hyphae **h, i** microconidia. Scale bars: 10 µm (**d–i**).

Coton & J.L. Jany and *B. penicilloides* O. Savary, M. Coton, E. Coton & J.L. Jany in the phylogenetic tree, *B. allantoides* had allantoidal macroconidia (Savary et al. 2021) and *B. penicilloides* had ellipsoidal and reniform macroconidia and absent microconidia (Savary et al. 2021). *Bisifusarium keratinophilum* can be distinguished from the other previously described species by having crescent and clavate macroconidia and cymbiform microconidia.

Our team found that *B. keratinophilum* has the ability to degrade chicken feathers. Specific method: the spore suspension ( $10^7$  spores per millilitre) was inoculated into the fermentation medium containing 1g chicken feathers and cultured in a shaking table at 150 rpm, 30 °C for 96 h, then the chicken feather residue was filtered, dried and weighed. This fungus had a good degradation effect on chicken feathers with the degradation rate of 52.02%.

**Sordariomycetes O.E. Erikss. & Winka**

**Sordariales Chadeff. ex D. Hawksw. & O.E. Erikss.**

**Chaetomiaceae G. Winter**

***Ovatospora* X. Wei Wang, Samson & Crous**

***Ovatospora sinensis* H.Y. Wang & Y.F. Han, sp. nov.**

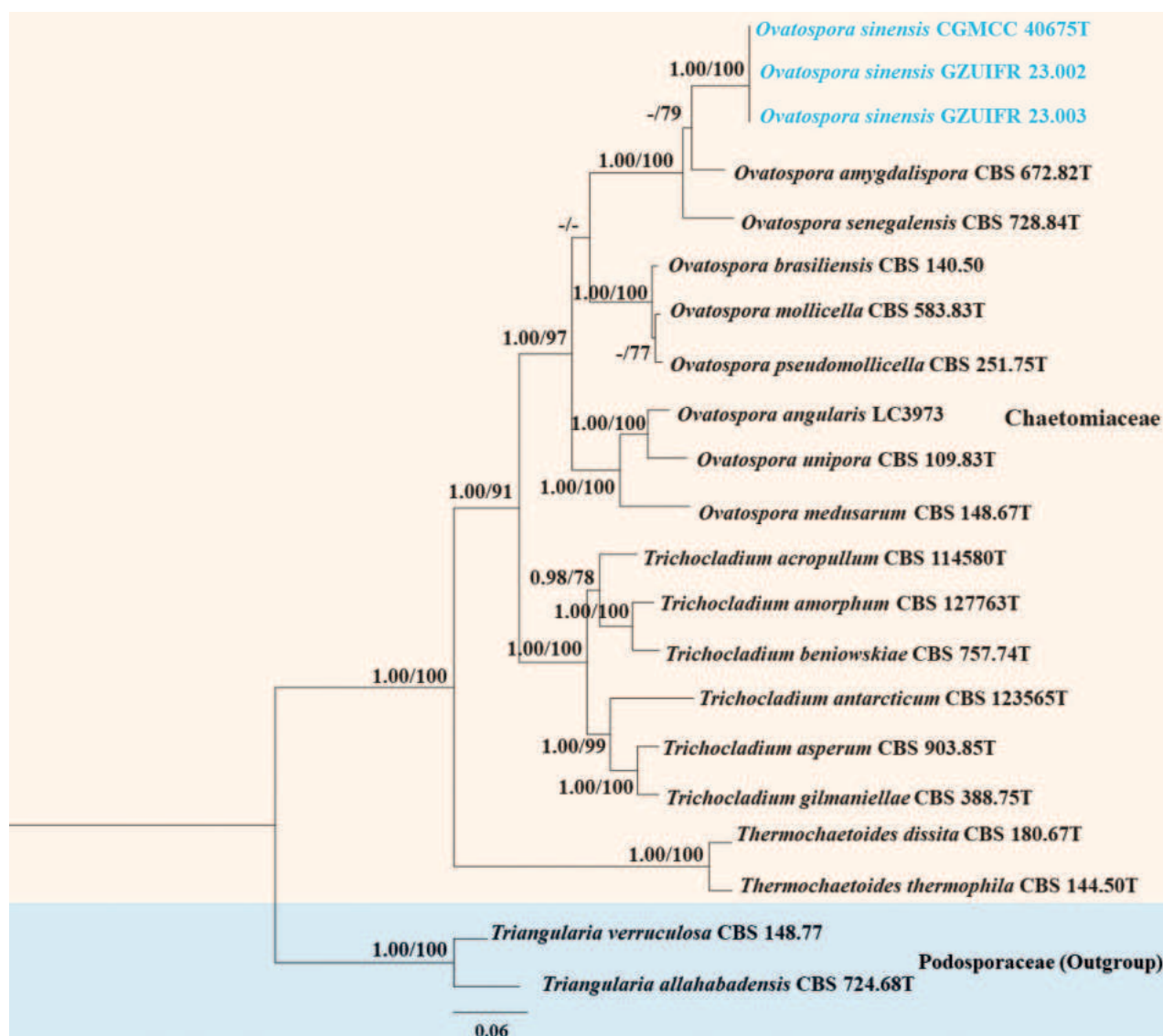
MycoBank No: 850259

Fig. 4

**Etymology.** Refers to China where the species was discovered.

**Type.** CHINA: Shandong Province, Qingdao City, Qingdao Zoo (35°59'14"N, 120°3'53"E), soil, July 2021, Hai-Yan Wang & Yan-Feng Han, ex-type CGMCC 40675=GZUIFR 23. 001, dried holotype GZAC 23. 001.

**Description.** Culture characteristics: Colonies growing on MEA, OA and PDA after 7 days of incubation at 45 °C. Colony on MEA reaching about 35–45 mm diam., pure white (RAL9010), densely villiform; irregular in the margin; reverse



**Figure 3.** Phylogenetic tree of the genus *Ovatospora* constructed from ITS, LSU, *tub2* and *rpb2*. Notes: Statistical support values (BI/ML) were shown at nodes. ML bootstrap values  $\geq 75\%$  and posterior probabilities  $\geq 0.90$  are shown above the internal branches. ‘-’ indicates the absence of statistical support ( $< 75\%$  for bootstrap proportions from ML analysis;  $< 0.90$  for posterior probabilities from Bayesian analysis). Three new strains are shown in blue. CBS: CBS-KNAW Fungal Biodiversity Centre, Utrecht, The Netherlands; CGMCC: The China General Microbiological Culture Collection Centre; GZUIFR: The Institute of Fungus Resources, Guizhou University, China; LC: Lei Cai’s personal culture collection, Beijing, China.

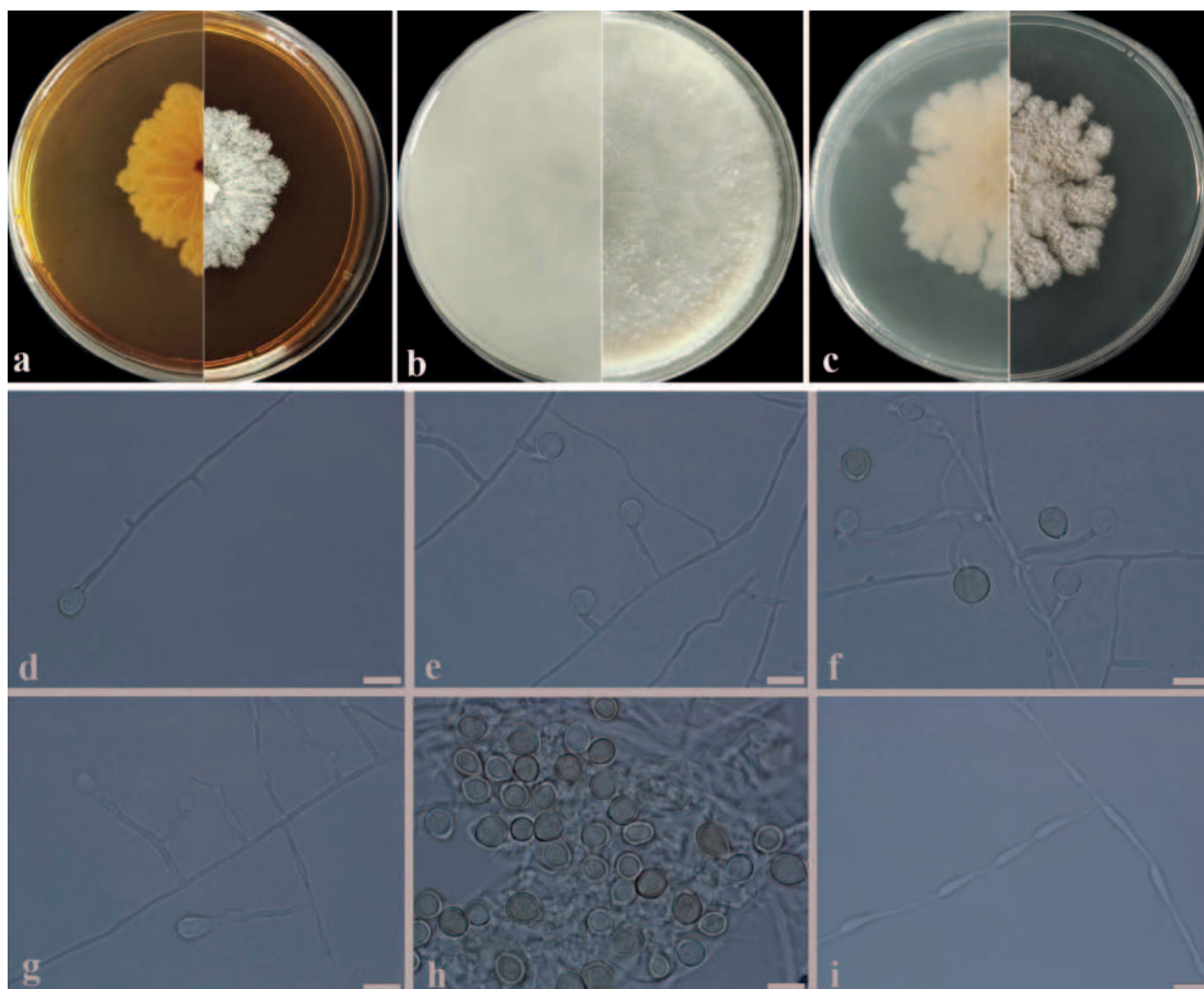


**Figure 4.** Morphological characteristics of *Ovatospora sinensis* sp. nov. **a–c** reverse and front of colony on MEA, OA and PDA after 7 days at 45 °C **d–h** conidiophores and conidia **i** hyphae. Scale bars: 10 µm (**d–i**).

light ivory (RAL1015), radial lines, irregular in the margin. Colony on OA reaching about 80–90 mm diam., grey white (RAL9002), sparsely aerial mycelium, mostly regular in the margin; reverse grey white (RAL9002). Colony on PDA reaching about 45–50 mm diam., creamy (RAL9001), densely villiform obviously powdery conidia group, sparsely spongy, irregular in the margin; reverse creamy (RAL9001), plicated at the centre, irregular in the margin.

**Hyphae** septate, hyaline, smooth, thin-walled, 1.5–3.5 µm wide. **Conidiophores** arising from hyphae, 2–30 × 1.5–3.5 µm, solitary or branched, smooth, mostly clavate, septate. **Conidiogenous cell** reduced to Conidiophores. **Conidia** on conidiogenous or acrogenous directly on the hyphae, hyaline or light-brown, mostly globose, rarely obovate, thick-walled, 6.0–10.5 µm diam. (av. 8.0 µm). Sexual morph unknown.

**Additional specimens examined.** CHINA. Shandong Province, Qingdao City, Qingdao Zoo (35°59'14"N, 120°3'53"E), soil, July 2021, Hai-Yan Wang & Yan-Yeng Han, living cultures GZUIFR 23.002, GZUIFR 23.003.

**Notes.** Phylogenetically, our three strains (CGMCC 40675, GZUIFR 23.002 and GZUIFR 23.003) of *Ovatospora sinensis* H.Y. Wang & Y.F. Han sp. nov. clustered together in a single clade with a high support value (BI/ML 1/100).

Although it was closely related to *O. amygdalispora* (Udagawa & T. Muroi) X. Wei Wang & Houbraken and *O. senegalensis* (Ames) X. Wei Wang & Samson, it has an apparent separate subclade. Morphologically, *O. amygdalispora* and *O. senegalensis* only have the sexual structures, while *Ovatospora sinensis* sp. nov. only produce an asexual morph with clavate and solitary or ramiform conidiophores and globose conidia. So far, *Ovatospora sinensis* sp. nov. is the only species that produces an asexual morph and is a thermophilic fungus in the genus *Ovatospora*.

## Discussion

Lombard et al. (2015) re-estimated the status of those genera lacking DNA sequence data in Nectriaceae, based on the morphology and multi-gene phylogenetic analyses and the new genus *Bisifusarium* with the type *B. dimerum* (Penz.) L. Lombard & Crous was proposed, which formed a well-supported clade (ML = 100%, BYPP = 1.0) and separated from the clade of *Fusarium*. Therefore, these fusarium-like species including *B. biseptatum* (Schroers, Summerbell & O'Donnell) L. Lombard & Crous, *B. delphinoides* (Schroers, Summerbell, O'Donnell & Lampr.) L. Lombard & Crous, *B. dimerum*, *B. domesticum* (Fr.) L. Lombard & Crous, *B. lunatum* (Ellis & Everh.) L. Lombard & Crous, *B. nectrioides* (Wollenw.) L. Lombard & Crous (Schroers, Summerbell & O'Donnell) and *B. penzigii* (Schroers, Summerbell & O'Donnell) L. Lombard & Crous, were transferred from the genus *Fusarium* Link to this new genus *Bisifusarium*. The genus *Bisifusarium* produces macroconidia below three septa and forms lateral phialidic pegs arising from the hyphae, which can be distinguished from the other species in the genus *Fusarium* (Schroers et al. 2009; Lombard et al. 2015). Recently, several new species in genus *Bisifusarium* have been published. Presently, *Bisifusarium* contains fifteen species records in the Index Fungorum (<http://www.indexfungorum.org/Names/Names.asp>, retrieval on 18 October 2023). Here, excluding synonyms and adding *B. keratinophilum* sp. nov., the genus *Bisifusarium* has a total of fourteen species.

Based on the morphology and phylogenetic analysis of a combined dataset of ITS, LSU, *rpb2* and *tub2* sequence data, Wang et al. (2016) redefined the generic concept of *Chaetomium* Kunze and *Ovatospora* X. Wei Wang, Samson & Crous with the type *O. brasiliensis* (Batista & Pontual) X. Wei Wang & Samson was proposed, which formed a well-supported clade and separated from the *Chaetomium* clade. Therefore, these chaetomium-like species included *O. brasiliensis* (Batista & Pontual) X. Wei Wang & Samson, *O. medusarum* (Meyer & Lanneau) X. Wei Wang & Samson, *O. mollicella* (Ames) X. Wei Wang & Samson, *O. senegalensis* (Ames) X. Wei Wang & Samson and *O. unipora* (Aue & Müller) X. Wei Wang & Samson. Simultaneously, *O. pseudomollicella* X. Wei Wang & Samson sp. nov. was introduced. In addition, based on the results of the phylogeny and molecular data analyses, two new combinations, *O. amygdalispora* (Udagawa & T. Muroi) X. Wei Wang & Houbraken and *O. angularis* (Yu Zhang & L. Cai) X. Wei Wang & Houbraken from *Chaetomium* were proposed by Wang et al. (2022a). As of October 2023, the genus *Ovatospora* contains nine species: *O. amygdalispora*, *O. angularis*, *O. brasiliensis*, *O. medusarum*, *O. mollicella*, *O. pseudomollicella*, *O. senegalensis*, *Ovatospora sinensis* and *O. unipora*.

## Additional information

### Conflict of interest

The authors have declared that no competing interests exist.

### Ethical statement

No ethical statement was reported.

### Funding

The work was supported by “Hundred” Talent Projects of Guizhou Province (Qian Ke He [2020] 6005), the National Natural Science Foundation of China (no. 32060011, 32160007, 32260003) and Guizhou Provincial Department of Education Characteristic Field Project [QianJiaohe KY character [2021]073].

### Author contributions

Sampling and fungal isolation: Hai-Yan Wang, Xin Li and Yan-Feng Han; molecular biology analysis and phylogenetic analysis: Chun-Bo Dong and Wan-Hao Chen; microscopy: Hai-Yan Wang and Yan-Wei Zhang; original draft preparation: Hai-Yan Wang and Yan-Feng Han; review and editing: Hai-Yan Wang, Xin Li, Chun-Bo Dong, Wan-Hao Chen, Jian-Dong Liang; Funding: Yan-Wei Zhang and Yan-Feng Han. All authors reviewed and approved the final manuscript.

### Author ORCIDs

Hai-Yan Wang  <https://orcid.org/0000-0001-9190-0490>

Xin Li  <https://orcid.org/0000-0001-7910-1469>

Chun-Bo Dong  <https://orcid.org/0000-0001-7074-5700>

Yan-Wei Zhang  <https://orcid.org/0000-0003-1251-5821>

Wan-Hao Chen  <https://orcid.org/0000-0001-7240-6841>

Jian-Dong Liang  <https://orcid.org/0000-0002-3939-3900>

Yan-Feng Han  <https://orcid.org/0000-0002-8646-3975>

### Data availability

All of the data that support the findings of this study are available in the main text or Supplementary Information.

## References

- Arsenault ER, Liew JH, Hopkins JR (2022) Substrate composition influences amino acid carbon isotope profiles of fungi: Implications for tracing fungal contributions to food webs. *Environmental Microbiology* 24(4): 1462–2912. <https://doi.org/10.1111/1462-2920.15961>
- Blackwell M (2011) The fungi: 1, 2, 3 ... 5.1 million species? *American Journal of Botany* 98(3): 426–438. <https://doi.org/10.3732/ajb.1000298>
- Carbone I, Kohn LM (1999) A method for designing primer sets for speciation studies in filamentous ascomycetes. *Mycologia* 91(3): 553–556. <https://doi.org/10.1080/00275514.1999.12061051>
- de Cassia Pereira J, Paganini Marques N, Rodrigues A, Brito de Oliveira T, Boscolo M, Da Silva R, Gomes E, Bocchini Martins DA (2015) Thermophilic fungi as new sources

- for production of cellulases and xylanases with potential use in sugarcane bagasse saccharification. *Journal of Applied Microbiology* 118(4): 928–939. <https://doi.org/10.1111/jam.12757>
- Driscoll DA, Bland LM, Bryan BA, Newsome TM, Nicholson E, Ritchie EG, Doherty TS (2018) A biodiversity-crisis hierarchy to evaluate and refine conservation indicators. *Nature Ecology & Evolution* 2(5): 775–781. <https://doi.org/10.1038/s41559-018-0504-8>
- Fisher MC, Henk DA, Briggs CJ, Brownstein JS, Madoff LC, McCraw SL, Gurr SJ (2012) Emerging fungal threats to animal, plant and ecosystem health. *Nature* 484(7393): 186–194. <https://doi.org/10.1038/nature10947>
- Fisher MC, Gurr SJ, Cuomo CA, Blehert DS, Jin H, Stukenbrock EH, Stajich JE, Kahmann R, Boone C, Denning DW, Gow NAR, Klein BS, Kronstad JW, Sheppard DC, Taylor JW, Wright GD, Heitman J, Casadevall A, Cowen LE (2020) Threats posed by the fungal kingdom to humans, wildlife, and agriculture. *mBio* 11(3): e00449–e20. <https://doi.org/10.1128/mBio.00449-20>
- Hawksworth DL, Lücking R (2017) Fungal diversity revisited: 2.2 to 3.8 million species. *Microbiology Spectrum* 5(4): 10–1128. <https://doi.org/10.1128/microbiolspec.FUNK-0052-2016>
- Hyde KD, Jeewon R, Chen YJ, Bhunjun CS, Calabon MS, Jiang HB, Lin CG, Norphanphoun C, Sysouphanthong P, Pem D, Tibpromma S, Zhang Q, Doilom M, Jayawardena RS, Liu J-K, Maharachchikumbura SSN, Phukhamsakda C, Phookamsak R, Al-Sadi AM, Thongklang N, Wang Y, Gafforov Y, Gareth Jones EB, Lumyong S (2020) The numbers of fungi: Is the descriptive curve flattening? *Fungal Diversity* 103(1): 219–271. <https://doi.org/10.1007/s13225-020-00458-2>
- Kurth T, Wübbels G, Portafaix A, Meyer zum Felde A, Zielcke S (2021) *The Biodiversity Crisis is a Business Crisis*. Boston Consulting Group, Boston, 50 pp.
- Li YQ, Cui ZQ, Hu DM (2014) Coprophilous Fungi from Different Fecal Substrates in Kunming Zoo. *Journal of Fungal Research* 12(2): 88–95. <https://doi.org/10.13341/j.jfr.2014.1001>
- Li X, Zhang ZY, Ren YL, Chen WH, Liang JD, Pan JM, Huang JZ, Liang ZQ, Han YF (2022a) Morphological characteristics and phylogenetic evidence reveal two new species of *Acremonium* (Hypocreales, Sordariomycetes). *Mycology* 91: 85–96. <https://doi.org/10.3897/mycokeys.91.86257>
- Li X, Zhang ZY, Chen WH, Liang JD, Huang JZ, Han YF, Ling ZQ (2022b) A new species of *Arthrographis* (Eremomycetaceae, Dothideomycetes), from the soil in Guizhou, China. *Phytotaxa* 538(3): 175–181. <https://doi.org/10.11646/phytotaxa.538.3.1>
- Liu YL, Ren GR, Liu S, Wang L, Li YH, Zhao J, Qiu JZ (2022) Macrofungal diversity in coniferous forests and grassland of Xinjiang. *Junwu Xuebao* 41(7): 1021–1034.
- Löbl I, Klausnitzer B, Hartmann M, Krell FT (2023) The silent extinction of species and taxonomists—An appeal to science policymakers and legislators. *Diversity* 15(10): 1053. <https://doi.org/10.3390/d15101053>
- Lombard L, van der Merwe NA, Groenewald JZ, Crous PW (2015) Generic concepts in Nectriaceae. *Studies in Mycology* 80(1): 189–245. <https://doi.org/10.1016/j.simyco.2014.12.002>
- Mapook A, Hyde KD, Hassan K, Kemkuignou BM, Čmoková A, Surup F, Kuhnert E, Pao-mephan P, Cheng T, de Hoog S, Song Y, Jayawardena RS, Al-Hatmi AMS, Mahmoudi T, Ponts N, Studt-Reinhold L, Richard-Forget F, Chethana KWT, Harishchandra DL, Mortimer PE, Li H, Lumyong S, Aiduang W, Kumla J, Suwannarach N, Bhunjun CS, Yu FM, Zhao Q, Schaefer D, Stadler M (2022) Ten decadal advances in fungal biology

- leading towards human well-being. *Fungal Diversity* 116(1): 547–614. <https://doi.org/10.1007/s13225-022-00510-3>
- Minh BQ, Nguyen MAT, von Haeseler A (2013) Ultrafast approximation for phylogenetic bootstrap. *Molecular Biology and Evolution* 30(5): 1188–1195. <https://doi.org/10.1093/molbev/mst024>
- Nguyen LT, Schmidt HA, von Haeseler A, Minh BQ (2015) IQ-TREE: A fast and effective stochastic algorithm for estimating maximum-likelihood phylogenies. *Molecular Biology and Evolution* 32(1): 268–274. <https://doi.org/10.1093/molbev/msu300>
- Niskanen T, Lücking R, Dahlberg A, Gaya E, Suz LM, Mikryukov V, Liimatainen K, Druzhinina I, Westrip JRS, Mueller GM, Martins-Cunha K, Kirk P, Tedersoo L, Antonelli A (2023) Pushing the frontiers of biodiversity research: Unveiling the global diversity, distribution, and conservation of fungi. *Annual Review of Environment and Resources* 48(1): 149–176. <https://doi.org/10.1146/annurev-environ-112621-090937>
- O'Donnell K, Cigelnik E (1997) Two divergent intragenomic rDNA ITS2 types within a monophyletic lineage of the fungus *Fusarium* are nonorthologous. *Molecular Phylogenetics and Evolution* 7(1): 103–116. <https://doi.org/10.1006/mpev.1996.0376>
- O'Donnell K, Kistler HC, Cigelnik E, Ploetz RC (1998) Multiple evolutionary origins of the fungus causing Panama disease of banana: Concordant evidence from nuclear and mitochondrial gene genealogies. *Proceedings of the National Academy of Sciences of the United States of America* 95(5): 2044–2049. <https://doi.org/10.1073/pnas.95.5.2044>
- O'Donnell K, Sarver BAJ, Brandt M, Chang DC, Noble-Wang J, Park BJ, Sutton DA, Benjamin L, Lindsley M, Padhye A, Geiser DM, Ward TJ (2007) Phylogenetic diversity and microsphere array-based genotyping of human pathogenic *Fusaria*, including isolates from the multistate contact lens-associated U.S. keratitis outbreaks of 2005 and 2006. *Journal of Clinical Microbiology* 45(7): 2235–2248. <https://doi.org/10.1128/JCM.00533-07>
- Park JH, Oh J, Song JS, Kim J, Sung GH (2019) *Bisifusarium delphinoides*, an emerging opportunistic pathogen in a burn patient with diabetes mellitus. *Mycobiology* 47(3): 340–345. <https://doi.org/10.1080/12298093.2019.1628521>
- Pejin B, Teanovi K, Jakovljevi D, Kaiarevi S (2019) The polysaccharide extracts from the fungi *Coprinus comatus* and *Coprinellus truncorum* do exhibit AChE inhibitory activity. *Natural Product Research* 33(6): 1478–6419. <https://doi.org/10.1080/14786419.2017.1405417>
- Ren YL, Zhang ZY, Chen WH, Liang JD, Han YF, Liang ZQ (2022) Morphological and phylogenetic characteristics of *Phaeomycocentrospora xinjangensis* (Pleosporales, Dothideomycetes), a new species from China. *Phytotaxa* 558(1): 125–132. <https://doi.org/10.11646/phytotaxa.558.1.9>
- Ronquist F, Teslenko M, van der Mark P, Ayres DL, Darling A, Höhna S, Larget B, Liu L, Suchard MA, Huelsenbeck JP (2012) MrBayes 3.2: Efficient bayesian phylogenetic inference and model choice across a large model space. *Systematic Biology* 61(3): 539–542. <https://doi.org/10.1093/sysbio/sys029>
- Savary O, Coton M, Frisvad JC, Nodet P, Ropars J, Coton E, Jany JL (2021) Unexpected Nectriaceae species diversity in cheese, description of *Bisifusarium allantoides* sp. nov., *Bisifusarium penicilloides* sp. nov., *Longinectria* gen. nov. *lagenoides* sp. nov. and *Longinectria verticilliforme* sp. nov. *Mycosphere* 12(1): 1077–1100. <https://doi.org/10.5943/mycosphere/12/1/13>
- Schroers HJ, O'Donnell K, Lamprecht SC, Kammcyer PL, Johnson S, Sutton DA, Rinaldi MG, Geiser DM, Summerbell RC (2009) Taxonomy and phylogeny of the *Fusarium dimerum* species group. *Mycologia* 101(1): 44–70. <https://doi.org/10.3852/08-002>

- Shao QY, Dong CB, Zhang ZY, Han YF, Liang ZQ (2021) Effects of *Perilla frutescens* on the fungal community composition and ecological guild structure in a hospital grass-plot soil. *Junwu Xuebao* 40(5): 1008–1022. <https://doi.org/10.13346/j.mycosystema.200261>
- Sun BD, Zhou YG, Chen AJ (2017) *Bisifusarium tonghuanum* (Nectriaceae), a novel species of Fusarium-like fungi from two desert oasis plants. *Phytotaxa* 317(2): 123–129. <https://doi.org/10.11646/phytotaxa.317.2.4>
- Sung GH, Sung JM, Hywel-Jones NL, Spatafora JW (2007) A multi-gene phylogeny of Clavicipitaceae (Ascomycota, Fungi): Identification of localized incongruence using a combinational bootstrap approach. *Molecular Phylogenetics and Evolution* 44(3): 1204–1223. <https://doi.org/10.1016/j.ympev.2007.03.011>
- Tamura K, Stecher G, Peterson D, Filipowski A, Kumar S (2013) MEGA6: Molecular evolutionary genetics analysis version 6.0. *Molecular Biology and Evolution* 30(12): 2725–2729. <https://doi.org/10.1093/molbev/mst197>
- Tan YP, Shivas RG (2023) Novel species of microfungi from Australia. *Index of Australian Fungi* No.5 1-12. <https://doi.org/10.5281/zenodo.7765160>
- Wang XW, Houbraken J, Groenewald JZ, Meijer M, Andersen B, Nielsen KF, Crous PW, Samson RA (2016) Diversity and taxonomy of *Chaetomium* and chaetomium-like fungi from indoor environments. *Studies in Mycology* 84(1): 145–224. <https://doi.org/10.1016/j.simyco.2016.11.005>
- Wang MX, Liu KY, Xing YJ (2018) Association Analysis of Soil Microorganism and Plant Species Diversity Under Climate Change. *Zhongguo Nongxue Tongbao* 34(20): 111–117. <http://www.casb.org.cn>
- Wang XW, Han PJ, Bai FY, Luo A, Bensch K, Meijer M, Kraak B, Han DY, Sun BD, Crous PW, Houbraken J (2022a) Taxonomy, phylogeny and identification of Chaetomiaceae with emphasis on thermophilic species. *Studies in Mycology* 101(1): 121–243. <https://doi.org/10.3114/sim.2022.101.03>
- Wang MM, Crous PW, Sandoval-Denis M, Han SL, Liu F, Liang JM, Duan WJ, Cai L (2022b) *Fusarium* and allied genera from China: Species diversity and distribution. *Persoonia* 48(1): 1–53. <https://doi.org/10.3767/persoonia.2022.48.01>
- Wang HY, Zhang ZY, Ren YL, Shao QY, Li X, Chen WH, Liang JD, Liang ZQ, Han YF (2023) *Multiverruca sinensis* gen. nov., sp. nov., a thermotolerant fungus isolated from soil in China. *International Journal of Systematic and Evolutionary Microbiology* 73(2): e005734. <https://doi.org/10.1099/ijsem.0.005734>
- White TJ, Bruns T, Lee S, Taylor J (1990) Amplification and direct sequencing of fungal ribosomal RNA genes for phylogenetics. *PCR protocols: a guide to methods and applications* 18(1): 315–322. <https://doi.org/10.1016/B978-0-12-372180-8.50042-1>
- Wijayawardene NN, Hyde KD, Al-Ani L, Tedersoo L, Ags SF (2020) Outline of Fungi and fungus-like taxa. *Mycosphere* 11(1): 1060–1456. <https://doi.org/10.5943/mycosphere/11/1/8>
- Woudenberg JHC, Aveskamp MM, de Gruyter J, Spiers AG, Crous PW (2009) Multiple *Didymella* teleomorphs are linked to the *Phoma clematidina* morphotype. *Persoonia* 22(1): 56–62. <https://doi.org/10.3767/003158509X427808>
- Yao ZT, Yang YC, Yao X, He T, Zheng X, Meng YC, Zou CW (2021) Effects of different crop rotation modes on fungal community in potato rhizosphere soil. *Nanfeng Nongye Xuebao* 52(5): 1255–1262. <https://doi.org/10.3969/j.issn.2095-1191.2021.05.015>
- Yokokawa D, Tatematsu S, Takagi R, Saga Y, Kushiro T (2021) Synthesis of aminoacylated ergosterols: A new lipid component of fungi. *Steroids* 169(26): e108823. <https://doi.org/10.1016/j.steroids.2021.108823>

- Zhang YW, Han YF, Liu X, Liang ZQ (2013) Screening of new resources of natural vitamin e producing fungi from soil. *Hubei Agricultural Sciences*. 52 (17): 4066–4068. [+4082.] <https://doi.org/10.14088/j.cnki.issn0439-8114.2013.17.045>
- Zhang D, Gao FL, Jakovlić I, Zou H, Zheng J, Li WX, Wang GT (2020) PhyloSuite: An integrated and scalable desktop platform for streamlined molecular sequence data management and evolutionary phylogenetics studies. *Molecular Ecology Resources* 20(1): 348–355. <https://doi.org/10.1111/1755-0998.13096>
- Zhang ZY, Li X, Chen WH, Liang JD, Han YF (2023) Culturable fungi from urban soils in China II, with the description of 18 novel species in Ascomycota (Dothideomycetes, Eurotiomycetes, Leotiomycetes and Sordariomycetes). *MycKeys* 98: 167–220. <https://doi.org/10.3897/mycokeys.98.102816>

## Supplementary material 1

### The alignments used in the phylogenetic analysis

Authors: Hai-Yan Wang, Yan-Feng Han

Data type: zip

Copyright notice: This dataset is made available under the Open Database License (<http://opendatacommons.org/licenses/odbl/1.0/>). The Open Database License (ODbL) is a license agreement intended to allow users to freely share, modify, and use this Dataset while maintaining this same freedom for others, provided that the original source and author(s) are credited.

Link: <https://doi.org/10.3897/mycokeys.102.114480.suppl1>



## Corrigendum: Hu H et al. (2023) Taxonomic and phylogenetic characterisations of six species of Pleosporales (in Didymosphaeriaceae, Roussoellaceae and Nigrogranaceae) from China. MycoKeys 100: 123–151. <https://doi.org/10.3897/mycokeys.100.109423>

Hongmin Hu<sup>1,2\*</sup>, Minghui He<sup>1,2\*</sup>, Youpeng Wu<sup>1</sup>, Sihan Long<sup>1</sup>, Xu Zhang<sup>1</sup>, Lili Liu<sup>3</sup>, Xiangchun Shen<sup>1,2</sup>, Nalin N. Wijayawardene<sup>4</sup>, Zebin Meng<sup>5</sup>, Qingde Long<sup>1</sup>, Jichuan Kang<sup>6</sup>, Qirui Li<sup>1,2</sup>

- 1 State Key Laboratory of Functions and Applications of Medicinal Plants, Guizhou Medical University, Guiyang, Guizhou province, China
- 2 The High Efficacy Application of Natural Medicinal Resources Engineering Center of Guizhou Province (The Key Laboratory of Optimal Utilization of Natural Medicine Resources), School of Pharmaceutical Sciences, Guizhou Medical University, University Town, Gui'an New District, Guiyang, Guizhou province, China
- 3 Key Laboratory of Infectious Immune and Antibody Engineering of Guizhou Province, Cellular Immunotherapy Engineering Research Center of Guizhou Province, Immune Cells and Antibody Engineering Research Center of Guizhou Province, School of Biology and Engineering, Guizhou Medical University, Guiyang, Guizhou province, China
- 4 Center for Yunnan Plateau Biological Resources Protection and Utilization, College of Biological Resource and Food Engineering, Qujing Normal University, Qujing, Yunnan province, China
- 5 Guizhou Tea Seed Resource Utilization Engineering Research Center, Guizhou Education University, Guiyang, Guizhou province, China
- 6 The Engineering and Research Center for Southwest Bio-Pharmaceutical Resources of National Education Ministry of China, Guizhou University, Guiyang, Guizhou province, China

Corresponding authors: Qingde Long ([longqingde@gmc.edu.cn](mailto:longqingde@gmc.edu.cn)); Qirui Li ([lqrnd2008@163.com](mailto:lqrnd2008@163.com))



Due to an error on our part, we mixed up the figures used in Form 3 of the manuscript, and it was only after the manuscript was published that we noticed that we had misplaced the figures. We therefore provide below a new Table 3 containing the corrected information.

Academic editor: Thorsten Lumbsch

Received: 8 December 2023

Accepted: 9 December 2023

Published: 7 March 2024

Copyright: © Hongmin Hu et al.

This is an open access article distributed under terms of the Creative Commons Attribution License (Attribution 4.0 International – CC BY 4.0).

**Citation:** Hu H, He M, Wu Y, Long S, Zhang X, Liu L, Shen X, Wijayawardene NN, Meng Z, Long Q, Kang J, Li Q (2024) Corrigendum: Hu H et al. (2023) Taxonomic and phylogenetic characterisations of six species of Pleosporales (in Didymosphaeriaceae, Roussoellaceae and Nigrogranaceae) from China. MycoKeys 100: 123–151. <https://doi.org/10.3897/mycokeys.100.109423>. MycoKeys 102: 317–322. <https://doi.org/10.3897/mycokeys.102.116896>

\* These authors contributed equally as co-first authors.

**Table 3.** Taxa and corresponding GenBank accession numbers of sequences used in the phylogenetic analysis of Didymosphaeriaceae, Roussoellaceae and Nigrogranaceae.

Species	Strain	GenBank accession numbers					References
		ITS	SSU	LSU	<i>tef1</i>	<i>rpb2</i>	
<i>Alloconiothyrium camelliae</i>	NTUCC 17-032-1 <sup>T</sup>	MT112294	MT071221	MT071270	MT232967	—	(Kolařík et al. 2017)
<i>Arthopyrenia</i> sp.	UTHSC DI16–362	LT796905	LN907505	—	LT797145	LT797065	(Crous et al. 2015)
<i>Austropleospora ochracea</i>	KUMCC 20-0020 <sup>T</sup>	MT799859	MT808321	MT799860	MT872714	—	(Dissanayake et al. 2021)
<i>A. keteleeriae</i>	MFLUCC 18-1551 <sup>T</sup>	NR_163349	MK347910	NG_070075	MK360045	—	(Mapook et al. 2020)
<i>Biatrispora antibiotica</i>	CCF 1998	LT221894	—	—	—	—	(Kolařík et al. 2017)
<i>B. carollii</i>	CCF 4484 <sup>T</sup>	LN626657	—	—	LN626668	—	(Kolařík et al. 2017)
<i>B. mackinnonii</i>	E9303e	—	—	—	LN626673	—	(Kolařík et al. 2017)
<i>B. peruviansis</i>	CCF 4485 <sup>T</sup>	LN626658	—	—	LN626671	—	(Kolařík et al. 2017)
<i>Bimuria omanensis</i>	SQUCC 15280 <sup>T</sup>	NR_173301	—	NG_071257	MT279046	—	(Wijesinghe et al. 2020)
<i>B. novae-zelandiae</i>	CBS 107.79 <sup>T</sup>	MH861181	AY016338	AY016356	DQ471087	—	(Vu et al. 2019)
<i>Chromolaenicola nanensis</i>	MFLUCC 17-1477	MN325014	MN325008	MN325002	MN335647	—	(Liu et al. 2014)
<i>C. siamensis</i>	MFLUCC 17-2527 <sup>T</sup>	NR_163337	MK347866	NG_066311	MK360048	—	(Mapook et al. 2020)
<i>C. thailandensis</i>	MFLUCC 17-1475	MN325019	MN325013	MN325007	MN335652	—	(Liu et al. 2014)
<i>C. lampangensis</i>	MFLUCC 17-1462 <sup>T</sup>	MN325016	MN325010	MN325004	MN335649	—	(Liu et al. 2014)
<i>Cylindroaseptospora leucaenae</i>	MFLUCC 17-2424	NR_163333	MK347856	NG_066310	MK360047	—	(Mapook et al. 2020)
<i>Deniquelata hypolithi</i>	CBS 146988 <sup>T</sup>	MZ064429	—	NG_076735	MZ078250	—	(Ariyawansa et al. 2020b)
<i>D. barringtoniae</i>	MFLUCC 16-0271	MH275059	—	MH260291	MH412766	—	(Tibpromma et al. 2018)
<i>Didymocrea sadasivanii</i>	CBS 438.65	MH858658	DQ384066	DQ384103	—	—	(Vu et al. 2019)
<i>Didymosphaeria rubi-ulmifolii</i>	MFLUCC 14-0023 <sup>T</sup>	—	NG_063557	KJ436586	—	—	(Jayasiri et al. 2019)
<i>Kalmusia erioi</i>	MFLU 18-0832 <sup>T</sup>	MN473058	MN473046	MN473052	MN481599	—	(Vu et al. 2019)
<i>K. italica</i>	MFLUCC 13-0066 <sup>T</sup>	KP325440	KP325442	KP325441	—	—	(Vu et al. 2019)
<i>K. variispora</i>	CBS 121517 <sup>T</sup>	NR_145165	NG_070452	—	—	—	(Wijesinghe et al. 2020)
<i>K. ebuli</i>	CBS 123120 <sup>T</sup>	KF796674	JN851818	JN644073	—	—	(Dissanayake et al. 2021)
<i>Kalmusibambusa triseptata</i>	MFLUCC 13-0232	KY682697	KY682696	KY682695	—	—	(Tibpromma et al. 2018)
<i>Karstenula rhodostoma</i>	CBS 690.94	—	GU296154	GU301821	GU349067	—	(Crous et al. 2021)
<i>Laburnicola hawksworthii</i>	MFLUCC 13-0602 <sup>T</sup>	KU743194	KU743196	KU743195	—	—	(Ariyawansa et al. 2014)
<i>Letendreaa helminthicola</i>	CBS 884.85	MK404145	AY016345	AY016362	MK404174	—	(Tibpromma et al. 2018)
<i>L. muriformis</i>	MFLUCC 16-0290 <sup>T</sup>	KU743197	KU743199	KU743198	KU743213	—	(Ariyawansa et al. 2014)
<i>L. padouk</i>	CBS 485.70	—	GU296162	AY849951	—	—	(Zhang et al. 2013)
<i>L. cordylinicola</i>	MFLUCC 11 0148 <sup>T</sup>	NR_154118	KM214001	NG_059530	—	—	(Wijayawardene et al. 2020)
<i>Montagnula chromolaenicola</i>	MFLUCC 17-1469 <sup>T</sup>	NR_168866	NG_070157	NG_070948	MT235773	—	(Liu et al. 2014)
<i>M. cirsi</i>	MFLUCC 13 0680	KX274242	KX274255	KX274249	KX284707	—	(Hyde et al. 2020)
<i>M. krabiensis</i>	MFLUCC 16-0250 <sup>T</sup>	MH275070	MH260343	MH260303	MH412776	—	(Tibpromma et al. 2018)
<i>M. thailandica</i>	MFLUCC 17-1508 <sup>T</sup>	MT214352	NG_070158	NG_070949	MT235774	—	(Liu et al. 2014)
<i>M. bellevaliae</i>	MFLUCC 14-0924 <sup>T</sup>	NR_155377	KT443904	KT443902	KX949743	—	(Ariyawansa et al. 2014)
<i>Neoroussoella alishanense</i>	FU31016	MK503816	MK503822	—	MK336181	MN037756	(Verkley et al. 2014)
<i>N. bambusae</i>	MFLUCC 11–0124	KJ474827	KJ474839	—	KJ474848	KJ474856	(Dissanayake et al. 2021)
<i>N. heveae</i>	MFLUCC 17–1983	MH590693	MH590689	—	—	—	(Wanasinghe et al. 2018)
<i>N. lenispora</i>	GZCC 16-0020 <sup>T</sup>	—	KX791431	—	—	—	(Hyde et al. 2020)
<i>N. leucaenae</i>	MFLUCC 18–1544	MK347767	MK347984	—	MK360067	MK434876	(Mapook et al. 2020)
<i>N. solani</i>	CPC 26331 <sup>T</sup>	KX228261	KX228312	—	—	—	(Wijayawardene et al. 2014)
<i>Neokalmusia arundinis</i>	MFLUCC 15-0463 <sup>T</sup>	NR_165852	NG_068372	NG_068237	KY244024	—	(Thambugala et al. 2015)
<i>N. brevispora</i>	KT2313 <sup>T</sup>	LC014574	AB524460	AB524601	AB539113	—	(Tanaka et al. 2015)

Species	Strain	GenBank accession numbers					References
		ITS	SSU	LSU	<i>tef1</i>	<i>rpb2</i>	
<i>N. brevispora</i>	KT1466	LC014573	AB524459	AB524600	AB539112	–	(Tanaka et al. 2015)
<i>N. didymospora</i>	MFLUCC 11-0613	–	KP091435	KP091434	–	–	(Haridas et al. 2020)
<i>N. jonahhulmei</i>	KUMCC 21-0819	ON007044	ON007040	ON007049	ON009134	–	(Wanasinghe et al. 2016)
<b><i>N. karka</i></b>	<b>GMB0494<sup>T</sup></b>	<b>OR120445</b>	<b>OR120442</b>	<b>OR120432</b>	<b>OR150020</b>	–	<b>This study</b>
<b><i>N. karka</i></b>	<b>GMB0500</b>	<b>OR120438</b>	<b>OR120433</b>	<b>OR120443</b>	<b>OR150021</b>	–	<b>This study</b>
<i>N. kunmingensis</i>	KUMCC 18-0120 <sup>T</sup>	MK079886	MK079887	MK079889	MK070172	–	(Vu et al. 2019)
<i>N. scabrispora</i>	KT1023	LC014575	AB524452	AB524593	AB539106	–	(Tanaka et al. 2015)
<i>N. thailandica</i>	MFLUCC 16-0405 <sup>T</sup>	NR_154255	KY706137	NG_059792	KY706145	–	(Thambugala et al. 2015)
<i>Nigrograna antibiotica</i>	CCF 4378 <sup>T</sup>	JX570932	–	–	JX570934	–	(Kolařík et al. 2018)
<i>N. antibiotica</i>	CCF 1998	LT221894	–	–	–	–	(Kolařík et al. 2018)
<i>N. cangshanensis</i>	MFLUCC15-0253 <sup>T</sup>	KY511063	–	–	KY511066	–	(Crous et al. 2015)
<i>N. carollii</i>	CCF 4484 <sup>T</sup>	LN626657	–	–	LN626668	–	(Kolařík et al. 2018)
<i>N. chromolaenae</i>	MFLUCC 17-1437 <sup>T</sup>	MT214379	–	–	MT235801	–	(Liu et al. 2014)
<i>N. fuscidula</i>	CBS 141556 <sup>T</sup>	KX650550	–	–	KX650525	–	(Feng et al. 2019)
<i>N. fuscidula</i>	CBS 141476	KX650547	–	–	KX650522	–	(Feng et al. 2019)
<i>N. hydei</i>	GZCC 19-0050 <sup>T</sup>	NR_172415	–	–	MN389249	–	(Zhang et al. 2020)
<i>N. impatientis</i>	GZCC 19-0042 <sup>T</sup>	NR_172416	–	–	MN389250	–	(Zhang et al. 2020)
<i>N. locuta-pollinis</i>	CGMCC 3.18784	MF939601	–	–	MF939613	–	(Ahmed et al. 2014)
<i>N. locuta-pollinis</i>	LC11690	MF939603	–	–	MF939614	–	(Ahmed et al. 2014)
<i>N. mackinnonii</i>	CBS 674.75 <sup>T</sup>	NR_132037	–	–	KF407986	–	(Ariyawansa et al. 2015)
<i>N. mackinnonii</i>	E5202H	JX264157	–	–	JX264154	–	(Phukhamsakda et al. 2018)
<i>N. mackinnonii</i>	E9303e	–	–	–	LN626673	–	(Kolařík et al. 2017)
<i>N. magnoliae</i>	GZCC 17-0057	MF399066	–	–	MF498583	–	(Zhang et al. 2020)
<i>N. magnoliae</i>	MFLUCC 20-0020 <sup>T</sup>	MT159628	–	–	MT159605	–	(Liu et al. 2014)
<i>N. mycophila</i>	CBS 141478 <sup>T</sup>	KX650553	–	–	KX650526	–	(Feng et al. 2019)
<i>N. mycophila</i>	CBS 141483	KX650555	–	–	KX650528	–	(Feng et al. 2019)
<i>N. norvegica</i>	CBS 141485 <sup>T</sup>	KX650556	–	–	–	–	(Feng et al. 2019)
<i>N. obliqua</i>	CBS 141477 <sup>T</sup>	KX650560	–	–	KX650531	–	(Feng et al. 2019)
<i>N. obliqua</i>	CBS 141475	KX650558	–	–	KX650530	–	(Feng et al. 2019)
<i>N. peruviansis</i>	CCF 4485 <sup>T</sup>	LN626658	–	–	LN626671	–	(Kolařík et al. 2018)
<i>N. rhizophorae</i>	MFLUCC 18-0397 <sup>T</sup>	MN047085	–	–	MN077064	–	(Poli et al. 2020)
<i>N. samueliana</i>	NFCCI-4383 <sup>T</sup>	MK358817	–	–	MK330937	–	(Poli et al. 2020)
<b><i>N. schinifolium</i></b>	<b>GMB0498<sup>T</sup></b>	<b>OR120434</b>	–	–	<b>OR150022</b>	–	<b>This study</b>
<b><i>N. schinifolium</i></b>	<b>GMB0504</b>	<b>OR120441</b>	–	–	<b>OR150023</b>	–	<b>This study</b>
<i>N. thymi</i>	MFLUCC 14-1096 <sup>T</sup>	KY775576	–	–	KY775578	–	(Crous et al. 2015)
<b><i>N. trachycarpus</i></b>	<b>GMB0499<sup>T</sup></b>	<b>OR120437</b>	–	–	<b>OR150024</b>	–	<b>This study</b>
<b><i>N. trachycarpus</i></b>	<b>GMB0505</b>	<b>OR120440</b>	–	–	<b>OR150025</b>	–	<b>This study</b>
<i>N. yasuniana</i>	YU.101026 <sup>T</sup>	HQ108005	–	–	LN626670	–	(Kolařík et al. 2018)
<i>Occultibambusa pustula</i>	MFLUCC 11-0502 <sup>T</sup>	KU940126	–	–	–	–	(Crous et al. 2014)
<i>O. bambusae</i>	MFLUCC 13-0855 <sup>T</sup>	KU940123	–	–	KU940193	–	(Crous et al. 2014)
<i>Paracamarosporium fagi</i>	CPC 24890 <sup>T</sup>	NR_154318	–	NG_070630	–	–	(Ariyawansa et al. 2014)
<i>P. cyclothyrioides</i>	CBS 972.95	JX496119	AY642524	JX496232	–	–	(Schoch et al. 2009)
<i>P. estuarinum</i>	CBS 109850 <sup>T</sup>	JX496016	AY642522	JX496129	–	–	(Verkley et al. 2014)
<i>P. hawaiiense</i>	CBS 120025 <sup>T</sup>	JX496027	EU295655	JX496140	–	–	(Verkley et al. 2014)
<i>P. robiniae</i>	MFLUCC 14-1119 <sup>T</sup>	KY511142	KY511141	–	KY549682	–	(Crous et al. 2015)
<i>P. rosarum</i>	MFLUCC 17-6054 <sup>T</sup>	NR_157529	NG_059872	–	MG829224	–	(Hyde et al. 2016)

Species	Strain	GenBank accession numbers					References
		ITS	SSU	LSU	<i>tef1</i>	<i>rpb2</i>	
<i>P. rosicola</i>	MFLUCC 15-0042	NR_157528	MG829153	MG829047	–	–	(Hyde et al. 2016)
<i>Paramassariosphaeria anthostomoides</i>	CBS 615.86	MH862005	GU205246	GU205223	–	–	(Vu et al. 2019)
<i>Paraphaeosphaeria rosae</i>	MFLUCC 17-2547 <sup>T</sup>	MG828935	MG829150	MG829044	MG829222	–	(Hyde et al. 2016)
<i>Pararousoella mukdahanensis</i>	KUMCC 18-0121	MH453489	MH453485	–	MH453478	MH453482	(Flakus et al. 2019)
<i>Parathyridaria ramulicola</i>	CBS 141479 <sup>T</sup>	KX650565	KX650565	–	KX650536	KX650584	(Feng et al. 2019)
<i>Phaeodothis winteri</i>	CBS 182.58	–	GU296183	GU301857	–	–	(Zhang et al. 2013)
<i>Pseudocamarosporium propinquum</i>	MFLUCC 13-0544 <sup>T</sup>	KJ747049	KJ819949	KJ813280	–	–	(Thambugala et al. 2017)
<i>Pseudodidymocyrtis lobariellae</i>	KRAM Flakus 25130 <sup>T</sup>	NR_169714	NG_070349	NG_068933	–	–	(Tanaka et al. 2015)
<i>Pseudoneoconiothyrium euonymi</i>	CBS 143426 <sup>T</sup>	MH107915	MH107961	–	–	MH108007	(Valenzuela-Lopez et al. 2017)
<i>Pseudopithomyces entadae</i>	MFLUCC 17-0917 <sup>T</sup>	–	MK347835	NG_066305	MK360083	–	(Mapook et al. 2020)
<i>Pseudorousoella chromolaenae</i>	MFLUCC 17-1492 <sup>T</sup>	MT214345	MT214439	–	MT235769	–	(Liu et al. 2014)
<i>P. elaeicola</i>	MFLUCC 15-0276a	MH742329	MH742326	–	–	–	(Liu et al. 2014)
<i>P. kunmingensis</i>	MFLUCC 17-0314	MF173607	MF173606	MF173605	–	–	(Mapook et al. 2020)
<i>P. pteleae</i>	MFLUCC 17-0724 <sup>T</sup>	NR_157536	MG829166	MG829061	MG829233	–	(Hyde et al. 2016)
<i>P. rosae</i>	MFLUCC 15-0035 <sup>T</sup>	MG828953	MG829168	MG829064	–	–	(Hyde et al. 2016)
<i>P. ulmi-minoris</i>	MFLUCC 17-0671 <sup>T</sup>	NR_157537	MG829167	MG829062	–	–	(Hyde et al. 2016)
<i>Rousoella acaciae</i>	CBS:138873 <sup>T</sup>	KP004469	KP004497	–	–	–	(Karunaratna et al. 2019)
<i>R. aquatic</i>	MFLUCC 18-1040 <sup>T</sup>	NR171975	NG073797	–	–	–	(Liu et al. 2014)
<i>R. chiangraina</i>	MFLUCC 10-0556 <sup>T</sup>	NR155712	NG059510	–	–	–	(Dissanayake et al. 2021)
<i>R. doimaesalongensis</i>	MFLUCC 14-0584 <sup>T</sup>	NR165856	NG068241	–	KY651249	KY678394	(Thambugala et al. 2015)
<b><i>R. doimaesalongensis</i></b>	<b>GMB0497</b>	<b>OR116188</b>	<b>OR117732</b>	–	<b>OR150026</b>	–	<b>This study</b>
<b><i>R. doimaesalongensis</i></b>	<b>GMB0503</b>	<b>OR120435</b>	<b>OR120444</b>	–	<b>OR150027</b>	–	<b>This study</b>
<i>R. elaeicola</i>	MFLUCC 15-15-0276a	MH742329	MH742326	–	–	–	(Crous et al. 2015)
<i>R. euonymi</i>	CBS:143426 <sup>T</sup>	MH107915	MH107961	–	–	MH108007	(Valenzuela-Lopez et al. 2017)
<i>R. guttulata</i>	MFLUCC 20-0102 <sup>T</sup>	NR172428	NG075383	–	–	–	(Senwana et al. 2018)
<i>R. hysteroioides</i>	CBS 546.94	MH862484	MH874129	–	KF443399	KF443392	(Vilgalys et al. 1990)
<i>R. intermedia</i>	CBS 170.96	KF443407	KF443382	–	KF443398	KF443394	(Crous et al. 2013)
<i>R. japonensis</i>	MAFF 239636 <sup>T</sup>	NR155713	–	–	–	–	(Dissanayake et al. 2021)
<i>R. kunmingensis</i>	HKAS 101773 <sup>T</sup>	MH453491	MH453487	–	MH453480	MH453484	(Flakus et al. 2019)
<i>R. magnatum</i>	MFLUCC 15-0185 <sup>T</sup>	–	KT281980	–	–	–	(Jiang et al. 2019)
<i>R. mangrovei</i>	MFLU 17-1542 <sup>T</sup>	MH025951	MH023318	–	MH028246	MH028250	(Jaklitsch and Voglmayr 2016)
<i>R. margidorensis</i>	MUT 5329 <sup>T</sup>	NR169906	MN556322	–	MN605897	MN605917	(Tibpromma et al. 2017)
<i>R. mediterranea</i>	MUT5369 <sup>T</sup>	KU314947	MN556324	–	MN605899	MN605919	(Tibpromma et al. 2017)
<i>R. mexicana</i>	CPC 25355 <sup>T</sup>	KT950848	KT950862	–	–	–	(Crous et al. 2015a)
<i>R. mukdahanensis</i>	MFLU 11-0237 <sup>T</sup>	NR155722	–	–	–	–	(Crous et al. 2014)
<i>R. multiplex</i>	GMB0316 <sup>T</sup>	ON479891	–	ON479892	–	–	(Dong et al. 2020)
<i>R. neopustulans</i>	MFLUCC 11-0609 <sup>T</sup>	KJ474833	KJ474841	–	KJ474850	–	(Dissanayake et al. 2021)
<b><i>R. neopustulans</i></b>	<b>GMB0496</b>	<b>OR120436</b>	<b>OR120446</b>	–	–	–	<b>This study</b>
<b><i>R. neopustulans</i></b>	<b>GMB0502</b>	<b>OR116176</b>	<b>OR117714</b>	–	–	–	<b>This study</b>
<i>R. nitidula</i>	MFLUCC 11-0634	KJ474834	KJ474842	–	KJ474851	KJ474858	(Dissanayake et al. 2021)
<i>R. padinae</i>	MUT 5503 <sup>T</sup>	–	MN556327	–	MN605902	MN605922	(Tibpromma et al. 2017)

Species	Strain	GenBank accession numbers					References
		ITS	SSU	LSU	<i>tef1</i>	<i>rpb2</i>	
<i>R. percutanea</i>	CBS 868.95	KF322118	KF366449	–	KF407987	KF366452	(Ahmed et al. 2014a)
<i>R. pseudohysterioides</i>	GMBC0009 <sup>T</sup>	MW881445	MW881451	–	–	MW883345	(Zhang et al. 2020)
<b><i>R. pseudohysterioides</i></b>	<b>GMB0495</b>	<b>OR116175</b>	<b>OR117737</b>	–	<b>OR150028</b>	–	<b>This study</b>
<b><i>R. pseudohysterioides</i></b>	<b>GMB0501</b>	<b>OR120447</b>	<b>OR120439</b>	–	<b>OR150029</b>	–	<b>This study</b>
<i>R. pustulans</i>	KT 1709	–	AB524623	–	AB539116	AB539103	(Zhang et al. 2020)
<i>R. scabrispora</i>	MFLUCC 14-0582	KY026583	KY000660	–	–	–	(Zhang et al. 2020)
<i>R. siamensis</i>	MFLUCC 11-0149 <sup>T</sup>	KJ474837	KJ474845	–	KJ474854	KJ474861	(Dissanayake et al. 2021)
<i>R. thailandica</i>	MFLUCC 11-0621 <sup>T</sup>	KJ474838	KJ474846	–	–	–	(Dissanayake et al. 2021)
<i>R. tuberculata</i>	MFLUCC 13-0854 <sup>T</sup>	KU940132	KU863121	–	KU940199	–	(Crous et al. 2014)
<i>R. verrucispora</i>	CBS 125434 <sup>T</sup>	KJ474832	–	–	–	–	(Dissanayake et al. 2021)
<i>R. yunnanensis</i>	HKAS 101762	MH453492	MH453488	–	MH453481	–	(Flakus et al. 2019)
<i>Roussoellopsis macrospora</i>	MFLUCC 12-0005	–	KJ474847	–	KJ474855	KJ474862	(Dissanayake et al. 2021)
<i>R. tosaensis</i>	KT 1659	–	AB524625	–	AB539117	AB539104	(Zhang et al. 2020)
<i>Setoarthopyrenia chromolaenae</i>	MFLUCC 17-1444	MT214344	MT214438	–	MT235768	MT235805	(Liu et al. 2014)
<i>Spegazzinia deightonii</i>	yone 212	–	AB797292	AB807582	AB808558	–	(Tanaka et al. 2015)
<i>S. radermacherae</i>	MFLUCC 17-2285 <sup>T</sup>	MK347740	MK347848	MK347957	MK360088	–	(Mapook et al. 2020)
<i>S. tessartha</i>	NRRL 54913	JQ673429	AB797294	AB807584	AB808560	–	(Tanaka et al. 2015)
<i>Thyridaria acaciae</i>	CBS 138873	KP004469	KP004497	–	–	–	(Liu et al. 2014)
<i>T. broussonetiae</i>	CBS 141481	NR_147658	KX650568	–	KX650539	KX650586	(Karunarathna et al. 2019)
<i>Torula herbarum</i>	CBS 111855	KF443409	KF443386	–	KF443403	KF443396	(Crous et al. 2013)
<i>T. hollandica</i>	CBS 220.69	KF443406	KF443384	–	–	KF443393	(Crous et al. 2013)
<i>Tremateia arundicola</i>	MFLU 16-1275	KX274241	KX274254	KX274248	KX284706	–	(Hyde et al. 2020)
<i>T. chromolaenae</i>	MFLUCC 17-1425 <sup>T</sup>	NR_168868	NG_070160	NG_068710	MT235778	–	(Tanaka et al. 2015)
<i>T. guiyangensis</i>	GZAAS01	KX274240	KX274253	KX274247	KX284705	–	(Hyde et al. 2020)
<i>T. murispora</i>	GZCC 18-2787	NR_165916	MK972750	MK972751	MK986482	–	(Feng et al. 2019)
<i>T. thailandensis</i>	MFLUCC 17-1430 <sup>T</sup>	NR_168869	NG_070161	NG_068711	MT235781	–	(Liu et al. 2014)
<i>Verrucoconiothyrium nitidae</i>	CBS:119209	EU552112	–	EU552112	–	–	(Wanasinghe et al. 2018)
<i>Xenocamarosporium acaciae</i>	CPC 24755 <sup>T</sup>	NR_137982	–	NG_058163	–	–	(Crous et al. 2015b)
<i>Xenorousoella triseptata</i>	MFLUCC 17-1438	MT214343	MT214437	–	MT235767	MT235804	(Liu et al. 2014)

## Additional information

### Conflict of interest

The authors have declared that no competing interests exist.

### Ethical statement

No ethical statement was reported.

### Funding

This research was supported by National Natural Science Foundation of China (31960005, 32000009 and 32170019); Science and Technology Department Foundation of Guizhou Province ([2018]2322); Qianhe Talents, Science and Technology Department of Guizhou Province ([2015]4029); Guizhou Provincial Education Department Scientific Research Project for Higher Education Institutions ([2022]064); National Natural Science Foundation of China Karst Centre Project U1812403-4-4.

### Author contributions

Jichuan Kang, Qirui Li, Xiangchun Shen; investigation, Hongmin Hu, Youpeng Wu, Qingde Long; morpho-logical examinations, molecular sequencing, and phylogenetic analyses, Xu Zhang, Sihan Long and Youpeng Wu; specimen identification, Hongmin Hu and Qirui Li; writing—original draft preparation, Hongmin Hu, Minghui He; writing—review and editing, Nalin N. Wijayawardene, Zebin Meng; supervision, Qirui Li. All authors have read and agreed to the published version of the manuscript

### Author ORCIDs

Hongmin Hu  <https://orcid.org/0000-0003-3894-3269>

Sihan Long  <https://orcid.org/0000-0002-8346-3646>

Nalin N. Wijayawardene  <https://orcid.org/0000-0003-0522-5498>

Jichuan Kang  <https://orcid.org/0000-0002-6294-5793>

Qirui Li  <https://orcid.org/0000-0001-8735-2890>

### Data availability

All of the data that support the findings of this study are available in the main text.